THE ORIGINS OF INORGANIC ACIDITY IN FOGS

Thesis by

Daniel James Jacob

In Partial Fulfillment of the Requirements

for the Degree of

Doctor of Philosophy

California Institute of Technology

Pasadena, California

1985

(submitted 15 January, 1985)

TABLE OF CONTENTS

TABLE OF CONTENTS (continued)

ACKNOWLEDGEMENTS

Completion of this thesis owes considerably to my "fog squad" coworkers, Jed Waldman and Bill Munger. They have been great friends and colleagues. I am deeply indebted to my adviser, Michael Hoffmann, who was always sensitive, enthusiastic and supportive, let me have a lot of freedom, and put me back on the right track when needed. I am also deeply indebted to my first adviser, Rick Flagan; in addition to providing great technical advice, he was sensitive and supportive in dealing with my first-year crises - research, courses, army. I am grateful to Jim Morgan, John Seinfeld, and Fred Shair for serving on my examining committee. My research was supported by the California Air Resources Board.

I thank the many faculty, students, and staff who helped me out at some point or the other. Special thanks go to Ted Russell, Glen Cass, and Greg McRae; they were full of great advice, and took the time to provide it. Don Buchholz did great work for the fog squad in the field. Thanks to Sandy Brooks and Elaine Granger for their help with paperwork. Thanks to Theresa Fall and coworkers for putting up with my deadlines and changes of mind. Thanks to Rayma Harrison and Gunilla Hastrup for their help in the library. Thanks to Elton Daly, Joe Fontana, Rich Eastvedt, and Leonard Montenegro for their great advice and for building worthwhile equipment from my vague designs.

Finally, I dedicate this thesis to my parents who loved me and supported me the whole way.

ABSTRACT

A rotating arm device to collect large samples of fogwater for chemical analysis was designed and fully characterized. This instrument was used to determine the chemical composition of fogwater at a large number of sites in California. Fogwater at both urban and non-urban sites was frequently found to contain important inorganic acidity. Chemical models were developed to interpret the origins of this acidity in terms of aqueous-phase S(IV) oxidation reactions and acid/base titration processes in the fog and the precursor atmosphere. These models were found to succesfully interpret the inorganic acidity in fogwater and aerosol during wintertime stagnation episodes in the San Joaquin Valley of California.

LIST OF TABLES

LIST OF TABLES (continued)

LIST OF TABLES (continued)

LIST OF FIGURES

LIST OF FIGURES (continued)

LIST OF FIGURES (continued)

LIST OF FIGURES (continued)

LIST OF FIGURES (continued)

OVERVIEW

The principal object of this thesis is to document the chemical composition of fogwater in California, explain the frequent occurrence of high-acidity fog events, and characterize the main processes determining fogwater acidity. Few attempts have been made prior to this work to collect fogwater for chemical analysis. Houghton (1955) observed pH values in the range 3.5 - 7.4 in coastal fogs of New England and Canada, and large concentrations of chloride and sulfate. Mrose (1960) sampled coastal and urban fogs in East Germany, and reported pH values in the range 3.8 - 4.2. Mack et al. (1977) found high sulfate and nitrate concentrations in fogwater collected off the shore of California. A few other investigators have collected cloudwater intercepting mountain slopes (Okita, 1968; Lazrus, 1970). The sparseness of data on the chemical composition of fogwater is rather surprising, since fogs have been associated with major health-threatening air pollution episodes: notorious examples are the fogs of London (Commins and Waller, 1967), the Meuse valley (Firket, 1936), and Donora, PA (Schrenk et al., 1949). Further, deposition of acid fogwater has been shown to damage crops (Thomas et al., 1952; Granett and Musselman, 1984) and forests (Scherbatskoy and Klein, 1983).

A likely reason for the sparseness of data is that collecting fogwater is not a trivial matter. Fog droplets range in size from 1 to 100 um, with a mass median diameter typically in the 10 - 30 μm range (Pruppacher and Klett, 1978). Droplets of this size are difficult to collect efficiently because of their inertia. A

fogwater sampling device must collect efficiently droplets up to at least 100 um; at the same time, it must exclude non-activated submicron particles which have physical and chemical properties different from those of the fog droplets. Further, large amounts of water must be provided for wet chemical analysis, while minimizing evaporation and condensation during the sampling process. These requirements cannot be satisfied by standard techniques for aerosol sampling.

The first step in this project was to develop a reliable instrument for fogwater sampling. The rotating arm collector designed in our laboratory (Chapter 1) has proven to be an effective means for collecting representative fogwater samples (Hering and Blumenthal, 1984). The instrument collects fog droplets by impaction on a slotted rod rotating at high velocity; impacted droplets are driven by centrifugal force into bottles mounted at the ends of the rod. In dense fog, collection rates of 1 ml min^{-1} are typically achieved. Droplet sizes are preserved at all stages of collection; i.e., no significant evaporation or condensation occurs over the course of the sampling process. The instrument was calibrated by releasing a single plume of SF_6 tracer and chemically tagged monodisperse aerosol in the atmosphere upwind of a scaled-down version of the instrument. By comparing the SF_6 concentration measured in the plane of collection to the amount of aerosol collected on the rod, the collection efficiency vs. particle size was determined. The lower size cut (50% collection efficiency) was found to be 20 μm diameter.

The rotating arm collector has drawbacks in that it does not

collect small fog droplets efficiently, it is not easily automatable, and it presents safety problems. Chapter 2 describes a screen collector which we recently developed to provide a simple. reliable instrument for routine monitoring of fogwater chemical composition.

The rotating arm collector was used in fogwater sampling programs at several locations in California. Fogwater samples collected along the California coast were found to be consistently acidic, even in rural areas (Chapter 3). Extremely high acidities (pH down to 1.69) were observed at sites in the Los Angeles basin and downwind. The main contributors to strong acidity were sulfuric and nitric acids; coastal urban activities and oil production operations are important sources of SO_2 and NO_x, precursors of these acids. Coastal atmospheres were found to have low acid-neutralizing capacities, and thus to be very sensitive to acid inputs.

A dynamic equilibrium model of fogwater chemistry was developed to study the effect on fogwater acidity of SO_2 oxidation in the fog droplet phase. Chapter 4 presents a review of the role of trace metals in catalyzing S(IV) aqueous-phase oxidation processes. It is shown with a simple model that the autoxidation reaction catalyzed by Fe^{3+} and Mn^{2+} in solution can be an important source of sulfuric acid production in fog. A model is developed in Chapter 5 which includes a large number of aqueous-phase equilibria and oxidation pathways, although it makes some crude assumptions regarding physical processes (e.g., transport, deposition, size-composition relationships are ignored). From the S(IV) oxidation rates derived in Chapter 4, it is shown that a fog droplet initially forming on non-acidic nuclei under conditions typical of the Los Angeles coastline may experience a

rapid drop in pH to below pH 3 as a result of SO_2 scavenging and aqueous-phase oxidation of S(IV) to S(VI). The main aqueous-phase oxidants are found to be H_2O_2 and O_2 (catalyzed by Fe^{3+} and Mn^{2+}). Ozone is an important oxidant at high pH, but becomes ineffective at pH < 4. The stable S(IV)-formaldehyde adduct is found to be the major form of S(IV) in the fogwater, but it forms too slowly to compete with S(IV) oxidation. The extent of S(IV) oxidation is mostly limited by the availability of H_2O_2 and the low solubility of SO_2 at low pH. When fog droplets form on acidic nuclei, it is found that the low initial pH prevents oxidation of S(IV) other than by H_2O_2. Aqueous-phase conversion of N(III) to N(V) in fog is found to be very slow.

The model of Chapter 5 was used to study the scavenging of trace gases in fog. Nitric acid is 100% scavenged under all conditions because of the large amounts of suspended liquid water. Ammonia is 100% scavenged at pH < 5, but at higher pH it mostly remains in the gas phase. Only a small fraction of SO_2 is initially scavenged, but this fraction increases as aqueous-phase S(IV) is oxidized to S(VI). Still, most of the SO_2 remains in the gas phase after 4 hours of fog. A small fraction of formaldehyde is scavenged in fog by formation of the S(IV)-formaldehyde adduct. Of the oxidants, O_3 is poorly soluble but H_2O_2 is highly soluble. Because H_2O_2 rapidly oxidizes S(IV) in the droplet, it is quickly depleted from the atmosphere.

Fogwater acidity may be neutralized if a sufficient amount of base is present in the atmosphere. Neutralization of fogwater acidity by ammonia was investigated in two field experiments

conducted in the San Joaquin Valley of California, where large inputs of strong acids are provided by oil and gas production (SO_2, NO_x), and large quantities of NH_3 are released by industrial farming and livestock feeding operations. Chapters 6 and 7 present the results of these field experiments. The H_2SO_4-HNO_3-NH_3 system contributed over 90% of the inorganic aerosol and fogwater ionic loading, and the fogwater alkalinity/mineral acidity could be correctly predicted from the local balance of sulfuric acid, nitric acid and ammonia in the atmosphere. The fogwater acidity directly reflected the relative proximities of oil fields and confined feeding operations.

Most of the fogs sampled in the San Joaquin Valley formed over the course of extended stagnation episodes. Progressive pollutant accumulation under stagnant conditions was documented under non-foggy stagnant conditions, and decreases in aerosol concentrations were observed following fogs. It is suggested that deposition of fog droplets provides a rapid sink of suspended pollutants, so that the occurrence of fogs limits pollutant accumulation in a stagnant atmosphere.

Accumulation profiles observed under stagnant conditions are discussed in detail in Chapter 7. Deposition was the principal means of removal for S(VI), N(V), and N(-III); the patterns of pollutant accumulation were consistent with deposition velocities < 0.1 cm sec^{-1} for secondary (SO_4^{2-}, NO_3^-, NH_4^+, H^+) aerosol, and deposition velocities > 1 cm sec^{-1} for $HNO_3(g)$. Slow scavenging of SO_2 by fog was documented, and an average SO_2 conversion rate of 2 % h^{-1} was determined in an overcast boundary layer. Production of HNO_3 was observed at the beginning of the stagnation episode, but was limited

by the availability of gas-phase oxidants. NO_x was found not to be significantly scavenged by fogwater. Overall, accumulation of strong acids H_2SO_4 and HNO_3 over the course of a stagnation episode resulted in a decrease of alkalinities at all sites in the southern San Joaquin Valley, and production of mineral acidities at the sites most distant from NH_3 emissions.

The San Joaquin Valley experiment provided simultaneous measurements of S(VI), N(V), and N(-III) concentrations in the gas phase, the aerosol, and the fogwater. These data were used in Chapter 8 to test the applicability of thermodynamic models for the H_2SO_4-HNO_3-NH_3-H_2O system at high humidities and in fogs. Under non-foggy alkaline conditions the aerosol was a neutralized mixture, alkalinity remained in the gas phase as $NH_3(g)$, and $HNO_3(g)$ concentrations were very low. Under non-foggy acidic conditions $NH_3(g)$ concentrations were very low, and the acidity was present both in the gas phase as $HNO_3(g)$ and in the aerosol phase as partly neutralized sulfuric acid. These findings are in qualitative agreement with the model results of Bassett and Seinfeld (1983). The dissociation constants $K=P_{NH3}P_{HNO3}$ predicted by Bassett and Seinfeld agreed to within one order of magnitude with the products of concentrations observed in the field, although they were systematically too low. Several possible explanations for this discrepancy were discussed.

In fog, concentrations of $HNO_3(g)$ were at or below the detection limit of 4 neq m^{-3} under non-acidic conditions, and were very low (although generally nonzero) under acidic conditions. The observation of detectable $HNO_3(g)$ in acidic fog was attributed to the

presence of unsaturated air parcels within the fog, and to the slow rate of diffusion of $HNO_3(g)$ to the fog droplets. No detectable $NH_3(g)$ was found under foggy acidic conditions, but substantial amounts were found under foggy non-acidic conditions. The observed $NH_3(g)$ concentrations were of the same magnitude as those predicted at equilibrium with fogwater.

REFERENCES

Bassett, M., and Seinfeld, J.H. 1983. Atmos.Environ. 17,2237-2252.

Commins, B.T., and Waller, R.E. 1967. Atmos.Environ. 1,49-68.

Firket, J. 1936. Trans.Faraday Soc. 32,1192-1197.

Granett, A.L., and Musselman, R.C. 1984. Atmos.Environ. 18,887-891.

Hering, S.V., and Blumenthal, D.L. 1984. "Fog Sampler Intercomparison Study: Final Report to the Coordinating Research Council." Available from Coordinating Research Council, 219 Perimeter Center Parkway, Atlanta, GA.

Houghton, H.G. 1955. J.Met. 12,355-357.

Lazrus, A.L., Baynton, H.W., and Lodge, J.P. 1970. Tellus 22,106-114.

Mack, E.J., Katz, U., Rogers, C.W., Gaucher, D.W., Piech, K.R., Akers, C.K., and Pilie, R.J. 1977. Report CJ-6017-M-1, Calspan Corp., Buffalo, NY.

Mrose, H. 1960. Tellus 18, 256-270.

Okita, T. 1968. J.Met.Soc.Japan 46,120-126.

Pruppacher, H.R., and Klett, J.D. 1978. Microphysics of Clouds and Precipitation. Reidel, Amsterdam,418-421.

Scherbatskoy, T., and Klein, R.M. 1983. J.Environ.Quality 12,189-195.

Schrenk, H.H., Heiman, H., Clayton, G.D., Gafefer, W.M., and Wexler, H. 1949. "Air Pollution in Donora, PA: Epidemiology of the Unusual Smog Episode of October 1948, Preliminary Report." Public Health Bulletin 306,pp 1-73, Public Health Science: Washington D.C.

Thomas, M.D., Hendricks, R.H., and Hill, G.R. 1952. in Air Pollution, L. McCabe ed., McGraw-Hill, New York, p.41-47.

CHAPTER I

FOGWATER COLLECTOR DESIGN AND CHARACTERIZATION

by Daniel J. Jacob, Rueen-Fang T. Wang, and Richard C. Flagan

Environmental Science and Technology 18, 827-833 (1984)

Reprinted from ENVIRONMENTAL SCIENCE & TECHNOLOGY, Vol. 18, Page 827, November, 1984

2

Fogwater Collector Design and Characterization

Daniel J. Jacob, Rueen-Fang T. Wang, and Richard C. Flagan*

Environmental Engineering Science, Keck Engineering Laboratories, California Institute of Technology, Pasadena, California 91125

■ The detailed characterization of a rotating arm collector to sample ambient fog droplets for chemical analysis is presented. Because of the large volume of sample required, and because fog droplets are of supermicron size and are sensitive to local thermodynamic disturbances, conventional methods for atmospheric aerosol sampling are not suitable for fogwater sampling. Design criteria for fogwater samplers are outlined. Devices used in previous investigations are evaluated in light of these criteria. The design of a rotating arm collector is discussed, and it is shown that this instrument performs adequately in preserving the physical and chemical integrity of the sample at all stages of collection. Limitations in the design due to mechanical constraints are discussed. Results of an in situ calibration experiment using a chemically tagged monodisperse aerosol indicate a size cut of 20-μm diameter.

Introduction

Supermicron particles contribute significantly to the total mass of a dry aerosol (*1*). This contribution increases considerably when the aerosol is wetted, especially under supersaturated conditions in which activated condensation nuclei grow rapidly to form cloud or fog droplets. Whereas the mass loading of an urban aerosol under nonsaturated conditions is of the order of 10^{-4} g m^{-3}, the liquid water content in a cloud or fog ranges from 0.01 to 1 g m^{-3}, with supermicron droplets constituting the bulk of the aerosol mass. In urban environments fogwater has been found to contain extremely high pollutant concentrations, often associated with high acidities (*2, 3*).

Supermicron particles are difficult to collect efficiently because their inertia may prevent them from following the air streamlines converging toward the inlet of the sampler (*4*). Furthermore, water droplets in the atmosphere are in a fragile thermodynamic balance with the ambient humidity which is very sensitive to perturbations by a sampling device. Conventional methods for collecting samples of total particulate matter may, therefore, lead to sampling biases due to anisokinetic sampling conditions or changes in temperature or pressure. Fog sampling is further complicated by the relatively large sample volume required for the study of the detailed aquatic chemistry. At least 10 mL of sample is needed for the standard inorganic analysis routinely carried out in our fog program (*3*). If the variation in chemical composition throughout the fog event is to be studied, sampling intervals should be short. For a typical liquid water content of 0.1 g m^{-3}, a sampling rate of over 1.7 m^3 min^{-1} is required to collect 10 mL for analysis in an hour. Larger sampling rates are required for the study of light fogs.

A rotating arm collector based on the principle of inertial impaction has been developed and used in our intensive fog sampling program. Major advances in the understanding of fog chemistry and the role of fogs in acid deposition have been made by using this device (*3, 5*). In a recent field intercomparison study of fogwater collectors (*6*), samples were collected simultaneously with instruments from five different research groups and analyzed for major ions. Ionic concentrations in samples collected by the rotating arm collector and a jet impactor (*7*) agreed within 5%; other collectors gave systematically either higher or lower concentrations. The rotating arm collector was found to collect water efficiently in both light and heavy fogs.

To date, the sampling characteristics of the rotating arm collector have only been qualitatively explored by measuring the change in the droplet size distribution in a cloud chamber which results from its operation. These measurements indicated that the minimum size of particles collected was at least 8 μm but did not provide sufficient resolution to determine the size-dependent collection efficiency (*8*). In this paper we first elaborate on the design criteria relevant to fogwater collection and then present a detailed examination of the design and operation of our rotating arm collector. Constraints on the design due to power requirements and possible sample biases due to aerodynamic heating are explored. Measurements of the collection efficiency as a function of particle size are presented.

Design Criteria for Fogwater Collectors

Size Cut. Fog droplets form by activation of atmospheric particles (condensation nuclei) under supersaturated conditions. At the levels of supersaturation found in the atmosphere, the lower size limit for particles to be activated is of the order of 0.1 μm (*9*). Figure 1 shows how fog formation can shift the size distribution of an urban aerosol; particles in the first mode (below 0.1 μm) are rather unaffected by the condensation process, but most particles in the two higher modes grow by condensation to much larger sizes. Therefore, two types of particles coexist in a fog: (1) supermicron fog droplets and (2) nonactivated, primarily submicron, particles. Being dilute aqueous solutions, fog droplets do not interact with their environment in the same way as the solid or concentrated submicron particles (*10, 11*). It is, therefore, important that a fogwater sampler differentiate between the two types of particles.

Fog droplets range in size from 1 to 100 μm, with a mass median diameter usually in the range 10–40 μm (*12–15*). The dependence of the fog droplet chemical composition on droplet size has not been rigorously investigated to date; general predictions from droplet growth theory (*16*) are difficult to make because humidities in fogs fluctuate rapidly in a manner that is still poorly understood (*17, 18*). Large droplets are not necessarily more dilute than smaller droplets because they generally result from condensation on larger nuclei. If the total pollutant burden associated with fogs is to be determined, droplets of all sizes should be collected with the same efficiency. Nonactivated submicron particles represent a very small fraction of the total aerosol mass but they could, if collected, contribute a sizable amount of solutes to the sample and result in a serious bias. A sharp lower size cut in the range 1–10-μm diameter is, therefore, desired. Furthermore, since most of the fog mass is associated with large droplets, droplets up to about 100-μm diameter must be collected without bias.

Three methods are available to collect the large particles while excluding the smaller particles: sedimentation, inertial separation, and removal of smaller particles by

0013-936X/84/0918-0827$01.50/0

Table I. Fogwater Collectors Reported in the Literature

reference	type	impaction velocity, cm s^{-1}	sampling rate, m^3 min^{-1}	characteristic width[a] inlet, cm	characteristic width[a] impaction surface, cm	lower size cut, μm	inlet Stokes no. for 100-μm droplets
passive							
Mrose (20)	cloth surface	ambient wind	variable		?[f]	variable	
Okita (21)	grid	ambient wind	variable		0.01	variable	
Lazrus et al. (22)	screen	ambient wind	variable		?	variable	
Sadasivan (23)	screen	ambient wind	variable		?	variable	
Falconer and Falconer (24)	grid	ambient wind	variable		0.02	variable	
active							
Houghton and Radford (12)	screen	600	102	30	0.01	3[c]	0.6
May (25)	grid	450	11	10	0.05	7[c]	1.4
May (25)	jet impactor	1700	0.05	0.85	0.4	?	13
Okita (21)	screen	94	1	7.5	?	?	0.3
Mack and Pilie (26)	rotating arm	1500–5000	7		0.45	?	
Katz (7)	jet impactor	2000	1.2	?	0.2	5[d]	?
Brewer et al. (27)	screen	320	1.5	5	0.02[e]	5[c]	2.0
this paper	rotating arm	3800–5600	5		0.48	20	

[a] Characteristic width of inlet: radius of circular inlet (12, 21, 25b, 27), half-width of square inlet (25a). Characteristic width of impaction surfaces: radius of wires (12, 21, 24, 25a, 27), half-width of jet (7, 25b), radius of rod (26, this paper). [b] Diameter of droplets collected with 50% efficiency. [c] Calculated from impaction theory for cylinders (19). [d] Calculated by Katz from theory and confirmed by experiment. [e] Obtained by personal communication from R. L. Brewer. [f] ? = not reported, or cannot be computed from available data.

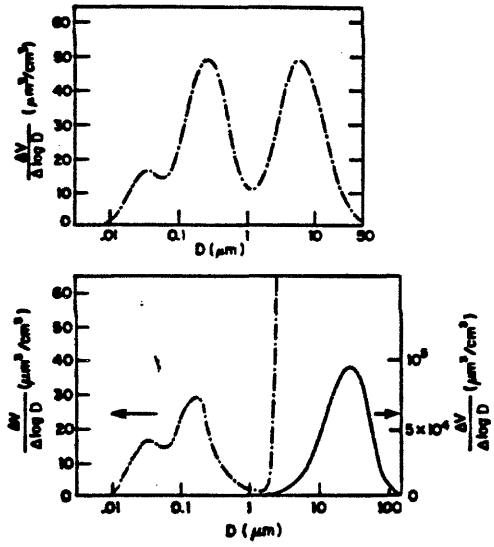

Figure 1. (Top) Typical urban aerosol size distribution profile (1). (Bottom) Expected shift in the size distribution profile as a result of fog formation.

diffusion. Of these, inertial separation, particularly impaction, most readily achieves sharp size cuts of a few microns and has been the method favored by past investigators. The efficiency of collection by impaction is a function of the Stokes number St (19):

$$\mathrm{St} = \frac{\rho_D D^2 U}{18 \mu a} \qquad (1)$$

where ρ_D is the droplet density, D is the droplet diameter, U is the velocity of approach, μ is the viscosity of air, and a is a characteristic width of the impaction surface. The size cut of a sampler is defined as the diameter D_{50} of droplets collected with 50% efficiency, and the cutoff Stokes number St_{50} is the corresponding Stokes number. Fogwater samplers used in past investigations (Table I) can be divided into two general groups: (1) passive collectors, where droplets impact on the collecting surface with the velocity of the ambient wind, and (2) active collectors, where droplets are accelerated to a certain velocity as they approach the collection surface. Passive collectors have the obvious drawback that the impaction velocity is not well-defined but instead fluctuates with the ambient wind. As a result the size cut varies with time, and the sample is not necessarily representative of the actual fogwater. Furthermore, at low wind speeds the minimum size of particles which will impact becomes large enough that the rate of sample collection becomes unacceptable, thereby precluding the use of these collectors in many locations. In active collectors, the size-dependent collection efficiency can be characterized for a given geometry of the impaction surface. However, modification of the ambient velocity of the droplets introduces two potentially important problems: perturbation of the ambient thermodynamic equilibrium and anisokinetic sampling.

Perturbation of the Ambient Thermodynamic Equilibrium. Modification of the flow field in active collectors may produce significant evaporation or condensation of the droplets as they approach the impaction surface. The total loss of water droplets has been reported past the first two stages of a cascade impactor (25). The extent to which droplet sizes are modified during approach can be estimated by simple mass transfer calculations, as shown in the next section. Unfortunately, no such calculations have been reported in the references of Table I.

Evaporation may also occur following collection if the droplets are not sheltered immediately from the flow of air past the impaction surface, because the air mass in a fog is thermodynamically inhomogeneous (29) and contains pockets of unsaturated air. Aside from evaporation, contact of the collected droplets with changing air masses may alter their compositions. It is therefore important that collected droplets be removed rapidly from the air flow. In the jet impactor designed by Katz (7), this is achieved with a rotating impaction surface; in the rotating arm collector, centrifugal force rapidly drives the impacted droplets into collection bottles where the air is stagnant. The screen collectors of Table I rely on gravity to draw the impacted droplets into storage bottles at the bottom of the

screen, but this is a slow process (especially in light fogs).

Anisokinetic Sampling. Recent studies of anisokinetic sampling biases (*30*, *31*) have indicated that a sampler oriented into the wind can lose over 30% of particles with inlet Stokes' numbers larger than 0.5. In a crosswind, losses are considerably greater. Losses are found to be maximum for sampling velocities 2–5 times the ambient wind velocity. In addition, deposition of most particles to the walls within a few inlet diameters from the inlet has been reported for Re > 5000 (*31*).

Although moderate sampling velocities have been used in the ducted devices listed in Table I, inlet Stokes' numbers are still high in most cases. In screen and grid collectors, the moderate sampling velocities used introduce the additional problem that very thin wires are required for impaction. Because the larger droplets in the fog are then comparable in size to the radius of the impaction cylinder, interception and aerodynamic interactions between the droplets and the wires become important. The impaction characteristics are then quite different from those of the point particles considered in most theoretical treatments of impaction on cylinders. The apparent geometry of a very thin wire also changes significantly as fog droplets collect on it, introducing uncertainty in the size cut.

Proper scaling of the inlet could allow the use of high impaction velocities with little anisokinetic sampling bias. However, droplets tend to fly off collection strings at velocities higher than about 8 m s^{-1} (*12*).

The anisokineticity effect can be suppressed by eliminating the inlet and, instead, generating an apparent velocity by moving the impaction surface at high speed through the ambient air. Such devices have been used in airborne sampling of clouds (*32*, *33*), where the speed of the aircraft constituted the apparent velocity. In ground-based collectors, high velocities can be generated by using a rotating system.

Design of a Rotating Arm Collector

Rotating arm collectors have been used for many years to collect biological particles on adhesive coated surfaces (*34–36*). Recently, a rotating arm virtual impactor has been developed to sample isokinetically giant atmospheric particles (*37*). In another device, the solid arms have been modified to collect fogwater by introducing a slot in the leading edges of a hollow arm (*26*). For the purpose of our field programs, we have developed an improved version of the latter collector.

Principle. The design of the rotating arm collector used in the Caltech fog sampling program is shown in Figure 2. A motor drives at high speed (1700 rpm) a type 304-L stainless steel solid rod of length $2L$ = 63 cm. Each end of the rod has a slot milled into its leading edge. Standard 30-mL VWR narrow mouth bottles are mounted at the ends of the arm to collect the water which impacts in the slots and flows outward by centrifugal force. Threaded Teflon tubes screwed onto the end of the arm and extending inside the collection bottles prevent the collected fogwater from running out after the instrument is stopped. Deflectors prevent water which impacts on the solid part of the arm from entering the slot since the collection of this water would bias the sample toward large droplet sizes. Small fins are welded to the back of the arm for extra strength. The entire arm is Teflon coated. In the absence of previous calibration data, the design was based on a cutoff Stokes number of unity. The cutoff size is weakly dependent on St_{50}; i.e., $D_{50} \propto St_{50}^{1/2}$, so even though the actual St_{50} may differ substantially from unity, the effect on D_{50} was not expected to be too large.

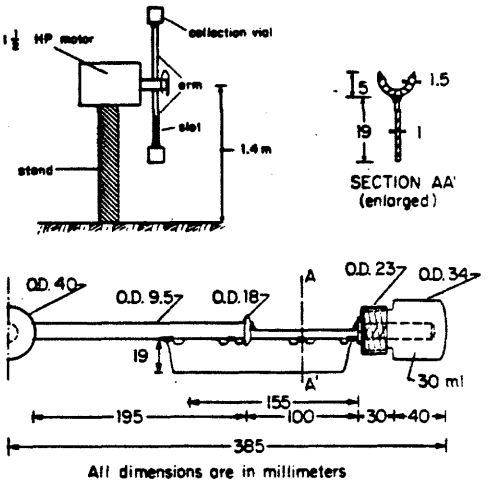

Figure 2. Caltech rotating arm collector. Full welds attaching the fin to the rod are shown in dark.

Mechanical Constraints. The size cut is determined by the choice of $(U/w)^{1/2}$, where w is the width of the slotted portion of the arm. Because reducing w leads to a proportional reduction in the sampling rate achieved with the instrument, a preferable way to obtain an acceptably low D_{50} is to operate at a high approach velocity. However, the resulting aerodynamic drag force F limits the extent to which U can be increased.

The arm consists of cylindrical sections and a half-cylinder cup. The drag coefficients C_d of these shapes at Reynolds numbers in the range 10^4–10^5 are approximately 1 and 2, respectively (*38*). The power P required to rotate the arm at a rotating speed ω (rps) is given by

$$P = 2\int_0^L \frac{dF}{dl}\, U(l)\, dl \qquad (2)$$

This may be separated into the components for the solid rod ($l < L_1$), the slot ($L_1 < l < L_2$), the bottle cap ($L_2 < l < L_3$), and the bottle ($L_3 < l < L$). Noting that the drag force is given by

$$F = C_d A \rho_a (U^2/2) \qquad (3)$$

where A is the projected area of the shape and ρ_a is the density of air, we find

$$P = 2\rho_a \omega^3 \pi^3 \sum_{i=1}^{4} C_{di} w_i (L_i^4 - L_{i-1}^4) \qquad (4)$$

where the w_i's are the widths of the corresponding portions of the arm, $L_0 = 0$, and $L_4 = L$. The power required to drive the arm is a strong function of the dimensions of the arm and the rotation frequency. To facilitate operation of the arm using readily available electrical circuits, the size and speed must be limited. Our rotating arm was designed to achieve an acceptable sampling rate and size cut, while not requiring more than a 110-V, 15-A circuit to drive the sampler. The power required when the collector is rotating at 1700 rpm is calculated from eq 4 to be 900 W. A 1.5-hp (1120-W) motor is sufficient to drive the collector, and this is still compatible with electrical circuits likely to be available in the field. The 30-mL cylindrical collection bottles are major contributors to the drag (450 W) because of their size, shape, and velocity. Collection vials are very small in the instrument described by Mack and Pilie (*26*), but the resulting samples are then too small for chemical determination, and the sampler is

inconvenient because of rapid overloading of the vials. Streamlined bottles or bottle casings could be adapted to the present design to minimize the drag while keeping the sample volume large enough to make the instrument practical.

Specifications. The slot velocities range from 38 to 56 m s^{-1}, and the Reynolds numbers at the slots range from 24 000 to 35 000. Laboratory tests under zero wind conditions indicate that air is drawn through both faces of the collector at a velocity of 1.5 m s^{-1} roughly uniform across the plane of collection (measured 25 cm away from the plane of collection). The sampled air is expelled radially (velocity of 4 m s^{-1} measured 25 cm away from the tip). This induced flow ensures that the sampled air is entirely renewed at every half-rotation of the arm, so that the sampling rate is 5 m^3 of air/min. Assuming 100% efficiency, a collection rate of 0.5 mL min^{-1} would be achieved in a fog of 0.1 g m^{-3} liquid water content. Collection rates of up to 2 mL min^{-1} have been obtained in the field.

Droplet Evaporation. Droplet evaporation may occur at the three stages of collection: (1) as the droplet approaches the impaction surface, (2) in the collection slots, and (3) in the collection bottles.

Evaporation during approach is most likely to occur as the droplet approaches the slot at high apparent velocity. Let us consider, as a worst case, the stagnation streamline; as air approaches the slot its velocity decreases from U_∞ in the free stream to 0 at the stagnation point. This deceleration leads to aerodynamic heating. We write the appropriate equations for mass transfer (*16*) and droplet trajectory: because we are concerned only with activated supermicron droplets, we neglect the effect of solutes on the physical properties of the droplets.

$$r\frac{dr}{dt} = \frac{s - y(T)}{\dfrac{\rho_W RT}{e_{sat}(T)DM_r} + \dfrac{\Delta H \rho_W}{kT}\left(\dfrac{\Delta H M_r}{RT} - 1\right)} \tag{5}$$

$$y(T) = \frac{2\sigma M_r}{RT\rho_W r}$$

$$\frac{dz}{dt} = -U_D \tag{6}$$

$$\frac{dU_D}{dt} = -\frac{3}{8}\left(\frac{\rho_a}{\rho_W}\right)C_d\frac{(U_D - U)^2}{r} \tag{7}$$

r is the droplet radius; $s = (e/e_{sat}(T)) - 1$ is the ambient supersaturation, where e is the water vapor pressure over the droplet and $e_{sat}(T)$ is the saturation water vapor pressure over a plane water surface at temperature T; σ is the surface tension of water against air; R is the universal gas constant; ρ_W and ρ_a are the densities of water and air, respectively; D is the diffusivity of water vapor in air; ΔH is the latent heat of vaporization of water; k is thermal heat conductivity of air; M_r is the molecular weight of water; z is the distance of the droplet to the collector; U is the velocity of the air flow; U_D is the velocity of the approaching droplet. The local Reynolds number Re_l of the droplet is

$$Re_l = \frac{2|U_D - U|r}{\nu} \tag{8}$$

where ν is the kinematic viscosity of air. The drag coefficient C_d can be approximated for $Re_l < 10^3$ by (*39*)

$$C_d = \frac{24}{Re_l}(1 + 0.158Re_l^{2/3}) \tag{9}$$

Under the assumption that the compression proceeds isentropically, the temperature and pressure fields for the approaching droplet are given by

$$T = T_\infty + \frac{U_\infty^2 - U^2}{2c_p} \tag{10}$$

$$P = P_\infty\left(\frac{T}{T_\infty}\right)^{\gamma/(\gamma-1)} \tag{11}$$

where c_p is the specific heat of air at constant pressure and γ is the ratio of specific heats. The water vapor pressure is calculated by assuming that the mixing ratio of water vapor remains constant as the air approaches the collector and that droplets in the free stream are at equilibrium with water vapor:

$$e(T) = \frac{P}{P_\infty}e_{sat}(T_\infty)[1 + y(T_\infty)] \tag{12}$$

For a given $U(z)$ along the stagnation streamline, the coupled eq 5–7 can readily be solved numerically. Unfortunately, the complicated potential flow around a cup has not yet been characterized to the authors' knowledge. It is assumed here that the flow (at least to within some distance of the impaction surface) should be comparable to that around a cylinder of diameter w, for which the potential flow solution along the stagnation streamline yields

$$U = U_\infty\left[1 - \left(\frac{w}{2z}\right)^2\right] \tag{13}$$

The system of eq 5–7 is then integrated with a fourth-order Runge–Kutta routine. Under the conditions U_∞ = 56 m s^{-1}, T_∞ = 283 K, and P_∞ = 1 atm, the percentage of loss in droplet mass by the time the droplet reaches the stagnation point (actually the time at which $(2z - w)/w < 0.001$) is less than 0.1% for activated supermicron droplets. Increasing U_∞ to 100 m s^{-1} does not significantly increase this loss; therefore, evaporation during approach to the slots is not a constraint in choosing higher approach velocities.

A similar mass transfer calculation was conducted to evaluate the effect of thermodynamic modifications as air is drawn through the sampler with a velocity U = 1.5 m s^{-1}. It was found that no significant change in droplet size occurs for supermicron droplets during that stage of approach.

Evaporation in the slot could also occur after impaction from the thin film of water in the slot to the unsaturated air above. Because the flow patterns in the slot originate mostly from turbulent eddies, an accurate description of the transfer phenomena would be very complicated. By using an oversimplified model of tangential flow of unsaturated air over a flat plate, we estimated that under the worst conditions the evaporation rate could be no more than 0.01 g min^{-1}. Even in this case, evaporation is still very small at typical collection rates (0.1–1 g min^{-1}).

Finally, evaporation in the collection bottles must be considered. As a test, the bottles were filled halfway with water (15 mL in each), mounted on the collector, and spun for 30 min in a dry atmosphere. This did not affect the volume of water in the bottles, which shows that evaporation in the bottles is negligible.

Safety. Safety is a primordial concern for a large diameter device rotating in the open. The collector must be carefully balanced to prevent vibrations and securely mounted to a rigid stand. The mechanisms for mounting the bottles must be able to withstand the loads due to high acceleration (1200*g*). Stainless steel caps with close tol-

erance threads were found to be satisfactory in laboratory tests. The operating site must be carefully selected and supervised to minimize the hazard.

The arm must be inspected to detect any mechanical flaws or stress concentration points which could lead to failure by fatigue. In the original design of the collector (*8*), the back fin was attached to a 304 steel rod with tack welds. This method of attachment produced a sharp angle with the rod, which served as an incipient crack. Stress concentration at that point led to one occasion of failure by fatigue. To prevent this from reoccurring we have modified the design of the fins; the points of contact with the rod are now smooth and fully welded. We have switched to 304-L steel, which is less prone to weakening at the weld points. Also, the instrument is now stress-relieved after welding to further reduce the risk of failure.

Calibration

Mack and Pilie (*26*) used theoretical results for impaction on cylinders to predict the collection efficiency of their rotating arm collector. However, they presented no justification for doing so. Because of the complicated flow inside the cavity, impaction in the slot may differ from impaction on a cylinder. Experimental calibration is necessary.

Scaling Considerations. At high flow Reynolds numbers and low interception numbers, the collection efficiency, η, of an impaction surface can be satisfactorily reduced to a function of the three dimensionless groups St, Re_D, and Mach number (*19*). Re_D is the droplet Reynolds number based on the droplet diameter and the free-stream velocity. When the Mach number based on the local sonic speed is smaller than 0.4, it has a negligible effect on the collection efficiency (*40*). As a good approximation

$$\eta = f(\mathrm{St}, \mathrm{Re_D}) \tag{14}$$

In the range $10^0 < Re_D < 10^3$, which is the range at which the droplets are collected in the slots, η is a strong function of both St and Re_D (*19*). To reduce the dependence of η to one dimensionless group, Israel and Rosner (*28*) have proposed a generalized Stokes number which accounts for the variation in the droplet drag coefficient at higher particle Reynolds numbers:

$$\mathrm{St}' = \frac{4}{3}\left(\frac{\rho_D}{\rho_a}\right)\left(\frac{D}{a}\right)\int_0^{\mathrm{Re_D}} \frac{d\mathrm{Re}'}{C_d(\mathrm{Re}')\mathrm{Re}'} \tag{15}$$

The generalized Stokes number reduces to the Stokes number for $Re_D \ll 1$. For higher particle Reynolds numbers St′ is related to St by

$$\mathrm{St}' = \mathrm{St}\psi(\mathrm{Re_D}) \tag{16}$$

where

$$\psi(\mathrm{Re_D}) = \frac{24}{\mathrm{Re_D}}\int_0^{\mathrm{Re_D}} \frac{d\mathrm{Re}'}{C_d(\mathrm{Re}')\mathrm{Re}'} \tag{17}$$

By substitution of St′ for St, the dependence of η on Re_D is reduced (*28*), so that the collection efficiency is a function of St′ alone, i.e.

$$\eta \simeq f(\mathrm{St}') \tag{18}$$

Calibration Method. Calibration of an aerosol sampling device involves dispersal of a calibration aerosol in a large volume of air under well-controlled conditions and would generally be conducted in a wind tunnel. Since a wind tunnel suitable for the rotating arm collector, or even a scaled-down version of the instrument, was not available, an alternate approach was taken. This method, which has recently been used to test sampler inlets (*41*), allows evaluation of the performance of the instrument under ambient conditions.

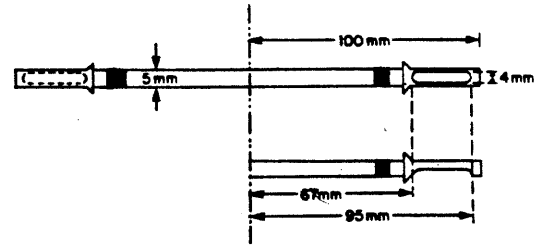

Figure 3. Model rotating arm collector used in calibration experiment.

A tracer gas is used to follow an aerosol plume as it is advected in the atmosphere from an aerosol generator to the collector to be tested. A chemically tagged monodisperse aerosol is released at a constant rate together with a tracer gas. The collection device is set one meter downwind of the point of release and samples the diluted aerosol plume. Prior to testing, the concentration of aerosol at the release point is measured. During testing, tracer gas samples are taken at the release point and next to the impaction surface of the sampler. Automatic continuous gas samplers give integrated measurements of tracer gas concentrations at both locations throughout the testing interval. If sedimentation of the particles is insignificant over the distance from the release point to the sampler, the trajectories of the particles and the gas are nearly identical over that distance. The average concentration C of aerosol crossing the collector path is then given by

$$C = C_0\left(\frac{C^*}{C^*_0}\right) \tag{19}$$

where the subscript 0 refers to the release point and the asterisk refers to the tracer gas. If a mass m of aerosol is collected by the sampler over a time interval Δt with a sampling rate Q, the collection efficiency is

$$\eta = \frac{m}{CQ\Delta t} \tag{20}$$

By running several tests over a range of St′ values, one obtains the dependency of η on St′.

In our tests a monodisperse sodium fluorescein solid aerosol was generated with a Berglund–Liu Model 3050 vibrating orifice generator. Sulfur hexafluoride (SF_6) was used as a tracer gas and connected to the upstream of the dilution air system of the aerosol generator (for which the flow rate was about 40 L min^{-1}) to ensure complete mixing. The aerosol production rate ranged from 10^{-9} to 10^{-7} g min^{-1}, and the flow rate of SF_6 ranged from 0.43 to 0.68 cm^3 min^{-1}. Due to the slow rate of aerosol release, the prototype collector had to be scaled down so that sufficient amounts of aerosol could be conveniently collected for analysis. The model collector (Figure 3) consists of two slotted ends screwed onto a solid rod. It was spun with a variable speed 0.5-hp 10000 rpm motor. Similarity of the Reynolds numbers was maintained, and the aspect ratio was kept as close as possible to that of the prototype. For structural reasons the width/length ratio for the slots is 0.15 in the model, whereas it is 0.095 in the prototype.

The experimental setup is shown in Figure 4. A fan generating a wind speed of about 5 m s^{-1} was used to advect the aerosol toward the collector. The experiments were conducted under conditions of low ambient winds. Dilution of the plume from the point of release to the

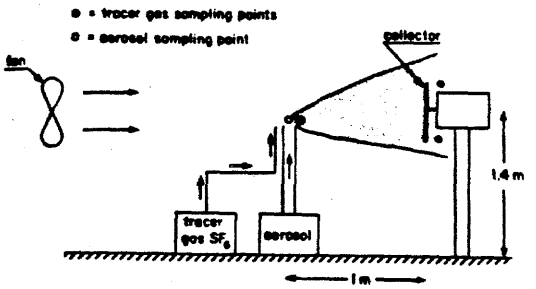

Figure 4. Calibration experiment setup.

sampling point, as measured by C^*/C^*_0, ranged from a factor of 30 to 1000 depending on the meteorological conditions. Particles ranging in diameter from 3 to 20 μm were generated to cover a wide range of Stokes numbers. The settling velocity of 20 μm particles is less than 1 cm s^{-1}, so that sedimentation is negligible over the distances of concern. Tests were run over 30-min intervals, which allowed collection of a sufficient amount of aerosol for accurate determination of the collected mass.

Two automatic continuous gas samplers, sampling over 5-min intervals, and one syringe pump, sampling over 30-min intervals, were used to obtain SF_6 samples. Comparison of the 5- and 30-min integrated measurements provided a check on the SF_6 levels and raised attention to any major changes in the ambient wind speed or turbulence over the course of testing. Analysis was done by gas chromatography using an electron capture detector (*42*). Samples were diluted to reach the optimal SF_6 detection range (100–300 ppt (parts per trillion)). The aerosol concentration at the release point was measured prior to testing by running a known volume of air through a glass-fiber filter. To restrict the aerosol loading on the model arm to the collecting slots, all other parts of the collector were covered with tape, which was removed prior to analysis. A coat of Vaseline grease was applied on one of the two slots to test against possible particle bounce-off. After testing, the sodium fluorescein was extracted in an ultrasonic bath for 30 min with a 0.1 N NH_4OH solution. For the greased slots extraction was first carried out with toluene for 30 min and then with the 0.1 N NH_4OH solution for another 30 min. The aqueous phase was then separated by centrifugation. The sodium fluorescein was analyzed by spectrofluorometry.

Results and Discussion. Figure 5 shows the observed dependence of the collection efficiency on St′ for the scaled-down model. The scale below the abscissa gives the droplet diameter as a function of St′ for a droplet impacting at the middle of the slot in the full-scale arm. Although there is some scatter in the data around $\eta = 50\%$, St'_{50} (based on the data from the greased slots) is about 5, which corresponds to $D_{50} = 20$ μm. Ungreased surfaces collect particles with lower efficiency, which indicates that some particle bounce-off occurs.

Each collection efficiency measurement corresponds to a range of Stokes numbers because velocities of approach vary from one end of the slot to the other. The spread in the Stokes numbers in the scaled-down model is 17% in each direction off the middle of the slot. In the prototype this spread is 19%, which leads to a 10% uncertainty on the size cut of the instrument. A way to eliminate this uncertainty would be to use a tapered slot, i.e., narrow close to the shaft and widening toward the tip, to maintain St′ constant over the whole length of the slot.

In ref 28, it is claimed that the use of St′ in interpreting inertial impaction on a surface greatly reduces the dependence of η on the geometry of that surface. Comparison of our calibration data to the curve obtained in ref 28 from previous calculations for cylinders and spheres shows similarity in shape, but our results are shifted toward the higher Stokes numbers (Figure 5). Because the largest discrepancies occur at low St′ values, this is not likely due to particle bounce. Recent studies of virtual impactors (*43*) have suggested an explanation for the larger St'_{50} in the rotating arm collector. In order to be collected, the particles must not only pass the virtual surface through which there is no mean air flow but also penetrate through the air in the cavity to reach the wall of the collector. Those particles which do not impact on the walls have a significant probability of being reentrained, particularly in the rotating arm collector where there is an induced flow along the length of the collector slot. This may explain the large Stokes numbers required for efficient collection.

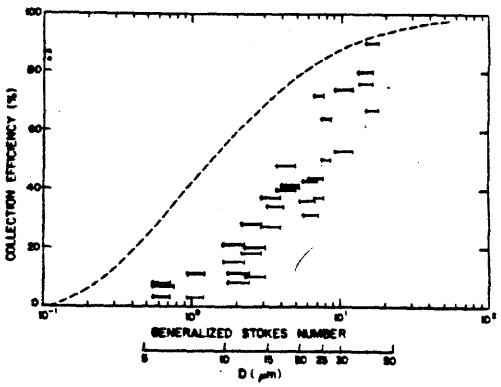

Figure 5. Collection efficiency of model collector vs. the generalized Stokes number, for greased (in bold) and ungreased impaction surfaces. The scale below the abscissa converts the generalized Stokes number to the diameter of droplets impacting in the middle of the slots of the prototype collector. The dashed curve represents theoretical collection efficiencies for cylinders and spheres (*28*).

Comparison with Field Results. Some liquid water content data were obtained at Bakersfield, CA, in Jan 1983 by drawing air with an open-faced Hi-Vol sampler through a paper filter. By measuring the difference in weight of the filters after a certain volume of air has been drawn through the Hi-Vol, one obtains an estimate of the liquid water content. At another location (Albany, NY, Oct 1982) the liquid water content was determined by infrared scattering using a laser transmissometer (*44*). It must be noted that uncertainties as large as 50% are commonly associated with these two liquid water content measurement methods. Figure 6 compares the amount of water collected per cubic meter of air sampled (assuming a sampling rate of 5 m^3 min^{-1}) to the actual liquid water content measured independently. A best fit to the data indicates an overall collection efficiency of 60%. The apparent decrease in collection efficiency when the liquid water content is high may be due to overloading of the bottles before the collector was stopped. To prevent premature overloading due to air lock in the bottles, we have since then added a small hole (0.36-mm diameter) on the upper part of the Teflon tube extending inside the bottle. This allows exchange of air in and out of the bottle during sampling and has been found to improve the collection characteristics in dense fog.

Conclusion

The performance of instruments to collect fogwater for chemical analysis can be assessed in the light of the fol-

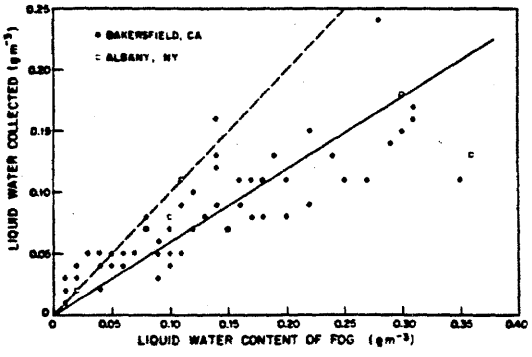

Figure 6. Collected water per cubic meter of air sampled vs. liquid water content. Liquid water content was measured with an open-faced Hi-Vol sampler (Bakersfield, CA) or with an infrared laser transmissometer (Albany, NY). (—) Linear best fit to the data. (---) 100% collection efficiency line.

lowing design criteria: (a) high collection efficiency for droplets in the size window 1–100 μm, (b) collection rate high enough to supply the sample volume required for chemical analysis, (c) conservation of droplet size during approach to the collection surface, and (d) rapid removal of the collected droplets away from the air flow into a quiescent environment.

We discussed in depth the design and characteristics of the rotating arm collector used in our ongoing fogwater chemistry field program and concluded that it performs well in preserving the chemical integrity of the collected droplets while providing large sample volumes. These results have been confirmed in the field (*6*). An in situ calibration indicated a size cut of 20 μm diameter, which is significantly higher than that desired. Because our sampler and the jet impactor designed by Katz (*7*) give consistent determinations of ionic concentrations in fogwater, there appears to be no obvious dependence of the chemical composition on the size of droplets collected. The rotating arm seems to collect samples representative of the fogwater chemistry in spite of its high lower size cut.

Our laboratory is currently investigating several promising designs of fogwater samplers that will collect efficiently droplets in the 1–10-μm size range while minimizing potential sample contamination. The objective is to build a reliable, fully automated instrument suitable for routine monitoring under a wide variety of field conditions. Results will be presented in a future report.

Acknowledgments

E. F. Daly and J. J. Fontana constructed the collectors and provided many valuable practical suggestions. Comments from D. S. Wood, J. M. Waldman, J. W. Munger, and M. R. Hoffmann are gratefully acknowledged.

Literature Cited

(1) Whitby, K. T. *Atmos. Environ.* **1978**, *12*, 135–159.
(2) Waldman, J. M.; Munger, J. W.; Jacob, D. J.; Flagan, R. C.; Morgan, J. J.; Hoffmann, M. R. *Science (Washington, D.C.)* **1982**, *218*, 677–680.
(3) Munger, J. W.; Jacob, D. J.; Waldman, J. M.; Hoffmann, M. R. *J. Geophys. Res.* **1983**, *88*, 5109–5123.
(4) Watson, H. H. *Am. Ind. Hyg. Assoc., Q.* **1954**, *15*, 21–25.
(5) Jacob, D. J.; Waldman, J. M.; Munger, J. W.; Hoffmann, M. R. *Tellus*, in press.
(6) Hering, S. V.; Blumenthal, D. L. "Fog Sampler Intercomparison Study: Final Report". Prepared for Coordinating Research Council, Atlanta, GA, 1984, Project STI 11 90063.
(7) Katz, U. "Communications de la 8eme Conference sur la Physique des Nuages". Clermont-Ferrand, France, July 15–19, 1980.
(8) Jacob, D. J.; Flagan, R. C.; Waldman, J. M.; Hoffmann, M. R. *Proc. Int. Conf. Precipitation Scavenging, Dry Deposition, Resuspension, 4th* **1983**, 125–136.
(9) Junge, C.; McLaren, E. *J. Atmos. Sci.* **1971**, *28*, 382–390.
(10) Jacob, D. J.; Hoffmann, M. R. *J. Geophys. Res.* **1983**, *88*, 6611–6621.
(11) Bassett, M.; Seinfeld, J. H. *Atmos. Environ.* **1983**, *17*, 2237–2253.
(12) Houghton, J. G.; Radford, W. H. *Pap. Phys. Ocean. Met. Mass. Inst. Technol. Woods Hole Ocean. Inst.* **1938**, *6* (4).
(13) Garland, J. A. *Q. J. R. Meteorol. Soc.* **1971**, *97*, 483–494.
(14) Mallow, J. V. *J. Atmos. Sci.* **1975**, *32*, 440–443.
(15) Goodman, J. *J. Appl. Meteorol.* **1977**, *16*, 1056–1067.
(16) Pruppacher, H. R.; Klett, J. D. "Microphysics of Clouds and Precipitation"; Reidel: Dordrecht, Netherlands, 1978; pp 141–142, 418–421.
(17) Roach, W. T. *Q. J. R. Meteorol. Soc.* **1976**, *102*, 355–359.
(18) Gerber, H. E. *J. Atmos. Sci.* **1981**, *38*, 454–458.
(19) Friedlander, S. K. "Smoke, Dust and Haze"; Wiley: New York, 1977; pp 95–109.
(20) Mrose, H. *Tellus* **1966**, *18*, 266–270.
(21) Okita, T. *J. Meteorol. Soc. Jpn.* **1968**, *46*, 120–126.
(22) Lazrus, A. L.; Baynton, H. W.; Lodge, J. P. *Tellus* **1970**, *22*, 106–114.
(23) Sadasivan, S. *Atmos. Environ.* **1980**, *14*, 33–38.
(24) Falconer, R. E.; Falconer, P. D. *J. Geophys. Res.* **1980**, *85*, 7465–7470.
(25) May, K. R. *Q. J. R. Meteorol. Soc.* **1961**, *87*, 535–548.
(26) Mack, E.; Pilie, R. U.S. Patent 3 889 532, 1975.
(27) Brewer, R. L.; Ellis, E. C.; Gordon, R. J.; Shephard, L. S. *Atmos. Environ.* **1983**, *17*, 2267–2271.
(28) Israel, R.; Rosner, D. E. *Aerosol Sci. Technol.* **1983**, *2*, 45–51.
(29) Roach, W. T.; Brown, R.; Caughey, S. J.; Garland, J. A.; Readings, C. J. *Q. J. R. Meteorol. Soc.* **1976**, *102*, 313–333.
(30) Durham, M. D.; Lundgren, D. A. *J. Aerosol Sci.* **1980**, *11*, 179–188.
(31) Davies, C. N.; Subari, M. *J. Aerosol Sci.* **1982**, *13*, 59–71.
(32) Petrenchuk, O. P.; Aleksandrov, N. N. *Glavnoi Geofiz. Obs., Leningr. Tr.* **1966**, *185*, 126–132.
(33) Mohnen, V. A. *Atmos. Technol.* **1980**, *12*, 20–25.
(34) Durham, O. C. *J. Allergy* **1947**, *18*, 231–238.
(35) Perkins, W. A. Stanford University, Palo Alto, CA, 1957, second semiannual report.
(36) Asai, G. N. *Phytopathology* **1960**, *50*, 535–541.
(37) Hameed, R.; McMurry, P. H.; Whitby, K. T. *Aerosol Sci. Technol.* **1983**, *2*, 69–78.
(38) Hoerner, S. "Fluid-Dynamic Drag"; Hoerner Fluid Dynamics: Brick Town, NJ, 1965; pp 3/9, 3/17.
(39) Serafini, J. S. 1954, NACA Report 1159.
(40) Biswas, P.; Flagan, R. C. *Environ. Sci. Technol.* **1984**, *18*, 611–616.
(41) Hofschreuder, P.; Vrins, E.; van Boxel, J. *J. Aerosol Sci.* **1983**, *14*, 65–68.
(42) Drivas, P. J.; Shair, F. H. *Atmos. Environ.* **1974**, *8*, 1155–1163.
(43) Biswas, P., California Institute of Technology, Pasadena, CA, personal communication, 1983.
(44) Jiusto, J. E.; Lala, G. G. State University of New York at Albany, Albany, NY, 1983, ASRC-SUNY Publication 869.

Received for review August 8, 1983. Accepted May 15, 1984. This research was funded by the California Air Resources Board (A2-048-32) and the President's Fund of the California Institute of Technology.

CHAPTER II

AN INSTRUMENT TO COLLECT FOGWATER FOR CHEMICAL ANALYSIS

by Daniel J. Jacob, Jed M. Waldman, M. Haghi, Michael R. Hoffmann,

and Richard C. Flagan

Submitted to Review of Scientific Instruments (December 1984)

ABSTRACT

An instrument is presented which collects large samples of ambient fogwater by impaction of droplets on screens. The collection efficiency of the instrument is determined as a function of droplet size, and it is shown that fog droplets in the range 3 - 100 μm are efficiently collected. No significant evaporation or condensation occurs at any stage of the collection process. Field testing indicates that samples collected are representative of the ambient fogwater. The instrument may easily be automated, and is suitable for use in routine air quality monitoring programs.

INTRODUCTION

Under supersaturated conditions in the atmosphere, fog droplets form by activation of condensation nuclei[1] and rapidly grow to sufficiently large diameters (1 - 100 μm) that the deposition to vegetation canopies is considerably enhanced[2]. Recent reports of extremely high acidities in fogs, and clouds intercepting mountain slopes, have raised concern regarding related environmental consequences[3]. Air quality control agencies in areas exposed to acidic fog have expressed the need to establish networks of sites monitoring the chemical composition of fog on a routine basis. A fogwater sampler to be used in such programs must meet four basic requirements: (1) collect efficiently fog droplets in the 1-100 μm size window while avoiding collection of the submicron non-activated aerosol, (2) preserve the size and chemical composition of fog droplets through all stages of collection, (3) rapidly collect large amounts of liquid water for wet chemical analysis, (4) be automated, inexpensive to construct, and require minimal maintenance. A recent paper from our group[4] has elaborated on design criteria for fogwater collectors, and reported that none of the currently available instruments is satisfactory in all respects. A rotating arm collector developed in our laboratory[4] has been shown to provide samples representative of the ambient fogwater[5], but it is not suitable for automation and presents safety problems. We describe herein a collector that we have recently developed explicitly to provide a simple, reliable, and inexpensive instrument for routine monitoring.

DESIGN

The instrument (shown in Figure 1) collects fogwater by inertial impaction of fog droplets on a series of screens. The screens are placed in a duct, through which a blower samples ambient fog-laden air at a velocity U_s = 9 m sec^{-1}. The screens consist of 330 μm diameter Teflon monofilament strung vertically between two Teflon-coated threaded rods. The pressure drop across one screen is 87 Pa. The screens slide into position along grooves carved in the wall of the duct, inclined at an angle $\theta = 35^{o}$ (Figure 1b). We have found that inclining the strings considerably reduces the residence time of droplets on the strings (as compared to strings set vertically), because aerodynamic drag pushes the impacted droplets to the bottom of the screen. Further, inclining the strings at 35^{o} prevents resuspension of the impacted droplets into the air flow; such resuspension would occur if the strings were set vertically[6]. Accumulation of water on the strings proceeds by formation of large droplets spaced at intervals along the strings; these droplets rapidly grow large enough (about 1-2 mm diameter) to flow down. A Teflon funnel drains the fogwater collected at the bottom of the screen into a storage bottle directly below. The instrument is set on a platform surmounted by a wind vane so that the inlet is oriented into the wind at all times. Automation of instrument start-up may be provided by a number of methods.

The flow of air through the instrument is 22 m^3 min^{-1}, but only a fraction of that air is actually sampled because of the spacing

between strings . Based on the dry diameter of the strings, each screen would sample 20 % of the air flowing through; in practice, accumulation of water on the strings will slightly increase the impaction surface area and therefore the amount of air sampled. With four screens, the instrument samples about $(1 - (0.8)^4) = 60\%$ of the air flowing through the duct. Thus, in a fog of typical liquid water content 0.1 g m^{-3}, 80 ml of sample is collected in an hour. This is sufficient for most analytical purposes.

The principle of operation is that inertia prevents droplets approaching the strings from following the curved flow streamlines around the strings. The deviations of droplet trajectories increase with droplet inertia, and droplets above a certain size deviate sufficiently to collect on the strings. The efficiency of this process is characterized by the Stokes number[7], St:

$$St = \frac{\rho D^2 U_s \cos\theta}{18\,\mu\,R} \qquad (1)$$

where ρ is the droplet density, D is the droplet diameter, μ is the viscosity of air, and R is the radius of the string. The Reynolds number of the flow through the duct is sufficiently high (10^5), and the Mach number is sufficiently low (0.03), that the collection efficiency can be satisfactorily described as solely a function of St and the droplet Reynolds number[7,8]. Experimental data are available for the collection efficiency of particles on cylinders as a function of these two dimensionless groups[8].

When U_s differs from the ambient wind velocity U_a, large droplets cannot follow the bending of the streamlines during approach

to the inlet. A collection bias is introduced at the upper end of the size distribution, which depends on the relative magnitudes and orientations of U_s and U_a, and on the inlet Stokes number (defined by R = half-width of the inlet). Inlet biases have been documented in detail[9]; they are considerably greater in a crosswind than when the inlet is oriented into the wind. In the latter case, the following pattern is found: (a) no sampling bias for $U_a = 0$ or $U_a = U_s$, (b) negative biases for $U_a < U_s$, which go through a maximum for $U_a/U_s \cong 0.3$, (c) positive biases for $U_a > U_s$, which approach an asymptotic limit equal to U_a/U_s at large inlet Stokes numbers.

The collection efficiency of our instrument was determined as a function of droplet size from the data of Refs. 8 and 9, for various ambient wind velocities and an inlet oriented into the wind (Figure 2). The impaction Stokes number was calculated by taking R equal to the radius of the dry strings. Droplets in the size window 3 - 100 μm diameter are efficiently collected, while collection of submicron aerosol is entirely avoided. Fog droplets below 3 μm are poorly collected, but represent only a very small fraction of the total suspended liquid water. The anisokinetic sampling bias for large droplet sizes depends considerably on the ambient wind speed. Although wind speeds in radiation fogs are in general less than 2 m sec^{-1}, we have frequently found higher velocities (up to 10 m sec^{-1}) in coastal advection fogs. Positive collection biases require even higher ambient wind velocities, which could be found in clouds intercepting mountain slopes but are unlikely in other situations.

Perturbation of the ambient relative humidity during the sampling process may change the size of the fog droplets by

condensation or evaporation, and therefore affect chemical concentrations in the sample. Aerodynamic cooling as the droplets are accelerated at the inlet leads to condensation, and aerodynamic heating as the droplets are decelerated during approach to the strings leads to evaporation. To determine the extent of the resulting droplet size modification, we simultaneously solved the equations for flow field, relative humidity, droplet trajectory, and mass transfer, from equations previously derived[4]. These calculations showed that no significant droplet growth or evaporation occurs for droplets above 1 μm. Therefore, droplet sizes are preserved at all stages of approach.

Evaporation on the strings must also be investigated. Aerodynamic heating near the strings leads to a localized subsaturation. Assuming that the compression is adiabatic, the maximum temperature gradient at the surface of the string is:

$$\Delta T = \frac{U_s^2}{2C_p} \qquad (2)$$

where C_p is the heat capacity of air. We find $\Delta T = 0.03^{o}K$, which corresponds to a decrease in relative humidity of about 0.2 %. More important as sources of thermodynamic modification are the fluctuations of the ambient relative humidity in fog: rapid oscillations of up to 1% relative humidity in amplitude have been reported in a radiation fog[10]. Mass transfer calculations for a flow of air at 99 % relative humidity past a bank of cylinders[11] indicate an overall rate of evaporation from the screens of 10^{-2} g min-1. This is small compared to the collection rates achieved.

FIELD TESTING

The collector, with only one screen installed, was first tested during a stratus cloud sampling program conducted on the mountain slopes above the Los Angeles basin[12]. Collection rates were in the range 0.5 - 1.5 ml min^{-1}. Four samples were collected simultaneously with the rotating arm collector, and the chemical compositions of the samples were compared (Table 1). Concentrations were not significantly different between the two instruments, and usually within the errors previously documented between two rotating arm collectors set side by side[5]. Exceptions were Na^{+}, Ca^{2+}, and Mg^{2+}, which were present at significantly higher concentrations in samples collected with the rotating arm collector. These cations may be substantially contributed by large insoluble soil dust particles collected along with the fog droplets; apparently, the rotating arm collector collects these dust particles more efficiently than the screen collector. After some time of operation, a black deposit was observed on the screens, which suggests that impacted dust particles stick to the strings and are not entrained by the water flow. The good agreement found for water-soluble constituents demonstrates that the screen collector provides representative samples of the fogwater itself.

ACKNOWLEDGEMENTS

Elton F. Daly and Joseph J. Fontana constructed the collector and offered valuable practical suggestions. This work was funded by the California Air Resources Board.

REFERENCES

1. H. R. Pruppacher and J. D. Klett, Microphysics of Clouds and Precipitation (Reidel, Amsterdam, 1978), p. 141-142, 418-421.

2. G. M. Lovett, Atmos.Environ. 18, 361 (1984).

3. B. Hileman, Environ.Sci.Technol. 17, 117A (1983).

4. D. J. Jacob, R.-F. T. Wang, and R. C. Flagan, Environ.Sci.Technol. 18, 827 (1984).

5. S. V. Hering and D. L. Blumenthal, Fog sampler intercomparison study: Final Report to Coordinating Research Council. Available from Coordinating Research Council, 219 Perimeter Center Parkway, Atlanta, GA (1984).

6. J. G. Houghton and W. H. Radford, Pap. Phys. Ocean. Met. Mass. Inst. Technol. and Woods Hole Ocean. Instn. 6, N^{O}4 (1938).

7. S. K. Friedlander, Smoke, Dust and Haze (Wiley, New York, 1977), p. 95-109.

8. R. Israel and D. E. Rosner, Aerosol Sci.Technol. 2, 45 (1983).

9. C. N. Davies and M. Subari, J.Aerosol Sci. 13, 59 (1982).

10. H. E. Gerber, J.Atmos.Sci. 38, 454 (1981).

11. R. B. Bird, W. E. Stewart, and E. N. Lightfoot, Transport Phenomena (Wiley, New York, 1960), p. 646.

12. J. M. Waldman, Ph.D. Thesis, California Institute of Technology, Pasadena, California (1985).

Table 1. Comparison of fogwater concentrations in samples collected sinultaneously with the screen collector (SC) and the rotating arm collector (RAC) set side by side[a].

	H^+	Na^+	Ca^{2+}	Mg^{2+}	NH_4^+	Cl^-	NO_3^-	SO_4^{2-}
SC/RAC	1.08±0.11	0.71±0.04	0.70±0.10	0.71±0.04	1.14±0.14	0.93±0.10	0.85±0.06	0.99±0.07

	Fe	Pb	Mn	Ni	V	CH_2O	fogwater collection rate
SC/RAC	1.11±0.34	1.12±0.18	0.85±0.28	1.05±0.27	0.99±0.12	1.04±0.08	2.34±0.24

(a) Comparison of 4 samples collected on 12 June 1984 at Henninger Flats[12].

FIGURE CAPTIONS

Figure 1. Screen collector to sample fogwater for chemical analysis. Air is aspirated through a leucite duct at a rate of 22 m^3 min^{-1} (blower: model 80A, 1/3 HP 115V motor, Central Blower Co., City of Industry, California). Fog droplets impact on Teflon FEP monofilament screens (13 mils, Dupont de Nemours Corp.) strung on threaded Teflon-coated brass frames. Fogwater collected on the screens flows down to a Teflon funnel and a polyethylene bottle directly underneath. (a) perspective view of the instrument, (b) side view (section), (c) detail of the screen frames.

Figure 2. Collection efficiency vs. droplet diameter. Anisokinetic sampling biases are considered for an inlet oriented into the wind and various ambient wind velocities (m sec^{-1}) indicated on the curves. No inlet bias occurs for $U_a = 0$ or $U_a = 9$ m sec^{-1}. Maximum negative bias occurs for $U_a \cong 3$ m sec^{-1}. Collection efficiencies in excess of 100% indicate positive sampling biases ($U_s < U_a$).

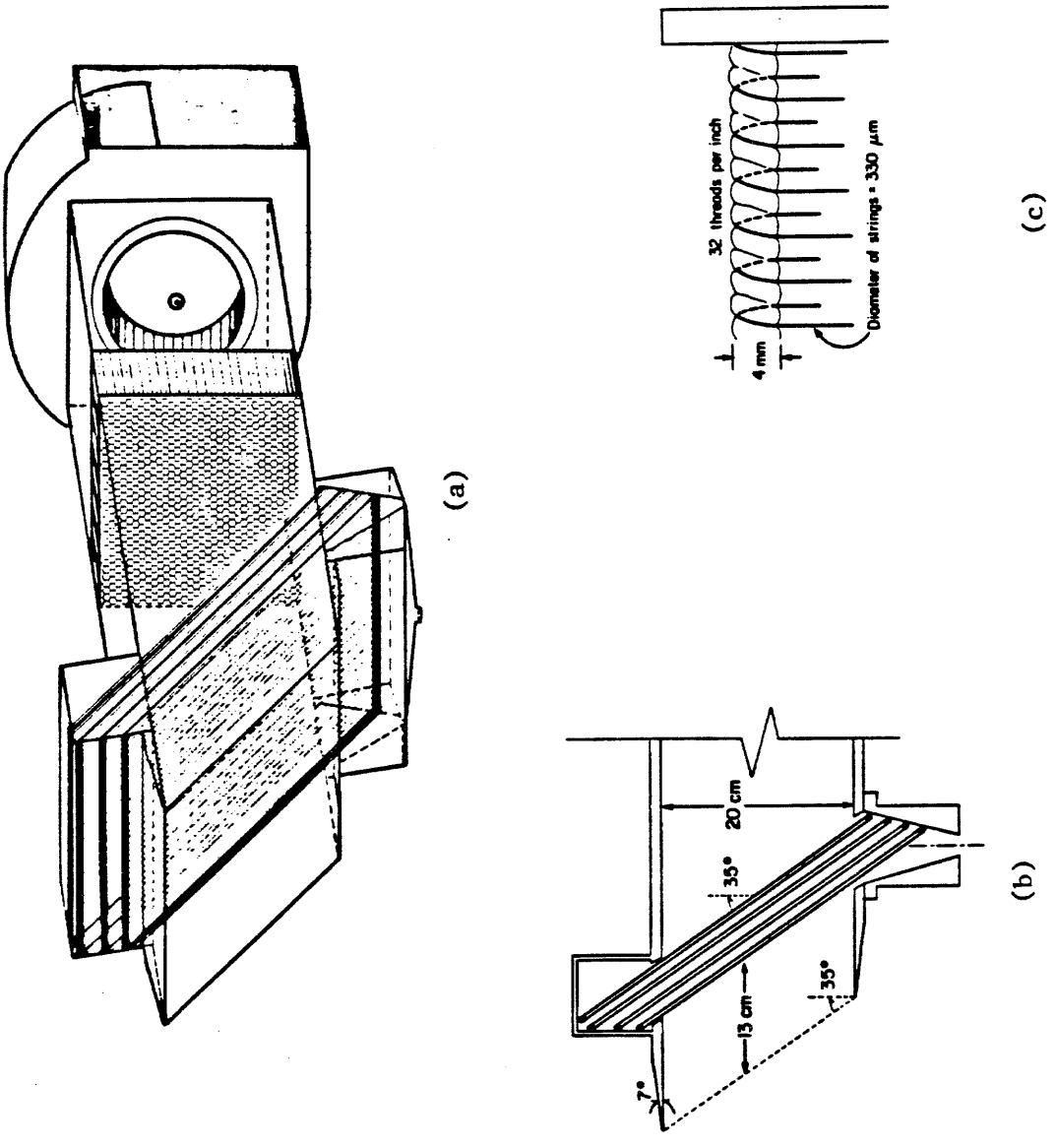
(a)
32 threads per inch
4 mm
Diameter of strings = 330 μm
(c)
20 cm
35°
35°
13 cm
7°
(b)

Figure 1

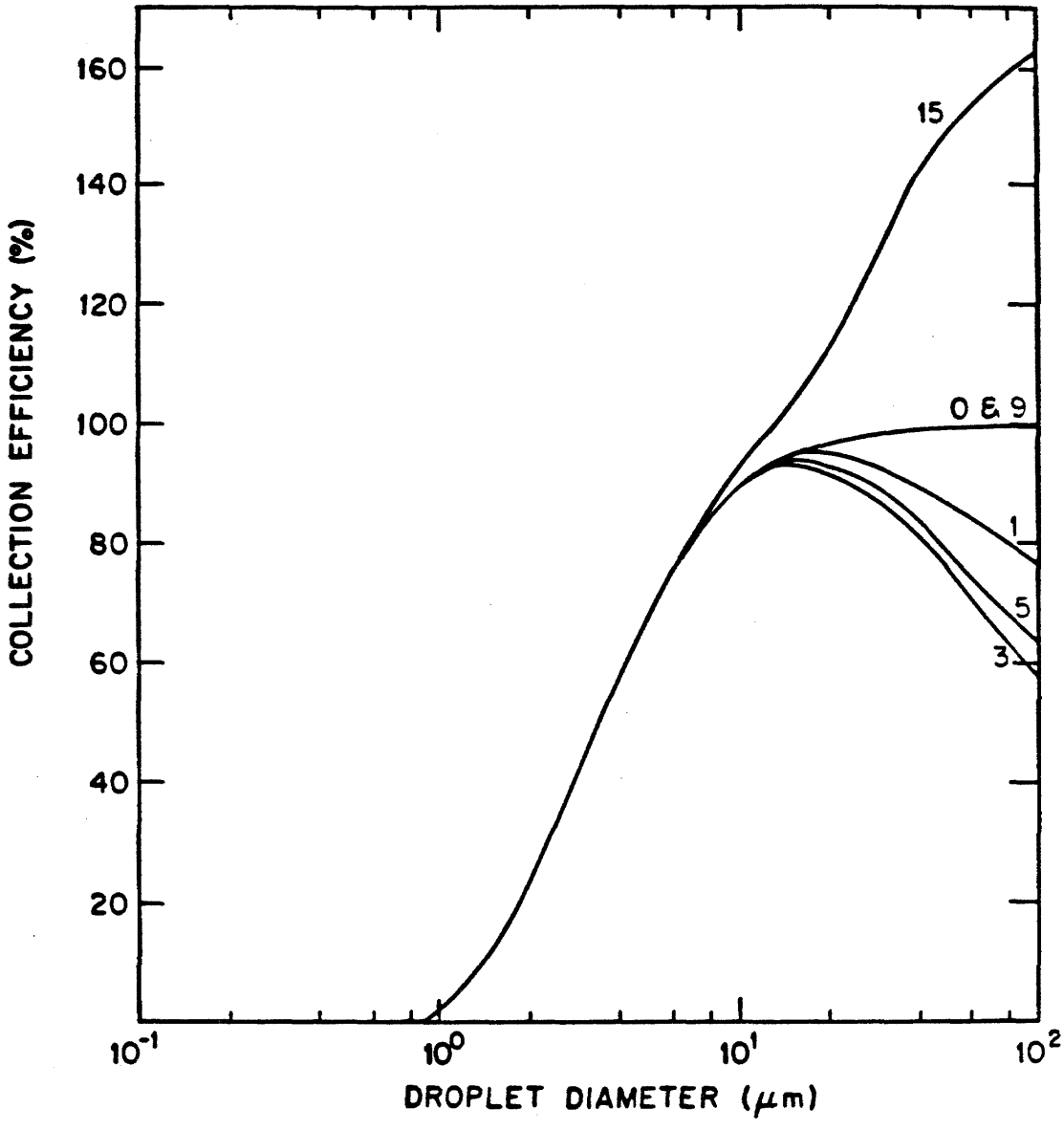
COLLECTION EFFICIENCY (%)
160
140
120
100
80
60
40
20
15
0 & 9
1
5
3
10^{-1}
10^{0}
10^{1}
10^{2}
DROPLET DIAMETER (μm)

Figure 2.

CHAPTER III

CHEMICAL COMPOSITION OF FOGWATER COLLECTED ALONG THE CALIFORNIA COAST

by Daniel J. Jacob, Jed M. Waldman, J. William Munger,

and Michael R. Hoffmann

Submitted to Environmental Science and Technology (September 1984)

ABSTRACT

Fogwater collected at both urban and non-urban coastal sites in California was found to be consistently acidic. The highest acidities (pH values down to 2) occurred at sites in the Los Angeles basin or downwind. Concentrations of acid-neutralizing constituents in coastal air were found to be very low, so that fogs were acidic even under relatively clean conditions. Chloride loss relative to its sea salt contribution was observed at sites furthest from anthropogenic sources.

INTRODUCTION

Recent investigations of fogwater chemical composition in the Los Angeles basin (1, 2) have revealed high ionic concentrations and, often, very high acidities (pH values typically in the range of 2 to 4). Comparable acidities have been observed in low stratus clouds collected by aircraft over the basin (3) and sampled on the slopes of the surrounding mountains (4). These high acidities have raised concern regarding potential damage to materials, vegetation (5), crops (6), and public health (7). Laboratory data indicate that conversion of SO_x to sulfate can proceed rapidly at the concentrations found in urban fog droplets (8) and in the precursor haze aerosol (9). Field studies have proposed evidence for aqueous-phase sulfate production in the atmosphere (10,11,12,13).

Fogs are frequent seasonal occurrences along the California coast. During the summer, coastal stations may report over 50% foggy days (14). These fogs are often coupled with land breeze/sea breeze systems, which recirculate the same air parcels several times across the shoreline (13). Tracer studies in the Santa Barbara Channel (15) have shown that emissions from offshore and coastal sources may reside several days along the coast. These humid, poorly ventilated conditions favor pollutant build-up and sulfate production.

As part of an extensive fog sampling program in California, we have collected fogwater at a number of coastal sites. Coastal fogs may be a major cause of sulfate pollution episodes in Southern California (16). Further, because impaction of fog droplets can be a significant source of water input to the coastal vegetation (17), the

chemical composition of the fogwater has important local implications for acid deposition. Recent interest in these problems has been stirred by federal plans to encourage oil exploration and production in the outer continental shelf off California (18).

SAMPLING SITES AND METHODS

Fogwater was sampled with a rotating arm collector (19) at eight coastal sites and one island site (Figure 1). The sites, and conditions during sampling, are described in Table 1. Samples were collected over intervals ranging from 30 minutes to 2 hours, and were analyzed for major ions and metals following the protocol described in Ref. 1. Concentrations of Na^+, K^+, Ca^{2+}, and Mg^{2+} were determined by atomic absorption spectroscopy on filtered aliquots; at some sites (Del Mar, Long Beach, Lennox, Morro Bay) we analyzed both filtered and unfiltered aliquots and did not observe significant differences in concentrations.

Determination of anions by ion chromatography revealed unidentified peaks eluting just before chloride in fogwater samples collected at some urban sites. When chloride concentrations were low, a positive interference from these peaks was noted; chloride concentrations reported are then an upper bound of true chloride concentrations and are indicated as such. The unidentified peaks were likely due to organic acids (20,21). We have measured formate and acetate at concentrations around 10^{-4} M in fog samples (J. W. Munger, unpublished results).

The contributions of different source types to the fogwater

chemical composition were determined from an emission matrix for primary California aerosol (Table 2). Concentrations of fly ash and automobile exhaust were calculated from the concentrations of vanadium and lead, respectively. Contributions from sea salt, soil dust, and cement dust were obtained by a balance on sodium, iron, and calcium, after subtraction of fly ash and automobile exhaust contributions. Because concentrations of the different elements analyzed in a sample spread over a wide range, we found that this apportionment method gave more reliable results than a least-squares fit of all elemental concentrations to the emission matrix (22). Secondary sulfate was calculated by subtraction of primary contributions from the total sulfate concentration. All nitrate was assumed to be of secondary origin.

RESULTS AND DISCUSSION

Fogwater concentrations. Table 3 gives liquid water-weighted average fogwater concentrations for each event; the detailed data set is available elsewhere (25). Contributions from the different source types are given in Table 4 in terms of fogwater loadings, which we define as the mass of material in fogwater per m^3 of air. Liquid water contents were estimated from the collection rate of our rotating arm collector, assuming a 60% overall collection efficiency (19). A number of methods have been used in field investigations to measure liquid water contents in fogs, but none has been reliably calibrated, and a field intercomparison has revealed systematic biases between different methods (4). Although the absolute error on

our liquid water content estimates cannot be ascertained at this time, we are satisfied that differences in the collection rate closely follow actual differences in the liquid water content (4).

In Table 5, elemental ratios in fogs are compared to those for sea salt. The observed Na/Mg ratios were close to that for sea salt; exceptions were the Long Beach, Lennox, and San Marcos sites, where sea salt constituted only a small fraction of the total loading and significant soil dust contributions of Na and Mg were apparent. Calcium and sulfate were partly of marine origin, but usually had larger contributions from dust (calcium) and secondary production (sulfate). The K/Na ratios were close to that for sea salt at Del Mar, San Nicholas Island, and Pt. Reyes; soil dust was an important source of potassium at other sites.

The sites in and around the Los Angeles basin were by far the most affected by anthropogenic sources (Table 4). The large contribution from automobile exhaust in the fog samples collected at Lennox can be attributed to the nearby freeway and airport traffic. The sulfate-to-nitrate equivalent ratio at Long Beach Harbor was much higher than that usually observed in the Los Angeles basin (0.2-0.5); non-sea salt (NSS) sulfate concentrations in the basin are known to peak in the Long Beach Harbor because of oil burning by ships (10).

The fogs on 7 and 18 December 1981 at Lennox and 7 December 1983 at Corona del Mar occurred during severe sulfate pollution episodes in the Los Angeles basin. Average fogwater pH values below 3 were observed on those nights. On the day following the Corona del Mar event, all coastal stations of the South Coast Air Quality Management District recorded their highest 24-hour sulfate

concentrations for 1982, ranging from 23 to 37 $\mu g\ m^{-3}$. The prevailing southward transport of pollutants on the night 6-7 December, 1982 (26) explains the extremely high acidities observed at Corona del Mar; a second sample (1 ml) collected as the fog dissipated had a pH = 1.69 (a value which was later confirmed in the laboratory).

High ionic concentrations and acidities were also found in samples collected at Del Mar on 8 January 1983 (Figure 2). The NW winds blowing over Del Mar at the beginning of the sampling period carried pollutants from Los Angeles which had been transported offshore by weak NE winds the previous morning (27). A developing land breeze led to flow reversal between 1900 and 2000 PST and advection over the site of inland air from suburban San Diego County. Sea salt concentrations dropped considerably as the land breeze developed; contributions from anthropogenic sources also decreased, although less, as the Los Angeles air was replaced by cleaner air.

Fogwater collected at San Marcos Pass (low stratus), Morro Bay, Mt. Sutro, and Pt. Reyes contained much less nitrate , NSS sulfate, and automobile exhaust than fogwater collected in the Los Angeles basin or downwind. However, except at Morro Bay, all samples were acidic; fogwater pH ranged from 4.21 to 4.69 at San Marcos Pass, and from 3.60 to 5.00 at Pt. Reyes. Significant concentrations of metals and NSS calcium at all sites show that the air sampled was of partly continental origin even under onshore wind conditions. This has previously been observed in aerosol collected elsewhere along the California coast (28). Fogwater collected at Pt. Reyes under offshore wind conditions (12 Aug. 1983) contained less sea salt, more

soil dust, and more automobile exhaust than fogwater collected on other nights under the more usual N-NW wind conditions.

Nitrate and NSS sulfate loadings at San Nicholas Island were higher than those at other non-urban sites, even though impact of Los Angeles pollutants is very unlikely under the wind conditions observed on that night. High concentrations of metals and NSS calcium indicated that the air over the island was of mixed marine/continental origin. The relatively high fly ash and low automobile exhaust loadings suggest that the high acidity could be due to advection by NNW winds of a plume from oil drilling operations off Pt. Conception or emissions from the Morro Bay power plant; dilution of the plume would be limited by the low mixing heights and slow horizontal dispersion over the ocean (15). Transport from the Pt. Conception area over San Nicholas Island has been previously documented (29).

The acidity of coastal fogs in California. Fogwater was often extremely acidic in and around the Los Angeles basin; elsewhere, relatively high "background" nitrate and NSS sulfate concentrations apparently led to ubiquitous acidic conditions along most of the California coastline. Pollutant transport with slow dispersion along the coast has been well documented (13, 15), and has been attributed to the dominant NW wind, the sea-breeze/land-breeze circulation system, the low surface roughness of the ocean, and the persistent strong inversions.

Acidities in non-urban coastal fogs were comparable to those found in fogs sampled in the inland San Joaquin Valley of California,

where much higher nitrate and sulfate loadings were observed (30). The non-neutralized fraction of the acidity, $[H^+]/([NO_3^-]+[(NSS)SO_4^{2-}])$, was typically less than 10% in San Joaquin Valley fogs (30); in comparison, the non-neutralized fraction of the acidity was on the average 25% at San Marcos Pass, 31% at Mt. Sutro, and 48% at Pt. Reyes.

Obviously, there is little alkalinity available in the coastal air to neutralize acid inputs. Ammonia was found to be the main acid-neutralizing component in San Joaquin Valley fogs (30). An excess of ammonia ($H = 50\ \underline{M}\ atm^{-1}$, $K_b = 1.7 \times 10^{-5}\ \underline{M}$ at 10^oC) maintains fogwater pH above 5. Fogwater below pH 5, as found along the coast, cannot support gaseous ammonia at equilibrium; ammonia is then expected to be nearly 100 % scavenged by the fog droplets. The relatively low ammonium fogwater concentrations (as compared to nitrate and sulfate concentrations) show that alkalinity from ammonia is lacking in coastal air. Soil dust is an alternate source of alkalinity, but the small amount present in the droplets (Table 4) limits the extent of H^+-neutralizing ion-exchange surface reactions. These reactions would mostly involve the cations Ca^{2+} and Mg^{2+}, but as mentioned previously we found these ions to be mostly dissolved. Alkalinity from scavenged soil dust was therefore exhausted.

The low nitrate concentrations observed at Pt. Reyes and Mt. Sutro on 10-13 August, 1982 suggest a source of acidity especially rich in H_2SO_4. Two likely sources are emission from ships and oxidation of dimethylsulfide volatilized from the ocean surface. Non-sea salt sulfate concentrations of 0.1 - 1 ug m^{-3} over the Pacific Ocean have been attributed to the oxidation of

dimethylsulfide (31), and oceanic dimethylsulfide production has been found to be maximum near coasts (32). Rapid photo-oxidation of alkyl sulfides in a sunlight-irradiated chamber has been reported (33). This source of sulfate could therefore possibly be a major contributor to the acidity at non-urban coastal sites in California.

Volatilization of HCl(g) from sea salt nuclei. A number of investigators of marine aerosols have observed chloride loss relative to its expected sea salt contribution (34,35). These investigators report chloride losses ranging from 0% (no loss) up to 100%. Chloride loss proceeds by incorporation of a strong acid in sea salt-containing aerosol, resulting in pH-lowering and volatilization of HCl(g). The strong acids can be HNO_3 (34) or H_2SO_4 (35,36). Displacement by NO_2(g) on NaCl(s) has been found to be effective at ppm concentrations of NO_2 (37).

Table 6 is a summary of thermodynamic data regarding the main reactions involved. If the sea salt particle is solid, the reaction may proceed by adsorption of HNO_3(g) and sublimation of HCl(g) from surface NaCl crystals, or by coagulation of sea salt aerosol with sulfuric acid or bisulfate droplets. Above the deliquescence point, volatilization of HCl(g) is given by the position of equilibrium (3). Both H_2SO_4 and HNO_3 added to a NaCl(aq) aerosol will displace HCl, but HNO_3 is less efficient than H_2SO_4 because it is only slightly less volatile than HCl. Hitchcock et al. (35) infer from field data that HSO_4^- does not displace Cl^-; however, equilibria (3) and (5) indicate that a substantial fraction of chloride could be released to the gas phase at the liquid water contents typical of haze (10^{-3} g

m^{-3}).

Although volatilization of HCl(g) proceeds effectively in acid haze, reaction (3) indicates that fog, even acidic, cannot support HCl(g). This is because of the higher liquid water contents, and because acidities in fogs are not as high as those reached in haze. If chloride was lost in the precursor aerosol, it could still be recovered in the fog by scavenging of HCl(g). Chloride deficiency with respect to its sea salt contribution in the fog therefore requires loss of chloride from the precursor aerosol followed by removal of the resulting HCl(g) from the air parcel during transport prior to droplet activation.

The fogs sampled in our study were acidic, and chloride loss in the precursor aerosol would be expected. However, measured chloride concentrations were in excess of the sea salt contribution at most of our sites; this would be due to (i) anthropogenic sources of chloride, (ii) organic acids interfering with chloride in analysis. Significant chloride loss was observed in 1 sample from Del Mar (18%), all samples from San Nicholas Island (12%-35%), and 4 samples from Pt Reyes (10%-28%). Therefore, chloride loss was observed in the fogwater only at those sites where long transport of acids over the ocean was involved. Transport may have led to separation of HCl(g) from the nuclei, possibly by removal of HCl(g) to the ocean surface. Because of its high reactivity with surfaces, HCl(g) should deposit faster than NaCl aerosol.

CONCLUSION

Fogwater samples collected at both urban and non-urban sites along the coast of California were consistently acidic. Apart from sea salt, the main constituents were sulfuric and nitric acids (partially neutralized by ammonia). Extremely high acidities (pH values down to 2) were observed at sites in the Los Angeles basin or downwind. The acid-neutralizing capacities were found to be much lower in the coastal air than in inland areas of Southern California, and insufficient to neutralize even low acid inputs at non-urban sites. Chloride loss in fogwater was observed at sites affected by acids advected from distant sources, even though hydrochloric acid volatilized by pH-lowering of the precursor sea salt aerosol would be scavenged upon fog formation. A possible explanation is that HCl(g) deposits faster than NaCl over ocean surfaces.

ACKNOWLEDGEMENTS. We thank the organizations who provided us with sampling sites: the U.S.Navy, the National Park Service, the South Coast Air Quality Management District, the San Luis Obispo and San Diego Air Pollution Control Districts. This research was funded by the California Air Resources Board (contract No. A2-048-32).

LITERATURE CITED

(1) Munger,J.W.; Jacob,D.J.; Waldman,J.M.; Hoffmann,M.R. J.Geophys.Res. 1983,88,5109-5123.

(2) Brewer,R.L.; Ellis,E.C.;Gordon,R.J.;Shepard,L.S. Atmos.Environ. 1983,17,2267-2271.

(3) Richards,L.W.; Anderson,J.A.; Blumenthal,D.L.; McDonald,J.A.;

Kok,G.L.; Lazrus,A.L. Atmos.Environ. 1983,17,911-914.

(4) Waldman,J.M.; Munger,J.W.; Jacob,D.J.; Hoffmann,M.R. submitted to Tellus.

(5) Scherbatskoy,T.; Klein,R.M. J.Environ.Quality.1983,12,189-195.

(6) Granett,A.L.; Musselman,R.C. Atmos.Environ. 1984,18, 887-891.

(7) Hoffmann,M.R. Environ.Sci.Technol. 1984,18,61-63.

(8) Martin, L.R. in "Acid Precipitation," J.G. Calvert ed., Butterworth, Boston, 1984,p.63-100.

(9) Crump,J.G.; Flagan,R.C.; Seinfeld,J.H. Atmos.Environ. 1983,17,1277-1289.

(10) Cass,G.R. Atmos.Environ. 1981,15,1227-1249.

(11) Hegg,D.A.; Hobbs,P.V. Atmos.Environ. 1982,16,2663-2668.

(12) Daum,P.H.; Schwartz,S.E.; Newman,L. in "Precipitation Scavenging, Dry Deposition, and Resuspension," H.R. Pruppacher et al. eds.,Elsevier, New York 1983,pp.31-44.

(13) Cass,G.R.; Shair,F.H. J.Geophys.Res. 1984,89,1429-1438.

(14) deViolini,R. 1974 Techn.Publ. TP/74/1, Pacific Missiles Range, Pt. Mugu, CA 1974.

(15) Reible,D.D.; Shair,F.H.; Lehrman,D.E. manuscript in preparation.

(16) Zeldin,M.D. et al. Evaluation and Planning rpt. 76-1, Southern California Air Pollution Control District, El Monte, CA, Aug. 1976.

(17) Azevedo,J.; Morgan,D.L. Ecology.1974,55,1135-1141.

(18) California Air Resources Board 1982 "Air quality aspects of the development of offshore oil and gas resources," Sacramento, CA.

(19) Jacob,D.J.; Wang,R.-F.T; Flagan,R.C. Environ.Sci.Technol. 1984 (in press).

(20) Nagamoto,C.T.; Parungo,F.; Reinking,R.; Pueschel,R.; Gerish,T. Atmos.Environ. 1983,17,1073-1082.

(21) Keene, W.C.; Galloway,J.N. Atmos. Environ. 1984 (in press).

(22) Friedlander,S.K. Environ.Sci.Technol. 1973,7,235-240.

(23) Cooper,J.A.; Watson,J.G.,Jr. J. Air Poll. Control Assoc. 1980,30,1116-1125.

(24) Weast,R.C. ed. 1975 "Handbook of Chemistry and Physics,"56th ed., p.F-199.

(25) Jacob,D.J. 1984 Ph.D. thesis, California Institute of Technology, Pasadena, CA .

(26) Unger,C.D. "An analysis of meteorological and air quality data associated with the occurrence of fogwater with high acidity in the Los Angeles basin," July 18, 1984 memorandum, California Air Resources Board, Sacramento, CA.

(27) Brown,H.W. 1983 "An analysis of air flow over the Southern California bight and northern San Diego county on January 8,1983," San Diego Air Pollution Control District, San Diego, CA.

(28) Whitby,K.T.; Sverdrup,G.M. Adv.Environ.Sci.Technol. 1980,9,477-517.

(29) Rosenthal,J.; Battalino,T.E.; Hendon,H.; Noonkester,V.R. Techn.Publ. TP/79/33, Pacific Missiles Test Center, Pt. Mugu, CA, 1979.

(30) Jacob,D.J.; Waldman,J.M.; Munger,J.W.; Hoffmann,M.R. Tellus (in press).

(31) Saltzman,E.S.; Savoie,D.L.; Zika,R.G.; Prospero,J.M. J.Geophys.Res. 1983,88,10897-10902.

(32) Andreae,M.O.; Raemdonck.H. Science (Washington, D.C.)

1983,221,744-747.

(33) Grosjean,D. Environ.Sci.Technol. 1984,18,460-468.

(34) Martens,C.S.; Welosowski,J.J.; Harriss,R.C.; Kaifer,R. J.Geophys.Res. 1973,78,8778-8792.

(35) Hitchcock,D.R.; Spiller,L.L.; Wilson,W.E. Atmos.Environ. 1980,14,165-182.

(36) Eriksson,E. Tellus.1960,12,63-109.

(37) Finlayson-Pitts,B.J. Nature 1983,306,676-677.

(38) Latimer,W.D. "The oxidation states of the elements and their potentials in aqueous solutions,"2nd ed.,Prentice-Hall, New York, 1952.

Table 1. Description of sampling sites.

Site		Conditions during sampling		
		Inversion base[a] (m)	Temp.[b] (°C)	Surface wind[b] (m s^{-1})
Del Mar	Coastal lagoon, residential surroundings. Collector set on ground, 800 m from shore.	surface	11	moderate NW shifting to moderate E
Corona del Mar	Residential area. Collector set on pier.	260	11	calm
Long Beach Harbor	Industrial area, ships. Collector set on dock, 10 m from water.	220	10	calm
Lennox	Industrial and residential area. Los Angeles Int'l Airport is 2 km NW, major freeway is 500 m E. Ocean is 4 km W. Collector set on roof of 1-story building.	surface	12 (7 Dec. 1981)	1NE
		surface	14 (18 Dec.1981)	1SE
		220	10 (7 Jan. 1983)	calm
San Nicholas Island	U. S. Navy base, 100 km offshore. No impact from local sources. Collector set at 50 m elevation, 400 m from shore.	150	14	5 NNW
San Marcos Pass	Mountain pass in coastal range, 700m elevation. No nearby sources.	1800	8-15	2S
Morro Bay	Rural town at the base of major power plant. Agriculture, ranches. Some local traffic. Collector set 500 m from shore, on roof of 1-story building.	450	11	0-2 SW
Mt. Sutro	250 m elevation hill in San Francisco. Radio towers, no local traffic. Ocean is 5 km W.	570	12	1 W
Pt. Reyes	National Seashore, no nearby sources. Collector set at tip of peninsula, 10 m elevation, 50 m from shore.	600	12 (9 Aug. 1982)	10-15 N
		420	11-12 (10 Aug. 1982)	10-15 N
		1800	12-14 (11 Aug. 1982)	10-15 N
		240	11-14 (12 Aug. 1982)	2 SE

(a) measured by the National Weather Service at San Diego, Los Angeles, Vandenberg AFB, or Oakland.
(b) measured at the site.

Table 2. Source concentrations of particulate matter[a].

	% mass				
	sea salt	soil dust	cement dust	fuel oil fly ash	automobile exhaust
Na	30.6	2.5[b]	0.4[b]	5[b]	0[b]
S	2.6	0.1[b]	0.1[b]	15[b]	2[b]
Ca	1.16	1.5	46.0	1.3	0.02[b]
V	9×10^{-7}[c]	0.006	0	7	0
Fe	0	3.2	1.09	6	0.4
Pb	10^{-5}[c]	0.02	0	0.07	40

(a) data from ref. 22 unless otherwise specified.
(b) ref. 23
(c) ref. 24

Table 3. Liquid water-weighted average fogwater concentrations.

Site	Date[a]	n	pH	H^+	Na^+	K^+	NH_4^+	Ca^{2+}	Mg^{2+}	Cl^-	NO_3^-	SO_4^{2-}	S(IV)[b]	CH_2O[b]	L[c]
				ueq l^{-1}									uM l^{-1}		
Del Mar	9 Jan. 83 1840-2300	5	2.85	1410	511	9	781	49	130	614[d]	1850	469	66	78	0.24
Corona del Mar	7 Dec. 82 2100-2300	1	2.16	6920	725	71	2860	197	188	1050	7900	1290	NA	NA	0.11
Long Beach	6 Jan. 83 0400-0500	2	4.90	12.7	62	12	759	45	26	221[d]	252	487	NA	71	0.25
Lennox[e]	7 Dec. 81 2305-0840	8	2.96	1100	65	12	1610	111	42	178[d]	2210	926	80	196	0.30
	18 Dec. 81 2315-0045	3	2.66	2190	131	30	1280	127	48	150[d]	2780	1280	NA	178	0.14
	6 Jan. 83 0000-0430	5	3.63	237	41	8	464	39	18	68[d]	365	126	34	68	0.17
San Nicholas Island	26 Aug. 82 2115-0755	7	3.86	138	6060	148	452	450	1500	5330	1580	1080	11	15	0.052
San Marcos Pass[f]	20 Aug. 83 2340-1200	14	4.49	32.1	10	3	97	3	4	19	74	55	2	8	0.43
Morro Bay	14 Jul. 82 0500-0900	2	6.17	0.67	746	64	107	120	221	1200	114	214	6	7	0.14
Mt. Sutro	13 Aug. 82 2125-2225	1	3.99	102	648	52	183	93	170	851	87	319	NA	NA	0.056
Pt. Reyes	9 Aug. 82 2200-0000	1	3.60	251	3520	91	327	242	890	3040	526	1280	10	19	0.054
	10 Aug. 82 0230-1115	3	4.48	33.4	3146	72	95	153	782	4576	38	463	4	2	0.081
	11 Aug. 82 0200-1155	7	3.88	132	498	12	59	27	118	645	36	208	5	3	0.13
	12 Aug. 82 0340-0815	6	4.69	20	42	1.6	43	3	10	57	6	54	5	3	0.19

(a) date is that of the a.m. samples, or that of the morning following the fog. Time is local time.
(b) averages for S(IV) and CH_2O may be based on incomplete data sets.
(c) average liquid water content (g m^{-3}), calculated from the total volume collected.
(d) $[Cl^-]$ may be overestimated due to interference from organic acids during analysis. At Del Mar, this uncertainty is significant only for the last three samples (see text).
(e) 1981 events at Lennox have been previously reported by Munger et al. (1983).
(f) stratus cloud.

Table 3 (continued)

Site	n	Fe	Mn	Pb	Cu	Ni	V
		----------ug l^{-1}----------					
Del Mar	4	354	36	310	NA	111	6
Long Beach	2	96	22	152	NA	17	1
Lennox							
7 Dec. 1981	7	1440[a]	37	1180	34	10	6
18 Dec. 1981	3	1330	51	NA	NA	NA	13
6 Jan. 1983	5	315[b]	127	447	NA	25[c]	5
San Nicholas Island	5	431	93	49	49	99	8
San Marcos Pass	9	22	3	23	12	6	NA
Morro Bay	1	192	21	11	57	21	3
Mt. Sutro	1	160	10	24	50	28	NA
Pt. Reyes							
9 Aug. 1982	1	484	67	67	87	209	NA
10 Aug. 1982	3	276	12	21	36	66	NA
11 Aug. 1982	4	301	10	38	151	59	NA
12 Aug. 1982	5	265	7	26	48	17	NA

NA: not analyzed.
Metal concentrations were not determined in the Corona del Mar fog.
(a) average from 6 samples
(b) average from 2 samples
(c) average from 4 samples

Table 4. Source contributions to fogwater loading.

Site	mass loading ($ug\ m^{-3}$)						
	sea salt	secondary nitrate	secondary sulfate	soil dust	cement dust	fuel oil fly ash	automobile exhaust
Del Mar	9.0	28	4.9	2.8	0.27	0.023	0.21
Corona del Mar	6.1	54	6.6		0.80		
Long Beach	1.2	3.9	5.8	0.58	0.45	0.0036	0.095
Lennox							
7 Dec. 1981	0.80	30	10	8.6	1.1	0.019	0.62
18 Dec. 1981	1.2	25	9.0	5.7	0.74	0.027	
6 Jan, 1983	0.51	3.9	1.0	1.8	0.26	0.012	0.20
San Nicholas Island	23	5.2	4.3	0.55	0.42	0.0074	0.0064
San Marcos Pass	0.34	1.9	1.1	0.27	0.047		0.023
Morro Bay	7.5	1.1	1.2	0.97	0.55	0.0086	0.0055
Mt. Sutro	2.7	0.30	0.74	0.22	0.16		0.0033
Pt. Reyes							
9 Aug. 1982	14	1.8	2.7	0.74	0.21		0.0090
10 Aug. 1982	17	0.16	0.95	0.79	0.038		0.0034
11 Aug. 1982	5.2	0.28	1.1	1.6	0.020		0.014
12 Aug. 1982	0.54	0.074	0.47	1.6	0.0049		0.013

Mass loadings defined as the mass of material in fogwater per m^3 of air. Numbers given are averages for each event. Contributions from soil dust, fly ash, or exhaust were not determined when the concentrations of their respective tracers (Fe,V,Pb) was missing. When Fe data was missing, all NSS Ca was attributed to cement dust.

Table 5. Equivalent ratios in coastal fogs.

Site	Mg^{2+}/Na^{+}	Cl^{-}/Na^{+}	Ca^{2+}/Na^{+}	SO_4^{2-}/Na^{+}	K^{+}/Na^{+}
Del Mar	0.25	1.2	0.096	0.92	0.018
Corona del Mar	0.26	1.4	0.27	1.8	0.098
Long Beach	0.42	3.6	0.73	7.9	0.20
Lennox					
7 Dec. 1981	0.65	2.7	1.7	14	0.19
18 Dec. 1981	0.36	1.1	0.96	9.7	0.23
6 Jan. 1983	0.43	1.6	0.95	3.04	0.21
San Nicholas Island	0.25	0.91	0.074	0.34	0.024
San Marcos Pass	0.40	1.96	0.33	5.64	0.265
Morro Bay	0.30	1.61	0.16	0.29	0.086
Mt. Sutro	0.26	1.31	0.14	0.49	0.080
Pt. Reyes					
9 Aug. 1982	0.25	0.86	0.069	0.36	0.026
10 Aug. 1982	0.25	1.45	0.049	0.15	0.023
11 Aug. 1982	0.24	1.30	0.054	0.42	0.025
12 Aug. 1982	0.24	1.37	0.063	1.29	0.039
sea salt	0.23	1.17	0.043	0.12	0.021

Table 6. Chemical equilibria of the $NaCl-H_2SO_4-HNO_3-H_2O$ system.

	Reaction	Equilibrium constant
1.	$HNO_3(g) + NaCl(s) = HCl(g) + NaNO_3(s)$	3.4×10^{0}
2.	$2NO_2(g) + NaCl(s) = NOCl(g) + NaNO_3(s)$	2.2×10^{3}
3.	$H^+(aq) + Cl^-(aq) = HCl(g)$	5.6×10^{-7}
4.	$H^+(aq) + NO_3^-(aq) = HNO_3(g)$	4.3×10^{-7}
5.	$H^+(aq) + SO_4^{2-}(aq) = HSO_4^-(aq)$	7.8×10^{1}

Equilibrium constants calculated at 298K from free enthalpies of formation (38).

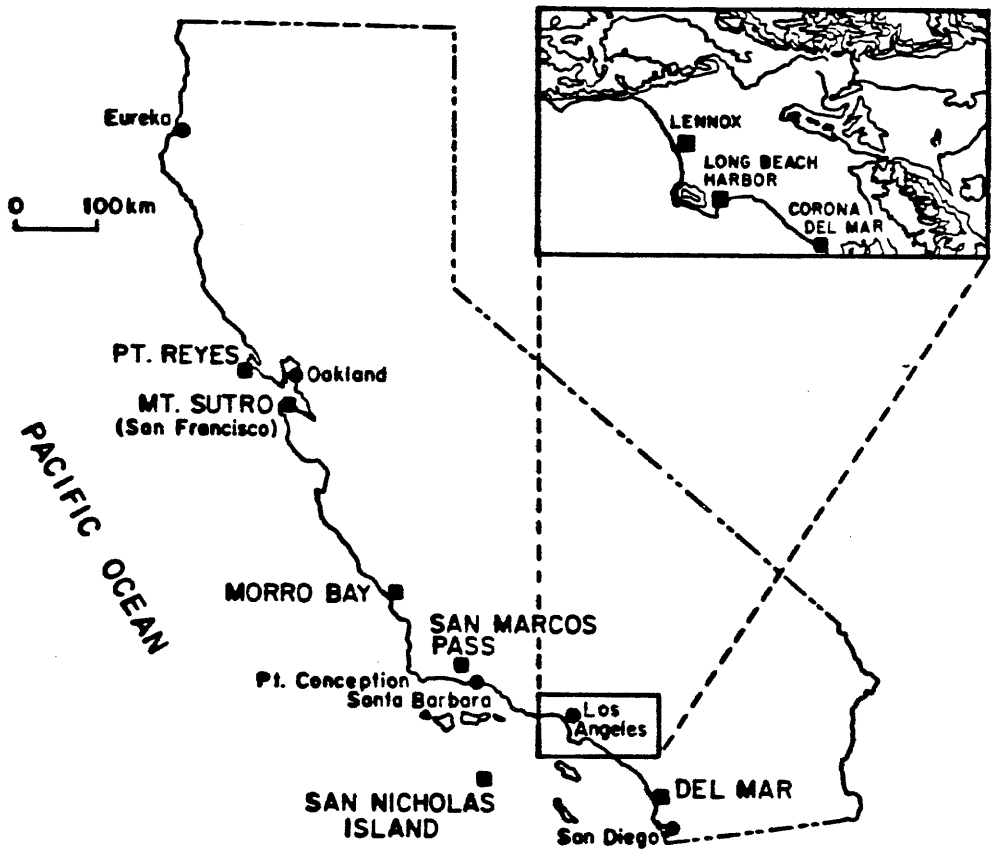

Figure 1. Fogwater sampling sites (■).

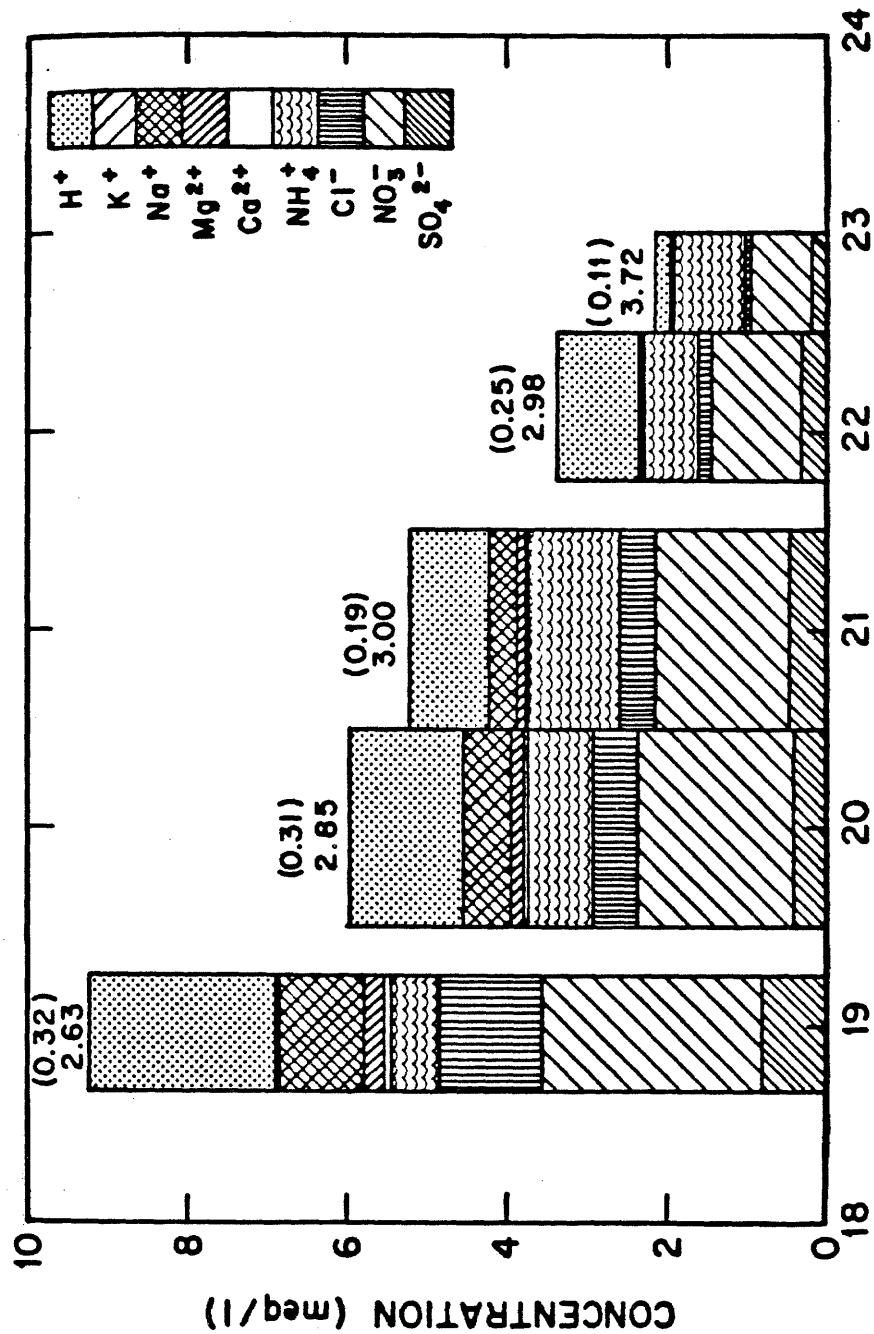

Figure 2a. Fogwater concentrations at Del Mar. pH values and liquid water contents (g m^{-3}, in parentheses) are indicated on top of each data bar.

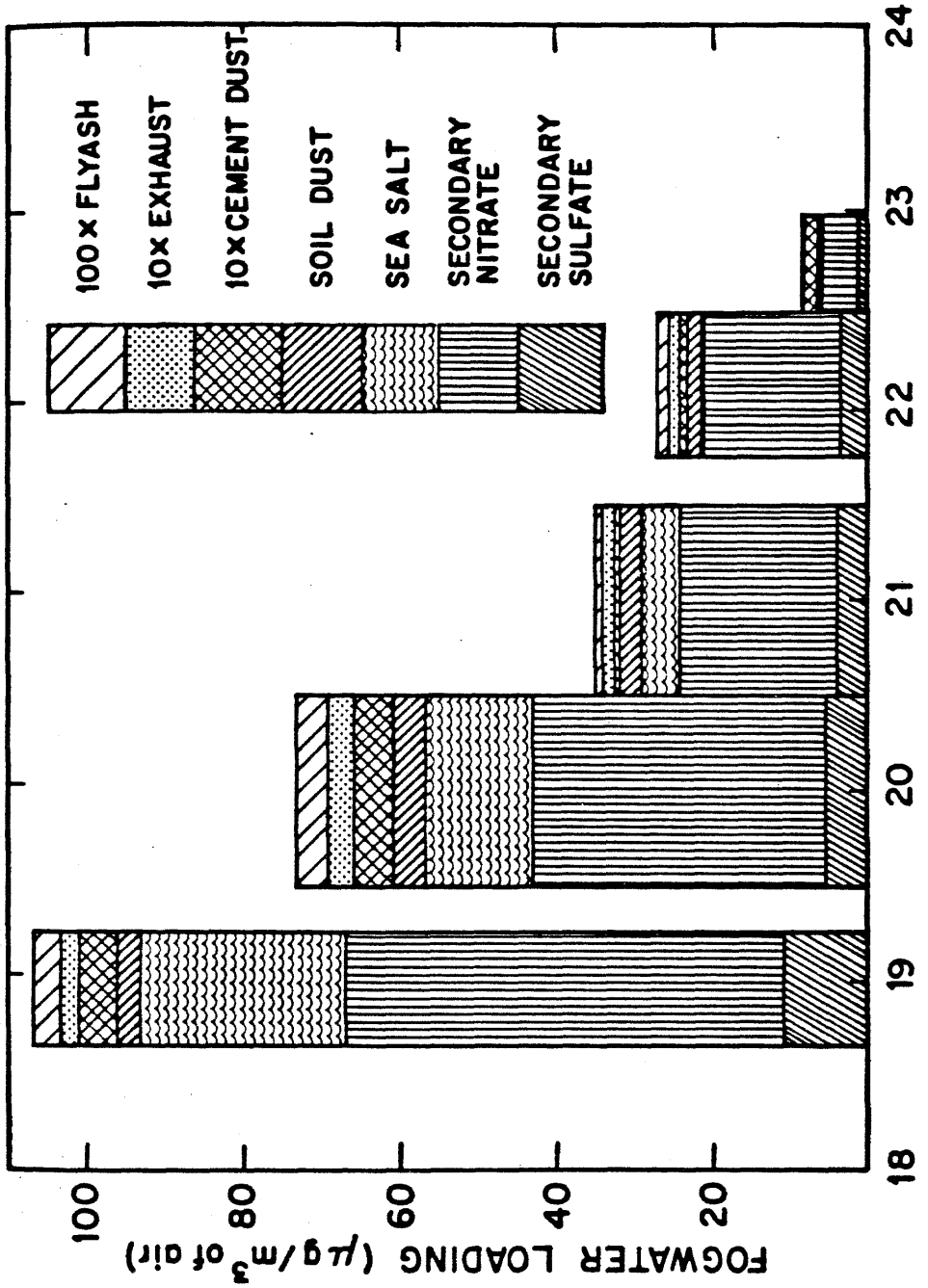

Figure 2b. Source contributions to the fogwater loading at Del Mar; contributions from soil dust, fly ash, and exhaust were not determined for the last sample.

CHAPTER IV

KINETICS AND MECHANISMS OF THE CATALYTIC OXIDATION OF DISSOLVED SULFUR DIOXIDE IN AQUEOUS SOLUTION: AN APPLICATION TO NIGHTTIME FOGWATER CHEMISTRY

by Michael R. Hoffmann and Daniel J. Jacob

Acid Precipitation: SO_2, NO, and NO_x Oxidation Mechanisms: Atmospheric Considerations. J.G. Calvert, ed., Butterworth, Boston, 101-172 (1984)

Kinetics and Mechanisms of the Catalytic Oxidation of Dissolved Sulfur Dioxide in Aqueous Solution: An Application to Nighttime Fog Water Chemistry

Michael R. Hoffmann
Daniel J. Jacob

Sulfur dioxide can be oxidized to sulfate aerosols either homogeneously in the gas phase or heterogeneously in atmospheric microdroplets [1–3]. Field studies indicate that the relative importance of homogeneous and heterogeneous processes depends on a variety of climatological factors, such as relative humidity and the intensity of incident solar radiation [4–9].

Cass [5] has shown that the worst sulfate pollution episodes in Los Angeles occur during periods of high relative humidity and when the day begins with low clouds or fog in coastal areas, while Cass and Shair [4] have reported that nighttime conversion rates (5.8%/h) for SO_2 in the Los Angeles sea breeze/land breeze circulation system are statistically indistinguishable from typical daytime conversion rates (5.7%/h) for the month of July. Liljestrand and Morgan [10], in their study of rainfall in the Los Angeles basin, have reported that light, misting precipitation events resulted in low pH values (e.g., pH 2.9) and correspondingly high SO_4^{2-} and NO_3^- concentrations.

Results of these investigations along with the results of other investigators [6–9,11–13] indicate that aqueous-phase oxidation of SO_2 is a significant pathway for the total transformation of SO_2.

Waldman et al. [14] characterized the chemistry of winter fogs in the Los Angeles basin; they reported that nighttime fog water has extremely low pH values (e.g., pH 2.2) and extremely high concentrations of sulfate, nitrate, ammonium ion and trace metals. Observed ranges reported by Waldman et al. [14] are summarized in Table I. Of special interest are the high values observed for SO_4^{2-}, NO_3^-, S(IV), CH_2O, and Fe, Mn, Pb and Cu ions in the fog water droplets. These values

Table I. Fog Water Composition in Southern California: Observed Concentration Ranges [12–14]

	Location					
					Los Angeles	
	Pasadena 11–23–81	*Lennox 12–18–81*	*Bakersfield 1–14–82*	*Extremes*	*Clouds 11–23–81*	*Rain 1981–1982*
pH	2.92–4.85	2.52–2.81	2.90–3.07	2.20	2.95–3.80	3.67–5.21
NO_3^- (μeq-L^{-1})	1,220–3,520	2,070–3,690	3,140–5,140	12,000	100–1,393	1.4–471
SO_4^{2-} (μeq-L^{-1})	481–944	510–1,970	2,250–5,000	5,060	113–544	3.1–125
NH_4^+ (μeq-L^{-1})	1,290–2,380	950–1,570	5,370–10,520	10,520	34–477	1–115
Fe (μg-L^{-1})	920–1,770	1,020–2,080	240–6,600	23,700	14–1,260	1.6–13.2
Mn (μg-L^{-1})	34–56	25–81		812	1.5–59	1–2.8
Pb (μg-L^{-1})	1,310–2,540	828–2,400	241–366	2,540	10–197	2–88
Cu (μg-L^{-1})	88–105	9–150	40–400	144	23–1,510	2.2–16.9
Ni (μg-L^{-1})	7.6–13.6	2.3–51.5	125–590	51.5	10–200	
CH_2O (mg-L^{-1})	3.1–3.4	3.9–7.6	6.1–14	12.8	0.13–1.6	
SO_3^{2-} (μeq-L^{-1})	151–235	30–250		250	54–258	

and their time-dependent changes [14] indicate that nighttime fogs provide a very reactive and complex environment for the incorporation and transformation of SO_2 and NO_x to their acidic products, H_2SO_4 and HNO_3. Concomitant incorporation of NH_3 gas and calcereous dust into the droplet phase results in the partial neutralization of the generated acidity. Later sections of this chapter will discuss models for the detailed thermodynamic speciation and possible reaction kinetics that lead to sulfate and nitrate production in these droplet systems.

Because of their similarity to clouds with respect to physical characteristics, fogs are likely to reflect the same chemical processes occurring in clouds and, to some degree, in aqueous microdroplets. Cloud and fog water droplets are in the size range 2–100 μm, whereas aqueous microdroplets will be in the range 0.01–1 μm. On the other hand, raindrops are approximately 100 times larger than cloud and fog water droplets (e.g., 0.1–3 mm). In the Los Angeles study, Waldman et al. [14] found that fog water was more concentrated in the primary constituents than was the overlying cloud water, which was in turn more concentrated than rain water during overlapping periods of time. These results suggest that fog and low-lying clouds may play an important role in the diurnal production of sulfate and nitrate in the Los Angeles basin during certain times of the year when the meteorological conditions are propitious for fog and cloud formation. Furthermore, Hegg and Hobbs [15] have observed sulfate production rates in cloud water over western Washington that ranged from 4.0 to 300%-h^{-1} and pH values from 4.3 to 5.9. The sulfate production rate appeared to increase with an increase in pH. Similar pH values and sulfate levels were observed in stratus clouds over the Los Angeles basin [15].

Historically, fog events have been correlated with severe pollution episodes in which elevated concentrations of SO_2 and particulate aerosol have been observed [16]. During many of these extended fog periods excess deaths were recorded [17–21]. The London fog of 1952 was particularly bad in this regard. For example, during the London fog of 1952 the daily mass emission rate of SO_2 has been estimated to be 1.82×10^9 g, the affected area to be 1.3×10^9 m^2, the height of the inversion layer to be 150 m and the liquid water content at 1.23×10^{12} g [22]. Given the daily observed increase in the gas-phase SO_2 concentration of 0.18 ppm and an established droplet residence time of 0.25 days [18], the sulfate concentration of the fog water can be estimated to be approximately 11.0 meq-L^{-1} with an apparent conversion rate of 12.5%-h^{-1}. This estimated value can be compared to the sulfate ranges observed in the Los Angeles fog water, which were 0.8–3 meq-L^{-1}. However, the London fog lasted for five days while the Los Angeles fogs of 1981–1982 persisted for no more than eight to ten successive hours.

As pointed out in Chapter 1, gas-phase reactions involving hydroxy radical oxidation of SO_2 are too slow to account for the very high transformation rates. Alternatively, the catalytic autoxidation of SO_2 in aqueous microdroplets has been suggested as a nonphotolytic pathway for rapid production of sulfuric acid in humid atmospheres [22–30]. In addition, H_2O_2 and O_3 have been given serious consideration as the major oxidants of dissolved SO_2 as discussed in Chapters 2 and 4. Oxidation by H_2O_2 seems to be most favorable because of its extremely

high rate of reaction [31–34] and its pH dependence which favors the reaction at low pH. In comparison, metal-catalyzed autoxidations tend to exhibit decreasing reaction rates with a decrease in pH [27]. Similarly, the reaction rate of O_3 with S(IV) decreases with a decrease in pH.

Limiting factors in the metal-catalyzed pathways will be the total concentration of the active metal catalyst and its speciation as a function of pH. As shown in Table I, Los Angeles fog water has high concentrations of Fe, Mn, Cu, Ni and Pb ions. Of these metals, Fe, Mn and Cu are expected to be the most effective catalysts for autoxidation of S(IV) [27,34]. The highest observed concentrations for Fe and Mn were 424 and 14.8 μM, respectively, while the average Fe and Mn concentrations in Los Angeles fog water were observed to be 51.6 and 1.7 μM, respectively. For comparison, Thornton [35] has reported that the worldwide mean concentrations for Fe in urban, rural and remote rainfall are 4.5, 3.1 and 0.13 μM, respectively. In many calculations of the droplet-phase SO_2 oxidation rate [2,36–39], the assumed Fe concentrations range from 1 to 360 μM and the assumed Mn concentrations range from 1 to 37 μM. At the upper range of the concentration scales, metal-catalyzed reactions may play an important role in the overall SO_2 oxidation rate in light of the rate laws discussed in Chapter 2. The role of metal ion speciation and kinetic models for fog water chemistry will be discussed later in this chapter.

To translate laboratory results on the kinetics of various pathways for SO_2 oxidation in aqueous systems to atmospheric droplet systems, detailed rate laws, mechanisms, activation energies and ionic strength dependencies should be determined. In only very few cases has this complete information been assembled. However, in the case of metal-catalyzed systems, there are numerous discrepancies among investigators concerning the detailed kinetic information [15]. Metal-catalyzed autoxidations can proceed via four distinctly different mechanistic pathways [40]. These include a thermally initiated free-radical chain reaction involving a series of one-electron transfer steps, an inner-sphere metal-sulfite complexation pathway involving a series of two-electron transfers, a surface complexation pathway involving metal oxides and oxyhydroxides in suspension, and photoassisted pathways in which the oxidation is initiated by absorption of light by S(IV), metal ions, metal oxide surfaces or a specific metal-sulfite complex. The details of these different reaction pathways will be discussed in the next section of this chapter.

The mechanism of the oxidation of S(IV) by hydrogen peroxide is fairly well understood [31–33,41,42]. This reaction proceeds via nucleophilic displacement of H_2O_2 on bisulfite (HSO_3^-) ion and is catalyzed by specific and general acid catalysis. The significance of this latter feature for open atmospheric systems has been discussed in Chapters 2 and 4. On the other hand, the mechanism of the oxidation of sulfite by ozone [32,43] and its various catalytic influences are less well understood. Most likely, the reaction with ozone proceeds via a free radical mechanism involving the sulfite radical and peroxymonosulfite radical species [32]. The details of the polar pathway involving H_2O_2 and the radical pathway involving O_3 will be presented in the next section. This discussion will be followed by presentation of a fog water chemistry model that will incorporate and test the various reaction pathways for an open nonphotolytic system.

S(IV) OXIDATION MECHANISMS

Metal-Catalyzed Pathways for Oxidation

Reactions of the triplet ground state of molecular oxygen with singlet ground state reductants such as SO_2 proceed slowly because they involve changes in spin multiplicity and a large degree of bond deformation or alteration in the formation of products. In many cases, the reactions of O_2 with organic and inorganic reductants can be accelerated in the presence of transition metal ions and their complexes. In particular, the first-row transition metal ions have been shown to be particularly effective as catalysts for autoxidation [44]. Catalysis by first-row transition metals may occur homogeneously or heterogeneously in the liquid phase. If the catalytic center involves a soluble metal ion or complex, the reaction can be classified as a homogeneous process; however, if the catalytic center involves a metal surface such as an oxide, oxyhydroxide or sulfide solid, then the reaction can be classified as a heterogeneous process in the liquid phase. Transition metal ions such as Co(II), Co(III), Cu(II), Fe(II), Fe(III), Mn(II), Ni(II), V(IV) (as VO^{2+}) and their soluble complexes have been shown to be effective homogeneous catalysts [44], while solid surfaces such as Fe_2O_3 [45], TiO_2 [45], CdS [45], ZnO [45], FeOOH [37], $Co(OH)_3$ [46], V_2O_5 [47], MnO_2 [48] and MnOOH [48] have been shown to be effective heterogeneous catalysts for certain redox reactions.

Numerous attempts have been made to characterize the kinetics and mechanisms of metal-catalyzed autoxidation of S(IV) in aqueous solution; however, these studies have been characterized by inconsistent reaction rates, rate laws and pH dependencies [27,40,44,49]. In this section, postulated mechanisms and their resulting theoretical rate expressions will be examined critically. In general, the homogeneous reaction mechanisms can be broken down into three general categories: (1) free radical chain mechanisms involving a sequence of one-electron transfer steps following a thermal initiation; (2) polar mechanisms involving inner-sphere complexation and two-electron transfer steps; and (3) photoassisted mechanisms. These mechanisms, their rate expressions and the empirical rate laws will be compared for consistency.

Free Radical Chain Reactions

Oxidation of S(IV) in aqueous solution proceeds according to the following simple stoichiometry:

$$H_nOSO_2^{(2-n)-} + 0.5\ O_2 \longrightarrow H_nSO_4^{(2-n)-} \qquad (1)$$

where n varies from 0 to 2 depending on pH. Bäckström [50] proposed that the reaction of Equation 1 involves a chain mechanism in which a metal ion, M^{n+}, of appropriate oxidation state initiates the radical sequence as follows:

$$\text{initiation} \qquad M^{n+} + SO_3^{2-} \xrightarrow{k_1} M^{(n-1)+} + SO_3^{-} \qquad (2)$$

$$\text{propagation} \quad SO_3^- + O_2 \xrightarrow{k_2} SO_5^- \tag{3}$$

$$\text{propagation} \quad SO_5^- + SO_3^{2-} \xrightarrow{k_3} SO_5^{2-} + SO_3^- \tag{4}$$

$$\text{oxidation} \quad SO_5^{2-} + SO_3^{2-} \xrightarrow{k_4} 2SO_4^{2-} \tag{5}$$

$$\text{termination} \begin{cases} 2SO_3^- \xrightarrow{k_5} S_2O_6^{2-} & (6) \\ SO_3^- + SO_5^- \xrightarrow{k_6} S_2O_6^{2-} + O_2 & (7) \\ SO_5^- + SO_5^- \xrightarrow{k_7} S_2O_6^{2-} + 2O_2 & (8) \end{cases}$$

where the initiation step involves a one-electron reducible metal ion as the catalytic initiator [for a truly closed catalytic sequence, $M^{(n-1)+}$ must be oxidized back to M^{n+}], the propagation steps involve SO_3^-, SO_5^- and SO_5^{2-} (peroxymonosulfite ion) as reactive intermediates, the oxidation step is invoked for stoichiometric reasons, and the termination steps result in the production of dithionate, a frequently observed but low-yield product.

Theoretical rate expressions for the overall stoichiometric reaction (Equation 1) (i.e., the summation of Equations 2–5) can be derived readily from the appropriate differential equations describing the total rate of appearance or of disappearance of each species involved in the mechanism provided that the steady-state approximation is used. For example, assuming that the chain mechanism involves Equations 2–5 and Equation 6 as the termination step the following rate expression can be derived [51].

$$-d[SO_3^{2-}]/dt = d[SO_4^{2-}]/dt = k_1[SO_3^{2-}][M^{n+}] + k_2(2k_1/k_5)^{0.5}[M^{n+}]^{0.5}[SO_3^{2-}]^{0.5}[O_2] \tag{9}$$

Since the sulfite chain reaction has a chain length of ~50,000, according to Bäckström [50], the long chain length approximation can be invoked (i.e., $\nu_p/\nu_i >> 1$ or the ratio of the rate of propagation to the rate of initiation is very large) and Equation 9 can be rewritten as:

$$-d[SO_3^{2-}]/dt = k'[M^{n+}]^{0.5}[SO_3^{2-}]^{0.5}[O_2] \tag{10}$$

where $k' = k_2(2k_1/k_5)^{0.5}$

Different theoretical rate expressions can be obtained if assumptions are made about the nature of the rate-determining propagation step and the corresponding termination step. In addition, the steady-state and the long chain length approxima-

Table II. Theoretical Rate Expressions Obtained from the Bäckström [50] Mechanism for Various Termination Steps[a]

Termination Step	*Rate Coefficient, k*	α	β	γ
k_5	$k_2(2k_1/k_5)^{1/2}$	1/2	1/2	1
k_6	$(2k_1k_2k_3/k_6)^{1/2}$	1/2	1	1/2
k_7	$k_3(2k_1/k_7)^{1/2}$	1/2	3/2	0

[a] α, β, and γ represent the reaction orders for the reaction rate given by the generalized rate expression $-d[SO_3^{2-}]/dt = k[M^{n+}]^{\alpha}[SO_3^{2-}]^{\beta}[O_2]^{\gamma}$.

tions for a free radical, closed-sequence catalytic [51,52] process can be used to simplify the algebraic manipulations. Theoretical rate expressions obtained with these procedures are listed in Table II [25,26,37,46,53–60].

The theoretically derived rate expressions can be compared to the empirical rate laws reported by other investigators (Table III). Perusal of this list indicates a considerable lack of agreement among these investigators as to the specific reaction orders; in particular, few empirical rate laws agree with the derived rate expressions shown in Table II. The empirical rate laws observed by Barron and O'Hern [66], Chen and Barron [58] and Bengtsson and Bjerle [60] at constant pH are in general agreement with the third rate expression of Table II. However, later results reported by Sawicki and Barron [59] using a thin-film reactor system contradicted earlier results reported by Barron and co-workers [58,66]. Most often the various investigators concur that the reaction order in oxygen is zero. However, it should be pointed out that an oxygen dependence in many cases was overlooked by using pseudo-order conditions in oxygen or, in other cases, mass-transfer limitations may have resulted in an apparent zero-order oxygen dependency. The first and second rate expressions of Table II show a nonzero reaction order in oxygen and a half-order metal ion dependence, whereas most investigators report a first-order metal ion dependence and a zero-order oxygen dependence. Nonetheless, many of these investigators cite the Bäckström [50] mechanism as a logical sequence of elementary reactions that is adequate to explain their empirical observations. Clearly, in many cases it appears to be inadequate. Finally, a caveat to this comparison is that few investigators used similar analytical and kinetic methodologies and fewer used identical concentration and pH ranges. As a result the lack of agreement is somewhat understandable and may suggest that parallel mechanistic pathways are followed which will result in complicated multiterm rate laws.

In most kinetic studies of the metal catalyzed autoxidation of S(IV), SO_3^{2-} has been identified as the reactive form of S(IV). If this is indeed the case, the apparent pH dependencies in part can be expressed as follows:

$$[S(IV)] = [H_2O \cdot SO_2] + [HSO_3^-] + [SO_3^{2-}] \quad (11)$$

Table III. Empirical Rate Laws Reported by Various Investigators for the Metal Catalyzed Autoxidation of SO_2.[a]

M^{n+}	α	β	γ	Δ	*Reference*
Mn^{2+}	2	0	0		53
	2	0	0	−1	Chapter 2[b]
	1	1	0	1	Chapter 2[b]
	1	1	0	1	54
	≤1	≤1	0		55
	1	1	0		56
Fe^{3+}	1	1	0	1	37
	1	2	0	1	25
	1	1–2	?	2	26
	1	1	0	−1	Chapter 2
	2	2	0	1/n	57[c]
	1	1	0	1/n	57[c]
Co^{3+}	1/2	3/2	0		58
	1/2	?	2		59
Co^{2+}	1/2	3/2	0	−1	60
	1	1	1		61
	2	1	1	−1	62
	1/2	1	0	1/n	63[c]
	1/2	3/2	0		64
Cu^{2+}	1	1	0	1/2	65
	1/2	3/2	0		66
	1/2	3/2	0		46
	1	1	0		56

[a] α, β, γ, and Δ represent the reaction orders for the reaction rate given by the generalized rate expression $-d[SO_3^{2-}]/dt = k[M^{n+}]^{\alpha}[SO_3^{2-}]^{\beta}[O_2]^{\gamma}[H^+]^{\Delta}$.

[b] Multiterm rate law.

[c] Multiterm rate law where n = 0, 1 or 2.

$$[H_2O \cdot SO_2] \overset{K_{a1}}{\rightleftharpoons} [HSO_3^-] + [H^+] \tag{12}$$

$$[HSO_3^-] \overset{K_{a2}}{\rightleftharpoons} [H^+] + [SO_3^{2-}] \tag{13}$$

$$[S(IV)] = [SO_3^{2-}]\left(\frac{[H^+]^2}{K_{a1}K_{a2}} + \frac{[H^+]}{K_{a1}} + 1\right) \tag{14}$$

$$[SO_3^{2-}] = [S(IV)]\left(\frac{K_{a1}K_{a2}}{[H^+]^2 + K_{a2}[H^+] + K_{a1}K_{a2}}\right) \tag{15}$$

Substitution into Equation 10 gives

$$\frac{-d[S(IV)]}{dt} = k'[M^{n+}][S(IV)]^{0.5}[O_2]\left(\frac{K_{a1}K_{a2}}{[H^+]^2 + K_{a2}[H^+] + K_{a1}K_{a2}}\right) \tag{16}$$

Alternative free-radical mechanisms have been postulated [67,68]. Hayon et al. [67] observed the formation of the sulfate radical ion, SO_4^-, during the flash photolysis and pulse radiolysis of oxygenated sulfite solutions, and they found no firm evidence for SO_5^-. If the flash photolysis experiments employed by Hayon et al. [67] truly give insight into more moderate energetic conditions anticipated in thermal reactions, the following mechanism can be postulated:

$$\text{initiation} \qquad M^{n+} + SO_3^{2-} \xrightarrow{k_1} M^{(n-1)+} + SO_3^- \tag{17}$$

$$SO_3^- + O_2 \xrightarrow{k_2} SO_5^- \tag{18}$$

$$\text{propagation} \qquad SO_5^- + SO_3^{2-} \xrightarrow{k_3'} SO_4^- + SO_4^{2-} \tag{19}$$

$$SO_4^- + SO_3^{2-} \xrightarrow{k_4'} SO_4^{2-} + SO_3^- \tag{20}$$

$$\text{termination} \qquad \begin{cases} SO_5^- + SO_5^- \xrightarrow{k_7} S_2O_6^{2-} + 2O_2 & (21) \\ SO_4^- + SO_4^- \xrightarrow{k_8} S_2O_6^{2-} + O_2 & (22) \\ SO_4^- + SO_4^- \xrightarrow{k_8'} S_2O_8^{2-} & (23) \end{cases}$$

This mechanism is similar in many respects to the Bäckström mechanism with the exception of the inclusion of the sulfate radical ion as a reactive propagation intermediate.

Once again, theoretical rate expressions can be derived from the mechanism above using the steady-state approximation, the long chain length assumption, and the assumption that the rate of initiation is equal to rate of termination at steady-state (i.e., $\nu_i = \nu_t$ when $d[SO_3^-]/dt = d[SO_4^-]/dt = d[SO_5^-]/dt = 0$). The resulting equations are listed in Table IV. Regardless of the basic assumptions,

Table IV. Theoretical Rate Expressions Obtained from the Hayon et al. [67] and Schmittkunz [68] Mechanisms[a]

Mechanism	*Termination Step*	*Rate Coefficient, k*	α	β	γ
Hayon et al.	k_7	$k_4'(2k_1/k_8)^{1/2}$	1/2	3/2	0
Hayon et al.	k_8 or k_8'	$k_3'(2k_1/k_7)^{1/2}$	1/2	3/2	0
Schmittkunz	k_{12}	$k_9(2k_1'/k_{12})^{1/2}$	1/2	1	1/2

[a] α, β, and γ represent the reaction orders for the reaction rate given by the generalized rate expression $-d[SO_3^{2-}]/dt = k[M^{n+}]^\alpha[SO_3^{2-}]^\beta[O_2]^\gamma$.

the mechanism of Hayon et al. [67] yields a single rate expression in which there is a half-order dependence on the metal ion concentration and a three-halves-order dependence on sulfite. The same result is obtained if the k_2 step is assumed to be the rate limiting propagation step.

The mechanism proposed by Schmittkunz [68] postulates two separate chain propagation sequences resulting from two different initiation steps. The first sequence is similar in form to the Bäckström mechanism and the second involves O_2^-, $HO_2\cdot$, $\cdot OH$ and $H\cdot$ as chain carriers. The postulated mechanism is:

$$\text{initiation} \begin{cases} M^{x+}L_3^{n-} + O_2 \xrightarrow{k_1'} M^{x+}L^{(n-1)-} + O_2^- & (24) \\ O_2^- + H^+ \overset{K_a^{-1}}{\rightleftharpoons} HO_2\cdot & (25) \end{cases}$$

$$\text{propagation} \begin{cases} O_2H\cdot + SO_3^{2-} \xrightarrow{k_9} SO_4^{2-} + \cdot OH & (26) \\ \cdot OH + SO_3^{2-} \xrightarrow{k_{10}} SO_4^{2-} + H\cdot & (27) \\ H\cdot + O_2 \xrightarrow{k_{11}} HO_2\cdot & (28) \end{cases}$$

$$\text{termination} \quad 2HO_2\cdot \xrightarrow{k_{12}} H_2O_2 + O_2 \quad (29)$$

where $M^{x+}L_3^{n-}$ is a metal(M)–ligand(L) complex of appropriate charge, x-n, and K_a is the acid dissociation constant for the hydroperoxyl radical/superoxide acid-base equilibrium. The second radical pathway involves SO_3^-, SO_4^- and SO_5^- as chain carriers accordingly:

$$M^{x+}L_3^{n-} + SO_3^{2-} \xrightarrow{k_1} M^{(x-1)+}L_3^{n-} + SO_3^- \quad (30)$$

$$SO_3^- + O_2 \xrightarrow{k_2} SO_5^- \quad (31)$$

$$SO_5^- + SO_3^{2-} \xrightarrow{k_3'} SO_4^{2-} + SO_4^- \quad (32)$$

$$SO_4^- + SO_3^{2-} \xrightarrow{k_4'} SO_3^- + SO_4^{2-} \quad (33)$$

$$2SO_4^- \xrightarrow{k_8'} S_2O_6^{2-} + O_2 \quad (34)$$

This two-part overall mechanism indicates that there are two transition states and, consequently, a two-term rate law. The rate expression obtained with the methods used above is

$$d[SO_4^{2-}]/dt = 2k_9(k_1'/2k_{12})^{0.5}[M^{x+}L_3^{n-1}]^{0.5}[O_2]^{0.5}[SO_3^{2-}] + 2k_4'(k_1/2k_8')^{0.5}[M^{x+}L_3^{n-1}]^{0.5}[SO_3^{2-}]^{1.5} \quad (35)$$

In this case, pH dependencies in terms of the acid base chemistry of $SO_2(aq)$ have been ignored. A complete analysis valid over broad pH ranges requires consideration of the roles of $SO_2 \cdot H_2O$, HSO_3^-, $SO_2 \cdot H_2O^+$ and $HSO_3 \cdot$ as reactive species. Larson et al. [29] used a hybrid mechanism involving two distinct chain propagation sequences with superimposed acid-base equilibria to obtain a rate expression that agreed moderately well with their empirical rate law.

Polar Mechanisms Involving Inner Sphere Complexation

Nonradical, polar mechanisms for metal-catalyzed autoxidation of $SO_2(aq)$ have been proposed [25,40,55,56,69]. The common features of the mechanisms include inner-sphere complexation of the catalytic metal by sulfite as a prelude to electron transfer, subsequent binding of dioxygen by the resulting metal-sulfito complex, and finally electron transfer via successive two-electron transfers as opposed to a series of one-electron transfer, chain propagation steps.

Catalytic Effect of Mn^{2+}. Bassett and Parker [69] found that Mn^{2+} salts had a pronounced catalytic effect on the rate of sulfite autoxidation with almost complete suppression of dithionate formation; that the nature of the Mn^{2+} counterion (i.e., SO_4^{2-} or Cl^-) strongly influenced the reaction rate due to competitive complexation; and that a similar catalytic sequence was observed for Co(II) and Ni(II) salts. Based on these observations they proposed the following polar mechanism:

$$Mn^{2+} + SO_3^{2-} \underset{k_{-1}}{\overset{k_1}{\rightleftharpoons}} MnSO_3^0 \quad (36)$$

$$MnSO_3^0 + SO_3^{2-} \underset{k_{-2}}{\overset{k_2}{\rightleftharpoons}} Mn(SO_3)_2^{2-} \quad (37)$$

$$Mn(SO_3)_2^{2-} + O_2 \underset{k_{-3}}{\overset{k_3}{\rightleftharpoons}} Mn(SO_3)_2O_2^{2-} \quad (38)$$

$$Mn(SO_3)_2O_2^{2-} \xrightarrow[\text{slow}]{k_4} Mn^{2+} + 2SO_4^{2-} \quad (39)$$

A theoretical rate expression can be derived from this sequence of elementary reactions using the vector method of King and Altman [70]. In this procedure the mechanism is written in a cyclic form that represents the closed nature of the catalytic cycle for the overall reaction. The number of intermediate complexes is readily identified and the concentration of each form of the catalyst can be shown to be proportional to the sums of the terms that are obtained from the

elementary reaction steps which individually or in sequence lead to the specific form of the catalyst. The number of rate constants (or products of individual rate constants and concentrations of species in excess) must be one less than the number of species in a particular cycle. The steady-state approximation is applied to the resultant equations for each reactive intermediate and the final rate expression is obtained by substitution into a designated rate-limiting step. Using this procedure, the following rate expression is obtained:

$$\nu = -\frac{d[SO_3^{2-}]}{dt} = \frac{k_4[Mn^{2+}]_0[SO_3^{2-}]^2[O_2]}{K_A + K_B[O_2] + K_C[SO_3^{2-}] + K_D[SO_3^{2-}][O_2] + K_E[SO_3^{2-}]^2 + [SO_3^{2-}]^2[O_2]} \quad (40)$$

where

$$K_A = K_1^{-1}K_2^{-1}(K_3^{-1} + k_4/k_3)$$
$$K_B = K_1^{-1}\,k_4/k_2$$
$$K_C = K_2^{-1}\,(K_3^{-1} + k_4/k_3)$$
$$K_D = k_4/k_2 + k_4/k_1$$
$$K_E = K_3^{-1} + k_4/k_3$$
$$[Mn^{2+}]_0 = \text{initial manganese concentration}$$
$$K_1, K_2, K_3 = \text{equilibrium constants for reactions 1, 2 and 3, respectively}$$

This cumbersome expression can be simplified for certain limiting cases if assumptions are made about the magnitude of individual terms, as shown in Table V. It

Table V. Rate Expressions for Limiting Cases of the Bassett and Parker [69] Mechanism[a]

$$\nu = -\frac{d[SO_3^{2-}]}{dt} = \frac{k_4[Mn^{2+}]_0[SO_3^{2-}]^2[O_2]}{K_A + K_B[O_2] + K_C[SO_3^{2-}] + K_D[SO_3^{2-}][O_2] + K_E[SO_3^{2-}]^2 + [SO_3^{2-}]^2[O_2]}$$

Dominant Term in Denominator	α	β	γ
A	1	2	1
B	1	2	0
C	1	1	1
D	1	1	0
E	1	0	1
$[SO_3^{2-}]^2[O_2]$	1	0	0

[a] α, β, and γ represent the reaction orders for the reaction rate given by the generalized rate expression $= d[SO_3^{2-}]/dt = k[M^{n+}]^\alpha[SO_3^{2-}]^\beta[O_2]^\gamma$.

should be emphasized, however, that these limiting cases are idealizations and that intermediate cases generally would be expected.

From laboratory studies of S(IV) oxidation in aqueous aerosols, Matteson et al. [55] reported that the following rate law was adequate to account for their environmental observations under certain conditions:

$$v_0 \equiv -\left(\frac{d[H_2O\cdot SO_2]}{dt}\right)_0 = \frac{k[Mn^{2+}]_0[H_2O\cdot SO_2]_0}{k_1[H_2O\cdot SO_2]_0 + k'[Mn^{2+}]_0 + K} \tag{41}$$

Here the concentration of S(IV) is expressed as $[H_2O\cdot SO_2]$ to reflect the condition of high acidity employed in the study. Equation 41 can be reduced to

$$v_0 = k''[Mn^{2+}]_0[SO_2]_0 \tag{42}$$

for the initial rate when $K >> k_1[H_2O\cdot SO_2]_0 + k'[Mn^{2+}]_0$. Indication of such behavior based on aerosol conversion experiments has been observed [22,28]. Similar kinetic behavior has been reported by Ibusuki [54] and in Chapter 2 for low concentrations of S(IV). These results have been summarized in Table VI.

Complexation by Fe(III). Freiberg [71] has proposed a polar catalytic cycle involving inner-sphere complexation of sulfite by Fe(III) as a prelude to electron transfer. His hypothetical mechanism, which was postulated in an effort to obtain an empirical rate law consistent with the experimental data of other investigators (Table VII) is as follows:

$$H_2O\cdot SO_2 \overset{K_{a1}}{\rightleftharpoons} H^+ + HSO_3^- \tag{43}$$

$$HSO_3^- \overset{K_{a2}}{\rightleftharpoons} H^+ + SO_3^{2-} \tag{44}$$

$$Fe(OH)^{2+} + H^+ \overset{K_h^{-1}}{\rightleftharpoons} Fe^{3+} + H_2O \tag{45}$$

$$Fe^{3+} + HSO_3^- \underset{k_{-1}}{\overset{k_1}{\rightleftharpoons}} Fe(HSO_3)^{2+} \tag{46}$$

$$Fe(HSO_3)^{2+} + SO_3^{2-} \underset{k_{-2}}{\overset{k_2}{\rightleftharpoons}} Fe(SO_3)_2H^o \tag{47}$$

$$Fe(SO_3)_2H^o + O_2 \underset{k_{-3}}{\overset{k_3}{\rightleftharpoons}} Fe(SO_3)_2HO_2^o \xrightarrow[H_2O]{k_4} Fe(OH)^{2+} + 2HSO_4^- \tag{48}$$

$$Fe(SO_3)_2H^o + Fe^{3+} + H_2O \xrightarrow{k_5} 2Fe^{2+} + HSO_4^- + HSO_3^- + H^+ \tag{49}$$

Equation 49 represents direct oxidation of S(IV) by 2Fe(III) to produce S(VI).

Table VI. Empirical Rate Laws for Mn^{2+}-Catalyzed Autoxidation of S(IV) in Aqueous Solution

Rate ($v = -d[S(IV)]/dt$)	*Rate Constant*	*Conditions*	*Reference*
$v = k[Mn^{2+}][S(IV)][H^+]^{-1}$	$k = 25\ s^{-1}$	pH 0–0.2 $[S(IV)] < 10^{-4}\ M$ T = 25.0 C	Chapter 2
$v = k[Mn^{2+}][HSO_3^-]$	$k = 5 \times 10^3\ M^{-1}\text{-}s^{-1}$	pH 3–7.5 T = 25 C	54
$v = k[Mn^{2+}]^2[H^+]^{-1}$	$k = 4.7\ s^{-1}$	pH 0–2 $[S(IV)] < 10^{-4}\ M$ T = 25 C	Chapter 2
$v = \dfrac{k_2k_1[Mn^{2+}][SO_{2(aq)}]}{k_1[SO_{2(aq)}] + k_1k'[Mn^{2+}] + k_2 + k_3}$	$k_1 = 2.4 \times 10^5$ mmol^{-1}-min^{-1}-cm^{-3} $k' = n\text{-}cm^3\text{-}m^{-3}$ $k_2 = 0.22\ min^{-1}$ $k_3 = 10\ min^{-1}$	pH <2 droplet study n = aerosol volume	55
$v_o = \dfrac{[Mn^{2+}]_o^2[SO_2]_o^{2.2}}{k_1[Mn^{2+}]^2 + k_2[SO_2]^{2.2}}$	$k_1 = 1.32 \times 10^{-3}\ M^{-1}\text{-}s^{-1}$ $k_2 = 3.2 \times 10^{-4}\ M^{-1}\text{-}s^{-1}$	$[Mn^{2+}]_o = 1\text{–}100\ \mu M$ $[SO_2] \sim 10\ \mu M$	72
$v = k[Mn^{2+}]^{1.7\sim2}$	$k \simeq 5 - 8 \times 10^2\ M^{-1}\text{-}s^{-1}$	T = 35 C pH 2.4–3.3	73
$v = k[Mn^{2+}][H^+]^{-1}$	$k = 8 \times 10^{-4}\ M\text{-}min^{-1}$	T = 10 C pH 1.4–2.0 $[S(IV)] \simeq 6 \times 10^{-4}\ M$	74
$v = k_1[Mn^{2+}]^2[H^+]^{-1} + k_2[Fe^{3+}][S(IV)][H^+]^{-1} \times \left(1 + \dfrac{1.7 \times 10^3[Mn^{2+}]^{1.5}}{6.31 \times 10^{-6} + [Fe(III)]}\right)$	$k_1 = 4.7\ s^{-1}$ $k_2 = 0.82\ s^{-1}$ Synergistic term	T = 25 C pH 0–3 $[S(IV)] > 10^{-4}\ M$ $[Mn^{2+}] = 10^{-4}\ M$ $[Fe^{3+}] > 1\ \mu M$	Chapter 2

Table VII. Empirical Rate Laws for Fe^{3+} Catalyzed Autoxidation of S(IV) in Aqueous Solution

Rate ($v = -d[S(IV)]/dt$)	*Rate Constant*	*Conditions*	*Reference*
$v = k[Fe(III)][S(IV)][H^+]^{-1}$	$k = 0.82\ s^{-1}$	pH 0–3 $[S(IV)] > 10^{-4}\ M$	Chapter 2
$v = k[Fe(III)][S(IV)]$	$k = 100\ M^{-1}\text{-}s^{-1}$	pH 4–8 $[Fe(III)] \sim 1\ \mu M$ $[S(IV)] \sim 1\ mM$	37
$v = k[Fe(III)][S(IV)] (v = f([H^+]) = [H^+]^{-1})$	$k = 8 \times 10^2\ M^{-1}\text{-}s^{-1}$ (pH 4) $k = 80\ M^{-1}s^{-1}$ (pH 3)	pH ≤ 4 T = 20 C SO_2 electrode	26
$v = k[Fe(III)][S(IV)]^2$		pH ≥ 5 T = 20 C SO_2 electrode	26
$v = k[Fe(III)][S(IV)]^2[H^+]^{-1}$	$k = 40\ M^{-1}\text{-}s^{-1}$	pH 1.5–3 T = 10 C $[Fe(III)] > 10^{-4}\ M$ $[S(IV)] > 10^{-4}\ M$	74
$v = k_1[Fe^{3+}][H^+]^{-1} \times (1 - k_2[Fe^{2+}]/2k_3[O_2])$	No constants reported	Derived from postulated mechanism $[Fe(III)] >> [S(IV)]$ pH ~ 0.6	75
$v = \dfrac{k_1[Fe(III)]^2[SO_3^{2-}]^2}{[Fe(III)][SO_3^{2-}]_o + k_2[SO_4^{2-}] + k_3[Fe(III)][SO_3^{2-}]}$	$k_1 = 3.6 \times 10^6\ M\text{-}s^{-1}$ $k_2 = 2.5 \times 10^{-7}\ M\text{-}s^{-1}$ $k_3 = 4.5 \times 10^5\ M\text{-}s^{-1}$	T = 10 C $\mu = 1.2\ M$ pH 1.3–3.3 $[Fe(III)] < 10^{-3}\ M$ $[S(IV)] < 10^{-3}\ M$	57

Freiberg [71] assumed that Equation 47, the formation of an iron-sulfito complex of 1:2 stoichiometry, was rate-limiting in the catalytic sequence of Equations 43–48. With this assumption, and use of the steady-state hypothesis, Freiberg [71] derived the following overall rate expression:

$$\frac{d[SO_4^{2-}]}{dt} = \frac{k_1k_2(2k_3k_4[O_2] + k_5[Fe^{3+}])[HSO_3^-][Fe^{3+}][SO_3^{2-}]}{k_{-1}(k_{-2} + k_3[O_2] + k_5([Fe^{3+}])} \tag{50}$$

Since

$$[SO_3^{2-}] = K_{a2}[HSO_3^-]/[H^+] = K_{a1}K_{a2}[SO_2(aq)]/[H^+]^2 \tag{51}$$

Equation 50 was then expressed as

$$\frac{d[SO_4^{2-}]}{dt} = \frac{K_TK_{a1}^2[Fe^{3+}][SO_2(aq)]^2}{[H^+]^3} \tag{52}$$

where

$$K_T = \frac{k_1k_2K_{a2}(2k_3k_4[O_2]/k_5 + [Fe^{3+}])}{k_{-1}[(k_{-2} + k_3[O_2])/k_4) + [Fe^{3+}]} \tag{53}$$

Equation 50 can be recast in terms of $[SO_3^{2-}]$ as follows:

$$\frac{d[SO_4^{2-}]}{dt} = k'[Fe^{3+}][SO_3^{2-}]^2[H^+] \tag{54}$$

where $k' = K_T/K_{a2}^2$

Since the rate-limiting step (Equation 47) presumably involves the slow substitution of a second SO_3^{2-} to the coordination sphere of $Fe(H_2O)_5HSO_3^{2+}$, there should be no observed kinetic dependence on $[O_2]$. In addition to a sequence of two-electron transfers involving oxygen as the oxidant, oxidation of S(IV) directly by Fe^{3+} via successive one-electron transfers is predicted thermodynamically (Equation 49) in acidic solution:

$$H_2O + 2Fe(III) + SO_2 \cdot H_2O \rightleftharpoons SO_4^{2-} + 4H^+ + 2Fe(II) \tag{55}$$

$$\Delta G^\circ = -115.97 \text{ kJ-mol}^{-1}$$

However, due to the extremely slow rate of oxidation of Fe(II) to Fe(III) at low pH [48] a loss of apparent catalytic activity would be predicted if Equation 49 were a predominant pathway in the $Fe(III)/O_2/SO_2$ system, unless Fe(II) also exhibits catalytic activity in a fashion similar to Mn(II), Co(II), Ni(II) and Cu(II).

In addition to direct oxidation of S(IV) by Fe(III) to produce SO_4^{2-} {S(VI)}, dithionate $S_2O_6^{2-}$ {S(V)} can be produced according to the following stoichiometry:

$$2SO_2 \cdot H_2O + 2Fe(III) \rightarrow S_2O_6^{2-} + 4H^+ + 2Fe^{2+}(II) \qquad (56)$$

$$\Delta G^\circ = -38.6 \text{ kJ-mol}^{-1}$$

The kinetics of this reaction have been studied by Pollard et al. [76]; they have proposed the following mechanism:

$$Fe(III) + SO_2 \cdot H_2O \underset{k_{-1}}{\overset{k_1}{\rightleftharpoons}} Fe(II) + HSO_3 \cdot + H^+ \qquad (57)$$

$$2HSO_3 \cdot \xrightarrow{k_2} H_2S_2O_6 \qquad (58)$$

$$HSO_3 \cdot + Fe(III) \xrightarrow{k_3} Fe(II) + SO_3 + H^+ \qquad (59)$$

$$SO_3 + H_2O \xrightarrow{k_4} H_2SO_4 \qquad (60)$$

where $k_1 = 2.7 \times 10^{-4}\ M^{-1} = s^{-1}$

Likewise, Karraker studied direct oxidation of S(IV) by Fe(III) under the conditions of $[Fe(III)]_o > [S(IV)]_o$ and proposed the following mechanism involving initial complexation of Fe(III) by HSO_3^-:

$$Fe(III) + HSO_3^- \underset{}{\overset{\beta}{\rightleftharpoons}} Fe(HSO_3)^{2+} \qquad (61)$$

$$Fe(HSO_3)^{2+} \xrightarrow{k_1} Fe(II) + HSO_3 \cdot \qquad (62)$$

$$HSO_3 \cdot + Fe(II) \xrightarrow{k_2} Fe(III) + HSO_3^- \qquad (63)$$

$$H_2O + HSO_3 \cdot + Fe(III) \xrightarrow{k_3} SO_4^{2-} + Fe(II) + 3H^+ \qquad (64)$$

where k_1 and k_2/k_3 were estimated from kinetic data to be 7 min^{-1} and 22, respectively. Further evidence for the formation of discrete iron-sulfito complexes as a prelude to electron transfer has been cited [57,77–80]. Additional work by Carlyle and Zeck [81] suggests that the following noncatalytic mechanism provides a pathway for direct oxidation of S(IV):

$$Fe^{3+} + H_2O \underset{}{\overset{K_1}{\rightleftharpoons}} FeOH^+ + H^+ \qquad (65)$$

$$Fe^{3+} + HSO_3^- \overset{K_2}{\rightleftharpoons} FeSO_3^+ + H^+ \quad (66)$$

$$FeSO_3^+ \overset{K_3}{\rightleftharpoons} Fe^{2+} + SO_3^- \quad (67)$$

$$FeOH^{2+} + SO_3^- \longrightarrow Fe^{2+} + HSO_4^- \quad (68)$$

$$H_2O + FeSO_3^+ + SO_3^- \longrightarrow Fe^{2+} + HSO_4^- + HSO_3^- \quad (69)$$

where

$$\frac{-d[S(IV)]}{dt} = 2k'[Fe(III)]^2 \quad (70)$$

$$k' = 1.7 \times 10^{-6}[HSO_3^-]/[H^+]^2[Fe^{2+}] + (5.7 \times 10^{-5}[HSO_3^-]^2/[H^+][Fe^{2+}] \times (1/0.19 + [SO_2]) \quad (71)$$

Catalysis By Cu(II). Direct oxidation of S(IV) by Fe(III) is sensitive to catalysis by Cu(II) [76,81,82]. In general, the catalytic cycle would proceed accordingly:

$$Fe(III) + S(IV) \rightleftharpoons Fe(II) + S(V) \quad (72)$$

$$2S(IV) \longrightarrow S_2O_6^{2-} \quad (73)$$

$$Fe(III) + S(V) \longrightarrow Fe(II) + SO_4^{2-} \quad (74)$$

$$Cu(II) + S(V) \longrightarrow Cu(I) + SO_4^{2-} \quad (75)$$

$$Cu(I) + Fe(III) \xrightarrow{\text{fast}} Cu(II) + Fe(II) \quad (76)$$

Equations 72–76 may constitute an important alternative catalytic cycle for oxidation of S(IV) to S(VI). As shown in Table I, fog and cloud water droplets have significant levels of Fe and Cu. At these levels, Cu(II) catalysis of the Fe(III)–S(IV) reaction may contribute to the overall conversion of SO_2 in the droplet phase. According to Carlyle and Zeck [81], the catalytic rate of oxidation of S(IV) is given by:

$$\frac{-d[S(IV)]}{dt} = 2k''[Fe(III)] \quad (77)$$

where

$$k'' = [Cu^{2+}][HSO_3^-][H^+] \times 1/(14.1[Fe^{2+}] + 2.2[Cu^{2+}] + 0.8[Cu^{2+}]^2/[H^+]) \quad (78)$$

The reaction sequence of Equations 72–76 is an example of a redox reaction that is accelerated by a catalyst that exists in more than one oxidation state. Catalysis in this case is due to the fact that Equations 75 and 76, which involve the Cu(II)/Cu(I) couple, are fast relative to Equations 72 and 74. The net result is the apparent catalysis of the overall reaction given in Equation 55.

In the case of catalysis by Cu^+, Lunak et al. [56] proposed that autoxidation of S(IV) proceeds via a two-electron polar pathway as follows:

$$Cu^+ + SO_3^{2-} \overset{K_1}{\rightleftharpoons} CuSO_3^- \tag{79}$$

$$CuSO_3^- + SO_3^{2-} \overset{K_2}{\rightleftharpoons} Cu(SO_3)_2^{3-} \tag{80}$$

$$Cu(SO_3)_2^{3-} + O_2 \overset{K_3}{\rightleftharpoons} Cu(SO_3)_2O_2^{3-} \tag{81}$$

$$Cu(SO_3)_2O_2^{3-} \xrightarrow{k} Cu^+ + 2SO_4^{2-} \tag{82}$$

where $K_1 = 10^{7.85}$
$K_2 = 10^{7.08}$

The rate law (Table VIII) that results from this mechanism is identical in form to that presented in Equation 40 for catalysis by Mn^{2+}.

In the scheme proposed by Lunak et al. [56], Cu^{2+} is reduced rapidly to Cu^+ by SO_3^{2-}; Cu^+ then acts as the active catalytic center when complexed by excess S(IV) in solution. These investigators established a relative order of catalytic activity as follows:

$$Fe(II) \sim Co(II) > Mn(II) \sim Cu(I) \sim Cu(II) >> Fe(III) \sim Co(III) >> Ni(II) \tag{83}$$

Unfortunately, Lunak et al. [56] failed to report the pH at which these studies were performed.

The mechanistic interpretation of Lunak et al. [56] is in direct opposition with the kinetic observations and mechanisms proposed by other investigators [46,65,66]. These investigators favor the free radical pathway of Equations 2–8 in which the Cu^{2+}/Cu^+ redox couple acts as an one-electron acceptor

$$Cu^{2+} + SO_3^{2-} \longrightarrow Cu^+ + SO_3^- \tag{84}$$

However, using the estimated value of E° (−0.89 V) for the SO_3^{2-}/SO_3^- redox couple and the E° (0.15 V) for the Cu(II)/Cu(I) couple, it can be shown that Equation 84 is thermodynamically unfavorable, since E_H° for this reaction is −0.74 V (ΔG° = 71 kJ-mol^{-1}) [85]. This fact tends to support the hypothesis that the Cu(II)-catalyzed reaction proceeds via the formation of copper-sulfito complexes,

Table VIII. Empirical Rate Laws for Cu^{2+}-Catalyzed Autoxidation of S(IV) in Aqueous Solution

Rate ($v = -d[S(IV)]/dt$)	*Rate Constant*	*Conditions*	*Reference*
$v = (k_1 + k_3[Cu^{2+}])[SO_3^{2-}]$	$k_1 = 1.3 \times 10^{-2}\ s^{-1}$ $k_3 = 2.5 \times 10^6\ M^{-1}\text{-}s^{-1}$	$pH_o = 8.7$ $[Cu^{2+}]_o > 10^{-9}\ M$ $Cu(OH)_2(s)$ T = 25 C	65
$v = 0.5\ k_1[Cu^{2+}]^{1/2}[SO_3^{2-}]^{3/2}$	$k_1 = 1.2 \times 10^3\ M^{-1}\text{-}s^{-1}$	pH 7–9 $E_a = 76\ kJ\text{-}mol^{-1}$ T = 25 C	66
$v = 0.5\ k_1[Cu^{2+}]^{1/2}[SO_3^{2-}]^{3/2}$		pH 8.5 $E_a = 78.2\ kJ\text{-}mol^{-1}$ T = 25 C $[Cu^{2+}] = 1\ \mu M$	46
$v = k[Cu^{2+}][SO_3^{2-}]/[INHIB]$	$k = 7.3 \times 10^4\ M^{-1}\text{-}s^{-1}$	INHIB = 2-propanal T = 20 C $[Cu^{2+}] = 10\ \mu M$ pH 8.5	56
$v = k[Cu^{2+}][SO_3^{2-}]$	$k = 2.3\ M^{-1}\text{-}s^{-1}$ (pH > 12)	pH 4–12 T = 25 C 1–10 *M* (NH_4OH)	83
$v = k[Cu^{2+}][SO_3^{2-}]$			84

which react subsequently with oxygen as suggested originally by Titoff [83] and confirmed later by the results of Reinder and Vles [82].

Metal Ion Redox Couples. Metal ion redox couples that would be suitable for 1 ē oxidation of S(IV) to S(V) (i.e., Equation 2) and for initiation of a chain reaction (Equations 2–8), are Co(III)/Co(II) (Table IX), Mn(III)/Mn(II) and V(V)/V(IV) with E° values of 1.82, 1.5 and 1.0 V, respectively [85]. The Fe(III)/Fe(II) couple with an E° of 0.77 V would be insufficient for one-electron production of SO_3^-. Likewise, initiation of a chain reaction by Equation 24, involving a first-row transition metal redox couple, will be thermodynamically unfavorable as shown below. For example, two appropriate half-reactions:

$$O_2 + H^+ + 1\bar{e} \rightleftharpoons HO_2\cdot \quad (E^\circ = -0.13) \tag{85}$$

$$Fe(II) \rightleftharpoons Fe(III) + 1\bar{e} \quad (E^\circ = -0.77) \tag{86}$$

can be combined to give an initiation step as envisioned by Schmittkunz [68]:

Table IX. Empirical Rate Laws for Co(III)/Co(II)-Catalyzed Autoxidation of S(IV)

Rate ($v = -d[S(IV)]/dt$)	*Rate Constant*	*Conditions*	*Reference*
$v = k[Co(II)][SO_3^{2-}][O_2]$	$k = 1.5 \times 10^7\ M^{-2}\text{-}s^{-1}$	T = 20 C pH 8–9.2 $[Co(II)] \leq 0.1\ \mu M$ $[S(IV)] \leq 0.01\ M$	61
$v = \frac{k_1[Co^{2+}]_o[SO_3^{2-}][O_2]}{1 + k_2[SO_3^{2-}]}$	$k_1 = 1.96 \times 10^9\ M^{-2}\text{-}s^{-1}$ $k_2 = 4.74 \times 10^2\ s^{-1}$	T = 20 C pH 8–8.3	86
$v = k[Co(H_2O)_6^{3+}]^{1/2}[SO_3^{2-}]^{3/2}$	No constant reported	$E_a = 73.15$ kJ-mol^{-1} pH 9–9.7	58
$v = k[Co^{2+}]^{1/2}[SO_3^{2-}]^{3/2}[H^+]^{-1}$	$k \sim 1 \times 10^{-3}\ s^{-1}$ $k[H^+]^{-1} = 10^3\text{–}10^4\ M^{-1}\text{-}s^{-1}$	T = 30–60 C pH 6–7.5 $[Co^{2+}]_o < 3\ \mu M$ $[S(IV)]_o < 1\ mM$	60
$v = k[Co(II)L_4O_2][SO_3^{2-}]$	$k = 1.3 \times 10^1\ M^{-1}\text{-}s^{-1}$	T = 22 C $E_a = 112.4$ kJ-mol^{-1}	87
$v = k_1[(Co(II)L_5)_2O_2][S(IV)][H^+]^{-1}$	$k_1 = 6.2 \times 10^4\ M^{-1}\text{-}s^{-1}$	T = 25 C $\mu = 0.5\ M$ pH 0.5–1.3	62

$$Fe(II) + O_2 + H^+ \rightleftharpoons Fe(III) + HO_2\cdot \qquad (87)$$

$$E^\circ = -0.9$$

$$\Delta G^\circ = 86.7\ \text{kJ-mol}^{-1}$$

However, from ΔG° it is evident that this is an unfavorable process. Similarly, the other one-electron couples involving the soluble metal ions of Co, Mn, Cu and V are unfavorable for the above free radical initiation step.

Catalysis by Specific Metal-Ligand Complexes

Hoffmann and Boyce [40] have studied kinetics and mechanisms of autoxidation of dissolved sulfur dioxide over the pH range of 4.5–11.0 in the presence of Co(II), Fe(II), Mn(II), Cu(II), Ni(II) and V(IV)-4,4′,4″,4‴-tetrasulfophthalocyanine complexes. Phthalocyanine ligands are macrocyclic tetrapyrrole compounds similar in structure to porphyrins that readily form square planar complexes in which the metal atoms are located in the plane of the phthalocyanine ring. Certain metal-phthalocyanine complexes, such as cobalt tetrasulfophthalocyanine [Co(II)-TSP] are known to actively bind dioxygen and to serve as reversible oxygen carriers [88,89]. Because of their relationship to naturally occurring organic macromole-

cules, coupled with their high stability, catalytic specificity and oxidase-like activity, metal-phthalocyanine complexes have been shown to be suitable models for studying the catalytic effects of trace metals in aqueous systems [90].

The rate law reported by Hoffmann and Boyce [40] for Co(II)-TSP at pH 6.7 was:

$$-\mathrm{d[S(IV)]/dt} = k'[\mathrm{Co(II)\text{-}TSP}]^{1/2}[\mathrm{S(IV)}] \tag{89}$$

and at pH 9.4:

$$-\mathrm{d[S(IV)]/dt} = k''[\mathrm{Co(II)\text{-}TSP}][\mathrm{S(IV)}] \tag{90}$$

where $k' = 1.62\ M^{-1/2}\text{-}s^{-1}$
$k'' = 1.83 \times 10^3\ M^{-1}\text{-}s^{-1}$

Based on additional experimental observations and kinetic data reported by Boyce et al. [91], a two-electron transfer, bisubstrate complexation pathway was postulated. The mechanism, which can be classified as an ordered ternary-complex mechanism in the terminology of Laidler and Bunting [92], is as follows:

$$(\mathrm{Co(II)\text{-}TSP})_2^{4-} \overset{K_d}{\rightleftharpoons} 2\mathrm{Co(II)\text{-}TSP}^{2-} \tag{91}$$

$$\mathrm{Co(II)\text{-}TSP}^{2-} + SO_3^{2-} \underset{k_{-0}}{\overset{k_0}{\rightleftharpoons}} \mathrm{SO_3Co(II)\text{-}TSP}^{4-} \tag{92}$$

$$\mathrm{SO_3Co(II)\text{-}TSP}^{4-} + O_2 \underset{k_{-1}}{\overset{k_1}{\rightleftharpoons}} \mathrm{SO_3Co(III)\text{-}TSPO_2}\cdot^{4-} \tag{93}$$

$$SO_3^{2-} + \mathrm{SO_3Co(III)\text{-}TSPO_2}\cdot^{4-} \underset{k_{-2}}{\overset{k_2}{\rightleftharpoons}} \mathrm{SO_3Co(III)\text{-}TSPO_2}\cdot SO_3^{6-} \tag{94}$$

$$H_2O + \mathrm{SO_3Co(III)\text{-}TSPO_2}\cdot SO_3^{6-} \xrightarrow{k_3} \mathrm{SO_3Co(II)\text{-}TSPO_2^{6-}} + H_2SO_4 \tag{95}$$

$$\mathrm{SO_3Co(II)\text{-}TSPO_2^{6-}} + 2H^+ \xrightarrow{k_4} \mathrm{SO_3Co(II)\text{-}TSP}^{4-} + H_2O_2 \tag{96}$$

$$H_2O_2 + SO_3^{2-} \xrightarrow{k_5} SO_4^{2-} + H_2O \tag{97}$$

This general reaction scheme is depicted graphically in Figure 1.

Equation 92 represents the formation of the reactive monomeric catalytic center, $\mathrm{SO_3Co(II)\text{-}TSP}^{4-}$, from the dominant dimeric form of the catalyst in solution. This sequence of events is consistent with observed spectral changes that

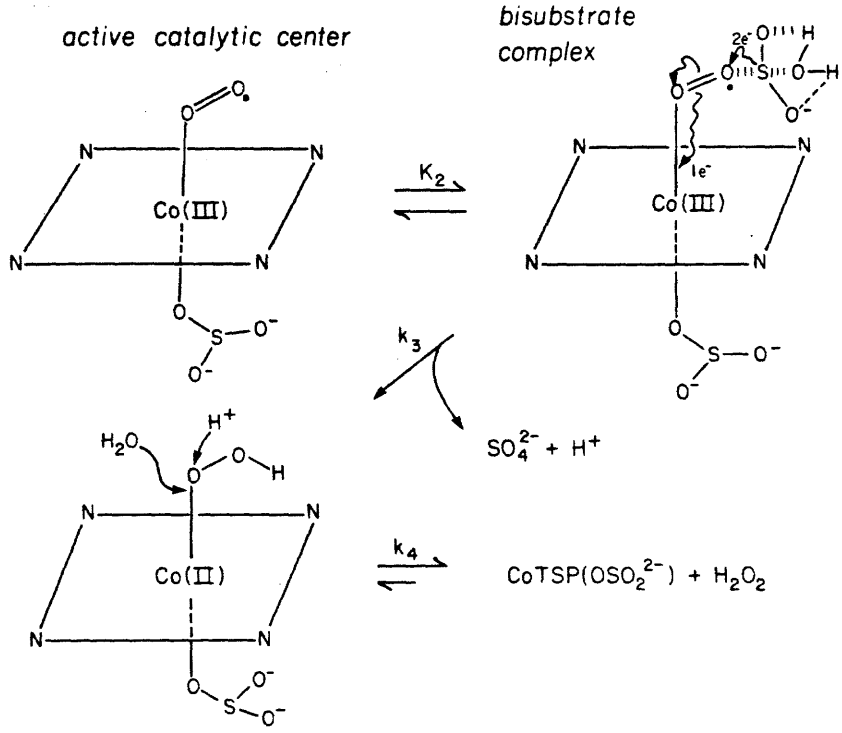

Figure 1. Schematic representation of the proposed catalytic reaction mechanism starting with the Co(II)-TSP sulfito complex as the active catalytic center. Reaction procedes via the formation of a ternary dioxygen adduct and results in the formation of hydrogen peroxide as an intermediate reduction product of oxygen.

indicate a shift in the dimer-monomer equilibrium (Equation 91) on complexation of the added substrate in an axial coordination position on Co(II) either above or below the plane of the phthalocyanine complex. Complexation of Co(II)-TSP by SO_3^{2-} in an axial coordination site enhances the subsequent complexation of dioxygen as written in Equation 93. Carter et al. [93] studied reversible binding of dioxygen by Co(II) complexes of the general form, Co(II)-(L)B, where L is a quadridentate planar ligand and B is an axial ligand, and they concluded that as the π-electron donating ability of B increased the electron density on the cobalt atom would be enhanced; this in turn results in a greater π-bonding electron flow from cobalt to oxygen. Rollman and Chan [94] reported that the imidazole complex of Co(II)-TSP rapidly complexed O_2, whereas the pyridine complex did not. Similar enhancements of the binding of dioxygen by Co(II)-TSP when complexed by an appropriate axial ligand have been reported [90,95,96]. In addition, studies of the catalytic properties of heme have shown that an axial ligand trans to dioxygen affects both the formation constant and the reversibility of oxygen transfer [89,97].

Electron spin resonance (ESR) studies [94,95] on Co(II)-TSP/O_2 complexes have been shown to be consistent with the formulation of the complex as Co(III)-TSPO_2^-. The intermediate complex given in Equation 93 is considered to be a mixed-ligand Co(III) complex with a superoxide ion (O_2^-) and a sulfite ion bound *trans* to one another in axial coordination positions. In the proposed mechanism, the O_2 adduct reacts with an additional SO_3^{2-} ion to form a ternary complex as indicated in Equation 94. This complex, in turn, undergoes a rate-limiting two-electron transfer from the second bound sulfite to the coordinated dioxygen-Co(II) system to form a SO_3 bound to a Co(II)-peroxide complex. The attached SO_3 hydrolyzes rapidly to give a coordinated H_2SO_4, which readily dissociates from the complex. After protonation, the coordinated O_2^{2-} is released as H_2O_2. This intermediate H_2O_2 reacts with another molecule of SO_3^{2-} to form SO_4^{2-} via an additional two-electron transfer in the final step. Hydrogen peroxide was identified positively as a reaction intermediate in this system using three different analytical procedures [98–100].

Schutten and Beelen [98] have observed directly the formation and accumulation of H_2O_2 as an intermediate reduction product of O_2 in Co(II)-TSP–catalyzed autoxidation of 2-mercaptoethanol in water. Davies et al. [62] have reported, on the basis of ^{18}O tracer experiments, that approximately half of the oxygen transferred to sulfite comes from a superoxo- complex, $(NH_3)_5$ Co(III)-O_2^--Co(II)NH_3^{5+}. The other half presumably comes from water. A compatible conclusion as to the origin of oxygen in the oxidized sulfite was reported by Holt et al. [101], who have shown conclusively that the ^{18}O content of the product sulfate for metal-catalyzed autoxidations of SO_3^{2-} was linearly related to the ^{18}O content of water, and that at least three of the four oxygen atoms in the sulfate products were isotopically controlled by the solvent water (the remaining atom of oxygen coming from O_2). Finally, Yatsimirskii et al. [87] found strong evidence for complexation of sulfite by the Co(II)-dioxygen complex, Co_2(L-histidine)O_2, as a prelude to electron transfer from S(IV) to O_2. In total, these results are consistent with the mechanism postulated in Equations 91–97.

The theoretical rate expression, that results from the above mechanism, was obtained by standard procedures [92]; it has the form:

$$\nu = \frac{-d[S(IV)]}{dt} = \frac{k'[SO_3Co(II)\text{-}TSP^{4-}]_T[SO_3^{2-}][O_2]}{K_A + K_B[O_2] + K_C[SO_3^{2-}] + [O_2][SO_3^{2-}]} \qquad (98)$$

where $k' = (k_3k_4)/(k_3 + k_4)$

$K_A = [k_4(k_{-1}k_2 + k_{-1}k_3)]/[k_1k_2(k_3 + k_4)]$

$K_B = [k_4(k_{-2} + k_3)]/[k_2(k_3 + k_4)]$

$K_C = (k_3k_4)/[k_1(k_3 + k_4)]$

When the monomer-dimer equilibrium of Equation 91 is considered, Equation 98 can be rewritten as:

$$\nu = \frac{k'K'[(Co(II)\text{-}TSP)_2^{4-}]^{1/2}[SO_3^{2-}][O_2]}{K_A + K_B[O_2] + K_C[SO_3^{2-}] + [O_2][SO_3^{2-}]} \tag{99}$$

where $K' = \beta K_d^{1/2}[SO_3^{2-}]$ when $[SO_3^{2-}]_o >> [(Co(II)\text{-}TSP)_2^{4-}]_o$

Equation 99 can be simplified for the experimental conditions $[O_2] >> [SO_3^{2-}]$ such that $K_B[O_2] >> K_A, K_C[SO_3^{2-}]$

$$\nu \simeq \frac{k'K'[(Co(II)\text{-}TSP)_2^{4-}]^{1/2}[SO_3^{2-}]}{K_B + [SO_3^{2-}]} \tag{100}$$

Two extremes can be considered for Equation 100. If $K_B >> [SO_3^{2-}]$,

$$\nu \simeq k'\beta K_d^{1/2}[(Co(II)\text{-}TSP)_2^{4-}]^{1/2}[SO_3^{2-}]K_B^{-1} \tag{101}$$

and if $[SO_3^{2-}] >> K_B$,

$$\nu \simeq k'\beta K_d^{1/2}[(CO(II)\text{-}TSP)_2^{4-}]^{1/2}[SO_3^{2-}] \tag{102}$$

The theoretical rate expressions for the limiting cases given in Equations 101 and 102 can be compared with the experimentally observed rate laws for pH 6.7 (Equation 89) and pH 9.4 (Equation 90). At pH 6.7 a half-order dependence on the catalyst concentration is observed, whereas Equation 101 predicts a half-order dependence on the dimeric form of Co(II)-TSP. Since, at pH 6.7, the dimer is the dominant catalyst species in solution, a half-order dependence on total added catalyst is consistent with the assumption that the monomer is actually the active form. Nonintegral reaction orders arise frequently in polar reactions when the principal reactive species is derived from the dissociation of a dimer [102]. At pH 9.4, a first-order dependence on the catalyst concentration is observed. This result is consistent with the kinetic formulation above if the dimeric form of the catalyst is no longer the dominant species. Cookson et al. [95] see evidence for a shift in the monomer-dimer equilibrium toward the monomer with an increase in pH. If this is the situation, the prior equilibrium can be neglected. Consequently, the theoretical rate expression would show a first-order dependence in catalysts as indicated in Equation 98.

Davies et al. [62] and Yatsimirskii et al. [87] have studied the oxidation of S(IV) by the μ-superoxo dimers, $(NH_3)_5Co(III)O_2Co(II)(NH_3)_5^{5+}$ and (L-histidine)$_2$ $Co(III)O_2Co(II)$(L-histidine)$_2$. Two mechanisms are possible for these systems. In these mechanisms the μ-superoxo complex, which can be symbolically written as $(CoL_n)_2O_2$, is the active catalytic center and it reacts either via a two-electron transfer sequence:

$$(CoL_n)_2O_2 + SO_3^{2-} \xrightarrow{\text{slow}} SO_4^{2-} + Co(II)L_n + Co(IV)L_nO \tag{103}$$

$$Co(IV)L_nO + SO_3^{2-} \rightarrow SO_4^{2-} + Co(II)L_n \quad (104)$$

$$Co(II)L_n + O_2 \rightleftharpoons Co(III)L_nO_2^- \quad (105)$$

$$Co(III)L_nO_2^- + Co(II)L_n \rightleftharpoons (CoL_n)_2O_2 \quad (106)$$

or via a one-electron transfer sequence:

$$(CoL_n)_2O_2 + SO_3^{2-} \rightarrow (CoL_n)_2O_2^- + SO_3^- \quad (107)$$

$$(CoL_n)_2O_2^- + SO_3^- \rightarrow CoL_nO_2^{2-} + CoL_n + SO_3 \quad (108)$$

$$SO_3 + H_2O \rightleftharpoons 2H^+ + SO_4^{2-}$$

$$2H^+ + CoL_nO_2^{2-} \rightleftharpoons CoL_n + H_2O_2 \quad (109)$$

Anast and Margerum [103] have reported that copper(III)-tetraglycine reacts rapidly with sulfite in two reversible one electron steps to give copper(II)-tetraglycine and aquated SO_3, which hydrolyzes to sulfate as follows:

$$Cu(III)(H_{-3}G_4)^- + SO_3^{2-} \underset{k_{-1}}{\overset{k_1}{\rightleftharpoons}} Cu(II)(H_{-3}G_4)^{2-} + SO_3^- \quad (110)$$

$$Cu(III)(H_{-3}G_4)^- + SO_3^- \underset{k_{-2}}{\overset{k_2}{\rightleftharpoons}} Cu(II)H_{-3}G_4)^{2-} + SO_3 \quad (111)$$

$$SO_3 + H_2O \rightarrow 2H^+ + SO_4^{2-} \quad (112)$$

In the presence of oxygen, Anast and Margerum [113] have proposed that the sulfite radical anion reacts with oxygen to give the peroxymonosulfite radical, SO_5^-, which in turn oxidizes the Cu(II) back to Cu(III)

$$SO_3^- + O_2 \rightarrow SO_5^- \quad (113)$$

$$Cu(II)(H_{-3}G_4)^{2-} + SO_5^- \rightarrow Cu(III)(H_{-3}G_4)^- + SO_5^{2-} \quad (114)$$

$$H_2O + 2Cu(II)(H_{-3}G_4)^{2-} + SO_5^{2-} \rightarrow 2Cu(III)(H_{-3}G_4)^- + SO_4^{2-} + OH^- \quad (115)$$

This mechanism is an example of an induced catalytic reaction in which the Cu(III)/Cu(II)-tetraglycine couple catalyzes the autoxidation of sulfite to sulfate, which can be described by the simple overall stoichiometry of:

$$2SO_3^{2-} + O_2 \xrightarrow{Cu(III)(H_{-3}G_4)^-} 2SO_4^{2-} \quad (116)$$

Values for k_1, k_2/k_{-1} and k_{-2}/k_3 were reported to be 3.7×10^4 M^{-1}-s^{-1}, 1.66 and 177 M^{-1}, respectively. In this reaction system, the oxidation of SO_3^{2-} by O_2 promotes an induced oxidation of Cu(II) to Cu(III) via an autocatalytic process in which there is a net gain in $Cu(III)(H_{-3}G_4)^-$ when $Cu(II)(H_{-3}G_4)^{2-}$, O_2 and SO_3^{2-} are present initially.

An induced oxidation mechanism of this type represents a conceptual alternative to a free radical chain sequence (Equations 2–8), even though SO_3^- and SO_5^- are postulated as reactive intermediates. Induced reactions occur when a relatively fast reaction between two substances (A + B → P) forces an otherwise slow reaction (A + C → P′) [103]. According to Edwards [104], the phenomenon of induced reactions provides a method for identifying unstable intermediates in reaction mechanisms; in this particular case, the unstable intermediate would be SO_3^-. Although similar to the free radical scheme of Equations 2–8, the above mechanism involves the regeneration of the initiator, Cu(III), whereas the Bäckström scheme does not.

Synergistic Catalysis

Barrie and Georgii [39] and Chapter 2 reported that an apparent synergism exists between Fe^{3+} and Mn^{2+} in the catalytic autoxidation of S(IV). Barrie and Georgii [39] noted that the addition of either Fe^{3+} or Fe^{2+} to an equimolar solution of Mn^{2+} in the presence of S(IV) and oxygen resulted in nonlinear increase in the absorption rate of SO_2. The net effect of adding iron was to increase the reaction rate tenfold. Chapter 2 examines this apparent synergism in greater detail, and finds that the mixed catalyst system exhibited an overall oxidation rate that was greater than the linear sum of the individual metal-catalyzed rates. This effect was quantitatively described in Chapter 2 with the following multiterm rate law obtained by an empirical force-fit of experimental data:

$$\frac{-d[S(IV)]}{dt} = k[Mn^{2+}]^2[H^+]^{-1} + k'[Fe(III)][S(IV)][H^+]^{-1} + k''[Fe(III)][Mn^{2+}][S(IV)][H^+]^{-1}/(K + [Fe(III)]) \quad (117)$$

Existence of a multiple-term rate law indicates that two or more transition states of different composition are involved in parallel in the overall reaction [102,105,106]. Furthermore, each term in the rate law gives the empirical composition and electric charge of the transition state for the rate-determining step for that particular parallel pathway (with the exception of chain mechanisms) [105,106].

With these fundamental rules of kinetics as guidelines, mechanisms for each term in the above rate can be proposed. Neither Chapter 2 nor Barrie and Georgii [39] proposed a hypothetical mechanism for the Fe-Mn synergism; therefore, mechanisms are suggested here for each term.

At the concentration levels used in Chapter 2, catalysis by Mn^{2+} alone exhibits a simple second-order rate law in $[Mn^{2+}]$ with zero-order dependencies on [S(IV)]

and $[O_2]$ as indicated in Equation 117. A mechanism consistent with the above term would be:

prior equilibrium $$Mn^{2+} + H_2O \underset{k_{-1}}{\overset{k_1}{\rightleftharpoons}} MnOH^+ + H^+ \quad (118)$$

rate determining dimerization $$MnOH^+ + Mn^{2+} \underset{k_{-2}}{\overset{k_2}{\rightleftharpoons}} MnOHMn^{3+} \quad (119)$$

$$Mn_2OH^{3+} + HSO_3^- \overset{K_3}{\rightleftharpoons} Mn_2OHSO_3^+ + H^+ \quad (120)$$

$$Mn_2OHSO_3^+ + HSO_3^- \overset{K_4}{\rightleftharpoons} Mn_2OH(SO_3)_2^- + H^+ \quad (121)$$

$$Mn_2OH(SO_3)_2^- + O_2 \overset{K_5}{\rightleftharpoons} Mn_2OH(SO_3)_2O_2^- \quad (122)$$

$$Mn_2OH(SO_3)_2O_2^- \xrightarrow{k_6} Mn_2OH^{3+} + 2SO_4^{2-} \quad (123)$$

where $k_1/k_{-1} = K_H^*$ ($= 10^{-10.24}$ at $\mu = 0.5\ M$ and T = 25 C) [107]
$k_2/k_{-2} = 10^4$ (at $\mu = 0.5\ M$ and T = 25 C) [107]

With the assumption that Equation 119 constitutes the rate-limiting step in the mechanism and that $k_2 > k_{-2}$, the following rate expression can be derived:

$$\nu_1 = \frac{-d[S(IV)]}{dt} = k_2K_1[Mn^{2+}]^2[H^+]^{-1} \quad (124)$$

This rate expression agrees well with the first term of the empirical rate law.

For the second term of the rate law, the following mechanism can be postulated:

rate determining complexation $$Fe(III) + HSO_3^- \underset{k_{-1}}{\overset{k_1}{\rightleftharpoons}} FeSO_3^+ + H^+ \quad (125)$$

rapid electron transfer $$Fe(III)S(IV)O_3^+ \underset{k_{-8}}{\overset{k_8}{\rightleftharpoons}} Fe(II)S(V)O_3^+ \quad (126)$$

$$Fe(II)S(V)O_3^+ + HSO_3^- \overset{K_9}{\rightleftharpoons} Fe(II)(S(V)O_3)(SO_3)^- + H^+ \quad (127)$$

$$Fe(II)(S(V)O_3)(SO_3)^- + O_2 \overset{K_{10}}{\rightleftharpoons} Fe(III)(S(V)O_3)(SO_3)O_2^- \quad (128)$$

$$Fe(III)(S(V)O_3)(SO_3)O_2^- \xrightarrow{k_{11}} Fe(V)(SO_3)O^+ + SO_4^{2-} \quad (129)$$

$$Fe(V)(SO_3)O^+ \xrightarrow{k_{12}} Fe(III) + SO_4^{2-} \quad (130)$$

In this mechanism, the first step, which involves the slow complexation of Fe^{3+} by HSO_3^- is rate determining; consequently, the theoretical rate expression that results is as follows if it is assumed that $[H^+] \simeq K_{a1}$ (i.e., ~ pH 2) and $k_7 >> k_{-7}$:

$$\nu_2 = \frac{-d[S(IV)]}{dt} = \frac{k_7 K_{a1}}{2}[Fe^{3+}][S(IV)][H^+]^{-1} \quad (131)$$

where $[S(IV)] = [HSO_3^-] + [H_2O \cdot SO_2]$

$K_{a1} = [H^+][HSO_3^-]/[SO_2(aq)]$

The overall kinetic coefficient $k_{obs} = k_7 K_{a1}/2$ can be estimated from known kinetic data on ligand substitution [108,109]. Using the water exchange rate constant [110] for Fe^{3+}, $k_{ex} \simeq 10^2\ s^{-1}$ and a calculated ion-pairing constant [111], $K_o \simeq 1\ M^{-1}$ for the Fe^{3+}:HSO_3^- ion pair, a value for k_7 ($\sim 10^2\ M^{-1}$-s^{-1}) can be obtained. At $\mu = 0$, $K_{a1} = 0.0123$. Using these values, the estimated value of k_{obs} is 0.62 s^{-1} at T = 25 C, pH 2 and $\mu = 0$. This value can be compared to the value of 0.82 s^{-1} reported in Chapter 2. However, if k_7 is estimated from the value of the overall second-order rate constant [112] for the complexation of Fe^{3+} by SO_4^{2-} ($k_7 \simeq 1 \times 10^3$), the value of k_{obs} would be predicted to be 6.2 s^{-1} at 25 C, pH 1.8 and $\mu = 0$. These estimates can be made in this fashion because the second-order rate of ligand substitution has been shown to be controlled most often by the water exchange rate of the central metal and to be relatively independent of the nature of the ligand [113].

The third term of the rate law indicates that Fe(III), Mn(II) and S(IV) are brought together in the transition state. One possible mechanism that would result in such a combination involves the formation of a reactive Mn(IV) intermediate from the interaction of the ferryl ion–sulfite complex [114] with Mn^{2+} as follows:

$$2H^+ + Fe(V)(SO_3)O^+ + Mn(II) \overset{K_{13}}{\rightleftharpoons} Fe(III)SO_3^+ + Mn(IV) + H_2O \quad (132)$$

$$H_2O + Mn(IV) + HSO_3^- \xrightarrow{k_{14}} Mn(II) + HSO_4^- + 2H^+ \quad (133)$$

where the rate-limiting step is the two-electron oxidation of Mn(II) by Fe(V). The activation energy for this mechanism should be significantly less than the two previous pathways. This conclusion is consistent with the low apparent activation energy reported by Barrie and Georgii [39] for the synergistic effect of Fe^{3+} on the catalysis by Mn^{2+}.

Alternatively, a one-electron oxidation of Mn^{2+} to Mn^{3+} could be envisioned:

$$Fe(V)SO_3O^+ + Mn^{2+} \overset{K_{15}}{\rightleftharpoons} Fe(IV)SO_3O + Mn^{3+} \quad (134)$$

This would be followed by a chain sequence (Equations 2–8) initiated by Mn^{3+}:

$$Mn^{3+} + HSO_3^- \overset{K_{16}}{\rightleftharpoons} Mn^{2+} + HSO_3; \tag{135}$$

The redox potential of the Mn^{3+}/Mn^{2+} couple ($E° \leq 1.5$ V) is sufficient to promote the one-electron oxidation of S(IV) to S(V)($E° \simeq 0.9$ V) and truly initiate a radical chain sequence. The rate law for this process would be one of the general forms given in Tables II or IV. This latter mechanistic possibility could readily explain the nonlinear concentration effects observed in Chapter 2 and by Barrie and Georgii [39].

Finally, a third possibility, involving the formation of mixed hydroxy-bridged complexes of Fe(III) and Mn(II), can be considered.

$$FeOH^{2+} + Mn^{2+} \overset{K_{17}}{\rightleftharpoons} Fe(OH)Mn^{4+} \tag{136}$$

$$Fe(OH)Mn^{4+} + 2HSO_3^- \rightleftharpoons Fe(OH)Mn(SO_3)_2 + 2H^+ \tag{137}$$

$$Fe(OH)Mn(SO_3)_2 + O_2 \rightleftharpoons Fe(OH)Mn(SO_3)_2O_2 \tag{138}$$

$$Fe(OH)Mn(SO_3)_2O_2 \rightarrow Fe(OH)Mn^{4+} + 2SO_4^{2-} \tag{139}$$

The rate expression obtained from this mechanism would have the following form if complexation of HSO_3^- by the hydroxy-bridged species is assumed to be rate limiting:

$$\nu = k'[Fe(III)][Mn(II)][S(IV)][H^+]^{-2} \tag{140}$$

Similar expressions involving the concentrations of Fe(III), Mn(II) and S(IV) are obtained for the other mechanisms given above. The rate expression of Equation 140 is not exactly of the form shown in Equation 117, but it does reflect some of the essential features.

Photoassisted Catalysis

Homogeneous Processes

The catalytic effect of light [50,62,115–125] on autoxidation of dissolved SO_2 has been acknowledged for years as an alternative mode of initiation of the chain reaction sequence given in Equations 2–8. UV irradiation of sulfite/bisulfite systems is thought to produce an aquated electron [62,121] and a sulfite radical ion:

$$SO_3^{2-} \xrightarrow{h\nu} SO_3^- + \bar{e}_{aq}$$

A transient electronic absorption maximum at $\lambda = 700$ nm has been assigned to the solvated electron and a similar transient maximum at $\lambda = 260$ nm has been assigned to the SO_3^- radical ion. The aquated electron decays by reaction with O_2 or HSO_3^- to produce a superoxide ion or sulfite ion and a hydrogen atom, respectively. However, only Lunak and co-workers [126–128] have systematically explored the possibility of metal-catalyzed photooxidation of sulfite, even though the phenomenon of homogeneous metal-assisted photooxidation/reduction processes has been reported previously for Fe(III) and Cu(II)-ligand systems [128–135].

The preliminary work of Lunak and Veprek-Siska [126] has shown a distinct photoassisted catalysis by Fe(III) at wavelengths higher than the cutoff for absorption by sulfite and bisulfite ion in aqueous solution. Quantum yields were shown to depend on the wavelength of irradiation and the concentration of Fe(III) in the system. They have proposed that a quantum of light is absorbed by a ferric-sulfito complex, thereby initiating the catalytic cycle through photoreduction of Fe(III) to Fe(II). In the absence of added Fe(III), the photochemical autoxidation of sulfite above $\lambda = 300$ nm did not proceed to a noticeable extent. A mechanism consistent with their findings would be:

$$Fe(OH)_n^{(3-n)+} + HSO_3^- \rightleftharpoons Fe(OH)_nSO_3^{(1-n)+} + H^+ \quad (141)$$

$$Fe(OH)_nSO_3^{(1-n)+} + HSO_3^- \rightleftharpoons Fe(OH)_n(SO_3)_2^{(n+1)-} + H^+ \quad (142)$$

$$Fe(III)(OH)_n(SO_3)_2^{(n+1)-} \xrightarrow{h\nu} {}^*Fe(II)(OH)_n(SO_3)(SO_3\cdot)^{(n+1)-} \quad (143)$$

$${}^*Fe(II)(OH)_n(SO_3)(SO_3\cdot)^{(n+1)-} \rightleftharpoons Fe(II)(OH)_nSO_3^{n-} + SO_3^- \quad (144)$$

or

$$Fe(III)(OH)_n(SO_3)_2^{(n+1)-} + O_2 \rightleftharpoons Fe(III)(OH)_n(SO_3)_2O_2^{(n+1)-} \quad (145)$$

$$Fe(III)(OH)_n(SO_3)_2O_2^{(n+1)-} \xrightarrow{h\nu} {}^*Fe(III)(OH)_n(SO_4)_2^{(n+1)-} \quad (146)$$

$$2H^+ + {}^*Fe(III)(OH)_n(SO_4)_2^{(n+1)-} \rightleftharpoons Fe(III)(OH)_n^{(3-n)+} + 2HSO_4^- \quad (147)$$

After photoinitiation, autoxidation would proceed via a free radical chain after Equation 86 or by inner-sphere electron transfer as shown in Equations 145–147.

Lunak and Veprek-Siska [127] also report that photoinitiated autoxidation of sulfite is influenced by the presence of Mn(II) at trace levels (10^{-8}–10^{-10} M) and that Cu(II) [125] does not exhibit a photocatalytic effect. On the other hand, Hoffmann and Boyce [40] have reported that cobalt(II)tetrasulfophthalocyanine catalyzed autoxidation of S(IV) is strongly influenced by visible light in the range

of 300–400 nm. They have interpreted their results in terms of formation of singlet oxygen due to a ligand-to-metal charge transfer absorption.

Heterogeneous Processes

A primary source of iron, manganese, zinc, titanium and other metals found in aerosol systems is from combustion of coal. These metals will be released to the atmosphere in their highest oxidation states in the form of metal oxides such as Fe_2O_3, MnO_2, ZnO and TiO_2. Taylor and Flagan [135] and Ouimette and Flagan [136] found direct evidence for significant mass fractions of Fe_2O_3 in submicrometer particle size fractions of fly ash from a coal-fired combustor and from ambient aerosol.

Barrie and Georgii [39] have used average values of Mn and Fe in urban aerosols of 0.2 and 1 $\mu g/m^3$, respectively, and an average liquid water content of 0.1 g/m^3 to estimate that the soluble concentration in the aqueous phase is on the order of 10 μM. In making these estimates they assumed that 25% of the total Mn was soluble and 10% of the total iron was soluble. The remaining solid phases are likely to exhibit some catalytic activity [137–141].

Frank and Bard [45] reported that Fe_2O_3 (hematite) surfaces catalyze photoassisted autoxidation of HSO_3^- to HSO_4^-. Irradiation at 400 nm of an oxygenated bisulfite solution with suspended Fe_2O_3 particles resulted in a rapid conversion of S(IV) and S(VI), whereas in the absence of light no conversion of sulfite to sulfate was observed. A sequence of stoichiometric reactions that offers one possible explanation for photoassisted catalysis on a metal oxide (semiconductor) surface is:

$$Fe_2O_3 + 2h\nu \xrightarrow{\text{surface}} (Fe_2O_3) + 2p^+ + 2e^- \tag{148}$$

$$H_2O + HSO_3^- + 2p^+ \xrightarrow{\text{surface}} HSO_4^- + 2H^+ \tag{149}$$

$$O_2 + 2e^- + 2H^+ \xrightarrow{\text{surface}} H_2O_2 \tag{150}$$

$$H_2O_2 + HSO_3^- \xrightarrow{\text{solution}} HSO_4^- + H_2O \tag{151}$$

where p^+ = charge vacancy created by the photoassisted excitation of an electron from the valence band of the metal oxide to the conduction band

Excited electrons in the conduction band and positive holes in the valence band migrate to the surface (presumably without recombination), where they react, respectively, with oxygen and bisulfite to produce hydrogen peroxide as the reduced product and bisulfate as the oxidized product.

Similar, but less effective, photocatalytic effects have been reported by Frank and Bard [45] for other semiconductor materials such as TiO_2, CdS and ZnO.

However, results for CdS and ZnO are obscured by the fact that at low pH (pH ~3) these solids dissolve to a certain extent; thus, any apparent photocatalytic effects may be due to dissolved metal species rather than due to inherent properties of the semiconductor material.

Faust and Hoffmann [142] studied photocatalytic autoxidation of HSO_3^- on synthetic Fe_2O_3 suspensions at pH 2.5; they report that the presence of Fe_2O_3 particles results in a slight rate enhancement as compared to the corresponding homogeneous photocatalytic system.

Childs [143] and Childs and Ollis [144] have addressed some of the fundamental considerations that are required to ascertain whether a heterogeneous photoreaction is truly photocatalytic according to Equations 148–151 or stoichiometrically photochemical. In a stoichiometric photochemical reaction, the observed conversion of sulfite to sulfate in irradiated systems may result from (1) direct photoactivation of an adsorbed sulfite on the surface; (2) a surface-prompted reaction of sulfite photoactivated in solution; (3) a noncatalytic reaction of the Fe_2O_3 surface with the adsorbed sulfite; or (4) homogeneous catalysis by Fe(III)/Fe(II) leached from the Fe_2O_3 surface. These questions remain to be resolved in the case of iron-catalyzed systems.

It is apparent [37,58,65,83,86] that the rate of autoxidation of S(IV) is most rapid in the concentration–pH domain where metal hydroxides are the dominant species such as $Ni(OH)_2$, $Co(OH)_3$, Co_3O_4, FeOOH, $Fe(OH)_3$ and $Cu(OH)_2$. For example, Brimblecombe and Spedding [37] have proposed that the oxyhydroxides FeOOH (α-FeOOH, β-FeOOH, γ-FeOOH) would be effective initiators for the production of SO_3^- (since $E°(FeOOH) = 0.91$ V) as follows:

$$H^+ + FeOOH_{(s)} + SO_3^{2-} \rightarrow Fe(OH)_{2(s)} + SO_3^- \qquad (152)$$

$$Fe(OH)_{2(s)} + SO_5^- \rightarrow FeOOH_{(s)} + SO_5^{2-} + H^+ \qquad (153)$$

Soot particles have been shown to be effective catalytic surfaces for autoxidation of S(IV) by Brodzinsky et al. [138], Chang et al. [139] and Benner et al. [145] although Cohen et al. [140] reported that the apparent catalysis by ambient fly ash particles was due to Fe(III) leached into aqueous solution. Furthermore, soot and powdered activated carbon surfaces provide moderately effective sites for adsorption of trace metals and these adsorbed metals may in turn be the active catalytic centers.

Ambient soot contains a significant level of polynuclear aromatic hydrocarbons (PAH). Certain PAH have been shown to be photosensitizers for the production of singlet oxygen, which will in turn react electrophilically with an oxidizable substrate rather than through a free radical pathway [146]. A sensitizer, such as PAH, is a molecule that can absorb a quantum of light and then transfer this energy to a second substrate. For example, benzophenone is an efficient producer of $^1O_2$ ($^1\Delta g$) [141]:

$$^1(C_6H_5)_2C=O \xrightarrow[366\text{ nm}]{h\nu} {}^1(C_6H_5)_2C=O^* \qquad (154)$$

$$^1(C_6H_5)_2C=O^* \longrightarrow {}^3(C_6H_5)_2C=O^* \tag{155}$$

$$^3(C_6H_5)_2C=O^* + {}^3O_2 \longrightarrow {}^1(C_6H_5)_2C=O + {}^1O_2 \tag{156}$$

$$Mn(SO_3)_2^{2-} + {}^1O_2 \longrightarrow Mn^{2+} + 2SO_4^{2-} \tag{157}$$

which in turn could oxidize S(IV) to S(VI) by a sequence of two-electron transfers. Energy transfer from an excited triplet state sensitizer to $^3O_2$ (Equation 156) to give $^1O_2$ is a spin-allowed process [146].

Fridovich and Handler [148] have shown that photosensitized dye molecules such as methylene blue and flavin mononucleotide are effective catalysts for autoxidation of S(IV); however, their early work was interpreted in terms of a free radical sequence rather than through production of $^1O_2$ as follows:

$$\text{dye} \xrightarrow{h\nu} \text{dye}^* \tag{158}$$

$$\text{dye}^* + HSO_3^- \longrightarrow \text{dyeH} + SO_3^- \tag{159}$$

$$\text{dyeH} + O_2 \longrightarrow \text{dye} + HO_2\cdot \tag{160}$$

Later work by McCord and Fridovich [149] showed that the autoxidation of S(IV) as catalyzed by dimethyl sulfoxide was inhibited by superoxide dismustase. This result indicates that $HO_2\cdot$ was a likely intermediate. However, in metal-catalyzed reactions, superoxide dismutase had no effect. In light of more recent work [150], the reaction observed by Fridovich and Handler [148] most likely involved the production of $^1O_2$. Srinivasan et al. [150] have shown that irradiated solutions of the dye rose bengal produce both O_2^- and $^1O_2$, which are quickly consumed by SO_3^{2-} at pH 7.8. They have estimated that 77% of the active oxygen generated is $^1O_2$ and 23% O_2^-.

Additional work by Srinivasan et al. [150] has shown that irradiated solutions of Ru(2,2′bipyridyl)$^{2+}$ produce O_2^-, which leads to rapid oxidation of S(IV)

$$Ru(bipy)^{2+} \xrightarrow{h\nu} {}^*Ru(bipy)^{2+} \tag{161}$$

$$^*Ru(bipy)^{2+} + O_2 \longrightarrow Ru(bipy)^{3+} + O_2^- \tag{162}$$

$$O_2^- + H^+ \rightleftharpoons HO_2 \tag{163}$$

$$HO_2\cdot + HSO_3^- \rightleftharpoons SO_3^- + H_2O_2 \tag{164}$$

Much work remains to be done on photocatalytic systems in aqueous systems to ascertain the role of condensed-phase photochemistry on total S(IV) conversion rates. If photoassisted pathways are shown to be important under ambient condi-

tions, differences between nighttime and daytime conversion rates may have a plausible explanation.

Oxidation by Hydrogen Peroxide, Ozone and Nitrous Acid: Catalytic Influences

As indicated in Chapters 2 and 4, hydrogen peroxide appears to be a potentially important oxidant in atmospheric droplets because of its favorable Henry's law constant ($K_H = 1 \times 10^5$ M-atm^{-1}), its rapid oxidation of S(IV), and its relative insensitivity to pH changes in an open two-phase system. Hydrogen peroxide is generated in the gas phase by the recombination of hydroperoxyl radicals, in the aqueous phase as an intermediate in metal-catalyzed autoxidations, and at air-water interfaces due to photoinduced redox processes [151]. Measurements by Kok and co-workers [152–155] indicate that steady-state aqueous-phase concentrations can be as high as 50 μM.

The kinetics of oxidation of S(IV) by H_2O_2 have been studied [31–33,41]. Mader [41] determined that over the pH range of 8–13 the rate of oxidation of S(IV) was characterized by a multiterm rate expression as shown in Table X. The first term accounts for uncatalyzed oxidation, the second term for general acid catalysis, and the third nominally for specific acid and other forms of unspeci-

Table X. Empirical Rate Laws for the Oxidation of S(IV) by Hydrogen Peroxide

Rate ($v = -d[S(IV)]/dt$)	*Rate Constant*	*Conditions*	*Reference*
$v = k_o[H_2O_2][SO_3^{2-}]$ $+ k_p[H^+][H_2PO_4^-][H_2O_2][SO_3^{2-}]$ $+ r_c$	$k_o = 0.2\ M^{-1}\text{-s}^{-1}$ $k_p = 1.7 \times 10^{10}\ M^{-3}\text{-s}^{-1}$ $E_a(k_o) = 63.5$ kJ-mol^{-1}	T = 25 C $\mu = 1.0\ M$ pH 7.9–12.8	41
$v = k[H^+][H_2O_2][S(IV)]$ $\{[H^+]/([H^+] + K_{a2})\}$ $+ k'[H_2PO_4^-][H_2O_2][S(IV)]$ $\{[H^+]/([H^+] + K_{a2})\}$	$k = 2.7 \times 10^8\ M^{-2}\text{-s}^{-1}$ $k' = 1.3 \times 10^3\ M^{-2}\text{-s}^{-1}$	T = 12 C $\mu = 1.0\ M$ pH 4–8	31
$v = k[H_2O_2][HSO_3^-][H^+]^{0.7}$ $+ k_a[H_2O_2][HSO_3^-][CH_3CO_2H]$ $k_1 = k[H_2O_2][H^+]^{0.7} + k_a[H_2O_2][HA]$	$k = 2.46 \times 10^6\ M^{-1}\text{-s}^{-1}$ (pH 4.6) $k_a = 1.9 \times 10^4\ M^{-2}\text{-s}^{-1}$ $E_a(k_1) = 24.9$ kJ-mol^{-1} (pH 4.6)	T = 20 C $\mu = 0.2\ M$ pH 4–8	32
$v = \dfrac{k[H_2O_2][HSO_3^-][H^+]}{K + [H^+]}$	$k = 5.6 \times 10^6\ M^{-1}\text{-s}^{-1}$ $K = 0.1\ M$	T = 25 C pH 0–3 μ (variable)	33
$v = \dfrac{k[H_2O_2][H_2O \cdot SO_2]}{K + [H^+]}$	$k = 8.3 \times 10^4\ M^{-1}\text{-s}^{-1}$ $K = 0.1\ M$ $E_a = 28$ kJ-mol^{-1}	T = 25 C pH 0–3 μ (variable)	33

fied catalysis. In addition to phosphate buffer catalysis, Mader observed carbonate and arsenate were effective as general acid catalysts. Mader offered no mechanistic interpretation of his kinetic results.

Earlier, Halperin and Taube [42] had suggested that the oxidation proceeded through the formation of a peroxymonosulfurous acid intermediate, which was followed by an intramolecular rearrangement to give sulfate and water. Their conclusions were based on double-isotope labeling experiments that showed that both of the labeled oxygens of $H^{18}O^{18}OH$ were incorporated to the product sulfate, even though the stoichiometry of the reaction requires the net addition of one oxygen atom.

$$H_2O_2 + H_2O \cdot SO_2 \rightarrow 2H^+ + SO_4^{2-} + H_2O \tag{165}$$

$$H^{18}O^{18}OH + H_2O \cdot SO_2 \rightarrow HO_2S^{18}O^{18}OH + H_2O \tag{166}$$

$$HO_2S^{18}O^{18}OH \rightarrow 2H^+ + SO_2^{18}O_2^{2-} \tag{167}$$

In a subsequent kinetic study of this reaction, Hoffmann and Edwards [31] found definitive evidence for both general acid and specific acid catalysis. They reported the following two-term rate law for the pH range of 4–8:

$$\frac{-d[S(IV)]}{dt} = k[H^+][H_2O_2][S(IV)]\{[H^+]/([H^+] + K_{a2})\} + k'[HA][H_2O_2][S(IV)]\{[H^+]/([H^+] + K_{a2})\} \tag{168}$$

where K_{a2} = second acid dissociation constant
[S(IV)] = sum of the concentration of sulfite and bisulfite within the pH range of 4–8
HA = weak acids used over this pH range as buffers

The first term of the rate law reflects the contribution of specific acid catalysis and the second term reflects the contribution of general acid catalysis to the overall rate.

Two alternative mechanisms that are consistent with the observed rate law and the isotopic labeling results of Halperin and Taube [42] are:

$$H^+ + SO_3^{2-} \underset{}{\overset{K_{a2}^{-1}}{\rightleftharpoons}} HSO_3^- \tag{169}$$

$$HSO_3^- + H_2O_2 \overset{K}{\rightleftharpoons} \begin{matrix} O^- \\ \diagdown \\ S - OOH \\ \diagup \\ O \end{matrix} + H_2O \tag{170}$$

$$\begin{matrix} O^- \\ \diagdown \\ \text{S-OOH} \\ \diagup \\ O \end{matrix} + HA \xrightarrow{k} H_2SO_4 + A^- \qquad (171)$$

where $HA = H_3O^+$ or a suitable weak acid such as phosphate, citrate, pivalate, acetate or phthalate

According to this mechanism, the reaction occurs via a nucleophilic displacement by H_2O_2 on sulfur of HSO_3^- to form a peroxymonosulfurous acid intermediate (Equation 170), which then undergoes a rate-determining rearrangement to HSO_4^- assisted by H_3O^+ or HA. Alternatively, a mechanism in which there would be an equilibrium protonation of the bisulfite followed by a proton transfer to A^- can be written as:

$$H^+ + SO_3^{2-} \overset{K_{a2}^{-1}}{\rightleftharpoons} HSO_3^- \qquad (172)$$

$$HSO_3^- + HA \overset{K'}{\rightleftharpoons} H_2O \cdot SO_2 + A^- \qquad (173)$$

$$A^- + H_2O_2 + H_2O \cdot SO_2 \xrightarrow[\text{slow}]{k_1} \begin{matrix} O^- \\ \diagdown \\ \text{S-OOH} \\ \diagup \\ O \end{matrix} + HA + H_2O \qquad (174)$$

$$\begin{matrix} O^- \\ \diagdown \\ \text{S-OOH} \\ \diagup \\ O \end{matrix} \xrightarrow[\text{rapid}]{k_2} HSO_4^- \qquad (175)$$

In this sequence, Equation 174, a termolecular step, in which A^-, H_2O_2 and $H_2O \cdot SO_2$ react to form peroxymonosulfurous acid, is rate-determining. In the first alternative mechanism (Equations 169–171), HSO_3^- is the reactive species of S(IV), and in the second mechanism (Equations 172–175) $H_2O \cdot SO_2$ is predicted to be the reactive species. The work of Martin and Damschen [33] appears to verify that HSO_3^- is in fact the reactive S(IV) species and that the mechanism of Equations 169–171 is valid over a broad range of pH (i.e., 0–8).

Penkett et al. [32] studied peroxide oxidation kinetics over the pH range 4.3–8.2 using acetate, citrate, phosphate and Tris buffers to maintain pH. They confirmed the role of these weak acids as general acid catalysts. However, Penkett et al. report a hydrogen ion dependence of $[H^+]^{0.7}$ over the pH range of 4–6 as noted in Table X. On the other hand, Martin and Damschen [33] report a first-order dependence on H^+ over the pH range of 1–3 and a reciprocal dependence below pH 1. This switch in pH dependence supports the notion that HSO_3^- is the reactive form of S(IV) in solution.

For the pH range of 1–5, Martin and Damschen [33] expressed the rate

law in a form that is convenient for application to open atmospheric systems as follows:

$$\frac{-d[S(IV)]}{dt} = 8.3 \times 10^5 [H_2O_2][H_2O \cdot SO_2] \tag{176}$$

or

$$\frac{-d[S(IV)]}{dt} = 8.3 \times 10^5 P_{H_2O_2} K_{H,H_2O_2} P_{SO_2} K_{H,SO_2} \tag{177}$$

The concentrations of H_2O_2 and $H_2O \cdot SO_2$ are expressed in terms of the products of their respective Henry's law constants and partial pressures. They also report that the oxidation reaction is apparently insensitive to the effects of metal catalysis (Fe^{3+} and Mn^{2+}) and organic inhibitors (hydroquinone, toluene, pinene and hexene).

However, in the case of H_2O_2, Fe^{2+} and Cu^{2+} would be the most likely metal ions to exert a catalytic effect on the reaction rate since these metals are well known initiators of the Fenton's reagent reaction [156–158]:

$$Fe^{2+} + H_2O_2 \rightarrow FeOH^{2+} + HO\cdot \tag{178}$$

$$Cu^{2+} + H_2O_2 \rightarrow CuOH^{2+} + HO\cdot \tag{179}$$

$$H^+ + HO\cdot + HSO_3^- \rightarrow HSO_3\cdot + H_2O \tag{180}$$

If oxygen were present in the reaction system a free radical pathway could be initiated by Equation 180 and proceed via Equations 3–8 or 18–23. Additional propagation steps can be envisioned to occur as follows:

$$HO\cdot + H_2O_2 \rightarrow HO_2\cdot + H_2O \tag{181}$$

$$HO_2\cdot + HSO_3^- \rightarrow HSO_4^- + HO\cdot \tag{182}$$

Future work on the H_2O_2–S(IV) reaction system should address the possibility of catalysis by Fe(II) and Cu(II).

There are few reports of catalytic influences on the oxidation of S(IV) by ozone. Barrie [159] has found that Mn^{2+} promotes the oxidation of S(IV) by ozone in aqueous droplets. In the absence of Mn^{2+}, gas-phase ozone alone failed to enhance SO_2 absorption rates in the aqueous phase. Chapter 2, in the section on ozone oxidation kinetics, reports no apparent catalysis due to Fe^{3+}, Mn^{2+}, VO^{2+} or Cu^{2+}; however, Harrison et al. [43] reported that additions of Mn^{2+} and Fe^{3+} at concentrations of 10 μM resulted in enhancements in the observed oxidation rates by factors of approximately 2 and 6, respectively. Addition of competitive complexing agents (phosphate or citrate) inhibits the apparent catalytic process. A maximum in cata-

lytic influence occurred at pH 4.5. This behavior suggests that ferric-sulfito and manganous-sulfito complexes play a role in the oxidation process.

$$O_3 + HSO_3^- \xrightarrow[Mn^{2+}]{Fe^{3+}} HSO_4^- + O_2 \tag{183}$$

Furthermore, Harrison et al. [43] indicate that the rate of oxidation increases linearly with an increase in Fe^{3+}. These results are summarized in Table XI.

Penkett [160] has proposed the following initiation of a radical mechanism to account for oxidation by ozone:

$$2O_3 + OH^- \rightarrow HO\cdot + O_2^- + 2O_2 \tag{184}$$

$$HO\cdot + HSO_3^- \rightarrow HSO_3\cdot + OH^- \tag{185}$$

The bisulfite radical of Equation 185 would proceed to react according to Equations 3–8, thereby completing the free radical sequence of the Bäckström mechanism.

Based on isotopic tracer experiments, Espenson and Taube [162] concluded that in acidic solution the reaction between ozone and sulfur dioxide could occur via a simple bimolecular process in which two atoms of oxygen are transferred from ozone to sulfur dioxide or via a radical reaction involving reactive intermediates or via both pathways in parallel. In basic solution, they concluded that the free radical pathway was more likely even though more than one oxygen atom was transferred from ozone to sulfite.

Table XI. Empirical Rate Laws for the Oxidation of S(IV) by Ozone

Rate ($\nu = -d[S(IV)]/dt$)	*Rate Constant*	*Conditions*	*Reference*
$\nu = k[O_3][HSO_3^-][H^+]^{-0.5}$	$k = 1.45 \pm 0.7 \times 10^4\ M^{-0.5}\text{-s}^{-1}$	pH 1–5 T = 25 C	32
$\nu = kP_{O_3}K_{H,O_3}[HSO_3^-][H^+]^{-0.1}$	$k = 4.4 \times 10^4\ M^{-0.9}\text{-s}^{-1}$ $K_{H,O_3} = 1.23\ M\text{-atm}^{-1}$	pH 4–7 T = 25 C	29
$\nu = k[O_3][S(IV)][H^+]^{-0.5}$	$k = 1.9 \times 10^4\ M^{-0.5}\text{-s}^{-1}$	pH 0–3 T = 25 C	Chapter 2
$\nu = k_1[HSO_3^-][O_3] + k_2[SO_3^{2-}][O_3]$	$k_1 = 3.1 \times 10^5\ M^{-1}\text{-s}^{-1}$ $k_2 = 2.2 \times 10^9\ M^{-1}\text{-s}^{-1}$ $E_{a,1} = 46\ \text{kJ-mol}^{-1}$ $E_{a,2} = 43.9\ \text{kJ-mol}^{-1}$	pH 0–4 T = 25 C	160
$\nu = k[Fe^{3+}][S(IV)][O_3][H^+]^n$	$k_{obs} = 6.8 \times 10^5\ M^{-1}\text{-min}^{-1}\text{-ppm}^{-1}$	T = 295 K pH 4–6 $[Fe^{3+}] \geq 10\ \mu M$	42

If a polar pathway were to occur as suggested by Espenson and Taube [162], a likely mechanism would be as follows:

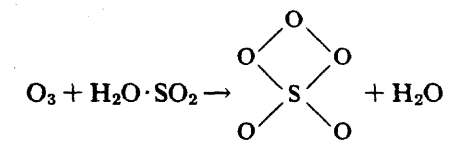

(186)

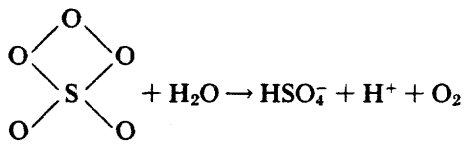

(187)

Catalysis by Fe^{3+} and Mn^{2+} may proceed through an initial metal sulfite complex followed by attachment of ozone to form a ternary complex.

$$Fe^{3+} + H_2O \overset{K_1}{\rightleftharpoons} FeOH^{2+} + H^+ \tag{188}$$

$$FeOH^{2+} + HSO_3^- \overset{K_2}{\rightleftharpoons} Fe(OH)SO_3^\circ + H^+ \tag{189}$$

$$Fe(OH)SO_3^\circ + O_3 \overset{K_3}{\rightleftharpoons} Fe(OH)SO_3O_3^\circ \tag{190}$$

$$Fe(OH)SO_3O_3^\circ \xrightarrow{k} FeOH^{2+} + SO_4^{2-} + O_2 \tag{191}$$

Finally, S(IV) in aqueous systems can be oxidized readily by N(III) and N(IV) species in the form of nitrite, nitrous acid and aquated nitrogen dioxide.

Nitrous acid will oxidize S(IV) in acidic solution according to the following stoichiometries:

$$2HNO_2 + H_2O \cdot SO_2 \rightarrow SO_4^{2-} + 2NO + 2H^+ + H_2O \qquad \Delta G^\circ = -160 \text{ kJ-mol}^{-1} \tag{192}$$

$$2HNO_2 + 2H_2O \cdot SO_2 \rightarrow 2SO_4^{2-} + N_2O + H_2O + 4H^+ \qquad \Delta G^\circ = -431 \text{ kJ-mol}^{-1} \tag{193}$$

Martin et al. [163] determined that the reaction was first-order in N(III), S(IV) and H^+, and insensitive to catalysis by Fe^{3+}, Mn^{2+} and VO^{2+} in the absence of O_2.

$$\frac{-d[S(IV)]}{dt} = k[HNO_2]_T[S(IV)][H^+] \quad (193)$$

where $[HNO_2]_T = [HNO_2] + [NO_2^-]$
$k = 142\ M^{-2}\text{-}s^{-1}$

They found that N_2O was the principal product at low pH.

Oblath et al. [164] found at higher pH (pH 5–7) that hydroxylamine disulfonate formed according to the following stoichiometry:

$$NO_2^- + 2HSO_3^- \rightarrow HON(SO_3)_2^{2-} + OH^- \quad (194)$$

Ross et al. [165] observed that a significant fraction of HNO_2 is converted to NO according to Equation 192 at higher acidities. They found that, in the presence of O_2, an apparent catalytic cycle involving NO is established. The stoichiometric equations for this sequence are as follows:

$$4NO(aq) + O_2 + 2H_2O \rightarrow 4HNO_2 \quad (195)$$

$$2HNO_2 + H_2O \cdot SO_2 \rightarrow 2NO(aq) + H^+ + HSO_4^- + H_2O \quad (196)$$

Latimer [85] suggested the following mechanism for the reduction of nitrous acid by S(IV):

$$HONO + HSO_3^- \longrightarrow HSO_3NO + OH^- \quad (197)$$

$$H_2O + HSO_3NO \rightarrow NOH + HSO_4^- + H^+ \quad (198)$$

$$2NOH \rightarrow N_2O + H_2O \quad (199)$$

$$NOH + HONO \rightarrow 2NO + H_2O \quad (200)$$

$$HSO_3NO + HSO_3^- \rightarrow HON(SO_3)_2^{2-} + H^+ \quad (201)$$

Oblath et al. [164] suggest the following mechanism:

$$HONO + HSO_3^- \rightleftharpoons NOSO_3^- + H_2O \quad (202)$$

$$NOSO_3^- + HSO_3^- \rightleftharpoons HON(SO_3)_2^{2-} \quad (203)$$

$$NO_2^- + S_2O_5^{2-} \rightleftharpoons ON(SO_3)_2^{3-} \quad (204)$$

$$H^+ + HONO \rightleftharpoons NO^+ + H_2O \quad (205)$$

$$NO^+ + HSO_3^- \rightleftharpoons NOSO_3^- + H^+ \tag{206}$$

which involves the formation of a nitrosonium ion, a fairly stable ionic species.

In acid solution, aquated nitrogen dioxide ($N(IV)O_2(aq)$) readily dimerizes to form nitrogen tetroxide, as reported in Chapter 4 and by Grätzel et al. [166]:

$$2NO_2(aq) \rightleftharpoons N_2O_4(aq) \qquad K_d = 7 \times 10^4\ M^{-1} \tag{207}$$

Nitrogen tetroxide, in turn, is a moderately strong oxidizing agent [84] with E° values of +1.07 and +1.03 V, respectively, for the following reactions:

$$N_2O_4 + 2H^+ + 2e^- \rightleftharpoons 2HNO_2 \tag{208}$$

$$N_2O_4 + 4H^+ + 4e^- \rightleftharpoons 2H_2O + 2NO \tag{209}$$

Takeuchi et al. [167] reported that the reaction of S(IV) with $NO_2(aq)$ proceeds rapidly according to the following stoichiometries and rate laws:

$$2OH^- + 2NO_2(aq) + SO_3^{2-} \rightarrow H_2O + 2NO_2^- + SO_4^{2-} \tag{210}$$

$$\frac{-d[S(IV)]}{dt} = k_1[NO_2(aq)][SO_3^{2-}] \tag{211}$$

$$H_2O + 2NO_2 + HSO_3^- \xrightarrow{Fe(II)} 2H^+ + HSO_4^- + 2NO_2^- \tag{212}$$

$$\frac{-d[S(IV)]}{dt} = k_2[NO_2(aq)][HSO_3^-] \tag{213}$$

where $t = 25°\ C$

$k_1 = 6.6 \times 10^5\ M^{-1}\text{-}s^{-1}$

$k_2 = 1.5 \times 10^4\ M^{-1}\text{-}s^{-1}$

Nash [168] described the role of Fe(II) catalysis in the above reactions in the nanomolar range.

As pointed out in Chapter 4, translation of the above rate laws for closed systems to open atmospheric systems requires that the concentrations of the important gases be expressed in terms of the product of the appropriate Henry's law constant times the observed partial pressures. In the case of HNO_2 and NO_2, their respective Henry's law constants are 49 and 0.01 M-atm^{-1}. These moderate values of K_H indicate that the partial pressures of each gas-phase species will determine to a large extent the contribution of the above pathways to the overall rate of S(IV) oxidation.

EQUILIBRIUM SPECIATION MODELS

To use the preceding kinetic information reliably in dynamic models of SO_2 transformation in the atmosphere, detailed chemical speciation in aqueous solution for reductant, oxidant and catalysts must be determined. Using data collected on the concentrations of chemical constituents in fog, cloud and rain water, equilibrium speciation models can be developed readily with the aid of the computer programs REDEQL2 and SURFEQL. Both REDEQL2 and SURFEQL are general-purpose programs for computation of multiple, simultaneous chemical equilibria involving acid-base, oxidation-reduction, precipitation-dissolution, complexation-dissociation and adsorption-desorption reactions [169–172]. As an example of the applicability of equilibrium models, we will consider the potential role of iron-sulfito complexes and sulfonic acid derivatives in increasing the apparent capacity of an aqueous droplet system for S(IV); the levels observed in fog and cloud water reported in Table I appear to be above those predicted by the observed partial pressures of SO_2.

Total S(IV) in the aqueous phase is given by:

$$S(IV)_T = [SO_2]_{aq} + [HSO_3^-] + [SO_3^{2-}] \tag{214}$$

$$S(IV)_T = K_H P_{SO_2}\left(1 + \frac{K_1}{[H^+]} + \frac{K_1K_2}{[H^+]^2}\right) \tag{215}$$

$$\alpha_0^{-1} = \left(1 + \frac{K_1}{[H^+]} + \frac{K_1K_2}{[H^+]^2}\right) \tag{216}$$

$$S(IV)_T = K_H P_{SO_2}/\alpha_0 \tag{217}$$

where K_H = Henry's law constant
K_1 = first acid dissociation constant for $H_2O \cdot SO_2$
K_2 = second acid dissociation constant for $H_2O \cdot SO_2$

Using the appropriate values for K_H, K_1 and K_2 [107], total [S(IV)] can be calculated to be approximately 1 μeq-L^{-1} at 16 ppbv SO_2 and pH 3. However, if the reactions of S(IV) with Fe^{3+} and CH_2O are considered the following expressions are valid:

$$HSO_3^- + CH_2O \overset{K_3}{\rightleftharpoons} HOCH_2SO_3^- \tag{218}$$

$$Fe^{3+} + SO_3^{2-} \overset{K_4}{\rightleftharpoons} FeSO_3^+ \tag{219}$$

$$S(IV)_T = [SO_2]aq + [HSO_3^-] + [SO_3^{2-}] + [HOCH_2SO_3^-] + [FeSO_3^+] \tag{220}$$

$$S(IV)_T = K_H P_{SO_2}\left(1 + \frac{K_1}{[H^+]} + \frac{K_1K_2}{[H^+]^2} + \frac{K_1K_3}{[H^+]}[CH_2O] + \frac{K_4K_2K_1}{[H^+]^2}[Fe^{3+}]\right)$$

In this case, for $K_3 = 10^5\ M^{-1}$ and $K_4 = 10^{12}\ M^{-1}$, the $[S(IV)]_T$ will be in the range of 100–600 μ eq-L^{-1} at 16 ppbv SO_2 and pH 3 if the observed concentrations of CH_2O and Fe are used as initial input values and approximate values for the equilibrium concentrations of CH_2O and Fe^{3+} are determined iteratively.

These computations can be performed readily using SURFEQL. To illustrate the applicability of this modeling approach, a sensitivity analysis on the value for K_4 was performed. Carlyle [77] has reported a value of $K_4 = 10^9$ while Hansen et al. [173] report a value of $K_4 = 10^{18.1}$. The actual value may lie somewhere between these two values.

Metal-sulfite complexes are notably strong compared to the corresponding metal-sulfate species, e.g. $\beta_2(Hg(SO_3)_2^{2-}) = 10^{24}$; $\beta_2(Hg(SO_4)_2^{2-}) = 10^4$. Results are shown in Figure 2. These results suggest that, if $K_4 \geq 10^{10}$, 50% of the total iron in a system initially 0.1 mM in Fe_T will be complexed at $FeSO_3^+$ over the pH range of 2–4. Furthermore, if $K_4 \geq 10^{15}$, the computer model predicts that all of the Fe will be found as the species $FeSO_3^+$. Similar computations can be

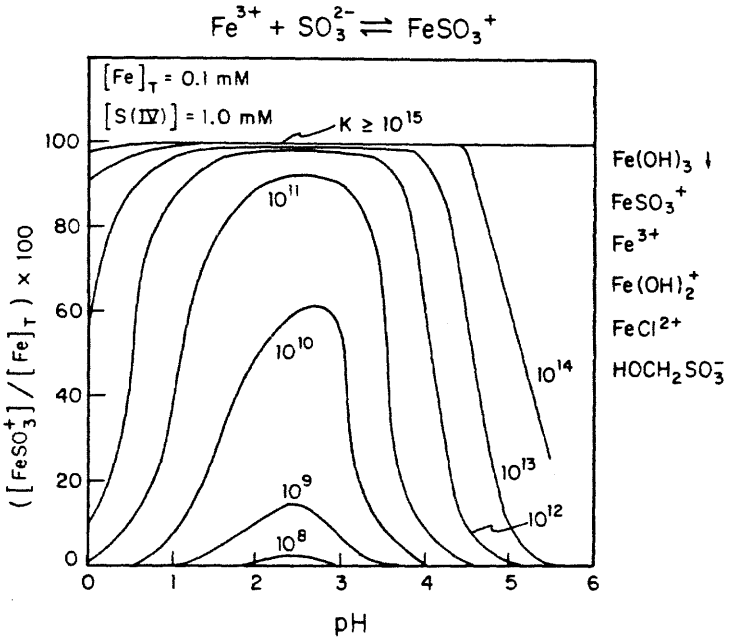

Figure 2. Speciation of Fe(III) vs pH in aqueous solution as a function of the stability constant of $FeSO_3^+$ as determined with SURFEQL. Other species that form are listed on the right side of the figure.

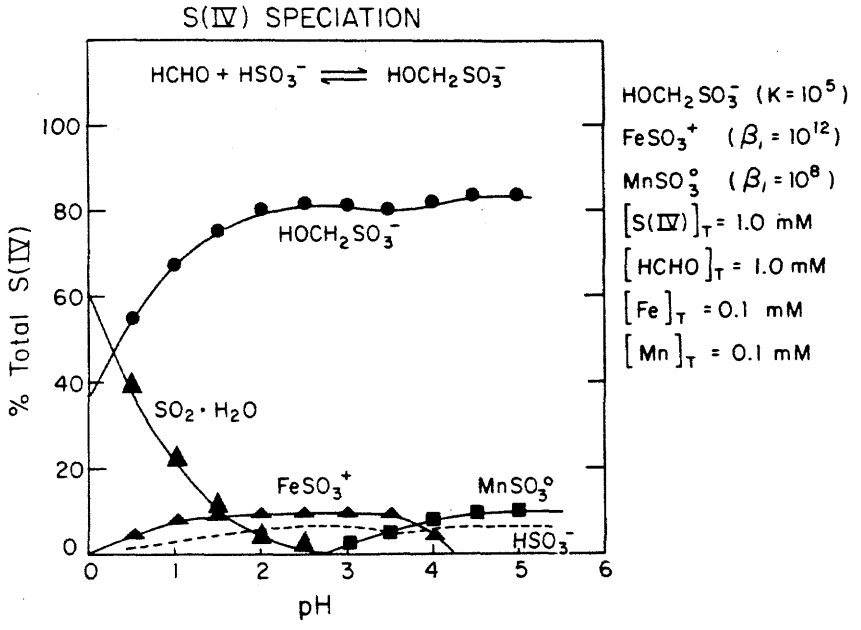

Figure 3. Speciation of S(IV) vs pH for the conditions on the far right of the figure as determined by SURFEQL.

performed on Mn^{2+} and HCHO. Figure 3 shows the total speciation for S(IV) over the pH range of 0 to 6 given the conditions listed on the right side of the figure.

In aqueous aerosol systems, important factors to consider are the nature and roles of dissolved organic molecules that can act as competitive complexing agents for metals. For example, liquid-phase autoxidation of benzaldehyde produces benzoic acid, which can act as a suitable complexing agent (e.g., $pK_{a1} = 3.97$, $\log\beta_{11} = 1.51$ for $Cu(C_7H_6O_2)^+$) and a similar oxidation of 2-hydroxybenzaldehyde to 2-hydroxybenzoic acid produces even a stronger potential ligand (e.g., $pK_{a1} = 2.78$, $\log\beta_{11} = 10.13$ for $Cu(C_7H_6O_4)^+$). The presence of complexing agents of this type and organic reductants will accelerate the dissolution of Fe_2O_3 and MnO_2, which are the likely sources of soluble iron and manganese in aerosol systems. As shown by Cohen et al. [40], the catalytic activity of soot-derived aerosols correlates well with the total iron released to the liquid phase. To illustrate this effect, oxalic acid/oxalate was added to the computation illustrated in Figure 2 at a concentration of 1.0 m*M*. Results are shown in Figure 4 for the effect of 1:1, 1:2 and 1:3 ferric oxalate complexes with $\log\beta_1 = 7.5$, $\log\beta_2 = 13.64$ and $\log\beta_3 = 18.49$ on the equilibrium distribution of $FeSO_3^+$. The net effect of the addition of oxalate was to lower the percentage contribution of $FeSO_3^+$ as a function of pH for a given stability constant. This effect is due to competitive complexation.

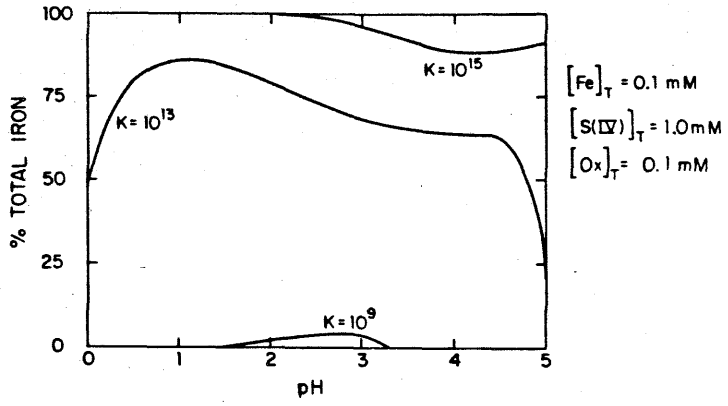

Figure 4. Speciation of Fe(III) perturbed by iron(III)oxalato complexes as a function of pH and stability constant (β_1) of the $FeSO_3^+$.

An additional effect that was not considered here is the possible formation of mixed ligand complexes of Fe^{3+}, S(IV) and oxalate.

As indicated above, certain metal-catalyzed autoxidations of sulfite proceed via the formation of discrete inner-sphere complexes between the reductant, SO_3^{2-} and the catalyst as a prelude to electron transfer. Few metal-sulfite stability constants have been determined because of the thermodynamic instability of sulfite toward oxidation in oxic systems; however, those that have been reported [107] are significantly larger than the corresponding constants for metal-sulfate complexes as shown in Table XII. Sulfite can form complexes by forming a bond either

Table XII. Comparison of Stability Constants[a] for Metal-Sulfito and -Sulfato Complexes at 25.0 C

Metal	μ	*log* β (SO_3^{2-})	μ	*log* β (SO_4^{2-})
Ag^+	0	$AgSO_3^-$, 5.6	0	$AgSO_4^-$, 1.3
Cd^{2+}	1.0	$Cd(SO_3)_2^{2-}$, 4.2	1.0	$Cd(SO_4)_2^{2-}$, 1.6
Hg^{2+}	1.0	$Hg(SO_3)_2^{2-}$, 24.1	0.5	$Hg(SO_4)_2^{2-}$, 2.4
Ce^{3+}	0	$CeSO_3^+$, 8.0	0	$CeSO_4^+$, 3.6
Fe^{3+}	0.1	$FeSO_3^+$, 18.1[b]	0	$FeSO_4^+$, 4.0
Fe^{2+}			0	$FeSO_4^0$, 2.2
UO_2^{2+}	1.0	$UO_2SO_3^0$, 5.3	1.0	UO_2SO_4, 1.8
Cu^+	1.0	$CuSO_3^-$, 7.8		
Cu^+	1.0	$Cu(SO_3)_2^{3-}$, 8.7		
Cu^{2+}			0	$CuSO_4^0$, 2.4

[a] All constants reported in this table were taken from Smith and Martell [106], except the stability constant for $FeSO_3^+$.

[b] Hansen et al. [172].

through sulfur [174,175] or through oxygen [176–178] whereas sulfate is restricted to bond formation through oxygen. Part of the increased metal-sulfite bond stability may be due to the availability of low lying "d" orbitals on sulfur for $p\pi$-$d\pi$ and $d\pi$-$d\pi$ metal to ligand backbonding. In addition to this added stability, sulfite can readily form bidentate [179] and bridging complexes with bond formation through two oxygen atoms or through an oxygen and sulfur.

Based on simple linear free energy correlations, reasonable estimates for the stability constants of Fe^{2+}, Mn^{2+}, Cu^{2+} and Ni^{2+} complexes with sulfite can be made using the data given in Table XII. With this information, models for the speciation of fog water (Table I) can be constructed with the aid of SURFEQL. These computations are particularly important in the case of Fe^{3+} since it can exist as a solid ($Fe(OH)_3$ or FeOOH) over a broad range of pH. Results of a speciation model for the chemical constituents and concentrations listed in Table I are illustrated in Figure 5 for Fe^{3+}, S(IV), Mn^{2+} and Cu^{2+}. Iron(III) above pH 4 is predicted to occur exclusively as amorphous $Fe(OH)_3$; below pH 4, Fe^{3+} is complexed by SO_3^{2-} ($\log\beta_1 \simeq 12$) and by F^-. Only a small fraction of total iron appears as free hexaquo iron(III). This fraction increases at pH <2.

Copper and manganese speciation are relatively straightforward. At the micro-

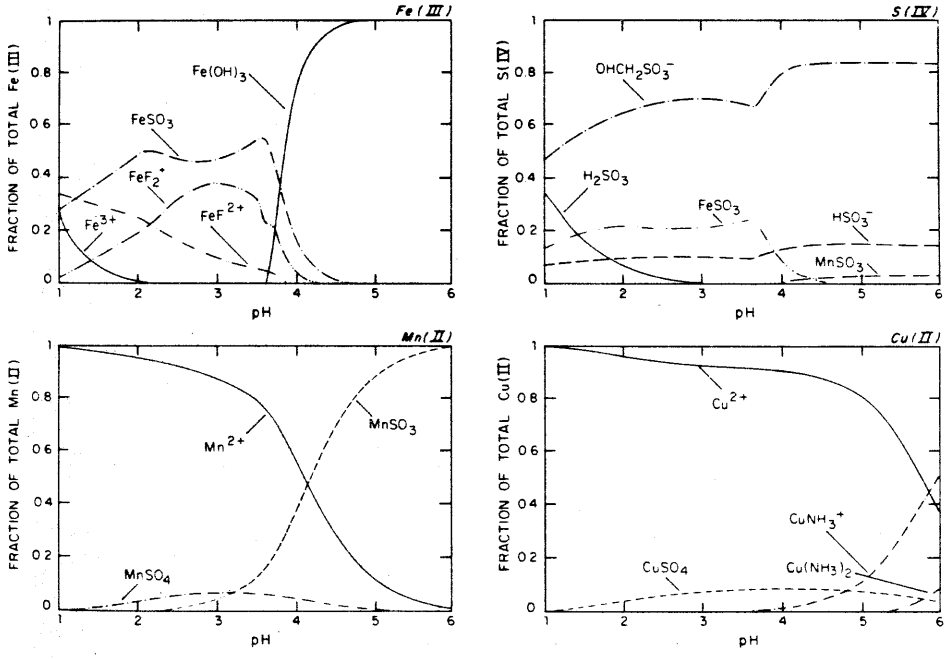

Figure 5. Speciation of Fe(III), S(IV), Cu(II) and Mn(II) in fog water as a function of pH. Input values were the high values for all measured components listed in Table I. (log β_1 $\{FeSO_3^+\} = 12$ and log β_1 $\{MnSO_3^o\} = 8$.)

molar concentration levels given in Table I, both Cu^{2+} and Mn^{2+} occur as soluble species over the pH range 1–6. Copper(II) forms amino complexes to some extent at pH >4. Manganese(II) is found primarily as a sulfite complex ($\log\beta_1 \simeq 8$) at pH 4–6 and as a free hexaquo metal at pH <4.

The speciation of S(IV) is of great interest. Bisulfite readily forms sulfonic acid derivatives, α-hydroxyalkanesulfonic acids (also known as bisulfite addition compounds) [180], as indicated in Equation 218, with aldehydes and ketones. Since relatively high levels of formaldehyde ($K_H = 6.3 \times 10^3$ M-atm^{-1}) (Chapter 4) and other aldehydes have been found in fog and cloud water in Los Angeles, the formation of these addition complexes must be considered in kinetic or thermodynamic model development. Dasgupta et al. [181] have established a conditional stability constant for the formation of α-hydroxymethanesulfonic acid of approximately $K = 10^{4.8}$ over the pH range 2–6. This constant can be used in the equilibrium computation. Results shown in Figure 5 for S(IV) indicate that the sulfonic acid derivative will be the predominant S(IV) species over a broad range of pH. Of secondary importance below pH 4 are $FeSO_3^0$, HSO_3^- and $H_2O{\cdot}SO_2$, respectively. The occurrence of S(IV) as stable sulfonic acid derivatives may retard the net oxidation of S(IV) to S(VI). Dasgupta et al. [181] and Fortune and Dellinger [182] have found that addition of CH_2O to sulfite solutions stabilizes S(IV) as hydroxymethanesulfonic acid (HMSO), and that HMSO was not significantly degraded and oxidized to S(VI) for at least one month.

In conclusion, equilibrium speciation models will prove to be an invaluable tool in determining the detailed chemistry of atmospheric water droplets when sufficient time is available for reactions under consideration to be in a steady-state or approximate equilibrium. The kinetic and mass transport limitations for these approximations have been discussed [170,183]. In the next section, the models discussed above will be interfaced with a kinetic model for nighttime fog water chemistry.

FOG WATER CHEMISTRY MODEL

Background

Fog and cloud droplets form by condensation of water vapor on the activated cloud condensation nuclei (ACCN) in the atmosphere and grow by accretion of water vapor. The soluble components of the ACCN on which the droplets form dissolve in the droplet and provide an initial chemical loading. As the droplets grow, they absorb gases from the atmosphere, and liquid-phase reactions occur within.

During fall and winter 1981, water from nighttime fogs in the Los Angeles basin were sampled and analyzed (Table I) [14]. The results of this study highlighted the efficiency of fog droplets as scavengers of air pollutants in the boundary layer; extremely high concentrations of sulfate ions, as well as nitrate and ammonium

ions, were routinely found. The Log Angeles basin is a highly polluted region, and the sulfate levels observed could be attributed to (1) scavenging by nucleation of the large primary sulfate ACCN; (2) scavenging by diffusion of the smaller secondary sulfate aerosol particles; and (3) absorption of atmospheric SO_2 and subsequent liquid-phase oxidation to S(VI).

As discussed above, several pathways for the heterogeneous S(IV) $\rightarrow$ S(VI) oxidation scheme must be considered. The most important oxidants appear to be H_2O_2, O_3 and O_2 catalyzed by the Fe^{3+} and Mn^{2+} present at less-than-millimolar concentrations in the aqueous droplets. Hydrogen peroxide and ozone are both absorbed from the gas phase according to their respective Henry's law equilibria; Fe^{3+} and Mn^{2+} originate from fly ash and soil dust ACCN on which the droplets have condensed. The object of this section is to present a dynamic model for the water chemistry of nighttime urban fogs with which the contributions of the various oxidation mechanisms to the total S(VI) concentrations in fog water can be evaluated.

A number of rain and cloud water chemistry models have been proposed in recent years. Adamowicz [184] modeled the chemistry of pure raindrops falling through a well mixed polluted layer with uniform and constant concentrations of SO_2, CO_2 and NH_3. He assumed that the aqueous-phase oxidation of S(IV) to S(VI) occurred exclusively through iron-catalyzed oxidation by O_2 according to the kinetic expression of Brimblecombe and Spedding [37]. Mass transfer at the surface of the drop was modeled with two-film theory, which Baboolal et al. [185] have since shown to be unsatisfactory in that it ignores the forced convection inside and outside the falling drop, which greatly enhances the rates of mass transfer. Durham et al. [186] added NO_x to the gas phase and considered O_3 to be the only liquid-phase oxidant, which greatly underestimates S(VI) formation rates. Easter and Hobbs [187] modeled cloud water chemistry by using a wave cloud model, an open atmosphere with trace concentrations of CO_2, SO_2 and NH_3, and a rudimentary S(IV) oxidation rate consisting of a simple first-order dependence on sulfite.

In the model presented here, the chemistry is more detailed than in the above models; recent evaluations for reaction mechanisms, rate constants, activation energies and thermodynamic data are used. ACCN chemistry and gas-phase reactions are included to simulate the coupling between gas-phase, liquid-phase and aerosol chemistries. The system is considered closed because of the significant depletion of trace gases due to absorption by the fog droplets, which would make the assumption of an open system very inaccurate. Also, the physical processes relevant to droplet chemistry are examined more rigorously than in the previous models; as shall be shown, restriction of the model to nighttime fogs allows one to account for these physical processes in a simple but fairly realistic manner, whereas in rains and clouds, the large temporal and spatial scales involved make detailed analysis exceedingly difficult. The proposed model is a potentially useful tool for prediction of fog water chemistry, even though the present discussion will mostly be limited to S(IV) aqueous-phase oxidation processes.

Model Development

Gas-Phase Chemistry

At nighttime the gas-phase chemistry is considerably simplified over that in the daytime because of the absence of sunlight and thus of the associated photochemical reactions. In the absence of OH, $O^3(P)$ and CH_3O_2 radicals, which disappear rapidly after sunset, SO_2 gas-phase oxidation is very slow [188] and negligible on the time scales of a fog event. Although oxidation by ozone of organics (especially olefins) may be important, it will not be considered at the present time. Gas-phase chemistry is assumed to be limited to NO_x oxidation, which proceeds through the following mechanism [189,190]:

$$NO + O_3 \longrightarrow NO_2 + O_2 \qquad k_1 = 3.38 \times 10^3 \exp(-1450/T) \quad (222)$$

$$NO_2 + O_3 \longrightarrow NO_3 + O_2 \qquad k_2 = 1.76 \times 10^2 \exp(-2450/T) \quad (223)$$

$$NO + NO_3 \longrightarrow 2NO_2 \qquad k_3 = 2.94 \times 10^4 \text{ (at 25 C)} \quad (224)$$

$$NO_2 + NO_3 \longrightarrow N_2O_5 \xrightarrow[H_2O]{\text{very fast}} 2HNO3 \qquad k_4 = 7.35 \times 10^3 \text{ (at 25 C)} \quad (225)$$

No data are given for the activation energies of Equations 224 and 225; a doubling of the reaction rates for a 10° C increase in temperature is assumed.

The kinetics of the hydrolysis of N_2O_5, which involves both water vapor and the fog droplets, is not well understood. The essential work in this problem area has been reviewed [191]. Hydrolysis of N_2O_5 appears to occur much faster at the surface of aerosol particles than homogeneously in the gas phase. In the presence of fog droplets the reaction is probably very fast, because of the large droplet surface area and the possibility of heterogeneous hydrolysis. Therefore, this step is assumed to be instantaneous. Reactions 222–225 yield a system of differential equations that is readily solved by a fourth-order Runge-Kutta routine. The overall reaction rate is essentially limited by the slow rate of oxidation of NO_2.

Liquid-Phase Chemistry

Droplet chemistry is determined primarily by ACCN chemistry and by absorption and subsequent aqueous-phase reactions of atmospheric gases. Gases are absorbed and react in the droplet according to the equilibria listed in Table XIII. The temperature dependence for all the equilibrium constants in Table XIII is determined by the Van't Hoff equation:

$$ln K_T = ln K_{298.15} - \frac{\Delta H^\circ}{R}\left(\frac{1}{T} - \frac{1}{298.15}\right) \quad (226)$$

Table XIII. Equilibria and Thermodynamic Data Considered in Fog Water Model [10, 32,196,197]

Reaction	$\Delta G°_{298.15}$ (*kcal-mol^{-1}*)	$\Delta H°_{298.15}$ (*kcal-mol^{-1}*)	$K_{(aq)}$ (*M-atm^{-1} or M*)
$H_2O(l) \rightleftharpoons H^+ + OH^-$	19.093	13.345	1.008×10^{-14}
$CO_2(g) + H_2O(l) \rightleftharpoons H_2CO_3(l)$	2.005	−4.846	3.390×10^{-2}
$H_2CO_3(l) \rightleftharpoons H^+ + HCO_3^-$	8.687	1.825	4.283×10^{-7}
$HCO_3^- \rightleftharpoons H^+ + CO_3^{2-}$	14.09	3.55	4.687×10^{-11}
$NH_3(g) \rightleftharpoons NH_3(l)$	−2.41	−8.17	5.844×10^{1}
$NH_3(l) \rightleftharpoons NH_4^+ + OH^-$	6.503	8.65	1.709×10^{-5}
$SO_2(g) \rightleftharpoons SO_2(l)$	−0.130	−6.247	1.245
$SO_2(l) \rightleftharpoons HSO_3^- + H^+$	2.578	−4.161	1.290×10^{-2}
$HSO_3^- \rightleftharpoons SO_3^{2-} + H^+$	9.850	−2.23	6.014×10^{-8}
$HNO_3(g) \rightleftharpoons H^+ + NO_3^-$	−8.92	−17.46	3.460×10^{5}
$H_2O_2(g) \rightleftharpoons H_2O_2(l)$		−14.5	7.1×10^{4}
$O_3(g) \rightleftharpoons O_3(l)$		−5.04	9.4×10^{-3}

It is interesting to note that at the pH commonly encountered in fogs (pH 2–6) all of the gaseous nitric acid and ammonia are absorbed by the droplets because of their acid-base chemistries in the liquid phase. For other gases absorption is limited.

Oxidation of S(IV) in the droplet is allowed to proceed along the major pathways discussed previously. The important oxidants are H_2O_2 and O_3; oxidation by dissolved O_2 may also be important if catalyzed by Fe^{3+} and Mn^{2+}, for which the catalytic synergism noted in Chapter 2 is considered. Oxidation by NO_x and by O_2 catalyzed by trace metals other than Fe^{3+} and Mn^{2+} is ignored for the present time.

Speciation of Fe and Mn within the droplets may control their catalytic effectiveness. Fe and Mn are effective catalysts as long as they are dissolved (as free ions or complexes in solution); however, their catalytic properties are totally altered if they occur as solid phases. Surface catalysis may occur, but this possibility will not be considered here. The distribution of Fe and Mn species inside the fog droplets was obtained from typical values for the concentration of all major components of Los Angeles fog water with SURFEQL [172]. The results were shown in Figure 5. Mn^{2+} remains totally in solution at the pH values found in fog water, but Fe^{3+} starts to precipitate as $Fe(OH)_3$ above pH 4. At pH values above 5 no Fe^{3+} remains in solution; therefore, high pH values quench the iron-catalyzed S(IV) oxidation mechanism. Total soluble Fe^{3+}, y, is given by the following relationship:

$$y \equiv {}^*K_{so}[H^+]^3\alpha_0 Fe_T$$

where y is the dissolved fraction of the total iron in the system, $^*K_{SO}$ is the solubility product constant for $Fe(OH)_{-3}$ (S), and α_O is defined as follows:

$$\alpha_O = (1 + \beta_1[F^-]^2 + \beta_2[F^-] + \beta_3[SO_3^{2-}] + {}^*K_1/[H^+] + {}^*K_2[H^+]^2)^{-1}$$

For all oxidation reactions the reaction rates and activation energies are chosen from the expressions suggested in Chapter 2 for atmospheric models, with speciation for Fe^{3+} added.

Physical Description

The model presented here uses a closed-box approximation. At t = 0, under conditions determined by the ambient saturation, size distribution and chemical composition of the CCN, water droplets suddenly form and grow subsequently by accretion of water vapor. Scavenging of the smaller aerosol particles by diffusion to the surface of the droplet is not included in the model.

The possible limitation of S(IV) oxidation reactions by mass transfer has been discussed [185,188,192,193]. Seinfeld [188] indicated that the liquid-phase chemical equilibria of concern are established very quickly and thus do not induce any rate limitations in the system. Schwartz and Freiberg [192,193] showed that, for stationary droplets smaller than 50 μm, the rate was limited by the chemical oxidation rates. Baboolal et al. [185] extended this analysis by showing that for the few fog water droplets larger than 50 μm that exhibit a significant sedimentation velocity (as opposed to the smaller quasistationary droplets), forced convection both inside and outside the droplet enhances significantly the rates of mass transfer as calculated for stationary droplets. Because of this enhancement the diffusion rate still is faster than the S(IV) oxidation rate. Therefore, the chemical changes in fog droplets are most likely limited by the specific reaction rates.

Because fogs are generally localized events and occur on time scales of a few hours, usually under low wind conditions, no consideration of long-term transport of condensing/evaporating droplets was included in the model; also, evolution of the droplet spectrum through coagulation can be neglected since mass transfer does not limit the reaction kinetics. Droplet growth can simply be accounted for by the input of a time-dependent liquid water content (LWC), which is measured experimentally. Thus a reasonable physical description of the system in the model can be limited to the input of temperature and of a time-dependent LWC.

Mathematical Formulation

At time t = 0, droplets are assumed to suddenly condense in an atmospheric "closed box" containing ACCN and trace atmospheric gases; the instantaneous formation of these droplets is associated with a certain LWC. This LWC may be made to vary with time following either experimental observations or theoretical predictions [194]. In the results presented here, LWC will be taken to be constant. When the droplets form they receive an initial chemical loading from the water-

soluble fraction of the ACCN, immediately absorb atmospheric gases according to Henry's law and the liquid-phase equilibria of Table XIII are established. The concentrations of the species at equilibrium are obtained by solving the electroneutrality equation for a closed system (see appendix for details of the calculation).

Formation of S(VI) in the liquid phase is calculated over small time increments Δt by a forward finite-difference technique:

$$[S(VI)]_{t+\Delta t} = [S(VI)]_t + \left(\sum_{ox}\left(\frac{d[S(VI)]}{dt}\right)_{ox}\right)\Delta t \tag{228}$$

After each time step, changes in gas-phase concentrations from fresh emissions and NO_x oxidation are calculated, and the electroneutrality equation is solved to obtain the new equilibrium concentrations for the species in the system.

Time increments are taken as $\Delta t = 2 \times 10^{-4}$ n (minutes) where n is the time step number; this expression allows for a better resolution at the beginning of the fog event, where chemical changes are rapid. The use of smaller time steps did not change the calculation results.

Results and Discussion

The model was designed to interpret the results of the 1981–1982 fog sampling program [14] and to shed light on the relative importances of the various liquid-phase S(IV) oxidation mechanisms in ambient fog droplets. The present discussion will be limited to the latter point, in light of the fog water data collected in the Los Angeles basin [14] and the permanent atmospheric chemistry records of the Air Quality Management District.

The following pre-fog nighttime gas-phase concentrations were assumed for all model runs:

- $CO_2 = 3.3 \times 10^5$ ppb,
- NO = 100 ppb,
- $NO_2 = 50$ ppb,
- $NH_3 = 5$ ppb,
- $HNO_3 = 3$ ppb, and
- $SO_2 = 20$ ppb.

In cases H and I, different levels and emission rates for NO and NO_2 are considered.

Gas emission sources per liter of basin air were taken to be

- $\delta_{NO} = 0.1$ ppb-min^{-1}-L^{-1},
- $\delta_{NO_2} = 0.01$ ppb-min^{-1}-L^{-1},
- $\delta_{SO_2} = 0.05$ ppb-min^{-1}-L^{-1}, and
- $\delta_{NH_3} = 0.005$ ppb-min^{-1}-L^{-1}.

Table XIV. Atmospheric Conditions for the Fog Events Simulated by the Model[a]

	Case								
	A	*B*	*C*	*D*	*E*	*F*	*G*	*H*	*I*
Concentrations of Atmospheric Gases (ppb)									
H_2O	1	1	1	5	1	1	1	1	1
O_3	10	10	10	10	10	10	10	10	10
NO	100	100	100	100	100	100	100	5	0
NO_2	50	50	50	50	50	50	50	10	0
Aqueous-Phase Metal Concentrations (μeq-L^{-1})									
Fe^{3+}	100	20	100	100	100	100	100	100	100
Mn^{2+}	5	1	5	5	5	5	5	5	5
Sources of NO_x (ppb-min^{-1})									
δ_{NO}	0.1	0.1	0.1	0.1	0.1	0.1	0.1	10^{-3}	0
δ_{NO_2}	0.01	0.01	0.01	0.01	0.01	0.01	0.01	10^{-4}	0
ACCN Composition	NaCl	NaCl	NaCl	NaCl	NaCl	HNO_3 1 μmol-m^{-3}	NaOH 1 μmol-m^{-3}	NaCl	NaCl
Synergysm, Fe/Mn	Yes	Yes	No	Yes	Yes	Yes	Yes	Yes	Yes
Temperature (C)	10	10	10	10	25	10	10	10	10

[a] Additional conditions: 330 ppm CO_2, 3 ppb HNO_3, 5 ppb NH_3, 20 ppb SO_2, $\delta_{SO_2} = 0.05$ ppb-min^{-1}, $\delta_{NH_3} = 0.005$ ppb-min^{-1} and LWC = 1 g-m^{-3}.

Concentrations of gas-phase ozone at night range from 0 to 30 ppb. There is some evidence of nighttime diffusion of ozone from the upper atmosphere down to the boundary layer as ozone is depleted near the ground by gas-phase oxidation reactions [195]; this source term will be ignored for now. Because NO is usually in excess of O_3, the additional ozone would merely oxidize part of the excess NO and thus have little effect on the droplet chemistry.

Hydrogen peroxide levels are poorly documented, and the reliability of the few existing measurements has been questioned; a concentration range of 1–5 ppb will be assumed. Hydrogen peroxide is not considered to be an important oxidant for nighttime gas-phase NO_x chemistry.

A major feature of the Los Angeles fog water as shown in Table I is the high levels of trace metals. The model calculations were performed for the ranges observed, which are 20–200 μeq-L^{-1} for Fe^{3+} and 1–10 μeq-L^{-1} for Mn^{2+}. For all runs a typical value of 20 was taken for the Fe/Mn ratio in equivalents. Table XIV gives concentration conditions imposed on the model calculations.

Calculations were first made under conditions typical of Los Angeles fog with a temperature of 10° C, a LWC of 1 g-m^{-3}, prefog conditions of 1 ppb H_2O_2 and 10 ppb O_3 and trace metal levels in the droplets of 100 μeq-L^{-1} for Fe and 5 μeq-L^{-1} for Mn. Synergism between Fe and Mn was considered for S(IV) oxidation, and the ACCN were assumed to be NaCl or some other neutral aerosol. The results of the calculations are shown in Figure 6.

A basic feature of S(IV) nighttime oxidation is that the strong oxidants (H_2O_2 and O_3) are not resupplied to the atmosphere in the absence of the daytime photochemical reactions. As seen in Figure 6, 10 min after fog formation, H_2O_2 and O_3 no longer contribute to S(IV) oxidation because they have been totally depleted from the atmosphere, H_2O_2 by S(IV) liquid-phase oxidation and O_3 by S(IV) liquid-phase oxidation and NO_x gas-phase oxidation. Hydrogen peroxide is an efficient liquid-phase oxidant because it is very soluble in water, has rapid oxidation rates at low pH, and is not depleted at a significant level by gas-phase oxidation reactions. On the other hand, O_3 is poorly soluble; its rate for oxidizing S(IV) drops dramatically as pH decreases; and it reacts quickly with NO in the gas phase to form NO_2. Hydrogen peroxide is thus a very effective oxidant for S(IV) in ambient fog water, whereas oxidation by O_3 is relatively insignificant.

In addition, it is apparent from the model calculations that rapid reaction of O_3 with NO not only prevents liquid-phase S(IV) oxidation by O_3 but also gas-phase NO_2 oxidation by O_3, which is the rate-limiting reaction for the formation of nitric acid at night; thus, there is no nitrate formation during a nighttime fog event (although the fog water may have a high nitrate concentration because of the scavenging of nitrate particles and of the prefog gaseous nitric acid).

Finally, the most striking result of the calculations is the dominating role of metal-catalyzed oxidation, which accounts for more than 90% of the S(VI) formed in the liquid phase four hours after the beginning of the fog event. Unlike H_2O_2 and O_3, there is an infinite supply of O_2, and concentrations of Fe and Mn in Los Angeles fog water are high enough to make O_2 an effective oxidant. Although the corresponding oxidation rates exhibit an inverse dependence on H^+

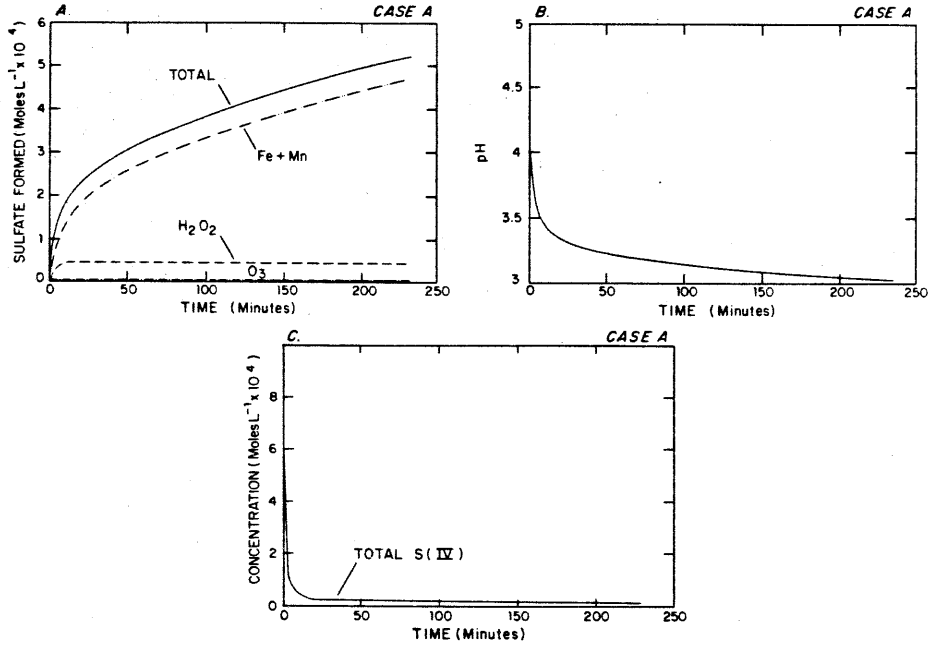

Figure 6. Sulfate formed, pH and total S(IV) for the fog water as a function of time after fog formation, under conditions typical of the Los Angeles atmosphere (case A): 20 ppb SO_2, 10 ppb O_3, 1 ppb H_2O_2 in the pre-fog gas phase, metal aqueous-phase concentrations of 100 μeq-L^{-1} Fe^{3+} and 5 μeq-L^{-1} Mn^{2+}.

concentration, dissolution of the ferric hydroxide precipitate below pH 4 maintains oxidation rates at a high level at the low pH values characteristic of Los Angeles fog water. Even at the lowest concentrations of metals found in the fog water (Case B, Figure 7) and in the absence of synergism between Fe and Mn catalytic effects (Case C, Figure 7), metal-catalyzed oxidation is still the major source of S(VI) formation.

It should not, however, be concluded from the above results that H_2O_2 is only a minor contributor to S(IV) oxidation. Because no reliable method exists for measuring gas-phase H_2O_2, its levels in the atmosphere are uncertain; at concentrations higher than the 1 ppb considered in Case A it may be an important oxidant. This is illustrated by Case D (Figure 8), where a pre-fog H_2O_2 level of 5 ppb is assumed; the contribution of H_2O_2 to S(IV) oxidation is then important, and dominates oxidation processes until two hours after fog formation. High levels of H_2O_2 also slow down the metal-catalyzed oxidation kinetics because of the abrupt pH drop associated with the rapid quantitative depletion of H_2O_2.

Temperature dependence of the chemical composition of the droplet was studied by raising the temperature in Case A from 10 to 25 C (Case E, Figure 8). At this higher temperature the oxidation rates are higher, but the solubilities

of the gases are lower. These opposite effects make the system rather stable to changes in temperature. Comparing Cases A and E 4 h after fog formation, somewhat more S(VI) has been produced at the higher temperature (700 μmol-L^{-1} at 25° C vs 520 μmol-L^{-1} at 10 C) while the pH is slightly lower (2.9 at 10° C vs 3.05 at 25° C). Oxidation of S(IV) by ozone becomes totally unimportant at 25° C, as ozone is even less soluble than at 10 C.

The effect of droplet "background" acidity was investigated by calculating the chemical content of the droplets in Case F of acid ACCN (1 μmol-m^{-3} of HNO_3) and in Case G of basic ACCN (1 μmol-m^{-3} of NaOH). These cases yielded "initial pH values" of 3.03 and 6.50, respectively; the calculated results are shown in Figure 9 (cases F and G). The effects of the pH changes are damped by the slow S(IV) metal catalyzed oxidation rates at low pH, and after 4 h, the pH values are reasonably close at 2.90 and 3.15, respectively. However, six times more sulfate is formed in the initially "basic" droplet. A main feature of this latter case is that the high initial pH allows for a much higher rate of S(IV) oxidation by O_3, which then becomes a major contributor to S(IV) oxidation.

In urban air, the levels of NO at dusk are generally higher than those of

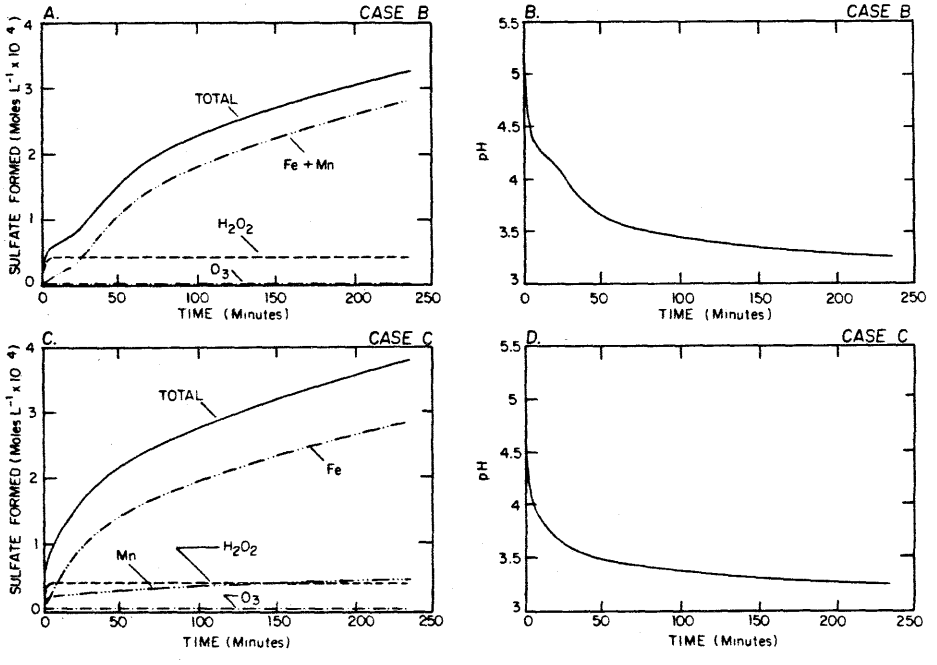

Figure 7. Sulfate formed and pH for the fog water as a function of time after fog formation, when Fe^{3+} = 20 μeq-L^{-1} and Mn^{2+} = 1 μeq-L^{-1} (case B) which are the lows observed in the Los Angeles fog water, or when no synergism for iron- and manganese-catalyzed oxidation mechanisms is considered (case C).

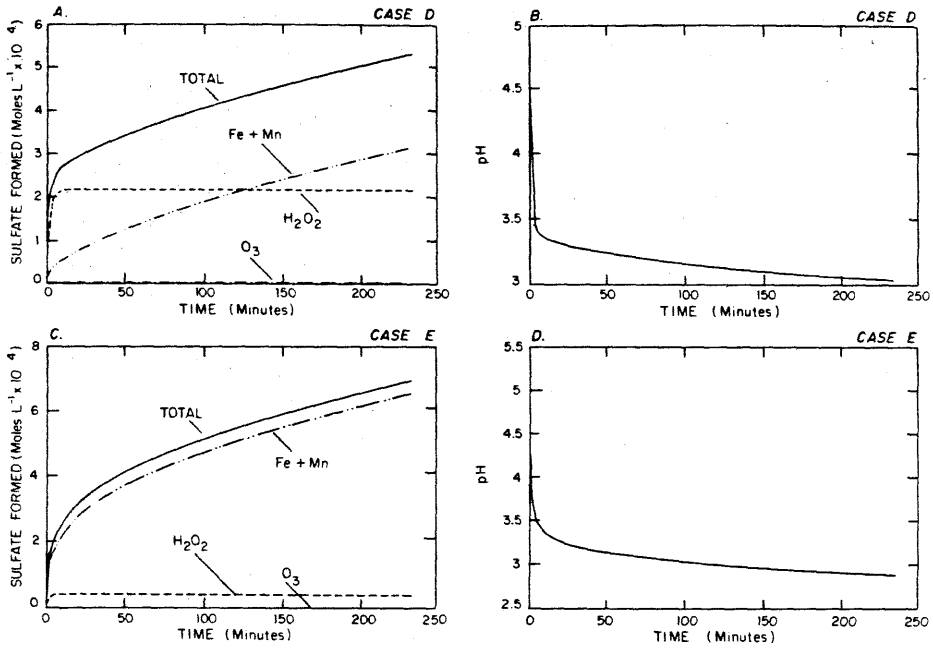

Figure 8. Sulfate formed and pH for the fog water as a function of time after fog formation, when H_2O_2 = 5 ppb in the pre-fog gas phase (case D), or when the temperature is 25 C (case E).

O_3, and the gas-phase oxidation of NO by O_3 depletes all the O_3 from the system. However, it may happen that ozone will be in excess of NO; in that case, after the oxidation of all the NO to form NO_2, there will be ozone available to oxidize both NO_2 in the gas phase to form nitric acid and S(IV) in the liquid phase to form S(VI). Figure 10 illustrates the chemical behavior of the fog under conditions of Case H, where ozone is in excess of NO. Comparing the results to those of Case A, one observes a slight increase in the ozone contribution to the S(IV) liquid-phase oxidation, but mostly a large amount of nitrate formed. After NO is depleted, the slow gas-phase oxidation of NO_2 to HNO_3 thus becomes the dominant pathway for ozone removal from the system. Less sulfate is then formed because of the drop in pH due to the incorporation in the droplet of the nitric acid. It is interesting to note that under conditions of a NO_x-free atmosphere (Case I, Figure 10) one does not observe an increase in the production of S(VI) by ozone as compared to Case H; this shows that production is not limited by competition from gas-phase NO_2 oxidation but rather by the inefficacy of ozone as a liquid-phase oxidant for S(IV) in low pH solutions. It is observed from the model calculations that there is no oxidation of S(IV) by ozone below pH 4 regardless of the NO_2 concentrations.

Overall the results of this dynamic model reveal some important features

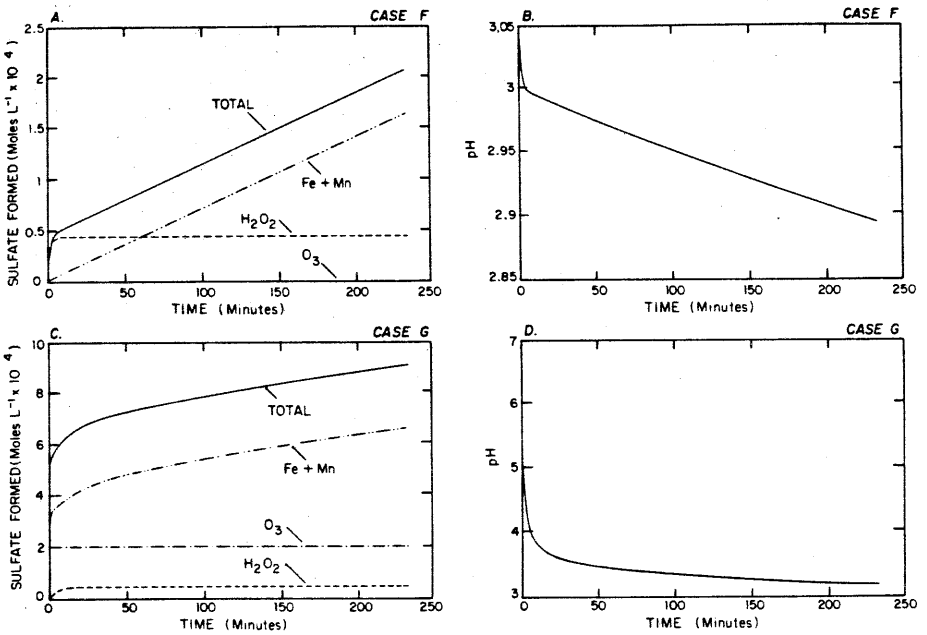

Figure 9. Sulfate formed and pH for the fog water as a function of time after fog formation, when condensation takes place on HNO_3 ACCN (case F), or on NaOH ACCN (case G).

of S(IV) liquid-phase oxidation in the fogwater of polluted atmospheres. They are:

1. The main contributor to S(VI) formation in the aqueous phase at night is metal-catalyzed oxidation of S(IV). This conclusion may be challenged because of the lack of definitive data for H_2O_2 concentrations in the atmosphere, which makes our estimated value of 1 ppb no more than an educated guess; it still appears that metal-catalyzed oxidation is more important in polluted atmospheres than has been hitherto recognized.
2. S(IV) oxidation by ozone is insignificant because of a combination of slow oxidation rates at low pH, poor ozone solubility and depletion of ozone in the gas phase by oxidation of NO.
3. S(IV) oxidation by H_2O_2 is very rapid, but is limited by the amount of H_2O_2 originally present in the system.
4. Precipitation of ferric hydroxide at pH 4, with the accompanying loss (or modification) of its catalytic properties, requires that Fe^{3+} speciation be taken into account in the development of atmospheric water chemistry models.
5. If the level of NO is higher than that of O_3, there is no nitrate formation in the fog. If it is lower than that of O_3, O_3 will first oxidize NO very quickly to form NO_2 and then slowly oxidize NO_2 to form NO_3, which

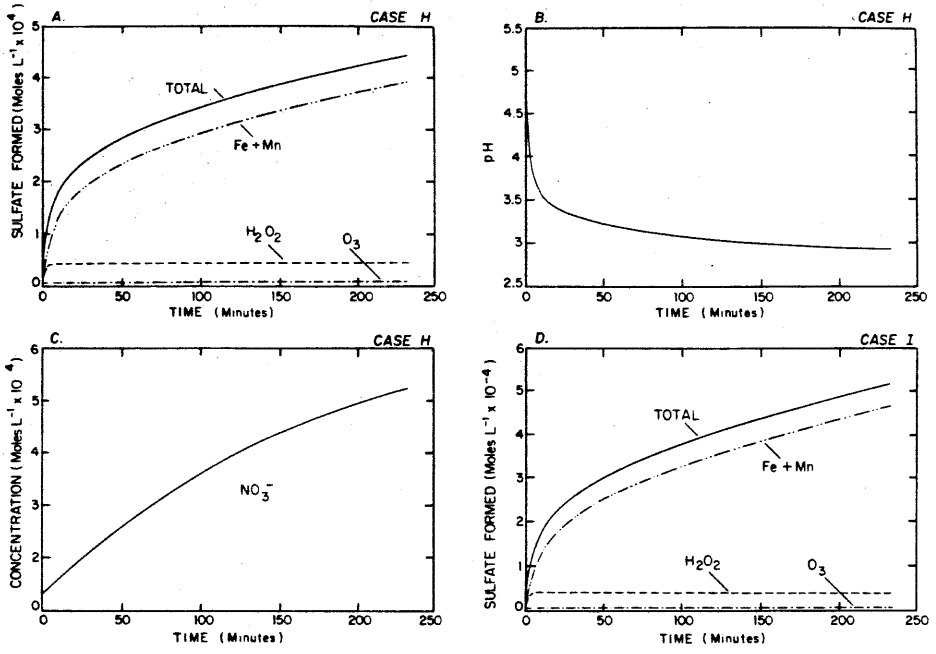

Figure 10. Sulfate formed, pH and nitrate for the fog water as a function of time after fog formation when ozone is in excess of NO (case H), and sulfate formed under conditions of a NO_x-free atmosphere (case I).

will then react to produce nitric acid. The rate of S(IV) oxidation by ozone in such a system is not limited by the amount of NO_2 in the atmosphere but by the pH of the fog water. Below pH 4 it is insignificant.

Conclusion

In heavily polluted atmospheric water droplets, such as those found in urban fogs, the model presented here shows that metal-catalyzed S(IV) oxidation is a significant contributor to formation of S(VI) in the liquid phase, and apparently is more important than oxidation by H_2O_2. Under conditions typical of the Los Angeles area, liquid-phase oxidation of S(IV) to S(VI) is found to account for sulfate concentrations in the range of 5×10^{-4} mole-L^{-1} 4 h after fog formation. Waldman et al. [14] found sulfate concentrations ranging from 5×10^{-4} to 2×10^{-3} mole-L^{-1} in the fog. Direct comparison of our calculated values with the field data is difficult, since Waldman et al. did not measure the LWC of the fogs they studied; nevertheless, it appears clearly that absorption of SO_2 followed by liquid-phase oxidation is an important mechanism for explaining the sulfate concentrations in polluted fog water.

The present model needs to be refined further; the main limitations now are the failure to include organic complexing agents and reductants and the rather simplistic treatment of the formation of complexes. Absorption of formaldehyde followed by formation of its sulfite complex ($HOCH_2SO_3^-$) must be considered in an advanced model; including this complex and others requires the use of multidimensional calculation routines such as SURFEQL to obtain the equilibrium concentrations of the species in the droplet.

ACKNOWLEDGMENTS

The authors acknowledge gratefully the financial support of the U.S. Environmental Protection Agency (Grant No. R808086-1) and the President's Fund/Sloan Foundation Grant administered by the California Institute of Technology. They are also grateful to S. Schwartz, J. Seinfeld and G. McRae for their helpful comments.

APPENDIX: THE ELECTRONEUTRALITY EQUATION

The ionic species in the fog droplets must satisfy the following electroneutrality equation:

$$[H^+] + [NH_4^+] + [Na^+] + 3[Fe^{3+}] + 2[Mn^{2+}] = [OH^-] + [HCO_3^-] + 2[CO_3^{2-}] + [HSO_3^-] + 2[SO_3^{2-}] + 2[SO_4^{2-}] + [NO_3^-] + [Cl^-]$$

where the iron and manganese complexes have been omitted for now to allow the equation to be solved by the one-dimensional Newton's method. Fe^{3+} and Mn^{2+} are assumed to be introduced in the liquid phase through ACCN containing $FeCl_3$ and $MnCl_2$.

In the closed two-phase system considered here the mass balance equation for component A can be written:

$$A_T = \frac{P_A}{RT} + L[A(aq)]$$

where P_A = atmospheric partial pressure of A
$[A(aq)]$ = concentration of A in the liquid phase (where A may be distributed among different species)
L = LWC (liters of water per liters of air)
A_T = total double-phase concentration of A in a liter of air (note that $L \ll 1$); a constant for the system

For sulfur(IV), for example,

$$S_T = \frac{P_{SO_2}}{RT} + L([SO_2(\ell)] + [HSO_3^-] + [SO_3^{2-}])$$

From Table XIII:

$$K_7 = \frac{[SO_2(\ell)]}{P_{SO_2}}$$

$$K_8 = \frac{[HSO_3^-][H^+]}{[SO_2(\ell)]}$$

$$K_9 = \frac{[SO_3^{2-}][H^+]}{[HSO_3^-]}$$

which yields

$$[SO_3^{2-}] = \frac{K_7K_8K_9}{[H^+]^2} S_T \left(\frac{1}{\frac{1}{RT} + L\left(K_7 + \frac{K_7K_8}{[H^+]} + \frac{K_7K_8K_9}{[H^+]^2}\right)} \right)$$

In this manner the electroneutrality equation can be rewritten:

$$[H^+] + \frac{K_5K_6[H^+]}{K_W} \left(\frac{[NH_3]_T}{\frac{1}{RT} + L\left(K_5 + \frac{K_5K_6[H^+]}{K_W}\right)} \right) + [Na^+] + 3[Fe^{3+}] + 2[Mn^{2+}]$$

$$= \frac{K_W}{[H^+]} + \frac{K_2K_3}{[H^+]} P_{CO_2} + \frac{2K_2K_3K_4}{[H^+]^2} P_{CO_2} + \frac{K_7K_8}{[H^+]}$$

$$\times \left(\frac{S_T}{\frac{1}{RT} + L\left(K_7 + \frac{K_7K_8}{[H^+]} + \frac{K_7K_8K_9}{[H^+]^2}\right)} \right)$$

$$+ \frac{2K_7K_8K_9}{[H^+]^2} \left(\frac{S_T}{\frac{1}{RT} + L\left(K_7 + \frac{K_7K_8}{[H^+]} + \frac{K_7K_8K_9}{[H^+]^2}\right)} \right)$$

$$+ 2[SO_4^{2-}] + \frac{K_{11}}{[H^+]} \frac{[NO_3]_T}{\frac{1}{RT} + \frac{LK_1}{[H^+]}} + [Cl^-]$$

which is of the form $f([H^+]) = 0$ and is readily solved by Newton's method.

REFERENCES

1. Calvert, J.G., F. Su, J.W. Bottenheim and O.P. Strausz. "Mechanisms of Homogeneous Oxidation of Sulfur Dioxide in the Troposphere," *Atmos. Environ.* 12:197–226 (1978).
2. Middleton, P., C.S. Kiang and V.A. Mohnen. "Theoretical Estimates of the Relative Importance of Various Urban Sulfate Aerosol Production Mechanisms," *Atmos. Environ.* 14:463–472 (1980).
3. Möller, D. "Kinetic Model of Atmospheric Oxidation Based on Published Data," *Atmos. Environ.* 14:1067–1076 (1980).
4. Cass, G.R., and F.H. Shair. "Transport of Sulfur Oxides Within the Los Angeles Sea Breeze/Land Breeze Circulation System," in *Proceedings of the Second Joint Conference on Applications of Air Pollution Meteorology* (American Meteorological Society, 1980), pp. 320–327.
5. Cass, G.R. "Methods for Sulfate Air Quality Management with Applications to Los Angeles," PhD Thesis, California Institute of Technology, Pasadena, CA (1977).
6. Cox, R.A. "Particle Formation from Homogeneous Reactions of Sulfur Dioxide and Nitrogen Dioxide," *Tellus* 26:235–240 (1974).
7. McMurry, P.H., D.J. Rader and J.L. Smith. "Studies of Aerosol Formation in Power Plant Plumes. I. Parameterization of Conversion Rate for Dry, Moderately Polluted Ambient Conditions," *Atmos. Environ.* 15:2315–2329 (1981).
8. Smith, F.B., and G.H. Jeffrey. "Airborne Transport of Sulphur Dioxide from the U.K.," *Atmos. Environ.* 9:643–659 (1975).
9. Wilson, J.C., and P.H. McMurry. "Studies of Aerosol Formation in Power Plant Plumes—I. Secondary Aerosol Formation in the Navajo Generating Station Plume," *Atmos. Environ.* 15:2329–2339 (1981).
10. Liljestrand, H.M., and J.J. Morgan. "Spatial Variation of Acid Precipitation in Southern California," *Environ. Sci. Technol.* 15:333–339 (1981).
11. Gartrell, J.E., J.W. Thomas and S.B. Carpenter. "Atmospheric Oxidation of SO_2 in Coal-Burning Power Plant Plumes," *Am. Ind. Hyg. Assoc. Quart.* 24:113–120 (1963).
12. Diffenhoeffer, A.C., and R.G. dePena. "A Study of Production and Growth of Sulfate Particles in Plumes from a Coal-Fired Power Plant," *Atmos. Environ.* 12:297–306 (1978).
13. Enger, L., and U. Hogstrom. "Dispersion and Wet Deposition of Sulfur from a Power Plant Plume," *Atmos. Environ.* 13:797–810 (1979).
14. Waldman, J.M., J.W. Munger, D.J. Jacob, R.C. Flagan, J.J. Morgan and M.R. Hoffmann. "Chemical Composition of Acid Fog," *Science* 218:677–680 (1982).
15. Hegg, D.A., and P.V. Hobbs. "Cloud Water Chemistry and the Production of Sulfates in Clouds," *Atmos. Environ.* 15:1597–1604 (1981).
16. "Guide for Air Pollution Avoidance. Appendix B. History of Episodes," PH-22-68-32, U.S. EPA (1971), pp. 123–135.
17. Wilkins, E.T. "Air Pollution and the London Fog of December, 1952," *J. Roy. San. Instit.* 74:1–21 (1954).
18. Wilkins, E.T. "Air Pollution Aspects of the London Fog of December, 1952," *J. Roy. Meteorol. Soc.* 80:267–278 (1954).
19. Holland, W.W. *Air Pollution and Respiratory Disease* (Westport, CT: Technomic Publishing Co., Inc., 1972), pp. 27–51.
20. Friedlander, S.K., and A.L. Ravimohan. "A Theoretical Model for the Effect of an

Acute Air Pollution Episode on a Human Population," *Environ. Sci. Technol.* 2:1101–1108 (1968).

21. Larsen, R.I. "Relating Air Pollutant Effects to Concentration and Control," *J. Air Poll. Control Assoc.* 20:214–225 (1970).
22. Cheng, R.T., M. Corn and J.O. Frohliger. "Contributions to the Reaction Kinetics of Water-Solubles and SO_2 in Air at ppm Concentrations," *Atmos. Environ.* 5:987–1008 (1971).
23. Beilke, S., and G. Gravenhorst. "Heterogeneous SO_2-Oxidation in the Droplet Phase," *Atmos. Environ.* 12:231–239 (1978).
24. Dasgupta, P.K., P.A. Mitchell and P.W. West. "Study of Transition Metal–S(IV) Systems," *Atmos. Environ.* 13:775–782 (1979).
25. Freiberg, J. "Effects of Relative Humidity and Temperature on Iron-Catalyzed Oxidation of SO_2 in Atmospheric Aerosols," *Environ. Sci. Technol.* 8:731–734 (1974).
26. Fuzzi, S. "Study of Iron(III) Catalyzed Sulphur Dioxide Oxidation in Aqueous Solution over a Wide Range of pH," *Atmos. Environ.* 12:1439–1442 (1978).
27. Hegg, D.A., and P.V. Hobbs. "Oxidation of Sulfur Dioxide in Aqueous Systems with Particular Reference to the Atmosphere," *Atmos. Environ.* 12:241–253 (1978).
28. Kaplan, D.J., D.M. Himmelblau and C. Kanaoka. "Oxidation of Sulfur Dioxide in Aqueous Ammonium Sulfate Aerosols Containing Manganese as a Catalyst," *Atmos. Environ.* 15:763–773 (1981).
29. Larson, T.V., N.R. Horike and H. Halstead. "Oxidation of Sulfur Dioxide by Oxygen and Ozone in Aqueous Solution: A Kinetic Study with Significance to Atmospheric Processes," *Atmos. Environ.* 12:1597–1611 (1978).
30. Penkett, S.A., B.M.R. Jones and A.E.J. Eggleton. "A Study of SO_2 Oxidation in Stored Rainwater Samples," *Atmos. Environ.* 13:139–147 (1979).
31. Hoffmann, M.R., and J.O. Edwards. "Kinetics and Mechanism of the Oxidation of Sulfur Dioxide by Hydrogen Peroxide in Acidic Solution," *J. Phys. Chem.* 79:2096–2098 (1975).
32. Penkett, S.A., B.M.R. Jones, K.A. Brice and A.E.J. Eggleton. "The Importance of Atmospheric Ozone and Hydrogen Peroxide in Oxidizing Sulfur Dioxide in Cloud and Rainwater," *Atmos. Environ.* 13:123–137 (1979).
33. Martin, L.R., and D.E. Damschen. "Aqueous Oxidation of Sulfur Dioxide by Hydrogen Peroxide at Low pH," *Atmos. Environ.* 15:1615–1622 (1981).
34. Martin, L.R., D.E. Damschen and H.S. Judeikis. "Sulfur Dioxide Oxidation Reactions in Aqueous Solution," EPA 600/7-81-085, U.S. EPA (1981).
35. Thornton, J.D. "The Metal and Strong Acid Composition of Rain and Snow in Minnesota: Land Use Effects," MS Thesis, University of Minnesota, Minneapolis, MN (1981).
36. Overton, J.H., V.P. Aneja and J.L. Durham. "Production of Sulfate in Rain and Raindrops in Polluted Atmospheres," *Atmos. Environ.* 13:355–367 (1979).
37. Brimblecombe, P., and D.J. Spedding. "The Catalytic Oxidation of Micromolar Aqueous Sulphur Dioxide," *Atmos. Environ.* 8:937–945 (1974).
38. Middleton, P., C.S. Kiang and V.A. Mohnen. "Theoretical Estimates of the Relative Importance of Various Urban Sulfate Aerosol Production Mechanisms," *Atmos. Environ.* 14:463–472 (1980).
39. Barrie, L.A., and H.W. Georgii. "An Experimental Investigation of the Absorption of Sulfur Dioxide by Water Drops Containing Heavy Metal Ions," *Atmos. Environ.* 10:743–749 (1976).
40. Hoffmann, M.R., and S.D. Boyce. "Catalytic Autoxidation of Aqueous Sulfur Dioxide

in Relationship to Atmospheric Systems." *Adv. Environ. Sci. Tech.* 12, 148–189 Wiley-Interscience, New York (1983).

41. Mader, P.M. "Kinetics of the Hydrogen Peroxide–Sulfite Reaction in Solution," *J. Am. Chem. Soc.* 80:2634 (1958).
42. Halperin, J., and H. Taube. "The Transfer of Oxygen Atoms in Oxidation-Reduction Reactions. IV. The Reaction of Hydrogen Peroxide with Sulfite and Thiosulfate, and of Oxygen, Manganese Dioxide and Permanganate with Sulfite," *J. Am. Chem. Soc.* 74:380–382 (1952).
43. Harrison, H., T.V. Larson and C.S. Monkman. "Aqueous Phase Oxidation of Sulfites by Ozone in the Presence of Iron and Manganese," *Atmos. Environ.* 16:1039–1041 (1982).
44. Hoffmann, M.R. "Trace Metal Catalysis in Aquatic Environments," *Environ. Sci. Technol.* 14:1061–1066 (1980).
45. Frank, S.N., and A.J. Bard. "Heterogeneous Photocatalytic Oxidation of Cyanide and Sulfite in Aqueous Solution at Semiconductor Powders," *J. Phys. Chem.* 81:1484–1488 (1977).
46. Mishra, G.C., and R.D. Srivastava. "Homogeneous Kinetics of Potassium Sulfite Oxidation," *Chem. Eng. Sci.* 31:969–971 (1976).
47. Boreskov, G.K., R.A. Buyanov and A.A. Ivanov. "Kinetics of Sulfur Dioxide on Vanadium Catalysts," *Kinetika Kataliz* 8:153–159 (1967).
48. Sung, W., and J.J. Morgan. "Kinetics and Products of Ferrous Iron Oxygenation in Aqueous Systems," *Environ. Sci. Technol.* 14:561–568 (1981).
49. Beilke, S., and G. Gravenhorst. "Heterogeneous SO_2-Oxidation in the Droplet Phase," *Atmos. Environ.* 12:231–239 (1978).
50. Bäckström, H. "Der Kettenmechanisms bei der Autoxydation von Natriumsulfitlösungen." *Z. Physik. Chem.* 25B:122–138 (1934).
51. Moore, J.W., and R.G. Pearson. *Kinetics and Mechanism* (New York: Wiley-Interscience, 1981).
52. Boudart, M. *The Kinetics of Chemical Processes* (Englewood Cliffs, NJ: Prentice-Hall, Inc., 1968), pp. 246.
53. Coughanowr, D.R., and F.E. Krause. "The Reaction of SO_2 and O_2 in Aqueous Solutions of $MnSO_4$," *Ind. Eng. Chem. Fund.* 4:61–66 (1965).
54. Ibusuki, T. "Manganese(II) Catalyzed Sulfur Dioxide Oxidation in Aqueous Solution at Environmental Concentrations over a Wide Range of pH," *Atmos. Environ.* (in press).
55. Matteson, J.J., W. Stöber and H. Luther. "Kinetics of the Oxidation of Sulfur Dioxide by Aerosols of Manganese Sulfate," *Ind. Eng. Chem. Fund.* 8:677–684 (1969).
56. Lunak, S., A. El-Wakil and J. Veprek-Siska. "Autoxidation of Sulfite Catalyzed by 3d Transition Metals and Inhibited by 2-Propanol: Mechanism of Inhibited and Induced Reactions," *Coll. Czech. Chem. Comm.* 43:3306–3316 (1978).
57. Aubuchon, C. "The Rate of Iron Catalyzed Oxidation of Sulfur Dioxide by Oxygen in Water," PhD Thesis, Johns Hopkins University, Baltimore, MD (1976).
58. Chen, T.I., and C.H. Barron. "Some Aspects of the Homogeneous Kinetics of Sulfite Oxidation," *Ind. Eng. Chem. Fund.* 11:466–470 (1972).
59. Sawicki, J.E., and C.H. Barron. "On the Kinetics of Sulfite Oxidation in Heterogeneous Systems," *Chem. Eng. J.* 5:153–159 (1973).
60. Bengtsson, S., and I. Bjerle. "Catalytic Oxidation of Sulphite in Dilute Aqueous Solutions," *Chem. Eng. Sci.* 30:1429–1435 (1975).

61. Yagi, S., and H. Inoue. "The Absorption of Oxygen into Sodium Sulfite Solution," *Chem. Eng. Sci.* 17:411–421 (1962).
62. Davies, R., A.K.E. Hagopian and A.G. Sykes. "Kinetic and Oxygen-18 Tracer Studies on the Reaction of Sulphite with the Superoxo-Complex $(NH_3)_5Co \cdot O_2 \cdot Co(NH_3)_5^{5+}$ in Aqueous Media," *J. Chem. Soc.* (A):623–629 (1969).
63. Linek, V., and J. Mayrhoferova. "The Kinetics of Oxidation of Aqueous Sodium Sulfite Solution," *Chem. Eng. Sci.* 25:787–800 (1970).
64. Mishra, G.C., and R.D. Srivastava. "Kinetics of Oxidation of Ammonium Sulfite by Rapid-Mixing Method," *Chem. Eng. Sci.* 30:1387–1390 (1975).
65. Fuller, E.C., and R.H. Crist. "The Rate of Oxidation of Sulfite Ions by Oxygen," *J. Am. Chem. Soc.* 63:1644–1650 (1941).
66. Barron, C.H., and H.A. O'Hern. "Reaction Kinetics of Sodium Sulfite by the Rapid-Mixing Method," *Chem. Eng. Sci.* 21:397–404 (1966).
67. Hayon, E., A. Treinin and J. Wilf. "Electronic Spectra, Photochemistry, and Autoxidation Mechanism of the Sulfite-Bisulfite-Pyrosulfite Systems. The SO_2^-, SO_3^-, and SO_5^- Radicals," *J. Am. Chem. Soc.* 94:47–57 (1972).
68. Schmittkunz, H. "Chemilumineszenz der Sulfitooxidation," Dissertation, Naturwissenschaftliche Fakultät, Frankfurt (1963).
69. Bassett, H., and W.G. Parker. "The Oxidation of Sulphurous Acid," *J. Chem. Soc.* (1951), pp. 1540–1560.
70. King, E.L., and C. Altman. "A Schematic Method of Deriving the Rate Laws for Enzyme Catalyzed Reactions," *J. Phys. Chem.* 60:1375–1378 (1956).
71. Freiberg, J. "The Mechanism of Iron-Catalyzed Oxidation of SO_2," *Atmos. Environ.* 9:661–672 (1975).
72. Bracewell, J.M., and D. Gall. "The Catalytic Oxidation of Sulfur Dioxide in Solution at Concentrations Occurring in Fog Droplets," paper presented at the Symposium on Physio-chemical Transformation of Sulfur Compounds in the Atmosphere and the Formation of Acid Smogs, Mainz, Germany, 1967.
73. Hoather, R.C., and C.F. Goodeve. "The Oxidation of Sulphurous Acid III. Catalysis by Manganous Sulphate," *Trans. Faraday Soc.* 30:1149–1156 (1934).
74. Neytzell-deWilde, F.G., and L. Taverner. "Experiments Relating to Possible Production of Air Oxidizing Acid Leach Liquor by Autoxidation for the Extraction of Uranium," *2nd U.N. Intl. Conf. Peaceful Uses for Atomic Energy Proc.* 3:303–317 (1958).
75. Karraker, D.G. "The Kinetics of the Reaction Between Sulfurous Acid and Ferric Ion," *J. Phys. Chem.* 67:871–874 (1963).
76. Pollard, F.H., P. Hanson and G. Nickless. "Chromatographic Studies on the Oxidation of Sulphurous Acid by Ferric Iron in Aqueous Acid Solution," *J. Chromatog.* 5:68–73 (1961).
77. Carlyle, D.W. "A Kinetic Study of the Aquation of Sulfitoiron(III) Ion," *Inorg. Chem.* 10:761–764.
78. Lancaster, J.M., and R.S. Murray. "The Ferricyanide-Sulphite Reaction," *J. Chem. Soc.* (1971), pp. 2755–2758.
79. Veprek-Siska, J., D.M. Wagnerova, and K. Eckschlager. "Einäequivalent-Oxydationen. II. Sulfitoxydation Durch Komplexionen," *Coll. Czech. Chem. Comm.* 31:1248–1255 (1966).
80. Veprek-Siska, J., A. Solcova and D.M. Wagnerova. "Einäequivalent-Oxydationen. III. Kinetik der Sulfitoxydation Mittels Pentacyanoaquoferrats(III)," *Coll. Czech. Chem. Comm.* 31:3287–3298 (1966).

81. Carlyle, D.W., and O.T. Zeck, Jr. "Electron Transfer Between Sulfur(IV) and Hexaaquoiron(III) Ion in Aqueous Perchlorate Solution. Kinetics and Mechanisms of Uncatalyzed and Cu(II)-Catalyzed Reactions," *Inorg. Chem.* 12:2978–2983.
82. Higginson, W.C.E., and J.W. Marshall. "Equivalence Changes in Oxidation-Reduction Reactions in Solution: Some Aspects of the Oxidation of Sulphurous Acid," *J. Chem. Soc.* (1957), pp. 447–458.
83. Reinders, W., and S.I. Vles. "The Catalytic Oxidation of Sulfites," *Rec. Trav. Chem.* 44:249–268 (1925).
84. Titoff, A. "Beiträge zur Kenntnis der Negativen Katalyse in Homogeneous System," *Z. Phys. Chem.* 45:641–683 (1903).
85. Latimer, W. M. *Oxidation Potentials* 2nd ed. (New York: Prentice-Hall, Inc., 1952).
86. Srivastava, R.D., A.F. McMillan and I.J. Harris. "The Kinetics of Oxidation of Sodium Sulphite," *Can. J. Chem. Eng.* 46:181–184 (1968).
87. Yatsimirskii, K., B. Bratushko, I. Yu and I.L. Zatsny. "Kinetics and Mechanism of the Reduction of Molecular Oxygen Coordinated in the Complex Co_2(L-histidine)$_4O_2$ by Sodium Sulphite in Aqueous Solution," *Zh. Neorgan. Khimii.* 22:1611–1616 (1977).
88. Abel, E.W., J.M. Pratt and R. Whelan. "Formation of a 1:1 Oxygen Adduct with the Cobalt(II)-Tetrasulphophthalocyanine Complex," *Chem. Commun.* (1971), pp. 449–450.
89. Jones, R.D., D.A. Summerville and F. Basolo. "Synthetic Oxygen Carriers Related to Biological Systems," *Chem. Revs.* 79:139–179 (1979).
90. Hoffmann, M.R., and B.C.H. Lim. "Kinetics and Mechanism of the Oxidation of Sulfide by Oxygen: Catalysis by Homogeneous Metal-Phthalocyanine Complexes," *Environ. Sci. Technol.* 13:1406–1413 (1979).
91. Boyce, S.D., M.R. Hoffmann, P.A. Hong and L.M. Moberly. "Catalysis of the Autoxidation of Aquated Sulfur Dioxide by Homogeneous and Heterogeneous Transition Metal Complexes," in *Acid Rain, Vol. 1, Meteorological Aspects* (Ann Arbor, MI: Ann Arbor Science Publishers, 1983).
92. Laidler, K.J., and P.S. Bunting. *The Chemical Kinetics of Enzyme Action* (Oxford: Clarendon Press, 1973).
93. Carter, J.J., D.P. Rillema and F. Basolo. "Oxygen Carrier and Redox Properties of Some Neutral Cobalt Chelates," *J. Am. Chem. Soc.* 96:392–400 (1974).
94. Rollmann, L.D., and S.I. Chan. "Electron Spin Resonance Studies of Low-Spin Cobalt(II) Complexes. Base Adducts of Cobalt Phthalocyanine," *Inorg. Chem.* 10:1978–1982 (1971).
95. Cookson, D.J., T.D. Smith, J.F. Boas, P.R. Hicks and J.R. Pilbrow. "Electron Spin Resonance Study of the Autoxidation of Hydrazine, Hydroxylamine and Cysteine Catalyzed by the Cobalt(II) Chelate Complex of 3,10,17,24-Tetrasulphophthalocyanine," *J. Chem. Soc.* (1977), pp. 109–114.
96. Przywarska-Boniecka, H., and K. Fried. "The Influence of Additional Ligands on Autoxidation of Cobalt and Iron 4,4′,4″,4‴-Tetrasulfonated Phthalocyanines," *Roczniki Chemii.* 50:43–52 (1976).
97. Basolo, F., B. M. Hoffmann and J.A. Ibers. "Synthetic Oxygen Carriers of Biological Interest," *Accts. Chem. Res.* 8:384–392 (1975).
98. Schutten, J.H., and T.P.M. Beelen. "The Role of Hydrogen Peroxide During the Autoxidation of Thiols Promoted by Bifunctional Polymer-Bonded Cobalt Phthalocyanine Catalysts," *J. Mol. Catal.* 10:85–97 (1981).

99. Zika, R., and E. Saltzman. "Interaction of Ozone and Hydrogen Peroxide in Water: Implications for Analysis of H_2O_2 in Air," *Geophys. Res. Lett.* 9:213–234 (1982).
100. Egerton, A.C., A.J. Everett, G.J. Minkoff, S. Rudrakanchana and K.C. Salooja. "Some Improvements in the Methods of Analysis of Peroxides," *Anal. Chim. Acta* 10:422–429 (1954).
101. Holt, B.D., R. Kumar and P.T. Cunningham. "Oxygen-18 Study of the Aqueous Phase Oxidation of Sulfur Dioxide," *Atmos. Environ.* 15:557–566 (1981).
102. Frost, A.A., and R.G. Pearson. *Kinetics and Mechanism.* (New York: John Wiley & Sons, Inc., 1961).
103. Anast, J.M., and D.W. Margerum. "Trivalent Copper Catalysis of the Autoxidation of Sulfite. Kinetics and Mechanism of the Copper (III/II) Tetraglycine Reactions with Sulfite," *Inorg. Chem.* 20:2319–2326 (1981).
104. Edwards, J.O. *Inorganic Reaction Mechanisms* (Reading, MA: W.A. Benjamin, Inc., 1965).
105. Edwards, J.O., E.F. Greene and J. Ross. "From Stoichiometry and Rate Law to Mechanism," *J. Chem. Educ.* 45:381–385 (1968).
106. Bunnet, J.F. "From Kinetic Data to Reaction Mechanism," in *Investigation of Rates and Mechanisms of Reactions Part I,* 3rd ed., E.S. Lewis, Ed. (New York: Wiley-Interscience, 1974).
107. Smith, R.M., and A.M. Martell. *Critical Stability Constants, Vol. 4, Inorganic Complexes* (New York, Plenum Press, 1976).
108. Langford, C.H., and H.B. Gray. *Ligand Substitution Processes.* (Reading, MA: W.A. Benjamin, Inc., 1966).
109. Bernasconi, C.F. *Relaxation Kinetics* (New York: Academic Press, Inc., 1976).
110. Taube, H. *Electron Transfer Reactions of Complex Ions in Solution* (New York: Academic Press, Inc., 1970).
111. Fuoss, R.M. "Ion Association III. The Equilibrium Between Ion Pairs and Free Ions," *J. Am. Chem. Soc.* 80:5059–5061 (1958).
112. Davis, G.G., and W.F. Smith. "The Kinetics of the Formation of the Monosulphate Complex of Iron(III) in Aqueous Solution," *Can. J. Chem.* 40:1836–1845 (1962).
113. Basolo, F., and R.G. Pearson. *Mechanisms of Inorganic Reactions* (New York: John Wiley & Sons, Inc., 1967).
114. Groves, J.T. In: *Metal Ion Activation of Dioxygen,* T.G. Spiro, Ed. (New York: John Wiley & Sons, Inc., 1979).
115. Mathews, H.J., and L.H. Dewey. "A Quantitative Study of Some Photochemical Effects Produced by Ultra-Violet Light." *J. Phys. Chem.* 17:211–218 (1912).
116. Mathews, H.J., and M.E. Weeks. "The Effect of Various Substances on the Photochemical Oxidation of Solutions of Sodium Sulfite," *J. Am. Chem. Soc.* 39:635–647 (1917).
117. Mason, R.B., and J.H. Mathews. "The Effect of Ultra-Violet Light on the Oxidation of Sodium Sulfite by Atmospheric Oxygen," *J. Phys. Chem.* 30:414–420 (1926).
118. Alyea, H.N., and L.J. Bäckström. "The Inhibition Action of Alcohols on the Oxidation of Sodium Sulfite," *J. Am. Chem. Soc.* 51:90–109 (1929).
119. Haber, F., and O.H. Wansbrough-Jones. "Uber die Einwirkung des Lichtes auf Sauerstoffreie und Sauerstoffhaltige Sulfitlösung," *Z. Phys. Chem.* B18:103–123 (1931).
120. Norman, R.O.C., and P.M. Storey. "Electron Spin Resonance Studies. Part XXXI. The Generation, and Some Reactions of the Radicals SO_3^-, $S_2O_3^-$, S^- and HS· in Aqueous Solution," *J. Chem. Soc.* (B):1009–1013 (1971).
121. Dogliotti, L., and E. Hayon. "Flash Photolysis Study of Sulfite, Thiocyanate and Thiosulfate Ions in Solution," *J. Phys. Chem.* 72:1800–1807 (1967).

122. Bäckström, H.L.J. "The Chain Reaction Theory of Negative Catalysis," *J. Am. Chem. Soc.* 49:1460–1472 (1927).
123. Bäckström, H.L.J. "Der Kettenmechanisms bei der Autoxydation von Aldehyden," *Z. Phys. Chem.* (Leipzig) B25:99–121 (1934).
124. Abel, E. "Zur Theorie der Oxydation von Sulfit zur Sulfat durch Sauerstoff," *Monatsch. Chem.* 82:815–834 (1951).
125. Matsuura, A., J. Harada, T. Akehata and T. Shirai. "Rate of Ammonium Sulfite Oxidation in Aqueous Solution," *J. Chem. Eng. Japan* 2:199–203 (1969).
126. Lunak, S., and J. Veprek-Siska. "Photochemical Autoxidation of Sulfite Catalyzed by Iron(III) Ions," *Coll. Czech. Chem. Commun.* 41:3495–3503 (1976).
127. Lunak, S., and J. Veprek-Siska. "Catalytic Effect of Metal Ions on Photochemical Reactions of Molecular Oxygen. III. Photochemical Autoxidation of Sulfite Catalyzed by Manganese(II) Ions," *Reac. Kin. Catal. Lett.* 5:157–161 (1976).
128. Veprek-Siska, J., S. Lunak and A. El-Wakil. "Catalytic Effect of Ferric Ions on the Photoinitiated Autoxidation of Sulfite," *Z. Naturforsch.* 29B:812–813 (1974).
129. Balzani, V., and V. Carassiti. *Photochemistry of Coordination Compounds* (New York: Academic Press, Inc., 1970).
130. Langford, C.H., M. Wingham and V.S. Sastri. "Ligand Photooxidation in Copper(II) Complexes of Nitrilotriacetic Acid," *Environ. Sci. Technol.* 7:820–822 (1973).
131. Langford, C.H., and J.H. Carey. "The Charge Transfer Photochemistry of the Hexaaquoiron(III) Ion, the Chloropentaaquoiron(III) Ion, and the μ-Dihydroxo Dimer Explored with tert-Butyl Alcohol Scavenging," *Can. J. Chem.* 53:2430–2435 (1975).
132. Lockhart, H.B., Jr., and R.V. Blakeley. "Aerobic Photodegradation of Fe(III)-(Ethylenedinitrilo) Tetraacetate (Ferric EDTA)," *Environ. Sci. Technol.* 12:1035–1038 (1975).
133. Miles, C.J., and P.L. Brezonik. "Oxygen Consumption in Humic-Colored Waters by a Photochemical Ferrous-Ferric Catalytic Cycle," *Environ. Sci. Technol.* 15:1089–1095 (1981).
134. Baker, A.D., A. Casadavell, H.D. Gafney and M. Gellender. "Photochemical Reactions of Tris(oxalato) Iron(III)," *J. Chem. Educ.* (1980), pp. 314–315.
135. Taylor, D.D., and R.C. Flagan. "Aerosols from a Laboratory Pulverized Coal Combustor," in *Atmospheric Aerosol: Source/Air Quality Relationships,* E.S. Macias and P.K. Hopke, Eds., ACS Symp. Ser No. 167 (Washington, DC: American Chemical Society, pp. 157–172 (1981).
136. Ouimette, J.R., and R.C. Flagan. "Chemical Species Contributions to Light Scattering by Aerosols at a Remote Arid Site," in *Atmospheric Aerosol: Source/Air Quality Relationships,* E.S. Macias and P.K. Hopke, Eds., ACS Symp. Ser. No. 167 (Washington, DC: American Chemical Society, 1981), pp. 125–156.
137. Adamson, A.W., and P.D. Fleischauer. *Concepts of Inorganic Photochemistry* (New York: Wiley-Interscience, 1975).
138. Brodzinsky, R., S.G. Chang, S.S. Markowitz and T. Novakov. "Kinetics and Mechanism for the Catalytic Oxidation of Sulfur Dioxide on Carbon in Aqueous Suspensions," *J. Phys. Chem.* 84:3354–3358 (1980).
139. Chang, S.G., R. Toosi and T. Novakov. "The Importance of Soot Particles and Nitrous Acid in Oxidizing SO_2 in Atmospheric Aqueous Droplets," *Atmos. Environ.* 12:297–306 (1981).
140. Cohen, S., S. Chang, S. Markowitz and T. Novakov. "Role of Fly Ash in Catalytic Oxidation of S(IV) Slurries," *Environ. Sci. Technol.* 15:1498–1502 (1981).

141. Kim, K.K., and J.S. Choi. "Kinetics and Mechanism of the Oxidation of Sulfur Dioxide on α-Fe_2O_3," *J. Phys. Chem.* 85:2447–2450 (1981).
142. Faust, B.C., and M.R. Hoffmann. "Photocatalytic Oxidation of Dissolved Sulfur Dioxide on Fe_2O_3 Surfaces" (in progress).
143. Childs, A.L. "Studies in Photoassisted Heterogeneous Catalysis," PhD Thesis, Princeton University, Princeton, NJ (1981).
144. Childs, L.P., and D.F. Ollis. "Is Photocatalysis Catalytic?" *J. Catal.* 66:383–390 (1980).
145. Benner, W.H., R. Brodzinsky and T. Novakov. "Oxidation of SO_2 in Droplets Which Contain Soot Particles," *Atmos. Environ.* 16:1333–1340 (1982).
146. Colton, F.A., and G. Wilkinson. *Advanced Inorganic Chemistry* (New York: John Wiley & Sons, Inc., 1980).
147. Roberts, J.D., S. Ross and M.C. Caserio. *Organic Chemistry* (Menlo Park, CA: W.A. Benjamin, Inc., 1971).
148. Fridovich, I., and P. Handler. "Detection of Free Radicals in Illuminated Dye Solutions by the Initiation of Sulfite Oxidation," *J. Biol. Chem.* 235:1835–1838 (1960).
149. McCord, J.M., and I. Fridovich. "The Utility of Superoxide Dismutase in Studying Free Radical Reactions," *J. Biol. Chem.* 214:6056–6063 (1969).
150. Srinivasan, V.S., D. Podolski, N.J. Westrick and D.C. Neckers. "Photochemical Generation of O_2^- by Rose Bengal and $Ru(bpy)_3^{2+}$," *J. Am. Chem. Soc.* 100:6513–6515 (1978).
151. Zika, R.G. "Photochemical Generation and Decay of Hydrogen Peroxide in Seawater," *Trans. Am. Geophys. Union* 61:1010 (1980).
152. Kok, G.L., T.P. Holler, M.B. Lopez, H.A. Nachtrieb and M. Yuan. "Chemiluminescent Method for Determination of Hydrogen Peroxide in the Ambient Atmosphere," *Environ. Sci. Technol.* 12:1072–1076 (1978).
153. Kok, G.L., K.R. Darnall, A.M. Winer, J.N. Pitts, Jr. and B.W. Gay. "Ambient Air Measurements of Hydrogen Peroxide in the California South Coast Basin," *Environ. Sci. Technol.* 12:1077–1080 (1978).
154. Kok, G.L. "Measurements of Hydrogen Peroxide in Rainwater," *Atmos. Environ.* 14:653–656 (1980).
155. Kok, G.L. "Measurements of Hydrogen Peroxide in Rainwater," *EOS Trans. Am. Geophy. Union* 45:884 (1981).
156. Walling, C. "Fenton's Reagent Revisited," *Accts. Chem. Res.* 12:125–131 (1975).
157. Baxendale, J. H. "Decomposition of Hydrogen Peroxide by Catalysts in Homogeneous Aqueous Solution," *Adv. Catal.* 4:31 (1952).
158. Uri, N. "Inorganic Free Radicals in Solution," *Chem. Rev.* 50:375 (1952).
159. Barrie, L.A. "An Experimental Investigation of the Absorption of Sulfur Dioxide by Cloud and Raindrops Containing Heavy Metals," PhD Thesis, University of Frankfurt (1975).
160. Penkett, S.A. "Oxidation of SO_2 and Other Atmospheric Gases by Ozone in Aqueous Solution," *Nature, Phys. Sci.* 240:105–106 (1972).
161. Erickson, R.E., L.M. Yates, R.L. Clark and D. McEwen. "The Reaction of Sulfur Dioxide with Ozone in Water and Its Possible Atmospheric Significance," *Atmos. Environ.* 11:813–817 (1977).
162. Espenson, J.H., and H. Taube. "Tracer Experiments with Ozone as Oxidizing Agent in Aqueous Solution," *Inorg. Chem.* 4:704–709 (1965).
163. Martin, L.R., D.E. Damschen and H.S. Judeikis. "The Reactions of Nitrogen Oxides with SO_2 in Aqueous Solution," *Atmos. Environ.* 15:191–195 (1981).
164. Oblath, S.B., S.S. Markowitz, T. Novakov and S.G. Chang. "Kinetics of Formation

of Hydroxylamine Disulfonate by Reaction of Nitrite with Sulfites," *J. Phys. Chem.* 85:1017–1021 (1981).

165. Ross, D.S., C.L. Gu, G.P. Hum and D.G. Hendry. "Catalytic Oxidation of SO_2 by NO_x in Aqueous Systems" (submitted).
166. Grätzel, M., S. Taniguchi and A. Henglein. "Pulsradiolytisch Untersuchung der NO-Oxydation und des Gleichgewichts $N_2O_3 \rightleftharpoons NO + NO_2$ in Wässriger Lösung," *Ber. Bunsenges. Phys. Chem.* 74:488–492 (1970).
167. Takeuchi, H., M. Ando and N. Kizawa. "Absorption of Nitrogen Oxides in Aqueous Sodium Sulfite and Bisulfite Solutions," *Ind. Eng. Chem. Des. Dev.* 16:303–308 (1977).
168. Nash, T. "The Effect of Nitrogen Dioxide and of Some Transition Metals on the Oxidation of Dilute Bisulfite Solutions," *Atmos. Environ.* 13:1149–1154 (1979).
169. Morel, F.M., and J.J. Morgan. "A Numerical Method for Computing Equilibria in Aqueous Chemical Systems," *Environ. Sci. Technol.* 6:58–67 (1972).
170. Hoffmann, M. R. "Thermodynamic, Kinetic and Extrathermodynamic Considerations in the Development of Equilibrium Models for Aquatic Systems," *Environ. Sci. Technol.* 15:345–353 (1981).
171. Westall, J.C., J.L. Zachary and F.M. Morel. "MINEQL, A Computer Program for the Calculation of Chemical Equilibrium Composition of Aqueous Solutions," Tech. Note 18, Department of Civil Engineering, Massachusetts Institute of Technology, Cambridge, MA (1976).
172. Westall, J.C., and H. Hohl. "A Comparison of Electrostatic Models for the Oxide/Solution Interface," *Adv. Coll. Interface Sci.* 12:265–294 (1980).
173. Hansen, L.D., L. Whiting, D.J. Eatough, T.E. Jensen and R.M. Izatt. "Determination of Sulfur(IV) and Sulfate in Aerosols by Thermometric Methods," *Anal. Chem.* 48:634–638 (1976).
174. Eider, R.C., M.J. Heeg, M.D. Payne, M. Trkula and E. Deutsch. "Trans Effect in Octahedral Complexes. 3. Comparison of Kinetic and Trans Effects Induced by Coordinated Sulfur in Sulfito- and Sulfinatopentaamminecobalt(III) Complexes," *Inorg. Chem.* 17:431–440 (1978).
175. Raston, C.L., A.H. White and J.K. Yandell. "Structural and Kinetic Effects in Cobalt(III) Complexes with Cobalt-Sulfur Bonds. The Crystal Structure of trans-Bis(ethylenediamine)-imidazolesulfitocobalt(III) Perchlorate Dihydrate," *Aust. J. Chem.* 31:993–998 (1978).
176. Magnusson, A., L.G. Johansson and O. Lindqvist. "The Structure of Manganese(II) Sulfite," *Acta Cryst.* B37:1108–1110 (1981).
177. Johansson, L.G., and E. Ljungström. "Structure of Iron(II) Sulfite 2.5 Hydrate," *Acta Cryst.* B36:1184–1186 (1980).
178. Johansson, L.G., and O. Lindqvist. "Manganese(II) Sulfite Trihydrate," *Acta Cryst.* B36:2739–2741 (1980).
179. Baldwin, M.E. "Sulphitobis(ethylenediamine)Cobalt(III) Complexes," *J. Chem. Soc.* (1961), pp. 3123–3128.
180. Bordwell, F.G. *Organic Chemistry* (New York: Macmillan Co., 1963).
181. Dasgupta, P.K., K. DeCesare and J.C. Ullrey. "Determination of Atmospheric Sulfur Dioxide without Tetrachloromercurate(II) and the Mechanism of the Schiff Reaction," *Anal. Chem.* 52:1912–1922 (1980).
182. Fortune, C.R., and B. Dellinger. "Stabilization and Analysis of Sulfur(IV) Aerosols in Environmental Samples," *Environ. Sci. Technol.* 16:62–66 (1982).
183. Pankow, J.F., and J.J. Morgan. "Kinetics for the Aquatic Environment," *Environ. Sci. Technol.* 15:1155–1164,1306–1313 (1981).
184. Adamowicz, R.F. "A Model for the Reversible Washout of Sulfur Dioxide, Ammonia

and Carbon Dioxide from a Polluted Atmosphere and the Production of Sulfates in Raindrops." *Atmos. Environ.* 13:105–121 (1979).

185. Baboolal, L.B., H.R. Pruppacher and J.H. Topalian. "A Sensitivity Study of a Theoretical Model of SO_2 Scavenging by Water Drops in Air," *J. Atmos. Sci.* 38:856–870 (1981).
186. Durham, J.L., J.H. Overton and V.P. Aneja. "Influence of Gaseous Nitric Acid on Sulfate Production and Acidity in Rain," *Atmos. Environ.* 15:1059–1068 (1981).
187. Easter, R.C., and P.V. Hobbs. "The Formation of Sulfates and the Enhancement of Cloud Condensation Nuclei in Clouds," *J. Atmos. Sci.* 31:1586–1594 (1974).
188. Seinfeld, J.H. *Lectures in Atmospheric Chemistry,* American Institute of Chemical Engineers Monograph Series 76 (1980).
189. Graham, R.A., and H.S. Johnston. "The Photochemistry of NO_3 and the Kinetics of the N_2O_5-O_3 System," *J. Phys. Chem.* 82:254–268 (1978).
190. Baulch, D.L., R.A. Cox, R.F. Hampson, Jr., J.A. Kerr, J. Troe and R.T. Watson. "Evaluated Kinetic and Photochemical Data for Atmospheric Chemistry," *J. Phys. Chem. Ref. Data* 9:295–471 (1980).
191. Richards, L.W. "Comments on the Oxidation of NO_2 to Nitrate—Day and Night," *Atmos. Environ.* (in press).
192. Schwartz, S.E., and J.E. Freiberg. "Mass-Transport Limitation to the Rate of Reaction of Gases in Liquid Droplets: Application to Oxidation of SO_2 in Aqueous Solutions," *Atmos. Environ.* 15:1129–1144 (1981).
193. Freiberg, J.E., and S.E. Schwartz. "Oxidation of SO_2 in Aqueous Droplets: Mass-Transport Limitation in Laboratory Studies and the Ambient Atmosphere," *Atmos. Environ.* 15:1145–1154 (1981).
194. Rodhe, B. "The Effect of Turbulence on Fog Formation," *Tellus* 14:49–86 (1962).
195. McRae, G.J. Personal communication.
196. *Kirk-Othmer Encyclopedia of Chemical Technology, Vol. 16,* 3rd ed., (1981), p. 701.
197. Beutier, D., and H. Renon. "Representation of NH_3-H_2S,H_2O-NH_3-CO_2-H_2O, and NH_3-SO_2-H_2O Vapor-Liquid Equilibria," *Ind. Eng. Chem. Process. Des. Dev.* 17:220–228 (1978).

CHAPTER V

A DYNAMIC MODEL FOR THE PRODUCTION OF H^+, NO_3^-, AND SO_4^{2-} IN URBAN FOG

by Daniel J. Jacob and Michael R. Hoffmann

Journal of Geophysical Research 88, 6611-6621 (1983)

JOURNAL OF GEOPHYSICAL RESEARCH, VOL. 88, NO. C11, PAGES 6611–6621, AUGUST 20, 1983

A Dynamic Model for the Production of H^+, NO_3^-, and SO_4^{2-} in Urban Fog

DANIEL J. JACOB AND MICHAEL R. HOFFMANN

Environmental Engineering Science, W. M. Keck Laboratories, California Institute of Technology, Pasadena, California 91125

The chemical composition of nighttime urban fog has been investigated using a hybrid kinetic and equilibrium model. Extremely high acidity may be imparted to the droplets by condensation and growth on acidic condensation nuclei or by in situ S(IV) oxidation. Important oxidants of S(IV) were found to be O_2 as catalyzed by Fe(III) and Mn(II), H_2O_2, and O_3. Formation of hydroxymethanesulfonate ion (HMSA) via the nucleophilic addition of HSO_3^- to CH_2O(l) significantly increased the droplet capacity for S(IV) but did not slow down the net S(IV) oxidation rate leading to fog acidification. Gas phase nitric acid, ammonia, and hydrogen peroxide were scavenged efficiently, although aqueous phase hydrogen peroxide was depleted rapidly by reduction with S(IV). Nitrate production in the aqueous phase was found to be dominated by HNO_3 gas phase scavenging. Major aqueous phase species concentrations were controlled primarily by condensation, evaporation, and pH.

INTRODUCTION

Concentrations of major ions in nonprecipitating clouds [*Hegg and Hobbs*, 1981] and fogs [*Waldman et al.*, 1982; *Munger et al.*, 1983] have been reported to be significantly higher than those commonly observed in acidic precipitation. In Los Angeles, fogwater [*Waldman et al.*, 1982; *Munger et al.*, 1983] was reported to have acidities 100 times higher than those observed previously in rainwater by *Liljestrand and Morgan* [1981]. Lower dilutions and higher scavenging efficiencies due to reduced mass transfer limitations of gas absorption and longer residence times may explain, in part, the higher concentrations found in fog (1–100 μm) than in rain (0.1–3.0 mm).

A number of rainwater and cloudwater chemistry models have been proposed recently. *Adamowicz* [1979] simulated the chemistry of raindrops falling through a well-mixed polluted layer with uniform and constant concentrations of SO_2, CO_2, and NH_3. Gas and aqueous phase equilibria were established at all times, and aqueous phase transformation of S(IV) to S(VI) was allowed to proceed through the iron-catalyzed oxidation by O_2 according to the kinetic expression of *Brimblecombe and Spedding* [1974]. Mass transfer at the surface of the drop was modeled by two-film theory, but *Baboolal et al.* [1981] have since shown this simple model to be unsatisfactory since it ignores forced convection inside and outside of the falling drop. *Durham et al.* [1981] added NO_x to the gas phase and allowed some NO_x gas phase chemistry, considered kinetic expressions for all reactions instead of equilibrium relationships, and assumed O_3 to be the only liquid phase oxidant of S(IV) using the rate law of *Erickson et al.* [1977]. *Easter and Hobbs* [1974] modeled cloudwater chemistry by using a wave cloud model, an open atmosphere with trace concentrations of CO_2, SO_2, and NH_3, and a rudimentary S(IV) oxidation rate consisting of a simple first-order dependence on sulfite. More recent models have been proposed by *Middleton et al.* [1980], *Chameides and Davis* [1982], and *Carmichael et al.* [1983].

With this work in mind, a dynamic model for fogwater chemistry has been developed. The model has a hybrid kinetic and equilibrium structure: reactions which rapidly come to equilibrium are considered separately from reactions that are kinetically controlled. Gas phase chemistry, particle scavenging by droplets, evolution of the droplet microphysics, and deposition were not included explicitly.

Paper number 3C0722.
0148-0227/83/003C-0722$05.00

STRUCTURE OF THE MODEL

Aqueous Phase Reactions

The chemical composition of a fog droplet is assumed to be determined by the following factors: (1) the composition of the activated cloud condensation nuclei (CCN) on which the droplet condenses, (2) the absorption of atmospheric gases at the droplet surface, and (3) the subsequent aqueous phase reactions of homogeneous and heterogeneous species. Proton transfer and most ligand substitution reactions proceed extremely fast compared to the time scales of interest in this study [*Hoffmann*, 1981]; therefore they are treated as dynamic equilibria. The same assumption is applied to gas absorption in accordance with Henry's law, although mass transfer may be retarded by the formation of an organic film at the droplet surface [*Graedel et al.*, 1983]. Equilibrium constants K_T have been adjusted for temperature T with the van't Hoff relationship:

$$\int_{K_{298}}^{K_T} d \ln K = \frac{\Delta H^\circ_{298}}{R} \int_{298}^{T} \frac{dT}{T^2} \qquad (1)$$

ΔH° values at 298°K were obtained from literature sources (see Table 1). The equilibrium composition was determined using a MINEQL subroutine [*Morel and Morgan*, 1972; *Westall et al.*, 1976]. In MINEQL the equilibrium constant approach is used to solve the chemical equilibrium problem, which is defined by a system of mass action equations. The computed concentrations of constituents are constrained to remain positive and to satisfy mole balance relationships provided by the analytical information. Given a set of chemical constituents which have been defined operationally as metals and ligands, along with the corresponding stoichiometric and thermodynamic data, all the possible chemical species in a model system can be defined. The concentrations of these chemical species are written as functions of the free con-

TABLE 1. Henry's Law and Aqueous-Phase Equilibria Relevant to the Droplet Chemistry

Reaction No.	Reaction	pK*	$\Delta H^\circ_{298.15}$, kcal mole^{-1}	Reference†
(R1)	$H_2O(l) \rightleftharpoons H^+ + OH^-$	14.00	13.35	SM
(R2)	$SO_2(g) + H_2O \rightleftharpoons SO_2 \cdot H_2O$	−0.095	−6.25	SM
(R3)	$SO_2 \cdot H_2O \rightleftharpoons H^+ + HSO_3^-$	1.89	−4.16	SM
(R4)	$HSO_3^- \rightleftharpoons H^+ + SO_3^{2-}$	7.22	−2.23	SM
(R5)	$HNO_3(g) \rightleftharpoons H^+ + NO_3^-$	−6.51	−17.3	SW
(R6)	$HNO_2(g) \rightleftharpoons HNO_2(l)$	−1.7	−9.5	SW
(R7)	$HNO_2(l) \rightleftharpoons H^+ + NO_2^-$	3.29	2.5	SW
(R8)	$CO_2(g) + H_2O \rightleftharpoons CO_2 \cdot H_2O$	1.47	−4.85	SM
(R9)	$CO_2 \cdot H_2O \rightleftharpoons H^+ + HCO_3^-$	6.37	1.83	SM
(R10)	$HCO_3^- \rightleftharpoons H^+ + CO_3^{2-}$	10.33	3.55	SM
(R11)	$CH_2O(g) + H_2O \rightleftharpoons CH_2O \cdot H_2O$	−3.85	−12.85	LB
(R12)	$HOCH_2SO_3H \rightleftharpoons H^+ + HOCH_2SO_3^-$	<0‡	U§	R
(R13)	$HOCH_2SO_3^- \rightleftharpoons H^+ + {}^-OCH_2SO_3^-$	11.7	U	SA
(R14)	$NH_3(g) + H_2O \rightleftharpoons NH_3 \cdot H_2O$	−1.77	−8.17	SM
(R15)	$NH_3 \cdot H_2O \rightleftharpoons NH_4^+ + OH^-$	4.77	0.9	SM
(R16)	$O_2(g) \rightleftharpoons O_2(l)$	2.90	−3.58	P
(R17)	$H_2O_2(g) \rightleftharpoons H_2O_2(l)$	−4.85	−14.5	MD
(R18)	$O_3(g) \rightleftharpoons O_3(l)$	2.03	−5.04	L-B
(R19)	$CaHCO_3^+ \rightleftharpoons Ca^{2+} + HCO_3^-$	11.6	−2.78	SM
(R20)	$CaSO_4(l) \rightleftharpoons Ca^{2+} + SO_4^{2-}$	2.30	−1.65	SM
(R21)	$NaSO_4^- \rightleftharpoons Na^+ + SO_4^{2-}$	0.70	−2.23	SM
(R22)	$FeSO_4^+ \rightleftharpoons Fe^{3+} + SO_4^{2-}$	4.20	5.4	SM
(R23)	$Fe(SO_4)_2^- \rightleftharpoons Fe^{3+} + 2SO_4^{2-}$	5.60	U	SM
(R24)	$FeCl^{2+} \rightleftharpoons Fe^{3+} + Cl^-$	1.40	−7.91	SM
(R25)	$FeOH^{2+} \rightleftharpoons Fe^{3+} + OH^-$	12.30	0.04	SM
(R26)	$Fe(OH)_2^+ \rightleftharpoons Fe^{3+} + 2OH^-$	23.3	U	SM
(R27)	$Fe(OH)_3\downarrow \rightleftharpoons Fe^{3+} + 3OH^-$	39.0	20.7	SM
(R28)	$Fe_2(OH)_2^{4+} \rightleftharpoons 2Fe^{3+} + 2OH^-$	25.7	16.2	SM
(R29)	$FeSO_3^+ \rightleftharpoons Fe^{3+} + SO_3^{2-}$	10.0	U	this laboratory
(R30)	$MnSO_4(l) \rightleftharpoons Mn^{2+} + SO_4^{2-}$	2.30	−3.39	SM
(R31)	$MnCl^+ \rightleftharpoons Mn^{2+} + Cl^-$	1.10	−8.01	SM
(R32)	$HSO_4^- \rightleftharpoons H^+ + SO_4^{2-}$	2.20	−4.91	SM

*K is in M atm^{-1} or M. Temperature is 298°K.

†Reference code: SM = *Sillén and Martell* [1964]; SW = *Schwartz and White* [1981]; LB = *Ledbury and Blair* [1925]; SA = *Sørensen and Andersen* [1970]; MD = *Martin and Damschen* [1981]; L-B = *Landolt-Börnstein* [1976]; R = *Roberts et al.* [1971]; P = *Perry* [1963].

‡The pK for this reaction is very low.

§Unknown, $\Delta H = 0$ is assumed in the calculation.

centrations of the constituents by mass action equations. These functions are substituted into the mole balance equations with elimination of solids. The problem is reduced to a system of nonlinear equations in which the unknowns are the concentrations of the metals and ligands. This system of equations is solved by the Newton-Raphson method. The initial solution is tested against the solubility products of the solids and a new set of solids, which includes those solids with the most exceeded solubility products, is selected for the next computation. A final solution is achieved when the difference between the imposed analytical concentrations for a constituent and the sum of all individual species containing that constituent is less than or equal to a set value which is very small. Corrections for ionic strength were made using the Davies equation [*Stumm and Morgan*, 1981]. The thermodynamic data base consisted of 1300 equilibria; those found to influence the droplet composition are listed in Table 1.

For slower reactions, empirical rate laws were used. Specific rate laws for oxidation reactions involving N(III) and S(IV) have been incorporated in the model; they are listed in Table 2. Hydrogen peroxide, N(III), and O_3 are potentially important oxidants, and O_2 may also be important if catalyzed by active sites on soot or by transition metals, such as Fe(III) and Mn(II). Iron(III) and manganese(II) are effective catalysts when dissolved as free ions or complexes [*Hoffmann and Jacob*, 1983] but their catalytic properties are altered if they are present as solid phases. Surface catalysis may occur but in the absence of reliable data it has been neglected. In the kinetic formulation of (R35), [Fe(III)] and [Mn(II)] represent the summation of concentrations of all dissolved iron and manganese species. It should be noted that the kinetic data for this reaction is not satisfactory around *p*H 4 because of the influence of $Fe(OH)_3(s)$ which starts dissolving near *p*H 4. Rate expressions given by *Martin* [1983] at high *p*H and low *p*H fail to extrapolate to the same value at intermediate *p*H. To minimize this problem, an average of the two expressions was used near *p*H 4.

The reactions of absorption and aqueous phase disproportionation of NO_x to form nitrous and nitric acid have been reviewed by *Schwartz and White* [1981]. These reactions could be major contributors to nitrate formation in fog droplets if allowed to reach equilibrium; however, because of second-order kinetics they are too slow to be important on the time scales of concern in fog. Alternative aqueous phase nitrate formation pathways involve the oxidation of N(III) by H_2O_2 and O_3 [*Damschen and Martin*, 1982].

Overall, the rate laws shown in Table 2 indicate that oxidation reactions proceed on time scales of minutes to hours under urban atmospheric conditions. These rate laws are integrated with a simple finite difference scheme using adjustable

p. 6613, reactions (R38) and (R39):

"$\frac{d[S(VI)]}{dt}$" should read "$\frac{d[N(V)]}{dt}$"

TABLE 2a. Kinetic Expressions for the Aqueous Phase Oxidation Reactions of S(IV) to S(VI) and N(III) to N(V)

Reaction No.	Reaction	Conditions	Rate, $M\ s^{-1}$ at 25°C*	Activation Energy, kcal $mole^{-1}$	Reference†
(R33)	S(IV) + H_2O_2		$\frac{d[S(VI)]}{dt} = \frac{8 \times 10^4[H_2O_2(l)][SO_2(l)]}{0.1 + [H^+]}$	7.3	M
(R34)	S(IV) + O_3	pH < 3	$\frac{d[S(VI)]}{dt} = \frac{1.9 \times 10^4[SO_2(aq)][O_3(l)]}{[H^+]^{1/2}}$	6	M
		pH > 3	$\frac{d[S(VI)]}{dt} = 4.19 \times 10^5\left(1 + \frac{2.39 \times 10^{-6}}{[H^+]}\right)[O_3(l)][SO_2(aq)]$	6	Ma
(R35)	S(IV) + O_2 (with Fe (III) and Mn(II))	$[SO_2(aq)] > 10^{-5}$, pH < 4	$\frac{d[S(VI)]}{dt} = \frac{4.7[Mn(II)]^2}{[H^+]} + \left(\frac{0.82[Fe(III)][SO_2(aq)]}{[H^+]} \cdot \left(1 + \frac{1.7 \times 10^3[Mn(II)]^{1.5}}{6.3 \times 10^{-6} + [Fe(III)]}\right)\right)$	21.8	M
		$[SO_2(aq)] < 10^{-5}$, pH < 4	$\frac{d[S(VI)]}{dt} = 3\left(5000[Mn(II)][HSO_3^-] + \frac{0.82[Fe(III)][SO_2(aq)]}{[H^+]}\right)$	21.8	M
		$[SO_2(aq)] > 10^{-5}$, pH > 4	$\frac{d[S(VI)]}{dt} = \frac{4.7[Mn(II)]^2}{[H^+]} + 1 \times 10^7[Fe(III)][SO_2(aq)]^2$	27.3	M
		$[SO_2(aq)] < 10^{-5}$, pH > 4	$\frac{d[S(VI)]}{dt} = 5000\ [Mn(II)][HSO_3^-]$	27.3	M
(R36)	S(IV) + O_2 (with soot)‡		$\frac{d[S(VI)]}{dt} = 2.54 \times 10^7[O_2(l)]^{0.69} \cdot C_x \frac{[SO_2(aq)]^2}{1 + 3.06 \times 10^6[SO_2(aq)] + 1.5 \times 10^{12}[SO_2(aq)]^2}$	11.7	B
(R37)	S(IV) + N(III)	pH < 3	$\frac{d[S(VI)]}{dt} = 142[H^+][HNO_2(aq)][SO_2(aq)]$	12§	M
		pH > 3	$\frac{d[S(VI)]}{dt} = 2.2[HNO_2(l)][HSO_3^-]$	12§	O
(R38)	N(III) + H_2O_2		$\frac{d[S(VI)]}{dt} = 4.6 \times 10^3[H^+][H_2O_2(l)][HNO_2(l)]$	13.2	DM
(R39)	N(III) + O_3		$\frac{d[S(VI)]}{dt} = 5 \times 10^5[O_3(l)][NO_2^-]$	13.8	DM

*$[SO_2(aq)] = [SO_2(l)] + [HSO_3^-] + [SO_3^{2-}]$; $[HNO_2(aq)] = [HNO_2(l)] + [NO_2^-]$.
†Reference code: M = *Martin* [1982]; Ma = *Maahs* [1982]; B = *Brodzinsky et al.* [1980]; O = *Oblath et al.* [1981]; DM = *Damschen and Martin* [1982].
‡C_x is the concentration of active carbon in g l^{-1}.
§Assumed.

time steps ranging from 10 s to 200 s:

$$[R_i]_{t+\Delta t} = [R_i]_t + \left(\sum_{ox}\left(\frac{d[R_i]}{dt}\right)_{ox}\right)\Delta t \qquad (2)$$

where $[R_i]$ represents the concentration of the reduced component R_i (i.e. N(III) or S(IV)).

Of special interest in urban fog is the reaction of HSO_3^- with CH_2O and with other aldehydes, RCHO, to form hydroxymethanesulfonate ion (HMSA) and the corresponding sulfonates, $HOCHRSO_3^-$ [*Munger et al.*, 1983]:

$$CH_2O + HSO_3^- \underset{k_r}{\overset{k_f}{\rightleftharpoons}} HOCH_2SO_3^- \qquad (3)$$

Dasgupta et al. [1980] determined a conditional equilibrium constant for HMSA to be $K_{298} = k_f/k_r = 7.5 \times 10^4\ M^{-1}$, while S. D. Boyce and M. R. Hoffmann (unpublished manuscript, 1983) have determined that $k_f = 3\ M^{-1}\ s^{-1}$. Production of HMSA will contribute to the droplet acidity indirectly by producing a droplet that is supersaturated with respect to $SO_2(g)$, and because of the slow reversibility of (3), HMSA formation may inhibit the production of S(VI). Reaction (3) is integrated at each time step by using the integrated form of the rate law:

$$\ln\left|\frac{[HSO_3^-]_{t+\Delta t} - p}{[HSO_3^-]_{t+\Delta t} - q}\right| = k_f(q - p)\,\Delta t + \ln\left|\frac{[HSO_3^-]_t - p}{[HSO_3^-]_t - q}\right| \qquad (4)$$

TABLE 2b. Reaction Stoichiometries for Reactions in Table 2a

Reaction No.	Reaction Stoichiometries
(R33)	$HSO_3^- + H_2O_2(l) \rightarrow HSO_4^- + H_2O$
(R34)	$HSO_3^- + O_3(l) \rightarrow HSO_4^- + O_2$
(R35)	$HSO_3^- + 1/2O_2(l) \rightarrow HSO_4^-$
(R37)	$2HNO_2(l) + H_2O \cdot SO_2 \rightarrow 2NO + H^+ + HSO_4^- + H_2O$ $2HNO_2(l) + 2H_2O \cdot SO_2 \rightarrow 2SO_4^{2-} + N_2O + H_2O + 4H^+$
(R38)	$HNO_2(l) + H_2O_2(l) \rightarrow NO_3^- + H_2O + H^+$
(R39)	$NO_2^- + O_3(l) \rightarrow NO_3^- + O_2$

$$[\mathrm{HMSA}]_{t+\Delta t} = [\mathrm{HMSA}]_t - ([\mathrm{HSO_3^-}]_{t+\Delta t} - [\mathrm{HSO_3^-}]_t) \quad (5)$$

where p and q are the solutions to the second-degree equation

$$KX^2 + (K([\mathrm{CH_2O(l)}]_t - [\mathrm{HSO_3^-}]_t) + 1)X - ([\mathrm{HSO_3^-}]_t + [\mathrm{HMSA}]_t = 0 \quad (6)$$

Gas Phase and Aerosol

At night the oxidation of nitrogeneous compounds and alkenes by ozone is important. The kinetics of these reactions are dependent on the downward diffusion of ozone to the boundary layer [*McRae*, 1981]. In the boundary layer, nitric acid may be produced [*Graham and Johnston*, 1978; *McRae and Russell*, 1983] by a variety of pathways. No attempt has been made to model gas phase chemistry. Instead, concentrations of gases and gas phase production rates (from emissions and homogeneous reactions) have been estimated from local field data and predictions from the Caltech air quality model for the Los Angeles basin [*McRae*, 1981].

The integrated mass and composition of the activated cloud condensation nuclei on which the fog droplets condense were estimated from field data. No subsequent scavenging of the interstitial aerosol by diffusion or impaction was considered.

Physical Description

A parcel of air is followed in which droplets form and grow by accretion of water vapor. The droplets are assumed to remain constantly within the air parcel (i.e., sedimentation and diffusion of the droplets are ignored).

The limitation of S(IV) oxidation rates by mass transfer has been discussed by *Schwartz and Freiberg* [1981] and *Baboolal et al.* [1981]. Schwartz and Freiberg have shown that for stationary droplets smaller than 50 μm the net rate of oxidation was limited strictly by oxidation. Baboolal et al. extended this analysis to droplets larger than 50 μm. These large droplets have a significant sedimentation velocity, which drives convection both inside and outside of the droplet. This mixing effect enhances the rate of mass transfer as calculated for stationary droplets. Therefore the chemical changes in fog droplets are most likely limited by the specific reaction rates.

Because fogs are localized events and occur on time scales of a few hours, advection of condensing and evaporating droplets can be ignored as a first approximation. Also, evolution of the droplet spectrum through coagulation can be neglected since mass transfer does not limit overall reaction rates. In this context the liquid water content of the air parcel and its time dependency are sufficient parameters for characterizing fog microphysics.

At $t = 0$, droplets are assumed to condense, receive an initial chemical loading from the water-soluble fraction of the activated nuclei, and immediately react with the gaseous environment. The growth and evaporation of the droplets is simulated by the external input of an evolving liquid water content. At each time step the equilibrium composition of the droplet is calculated along with the HMSA formation rate and the changes in component concentrations due to oxidation reactions.

RESULTS AND DISCUSSION

Sulfate and Nitrate Oxidation Pathways

In this section the relative contributions of the various S(IV) and N(III) oxidation mechanisms to the droplet chemistry are discussed. For this specific purpose a closed parcel of air with a constant liquid water content has been assumed (i.e., droplets condense on the activated condensation nuclei at $t = 0$ with no droplet growth or evaporation). A nighttime air mass typical of the industralized coastline of the Los Angeles basin has been chosen. Concentrations of gases and preexisting nuclei were estimated from local field data and transport models (Table 3). Gases are depleted by absorption except for CO_2 and O_2, which are held constant at a fixed partial pressure. The liquid water content is $L = 0.1$ g m^{-3} and the temperature is $T = 283$ K.

Kinetic results shown in Figure 1 clearly show that H_2O_2 and O_2 (catalyzed by Fe and Mn) are the principal oxidants for S(VI) production in situ. Hydrogen peroxide is highly soluble in water and rapidly oxidizes S(IV) at low pH; however, if not replenished, it is quickly depleted from the parcel of air by reduction to water. In this case, in the absence of gas phase or aqueous phase H_2O_2 formation, no H_2O_2 remains in the system after 10 minutes.

The catalytic effectiveness of both Fe(III) and Mn(II) is dependent on their speciation in the droplet (Figure 2). The principal manganese species are $Mn(H_2O)_6^{2+}$ and $MnSO_4$(aq). Both of these species are assumed to be equally effective as catalysts for S(IV) autoxidation. On the other hand, Fe(III) above pH 4 is found primarily as an iron(III) hydroxide solid, which has been assumed to be catalytically inactive. As the pH decreases below 4, the solid phase dissolves and soluble Fe(III), the active catalyst, is released. The rate law indicates a decrease of the oxidation rate with pH but the dissolution of Fe(III) at low pH offsets this effect and the calculated rate actually increases between pH 4 and 3.5.

Oxidation by ozone contributes ~4% of the total S(VI)

TABLE 3. Composition of the Air Mass (Trace Gases and Condensation Nuclei) Prior to Fog Formation at a Polluted Site

Atmospheric Trace Gases		
	Concentration, ppb	Reference
SO_2	20	SCAQMD data*
HNO_2	1	*Hanst et al.* [1982]
HNO_3	3	id.
NH_3	5	id.
CH_2O	30	*Grosjean* [1982]
O_3	10	SCAQMD data
H_2O_2	1	*Graedel et al.* [1976]

Condensation Nuclei†			
	Concentration μg m^{-3}		Concentration, μg m^{-3}
SO_4^{2-}	10	NH_4^+	6.65
NO_3^-	10	Na^+	.61
Cl^-	1.1	Fe(III)	.5
CO_3^{2-}	1.83	Mn(II)	.02
C_x(soot)	30	Ca^{2+}	1.22

The air mass is typical of the industrial coastline of the Los Angeles basin for an inversion height of about 50 m. $P_{O_2} = 0.21$ atm, $P_{CO_2} = 330$ ppm.

*Data from the permanent records of the South Coast Air Quality Management District.

†$(NH_4)_2SO_4$, NH_4NO_3, NaCl, $CaCO_3$, metal oxides, and soot. References: *Gartrell et al.* [1980]; *Appel et al.* [1980].

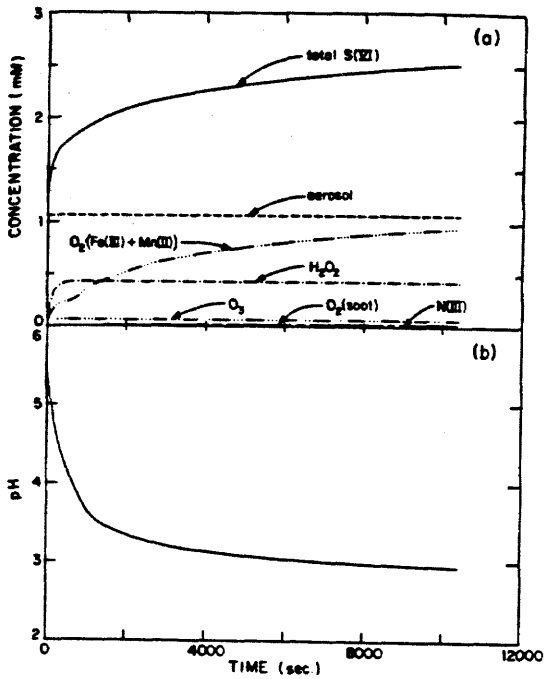

Fig. 1. (*a*) Profile versus time of total sulfate in the fogwater and of the individual contributions to the total sulfate of sulfate aerosol and different S(IV) oxidants. (*b*) Profile of *p*H versus time. The fog formed under the conditions of Table 3, with liquid water content = 0.1 g m^{-3}, temperature = 10°C.

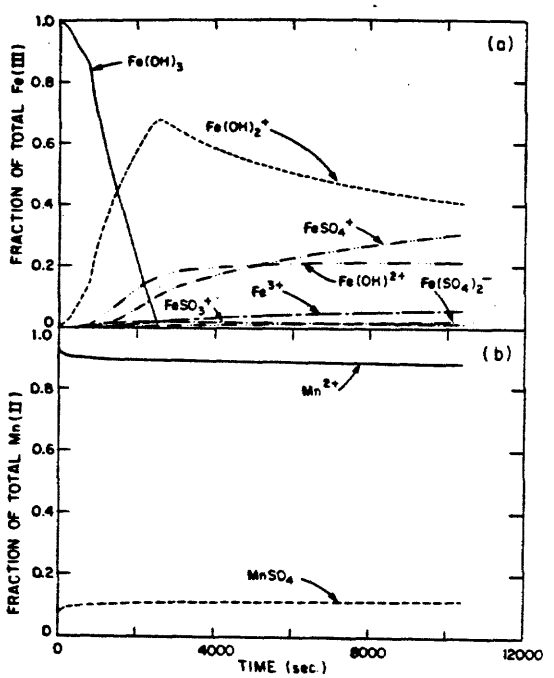

Fig. 2. Speciation of (*a*) Fe(III) and (*b*) Mn(II) in the fogwater as a function of time under conditions of Table 3, with liquid water content = 0.1 g m^{-3} and temperature = 10°C.

produced after 3 hours of fog. This is due to the low water solubility of ozone and the reciprocal hydrogen ion dependency of its reaction rate. Therefore little oxidation by ozone occurs below *p*H 4. Catalytic carbon sites in soot contribute <5% of the total S(VI) produced, even at the high carbon levels of urban environments. Oxidation by N(III) appears to be insignificant due to the low solubility of HNO_2(g) at *p*H < 4.

Oxidation of N(III) does not contribute appreciably to nitrate production. At t = 180 minutes, reaction with O_3 had generated less than 10^{-7} M NO_3^- and reaction with H_2O_2 less than 10^{-10} M NO_3^-.

The aqueous phase oxidation of S(IV) has an important consequence on the droplet acidity. Between *p*H 2 and 6 the principal reactive species of S(IV) is HSO_3^- [*Hoffmann and Jacob*, 1983]. The oxidation product, HSO_4^-, is completely dissociated above *p*H 3. Therefore the oxidation directly produces one free proton. Depletion of HSO_3^- leads to further dissolution of SO_2(g) which then dissociates to give HSO_3^- and H^+ in the droplet. Because the solubility of SO_2 decreases with *p*H, each depleted HSO_3^- molecule is not replaced in the droplet. Depending on the overall droplet chemistry, oxidation of one molar unit of S(IV) thus leads to the production of one- to two-fold that molar unit of free acidity. The impact on the droplet *p*H is dramatic, as shown in Figure 1*b*. In the first half hour of the fog, S(VI) production is the fastest and causes a pH drop of over two units. Field observations are consistent with these predictions [*Munger et al.*, 1983].

Components in the gas phase are scavenged by the droplets with efficiencies dependent on their Henry's law constants and aqueous phase chemistry. Table 4 shows the fraction of each gas scavenged at t = 0, t = 30 min, and t = 180 min. It must be kept in mind that these numbers vary with the liquid water content of the fog [*Schwartz*, 1983]. Nitric acid is totally dissolved and dissociated, while NH_3 dissolves totally at *p*H < 5. These two components essentially titrate each other in the aqueous phase. Formation of HMSA over the course of a fog event was found not to significantly increase the fraction of CH_2O scavenged; therefore the CH_2O partial pressure remains approximately constant throughout the simulation. Likewise, hydroxymethanesulfonate formation cannot be a significant sink for gas phase SO_2. The solubility of SO_2 is limited, but because $SO_2 \cdot H_2O$ is a weak acid, ~5% dissolves with the formation of the fog. S(IV) oxidation reactions further increase the fraction scavenged over the lifetime of the fog. Three hours after fog formation, over 80% of the initial SO_2 still remains in the gas phase, indicating that fog has little impact on the gaseous SO_2 concentration. Hydrogen peroxide

TABLE 4. Scavenging of Gases by Fog Droplets Under Conditions of Table 3

Gas	Fraction Scavenged From Gas Phase, %		
	t = 0	t = 30 min	t = 180 min
HNO_3	100	100	100
NH_3	43.9	99.5	100
CH_2O	5.0	5.3	5.3
SO_2	2.7	11.8	17.5
H_2O_2	32.1	100	100
O_3	0.0	1.5	1.5
HNO_2	3.8	0.0	0.0

Liquid water content = 0.1 g m^{-3}, temperature = 283 K.

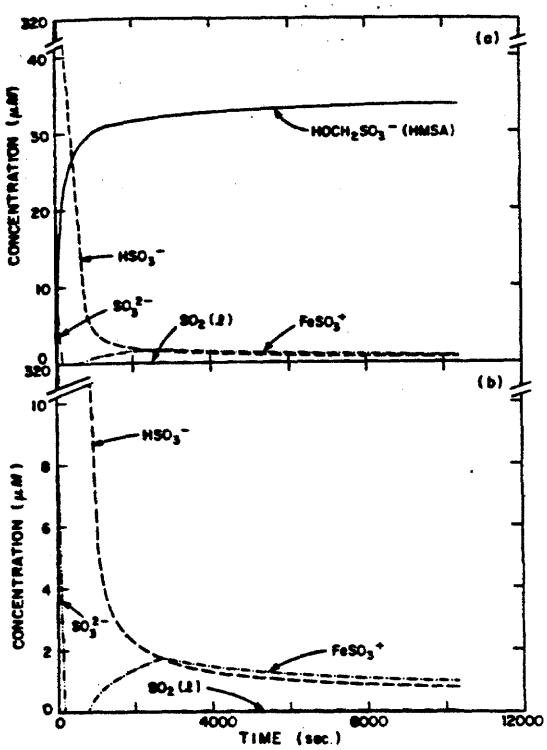

Fig. 3. (*a*) Concentrations of S(IV) species in the fogwater as a function of time under conditions of Table 3, with liquid water content = 0.1 g m^{-3} and temperature = 10°C. (*b*) Same as (*a*) but with no formaldehyde in the atmosphere.

is highly soluble in water. As was discussed above, reduction of H_2O_2 in the droplet is an efficient sink which depletes H_2O_2 from the system. Ozone, on the other hand, is poorly scavenged, as is HNO_2. Both react slowly in the droplet below *p*H 4.

The impact of HMSA formation on the droplet chemistry is worth discussing in some detail, as it has been the subject of recent interest [*Munger et al.*, 1983; *Boyce and Hoffmann*, 1983; *Richards et al.*, 1983]. Figure 3*a* shows the concentration profiles versus time for HSO_3^- and HMSA. The formation of HMSA is rapid but still slower than S(IV) oxidation. Consequently, the amount of HMSA produced is smaller than that of sulfate. Hydroxymethanesulfonate is the most important S(IV) species in solution; if formaldehyde was not present, the S(IV) concentration in the droplet would be much lower (Figure 3*b*).

It has been suggested that HMSA may inhibit S(IV) oxidation in atmospheric droplets by limiting the availability of reactive S(IV) species. This does not appear to be the case, since oxidation proceeds faster than adduct formation; furthermore, since the partial pressure of SO_2 remains approximately constant throughout the fog, the limiting concentrations of reactive S(IV) species are independent of the HMSA formation rate. However, the direct effect of HMSA on the fogwater acidity is of interest. Hydroxymethanesulfonate is the conjugate base of hydroxymethanesulfonic acid, which is a strong acid [*Roberts et al.*, 1971]. Hydroxymethanesulfonate is a weak acid (see Table 1). Between *p*H 2 and 10 and in a system open to SO_2, HMSA is stable and complexation of HSO_3^- leads to further dissolution of SO_2, which then dissociates and releases free acidity in the droplet. Because of the small amounts of HMSA produced with respect to the droplet $[H^+]$ concentration, this contribution is small.

In the first simulation, S(VI) formation buffered the droplet acidity at about *p*H 3, whereas in some extremely polluted atmospheres, higher acidity can be imparted to the droplet at $t = 0$ by simple dissolution of the activated nuclei. *Cass* [1975] reports some cases for Los Angeles, mostly under high humidity conditions, where the aerosol sulfate concentration was as high as 75 μg m^{-3}. A second simulation was run (Figures 4 and 5) under the same conditions as the first but with 75 μg m^{-3} SO_4^{2-} in the air mass as NH_4HSO_4 nuclei instead of 10 μg m^{-3} SO_4^{2-} as $(NH_4)_2SO_4$.

The *p*H of 2.4 at $t = 0$ (Figure 4) indicates the impact of the acid nuclei. At this low *p*H there is very little S(IV) in the droplet (Figure 5) and the only S(IV) oxidation reaction to proceed at a significant rate is that with H_2O_2. Therefore less sulfate and hydrogen ion are produced in situ. In the case of acidic condensation nuclei the *p*H of the fog may be controlled strictly by the nuclei composition instead of by S(VI) aqueous phase production. It should be mentioned that fogwater *p*H in the range of 2 to 2.5 has been observed in the Los Angeles basin following heavy 'smog' days. The lowest *p*H recorded was 1.69 in a dissipating fog along the coastline; in that case the dilution was probably less than the $L = 0.1$ g m^{-3} considered in the simulation.

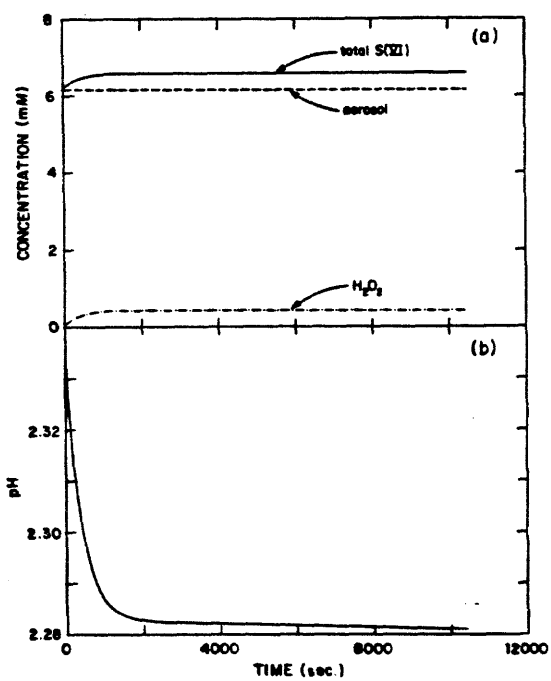

Fig. 4. (*a*) Profile versus time of total sulfate and of the individual contributions to the total sulfate of sulfate aerosol and different S(IV) oxidants. (*b*) Profile of *p*H versus time. The fog formed by condensation on highly acidic nuclei (75 μg m^{-3} NH_4HSO_4), other conditions as in Table 3, with liquid water content = 0.1 g m^{-3} and temperature = 10°C.

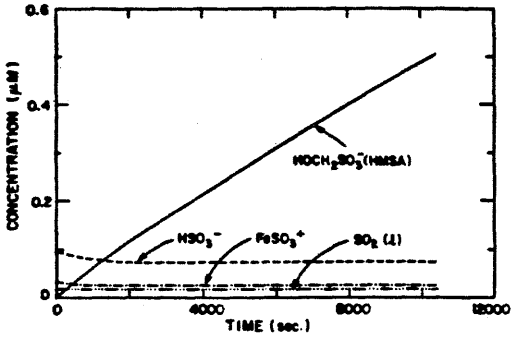

Fig. 5. Concentration of S(IV) species in the fogwater as a function of time. The fog formed by condensation on highly acidic nuclei (75 $\mu g\ m^{-3}$ NH_4HSO_4), other conditions as in Table 3, with liquid water content = 0.1 $g\ m^{-3}$ and temperature = 10°C.

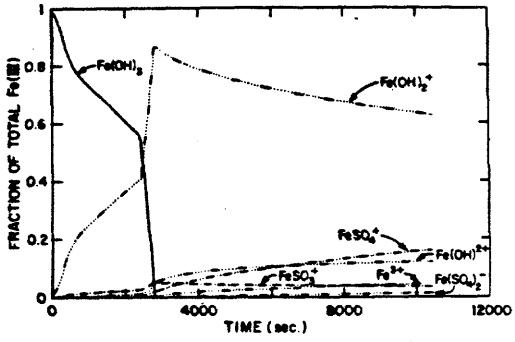

Fig. 7. Speciation of Fe(III) in the fogwater as a function of time under conditions of Table 3, with liquid water content = 0.1 $g\ m^{-3}$ and temperature = 1°C.

Fog frequently forms at temperatures lower than 10°C. Radiation fogs, in particular, often form near freezing. To check the chemical sensitivity of the system to temperature, a simulation was run at 1°C with $L = 0.1\ g\ m^{-3}$ and conditions given in Table 3. Reaction rates are slower at 1°C, but gas solubility increases. Solution equilibria are shifted in either direction depending on the sign of $\Delta H°$. The combination of these effects has an interesting impact on the sulfate production rates and the *p*H profile (Figure 6). The rate of S(IV) oxidation by H_2O_2 is relatively unaffected because of its low activation energy E_a, but metal-catalyzed oxidation by O_2, which has a high E_a, is much slower at 1°C than at 10°C. Oxidation by ozone becomes appreciable at the beginning of the fog because of its low E_a and the increased ozone solubility. However, between *p*H 4.5 and *p*H 4, H_2O_2 is totally depleted and oxidation by ozone becomes insignificant; the S(IV) autoxidation reaction is also very slow. The sulfate concentration and *p*H profiles are almost at a plateau in this *p*H range. Then, as the *p*H drops below 4, $Fe(III)(OH)_3$ starts dissolving and the rate of oxidation by O_2 increases, such that sulfate and acidity are again produced at an appreciable rate. After 3 hours of fog the values for *p*H and sulfate concentration are close to what they were at 10°C. The speciation profile of Fe(III) (Figure 7) is similar to that at 10°C, but dissolution of $Fe(OH)_3$ is retarded because of the slow drop in *p*H from 4.5 to 4. The speciation of Mn(II) is essentially the same as at 10°C.

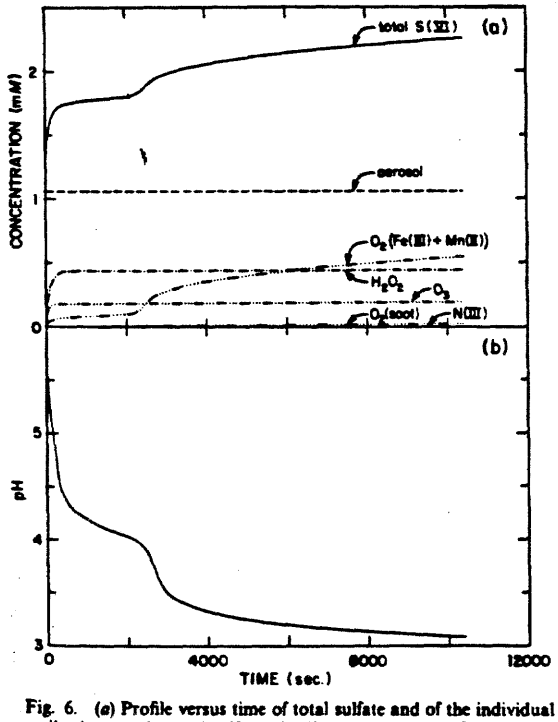

Fig. 6. (*a*) Profile versus time of total sulfate and of the individual contributions to the total sulfate of sulfate aerosol and different S(IV) oxidants. (*b*) Profile of *p*H versus time. The fog formed under the conditions of Table 3, with liquid water content = 0.1 $g\ m^{-3}$ and temperature = 1°C.

The scavenging efficiency of gases (Table 5) reflects their increased solubility; however, because the aqueous phase reactions are slower, little increase is seen between $t = 0$ and $t = 30$ min. After 3 hours the scavenging efficiency for SO_2 is similar to that at 10°C.

An interesting feature of the chemistry at 1°C is the high concentration of HMSA (Figure 8), which is due to the increased solubility of SO_2 and CH_2O. The reaction proceeds via a nucleophilic substitution of methylene glycol (S. D. Boyce and M. R. Hoffmann, unpublished manuscript, 1983) with an activation energy near 12 kcal $mole^{-1}$. Consequently, the reaction still proceeds rapidly at 1°C.

TABLE 5. Scavenging of Gases by Fog Droplets Under Conditions of Table 3

Gas	Fraction Scavenged From Gas Phase, %		
	$t = 0$	$t = 30$ min	$t = 180$ min
HNO_3	100	100	100
NH_3	76.0	97.0	100
CH_2O	9.8	10.3	10.5
SO_2	10.7	13.0	18.2
H_2O_2	58.0	100	100
O_3	0.0	4.2	4.2
HNO_2	10.2	3.4	0.0

Liquid water content = 0.1 $g\ m^{-3}$; temperature = 274 K.

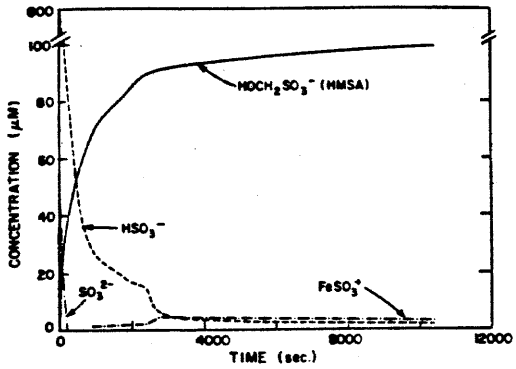

Fig. 8. Concentrations of S(IV) species in the fogwater as a function of time under conditions of Table 3, with liquid water content = 0.1 g m^{-3} and temperature = 1°C.

Simulation of a Fog Event

The simulation with the present model of an actual fog event necessitates the knowledge of input variables such as the condensation nuclei composition, the evolution of liquid water content with time, and the gas phase concentrations. Unfortunately, our field investigations [*Waldman et al.*, 1982; *Munger et al.*, 1983] so far have been limited to the determination of fogwater composition. Field data for the above parameters is incomplete; therefore a direct comparison of calculated and observed values is not possible at this time. In addition the current model neglects gas phase chemistry, transport mechanisms, and aerosol scavenging by droplets.

Fogwater composition and its variation with time for fog events at Lennox, a site in an industrial area near the Los Angeles coastline, have been documented thoroughly [*Waldman et al.*, 1982; *Munger et al.*, 1983]. In this section, a fog occurring under conditions typical of this highly impacted site has been simulated.

A plausible scenario for the evolution of liquid water content in fogs can be obtained from existing data [*Jiusto and Lala*, 1983]. The liquid water content often rises linearly following fog formation (neglecting small time scale oscillations), reaches a stable value after about an hour, and decreases linearly when the fog evaporates. Liquid water contents range from 0.01 g m^{-3} in very light fogs to 0.5 g m^{-3} in dense fogs. The profile chosen here is shown in Figure 9.

Concentrations of condensation nuclei and atmospheric gases prior to fog formation are given in Table 3. From the discussion of the previous section, it appears that some gas-phase emissions should be included. Hydrogen peroxide is not produced in the gas phase at night and thus actually disappears when the fog forms. Ammonia and HNO_3, which are scavenged efficiently by the droplets, are, on the other hand, continuously emitted into the atmosphere from a variety of sources. Because fog droplets are a sink for these two gases, fresh inputs into the parcel of air must be considered. At Lennox, plausible values associated with an inversion height of 50 m are 0.01 ppb min^{-1} for HNO_3 [*McRae and Russell*, 1983] and 0.01 ppb min^{-1} for NH_3 [*Russell et al.*, 1983]. Other gases included in the simulation are not depleted by fog, and a reasonable assumption is that their concentrations remain constant throughout the event. A constant temperature of 10°C has been chosen. Temperature changes during the course of fog events [*Jiusto and Lala*, 1983] are minimal.

The concentrations predicted for the major ions (Figure 10) are in the range of those reported by *Waldman et al.* [1982] and *Munger et al.* [1983], but no precise comparison should be made because of the reasons stated at the beginning of this section. The concave profiles observed (except for $[H^+]$) confirm the important role of dilution and evaporation that was suggested initially by Waldman et al. Aqueous phase oxidation of N(III) to N(V) is negligible and the only nitrate source is the slow gas phase production of HNO_3 followed by dissolution and dissociation. As a result, the nitrate concentration is controlled primarily by droplet growth. Similar behavior is predicted for ammonium ion, although in the initial stage of the fog the *p*H drop from a high value increases the NH_4^+ concentration. From equilibria described by (14) and (15), it is seen that scavenging of gaseous ammonia is highly *p*H-dependent over the range of 5 to 8, which is typical of fog forming in rural environments (D. J. Jacob, unpublished data, 1983) or influenced by alkaline atmospheric components [*Munger et al.*, 1983]. In such fogs, the NH_4^+ levels are expected to be controlled by acidity as well as dilution.

Oxidation of S(IV) contributes substantially to the sulfate level and the acidity in the early stages of the fog, and in the fully developed fog, 50% of the total sulfate present has been produced in the aqueous phase. During the first few minutes of the fog, S(IV) oxidation is in fact rapid enough to compensate for dilution; after H_2O_2 is depleted and the *p*H has dropped, the oxidation rate slows down and the role of dilution becomes predominant. Even with dilution the *p*H of the droplets does not rise because metal-catalyzed S(IV) oxidation by O_2 produces significant acidity in the droplet; instead, *p*H stabilizes at about 3.5. As the fog evaporates, concentration leads to a further *p*H decrease. The speciation of Fe(III) (Figure 11) correlates with *p*H in the manner discussed in the previous section. $FeSO_4^+$ becomes an important species as the fog evaporates because the sulfate concentration is so high. Speciation of Mn(II) (not shown) is similar to that in Figure 2.

An important question is, 'Is the sulfate formation predicted theoretically actually seen in the field?' The data of *Waldman et al.* [1982] and *Munger et al.* [1983] do not show obvious evidence for this. However, the bulk of the aqueous phase sulfate production is predicted to occur in the first hour of the fog, so that it could not be detected given the time resolution of the field study. A way to obtain experimental confirmation of this process would be to compare the amount of sulfate present in the atmosphere just before fog formation to that right after fog formation.

The HMSA concentration profile (Figure 12) shows the dominant effect of droplet growth and evaporation, except in

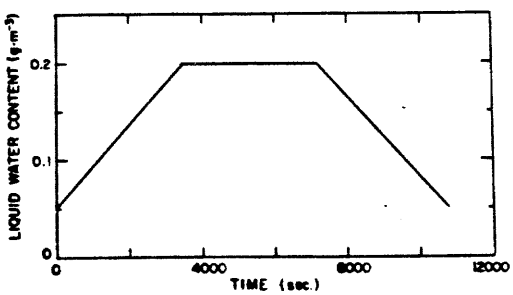

Fig. 9. Liquid water content profile versus time chosen for the simulation of a fog event in the Los Angeles basin.

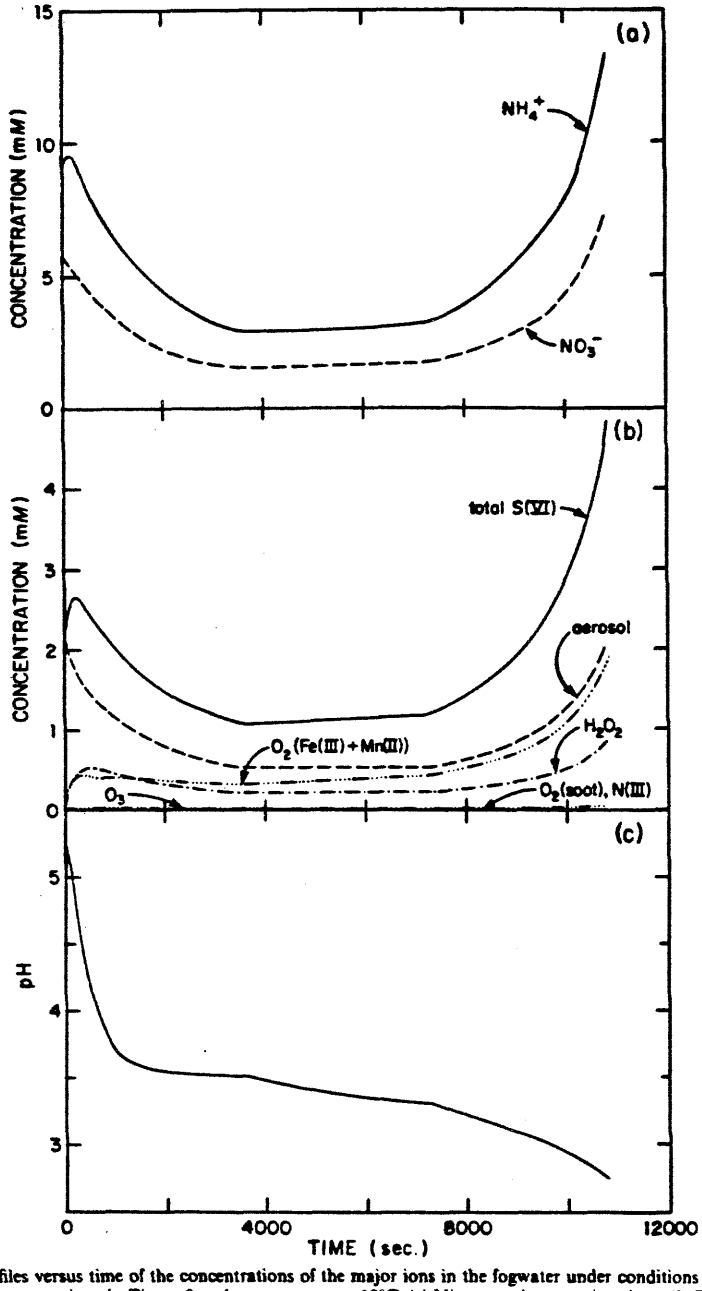

Fig. 10. Profiles versus time of the concentrations of the major ions in the fogwater under conditions of Table 3, with liquid water content as given in Figure 9 and temperature = 10°C. (*a*) Nitrate and ammonium ions. (*b*) Total sulfate and individual contributions of the different sulfate production mechanisms. (*c*) *p*H.

the first few minutes of the fog. Hydroxymethanesulfonate is the major S(IV) species, and its formation may explain the high S(IV) levels found in fogwater [*Munger et al.*, 1983]. It should be noted that in addition to formaldehyde, sulfite is known to readily form sulfonates with other aldehydes, some of which have been found in fog at concentrations comparable to formaldehyde [*Grosjean and Wright*, 1983]. These reactions would further explain the high S(IV) concentrations observed.

CONCLUSION

The chemistry of fogs forming in an urban environment has been investigated using a hybrid kinetic and equilibrium model. The most important conclusions are as follows.

1. Aqueous phase oxidation of S(IV) is an important source of sulfate in the droplet. The principal oxidants are H_2O_2 and O_2 (catalyzed by Fe(III) and Mn(II)), although ozone can also be an important oxidant above *p*H 5. Oxida-

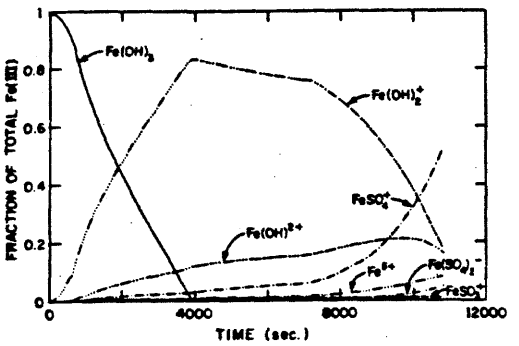

Fig. 11. Speciation of Fe(III) in the fogwater as a function of time under conditions of Table 3, with liquid water content as given in Figure 9 and temperature = 10°C.

tion by H_2O_2 is very fast but limited by its availability in the atmosphere. Most of the sulfate production occurs within the first hour following fog formation.

2. When fog condenses on alkaline to slightly acid nuclei, important acidification occurs as a result of S(IV) oxidation. In the first case simulated, the *p*H dropped two units from its initial value of 5.5 during the first half hour of the fog; it then stabilized around *p*H 3. When the fog formed on highly acidic condensation nuclei, however, the *p*H drop due to S(IV) oxidation was very small because of the high acidity initially present in the droplet.

3. Oxidation of N(III) in the droplet does not lead to significant production of nitrate. Production of nitrate proceeds through gas phase formation of HNO_3 followed by dissolution and dissociation in the droplet. Nitric acid is scavenged efficiently by the droplets as it is formed in the gas phase.

4. NH_4^+ concentration is dependent both on the liquid water content of the fog and the solubility of NH_3. Below *p*H 5 the droplets are essentially a total sink for NH_3, but above *p*H 5 the gas is partitioned between the two phases in a highly *p*H-dependent manner.

5. Over 90% of the S(IV) present in the droplet is complexed as HMSA, and this may explain the high S(IV) concentrations observed by *Munger et al.* [1983]. Formation of HMSA releases free acidity, but its effect on the droplet *p*H is negligible.

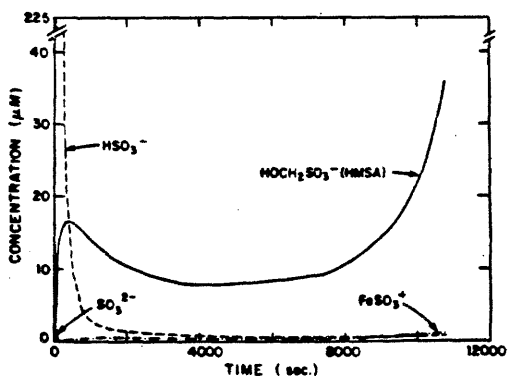

Fig. 12. Concentrations of S(IV) species in the fogwater as a function of time under conditions of Table 3, with liquid water content as given in Figure 9 and temperature = 10°C.

6. Fog does not affect the SO_2 gas phase concentrations greatly; as a result the supply of reactive S(IV) species for S(VI) and HMSA formation is determined primarily by the droplet *p*H. S(VI) formation proceeds faster than HMSA formation at all times and limits HMSA formation by causing the *p*H to drop and thus reducing the S(IV) supply.

7. At lower temperatures (1°C versus 10°C), metal-catalyzed oxidation by O_2 is slower and the importance of ozone as an S(IV) oxidant increases. Overall, sulfate and acidity are not produced as fast in the early stages of the fog but catch up later and become comparable in the later stage of the fog. Much more HMSA is produced at the lower temperature.

The model has thus revealed some important features of the chemistry and production of acidity in urban fogs. Gas phase and aerosol chemistry, droplet microphysics, and wind fields will have to be incorporated in future versions to give the simulations a predictive capability. These theoretical advances will have to be accompanied by concomitant sets of field measurements.

REFERENCES

Adamowicz, R. F., A model for the reversible washout of sulfur dioxide, ammonia and carbon dioxide from a polluted atmosphere and the production of sulfates in raindrops, *Atmos. Environ.*, *13*, 105–121, 1979.

Appel, B. R., E. L. Kothny, E. M. Hoffer, and J. J. Wesolowski, Sulfate and nitrate data from the California Aerosol Characterization Experiment (ACHEX), *Adv. Environ. Sci. Technol.*, *9*, 315–335, 1980.

Baboolal, L. B., H. R. Pruppacher, and J. H. Topalian, A sensitivity study of a theoretical model of SO_2 scavenging by water drops in air, *J. Atmos. Sci.*, *38*, 856–870, 1981.

Brimblecombe, P., and D. J. Spedding, The catalytic oxidation of micromolar aqueous sulphur dioxide, *Atmos. Environ.*, *8*, 937–945, 1974.

Brodzinsky, R., S. G. Chang, S. S. Markowitz, and T. Novakov, Kinetics and mechanism for the catalytic oxidation of sulfur dioxide on carbon in aqueous suspensions, *J. Phys. Chem.*, *84*, 3354–3358, 1980.

Carmichael, G. R., T. Kitada, and L. K. Peters, The effects of in-cloud and below-cloud scavenging on the transport and gas phase reactions of SO_x, NO_y, HC_z, H_2O_y, and O_3 compounds, in *4th International Conference on Precipitation Scavenging, Dry Deposition, and Resuspension*, Santa Monica, December 1982, Elsevier, New York, in press, 1983.

Cass, G. R., Dimensions of the Los Angeles SO_2/sulfate problem, *Environ. Qual. Lab. Memo. 15*, Calif. Inst. of Technol., Pasadena, 1975.

Chameides, W. L., and D. D. Davis, The free radical chemistry of cloud droplets and its impact upon the composition of rain, *J. Geophys. Res.*, *87*, 4863–4877, 1982.

Damschen, D. E., and L. R. Martin, Aqueous aerosol oxidation of nitrous acid by O_2, O_3, and H_2O_2, *Atmos. Environ.*, in press, 1983.

Dasgupta, P. K., K. De Cesare, and J. C. Ullrey, Determination of atmospheric sulfur dioxide without tetrachloromerurate(II) and the mechanism of the Schiff reaction, *Anal. Chem.*, *52*, 1912–1922, 1980.

Durham, J. L., J. M. Overton, and V. P. Aneja, Influence of gaseous nitric acid on sulfate production and acidity in rain, *Atmos. Environ.*, *15*, 1059–1068, 1981.

Easter, R. C., and P. V. Hobbs, The formation of sulfate and the enhancement of cloud condensation nuclei in clouds, *J. Atmos. Sci.*, *31*, 1586–1594, 1974.

Erickson, R. E., L. M. Yates, R. L. Clark, and D. McEwen, The reaction of sulfur dioxide with ozone in water and its possible atmospheric significance, *Atmos. Environ.*, *11*, 813–817, 1977.

Gartrell, G., Jr., S. L. Heisler, and S. K. Friedlander, Relating particulate properties to sources: The results of the California Aerosol Characterization Experiment, *Adv. Environ. Sci. Technol.*, *9*, 665–713, 1980.

Graedel, T. E., L. A. Farrow, and T. A. Weber, Kinetic studies of the photochemistry of the urban atmosphere, *Atmos. Environ.*, *10*, 1095–1116, 1976.

Graedel, T. E., P. S. Gill, and C. J. Wechsler, Effects of organic surface films on the scavenging of atmospheric gases by raindrops and aerosol particles, in *4th International Conference on Precipitation Scavenging, Dry Deposition, and Resuspension, Santa Monica, December 1982*, Elsevier, New York, in press, 1983.

Graham, R. A., and H. S. Johnston, The photochemistry of NO_3 and the kinetics of the N_2O_5–O_3 system, *J. Phys. Chem., 82*, 254–268, 1978.

Grosjean, D., Formaldehyde and other carbonyls in Los Angeles ambient air, *Environ. Sci. Technol., 16*, 254–262, 1982.

Grosjean, D., and B. Wright, Carbonyls in urban fog, ice fog, cloudwater and rain water, *Atmos. Environ.*, in press, 1983.

Hanst, P. L., N. W. Wong, and J. Bragin, A long-path infra-red study of Los Angeles smog, *Atmos. Environ., 16*, 969–981, 1982.

Hegg, D. A., and P. V. Hobbs, Cloudwater chemistry and the production of sulfates and clouds, *Atmos. Environ., 15*, 1597–1604, 1981.

Hoffmann, M. R., Thermodynamic, kinetic and extrathermodynamic considerations in the development of equilibrium models for aquatic systems, *Environ. Sci. Technol., 15*, 345–353, 1981.

Hoffmann, M. R., and D. J. Jacob, Kinetics and mechanisms of the catalytic oxidation of dissolved sulfur dioxide in aqueous solution: An application to nighttime fogwater chemistry, in *Acid Precipitation*, edited by J. G. Calvert, Ann Arbor Science, Ann Arbor, Mich., in press, 1983.

Jiusto, J. E., and G. G. Lala, Radiation fog field programs—Recent studies, *ASRC-SUNY Publ. 869*, State Univ. of N. Y., Albany, 1983.

Landolt-Börnstein, *Zahlenwerte und Funktionen. Gleichgewicht der Absorption von Gasen in Flüssigkeiten von niedrigem Dampfdruck*, 6th ed., vol. 4, part 4, sect. C, Springer Verlag, Heidelberg, Federal Republic of Germany, 1976.

Ledbury, W., and E. W. Blair, The partial formaldehyde vapour pressure of aqueous solutions of formaldehyde, 2, *J. Chem. Soc., 127*, 2832–2839, 1925.

Liljestrand, H. M., and J. J. Morgan, Spatial variations of acid precipitation in Southern California, *Environ. Sci. Technol., 15*, 333–339, 1981.

Maahs, H. G., The importance of ozone in the oxidation of sulfur dioxide in nonurban tropospheric clouds, paper presented at the 2nd Symposium on the Composition of the Nonurban Troposphere, Am. Meteorol. Soc., Williamsburg, Va., 1982.

Martin, L. R., Kinetic studies of sulfite oxidation in aqueous solution, in *Acid Precipitation*, edited by J. G. Calvert, Ann Arbor Science, Ann Arbor, Mich., in press, 1983.

McRae, G. J., Mathematical modeling of photochemical air pollution, Ph.D. thesis, Calif. Inst. of Technol., Pasadena, 1981.

McRae, G. J., and A. G. Russell, Dry deposition of nitrogen containing species, in *Acid Deposition: Wet and Dry*, vol. 6, edited by B. B. Hicks, Ann Arbor Science, Ann Arbor, in press, 1983.

Middleton, P., C. S. Kiang, and V. A. Mohnen, Theoretical estimates of the relative importance of various urban sulfate aerosol production mechanisms, *Atmos. Environ., 14*, 463–472, 1980.

Morel, F., and J. J. Morgan, A numerical method for computing equilibria in aqueous chemical systems, *Environ. Sci. Technol., 6*, 58–67, 1972.

Munger, J. W., D. J. Jacob, J. M. Waldman, and M. R. Hoffmann, Fogwater chemistry in an urban atmosphere, *J. Geophys. Res., 88*, 5109–5121, 1983.

Oblath, S. B., S. S. Markowitz, T. Novakov and S. C. Chang, Kinetics of the formation of hydrozylamine disulfonate by reaction of nitrite with sulfites, *J. Phys. Chem., 85*, 1017–1021, 1981.

Perry, J. M., *Chemical Engineer's Handbook*, 4th ed., McGraw-Hill, New York, 1963.

Richards, L. W., J. A. Anderson, D. L. Blumenthal, J. A. McDonald, G. L. Kok, and A. L. Lazrus, Hydrogen peroxide and sulfur (IV) in Los Angeles cloud water, *Atmos. Environ.*, 17, 911–914, 1983.

Roberts, J. D., R. Stewart, and M. C. Caserio, *Organic Chemistry*, W. A. Benjamin, Menlo Park, Calif., 1971.

Russell, A. G., G. J. McRae, and G. R. Cass, Mathematical modeling of the formation and transport of ammonium nitrate aerosol, *Atmos. Environ.*, in press, 1983.

Schwartz, S. E., Gas-aqueous reactions of sulfur and nitrogen oxides in liquid-water clouds, in *Acid Precipitation*, edited by J. G. Calvert, Ann Arbor Science, Ann Arbor, Mich., in press, 1983.

Schwartz, S. E., and J. E. Freiberg, Mass-transport limitation to the rate of reaction of gases in liquid droplets: Application to oxidation of SO_2 in aqueous solutions, *Atmos. Environ., 15*, 1129–1144, 1981.

Schwartz, S. E., and W. H. White, Solubility equilibria of the nitrogen oxides and oxyacids in dilute aqueous solution, *Adv. Environ. Sci. Eng., 4*, 1–45, 1981.

Sillén, G. L. and A. E. Martell, Stability constants of metal-ion complexes, *Spec. Publ. 17*, Chem. Soc., London, 1964.

Sørensen, P. E., and V. S. Andersen, The formaldehyde-hydrogen sulphite system in alkaline aqueous solution: Kinetics, mechanisms, and equilibria, *Acta Chem. Scand., 24*, 1301–1306, 1970.

Stumm, W., and J. J. Morgan, *Aquatic Chemistry*, 2nd ed., Wiley-Interscience, New York, 1981.

Waldman, J. M., J. W. Munger, D. J. Jacob, R. C. Flagan, J. J. Morgan, and M. R. Hoffmann, Chemical composition of acid fog, *Science, 218*, 677–680, 1982.

Westall, J. C., J. L. Zachary, and F. M. Morel, MINEQL, a computer program for the calculation of chemical equilibrium composition of aqueous solutions, *Tech. Note 18*, Dep. of Civ. Eng., Mass. Inst. of Technol., Cambridge, Mass., 1976.

(Received October 4, 1982;
revised April 14, 1983;
accepted April 14, 1983.)

CHAPTER VI

A FIELD INVESTIGATION OF PHYSICAL AND CHEMICAL MECHANISMS AFFECTING POLLUTANT CONCENTRATIONS IN FOG DROPLETS

by Daniel J, Jacob, Jed M. Waldman, J. William Munger,

and Michael R. Hoffmann

Tellus 36B, 272-285

Tellus (1984), *36B*, 272–285

A field investigation of physical and chemical mechanisms affecting pollutant concentrations in fog droplets

By DANIEL J. JACOB, JED M. WALDMAN, J. WILLIAM MUNGER and MICHAEL R. HOFFMANN, *Environmental Engineering Science, W. M. Keck Laboratories, California Institute of Technology, Pasadena, CA 91125, USA*

(Manuscript received November 8, 1983; in final form February 15, 1984)

ABSTRACT

High ionic loadings were found in fogwater collected at Bakersfield, California during an extended stagnation episode. The major ions were NH_4^+, NO_3^-, and SO_4^{2-}, with concentrations usually in the millimolar range. Droplet growth played an important rôle in determining fogwater concentrations. The amount of solute decreased substantially over the course of each fog event: this was attributed, at least in part, to deposition of fog droplets on surfaces. The occurrence of dense fogs thus seemed to limit particle build-up during stagnation episodes. The sulfate fraction in the aerosol increased appreciably over several days of stagnation, but no statistical evidence for in situ S(IV) aqueous-phase oxidation was found. The high ammonia concentrations present were sufficient to neutralize a large fraction of the ambient acidity. As a result, fogwater pH values rarely attained the extremely low values found in other polluted environments.

1. Introduction

Concern about acidic precipitation has stimulated research efforts to understand the chemistry of non-precipitating clouds (Petrenchuk and Drozdova, 1966; Lazrus et al., 1970; Hegg and Hobbs, 1982; Hegg, 1983). Ionic concentrations higher than those found in rain have been observed in clouds and fogs (Munger et al., 1983). In fog, the condensation of water vapor on pre-existent particles in the boundary layer shifts the aerosol size distribution towards larger sizes and produces a dilute aqueous aerosol. These physical and chemical changes in the aerosol may significantly affect its characteristics with regard to air pollution potential and deposition.

Even though fogs have been linked in the past to health-threatening pollution episodes (Commins and Waller, 1967), few field studies of fogwater chemistry have been made. Houghton (1955) sampled fog at several sites in New England and observed high concentrations of components that he attributed to the dissolution of activated nuclei. He found relatively high acidities and suggested that they were due to the scavenging of free sulfuric acid nuclei. Mrose (1966) and Okita (1968) also found elevated ionic concentrations and acidities in East Germany and Japan, respectively. Mader et al. (1949) reported sulfuric acid aerosol concentrations as high as 150 $\mu g\ m^{-3}$ during fog events in Los Angeles. These values were comparable to those observed during some London fogs (Goodeve, 1936). Waldman et al. (1982) and Munger et al. (1983) found extremely high ionic concentrations in Los Angeles area fogwater; solute concentrations were in the millimolar range for the major components, and pH values were usually in the range of 2 to 4.

Fog droplets appear to be efficient scavengers of boundary layer pollutants, and could provide a favorable environment for aqueous-phase reactions leading to the production of strong acids (Jacob and Hoffmann, 1983). The oxidation of absorbed S(IV) to form S(VI), with the concomitant production of acidity, is suspected as being an important reaction in the aqueous phase. Cass (1979) has observed that the worst sulfate pollution episodes in Los Angeles occur during periods of high

humidities and coastal fog, and Hegg and Hobbs (1982) have reported SO_2 conversion rates of up to 1900% h^{-1} in clouds. Laboratory studies (Martin, 1984) indicate that the oxidation of S(IV) can proceed rapidly at atmospheric concentrations in the presence of strong oxidants.

This paper presents results of a field investigation of fogwater composition in the southern San Joaquin Valley of California. The San Joaquin Valley is a site of both agricultural activity and oil recovery operations, which lead to high atmospheric loadings of particulate matter and trace gases. Fogs are common in the Valley during the winter months and can form every night under near-stagnant conditions caused by mesoscale subsidence. Because of the unusual stability in the local weather pattern and air masses, as well as the identification of emission sources (California Air Resources Board (CARB), 1982), it was possible to study the physical and chemical parameters influencing the fogwater composition, and to evaluate the cumulative effect of repeated fog occurrences on the chemical loading of an air mass.

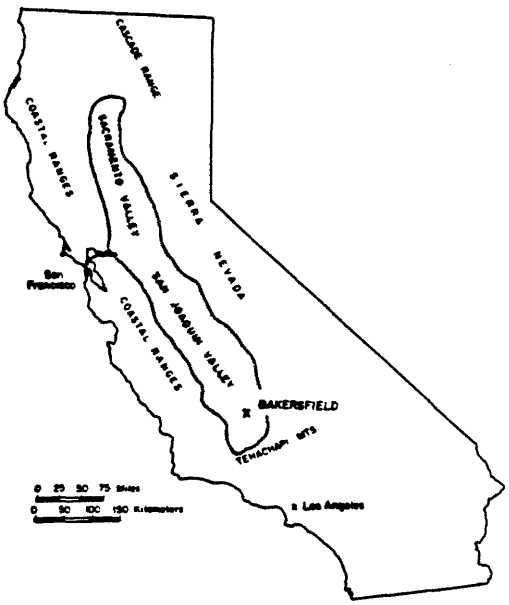

Fig. 1. The Central Valley of California.

2. Site description and measurement techniques

2.1. Site description

All measurements were made at Bakersfield (Kern county) from 30 December 1982 to 15 January 1983. Kern county is located at the southern tip of the Central Valley of California, which extends north about 700 km. The Valley is approximately 80 km wide over its entire length and is encompassed by mountain ranges (Fig. 1). Apart from a narrow gap at the Sacramento river delta, egress from the Valley is possible only through mountain passes. The lowest passes to the east and south are above 1000 m elevation. The Valley is subdivided into the San Joaquin and Sacramento Valleys, south and north of the Sacramento gap respectively. In the southern part of the San Joaquin Valley the lowest pass to the west is at 600 m elevation.

The wintertime meteorology of the Central Valley is dominated by the Basin High, which creates a very strong subsidence inversion (Holets and Swanson, 1981). The base of the inversion is typically 200 m to 500 m above ground level (AGL), although it occasionally comes down to the ground. This stable synoptic pattern is interrupted periodically by a frontal passage which often leads to precipitation on the Valley floor. As the subsidence resumes, the moist air is trapped inside the Valley. Loss of heat by radiation eventually leads to the formation of a widespread fog layer. Under these conditions, fog (locally called "Tule" fog) can form nightly and last into the late morning, with a persistent haze lasting through the afternoon.

Because the mixing height is usually lower than the natural boundaries of the Valley, the transport of air masses in and out of the Valley during these episodes is very limited. A weak net flow north out of the San Joaquin Valley leads to a residence time of 8 to 12 days for an air mass in the San Joaquin Valley (Reible et al., 1984). The daytime up-slope flow and the night-time drainage flow associated with the heating and cooling of the mountain slopes dominate the wind patterns in the Valley itself. Flow divergence from the Valley floor in the day, and convergence at night, has been observed by Smith et al. (1981). In the winter, because of the reduced insolation, this flow is probably too weak to ventilate the Valley by transport over the mountain ridges (Reible et al., 1983). As a result, between frontal passages and the ensuing at-

mospheric cleansing, the air in the Valley is near-stagnant.

Major oil fields are located in Kern county, and large amounts of SO_2 and NO_x are released in the steam-injection oil recovery operations (CARB, 1982). In addition, most of the Valley floor is occupied by farming and ranching activities, which are important sources of primary particulate matter (CARB, 1982) and ammonia. At the high humidities prevalent in the winter months, primary and secondary H_2SO_4 and HNO_3 react with NH_3 and H_2O to form ammonium sulfate and nitrate droplets (Stelson, 1982). Because of the production of this secondary aerosol, Kern county experiences severe sulfate pollution episodes in the winter months (Duckworth and Crowe, 1979).

2.2. *Measurement techniques*

Fog and aerosol samples were collected from the roof of a three-story building in downtown Bakersfield, above a CARB air monitoring station. The surroundings are residential and commercial, with no major point pollutant sources. There are no nearby structures taller than the site. An east–west highway, with usually moderate traffic, is located 500 m south of the site.

Fogwater was sampled with a rotating arm collector, which has been characterized in detail elsewhere (Jacob et al., 1984). This instrument samples air at a rate of 5 m^3 min^{-1}, performs well in preserving the chemical integrity of the sample at all stages of collection, and has a lower size cut of 20 μm diameter (determined by experimental calibration). Jacob et al. (1984) have estimated that on the average, 60% of the total liquid water is collected with this device. Fogwater samples were collected over periods ranging from 30 min to 3 h, and were analyzed for major ions, trace metals, S(IV), formaldehyde, and total organic carbon. Sample handling and analytical procedures were identical to those described previously (Munger et al., 1983).

Aerosol between fog events was collected on a set of two Gelman Zefluor Teflon filters. One filter, which was surmounted by a cap to prevent preferential sampling of large particles by sedimentation, was open-faced and collected total particulate matter; the other was set downstream of a cyclone separator which removed particles larger than 2 μm. After 11 January, only the open-faced filter was used. Filter samples were taken over time intervals ranging from 2.5 to 8 h. The filters were extracted in 10 ml of water on a reciprocating shaker for 60 min, and analyzed for major ions using the same analytical methods as for the fogwater.

Gaseous ammonia was collected by absorption on an oxalic acid impregnated Gelman glass fiber filter set downstream of the open-faced Teflon filter. Ammonium ion was determined by the phenol-hypochlorite method on a water extract using a modification described by Russell (1983).

Liquid water content was measured by drawing air at a rate of 1 m^3 min^{-1} through open-faced paper filters. The filters were exposed to the fog prior to use to equilibrate them with the ambient humidity. The liquid water content was determined by weight. This method has been found (Calspan Corp., Buffalo, NY, private communication) to yield results comparable to those obtained with more sophisticated optical methods (Chylek, 1978). It must be stressed that no fully reliable method for measuring absolute liquid water content exists to date, and that variations in results of up to 50% commonly occur from one method to another; therefore measurements must be interpreted with caution.

The CARB air monitoring station located at the site provided hourly averages of gas-phase NO, NO_x, SO_2, O_3, and CO concentrations. Hourly mixing height measurements (from 30 m up to 1000 m) were obtained at Bakersfield by acoustic sounding (Western Oil and Gas Association, Los Angeles, private communication). Hourly weather observations were recorded 8 km north of our site by the Bakersfield National Weather Service office (National Oceanic and Atmospheric Administration, 1983).

2.3. *Weather pattern*

On 22–23 December, a frontal passage over the Valley deposited 7.6 mm of rain on Bakersfield. A strong subsidence associated with the Basin High followed, and a stratus deck started forming on 26 December. Temperatures dropped and were 3 to 7 °C lower than normal during the period 30 December–15 January. Daily highs ranged from 4 to 8 °C and daily lows from −2 to 3 °C. Fog was reported at the Bakersfield site on 29 and 30 December, but was patchy in the surrounding area. In the text, the date of the fog will be given as that of the morning on which it occurred, even though it

may have already been formed the previous evening. On 31 December and 1 January, dense widespread fogs persisted through the night and well into the morning. The following three days, 2–4 January, thin radiation fogs formed at the site for a brief period in the early morning as the temperature dropped sharply. Dense widespread fog through the night again occurred on 5 January (not sampled) and on 6–8 January. On 9–10 January, a weak front passed through the Valley, resulting in some clear sunshine, high cloudiness, and drizzle in the morning of 9 January which deposited a trace amount of rain. On the morning of 10 January, a drop in temperature down to −2 °C at the site caused the formation of a thin, shallow fog which lasted for 3 h. After 1600 on 10 January, the subsidence inversion again limited the mixing heights to less than 500 m AGL and dense, all-night fogs formed every night from 11 January to 15 January. Sampling was discontinued after 15 January. All fogs were sampled from beginning to end, except the 31 December and 11 January fogs, for which sampling did not start until a few hours after fog formation.

3. Results and discussion

3.1. Fogwater concentrations

Table 1 gives the range and median value of fogwater concentrations for the entire data set (n = 108). Close ionic balances for most fogwater samples (±10% in over 80% of the cases) indicate that no important ions were missed in analysis. Ammonium, nitrate, and sulfate ions, by far the most important components present, had concentrations usually in the millimolar range. These high concentrations indicate the dominant impact of agriculture (NH_4^+) and fuel combustion (NO_3^-, SO_4^{2-}) on the fogwater composition. Occasionally, H^+, Ca^{2+}, and Cl^- contributed significantly to the total equivalent loading of the droplets. Ratios of concentrations of Na^+ to other ions indicated that sea salt was not a major source. Iron and lead were the most prominent trace metals.

Fig. 2 shows the evolution of fogwater concentrations with time during the 7 January fog. Winds were light and variable throughout the night, and temperatures ranged from 1 to 3 °C. As droplets grew at the beginning of the fog, they

Table 1. *Fogwater concentrations at Bakersfield, California**

Component	H^+	Na^+	K^+	NH_4^+	Ca^{2+}	Mg^{2+}	Cl^-
Range of concentrations (μeq l^{-1})	0.1–2750	1.4–325	1.6–368	490–13,300	7–3500	1.1–430	1–980
Median concentration (μeq l^{-1})	60	19.5	9.3	1440	47	6.3	47

Component	NO_3^-	SO_4^{2-}	S(IV)	CH_2O	TOC†
Range of concentrations (μeq l^{-1})	200–6800	194–9400	45–3000‡	53–710‡	710–23,000‡
Median concentration (μeq l^{-1})	850	1160	515‡	165‡	4000‡

Component	Fe	Mn	Pb	Cu	Ni	V
Range of concentrations (μg l^{-1})	81–10,700	3–525	48–3340	6–717	22–1232	7–850
Median concentration (μg l^{-1})	400	14	330	34	61	55

(a) Hydroxymethanesufonate ion coelutes with nitrate in the ion chromatographic column, so that nitrate concentrations could be overestimated.

* 108 samples over the period 30 December 1982–15 January 1983.

† Total organic carbon.

‡ For S(IV), CH_2O, and total organic carbon, concentrations are in μ moles l^{-1}.

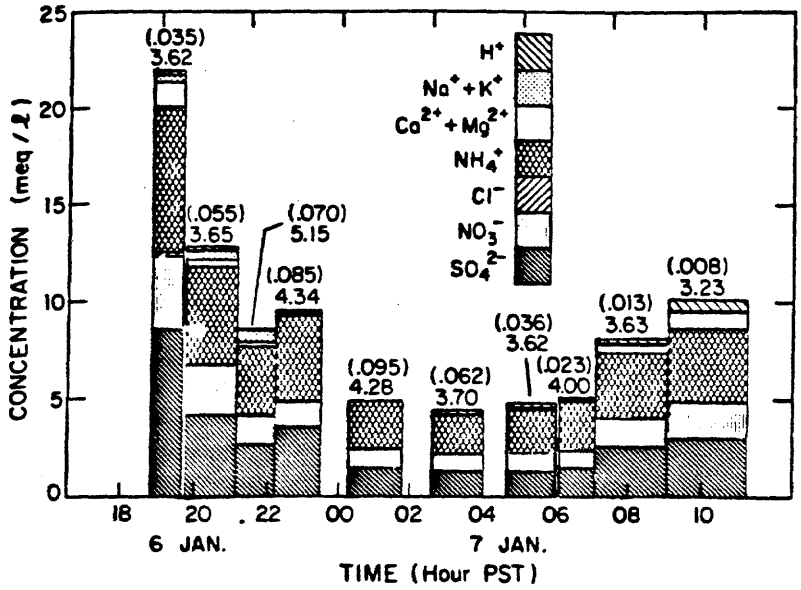

Fig. 2. Evolution of fogwater concentrations over the course of the 7 January 1983 fog event at Bakersfield. Fogwater pH and average liquid water contents (g m^{-3}, in parentheses) are indicated on top of each data bar.

became more dilute, and conversely as the fog dissipated, evaporation concentrated the droplets. The resulting concave profile for fogwater concentrations was evident in all the events sampled over the course of this investigation, and has been found to be a characteristic of fogs in other locations as well (Waldman et al., 1982). Droplet growth is therefore a dominant process in controlling fogwater concentrations. Accordingly, acidities were usually the highest at the beginning and end of fog events. The ratio of concentrations of one component to another was not subject to large variations from sample to sample within one event, which implies that the air masses were generally homogeneous. A trend of decreasing concentrations, superimposed on the concave profile, was noted. We will see that this can be attributed, at least in part, to deposition of fog droplets on surfaces.

3.2. Atmospheric particulate loadings in relation to fog occurrences

The major components of the daytime aerosol were NO_3^-, SO_4^{2-}, and NH_4^+. No significant differences were observed between the total aerosol and fine aerosol filters for NH_4^+, NO_3^-, SO_4^{2-}, and Cl^- concentrations. On the other hand, concentrations of Na^+, Ca^{2+}, and Mg^{2+} were higher in the total aerosol than in the fine aerosol; coarse soil dust is probably a major source of these components. Fig. 3 summarizes the evolution of atmospheric loadings over the 17-day sampling period. Mixing height data and concentrations of trace gases are given as hourly averages. Ozone concentrations were at or below the detection limit of 10 ppb in 96% of the hourly measurements. Time-averaged fogwater loadings/m^3 of air (calculated from liquid water content measurements) are given for each fog event, along with the aerosol loadings and gaseous ammonia concentrations between fog events. Prior to 6 January, the liquid water content was not directly measured; we estimated it by measuring the amount of water collected and assuming a 60% collection efficiency. In our calculations of the fogwater loadings, we assume that the collected samples are representative of the ambient fogwater in spite of the high lower size-cut of the sampler. The individual contributions of droplets of different sizes to the overall fogwater loading have not yet been rigorously investigated; they are difficult to predict from droplet growth theory (Pruppacher and Klett,

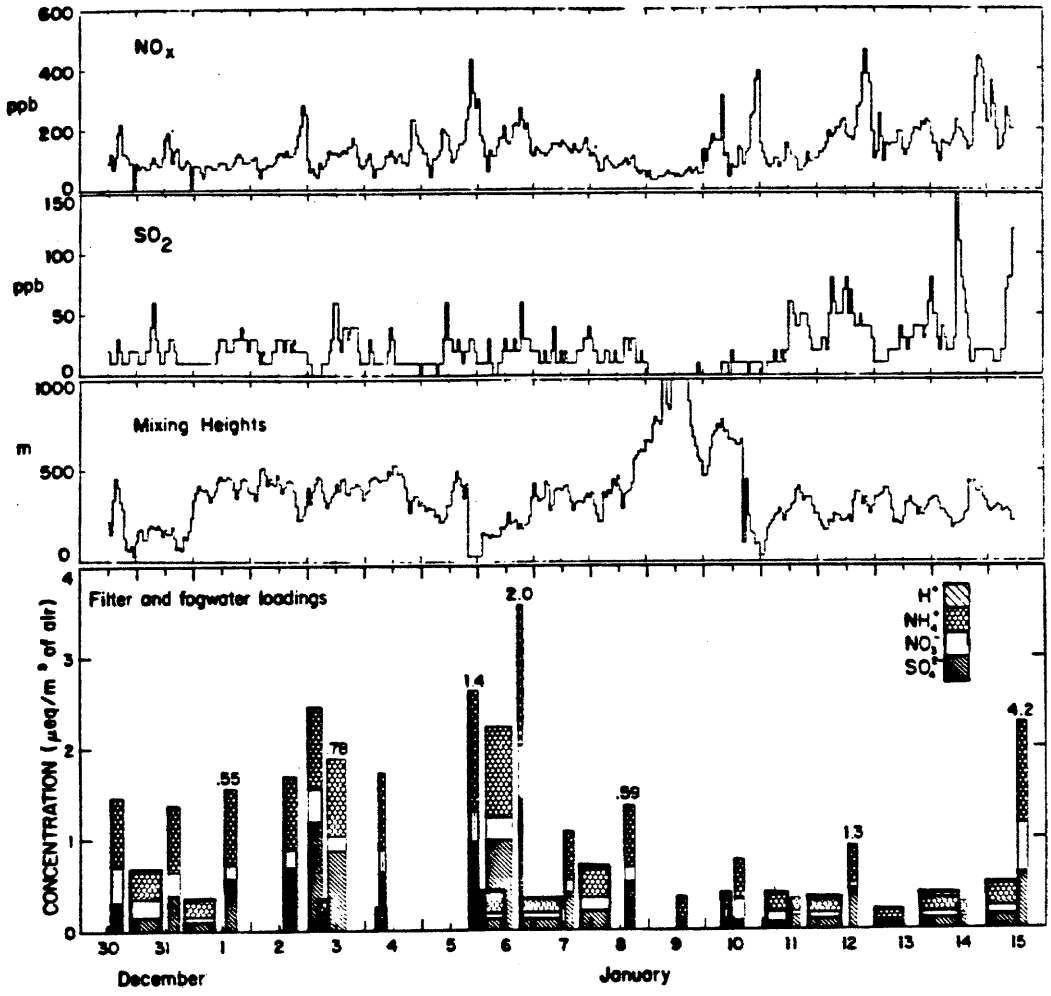

Fig. 3. Fogwater (in bold) and aerosol loadings of NH_4^+, NO_3^-, SO_4^{2-} and H^+ (fogwater) measured at Bakersfield during the period 30 December 1982–15 January 1983. When measured, gaseous ammonia concentrations (p.p.b.: 1 p.p.b. = 0.044 μmoles m^{-3} at 1 °C) are indicated on top of the aerosol data bars. Mixing heights are given in (m) above ground level.

1978) because supersaturations in fogs fluctuate rapidly in a poorly understood manner (Roach, 1976; Gerber, 1981). The large droplets in the fog are likely to have condensed on large nuclei, and therefore are not necessarily more dilute than the smaller droplets. A recent field intercomparison study of fogwater sampling devices (Hering and Blumenthal, 1983) seems to indicate that variations in the composition of the fogwater collected by instruments with different droplet size-cuts are insignificant.

The mixing height data show that two distinct air masses were involved during the 17-day period. The base of the inversion layer usually oscillated between 100 m and 500 m AGL. However, on 9 January, the inversion layer rose to above 1000 m and possibly vanished (no measurements were available above 1000 m). This allowed mixing with air from outside the Valley, and, with the added contribution of the 9 January morning drizzle, effectively renewed the air mass in the Valley. After the afternoon of 10 January, stagnation conditions resumed and no mixing heights above 500 m were recorded until after 15 January.

Aerosol and trace gas loadings reflected the apparent change in air masses. Since emission sources are located close to the ground, the majority of pollutants were released below the base of the inversion layer. Due to the lack of ventilation, accumulation of pollutants proceeded. During the period of 30 December to 9 January, the stagnant air mass was well-aged; high particulate and SO_2 levels were observed. After the effective cleansing of the atmosphere on 9–10 January, aerosol and SO_2 loadings dropped sharply.

On several occasions, aerosol samples were taken a few hours before a fog formation. The fraction of the afternoon aerosol found in the first fogwater sample collected the following night ranged from 0.1 to 0.8 and from 0.2 to 2.0 for sulfate and nitrate, respectively. These numbers varied considerably from fog to fog, and this can be attributed to variations in nucleation scavenging efficiencies and differences in the air masses advected over the site in the afternoon and at night. It is therefore not possible to make quantitative conclusions with regard to aerosol scavenging efficiencies, but it appears that a substantial fraction of the aerosol is incorporated into the fog droplets.

Scavenging of trace gases is an additional source of chemical input to the fogwater. The solubility of several gases in fog droplets has been discussed by Jacob and Hoffmann (1983). Nitric acid is 100% scavenged, and so is ammonia below pH 5. From the gas phase data, it appears that the occurrence of fog does not by itself affect partial pressures of SO_2; thermodynamic considerations indicate that, in spite of the dissociation of $SO_2 \cdot H_2O$ in solution and the formation of S(IV) adducts, absorption of $SO_2(g)$ by fog droplets is limited to a few % because of the small amount of water present. No correlation appears either between NO_x levels and fog occurrences. This agrees with the results of Schwartz and White (1981), who show that the dissolution of NO_x at atmospheric concentrations is too slow to be of relevance over the lifetime of the fog.

All the extended fog events sampled over the 17-day period showed a substantial decrease in the fogwater loadings over the course of the fog (Fig. 4). Loadings of major ions at the end of the fog ranged from 4% to 36% (median 17%) of those at the beginning of the fog, depending on the event. However, the steady decreasing pattern was not established until a few hours after fog formation; in the initial stage of the fog, the evolution of fogwater loadings was irregular. Changes in the fogwater loadings over the course of the fog could be

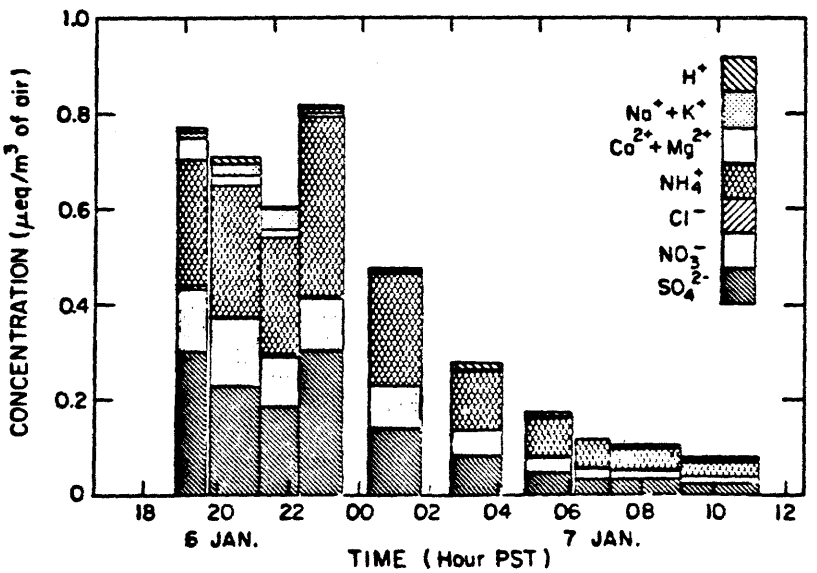

Fig. 4. Evolution of fogwater ionic loadings over the course of the 7 January fog event.

attributed to deposition of the coarse fog droplets, short-range transport, or displacement of the inversion base. Comparison of daytime aerosol or nighttime fog loadings to the mixing heights over the same time period did not show any strong correlation for mixing heights below 600 m. In addition, oscillations of the mixing height over the course of the fogs did not show a consistent trend which could be associated with a decrease in fogwater loadings. Therefore, this factor is probably not critical. Characterization of short-range transport at night is made difficult by the complex drainage flows converging to the center of the Valley. Because Bakersfield is located in the convergence zone, local winds oscillate considerably from hour to hour in both direction and speed (National Oceanic and Atmospheric Administration, 1983). Concentrations of CO, NO_x, and SO_2 during fog events did not show the strong decreases that would be associated with the advection of much cleaner air masses over the site. Therefore, it is unlikely that short-range transport could fully account for the considerable decrease of fogwater loadings with time.

Deposition of fog droplets on surfaces, on the other hand, could lead to the observed decreases in fogwater loading. Fog formation results in an important shift of the aerosol distribution towards larger particle sizes; because the residence time in the atmosphere of particles above 10 μm is of the order of hours, and rapidly decreases with increasing size (Muller, 1982), the deposition rate of the aerosol must be enhanced. During the early stage of the fog, the droplets presumably do not grow to a size large enough to be effectively deposited; factors other than deposition influence the fogwater loading, and hence the irregular behaviour of the profile of fogwater loadings with time. As a population of large droplets is later established, deposition becomes more rapid and overcomes other factors. Turbulent diffusion to the ground, impaction and sedimentation are probably all important in contributing to the removal of fog droplets. The numerical study of Brown and Roach (1976) has shown that important droplet settling must occur to explain the low liquid water content observed in fogs; Brown (1980) finds that the settling process does not become important until a few hours after fog formation, which is consistent with our observations. If scavenging of gases and particles by the droplets is followed by deposition, pollutants will effectively be removed from the atmosphere.

Particle concentrations in the Valley are determined by sources (fresh input of primary and secondary aerosol), sinks (transport aloft and out of the Valley, deposition), and intra-Valley transport. Under stagnant conditions, one would expect a pollutant build-up until a steady state is reached due to an eventual balance of sources and sinks. The characteristic time for deposition of haze particles (0.05–2 μm) is 3–6 days (Muller, 1982), but under fog conditions, particles scavenged by the fog droplets will deposit much more quickly. Dense fogs can therefore limit particle accumulation. The overall higher loadings during the 26 December–8 January stagnation episode (where dense fog did not form every night) compared to those during the 10 January–15 January episode (where dense fog formed every night) could then be explained by a pollutant build-up due to the predominance of haze but limited fog. This accumulation is obvious for ammonium nitrate and sulfate salts, which are the main constituents of the haze aerosol; on the other hand, concentrations of Ca^{2+} in the aerosol did not increase during the stagnation episodes. Calcium mostly originates from coarse dust particles with a residence time shorter than one day, and will settle out regardless of fog formation.

3.3. Heterogeneous S(IV) oxidation

Because of the high $SO_2(g)$ concentrations in Bakersfield and the presence of an aquated aerosol, there is a potential for aqueous-phase oxidation of S(IV) to S(VI) by the strong oxidants H_2O_2, O_3, and O_2 (Jacob and Hoffmann, 1983; Martin, 1984). Evolution of sulfate concentrations in the fogwater between times t_1 and t_2 can be expressed by:

$$[\mathrm{S(VI)}]_{t_2} L(t_2) = \{[\mathrm{S(VI)}]_{t_1} L(t_1) + \int_{t_1}^{t_2} \frac{\mathrm{d}[\mathrm{S(VI)}]}{\mathrm{d}t} L(t)\,\mathrm{d}t\}(1 - r), \quad (1)$$

where $L(t)$ is the liquid water content of the fog, and r characterizes changes in [S(VI)] (assumed first-order) due to physical mechanisms such as deposition. We assume as a first approximation that $L(t)$ and r control the evolution of the chemically conservative quantity $[T]$, defined as the sum of the equivalent concentrations of all

components A_i in solution minus sulfate and its counter-ion:

$$[T] = \sum_{i=1}^{n} [A_i]. - 2[\mathrm{S(VI)}] \tag{2}$$

With this assumption, we can write for a homogeneous air mass:

$$[T]_{t_2} L(t_2) = [T]_{t_1} L(t_1)\,(1 - r), \tag{3}$$

and substitute (3) into (1):

$$\int_{t_1}^{t_2} \frac{\mathrm{d[S(VI)]}}{\mathrm{d}t} L(t)\mathrm{d}t = L(t_1)\left([\mathrm{S(VI)}]_{t_2} \times \frac{[T]_{t_1}}{[T]_{t_2}} - [\mathrm{S(VI)}]_{t_1}\right). \tag{4}$$

A major difficulty in solving (4) for $\mathrm{d[S(VI)]}/\mathrm{d}t$ and using statistical analysis to verify or derive a rate law is that the variables on which $\mathrm{d[S(VI)]}/\mathrm{d}t$ depends are not satisfactorily quantified. Reactions of S(IV) with H_2O_2 and O_3 are expected to be first-order in oxidant concentrations (Martin, 1984), but H_2O_2 and O_3 concentrations were not measured at Bakersfield (ozone below the detection limit of 10 ppb, as observed, still cannot be neglected as an oxidant in droplets with high pH). Oxygen has been predicted to be an effective oxidant in solution when catalyzed by trace metals (Jacob and Hoffmann, 1983), but the form of the rate law has not been satisfactorily established at the pH and free S(IV) concentration ranges typical of the Bakersfield fogwater (Martin, 1984); furthermore, it may be complicated because of aqueous-phase speciation of metals and S(IV) (Hoffmann and Jacob, 1984).

Rates of sulfate production in the atmosphere have previously been derived from field data by Cass (1981) and Hegg and Hobbs (1981, 1982). These investigators expressed this rate in terms of a pseudo first-order rate constant k (% h^{-1}) referenced to gas-phase SO_2:

$$\frac{\mathrm{d[S(VI)]_{air}}}{\mathrm{d}t} = \frac{k}{100}[\mathrm{SO_2(g)}], \tag{5}$$

where $[\mathrm{S(VI)}]_{air}$ and $[\mathrm{SO_2(g)}]$ are concentrations per unit volume of air. Eq. (5) is obviously unjustified from a chemical standpoint, because it ignores the rate dependence on droplet pH, concentrations of oxidants and catalysts, temperature, and photochemical activity. Still, it provides a convenient parameterization of sulfate production and will be adopted here in the absence of a more reliable expression. Substituting (5) into (4):

$$\int_{t_1}^{t_2} \frac{k}{100}[\mathrm{SO_2(g)}]\mathrm{d}t = L(t_1)\left([\mathrm{S(VI)}]_{t_2} \frac{[T]_{t_1}}{[T]_{t_2}} - [\mathrm{S(VI)}]_{t_1}\right). \tag{6}$$

Assuming that $[\mathrm{SO_2(g)}]$ varies linearly with time over the interval considered:

$$k = \frac{200}{t_2 - t_1} \frac{L(t_1)}{[\mathrm{SO_2(g)}]_{t_2} + [\mathrm{SO_2(g)}]_{t_1}} \times \left([\mathrm{S(VI)}]_{t_2} \frac{[T]_{t_1}}{[T]_{t_2}} - [\mathrm{S(VI)}]_{t_1}\right). \tag{7}$$

Table 2 shows that the k values calculated from our data set with eq. (7) are lower than those obtained by Hegg and Hobbs (1981, 1982) for clouds over western Washington State, and are of the order of those observed in the Los Angeles aerosol by Cass (1981). However, both ozone concentrations and pH were higher in the clouds sampled by Hegg and Hobbs (1981, 1982) than in the Bakersfield fogs sampled in this study: in the same way, temperature, solar irradiation, and oxidant concentrations are all lower in Bakersfield (in the wintertime) than in Los Angeles. Therefore, comparison of the data sets in terms of k is difficult.

Cass (1981) noted that gas phase oxidation could not be sufficiently rapid to explain the S(IV) conversion rates in Los Angeles, and suggested aqueous-phase oxidation as an alternate mechanism. Hegg and Hobbs (1982) pointed to S(VI) in-cloud production from some basic statistical analysis of their data, a conclusion which has been disputed by Schwartz and Newman (Schwartz et al., 1983). Our data set does not allow us to conclude that k is significantly different from zero. Fig. 5 shows the frequency distribution we observed for k; the near symmetrical deviations about k = 0% h^{-1} can be simply attributed to the non-Lagrangian nature of the sampling procedure. The presence of a few outliers on the positive side of the distribution could suggest that S(IV) in-fog oxidation proceeds under certain conditions, but these points are associated with SO_2

Table 2. *SO_2 oxidation rates in the atmosphere*

Location	k (% h^{-1})*	Reference
Western Washington (wave clouds)	0–300	Hegg and Hobbs (1981)
Western Washington (clouds)	−600 ± 1000–1900 ± 1900	Hegg and Hobbs (1982)
Los Angeles (aerosol, summer)	6.0†	Cass (1981)
Los Angeles (aerosol, winter)	2.0†	Cass (1981)
Bakersfield (fogs)	0.9 ± 5.5‡	This study

* k is a pseudo first-order rate constant expressing sulfate production as a % of $[SO_2(g)]$.

† Hourly production rates averaged over 3 years.

‡ Calculated from one fog sample to the next using equation (7). Data for n = 80 samples. Samples were excluded from the data set when: (i) SO_2 partial pressure was below the detection limit of 10 ppb; (ii) ionic balances were off by over 30%; or (iii) only one sample was collected during the event (2 January).

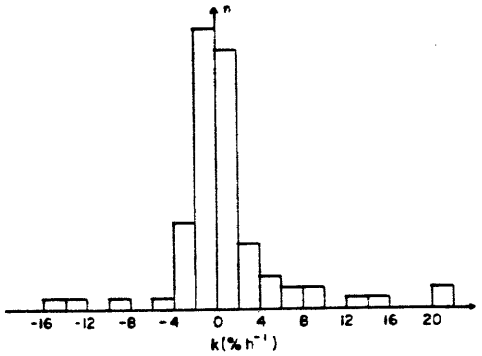

Fig. 5. Frequency distribution of the pseudo first-order rate constant for S(VI) in-fog production, k (% h^{-1}). Data from n = 80 fogwater samples collected at Bakersfield during the period 30 December 1982–15 January 1983.

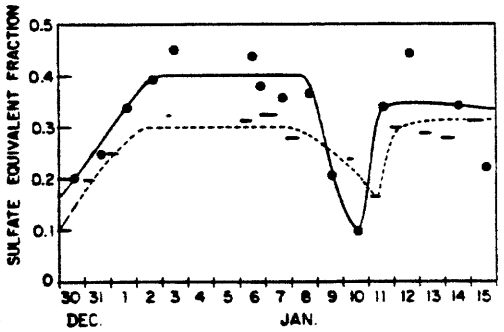

Fig. 6. Evolution of the sulfate equivalent fraction in the fogwater (—) and in the aerosol (●) at Bakersfield during the period 30 December 1982–15 January 1983. Lines have been added to show trends.

concentrations at, or close to, the detection limit of 10 ppb. The uncertainty on $[SO_2(g)]$ can then be as great as 50%, so that these outliers cannot be considered significantly different from the population as a whole.

Sulfate production was also analyzed in terms of k/L, which characterizes sulfate production referenced to the aqueous phase, and in terms of a zero-order dependence on $[SO_2(g)]$ (oxidation limited by mass transfer). Neither of these analyses showed evidence of S(VI) in-fog production.

In spite of this, the sulfate fraction of the aerosol increased over the course of the stagnation episodes (Fig. 6). After the two widespread fogs and persistent thick haze of 31 December and 1 January, the sulfate equivalent fraction (SEF) of the aerosol (defined as SEF = $[S(VI)]/[T]$) rose and stabilized at 0.40 ± 0.05. In comparison, the two-month aerosol averages reported by Heisler and Baskett (1981) for November–December 1978 at Bakersfield show an SEF of 0.22. The highest sulfate concentration we observed, 76 $\mu g\ m^{-3}$ on 6 January, is close to the highest 24-h value recorded in the area, 80 $\mu g\ m^{-3}$ (Duckworth and Crowe, 1979). On 9–10 January, along with the removal of the stagnant air mass from the Valley, the SEF dropped sharply, down to 0.10 on the afternoon of 10 January. After the inversion trapped the renewed air mass in the Valley, the SEF rose again to values similar to those before 10 January. The SEF values for the fogwater were lower than those

for the afternoon haze, but behaved qualitatively in the same way.

Preferential deposition of components other than sulfate would result in an increase in the sulfate content at the beginning of the stagnation episode. Because nitrate does not show the increase observed for sulfate, even though both components are mostly present in the same type of particles, it seems unlikely that preferential deposition alone could result in such a rise of the SEF. It therefore appears that S(VI) production reactions proceed in the stagnant air mass, and that the stabilization of the sulfate content then indicates the attainment of a steady-state between sulfate production and the sinks discussed previously. In-fog oxidation at an average rate of 0.9% h^{-1} (Table 2) with $P_{SO_2} = 20$ ppb would produce 16 neq m^{-3} S(VI)/h of fog. This is not sufficient to explain the increases in the SEF of the daytime aerosol, especially since a large fraction of the sulfate that could be produced in fog is expected to be lost by deposition. Gas-phase oxidation of SO_2 by radicals is expected to be unimportant because of the limited photochemical activity (reflected by the low O_3 levels). Instead, the higher SEF values in the daytime aerosol than in the fog suggest that sulfate production mostly occurs in the haze droplets forming at high humidities. This could be expected because of the higher catalyst concentrations in haze droplets, and because both temperatures and SO_2(g) concentrations usually peak in the afternoon. Oxidation of S(IV) in haze droplets should proceed along similar pathways as for fog droplets, and has been observed to proceed rapidly under controlled conditions (Matteson et al., 1969; Crump et al., 1983).

3.4. Fogwater acidity

Extreme acidity in fogwater, as has been documented in the Los Angeles area, may pose specific environmental problems because of the potential for injury to materials, vegetation (Scherbatskoy and Klein, 1983), and human health (Hoffmann, 1984). Sulfuric acid and nitric acid (which are the main strong acids present) can be emitted into the atmosphere as primary pollutants, or alternatively be produced in situ (Calvert, 1984). Alkaline components in the atmosphere will titrate free acidity. Gaseous ammonia, which is the most important alkaline component in the Valley, reacts with H_2SO_4 and HNO_3 at high humidities to form concentrated ammonium salt droplets (Stelson, 1982). Dissolution of SO_2(g) in the aquated aerosol leads to S(IV), which can then be oxidized to S(VI) as discussed in the previous section. Alternatively, S(IV) can be stabilized in the lower oxidation state by complexation with carbonyl compounds (Munger et al., 1984). The production of one molar unit of S(VI) releases one to two molar units of H^+; formation of S(IV) adducts also produces H^+ (Jacob and Hoffmann, 1983). The resulting input of acidity can be subsequently titrated by absorption of NH_3(g) in the droplet. Therefore, the acidity of liquid water in an air mass under high sulfate and nitrate conditions is limited by the availability of NH_3(g) (and other alkaline components) to neutralize the strong acids present. This has previously been observed for rainwater in the north-central United States (Munger, 1982).

In Los Angeles, where NH_3 emissions are relatively low (Russell et al., 1983), extremely high acidities are frequently found in the fogwater. In the Bakersfield fogwater, nitrate and sulfate concentrations are comparable to those in Los Angeles, but high acidities are much less common (Fig. 7). This is because ammonium concentrations are

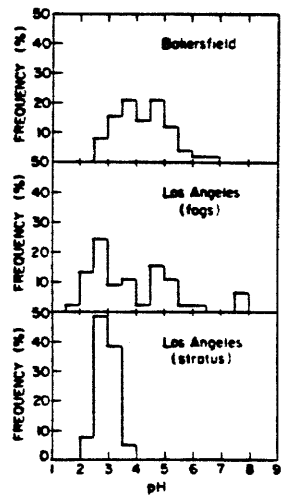

Fig. 7. pH frequency distribution for $n = 108$ fogwater samples collected at Bakersfield during the period 30 December 1982–15 January 1983. Results are compared with those obtained in the Los Angeles basin for fogs ($n = 45$) and stratus clouds ($n = 156$) (this laboratory, unpublished results, 1981–1983).

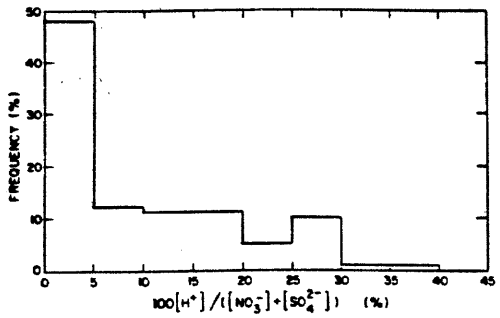

Fig. 8. Frequency distribution of the non-neutralized fraction of the acidity, as expressed by $[H^+]/([NO_3^-] + [SO_4^{2-}])$, for $n = 108$ fogwater samples collected at Bakersfield during the period 30 December 1982–15 January 1983.

considerably higher than in Los Angeles. A few samples at Bakersfield also had high concentrations of Ca^{2+}, indicating an alternative neutralization pathway by scavenging of alkaline dust.

Fig. 8 shows the fraction of non-neutralized acidic anions in our fog samples. In almost half of the samples, over 95% of the acidity was neutralized. At the same time, very low concentrations of gaseous ammonia were observed throughout the 17 days (Fig. 3). Most of the fogwater samples had pH values below 5, which suggests an absence of ammonia in the atmosphere from chemical equilibrium considerations. Ostensibly, the acidities present were sufficient to totally exhaust ammonia from the gas phase, and production of additional acidity resulted in a pH drop.

4. Conclusion

High ionic concentrations in the fogwater were observed at Bakersfield, California over the course of two stagnation episodes. The main contributors to the ionic loading of the fogwater were NH_4^+, NO_3^-, and SO_4^{2-}; this can be attributed to agricultural activity and oil recovery processes. Droplet growth was found to strongly influence the observed concentrations. Comparison of ionic loadings in the fogwater with those in the aerosol of the previous afternoon indicated that a sizable fraction of the aerosol was scavenged by the fog droplets. Fogwater ionic loadings decreased considerably over the course of the fog, and this was attributed to deposition of the large droplets on surfaces. In this manner, it was observed that a large fraction of the pollutants scavenged in the fog could be removed from the atmosphere. Deposition of fog droplets proceeds much more rapidly than deposition of the haze particles present at the high humidities between fog events, so that the occurrence of fog could slow down or limit the accumulation of particulate matter in a stagnant air mass.

Evolution of the sulfate content over the 17-day sampling period indicated an important increase of the sulfate fraction in the aerosol during stagnation episodes, but no statistical evidence for S(IV) oxidation in the fogwater was found. Most of the sulfate appeared to be produced in the daytime haze droplets. Preferential deposition of components other than sulfate could also partly explain the increase in the sulfate fraction.

High concentrations of acidic anions were present in the fogwater, but most of the acidity was neutralized by ammonia. In most cases, the neutralization of acidic components totally depleted NH_3 from the atmosphere; although the excess of acidity was usually not enough to lead to highly acidic conditions, 8% of the samples had pH values below 3.

5. Acknowledgements

This research was funded by the California Air Resources Board (CARB). We thank the staff of the CARB for their help and cooperation relating to our use of their facility at Bakersfield. We also acknowledge gratefully the CARB and the Western Oil and Gas Association for letting us use their data in this paper. Discussions with A. G. Russell were most helpful in the interpretation of some of the data.

REFERENCES

Brown, R. and Roach, W. T. 1976. The physics of radiation fog (II). A numerical study. *Q. J. R. Meteorol. Soc. 102*, 335–354.

Brown, R. 1980. A numerical study of radiation fog with an explicit formulation of the microphysics. *Q. J. R. Meteorol. Soc. 106*, 781–802.

California Air Resources Board 1982. Emission Inventory 1979, Stationary Source Control Division, Emission Inventory Branch, Sacramento, California.

Calvert, J. G. (ed.) 1984. *Acid precipitation*. Butterworth Publications, Boston.

Cass, G. R. 1979. On the relationship between sulfate air quality and visibility with examples in Los Angeles. *Atmos. Environ. 13*, 1069–1084.

Cass, G. R. 1981. Sulfate air quality control strategy design. *Atmos. Environ. 15*, 1227–1249.

Chylek, K. P. 1978. Extinction and liquid water content of fogs and clouds. *J. Atmos. Sci. 35*, 296–300.

Commins, B. T. and Waller, R. E. 1967. Observations from a ten-year study of pollution at a site in the city of London. *Atmos. Environ. 1*, 49–68.

Crump, J. G., Flagan, R. C. and Seinfeld, J. H. 1983. An experimental study of the oxidation of sulfur dioxide in aqueous manganese sulfate aerosols. *Atmos. Environ. 17*, 1277–1289.

Duckworth, S. and Crowe, D. 1979. Sulfur dioxide and sulfate trends, Bakersfield, 1977–1978. Technical Services Division, California Air Resources Board, Sacramento, California.

Gerber, H. E. 1981. Microstructure of a radiation fog. *J. Atmos. Sci. 38*, 454–458.

Goodeve, C. F. 1936. Discussion in "Sulphuric acid as a disperse phase in town air". *Trans. Faraday Soc. 32*, 1201–1202.

Hegg, D. A. and Hobbs, P. V. 1981. Cloud water chemistry and the production of sulfates in clouds. *Atmos. Environ. 15*, 1597–1604.

Hegg, D. A. and Hobbs, P. V. 1982. Measurements of sulfate production in natural clouds. *Atmos. Environ. 16*, 2663–2668.

Hegg, D. A. 1983. The sources of sulfate in precipitation (I). Parameterization scheme and physical sensitivities. *J. Geophys. Res. 88*, 1369–1374.

Heisler, S. and Baskett, R. 1981. Particle sampling and analysis in the California San Joaquin Valley. Research report CARB-RR-81-14, December 1981, available from Environmental Research and Technology, Westlake Village, California.

Hering, S. V. and Blumenthal, D. L. 1983. Field comparison of fog/cloud water collectors: preliminary results. Proceedings, Air Pollution Control Association Specialty Conference on the Meteorology of Acid Deposition, Hartford, Connecticut, 17 October 1983. Published by the Air Pollution Control Association, Pittsburgh.

Hoffmann, M. R. and Jacob, D. J. 1984. Kinetics and mechanisms of the catalytic autoxidation of dissolved sulfur dioxide in aqueous solution: an application to night-time fogwater chemistry. In *Acid precipitation* (ed. J. G. Calvert). Boston: Butterworth Publications, 101–172.

Hoffmann, M. R. 1984. Comment on acid fog. *Environ. Sci. Technol. 18*, 61–64.

Holets, S. and Swanson, R. N. 1981. High-inversion fog episodes in central California. *J. Appl. Meteorol. 20*, 890–899.

Houghton, H. G. 1955. On the chemical composition of fog and cloud water. *J. Meteorol. 12*, 355–357.

Jacob, D. J. and Hoffmann, M. R. 1983. A dynamic model for the production of H^+, NO_3^-, and SO_4^{2-} in urban fog. *J. Geophys. Res. 88*, 6611–6621.

Jacob, D. J., Wang, R.-F. T. and Flagan, R. C. 1984. Fogwater collector design and characterization. *Environ. Sci. Technol. 18*, (in press).

Lazrus, A. L., Baynton, H. W. and Lodge, J. P. 1970. Trace constituents in oceanic cloud water and their origin. *Tellus 22*, 106–114.

Mader, P. P., Hamming, W. J. and Bellin, A. 1949. Determination of small amounts of sulfuric acid in the atmosphere. *Anal. Chem. 22*, 1181–1183.

Martin, L. R. 1984. Kinetic studies of sulfite oxidation in aqueous solution. In *Acid precipitation* (ed. J. G. Calvert), Boston: Butterworth Publications, 63–100.

Matteson, M. J., Stober, W. and Luther, H. 1969. Kinetics of the oxidation of sulfur dioxide by aerosols of manganese sulfate. *I. & E. C. Fund. 8*, 677–686.

Mrose, H. 1966. Measurements of pH, and chemical analyses of rain-, snow-, and fog-water. *Tellus 18*, 266–270.

Muller, J. 1982. Rules in atmospheric behaviour of particulate substances. GAF-conference, Bologna, 14–17 September 1982, Fraunhofer Ges., Grafschaft/Schmallenberg, F. R. Germany.

Munger, J. W. 1982. Chemistry of atmospheric precipitation in the north central United States: influence of sulfate, nitrate, ammonia, and calcareous soil particulates. *Atmos. Environ. 16*, 1633–1645.

Munger, J. W., Jacob, D. J., Waldman, J. M. and Hoffmann, M. R. 1983. Fogwater chemistry in an urban atmosphere. *J. Geophys. Res. 88*, 5109–5123.

Munger, J. W., Jacob, D. J. and Hoffmann, M. R. 1984. The occurrence of bisulfite aldehyde addition products in fog- and cloudwater. *J. Atmos. Chem.* (in press).

National Oceanic and Atmospheric Administration 1983. Local climatological data (monthly summary) for Bakersfield, CA, Kern County air terminal, December 1982 and January 1983. Published by US Dept. of Commerce, National Climatic Data Center, Asheville, North Carolina, USA.

Okita, T. 1968. Concentration of sulfate and other inorganic materials in fog and cloud water and in aerosol. *J. Meteorol. Soc. Japan 46*, 120–126.

Petrenchuk, O. P. and Drozdova, V. M. 1966. On the chemical composition of cloudwater. *Tellus 18*, 260–286.

Pruppacher, H. R. and Klett, J. D. 1978. *Microphysics of clouds and precipitation*. Amsterdam: Reidel, 418–421.

Reible, D. D., Shair, F. H., Smith, T. B. and Lehrman, D. E. 1984. The origin and fate of air pollutants in California's San Joaquin Valley (I). Winter. *Atmos. Environ.* (in press).

Roach, W. T. 1976. On some quasi-periodic oscillations observed during a field investigation of radiation fog. *Q. J. R. Meteorol. Soc. 102*, 355–359.

Russell, A. G. 1983. Analysis of oxalic acid impregnated

filters for ammonia determination. Environmental Quality Lab open file report 83–1, California Institute of Technology, Pasadena, California.

Russell, A. G., McRae, G. J. and Cass, G. R. 1983. Mathematical modeling of the formation and transport of ammonium nitrate aerosol. *Atmos. Environ. 17*, 949–964.

Scherbatskoy, T. and Klein, R. M. 1983. Response of spruce and birch foliage to leaching by acidic mists. *J. Environ. Qual. 12*, 189–195.

Schwartz, S. E. and White, W. H. 1981. Solubility equilibria of the nitrogen oxides and oxyacids in dilute aqueous solution. *Adv. Environ. Sci. Eng. 4*, 1–45.

Schwartz, S. E., Newman, L., Hegg, D. A. and Hobbs, P. V. 1983. Measurements of sulfate production in natural clouds (discussion). *Atmos. Environ. 17*, 2629–2633.

Smith, T. B., Lehrman, D. E., Reible, D. D. and Shair, F. H. 1981. The origin and fate of airborne pollutants within the San Joaquin Valley. Final report to the California Air Resources Board, Sacramento, California.

Stelson, A. W. 1982. Thermodynamics of aqueous atmospheric aerosols. Ph.D. thesis, California Institute of Technology, Pasadena, California.

Waldman, J. M., Munger, J. W., Jacob, D. J., Flagan, R. C., Morgan, J. J. and Hoffmann, M. R. 1982. Chemical composition of acid fog. *Science 218*, 677–680.

CHAPTER VII

THE H_2SO_4 - HNO_3 - NH_3 SYSTEM AT HIGH HUMIDITIES AND IN FOGS: A FIELD STUDY OF A WINTERTIME STAGNATION EPISODE IN THE SAN JOAQUIN VALLEY OF CALIFORNIA

by Daniel J. Jacob, J. William Munger, Jed M. Waldman,

and Michael R. Hoffmann

Submitted to Journal of Geophysical Research (January 1985)

ABSTRACT

Atmospheric acidity in the San Joaquin Valley of California was interpreted from a systematic study at a network of sites of the H_2SO_4 - HNO_3 - NH_3 system in fogwater, aerosol, and the gas phase. Spatial patterns of atmospheric concentrations were established that reflect the distribution of emissions within the valley. Fogwater was acidic - or not - depending on the relative proximities of local oil recovery operations (SO_2, NO_x), and agricultural and livestock feeding activities (NH_3). The valley was efficiently ventilated when the temperature inversion broke up at some point in the day, but a severe stagnation episode was documented when a subsidence inversion based below the surrounding mountain ridges persisted for over five days. Progressive pollutant accumulation over the course of the stagnation episode was observed and interpreted in terms of production and removal mechanisms. An average SO_2 conversion rate of 2 % h^{-1} was determined in the overcast and stagnant boundary layer. Alkalinities decreased over the course of the episode due to the secondary production of strong acids, and inorganic acidities were observed at sites furthest from NH_3 emissions. The stratus cloud topping the boundary layer was found to slowly scavenge SO_2, but not NO_x. The occurrence of fog during the stagnation episode led to general decreases in aerosol concentrations, probably as a result of enhanced removal by deposition.

INTRODUCTION

Extremely high acidities have been reported in fogs and stratus clouds collected in Southern California (Munger et al., 1983; Brewer et al., 1983; Waldman et al., 1984; Jacob et al., 1984a,b). The acidity of these fogs was due to sulfuric acid and nitric acid, which had been partially neutralized by ammonia (Jacob et al., 1984a; Waldman et al., 1984). Therefore, one can attempt to interpret the "acid fog" phenomenon from the consideration of acid-base neutralization processes in the H_2SO_4-HNO_3-NH_3 system.

Ammonia is directly released to the atmosphere from a variety of sources, but H_2SO_4 and HNO_3 are mostly produced in the atmosphere itself by oxidation of reduced sulfur and nitrogen compounds. Oxidation of SO_2 to sulfate proceeds in the gas phase (Calvert and Stockwell, 1984), in concentrated aerosol (Kaplan et al., 1981; Crump et al., 1982), and in dilute aqueous solutions (Martin, 1984). Oxidation of NO_x to HNO_3 may proceed photochemically in the gas phase, or at the surface of particles, e.g., water droplets (Heikes and Thompson, 1983). Nitrite is slowly oxidized to NO_3^- in dilute solutions (Damschen and Martin, 1983). Using data available for S(IV) and N(III) oxidation, Jacob and Hoffmann (1983) found that aqueous-phase oxidation of S(IV) in fog droplets could be an important source of sulfate under polluted conditions; they found that, on the other hand, aqueous-phase oxidation of N(III) provided only a very small source of nitrate.

The residence times of H_2SO_4, HNO_3, and NH_3 in the atmosphere depend on the way they are partitioned between the gas phase and the

aerosol. Sulfuric acid is present as aerosol under usual atmospheric conditions, but HNO_3 and NH_3 may have significant vapor pressures over ammonium nitrate (Stelson and Seinfeld, 1982). The gaseous species are reactive and should be quiclky removed by deposition; Huebert (1983) has found deposition velocities of 1 - 5 cm s^{-1} for $HNO_3(g)$ over grass. On the other hand, the secondary particles formed from H_2SO_4 - HNO_3 - NH_3 - H_2O mixtures are typically in the size range 0.1 - 1 μm and have low deposition velocities, of the order of 0.01 -0.1 cm s^{-1} (Sehmel, 1980; Slinn, 1982). Under supersaturated conditions, however, deposition velocities of aerosol particles increase considerably if the particles grow to fog droplet size.

A general mechanism for the occurrence of fogwater acidity in polluted atmospheres must include five fundamental processes: (i) emissions of SO_2, NO_x, and NH_3, (ii) pollutant transport, (iii) atmospheric production of H_2SO_4 and HNO_3, (iv) detailed chemical speciation within the H_2SO_4 - HNO_3 - NH_3 - H_2O system, and (v) scavenging within fogs. To attempt an interpretation of fogwater acidity in terms of the above processes, we have conducted a detailed field study of aerosol and fogwater chemical composition in the San Joaquin Valley of California.

The San Joaquin Valley is the site of major oil recovery operations, which release large amounts of SO_2 and NO_x. In addition, agricultural and livestock feeding activities provide important sources of NH_3. Severe stagnation episodes, which are associated with fog and low-lying stratus clouds, occur frequently during the winter

months. They are caused by persistent subsidence inversions based a few hundred meters above the ground and below the surrounding mountain ridges (Holets and Swanson, 1981). Tracer studies have documented the lack of ventilation in the valley during these prolonged episodes (Reible, 1982).

In a preliminary study at a single site in December 1982 - January 1983, Jacob et al. (1984a) documented the main features of aerosol and fogwater chemical composition during stagnation episodes in the San Joaquin Valley. The main features observed were as follows: (i) important accumulation of secondary aerosol proceeded under non-foggy but stagnant conditions, (ii) significant pollutant deposition occurred over the course of fog events, (iii) SO_2 conversion in fogs did not exceed a few percent per hour, and (iv) the pH of the fogs was determined by the availability of ammonia to neutralize the sulfuric and nitric acids present.

In this paper, we report the results of a more comprehensive study conducted at multiple sites during January 1984. Spatial and temporal variations of aerosol and fogwater concentrations have been established that reflect both the geographical distribution of emission sources and the meteorological conditions. Pollutant accumulation and removal over the course of a stagnation episode have beem characterized under both foggy and non-foggy conditions. The H_2SO_4 production rate has been estimated. A thermodynamic interpretation of the partitioning of the H_2SO_4-HNO_3-NH_3 system between the gas phase, the aerosol, and the fogwater is presented in a companion paper (Jacob et al., 1985). Deposition data are discussed by Waldman (1985).

EXPERIMENTAL

The volumetric concentrations of aerosol, $HNO_3(g)$, and $NH_3(g)$ were monitored at eight sites over the period 31 December, 1983 - 14 January, 1984 (Figure 1). Samples were collected twice daily (0000 - 0400 PST and 1200 - 1600 PST) at the six valley sites and once daily (1000 - 1600 PST) at the two mountain sites (Tehachapi, Lake Isabella). The sampling stations were located on platforms 15 m above the ground (Wasco, Tehachapi), on the roof of a building or trailer (Bakersfield, Lost Hills, Buttonwillow, McKittrick, Visalia), or on the ground, 1.5 m above a grassy area (Lake Isabella). Two open-faced 47 mm Gelman Zefluor Teflon filters (1 um pore size) were operated side-by-side (10 lpm) to provide duplicate determinations of the inorganic content of the aerosol. The Stokes number at the filter inlet is 0.1 for a 50 μm diameter particle, so that even very large fog droplets should be sampled efficiently (Davies and Subari, 1982). A 47 mm Gelman Nylasorb nylon filter collected gaseous nitric acid immediately downstream of one of the Teflon filters, and an oxalic acid-impregnated glass fiber filter collected gaseous ammonia immediately downstream of the other Teflon filter. The filters were sealed in Petri dishes and kept at $4^{o}C$ following collection. The Teflon filters were extracted in 10 ml of distilled deionized water (Corning Megapure) for 90 minutes using a reciprocating shaker; subsequent extractions gave satisfactory blanks. The extracts were analyzed for major ions using standard methods previously described by Munger et al. (1983). The nylon filters were extracted in a solution 3 $\underline{m}M$ HCO_3^- and 2.4 $\underline{m}M$ CO_3^{2-} (a conventional ion chromatography

eluent), using the extraction procedure described above. Oxalic acid-impregnated filters were extracted and analyzed following the protocol of Russell (1983). Sulfur(IV) was found at low levels in the Teflon filter extracts, but since the S(IV) concentrations were small compared to S(VI), their contributions were ignored. Although most of the aerosol sulfur is expected to be present as sulfate, some of the measured sulfate may have resulted from the in situ oxidation of reduced sulfur species on the filter or in the extract.

Fogs were sampled by event at four sites (Figure 1). Fogwater samples were collected with a rotating arm collector (Jacob et al., 1984c) for intervals ranging from 30 minutes to 3 hours. The rotating arm collector has a theoretical sampling rate of 5 m^3 min^{-1}, and has been shown to collect fogwater samples without evaporation or condensation. Laboratory calibration has indicated a lower size cut (50% collection efficiency) of 20 μm diameter. Because the instrument collects fog droplets by direct impaction and does not require drawing air through an inlet, large fog droplets are efficiently collected. Liquid water content in the fog was determined from the sampling rate of the instrument, assuming that 60% of the total liquid water sampled was actually collected (Jacob et al., 1984c).

Fogwater samples were preserved and analyzed for major ions and trace metals following the protocol described by Munger et al. (1983), with the exception described below. In fogwater samples, significant S(IV) concentrations are found during conventional anion analysis by ion chromatography. A possible explanation is the formation of stable but reversible S(IV)-aldehyde adducts, such as hydroxymethanesulfonate (Munger et al., 1984). The standard ion chromatographic method

(Dionex AS-3 column, [3 mM HCO_3^- + 2.4 mM CO_3^{2-}] eluent, 3 ml min^{-1} flow rate) proposed by Dionex (1981) and used by Munger et al. (1983) does not clearly separate S(IV) and NO_3^-. Better separation is achieved with a weaker eluent or with the Dionex AS-4 column, but quantification of S(IV) remains unsatisfactory. To solve this problem, aliquots for anion determination were spiked to 0.09 M H_2O_2 several minutes prior to injection; this addition resulted in the quantitative oxidation of bisulfite and hydroxymethanesulfonate to sulfate. Oxidation of hydroxymethanesulfonate by H_2O_2 was probably facilitated by the presence in fogwater of metal catalysts (McArdle and Hoffmann, 1984). Sulfur(IV) concentrations were separately determined by a pararosaniline colorimetric method on aliquots preserved with buffered (pH 4) formaldehyde immediately upon sample collection (Dasgupta et al., 1980). Fogwater sulfate concentrations were calculated by subtracting the S(IV) concentrations thus obtained from the sulfate concentrations determined by ion chromatography.

To date, there are no standardized sampling procedures for the collection of fogwater and aerosol samples for chemical analysis. Therefore, it is important to assess the errors associated with our methods. A detailed discussion of sampling biases, artifacts, and standard errors on our data is presented in the Appendix.

Hourly average concentrations of SO_2 and NO_x were measured at Bakersfield and Visalia by the California Air Resources Board, and at McKittrick, Kernridge, and Lost Hills by the West Side Operators (WSO). Hourly average CO concentrations and mixing heights were measured at Kernridge by WSO. Surface winds were measured by WSO (Lost Hills, Kernridge, McKittrick, Maricopa), Getty Oil Company

(Bakersfield), National Weather Service (Bakersfield), Lemoore Naval Air Force base, Visalia airport, and Kern County Fire Department (Tehachapi). Upper-level winds were measured at Edwards Air Force Base, located in the Mojave desert on the other side of the Tehachapi mountains. Additional weather data were available from the National Weather Service station at Bakersfield.

To account for the equilibria between gas and aerosol phases, we define N(-III), N(V), and S(VI) to represent the element at the given oxidation state, both in the gas and aerosol phases. Thus N(-III) includes $NH_3(g)$ and NH_4^+, and N(V) includes $HNO_3(g)$ and NO_3^-. We further define [A] as the concentration of constituent A in fogwater ($\mu eq\ l^{-1}$ of water), and (A) as the concentration of A in the air ($neq\ m^{-3}$ of air). The fogwater loading $(A)_f$ is the concentration of A in fogwater per m^3 of air, and is obtained by multiplying [A] by the liquid water content of the fog.

WEATHER PATTERN AND POLLUTANT TRANSPORT

Figure 2 shows the profile vs. time of boundary layer mixing heights and stratus cloud bases over the valley floor during the winter 1984 sampling program. Two types of mixing height diurnal patterns were observed.

In the first pattern (the days of 31 December, 1 January, 10 - 12 January, 14 January), ground-based inversions formed by radiation at night and broke up briefly the following afternoon, leading to mixing heights in excess of 1000 m above ground level (AGL). This pattern was usually associated with clear skies or high cloudiness, but fogs in ground-based inversions were occasional occurrences (e.g., Bakersfield, 31 January). Figure 3a gives the average wind vectors on the days when this pattern was observed. A net slow NW flow was observed on the valley floor, consistent with NW winds at upper levels reflecting the circulation around the Pacific High. Terrain influences in the southern end of the valley led to convergence of the flow in the SE corner of the valley. Surface winds frequently shifted in direction, and erratic patterns of low winds were typically observed under nighttime stable conditions.

Concentrations of trace gases at Kernridge were lowest on the days when this pattern was observed (Figure 2), and so were aerosol concentrations (Jacob, 1985). Because of the weakness of the NW flow on the valley floor, it is unlikely that surface winds ventilated the valley by transport over the mountain ridges in the southeast corner of the valley. Aerosol concentrations at Tehachapi and Lake Isabella remained much lower than in the valley, which is evidence against such

transport. Instead, pollutant removal was due to rapid vertical mixing as the inversion broke up in the afternoon; this vertical mixing diluted the polluted air parcels and allowed their rapid transport by strong upper-level NW winds to the surrounding air basins.

A different mixing height pattern was observed on 2 - 7 January; during that period, a very strong subsidence inversion based a few hundred meters above the ground persisted over the valley. Subsidence was due to the presence of a stationary high-pressure center (Great Basin High) over the valley. Upper-level winds at Edwards AFB switched from the usual NW (circulation around the Pacific High) to E (circulation around the Great Basin High). A stratus cloud persisted in the valley below the inversion (Figure 2), and frequently intercepted the McKittrick site 250 m above the valley floor. On the night of 4 - 5 January, the stratus base lowered sufficiently to cause fog at elevated sites on the valley floor (Kernridge, Bakersfield NWS). On the nights of 5 - 6 and 6 - 7 January, the stratus base lowered sufficiently to fill the entire boundary layer, and dense fog was observed everywhere in the valley. The cloud layer deepened considerably on 7 - 8 January, and mixing heights rose to above 1000 m AGL; drizzle fell on the valley floor. On 9 January the inversion base dropped again, but upper-level winds had switched back to NW. After 10 January, the first mixing height pattern (surface inversions at night breaking up in the afternoon) was observed.

The capping of the valley by a persistent inversion based at a lower altitude than the surrounding mountain ridges obviously restricted ventilation. Concentrations of trace gases at Kernridge

(Figure 2) rose to high levels during the period 2 - 7 January, but dropped to low levels on 8 January when the mixing height rose above the mountain ridges. Concentrations began increasing again on 9 - 10 January, and dropped on 10 January.

The resultant winds in the valley during the 2 - 7 January period are shown in Figure 3b. Cross-valley winds were dominant in the southern end; further north, however, a slow net southerly flow out of the valley was apparent. Such a flow pattern has been previously documented during stagnation episodes by Reible (1982), who found from tracer studies that pollutant transport in the southern San Joaquin Valley (SSJV; see Figure 1 for definition) was extremely complex because of the upslope flow/downslope flow system associated with the mountain/valley breeze. Reible suggested that the SSJV could be crudely modeled as a stirred-tank reactor that was ventilated by the weak southerly air flow. He reported residence times of 2 - 8 days for air parcels in the SSJV.

A net flow of air into the SSJV was observed on the west side. The dominant westerly surface winds in the southern end of the SSJV suggest that upslope transport over the ridges of the Tehachapi mountains and southern Sierra Nevada could have been a significant source of outflow for the SSJV air. However, the inversion did not break down or lift near the slopes: the stratus cloud intercepted the Bakersfield - Tehachapi highway as a well-defined fog layer, and the community of Tehachapi always remained sunny and very clear. Winds in the SSJV were entirely decoupled from the circulation aloft, as determined by the E upper-level winds at Edwards AFB and the SE afternoon winds at Tehachapi. Aerosol concentrations remained very

low at Tehachapi and Lake Isabella throughout the episode, confirming that upslope transport was not an efficient ventilation pathway. It is likely that shifts in wind direction occurred along the slope. Considerable fluctuations of both wind direction and speed with altitude have been previously documented during stagnation episodes in the SSJV (Aerovironment, Inc., 1982).

Therefore, slow transport north out of the valley was the main outflow for SSJV air. Average winds at Lemoore, Fresno, and Lost Hills were consistent (Figure 3b). Projections of these winds on the valley axis (150^{o}) yielded average speeds of 0.24 m s^{-1}, 0.26 m s^{-1}, and 0.22 m s^{-1} at each site, respectively. Since the SSJV is about 100 km long, this flow led to an average residence time of 5 days for an air parcel within the SSJV. The accumulation pattern for CO at Kernridge (Figure 2) suggests approach of a steady-state on 6 - 7 January, which is consistent with a residence time of 5 days.

AVERAGE AEROSOL AND FOGWATER CONCENTRATIONS AT EACH SITE

1. Aerosol and fogwater concentrations

The SSJV is the site of important SO_2, NO_x, and NH_3 emissions (Table 1). The geographical distribution of emissions is shown in Figure 1. Most of the NH_3 is emitted from confined feeding operations concentrated on the east side of the valley, especially around Bakersfield and Visalia. Another important source of NH_3 is cropland, which occupies most of the land in the valley floor not used for oil recovery operations, and the associated fertilizer use. Emissions of SO_2 and NO_x are concentrated in the east side and west side oil fields of the SSJV; the oil field emissions originate mostly from small boilers, which release their exhausts 10 - 20 m above the ground and therefore affect primarily the surrounding air. Mobile sources (two major highways, off-road farm equipment, city traffic) also contribute to NO_x emissions.

Spatial patterns of aerosol concentrations and fogwater loadings (Tables 2 and 3) directly reflected the distribution of emission sources. The ionic content of aerosol in the valley was dominated by SO_4^{2-}, NO_3^-, and NH_4^+, which contributed over 90% of the total measured ionic loading. Concentrations of N(-III) were highest at Bakersfield and Visalia, and lowest on the west side (Lost Hills, McKittrick). Mountain sites (Lake Isabella, Tehachapi), which have no important local NH_3 sources, had very low N(-III) concentrations. Concentrations of S(VI) were highest at Bakersfield, which is in the immediate vicinity of the largest oil field in the valley; they were

also very high at McKittrick, which is located within the west side oil fields, and at Buttonwillow, which is directly downwind. Concentrations of S(VI) at Wasco, Lost Hills, and Visalia were lower, which reflects their respective distances from oil recovery operations. A chemical balance on primary aerosol (based on Cooper and Watson, 1980) showed that all but a negligible fraction of the total S(VI) in the valley was of secondary origin. However, in spite of the time required for SO_2 conversion to sulfate, the areas of SO_2 emissions matched the areas of high S(VI) concentrations. Concentrations of S(VI) at the two mountain sites were very low and indicated little impact of the valley air.

Because most of the NO_x was emitted from the same sources as SO_2, one would expect the spatial distribution of N(V) concentrations to be similar to that of S(VI). Indeed, N(V) concentrations were highest at Bakersfield; however, concentrations at McKittrick were low. The lack of NH_3 at McKittrick led to frequently acidic conditions, in which N(V) would be mostly present as HNO_3(g) and therefore quickly removed by deposition. This point will be addressed in more detail below. Concentrations of N(V) were higher at Visalia than would be expected from the spatial distribution of S(VI); Visalia is an important population center, and it is therefore likely that emissions from mobile sources were the dominant source of N(V) at that site.

Fogwater loadings of Ni and V, which are almost exclusively associated with residual oil burning (Cooper and Watson, 1980), were high at Bakersfield, McKittrick, and Buttonwillow, and low at Visalia. Loadings of Pb, a tracer for automobile exhaust, were higher in the

population centers (Bakersfield, Visalia) than at rural sites (McKittrick, Buttonwillow).

Overall, the large differences in S(VI), N(V), and N(-III) concentrations, that were observed from one site to another over distances of only a few tens of kilometers, show that the composition of the H_2SO_4 - HNO_3 - NH_3 system at each site was strongly determined by the nature of emission sources in the immediate vicinity. This is especially interesting in regard to the secondary constituents S(VI) and N(V), and supports our observation that there was little net horizontal pollutant transport on the valley floor. The spatial distributions of SO_2, NO_x, and NH_3 emissions are such that the acid-neutralizing capacity of the atmosphere should vary considerably within the valley. Indeed, Table 3 shows that fogwater acidity differed greatly from site to site, with low pH values at McKittrick and very high pH values at Visalia. Fog samples collected simultaneously at four sites during a widespread fog event clearly showed this spatial pattern (Figure 4). Acid fog was consistently observed at McKittrick, but never at the other sites.

2) Alkalinity and inorganic acidity

We explore further the spatial variations in the acid-neutralizing capacity of the atmosphere by calculating the alkalinities at each site. Although alkalinities were not directly measured, they can be estimated from our data. We define the alkalinity of fogwater [ALK] as the deficiency of protons with reference to the system of "neutralized" fogwater species (CAT^{n+}, Cl^-,

NO_3^-, SO_4^{2-}, $S(IV)^-$, HA). The symbol HA refers to undissociated weak acids in solution. In the pH 2 - 7 range, the main S(IV) species in the fog are expected to be HSO_3^- and stable monovalent S(IV)-aldehyde adducts (Jacob and Hoffmann, 1983; Munger et al., 1984; Boyce and Hoffmann, 1984). Therefore, the monovalent form of S(IV) is most appropriate for use as reference. For the subset of samples analyzed for carboxylic acids, we have calculated the fogwater alkalinity [ALK] as follows:

$$[ALK] = [HCOO^-] + [CH_3COO^-] + [CH_3CH_2COO^-] + [CH_3CH(OH)COO^-] + [HCO_3^-] + [NH_3(aq)] + [OH^-] - [H^+] \quad (1)$$

where $[H^+]$ was directly measured and the concentrations of alkalinity-contributing species were determined from the aqueous concentrations and the equilibrium constants at 5°C (see Appendix). For $NH_3(aq)$, the equilibrium constants at 5°C are $K_{b,NH3} = 1.5 \times 10^{-5}$ M, $K_w = 2.0 \times 10^{-15}$ M^2 (Smith and Martell, 1976).

Estimating the alkalinity of aerosol $(ALK)_a$ is less straightforward. We assume that the ions on the right-hand side of (1), plus possibly additional weak acid anions, constituted most of the aerosol ionic content unaccounted for in our chemical analysis. By a charge balance on the aerosol (concentrations in neq m^{-3}), we obtain:

$$(ALK)_a = (Na^+) + (K^+) + (NH_4^+) + (Ca^{2+}) + (Mg^{2+}) - (Cl^-) - (NO_3^-) - (SO_4^{2-}) . \quad (2)$$

We define the atmospheric alkalinity (ALK) by considering, in addition to aerosol alkalinity, the gaseous species $HNO_3(g)$ and $NH_3(g)$:

$$(ALK) = (ALK)_a + (NH_3(g)) - (HNO_3(g)) \ . \qquad (3)$$

Negative values of ALK correspond to a situation where strong acids (mostly H_2SO_4 and HNO_3) are not neutralized. When ALK is negative, we will refer to the absolute value of ALK as the inorganic acidity. This quantity is also sometimes referred to in the literature as the "mineral acidity" (Stumm and Morgan, 1981).

Average alkalinities at each site are given in Table 4a. Due to the possibility of HNO_3 or NH_3 volatilization from filters collected in fog (see appendix), (ALK) and $(ALK)_a$ were calculated only for non-foggy conditions. (ALK) and $(ALK)_a$ were usually small numbers determined by the difference of two large numbers, and so the errors are fairly large. The calculation of the fogwater alkalinity [ALK] involved subtracting a small number from a large number; the resulting standard errors are small and not indicated explicitly.

On the average, the air contained substantial alkalinity at all sites except McKittrick and Lost Hills. This clearly reflected the spatial distribution of NH_3, SO_2, and NO_X emissions, and the deficiency in ammonia on the west side of the SSJV. Alkalinities were considerably higher at Visalia than at Bakersfield, even though N(-III) concentrations were similar at both sites. Further, alkalinities at Buttonwillow and Bakersfield were comparable even though N(-III) concentrations were much higher at Bakersfield. Most of the alkalinity at Bakersfield was depleted by high H_2SO_4 and HNO_3

inputs.

The partitioning of alkalinity between the gas phase and the aerosol is of interest. Scavenging of $NH_3(g)$ to form ammonium salts of weak acids could be a source of important alkalinity in the aerosol. Significant fogwater alkalinities were found at Bakersfield, Buttonwillow, and Visalia; however, under non-foggy conditions, the aerosol was never significantly alkaline. Although the error bars on the determinations of $(ALK)_a$ are large, the absence of positive $(ALK)_a$ values even in the presence of large excesses of $NH_3(g)$ (as at Visalia) strongly suggests that the alkaline ammonium salts are volatile under non-foggy conditions. This hypothesis is supported by concurrent sampling of aerosol and fogwater at Visalia, where NH_4^+ was in excess of NO_3^- and SO_4^{2-} in the fog but not in the aerosol (Jacob et al., 1985).

Under non-foggy acidic conditions, the aerosol contained significant mineral acidity when S(VI) was present in excess of N(-III). This occurred in 6 of the samples, all at McKittrick. In the remainder of the samples collected under acidic conditions, the aerosol was neutralized and the inorganic acidity was present exclusively in the gas phase as $HNO_3(g)$. This observation is in agreement with aerosol equilibrium models (Bassett and Seinfeld, 1983); $NH_3(g)$ is scavenged by acid sulfate aerosol until this aerosol is neutralized as $(NH_4)_2SO_4$. Excess NH_3 may then combine with HNO_3 to add NH_4NO_3 to the aerosol phase, but HNO_3 in excess of NH_3 remains in the gas phase.

The contributions of different species to fogwater alkalinity are shown in Table 4b. The main contributors to [ALK] at Bakersfield

and Buttonwillow were formate and acetate. Formic and acetic acids are efficiently scavenged in fogwater at pH > 5; they are highly soluble as indicated by their large Henry's law constants ($H_{FOR,298}$ = 3.7×10^3 M atm^{-1}; $H_{ACET,298}$ = 8.8×10^3 M atm^{-1}; JANAF, 1971) and they are mostly dissociated ($pK_{FOR,278}$ = 3.77; $pK_{ACET,278}$ = 4.77; Martell and Smith, 1977). At Visalia, the fogwater pH was much higher than at Bakersfield or Buttonwillow, and the contribution from HCO_3^- to [ALK] was correspondingly larger. Carboxylate anions did not provide higher contributions at Visalia than at Bakersfield or Buttonwillow, since carboxylic acids are already efficiently scavenged at pH 5 - 6, raising the pH higher leads to little additional scavenging.

The speciation of N(-III) and N(V) in the atmosphere was directly related to the ambient alkalinity. Under alkaline conditions, only a small fraction of N(V) was present in the gas phase. At Bakersfield, Wasco, Buttonwillow, and Visalia, the average fraction of N(V) as HNO_3(g) was less than 10%. Even under neutral to acidic conditions (Lost Hills, McKittrick) there was sufficient N(-III) available to draw most of the N(V) into the aerosol phase. At Lost Hills and McKittrick, less than 15% of the total N(-III) was in the gas phase, but this fraction was larger at other sites. Gaseous ammonia constituted 64% of the total N(-III) at Visalia, which reflects the considerable excess of N(-III) over N(V) and S(VI) at that site.

EVOLUTION OF THE H_2SO_4-HNO_3-NH_3 SYSTEM OVER THE COURSE OF A SEVERE STAGNATION EPISODE

Figure 5 shows the evolution of concentrations at the six valley sites over the period 1 - 8 January. With a few exceptions (discussed below), concentrations increased over the 2 - 7 January stagnation episode and dropped on 7 - 8 January. The decrease of CO concentrations at Kernridge indicates that the increase in mixing heights on 7 - 8 January ventilated the valley; S(VI), N(V), and N(-III) were removed more efficiently than CO, which indicates that wet deposition was also an important contributor to pollutant removal.

Dense widespread nighttime fogs on the valley floor (6, 7 January) were also associated with decreases in S(VI), N(V), and N(-III) concentrations. No drizzle or increase in mixing heights was observed on those days which could account for these decreases; therefore, they were likely due to rapid deposition of fog droplets. Jacob et al. (1984a) have previously suggested that fogs efficiently limit pollutant accumulation during stagnation episodes. In the winter 1982 - 1983 study, Jacob and co-workers compared fogwater loadings in successive samples collected during the same event and found rapid decreases with time of the amount of material suspended in the fogwater. Unfortunately, such an analysis could not be adequately conducted for this year because of the paucity of extended fogs on the valley floor. Figure 4 suggests that fogwater loadings decreased with time at Bakersfield, Buttonwillow, and Visalia during the 7 January fog event; however, this evidence is not conclusive because liquid water contents were also decreasing. The apparent decrease in

fogwater loadings could possibly have simply been due to evaporation of fog droplets to below the collector size cut.

Scavenging of NO_x and SO_2 by fog can be evaluated from their concentration profiles. Concentrations of NO_x at Kernridge increased steadily throughout the episode, even during the foggy 5 - 7 January period (Figure 2); NO_x at Kernridge behaved similarly to CO, which is not water-soluble. At McKittrick, NO_x concentrations increased steadily (Figure 6), even though the stratus cloud frequently intercepted the site during the 2 - 7 January period. Therefore, it appears that NO_x was not scavenged by fog droplets. This is consistent with laboratory data documenting the poor solubility of NO_x in water at atmospheric concentrations (Schwartz and White, 1981).

The profile of SO_2 concentrations at Kernridge was very different from that of NO_x, even though both gases originated from the same combustion sources. Concentrations of SO_2 rapidly reached a steady-state after an initial increase, and this is consistent with fairly high deposition velocities of SO_2 over grass-type surfaces (1 cm s^{-1}; Sehmel, 1980). Concentrations of SO_2 then decreased progressively over the 5 - 7 January foggy period, in contrast to CO and NO_x. This is strong evidence that SO_2 was being slowly scavenged by fog droplets. We infer from the SO_2 concentration profile at Kernridge that the rate of SO_2 scavenging was of the order of a few percent per hour. At McKittrick (Figure 6), concentrations of SO_2 fluctuated considerably while NO_x concentrations increased relatively steadily; this is consistent with SO_2 scavenging by the frequent fogs at that site.

Steady increases in S(VI) concentrations were observed at

Bakersfield, Wasco, and Lost Hills over the period 2 - 5 January, when no fog or drizzle occurred to limit pollutant accumulation. Sulfate concentrations did not appear to reach a steady state over that period. We have argued previously that a stirred-tank reactor approximation could be used to interpret pollutant accumulation in the SSJV. For the period 3 - 5 January, the average mixing height h was about 400 m AGL. The characteristic time τ_r for S(VI) removal is given by:

$$\frac{1}{\tau_r} = \frac{v_{SO4}}{h} + \frac{1}{\tau_a} \qquad (4)$$

where τ_a is the characteristic time for advection out of the SSJV (5 days), and v_{SO4} is the deposition velocity for sulfate aerosol. Considering that there was still no evidence of a S(VI) steady state on 5 January, v_{SO4} should be smaller than 0.05 cm s^{-1}. This is in agreement with deposition velocities for particles in the 0.05 - 1 μm size range at low wind velocities (Sehmel, 1980). Deposition velocities for SO_2(g) are of the order of 1 cm s^{-1} (Sehmel, 1980); therefore, we expect roughly steady-state SO_2(g) concentrations to be reached on a time scale of about one day after the onset of the stagnation episode, as was observed at Kernridge. We can then estimate the average rate of sulfate production from the increase in sulfate concentrations over the period 3 - 5 January, assuming that sulfate deposition can be ignored over that period. The average rates

of (S(VI)) increase were 9 neq m^{-3} h^{-1} at Bakersfield, 3 neq m^{-3} h^{-1} at Wasco, and 3 neq m^{-3} h^{-1} at Lost Hills. Modeling of SO_2 concentrations (Aerovironment, Inc., 198) indicate that the SO_2 concentration field in the SSJV during a stagnation episode should be bounded on the lower end by the concentrations at Wasco and Lost Hills, and on the upper end by concentrations at Bakersfield and McKittrick. Over the period 3 - 5 January, SO_2 concentrations averaged 3 ppb at Lost Hills and 25 ppb at Bakersfield. Therefore, the average pseudo first-order SO_2 conversion rate k should lie between 0.8 and 2.5 % h^{-1}. Alternatively, we can calculate the SO_2 conversion rate from an estimate of the average SO_2 concentration in the SSJV based on steady-state attainment in a stirred-tank model:

$$(SO_2)_{av} = \frac{E_{SO2}}{k + \frac{v_{SO2}}{h} + \frac{1}{\tau_a}} \qquad (5)$$

where E_{SO2} = 0.95 μeq m^{-3} day^{-1} is taken from Table 3. We obtain by this method $(SO_2)_{av}$ = 9 ppb, and 1 % h^{-1} < k < 3 % h^{-1}. This is consistent with the above result.

During the period 3 - 5 January, the stratus cloud filled a large fraction of the boundary layer. Although we have presented evidence that SO_2 was slowly scavenged in fog, this does not necessarily imply enhanced sulfate production in fog; S(IV) may be stabilized in the aqueous phase by adduct formation (Munger et al., (1984), or removed by deposition before being oxidized. In-cloud sulfate production cannot be reliably interpreted

from our fogwater sulfate data, because we cannot ascertain the history and fate of droplets collected in successive samples at a given site. We tried to account for transport by using Ni and V as tracers for sulfur, but were unsuccessful at obtaining a significant rate of sulfate production in fogwater. Details of the calculation are given by Jacob (1985).

In addition to H_2SO_4, HNO_3 was produced in the boundary layer. Under the alkaline to neutral conditions found at Bakersfield, all S(VI) and N(V) combined with N(-III) to produce a neutralized (NH_4^+, NO_3^-, SO_4^{2-}) aerosol. However, S(VI) and N(V) did not accumulate in the same way (Figure 5). Concentrations of S(VI) did not begin increasing until 3 January, showing a time lag consistent with the slow rate of SO_2 conversion: SO_2 must first build up before important S(VI) production proceeds. After 3 January, S(VI) concentrations rose steadily, consistent with the slow deposition velocity for sulfate aerosol. On the other hand, N(V) concentrations rose rapidly on the first day of the episode but did not increase after 3 January. This could be explained if nitrate was present in coarser particles than sulfate and therefore deposited more rapidly; attainment of a steady state on a time scale of 1 day would indicate a deposition velocity for nitrate over one order of magnitude higher than that for sulfate. The presence of nitrate in coarse aerosol has been documented in the Los Angeles basin (Appel et al., 1978) and can be explained by absorption of $HNO_3(g)$ onto primary aerosol. In the San Joaquin Valley, however, the relative paucity of cations other than NH_4^+ indicates that nitrate should be present mostly as secondary ammonium salt particles. The Kelvin effect leads to accumulation of

nitrate in particles larger than sulfate, but the resulting difference in sizes is very small at high relative humidities (Bassett and Seinfeld, 1984) and could not explain an order of magnitude difference in deposition velocities. Previous wintertime aerosol measurements in the San Joaquin Valley (Heisler and Baskett, 1982) did not reveal differences in the distributions of nitrate and sulfate between the coarse and fine aerosol.

A better explanation for the constancy of N(V) concentrations after 3 January is that conversion of NO_x to N(V) was limited by the lack of appropriate oxidants such as OH or O_3. Little photochemical activity is expected under overcast conditions; ozone concentrations at Bakersfield were below the detection limit of 10 ppb. The lack of nitrate production would explain the persistent accumulation of NO_x observed over the course of the stagnation episode. Low photochemical activity indicates that conversion of SO_2 to sulfate proceeded predominantly via heterogeneous processes.

As H_2SO_4 was produced over the course of the stagnation episode, alkalinities decreased at all SSJV sites. At Wasco, Lost Hills, and McKittrick, significant inorganic acidities were eventually produced; at Bakersfield, alkalinities were neutralized but no significant excess acidity was found. Strong acids titrated N(-III) into the aerosol, and consequently the air parcel became acidic when the supply of $NH_3(g)$ was exhausted. At Lost Hills, acidification coincided with a brief increase in $HNO_3(g)$ concentrations, followed by a drop in total N(V) concentration. This can be explained by displacement of NO_3^- by SO_4^{2-} in the acidic aerosol, followed by rapid deposition of $HNO_3(g)$. Because of its high deposition velocity, $HNO_3(g)$ should be

removed from the boundary layer on a time scale of less than a day.

McKittrick frequently intercepted stratus clouds after 3 January, and received occasional drizzle. Concentrations of N(-III) peaked on 2 - 3 January, and decreased afterward; the decrease may have been due to removal by fog and drizzle, but also to advection by dominant westerly winds of ammonia-poor air parcels from the coastal mountain ranges. Concentrations of S(VI) at McKittrick rose at the beginning of the episode, but accumulation was apparently limited by fog deposition. Concentrations of N(V) did not stabilize in the same way as concentrations of S(VI), and fell to low levels after 3 January. Transport is not by itself a satisfactory explanation for this behavior since N(V) and S(VI) at McKittrick are expected to originate from the same sources, and NO_x concentrations did not show the drop observed for N(V) (Figure 6). As in the case of Lost Hills, the drop in N(V) concentration coincided with acidification of the air parcel and was preceded by a brief increase in $HNO_3(g)$ concentration. Displacement of NO_3^- by SO_4^{2-} in the aerosol followed by rapid removal of $HNO_3(g)$ is a likely explanation. An additional explanation is that conversion of NO_x was limited by the low availability of oxidants; that is, N(V) was removed in the fog by deposition and was not replenished in the atmosphere. As opposed to N(V), S(VI) concentrations did not decrease because of continual production by heterogeneous processes.

Concentrations of N(-III), N(V), and S(VI) at Visalia (Figure 5) did not show the same patterns as in the SSJV. Visalia was overcast until 5 January except for a 1-h fog on 3 January, but dense, precipitating fog occurred on the morning of 5 January from 0200 PST

on. Concentrations of S(VI) remained low throughout the stagnation episode, reflecting the distance of Visalia from the SSJV oil fields. Nitric acid was not produced in sufficient amounts to deplete the very high alkalinity at Visalia, and large amounts of N(-III) remained in the gas phase. On 5 January, precipitating fog efficiently removed aerosol NH_4^+ and NO_3^- from the atmosphere, but did not affect the concentration of $NH_3(g)$. At the very high pH values found in Visalia fogwater, $NH_3(g)$ is not scavenged by fog droplets (Jacob et al., 1985).

The above discussion has shown that the profiles of concentrations vs. time during a stagnation episode can be succesfully interpreted based on stirred-tank considerations of pollutant accumulation and removal; however, the differences in concentrations from site to site clearly indicate that a stirred-tank model for the SSJV as a whole is not an adequate modeling tool. The major reason for that is the lack of internal mixing, and therefore the persistence of concentration patterns directly reflecting the local emissions. Modeling could possibly be approached by subdividing the SSJV into a number of cells where the stirred-tank approximation could be invoked. Such an exercise is beyond the scope of this paper; however, for the sake of illustrating the above discussion. we will describe two different patterns to be expected from such modeling.

The accumulation of constituent A in a stirred-tank is described by equation (6):

$$\frac{d(A)}{dt} = E_A + k(B) - k'(A) - \frac{1}{h}\left((A_g)v_{A_g} + (A_a)v_{A_a} + (A_f)v_{A_f} \right) - \frac{1}{\tau_a} \qquad (6)$$

where A_g, A_a, and A_f are the gas-phase, aerosol-phase, and fogwater-phase species, respectively, k is the pseudo first-order rate of conversion from precursor B to A, k' is the pseudo first-order rate of destruction of A, and E_A is the emission rate. We simultaneously solved the coupled stirred-tank equations for SO_2, NO_x, S(VI), N(V), and N(-III), under the conditions of Table 5. An exponential decay for the N(V) production rate was arbitrarily chosen to account for the limitation of the reaction by the availability of oxidants. We assumed that the aerosol was a neutralized mixture under non-foggy conditions if N(-III) was in excess of S(VI), and that the formation of NH_4NO_3 aerosol was sufficiently favored to prevent HNO_3 and NH_3 from coexisting in the gas phase. Further, based on the results presented in Jacob et al. (1985), we assumed that (a) 30% of the aerosol is present in the fogwater at any given time, (b) $HNO_3(g)$ is 100% scavenged under all foggy conditions, (c) $NH_3(g)$ is not scavenged in fog under alkaline conditions (N(-III) > N(V) + S(VI)).

Figure 7a was obtained from Case I of Table 5, which considers average SSJV emissions as calculated from Table 3. Aerosol accumulates rapidly under non-foggy conditions, and is partially removed by fog. Concentrations of N(V) and S(VI) show a short time lag at the beginning of the episode: SO_2 and NO_x must first build up before significant production can occur. Excess alkalinity as $NH_3(g)$ remains present throughout the episode.

Acidic conditions as observed at McKittrick and Lost Hills can

be interpreted by a simulation which assumes higher SO_2 and NO_x emissions, and lower NH_3 emissions, than the average SSJV values (Case II of Table 5, Figure 7b). Under such conditions, inorganic acidity appears early into the episode, and a large fraction of N(V) remains in the gas phase. Because $HNO_3(g)$ is rapidly removed by deposition, N(V) concentrations drop after a brief initial increase. The presence of N(V) as $HNO_3(g)$ also increases the scavenging efficiency of N(V) by fog, and the subsequent rapid deposition.

CONCLUSION

Fogwater acidity in the wintertime atmosphere of the San Joaquin Valley of California was interpreted from the composition of the H_2SO_4 - HNO_3 - NH_3 system at a network of sites. Fogwater acidity was found to be directly determined by the proximity of oil recovery operations (SO_2, NO_x) and livestock feeding activities (NH_3). Thus, a region of prevailing acidic conditions was identified on the western edge of the valley; alkaline conditions were found elsewhere. Considerable alkalinity and very high fogwater pH were found at a site distant from the oil fields but near major confined feeding operations. In view of the close balance of acidic and alkaline species presently found in the southern San Joaquin Valley, changes in the activities of either the oil industry or the cattle and dairy industry could dramatically affect fogwater acidity. This can explain why fog collected at Bakersfield was often acidic in December 1982 - January 1983 (Jacob et al.,1984a), but not in January 1984.

Pollutant concentrations were strongly affected by atmospheric stability, and by the occurrence of drizzle and fog. Instability in the boundary layer extending to above 1000 m AGL efficiently ventilated the valley. Accumulation in the boundary layer was evident under non-foggy conditions when strong and persistent inversions limited the ventilation, but decreases in concentrations were observed following fog. Aerosol removal in fogs was attributed to rapid deposition of material scavenged by the fog droplets.

Concentration profiles at each site followed a stirred-tank type of behavior over the course of a severe stagnation episode. The

accumulation patterns were consistent with very low deposition velocities for secondary ammonium sulfate and nitrate aerosol (< 0.05 cm s^{-1}), and a high deposition velocity for $HNO_3(g)$ (> 1 cm s^{-1}). In the absence of fog, slow sulfate production (of the order of 2 % h^{-1}) was observed on the valley floor, and enhanced scavenging of SO_2 was apparent in the stratus cloud above the valley floor. Sulfate appeared to be produced by heterogeneous processes, but we were not able to obtain statistical evidence of in-cloud sulfate production. Nitrogen oxides were not scavenged in fog, and the conversion of NO_x to HNO_3 was limited by the low degree of photochemical activity. Steady decreases in alkalinity associated with H_2SO_4 accumulation were observed over the course of a stagnation episode, and inorganic acidities were observed at sites distant from ammonia sources. Under acidic conditions, nitrate was displaced from the aerosol and $HNO_3(g)$ was apparently quickly removed by deposition. As a result, decreases in total nitrate were observed as the air parcel became acidic.

ACKNOWLEDGEMENTS

We thank the organizations that provided us with sampling sites: California Air Resources Board, Western Oil and Gas Association, Buttonwillow Park and Recreation, Kern County Fire Department, and U.S. Army Corps of Engineers. We further thank the organizations who provided us with atmospheric data: West Side Operators, California Air Resources Board, Getty Oil Company, Lemoore Naval Air Station, Tehachapi Fire Staion, Edwards Air Force Base, and Kern county Air Pollution Control District. We express our gratitude to D. Buchholz

and K. Mayer for their help in the field, and to M. Lemons of Getty Oil Company and K. Carter of the Boy Scouts of Lake Isabella for their contributions to the success of the sampling program. G. R. Cass (Caltech) provided many helpful discussions. This work was funded by the California Air Resources Board (contract No. A2-048-32).

REFERENCES

Aerovironment, Inc. 1982. Development, validation, and application of the AVKERN model. Report AV-FR-80/603R, Aerovironment, Inc., Pasadena, CA.

Aerovironment, Inc. 1983. AVKERN application report. Report AV-FR-83/501R2, Aerovironment, Inc., Pasadena, CA.

Appel, B.R., Kothny, E.L., Hoffer, E.M., Hidy, G.M., and Wesolowski, J.J. 1978. Sulfate and nitrate data from the California Aerosol Characterization Experiment (ACHEX). Environ.Sci.Technol. 12,418-425.

Appel, B.R., Wall, S.M., Tokiwa, Y., and Haik, M. 1980. Simultaneous nitric acid, particulate nitrate, and acidity measurements in ambient air. Atmos.Environ. 14, 549-554.

Bassett, M.E., and Seinfeld, J.H. 1983. Atmospheric equilibrium model of sulfate and nitrate aerosols. Atmos.Environ. 17,2237-2252.

Bassett,M.E. and Seinfeld,J.H. 1984. Atmospheric equilibrium model for sulfate and nitrate aerosols-II. Particle size analysis.

Atmos.Environ. 18,1163-1170.

Boyce, S.D. and Hoffmann, M.R. 1984. Kinetics and mechanism of the formation of hydroxymethanesulfonic acid at low pH. J.Phys.Chem. 88, 4740-4746.

Brewer,R.L., Ellis,E.C., Gordon,R.J. and Shepard,L.S. 1983. Chemistry of mist and fog from the Los Angeles urban area. Atmos.Environ. 17,2267-2271.

California Air Resources Board 1982. Emission Inventory 1979, Stationary Source Control Division, Emission Inventory Branch, Sacramento, CA.

Calvert,J.G. and Stockwell,W.R. 1984. Mechanism and rates of the gas-phase oxidations of sulfur dioxide and nitrogen oxides in the atmosphere. in Acid Precipitation: SO_2, NO, AND NO_2 Oxidation Mechanisms: Atmospheric Considerations. Calvert,J.G., ed. Butterworth publ., Boston, 1-62.

Cooper,J.A. and Watson,J.G.Jr. 1980. Receptor-oriented methods of air particulate source apportionment. J.Air Pollution Control Assoc. 30,1116-1125.

Crump,J.G., Flagan,R.C. and Seinfeld,J.H. 1983. An experimental study of the oxidation of sulfur dioxide in aqueous manganese sulfate

aerosols. Atmos.Environ. 17,1277-1289.

Damschen,D.E. and Martin.L.R. 1983. Aqueous aerosol oxidation of nitrous acid by O_2, O_3, and H_2O_2. Atmos.Environ. 17,2005-2011.

Dasgupta,P.K., DeCesare,K. and Ullrey,J.C. 1980. Determination of atmospheric sulfur dioxide without tetrachlormercurate(II) and the mechanism of the Schiff reaction. Anal.Chem. 52,1912-1922.

Daum,P.H., Schwartz,S.E. and Newman,L. 1984. Acidic and related constituents in liquid water stratiform clouds. J.Geophys.Res. 89,1447-1458.

Davies, C.N., and Subari, M. 1982. Aspiration above wind velocity of aerosols with thin-walled nozzles facing and at right angles to the wind direction. J.Aerosol Sci. 13,59-71.

Dionex,1981. Determination of anions in acid rain. Application note 31, July 1981. Dionex Corp., Sunnyvale, CA.

Heikes, B.G., and Thompson, A.M. 1983. Effects of heterogeneous processes on NO_3, HONO, and HNO_3 chemistry in the troposphere. J.Geophys.Res. 88,10883-10896.

Heisler, S. and Baskett, R. 1982. Particle sampling and analysis in the California San Joaquin Valley. ERT Document P-5381-700, Environmental Science and Technology, Inc., Westlake Village,

California.

Hering,S.V. and Blumenthal,D.L. 1984. Fog sampler intercomparison study: final report. Coordinating Research Council, 219 Perimeter Parkway, Atlanta,GA.

Holets,S. and Swanson,R.N. 1981. High-inversion fog episodes in central California. J.Appl.Met. 20,890-899.

Huebert, B.J. 1983. Measurements of the dry-deposition flux of nitric acid vapor to grasslands and forest. in Precipitation Scavenging, Dry Deposition, and Resuspension H.R.Pruppacher, R.G. Semonin, and W.G.N. Slinn, eds.2,785-794.

Jacob, D.J. and Hoffmann,M.R. 1983. A dynamic model for the production of H^+, NO_3^-, and SO_4^{2-} in urban fog. J.Geophys.Res. 88, 6611-6621.

Jacob,D.J., Waldman,J.M., Munger,J.W. and Hoffmann,M.R. 1984a. A field investigation of physical and chemical mechanisms affecting pollutant concentrations in fog droplets. Tellus.36B,272-285.

Jacob, D.J., Waldman,J.M., Munger,J.W. and Hoffmann,M.R. 1984b. Chemical composition of fogwater collected along the California coast. Environ.Sci.Technol. (submitted).

Jacob,D.J., Wang,R.-F.T. and Flagan,R.C. 1984c. Fogwater collector design and characterization. Environ.Sci.Technol. 18,827-833.

Jacob, D.J. 1985. The origins of inorganic acidity in fogs. Ph.D. thesis, California Institute of Technology, Pasadena, CA.

Jacob, D.J., Waldman, J.M., Munger, J,W., and Hoffmann, M.R. 1985. Comparison of field data with thermodynamic calculations for the H_2SO_4 - HNO_3 - NH_3 system at high humidities and in fogs. Submitted to J.Geophys.Res.

Kaplan,D.J., Himmelblau,D.M. and Kanaoka,C. 1981. Oxidation of sulfur dioxide in aqueous ammonium sulfate aerosols containing manganese as a catalyst. Atmos.Environ. 15,763-773.

Katz,U. 1980. A droplet impactor to collect liquid water from laboratory clouds for chemical analysis. in Communications a la 8eme Conference Internationale sur la Physique des Nuages. Publ. by Laboratoire Associé de Météorologie Physique, B.P. 45, 63170 Aubiere, France, pp. 697-700.

Martell, A.E., and Smith, R.M. 1977. Critical stability constants, vol.3. Plenum, New York.

Martin, L.R. 1984. Kinetic studies of sulfite oxidation in aqueous solution. in Acid Precipitation: SO_2, NO, and NO_x Oxidation Mechanisms: Atmospheric Considerations. Calvert,J.G., ed., Butterworth Publ., Boston,pp.63-100.

McArdle, J.V., and Hoffmann, M.R. 1984. Kinetics and mechanism of the oxidation of aquated sulfur dioxide by hydrogen peroxide at low pH. J.Phys.Chem. 87, 5425-5429.

Munger,J.W., Jacob,D.J., Waldman,J.M. and Hoffmann,M.R. 1983. Fogwater chemistry in an urban atmosphere. J.Geophys.Res. 88,5109-5121.

Munger,J.W., Jacob,D.J. and Hoffmann,M.R. 1984. The occurrence of bisulfite-aldehyde addition products in fog and cloudwater. J.Atmos.Chem. 1, 335-350.

Reible,D.D. 1982. Investigations of transport in complex atmospheric flow systems. Ph.D. Thesis, California Institute of Technology, Pasadena, California.

Russell, A.G. 1983. Analysis of oxalic acid impregnated filters for ammonia determination. Environmental Quality Laboratory open file report 83-1, California Institute of Technology, Pasasdena, California.

Russell,A.G. and Cass,G.R. 1984. Acquisition of regional air quality model validation data for nitrate, sulfate, ammonium ion and their precursors. Atmos.Environ. 18, 1815-1827.

Schwartz,S.E. and White,W.H. 1981. Solubility equilibria of the nitrogen oxides and oxyacids in dilute aqueous solution. Adv.Env.Eng.Sci. 4,1-45.

Sehmel,G.A. 1980. Particle and gas dry deposition: a review. Atmos.Environ. 14,983-1011.

Slinn,W.G.N. 1982. Predictions for particle deposition on vegetative canopies. Atmos.Environ. 16,1785-1794.

Smith, R.M., and Martell, A.E. 1976. Critical stability constants, vol.4. Plenum, New York.

Spicer, C.W. and Schumacher, P.M. 1979. Particulate nitrate: laboratory and field studies of major sampling interferences. Atmos.Environ. 13, 543-552.

Spicer,C.W., Howes,J.E., Bishop,T.A. and Arnold,L.H. 1982. Nitric acid measurement methods: an intercomparison. Atmos.Environ. 16,1487-1500.

Stelson,A.W. and Seinfeld,J.H. 1982. Relative humidity and temperature dependence of the ammonium nitrate dissociation constant. Atmos.Environ. 16,983-992.

Stumm,W. and Morgan,J.J. 1981. Aquatic Chemistry, 2nd ed., Wiley Interscience, New York.

Waldman,J.M., Munger,J.W., Jacob,D.J. and Hoffmann,M.R. 1984. Chemical characterization of stratus cloudwater and its role as a vector for pollutant deposition in a Los Angeles pine forest. Tellus 37B (in

press).

Waldman, J.M. 1985. Contribution of fog to the depositional flux of acidity. Ph.D.Thesis, California Institute of Technology, Pasadena, California.

Table 1. SO_2, NO_x, and NH_3 emission inventories for the southern San Joaquin Valley (SSJV; see Figure 1 for definition).

Area: 7930 km^2

SO_2 (tons/day)[a]

source	emissions (tons/day)
Oil production	
East side	116
West side	69
Agriculture	1
Mobile sources	6
TOTAL	192 tons/day

NO_x[b]

source	emissions (tons/day)
Stationary sources[c]	138
Mobile sources	52
TOTAL	190 tons/day

NH_3[d]

source	emissions (tons/day)
Livestock	46
Soil	18
Fertilizer use	10
Domestic	3
Fuel combustion	2
TOTAL	79 tons/day

(a) Aerovironment, Inc. (1984) - December 1982 data.
(b) California Air Resources Board (1982) - 1979 data.
(c) mostly oil and gas production.
(d) Jacob (1985) - January 1984 data.

Table 2. Aerosol, $HNO_3(g)$, and $NH_3(g)$ data, 31 December 1983 - 14 January 1984[a].

Site	n	Na^+	K^+	NH_4^+	Ca^{2+}	Mg^{2+}	Cl^-	NO_3^-	SO_4^{2-}	$HNO_3(g)$	$NH_3(g)$	N(V)	N(-III)
		neq m^{-3}											
Bakersfield													
range	30	<4-56	<4-19	144-1149	6-75	<4-12	<20-67	85-467	78-855	<4-46	19-483	93-471	209-1204
mean		15	4	560	35	6	27	276	336	16	146	292	706
Wasco													
range	29	<4-86	<4-20	74-584	4-43	<4-10	<20-93	23-419	19-312	<4-54	<17-273	54-431	95-648
mean		12	<4	308	16	<4	22	195	137	19	70	214	378
Lost Hills													
range	25	<4-48	<4-7	55-553	4-57	<4-11	<20-43	4-310	16-314	<4-174	<17-88	40-414	55-617
mean		11	<4	223	17	<4	<20	132	108	40	31	172	254
McKittrick													
range	29	5-70	<4-13	28-424	6-43	<4-10	<20-71	10-246	36-802	<4-164	<17-205	21-347	37-457
mean		17	<4	224	20	4	21	89	195	34	34	123	258
Buttonwillow[b]													
range	18	4-51	<4-10	36-663	6-68	<4-11	<20-41	34-400	31-579	<4-37	18-645	77-406	135-1001
mean		19	<4	306	31	5	23	184	188	12	131	196	437
Visalia[c]													
range	14	<4-16	<4-7	108-359	6-37	2-5	<20-41	73-318	35-129	<4-15	184-662	73-322	484-869
mean		7	<4	239	20	<4	<20	175	83	7	450	182	689
Lake Isabella													
range	11	<4-28	<4-4	<8-32	6-32	<4	<20	<4-23	<4-23	5-36	<17-44	<8-59	<8-44
mean		10	<4	8	11	<4	<20	9	9	16	19	25	27
Tehachapi													
range	13	<4-93	<4-140	<8-73	10-126	<4-43	<20-252	<4-50	<4-47	<4-18	<17-74	<8-68	<8-84
mean		17	12	11	46	8	32	11	17	7	34	18	45

(a) see Jacob (1985) for the complete data set.
(b) from 5 January to 14 January
(c) from 31 December to 7 January

Table 3. Liquid water-weighted average fogwater concentrations, December 31 1983–14 January 1984[a].

Site	n	pH range	H^+	Na^+	NH_4^+	Ca^{2+}	Mg^{2+}	Cl^-	NO_3^-	SO_4^{2-}	S(IV)	L [b]
			μeq l^{-1}								μM	g m^{-3}
Bakersfield	16	5.10–6.92	2.0	42	3270	169	33	122	819	2070	384	0.057
McKittrick	58	2.68–5.23	93	11	480	39	5	15	250	345	43	0.11
Buttonwillow	7	5.01–6.79	5.6	13	1067	82	10	47	522	760	74	0.050
Visalia	13	5.51–7.23	0.1	5.5	1080	17	2	115	341	265	12	0.049

Site	n	Fe	Mn	Pb	Cu	Ni	V	n	formate	acetate	lactate	propionate
		μg l^{-1}							μM			
Bakersfield	5	438	31	134	19	39	41	2	45	155	15	9
McKittrick	42	76	6	27	12	48	91	26	22	3	2	0
Buttonwillow	6	142	17	44	82	44	32	2	144	59	3	0
Visalia	6	144	7	61	7	11	8	6	53	65	7	0

(a) see Jacob (1985) for the complete data set.
(b) average liquid water content, based on the total amount of water collected and the total sampling time.

Table 4a. Average alkalinities at each site.

Site	n	ALK	ALK_a	n	ALK_f	$L^{(a)}$
		neq m^{-3}			$\mu eq\ l^{-1}$	$g\ m^{-3}$
Bakersfield	28	111±31	-20±30	2	210	0.11
Wasco	27	46±19	-13±18			
Lost Hills	23	-11±16	-2±16			
McKittrick	21	-12±18	-20±17	38	-98	0.11
Buttonwillow[(b)]	17	131±31	-14±28	2	183	0.05
Visalia[(c)]	11	441±30	-7±18	6	220	0.03

ALK is the alkalinity of the air parcel, ALK_a is the aerosol alkalinity, ALK_f is the fogwater alkalinity. ALK and ALK_a were calculated only for non-foggy periods. $^aALK_f$ was calculated for the subset of samples analyzed for organic acids. Error bounds are the standard errors on the determinations of the means.
(a) average liquid water content for the subset of fogwater samples.
(b) from 5 January to 14 January
(c) from 31 December to 7 January

Table 4b. Contributions of different species to fogwater alkalinity.

Site	n	free acidity[(a)]	formate	acetate	lactate	propionate	HCO_3^-	$NH_3(aq)$
		contribution to alkalinity ($\mu eq\ l^{-1}$)						
Bakersfield	2	-1.1	45	134	15	9.5	6.3	0.2
McKittrick	38	-123	22	1.1	1.6	0.0	0.2	0.0
Buttonwillow	2	-7.7	142	44	3.7	0.0	1.1	0.0
Visalia	6	0.0	53	66	7.7	0.0	92	1.5

(a) free acidity = $[H^+] - [OH^-]$

Table 5 . Parameters for stirred-tank model simulation .

Deposition velocities	cm sec^{-1}
SO_2	1
NO_x	0.1
aerosol (H^+, NH_4^+, NO_3^-, SO_4^{2-})	0.05
fog droplets	4
$HNO_3(g)$	3
$NH_3(g)$	1

Residence time of air parcels: 5 days.

Mixing height: 400 m

Initial conditions: $(H_2SO_4) = (HNO_3) = (NH_3) = 0$ at $t = 0$.

Fog from $t = 2$ days to $t = 3$ days.

Conversion rates	% h^{-1}
$SO_2 \rightarrow SO_4^{2-}$ (no fog)	2
$SO_2 \rightarrow SO_4^{2-}$ (fog)	10
$NO_x \rightarrow NO_3^-$	10 exp(-2t) (t in days).

Emission rates

Case I: $E_{SO2} = 0.95\,\mu M\ m^{-3}\ day^{-1}$, $E_{NOx} = 1.3\,\mu M\ m^{-3}\ day^{-1}$, $E_{NH3} = 1.4\,\mu M\ m^{-3}\ day^{-1}$

Case II: $E_{SO2} = 1.9\,\mu M\ m^{-3}\ day^{-1}$, $E_{NOx} = 2.6\,\mu M\ m^{-3}\ day^{-1}$, $E_{NH3} = 0.5\,\mu M\ m^{-3}\ day^{-1}$

APPENDIX: ERROR ANALYSIS

1. Fogwater concentrations

A recent intercomparison study of fogwater collectors (Hering and Blumenthal, 1984) has demonstrated that the Caltech rotating arm collector provides reproducible and representative samples under both light and heavy fog conditions. The uncertainty on the concentrations of major ions (determined from samples collected with two collocated rotating arm collectors) was found to be about 15%. Errors due to chemical analysis in the laboratory were about 5% for all analyzed ions. Hering and Blumenthal (1984) found that our rotating arm collector (lower size cut 20 μm) and a jet impactor (lower size cut of 2-5 μm; Katz, 1980) yielded samples with statistically undistiguishable concentrations of major ions, in spite of the difference between the lower size cuts of the two instruments. This suggests that small fog droplets are not sufficiently different in composition to affect the total solute loading.

Ionic balances are an indicator of whether all ionic components in the sample have been accounted for in analysis. Ionic balances in the fogwater samples were 0.98 $\pm$ 0.18 at Bakersfield (n=15), 1.02 $\pm$ 0.09 at McKittrick (n=53), 1.11 $\pm$ 0.18 at Buttonwillow (n=7), and 0.60 $\pm$ 0.17 at Visalia (n=12). The ionic balances were calculated from the following equivalent ratio:

$$\text{Ionic balance} = \frac{[Cl^-]+[NO_3^-]+[SO_4^{2-}]+[S(IV)]}{[H^+]+[Na^+]+[NH_4^+]+[Ca^{2+}]+[Mg^{2+}]} \qquad (A1)$$

where each mole of S(IV) was assumed to provide one equivalent (Jacob and Hoffmann, 1983). The most reliable ionic balances were found at McKittrick, while at Visalia there was a considerable and consistent anion deficiency. Fogwater at Visalia had a consistently high pH, and as a consequence could contain important alkalinity; therefore, additional weak acid anions must be considered in an ionic balance. In fogwater with low pH such as at McKittrick, weak acids are mostly present in undissociated form and thus equation (1) represents a reasonably good balance of cations to anions.

The principal ionic contributors to alkalinity in the pH range 4 - 8 are expected to be HCO_3^- ($H \times K_{a1} = 7.07 \times 10^{-12}$ $\underline{M}^2$ atm^{-1} at 5^oC) and carboxylate ions. Fogwater concentrations of some carboxylate ions in the fogwater were determined by J. W. Munger (unpublished data; average values are given in Table 3). The acidity constants of these ions at 5^oC are 1.3×10^{-4} for lactic acid, 1.7×10^{-4} for formic acid, 1.7×10^{-5} for acetic acid, and 1.3×10^{-5} for propionic acid (Martell and Smith, 1977). For the data set where carboxylate ion concentrations were determined, we calculated the dissociated fraction by assuming equilibrium at the fogwater pH; we then added the resulting anion equivalents (plus bicarbonate with P_{CO2}= 340 ppm) to equation (1). Before inclusion of weak acids, the ionic balances for that data set were 1.03 $\pm$ 0.09 at McKittrick (n=25) and 0.49 $\pm$ 0.15 at Visalia (n=6); after inclusion of weak acids, the ionic balances were 1.06 $\pm$ 0.11 at McKittrick and 0.75 $\pm$ 0.15 at Visalia. The McKittrick samples have little alkalinity, and the ionic balance remained close to unity. At Visalia, on the other hand, ionic balances were greatly

improved. There was still an anion deficiency at Visalia, likely due to undetermined weak acids or to an underestimate of HCO_3^- (equilibrium may not be reached).

2. Liquid water content

We determined the liquid water content in fogs from the collection rate of the Caltech rotating arm collector, with an empirical correction factor of 60%. This method has been found to provide reasonable agreement with Hi-Vol filter and laser transmissometer measurements (Jacob et al., 1984c; Hering and Blumenthal, 1984; Waldman, 1985). Further, this method provides measurements which coincide in time and space with our chemical characterization of fogwater. The correction factor of 60% is consistent with the lower size cut of 20 μm for the rotating arm collector, in view of typical fog droplet size distributions (Waldman, 1985). At the present time, there is no standard method for ground-based measurements of liquid water content; Hering and Blumenthal (1984) have found that biases between different methods are usually systematic; i.e., there is a good correlation between liquid water contents obtained by different methods. Although the absolute error on our liquid water content estimates cannot be ascertained, we are satisfied that the collection rate of the rotating arm collector adequately follows variations in liquid water content over the course of the fog.

3. Aerosol, $HNO_3(g)$, and $NH_3(g)$ measurements

There are two major errors incurred in the filter method used in this study: (i) N(V) and N(-III) artifacts, (ii) random errors from the sampling process. We will address each in order.

Stelson and Seinfeld (1982) have shown that an increase in temperature at constant dew point during sampling may volatilize ammonium nitrate collected on Teflon filters and result in artifact $HNO_3(g)$ and $NH_3(g)$. Further, absorption of gaseous nitric acid on the Teflon filter may result in artifact aerosol nitrate (Spicer and Schumacher, 1979; Appel, 1980). In an intercomparison study of gaseous nitric acid measurement methods, Spicer et al. (1982) found good agreement between the dual filter method (used here) and other methods. Further, Spicer et al. (1982) found that the dual filter method was accurate in measuring total N(V).

The study of Spicer et al. (1982) was conducted under hot, dry conditions. Potential biases are different under the cool, humid conditions found in the San Joaquin Valley. Nighttime samples (0000-0400 PST) were probably unaffected by volatilization because temperatures during the sampling period either remained constant or decreased. During the day, temperature changes were usually small because of the overcast conditions; temperatures recorded hourly at Bakersfield between 1200 and 1600 PST increased on only 5 of the 15 sampling days, and never increased by more than $1^{o}C$ except on 14 January (when a $3^{o}C$ increase was observed). Still, an increase of $1^{o}C$ in temperature at constant dew point may increase the dissociation constant $K = P_{HNO3} x P_{NH3}$ by a factor of 2 under high humidity conditions (Stelson and Seinfeld, 1982). The formation of aerosol

ammonium nitrate is strongly favored thermodynamically, and aerosol concentrations could not have been significantly affected by volatilization; on the other hand, high relative errors may have occurred on the determination of the gas present at the lowest concentration. That concentration was often near or below the detection limit, in which case the error was inconsequential.

Teflon filters run in dense fogs accumulated drops of liquid water at the surface. In those particular cases, samples were dried in the open before being sealed. Nitric acid scavenged in acidic fog volatilizes during drying, leading to underestimate of total aerosol nitrate. No significant nitrate loss should occur in non-acidic fog, because in that case NO_3^- remains in the aerosol phase as the fog dissipates. Similarly, ammonium aerosol should not volatilize in acidic fog. Volatilization of aerosol ammonium from filters collected in alkaline fog depends on the stability of the ammonium salts of weak acids. Some volatilization was found to occur (Jacob et al., 1985).

There are three types of "random" errors: (i) uncertainty in the flow rate through the filter, (ii) uncertainty in the efficiency of recovery by extraction, and (iii) analytical error. Because the first two sources of error affect the aerosol sample as a whole, we expect a correlation to exist between the errors on the different species. To test for these errors, concentrations of SO_4^{2-}, NO_3^-, and NH_4^+ were determined in duplicate for 45 pairs of filter samples "1" and "2" collected side by side. Concentrations of Cl^- were also determined, but the errors on those were generally controlled by the filter blank. The relative differences on the determinations of X for the 45 pairs of duplicate samples were statistically analyzed as follows:

$$DX = \frac{2\,|X_2 - X_1|}{X_1 + X_2} \quad . \qquad (A2)$$

Standard deviations S_{DX} on the determinations of SO_4^{2-}, NO_3^-, and NH_4^+ were 18.6%, 18.8%, and 19.1%, respectively. These results are comparable to those reported by Russell and Cass (1984) for similar measurements. Student "t" tests for paired data at the 5% level of significance did not show significant differences between sampling locations 1 and 2 for SO_4^{2-}, NO_3^-, or NH_4^+ at any site; therefore,no significant effects from the differences in backup filters were apparent.

The standard deviation S_{DX} was resolved into its component S_P associated with pump operation and filter extraction, and its component $S_{A,X}$ associated with chemical analysis. The error characterized by S_P was assumed to be the same for SO_4^{2-}, NO_3^-, and NH_4^+, while the errors due to analysis were assumed not to be correlated. Because S_{DX} is small, we can write as an approximation:

$$S_{DX}^2 = S_P^2 + S_{A,X}^2 \quad . \qquad (A3)$$

By statistical analysis of the differences between NH_4^+, NO_3^-, and SO_4^{2-} concentrations, we obtained S_P= 18.1%, $S_{A,SO4}$= 4.4%, $S_{A,NO3}$= 4.0%, and $S_{A,NH4}$= 6.3% Most of the error in aerosol determination was due to uncertainty in the amount of sample collected and recovered, and the errors on different species were thus strongly correlated. This correlation is an important point to take into account when

assigning error bounds to alkalinity calculations, or when predicting gas-phase concentrations from aerosol equilibrium models (Jacob et al., 1985).

No duplicate analyses were made for Na^+, K^+, Ca^{2+}, and Mg^{2+}. Replicate analyses of standards indicate $S_{A,X}$ of about 5% for these four ions. Duplicates for $NH_3(g)$ and $HNO_3(g)$ determinations were not collected, but the $S_{A,X}$ values should be the same as for NH_4^+ and NO_3^-, respectively. In addition to the analytical error, concentrations of all constituents were assumed to be subject to the same error S_p. This assumption implies that the variability of the flow rate through the filter is the major contributor to S_p, which seems justified since filter extraction efficiencies are better than 95% (Russell and Cass, 1984).

Filter blanks for all constituents except Cl^- and $NH_3(g)$ were below the detection limit of the analytical methods. For a 4-hour sample, the detection limits from the analytical methods corresponded to 4 neq m^{-3} for $NO3^-$, SO_4^{2-}, $HNO_3(g)$, and cations other than NH_4^+, and 8 neq m^{-3} for NH_4^+. Because of substantial filter blanks, effective detection limits for $NH_3(g)$ and Cl^- were 17 neq m^{-3} and 20 neq m^{-3}, respectively.

FIGURE CAPTIONS

Figure 1. Sampling sites in the San Joaquin Valley of California. Important emission sources (oil fields, major highways, confined feeding operations) are highlighted. The dashed line is the Kern county line, which is the northern boundary of the area referred to in the text as the "southern San Joaquin Valley" (SSJV). Altitudes in meters are given for each site; reference elevation is Lost Hills, the lowest site.

Figure 2. Concentrations of SO_2, NO_x, and CO at Kernridge (the bold lines were obtained by smoothing the data with a digital filter). Mixing heights at Kernridge and stratus cloud bases over the Bakersfield National Weather Service station. Kernridge hourly mixing height data were missing for 8 - 9 January (dotted line in the mixing height profile), and mixing heights for that period were interpolated from scattered measurements at Kernridge and cloud top data from pilot reports. Discontinuities in the mixing height profile at the altitude of Kernridge indicate a surface inversion at Kernridge. Discontinuities in the mixing height profile at 1000 m AGL indicate a mixing height in excess of 1000 m AGL.

Figure 3. Flow patterns during the sampling program. The wind roses indicate the frequencies of wind directions. The wind vector is the resultant wind (calculated by averaging the hourly wind vectors). (a) Non-stagnant conditions (31-1 Jan., 11-12 Jan., 14 Jan.). (b) Stagnant conditions (2-7 Jan.).

Figure 4. Fogwater composition determined simultaneously at four sites. pH values are indicated on top of each data bar. Concentrations of S(IV) were not determined in the last two samples at Bakersfield.

Figure 5. Aerosol and gas-phase concentrations, and atmospheric alkalinities, at the six valley sites over the period 1 - 8 January. (*) on top of the data bar indicates that the gas phase species was not measured. (†) on top of the data bar indicates that volatilization from the filter in fog could have affected the aerosol measurement (see Appendix).

Figure 6. Concentrations of SO_2 and NO_x at McKittrick. The bold lines were obtained by smoothing the data with a digital filter.

Figure 7. Stirred-tank simulations of aerosol accumulation over the course of a stagnation episode. Conditions adopted are given in Table 5. Two patterns of emissions are considered: (a) alkaline atmosphere (Case I of Table 5), and (b) acidic atmosphere (Case II of Table 5).

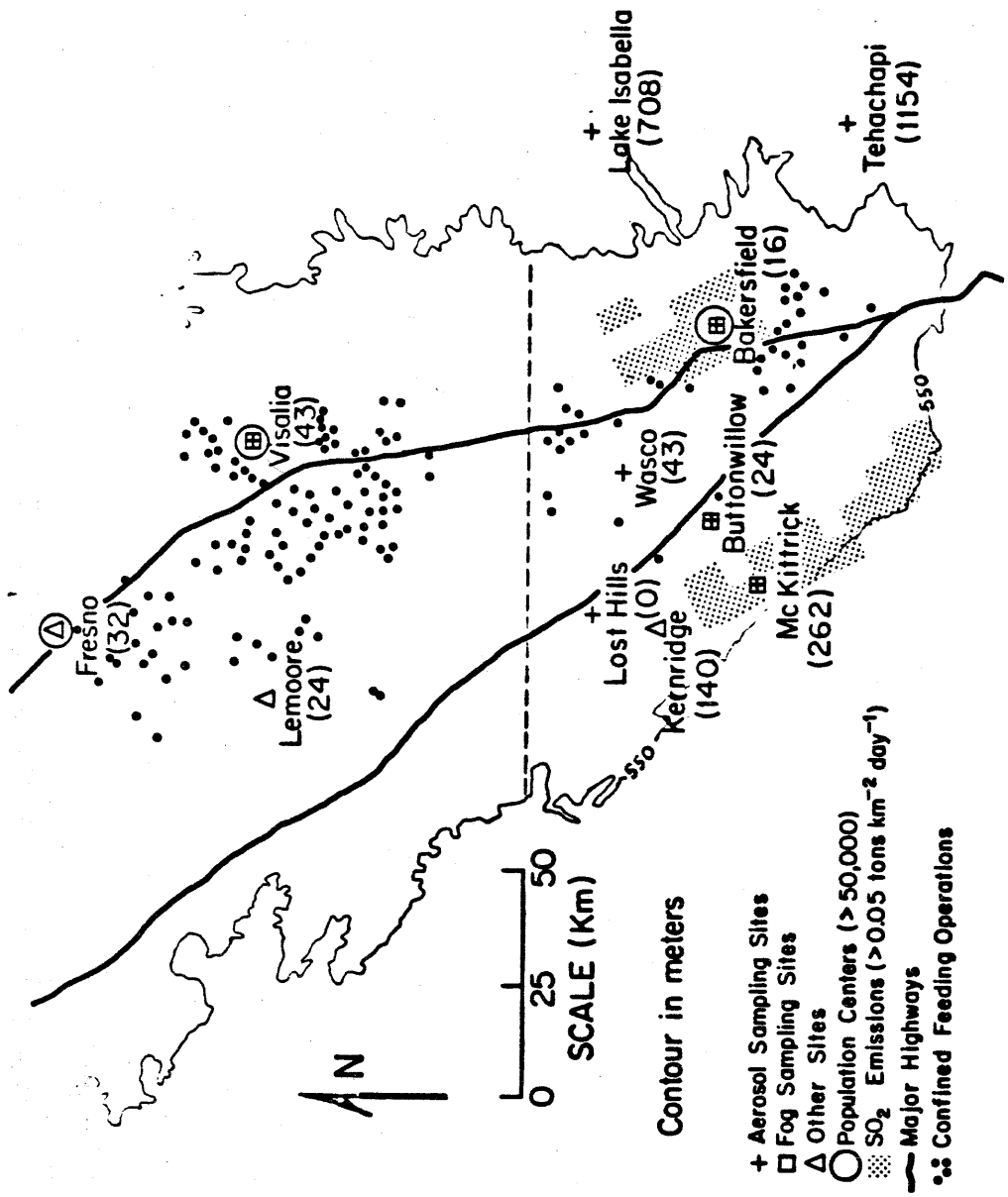
Fresno
(32)
Visalia
(43)
Lemoore
(24)
Lost Hills
(0)
Kettleman
(140)
Wasco
(43)
Buttonwillow
(24)
Mc Kittrick
(262)
Bakersfield
(16)
Lake Isabella
(708)
Tehachapi
(1154)
550
550
N
0
25
50
SCALE (Km)
Contour in meters
+ Aerosol Sampling Sites
□ Fog Sampling Sites
Δ Other Sites
○ Population Centers (>50,000)
SO_2 Emissions (>0.05 tons km^{-2} day^{-1})
Major Highways
Confined Feeding Operations

Figure 1

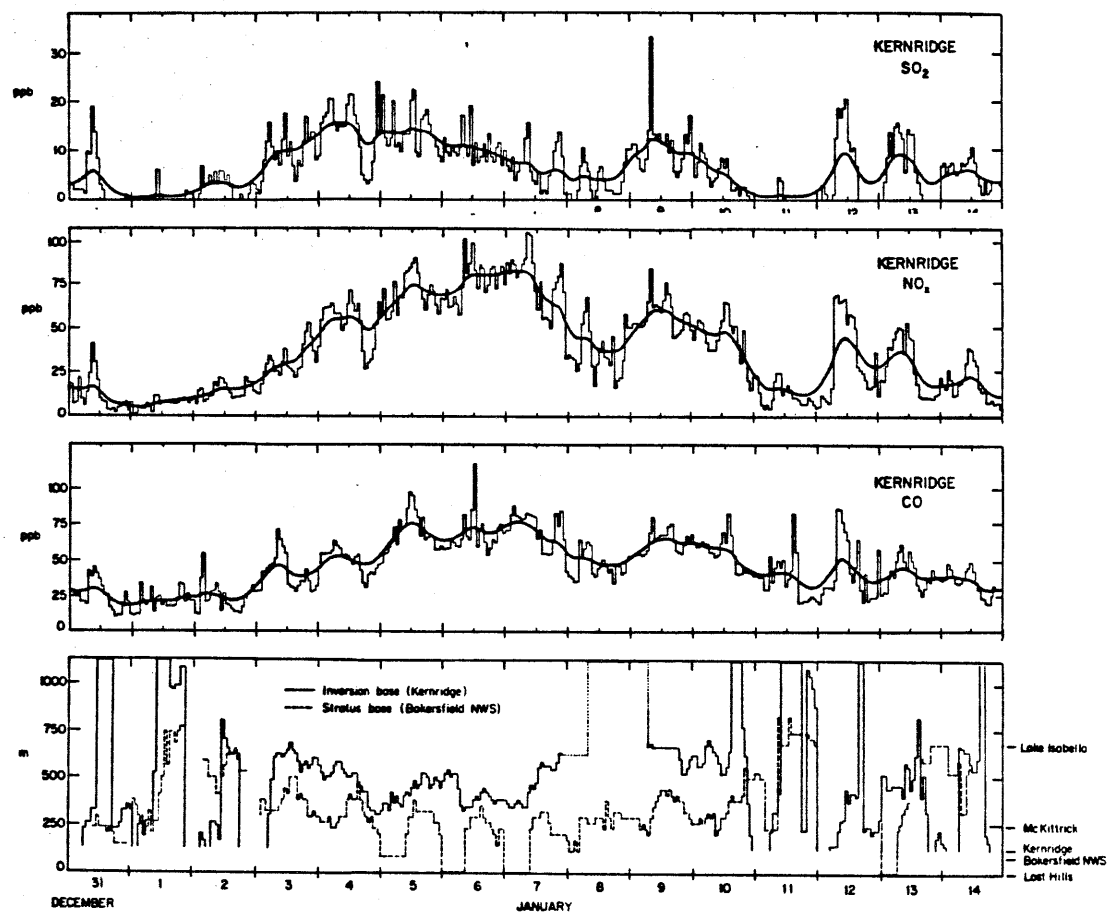
KERNRIDGE
SO_2
ppb
KERNRIDGE
NO_x
ppb
KERNRIDGE
CO
ppb
Inversion base (Kernridge)
Stratus base (Bakersfield NWS)
m
Lake Isabella
McKittrick
Kernridge
Bakersfield NWS
Lost Hills
DECEMBER
JANUARY

Figure 2

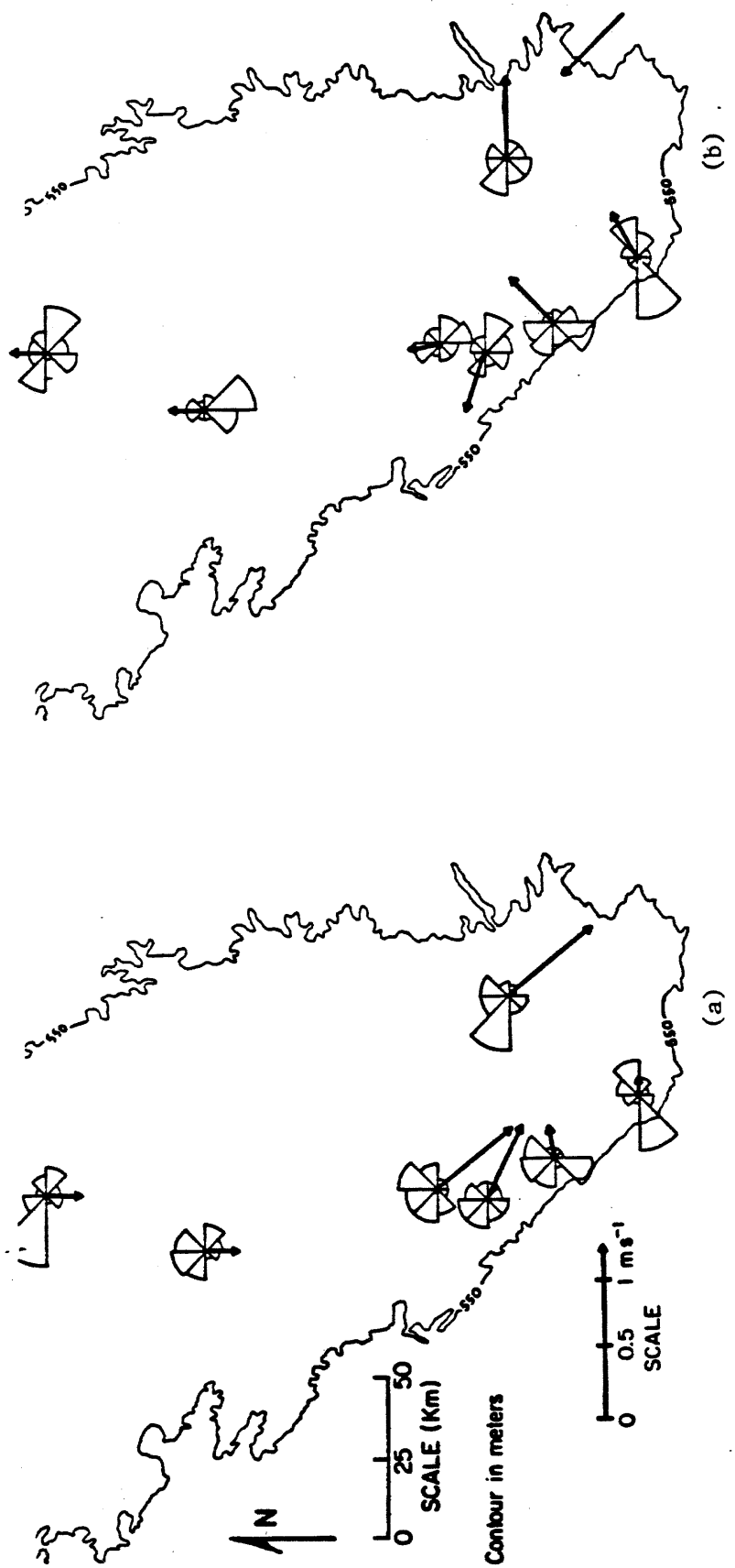

Figure 3

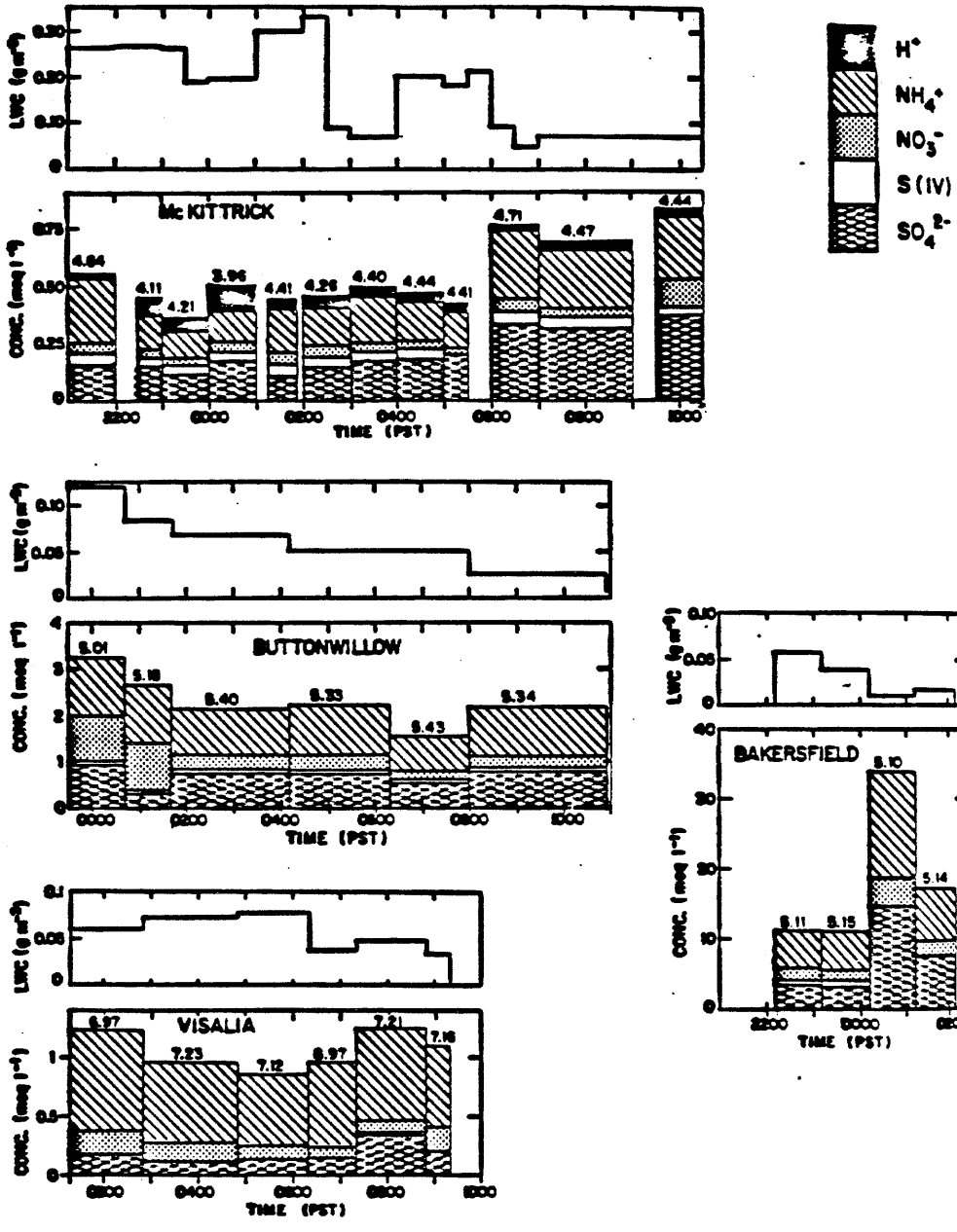
H+
NH4+
NO3-
S(IV)
SO4 2-
Mc KITTRICK
4.84
6.11
4.21
3.96
4.41
4.26
4.40
4.44
4.41
4.71
4.47
4.44
TIME (PST)
BUTTONWILLOW
5.01
5.18
5.40
5.33
5.43
5.34
TIME (PST)
BAKERSFIELD
5.11
5.15
5.10
5.14
TIME (PST)
VISALIA
6.97
7.23
7.12
6.97
7.21
7.16
TIME (PST)

Figure 4

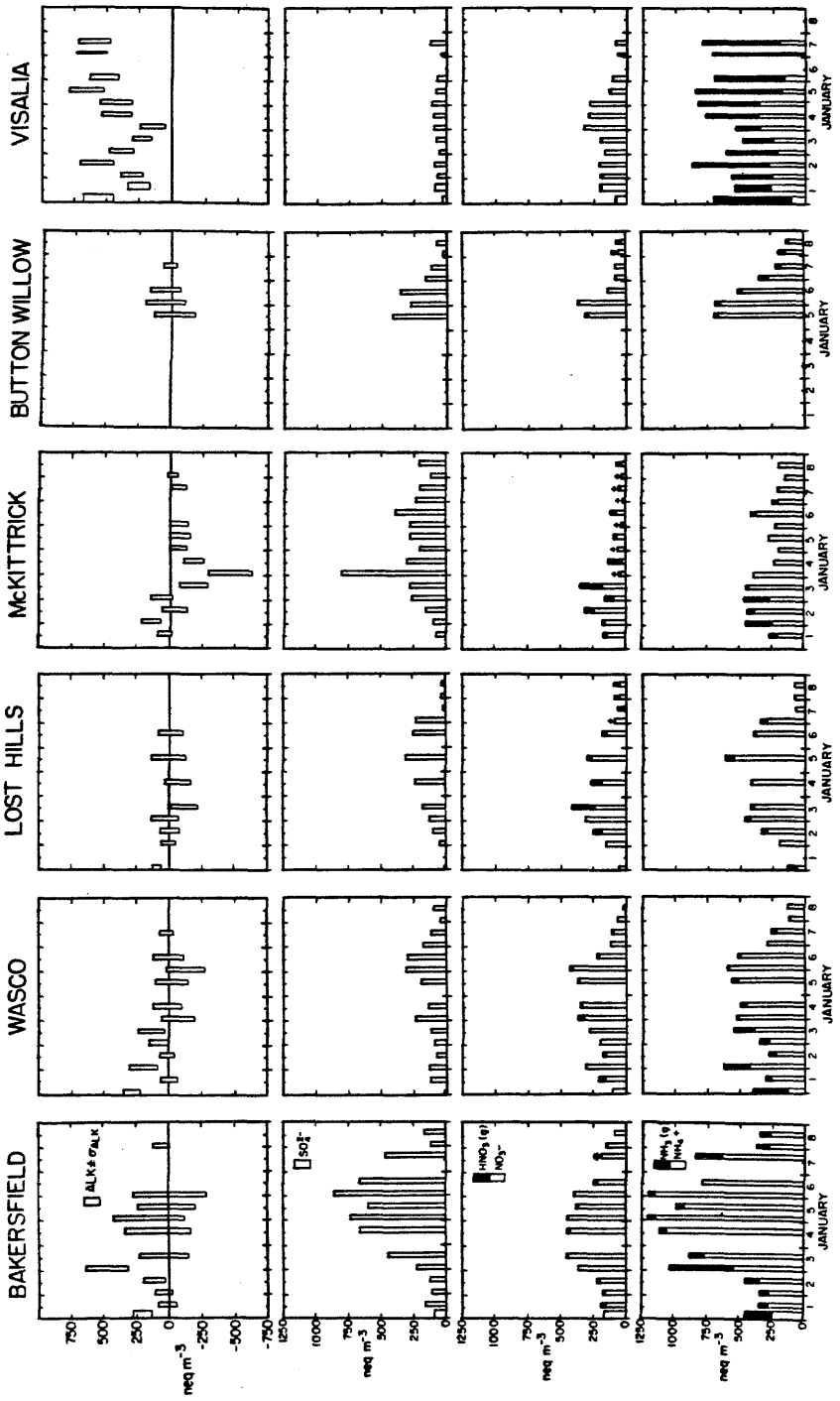
BAKERSFIELD
WASCO
LOST HILLS
McKITTRICK
BUTTON WILLOW
VISALIA
neq m-3
JANUARY

Figure 5

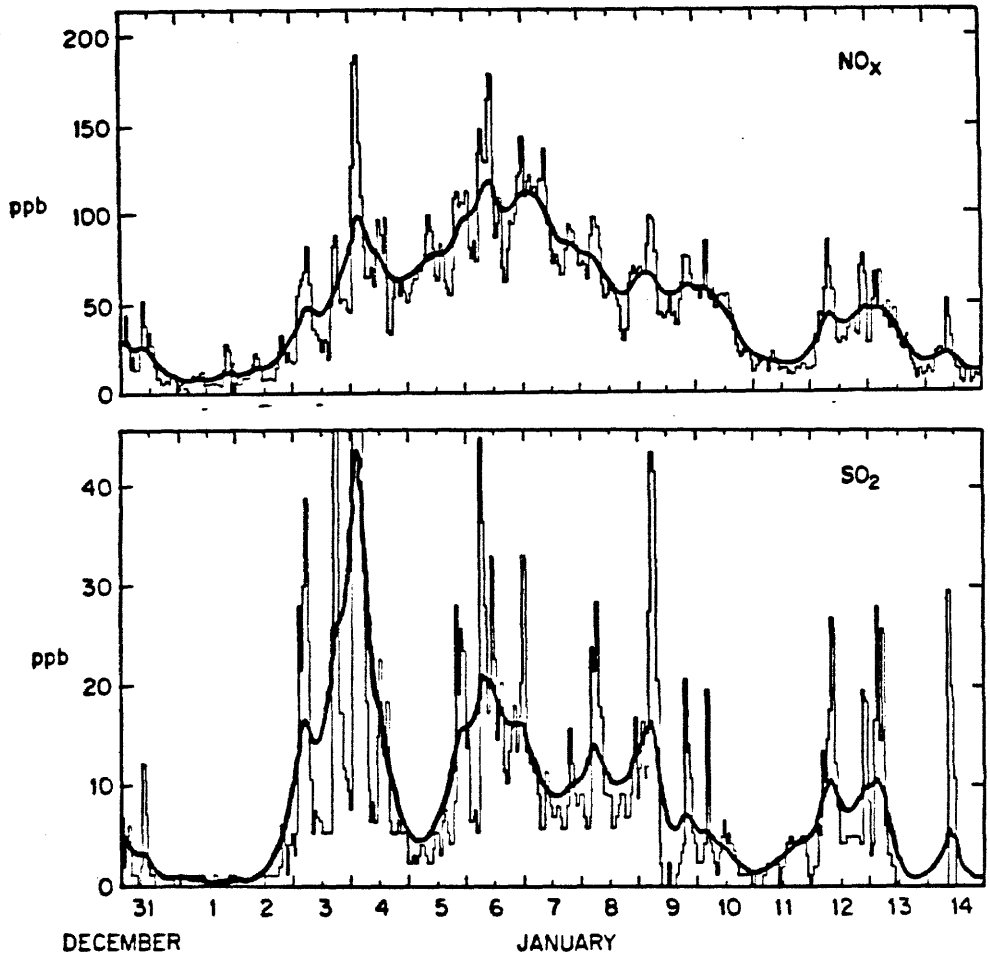
200
150
100
50
0
ppb
NOx
40
30
20
10
0
ppb
SO2
31
1
2
3
4
5
6
7
8
9
10
11
12
13
14
DECEMBER
JANUARY

Figure 6

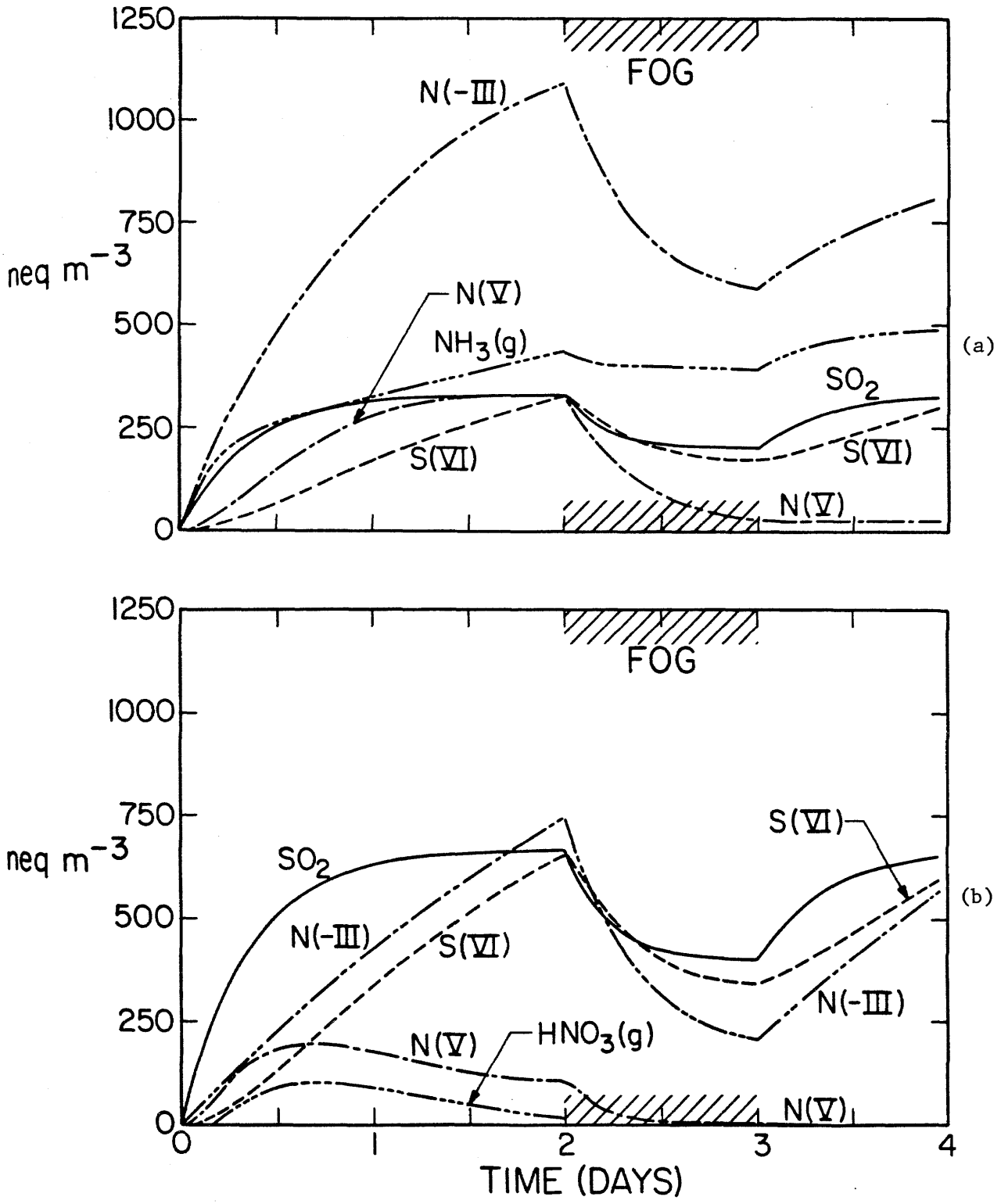
1250
1000
750
500
250
0
neq m^{-3}
FOG
N(-III)
N(V)
NH$_3$(g)
SO$_2$
S(VI)
S(VI)
N(V)
(a)
1250
1000
750
500
250
0
neq m^{-3}
FOG
S(VI)
SO$_2$
N(-III)
S(VI)
N(-III)
N(V)
HNO$_3$(g)
N(V)
(b)
0
1
2
3
4
TIME (DAYS)

Figure 7

CHAPTER VIII

COMPARISON OF FIELD DATA WITH THERMODYNAMIC CALCULATIONS FOR THE H_2SO_4 - HNO_3 - NH_3 SYSTEM AT HIGH HUMIDITIES AND IN FOGS

by Daniel J. Jacob, Jed M. Waldman, J. William Munger,

and Michael R. Hoffmann

Submitted to Journal of Geophysical Research (January 1985)

ABSTRACT

Aerosol and fogwater concentrations of SO_4^{2-}, NO_3^-, and NH_4^+, and gas-phase concentrations of HNO_3 and NH_3, were determined simultaneously in the field under cool and humid conditions. The data were compared to thermodynamic predictions for the chemical speciation of the H_2SO_4 - HNO_3 - NH_3 system between atmospheric phases. The observed products of $HNO_3(g)$ and $NH_3(g)$ concentrations under non-foggy conditions were usually of the same magnitude as the ammonium nitrate dissociation constants predicted by a recently developed model, but the model predictions were consistently too low. Concentrations of $HNO_3(g)$ in fog were below the detection limit under non-acidic conditions, but detectable concentrations were found under acidic conditions. Concentrations of $NH_3(g)$ observed in fog were of the same magnitude as those predicted at equilibrium with the fogwater.

INTRODUCTION

The partitioning of the H_2SO_4-HNO_3-NH_3-H_2O system between different phases in the atmosphere has been the subject of much recent interest. Concentrated sulfuric acid droplets form by homogeneous heteromolecular nucleation under usual atmospheric conditions (Kiang et al., 1973), but nitric acid remains in the gas phase at relative humidities up to about 98% (Nair et al., 1983). Ammonia is scavenged by acidic sulfate aerosols until eventual neutralization is achieved, and combines with nitric acid to form an aerosol of ammonium nitrate or mixed ammonium-nitrate-sulfate salts. Tang (1980) and Stelson and Seinfeld (1982a) studied the effect of relative humidity and droplet pH on the vapor pressures of HNO_3 and NH_3 over aqueous aerosol. Stelson and Seinfeld (1982b) determined the dependence on temperature and relative humidity of the ammonium nitrate aerosol dissociation constant $K_N = P_{HNO3} x P_{NH3}$, and later reported (Stelson and Seinfeld, 1982c) that addition of H_2SO_4 to the mixture does not lower K_N greatly unless the H_2SO_4/HNO_3 ratio is very large. However, addition of H_2SO_4 upsets the acid-base balance and may therefore considerably affect the individual concentrations of $HNO_3(g)$ and $NH_3(g)$. Saxena et al. (1983) and Bassett and Seinfeld (1983) incorporated thermodynamic equilibrium calculations into comprehensive multiphase models. Bassett and Seinfeld (1984) reported that droplet curvature did not increase significantly the vapor pressures of HNO_3 and NH_3.

A number of investigators have tested the applicability of the above thermodynamic calculations to field data. Stelson and Seinfeld (1982b) and Hildemann et al. (1984) calculated the products of $HNO_3(g)$

and $NH_3(g)$ concentrations from data collected under warm, usually dry conditions, and found numbers of the same magnitude as the predicted dissociation constants. Hildemann et al. (1984) reported that agreement could generally be improved by taking into account the association of NO_3^- with cations other than NH_4^+. Tanner (1983) found good agreement for one series of samples collected at a temperature of 14°C and relative humidities 55 - 70%, but large discrepancies in another series of samples collected at temperatures 5.5 - 8°C and relative humidities 75 - 85%. Harrison and Pio (1983) reported measurements consistent with thermodynamic predictions under cool and humid conditions.

The hygroscopic aerosol is an aqueous solution at high humidities, and Table 1 gives the reactions determining the speciation of HNO_3 and NH_3 under those conditions. K_N decreases rapidly with increasing humidity above the deliquescence point (Stelson and Seinfeld, 1982a). At relative humidities in excess of 100%, fog droplets grow on activated nuclei and the considerable increase in the atmospheric liquid water content leads to enhanced heterogeneous condensation of HNO_3 and NH_3. Even though fog droplets are generally in disequilibrium with the surrounding water vapor, the speciation of HNO_3 and NH_3 can be conveniently determined as a function of liquid water content from the reactions of Table 1. Fog droplets are sufficiently dilute solutions that simple activity correction expressions (Stumm and Morgan, 1981) can be used. One readily finds that HNO_3 is exclusively present as NO_3^- at the ranges of liquid water contents and pH values found in fog; i.e., $HNO_3(g)$ is 100% scavenged under all foggy conditions. On the other hand, the speciation of NH_3

is strongly dependent on droplet pH, liquid water content, and temperature, as shown in Figure 1.

Measurements of $HNO_3(g)$ and $NH_3(g)$ in fogs or clouds are few. Daum et al. (1984) found concentrations of both gases to be below the detection limit of 0.4 ppb in acidic stratus clouds (pH 3.2 - 4.2). Measurements in acidic fogs (pH 2 - 4) showed no detectable $NH_3(g)$, and very low concentrations of $HNO_3(g)$ (Hering and Blumenthal, 1984; Waldman, 1985). No measurements are available in non-acidic fogs, where a substantial vapor pressure of NH_3 is expected to persist.

This paper reports on simultaneous measurements of gas-phase, aerosol, and fogwater concentrations in the H_2SO_4-HNO_3-NH_3 system, obtained over the course of a field experiment in the San Joaquin Valley of California (Jacob et al., 1985). The observed speciation of the H_2SO_4-HNO_3-NH_3 system will be compared to that predicted by thermodynamic equilibrium calculations. Concentrations of $HNO_3(g)$ and $NH_3(g)$ were determined by dual filter methods as described in Russell and Cass (1984). The reader is referred to Jacob et al. (1985) for a description of sampling sites, sampling methods, and a detailed analysis of measurement errors.

NON-FOGGY CONDITIONS

We applied the Bassett and Seinfeld (1983) model to data collected at Bakersfield (Table 2). The Bassett and Seinfeld(1983) model determines the equilibrium composition of the atmospheric H_2SO_4-HNO_3-NH_3 system as a function of temperature and relative humidity. It does so by minimizing the Gibbs free energy of a system composed of the gas-phase species $H_2SO_4(g)$, $HNO_3(g)$, $NH_3(g)$, the aqueous-phase species H^+, HSO_4^-, SO_4^{2-}, NO_3^-, NH_4^+, and the solid phases $NH_4HSO_4(s)$, $(NH_4)_3H(SO_4)_2(s)$, $(NH_4)_2SO_4(s)$, $NH_4NO_3(s)$, $(NH_4)_2SO_4 \cdot 3NH_4NO_3(s)$, $(NH_4)_2SO_4 \cdot 2NH_4NO_3(s)$. In the special case of the HNO_3 - NH_3 - H_2O system, the model reduces to the model of Stelson and Seinfeld (1982b), which uses the same thermodynamic data and ionic strength correction procedures. The advantage of the Bassett and Seinfeld model is that it takes into account the presence of a number of sulfate-containing species.

The Bakersfield data set is well suited for comparison with thermodynamic models, because the ions SO_4^{2-}, NO_3^-, NH_4^+, and H^+ typically contributed over 90% of the total ionic content of the aerosol (Jacob et al., 1985). Therefore, the effect of other ions on the thermodynamics of the system are minimized. Further, temperatures and relative humidities remained stable over the 4-hour collection periods because of the prevalent low overcast conditions. We applied the model to describe two different partitioning modes for SO_4^{2-} and NO_3^-: (i) SO_4^{2-} and NO_3^- present exclusively in different aerosol phases ("external mixture"), (ii) SO_4^{2-} and NO_3^- present in the same aerosol phase ("internal mixture"). Because ammonium ion was always in excess of

sulfate, the "external mixture" case was treated by assuming all sulfate to be present as $(NH_4)_2SO_4$ and conducting the equilibrium calculation for the remaining HNO_3 and NH_3 with no sulfate present. The presence in the same phase of SO_4^{2-} and NO_3^- increases the solubility of HNO_3 and NH_3 (Stelson and Seinfeld, 1982c).

Temperature and dew point were measured hourly at the National Weather Service (NWS) station 8 km north of our Bakersfield sampling site, and standard deviations for temperature over the 4-hour period were calculated from the hourly temperature record; 0.5^oC was added to the standard deviation to account for the sensitivity of the readings. The dew point did not change significantly during the sampling periods.

The model requires as input the total concentrations of H_2SO_4, HNO_3, and NH_3, the temperature, and the relative humidity. The standard errors on the determinations of concentrations were about 20% for all species, and strongly inter-correlated (Jacob et al., 1985). To calculate the errors on the predictions from the errors on the measurements, 100 sets of input variables were generated for each data point from the observed values and standard errors for each variable; the correlations between measurement errors were accounted for with the scheme described by Jacob et al. (1985). The expected values and standard errors for the output variables were determined from the outputs for the 100 sets of input variables. Results are shown in Figure 2 (external mixture) and Figure 3 (internal mixture). The aerosol was predicted to be entirely aqueous except in a few cases (indicated on the figures).

The standard errors on the predicted values of K_N were mostly

due to errors on the determinations of temperature and relative humidity. They were not affected by errors on H_2SO_4, HNO_3, and NH_3 concentrations in the external mixture assumption, and only very weakly so in the internal mixture assumption. On the other hand, errors on the concentrations of the individual gases were often strongly affected by errors on the determinations of concentrations; as a result, error bars were sometimes very large.

The products of partial pressures observed in the field were usually of the same magnitude as the values of K_N predicted by the model, but the model was consistently too low. Predictions from the "external mixture" assumption were closer than those from the "internal mixture" assumption. The model appeared to give better predictions for individual gases than for K_N, but this is deceiving. First, the errors on the predicted gas concentrations were large; second, K_N was often so small that one of the gases was almost entirely depleted, and the remaining gas was then simply present at its concentration in excess of the neutralized aerosol.

Stelson and Seinfeld (1982b) also found that the products of vapor pressures over aqueous aerosol were systematically underpredicted by the model, by factors similar to the ones we observed. Harrison and Pio (1983) did not find such a systematic trend, although their determinations may have been subject to large errors because of the considerable fluctuations in temperatures and relative humidities over the course of the sampling periods. Bacause of the many complicated processes occurring in the atmosphere, it is difficult to assess the significance of the relatively small model underpredictions. Laboratory data of vapor pressures over

concentrated ammonium nitrate solutions would provide a check on the accuracy of the thermodynamic calculations, but are not available at this time.

Systematic experimental biases could not satisfactorily explain the larger discrepancies between our measurements and the predicted values of K_N. A systematically higher temperature at our site (located in downtown Bakersfield, pop.122,000) than at the NWS station (located on the outskirts) could occur because of the "heat island" effect; however, a few temperature measurements taken at our sampling site were within 1^oC of those taken by NWS. Measurements by the NWS confirm that temperatures and relative humidities at the NWS station are the same as in downtown Bakersfield (D. Gudgel, Bakersfield NWS, private communication). In comparison, an increase of K_N by a factor of 5 would require a difference in temperature of about 5^oC at constant dew point. Such a discrepancy is not realistic.

The dual filter method is known to be subject to positive interferences i.e., concentrations of $HNO_3(g)$ and $NH_3(g)$ may be overestimated. Volatilization of NH_4NO_3 from the Teflon pre-filter leads to artifact $HNO_3(g)$ and $NH_3(g)$, but in our case this problem is minimized because temperatures and relative humidities remained stable over the course of the sampling periods (Table 2). Another source of positive interference is the displacement of NO_3^- or NH_4^+ by non-volatile material collected on the filter, e.g., acid sulfates or alkaline carbonates. However, if such displacement reactions occurred on the filter it would mean that the atmosphere itself was not at equilibrium; in that case, $HNO_3(g)$ and $NH_3(g)$ concentrations could have differed substantially from their equilibrium values.

Indeed, one cannot exclude the possibility that the atmosphere was out of equilibrium with respect to $HNO_3(g)$ and $NH_3(g)$. To illustrate this possibility, we assume a monodisperse aerosol (particle radius a, number concentration N), and calculate an upper limit of the equilibration time τ by considering the rate at which a gas of very low vapor pressure is scavenged by the aerosol. From the equations of Fuchs and Sutugin (1971), we find:

$$\tau = \frac{1 + \left(\frac{1.3+0.7Kn^{-1}}{1 + Kn^{-1}} + \frac{4(1-\alpha)}{3\alpha}\right)Kn}{\frac{4}{3}\pi a^2 N Kn \left(\frac{8RT}{\pi M}\right)^{1/2}} \qquad (1)$$

where Kn is the Knudsen number, α is the accommodation coefficient, and M is the molecular weight. Depending on the value of the various parameters, τ may be rather large. For example, with a = 0.1 um (Kn = 1), $N = 10^4$ cm^{-3}, $\alpha = 10^{-2}$, and M = 63 g (nitric acid), we find τ = 17 minutes.

FOGGY CONDITIONS

Samples of fogwater, aerosol, $HNO_3(g)$, and $NH_3(g)$ were collected concurrently on 10 occasions. Aerosol, $HNO_3(g)$, and $NH_3(g)$ were simultaneously sampled, over intervals of about 4 hours; fogwater samples were collected over shorter intervals, covering in general all of the corresponding aerosol sampling period. The fogwater data are given in Table 3a. Fogwater was acidic at only one of the four sites (McKittrick). High alkalinities were found at the Visalia site (Jacob et al., 1985). Concentrations of $NH_3(g)$ at equilibrium with the fogwater were calculated from the overall reaction (Table 1):

$$NH_3(g) + H^+(aq) \overset{K'}{=\!=} NH_4^+(aq) \tag{2}$$

where

$$K' = \frac{K_3 K_4}{K_5} \tag{3}$$

$$(NH_3(g)) = \frac{1}{RTK'} \frac{[NH_4^+]}{[H^+]} \exp\left(\frac{(\Delta H_3 + \Delta H_4 - \Delta H_5)}{R} \left(\frac{1}{T} - \frac{1}{298} \right) \right). \tag{4}$$

$[NH_4^+]$ and $[H^+]$ are in ueq l^{-1}, and $(NH_3(g))$ is in ueq m^3. The standard errors on $(NH_3(g))$ were determined from standard errors of $\pm$ 1^oC on temperature and 15% on the determinations of $[NH_4^+]$ and $[H^+]$ (Jacob et al., 1985). Time-weighted averages of predicted $NH_3(g)$

concentrations and fogwater loadings are compared to the aerosol, $HNO_3(g)$, and $NH_3(g)$ data in Table 3b.

Total aerosol concentrations of NO_3^- and NH_4^+ in fog may be underestimated under acidic and alkaline conditions, respectively, because the aerosol filters that were run in fog were allowed to dry in the open before being sealed. This was not a problem for SO_4^{2-}, and fogwater was found to contain between 10 % and 60 % of total aerosol SO_4^{2-}. At Visalia, NH_4^+ was in excess of NO_3^- and SO_4^{2-} in the fog but not on the filter; this suggests evaporation of $NH_3(g)$ from alkaline fog droplets drying on the filter. Alkalinity present in the Visalia fogwater (in our case, mostly as ammonium carboxylate and bicarbonate salts) would thus return to the gas phase upon fog dissipation, explaining the absence of aerosol alkalinity observed under non-foggy conditions (Jacob et al., 1985). The ratio of aerosol/fogwater NO_3^- concentrations was much higher at McKittrick than at other sites, and this similarly suggests volatilization of HNO_3 as acid fog dries on the filter.

Concentrations of $HNO_3(g)$ in fogs were at or below the detection limit of 4 neq m^{-3} under non-acidic conditions (Bakersfield, Buttonwillow, Visalia). Fog was present for less than half of the time that the filter sample was collected at Bakersfield on 31 December, and the non-zero $HNO_3(g)$ concentrations on that night can be satisfactorily explained from the average relative humidity of 96% observed during sample collection. Concentrations of $HNO_3(g)$ in the range 5 - 11 neq m^{-3} were observed under foggy acidic conditions (McKittrick). These concentrations were much lower than those typically measured at that site under non-foggy conditions (Jacob et

al., 1985), but still were significantly different from zero. Although $HNO_3(g)$ is totally scavenged at equilibrium with fog under acidic conditions, equilibrium may not be fully reached because of the slow rate of gas-phase diffusion to droplets (Chameides, 1984). Further, air parcels undersaturated with respect to water vapor are likely to exist within the fog (Gerber, 1981); in such acidic air parcels, $HNO_3(g)$ would be present at equilibrium. Further, if fogwater collected on the aerosol filter was evaporated by undersaturated air during sampling, HNO_3 would have volatilized and caused artifact $HNO_3(g)$.

Concentrations of $NH_3(g)$ at McKittrick were below the detection limit at all times, whereas substantial concentrations were observed at other sites. This is consistent with the low fogwater pH at McKittrick, and the high pH at other sites. Although there were discrepancies between observations and equilibrium calculations, the magnitude of $NH_3(g)$ concentrations was correctly predicted. In comparison, several investigators of rainwater chemistry (e.g., Ayers et al., 1984) have reported $[NH_4^+]$ rainwater concentrations that differed by orders of magnitude from those expected from equilibrium with ground-level $NH_3(g)$. As pointed out by Ayers et al.(1984), a number of factors could prevent attainment of equilibrium between rainwater NH_4^+ and ground-level $NH_3(g)$. Fogs are more likely than rain to be near equilibrium with the surrounding gases because of longer contact times and smaller drop sizes. Due to the low solubility of NH_3 at pH > 5, equilibration of NH_3 with the fog droplets should proceed within seconds (Chameides, 1984). The discrepancies between observed and equilibrium $NH_3(g)$ concentrations

can be explained by non-uniformities in droplet pH, fluctuations in liquid water content, or formation of aqueous-phase ammonia-complexes which complicate the thermodynamics of the system (Hales and Drewes, 1979; Nielsen et al., 1979).

CONCLUSION

Aerosol and fogwater concentrations of SO_4^{2-}, NO_3^-, and NH_4^+, and gas-phase concentrations of HNO_3 and NH_3, were determined simultaneously in the field under cool and humid conditions. Data collected under both non-foggy and foggy conditions were compared to predictions from thermodynamic calculations.

Measurements under non-foggy, cool and humid conditions (temperatures 3 - 13°C, relative humidities 60% - 100%) were compared to predictions from the Bassett and Seinfeld (1983) model. The predicted ammonium nitrate dissociation constants were usually of the same magnitude as the observed products of $HNO_3(g)$ and $NH_3(g)$ concentrations; however, the predictions were consistently too low.

In fog, concentrations of $HNO_3(g)$ were at or below the detection limit of 4 neq m^{-3} under non-acidic conditions, and were very low (although generally non-zero) under acidic conditions. The observation of detectable $HNO_3(g)$ in acidic fog was attributed either to the presence of undersaturated air parcels within the fog or to the slow rate of $HNO_3(g)$ diffusion to the fog droplets. No detectable $NH_3(g)$ was found under foggy acidic conditions, but substantial amounts were found under foggy non-acidic conditions. The observed $NH_3(g)$ concentrations were of the same magnitude as those predicted at equilibrium with fogwater, but significant discrepancies were noted. These discrepancies can be explained by non-uniformities in droplet pH, fluctuations of liquid water content, and formation of ammonia-complexes.

ACKNOWLEDGEMENTS

A.G. Russell and G.R. Cass (Caltech) are thanked for many helpful discussions. This work was funded by the California Air Resources Board (A2-048-32).

REFERENCES

Ayers,G.P., Gras,J.L., Adriaansen,A. and Gillett,R.W. 1984. Solubility of ammonia in rainwater. Tellus· 36B,85-91.

Bassett,M. and Seinfeld,J.H. 1983. Atmospheric equilibrium model of sulfate and nitrate aerosols. Atmos.Environ. 17,2237-2252.

Bassett,M.E. and Seinfeld,J.H. 1984. Atmospheric equilibrium model for sulfate and nitrate aerosols-II. Particle size analysis. Atmos.Environ. 18,1163-1170.

Chameides, W.L. 1984. The photochemistry of a remote marine stratiform cloud. J.Geophys.Res. 89,4739-4755. See also Discussion by D.J. Jacob, same journal (in press).

Daum,P.H., Schwartz,S.E. and Newman,L. 1984. Acidic and related constituents in liquid water stratiform clouds. J.Geophys.Res. 89,1447-1458.

Fuchs,N.A., and Sutugin, A.G. 1971. High-dispersed aerosols, in

International Reviews of Aerosol Physics and Chemistry, vol.2, G.M. Hidy and J.R. Brock ed., p.1-60, Pergamon, New York.

Gerber,H.E. 1981. Microstructure of a radiation fog. J.Atmos.Sci. 38,454-458.

Hales,J.M. and Drewes,D.R. 1979. Solubility of ammonia in water at low concentrations. Atmos.Environ. 13,1133-1147.

Harrison, R.M. and Pio, C.A. 1983. An investigation of the atmospheric HNO_3-NH_3-NH_4NO_3 equilibrium relationship in a cool, humid climate. Tellus.35B,155-159.

Hering, S.V. and Blumenthal, D.L. 1984. Fog sampler intercomparison study: final report to the Coordinating Research Council. Available from Coordinating Research Council, 219 Perimeter Center Parkway, Atlanta, GA.

Hildemann,L.M., Russell,A.G. and Cass,G.R. 1984. Ammonia and nitric acid concentrations in equilibrium with atmospheric aerosol: experiment vs. theory. Atmos.Environ. 18, 1737-1750.

Jacob, D.J., Wang, R.-F. T., and Flagan, R.C. 1984. Fogwater collector design and characterization. Environ.Sci.Technol. 18,827-833.

Jacob, D.J., Munger, J.W., Waldman, J.M., and Hoffmann, M.R. 1985.

The H_2SO_4 - HNO_3 - NH_3 system at high humidities and in fogs: a field study of wintertime stagnation in the San Joaquin Valley of California. Submitted to J.Geophys.Res.

Kiang, C.S., Mohnen, V.A., Bricard, J., and Vigla, D. 1973. Heteromolecular nucleation theory applied to gas-to-particle conversion. Atmos.Environ. 7,1279-1283.

Nair, P.V.N., Joshi, P.V., Mishra, U.C., and Vohra, K.G. 1983. Growth of aqueous solution droplets of HNO_3 and HCl in the atmosphere. J.Atmos.Sci. 40,107-115.

Nielsen,A.T., Moore,D.W., Ogan,M.D., and Atkins,R.L. 1979. Structure and chemistry of the aldehyde ammonias. 3. Formaldehyde-ammonia reaction. 1,3,5 - hexahydrotriazine. J.Org.Chem. 44, 1678-1684.

Russell, A.G. and Cass, G.R. 1984. Acquisition of regional air quality model validation data for nitrate, sulfate, ammonium ion and their precursors. Atmos.Environ. 18, 1815-1827.

Saxena,P., Seigneur,S. and Peterson,T.W. 1983. Modeling of multiphase atmospheric aerosols. Atmos.Environ. 17,1315-1329.

Schwartz,S.E. and White,W.H. 1981. Solubility equilibria of the nitrogen oxides and oxyacids in dilute aqueous solution. Adv.Env.Eng.Sci. 4,1-45.

Smith,R.M. and Martell,A.E. 1976. Critical Stability Constants, vol. 4. Plenum, New York.

Stelson, A.W., and Seinfeld, J.H. 1982a. Relative humidity and pH dependence of the vapor pressure of ammonium nitrate-nitric acid solutions at 25°C. Atmos.Environ. 16, 993-1000.

Stelson,A.W. and Seinfeld,J.H. 1982b. Relative humidity and temperature dependence of the ammonium nitrate dissociation constant. Atmos.Environ. 16,983-992.

Stelson,A.W. and Seinfeld,J.H. 1982c. Thermodynamic prediction of the water activity, NH_4NO_3 dissociation constant, density and refractive index for the system NH_4NO_3-$(NH_4)_2SO_4$-H_2O at 25°C. Atmos.Environ. 16,2507-2514.

Stumm,W. and Morgan,J.J. 1981. Aquatic Chemistry, 2nd ed., Wiley Interscience, New York.

Tang, I.N. 1980. On the equilibrium partial pressures of nitric acid and ammonia in the atmosphere. Atmos.Environ. 14,819-828.

Tanner, R.L. 1983. An ambient experimental study of phase equilibrium in the atmospheric system: aerosol H^+, NH_4^+, SO_4^{2-}, NO_3^-, $NH_3(g)$, $HNO_3(g)$. Atmos.Environ. 17,2935-2942.

Waldman, J.M. 1985. Contribution of fog to the deposition flux of acidity. Ph.D. thesis, California Institute of Technology,Pasadena,CA.

Table 1. Dissociation and vapor pressure equilibria of HNO_3 and NH_3.

Reaction	K_{298} M or M atm^{-1}	ΔH_{298} kcal mole^{-1}	reference
1. $HNO_3(g) = HNO_3(aq)$	2.1×10^{5}	-17.3	Schwartz and White (1981)
2. $HNO_3(aq) = NO_3^- + H^+$	15		
3. $NH_3(g) = NH_3(aq)$	74	-6.80	Hales and Drewes (1979)
4. $NH_3(aq) + H_2O(l) = NH_4^+ + OH^-$	1.7×10^{-5}	0.9	Smith and Martell (1976)
5. $H_2O(l) = H^+ + OH^-$	1.0×10^{-14}	13.35	Smith and Martell (1976)

Table 2. Bakersfield data for aerosol and gaseous H_2SO_4 - HNO_3 - NH_3 species.

Date	Time[a]	NH_4^+	NO_3^-	SO_4^{2-}	$NH_3(g)$	$HNO_3(g)$	T	RH[b]
		neq m^{-3}					°C	%
31 Dec.	0000-0345	573	351	351	19	17	7.8±0.9	96
	1200-1610	669	467	297	158	4	10.8±0.6	93
1 Jan.	-0215-0815	242	170	89	212	<4	10.4±0.6	96
	1200-1615	275	161	161	68	35	13.3±0.7	76
2 Jan.	0000-0415	273	168	109	67	14	7.2±1.1	89
	1200-1620	344	201	124	107	25	11.8±0.7	74
3 Jan.	0000-0415	545	370	226	483	<4	9.1±0.8	87
	1200-1615	769	445	445	113	11	9.2±0.6	81
4 Jan.	1200-1700	1057	427	660	55	24	9.9±1.3	80
5 Jan.	0100-0510	1141	442	731	63	6	6.9±0.8	95
	1200-1615	923	362	596	60	19	8.8±0.6	85
6 Jan.	0000-0415	1149	388	855	47	7	7.4±0.6	95
8 Jan.	0000-0405	272	142	118	52	6	6.8±0.6	95
9 Jan.	1420-1825	260	85	219	139	8	7.3±0.6	86
10 Jan.	0000-0415	621	117	570	60	46	6.2±0.6	89
	1200-1615	533	152	417	48	14	6.9±0.8	85
11 Jan.	1200-1615	144	105	78	65	46	9.0±0.7	71
12 Jan.	0000-0415	345	204	149	157	<4	3.0±0.9	91
	1200-1615	331	244	169	334	26	11.2±1.0	66
13 Jan.	0000-0400	486	283	407	208	<4	4.6±0.7	96
	0700-1115	729	349	475	122	6	5.9±0.8	91
	1200-1615	855	437	507	240	14	9.9±1.1	73
	1800-2210	692	402	306	161	10	6.4±0.8	85
14 Jan.	0050-0410	567	423	229	180	5	4.9±1.2	89
	0735-1130	641	423	214	470	6	6.4±1.0	85
	1200-1615	318	263	129	118	43	10.7±1.5	61

(a) local time (PST)
(b) calculated from the expected temperature value and the dew point.

Table 3a. Chemical composition of fogwater samples used in comparison.

Site	Time	L[(a)]	pH	Na^+	NH_4^+	Ca^{2+}	Mg^{2+}	Cl^-	NO_3^-	SO_4^{2-}	$NH_3(g)$[(b)]
		$g\ m^{-3}$		———			$\mu eq\ l^{-1}$	———			neq m-3
Bakersfield	0115-0230	0.13	5.99	40	1590	73	13	38	285	799	76 ± 20
31 Dec. 1983	0305-0415	0.10	5.63	27	2510	75	14	40	519	2360	52 ± 13
T = 8 °C											
Bakersfield	0130-0200	0.11	6.38	59	3190	143	9	314	502	3250	227 ± 59
13 Jan. 1984	0200-0300	0.11	5.92	83	2800	175	16	180	425	2560	72 ± 19
T = 4 °C	0300-0330	0.03	6.72	ND	5920	492	52	211	1100	4920	957 ± 221
	0330-0400	0.07	6.74	ND	3300	294	123	147	662	2940	521 ± 142
McKittrick	0005-0100	0.32	4.02	4	399	13	1	4	245	267	< 1
5 Jan. 1984	0100-0200	0.16	4.00	6	347	21	2	3	256	272	< 1
T = 5 °C	0200-0300	0.24	4.02	96	344	10	1	3	229	253	< 1
	0300-0435	0.21	4.21	2	357	8	1	21	175	255	< 1
McKittrick	0035-0100	0.25	4.23	8	241	10	1	8	59	250	< 1
6 Jan. 1984	0100-0200	0.22	4.03	7	294	15	2	15	121	317	< 1
T = 5 °C	0200-0300	0.17	4.22	6	499	9	1	9	196	371	< 1
	0300-0400	0.15	4.20	11	333	10	1	8	158	310	< 1
	0400-0500	0.12	4.14	6	345	9	1	3	142	290	< 1
McKittrick	0000-0100	0.19	3.96	ND	136	47	2	26	46	250	< 1
7 Jan. 1984	0115-0150	0.30	4.41	ND	186	10	1	4	51	210	< 1
T = 5 °C	0200-0300	0.21	4.26	ND	162	14	2	12	50	223	< 1
	0300-0400	0.07	4.40	ND	204	36	6	7	43	255	< 1
	0400-0500	0.20	4.44	ND	166	24	3	7	29	278	< 1
McKittrick	1030-1230	0.10	4.23	ND	683	116	12	13	178	806	< 1
7 Jan. 1984	1230-1440	0.07	4.24	ND	870	145	14	24	313	827	< 1
T = 5 °C	1440-1540	0.17	4.28	ND	740	71	8	7	260	630	< 1
	1540-1655	0.22	4.12	ND	522	27	3	4	209	467	< 1
McKittrick	2035-0035	0.07	4.18	12	599	12	2	9	222	546	< 1
7-8 Jan. 1984	0035-0205	0.07	4.50	6	555	6	1	9	148	606	< 1
T = 5 °C	0205-0405	0.02	5.01	16	658	15	10	10	152	600	2 ± 1
McKittrick	0010-0120	0.10	3.71	28	845	78	8	30	270	842	< 1
10 Jan. 1984	0120-0525	0.07	3.85	7	351	16	2	16	131	418	< 1
T = 5 °C											
Buttonwillow	0040-0140	0.08	5.18	15	1270	18	4	56	1006	492	7 ± 2
7 Jan. 1984	0140-0410	0.07	5.40	8	969	29	5	18	331	916	10 ± 3
T = 6 °C	0410-0620	0.05	5.33	11	1070	27	5	27	318	900	9 ± 3
Visalia	0120-0250	0.06	6.97	9	860	11	2	25	198	176	300 ± 76
7 Jan. 1984	0250-0430	0.07	7.23	4	678	6	1	2	162	122	433 ± 120
T = 6 °C											

(a) calculated from sampling rate of rotating arm fogwater collector, assuming 60% collection efficiency (Jacob et al., 1984).
(b) calculated from equation (1).

Table 3b. Comparison of fogwater data with aerosol, $HNO_3(g)$, and $NH_3(g)$ data.

Site	Time		pH	Na^+	NH_4^+	Ca^{2+}	Mg^{2+}	Cl^-	NO_3^-	SO_4^{2-}	L[a]	$NH_3(g)$[b]	$HNO_3(g)$[b]
				neq m^{-3}							g m^{-3}	neq m^{-3}	
Bakersfield	000-0400	fog	5.84	4	223	9	2	5	43	153	0.12	(68±19)	(<1)
31 Dec.		aerosol		NA	573	8	28	6	67	351		$\overline{19}$	17
Bakersfield	0000-0400	fog	6.11	6	270	17	2	18	45	250	0.08	(370±86)	(<1)
13 Jan.		aerosol		14	486	29	5	33	283	407		$\overline{208}$	4
McKittrick	0045-0415	fog	4.08	1	71	2	0.3	2	44	53	0.20	(<1)	(<1)
5 Jan.		aerosol		10	187	12	<4	<20	62	202		<17	<4
McKittrick	0000-0410	fog	4.14	2	65	2	0.3	2	26	59	0.19	(<1)	(<1)
6 Jan.		aerosol		10	208	10	<4	<20	28	276		<17	7
McKittrick	0000-0415	fog	4.18	NA	30	5	0.4	2	9	42	0.18	(<1)	(<1)
7 Jan.		aerosol		15	194	12	<4	28	12	229		NA	9
McKittrick	1200-1615	fog	4.22	NA	85	10	1	1	30	78	0.12	(<1)	(<1)
7 Jan.		aerosol		8	197	10	<4	24	47	205		<17	11
McKittrick	0000-0410	fog	4.60	0.4	24	0.4	0.2	0.4	6	25	0.04	(1±1)	(<1)
8 Jan.		aerosol		8	144	6	<4	32	28	120		$\overline{17}$	5
McKittrick	0045-0445	fog	3.82	0.8	34	2	0.2	1	12	38	0.08	(<1)	(<1)
10 Jan.		aerosol		9	227	19	<4	29	37	294		NA	10
Buttonwillow	0100-0500	fog	5.43	0.7	69	2	0.3	2	31	54	0.07	(9±4)	(<1)
7 Jan.		aerosol		25	274	6	<4	30	73	171		$\overline{69}$	4
Visalia	0145-0335	fog	7.06	0.4	50	0.6	0.1	1	12	10	0.06	(355±90)	(<1)
7 Jan.		aerosol		8	128	18	5	<20	73	46		$\overline{592}$	<1

Fogwater loadings per m^3 of air were obtained by multiplying fogwater concentrations by the liquid water content. Measurement errors were about 20% for all species (Jacob et al., 1985). Detection limits were 17 neq m^{-3} for $NH_3(g)$, 4 neq m^{-3} for $HNO_3(g)$, 8 neq m^{-3} for NH_4^+, 20 neq m^{-3} for Cl^-, and 4 neq m^{-3} for all other aerosol species.

(a) time-weighted averages from Table 3a.

(b) numbers in parentheses are gas-phase concentrations at equilibrium with fogwater, calculated by time-weighted average of concentrations predicted in Table 3a. Errors are standard errors on the average, calculated from Table 3a.

FIGURE CAPTIONS.

Figure 1. Fraction of gaseous ammonia scavenged by fogwater. All fog droplets are assumed to be at the same pH. Liquid water contents of 0.05 g m^{-3} (——) and 0.5 g m^{-3} (---) are considered.

Figure 2. Comparison of Bakersfield field data to the Bassett and Seinfeld (1983) equilibrium model: products of concentrations $(HNO_3(g))x(NH_3(g))$, and individual concentrations of $HNO_3(g)$ and $NH_3(g)$. The aerosol is predicted by the model to be an aqueous solution in all cases, except when indicated by (*) (mixed aqueous/solid) or (†) (solid). Two limiting cases are considered: (a) sulfate and nitrate present exclusively in <u>different</u> aerosol phases (external mixture assumption), and (b) sulfate and nitrate present exclusively in <u>the same</u> aerosol phases (internal mixture assumption).

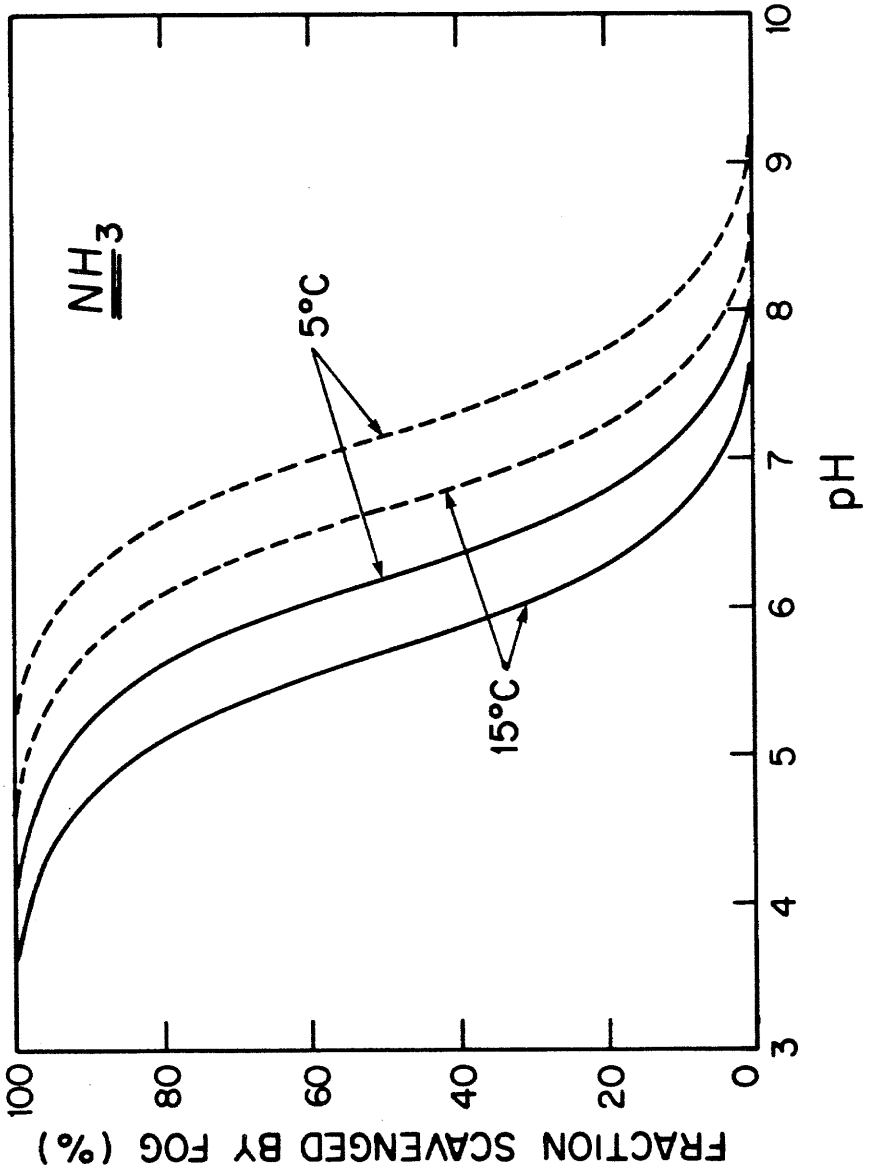
FRACTION SCAVENGED BY FOG (%)
100
80
60
40
20
0
3
4
5
6
7
8
9
10
pH
NH_3
5°C
15°C

Figure 1

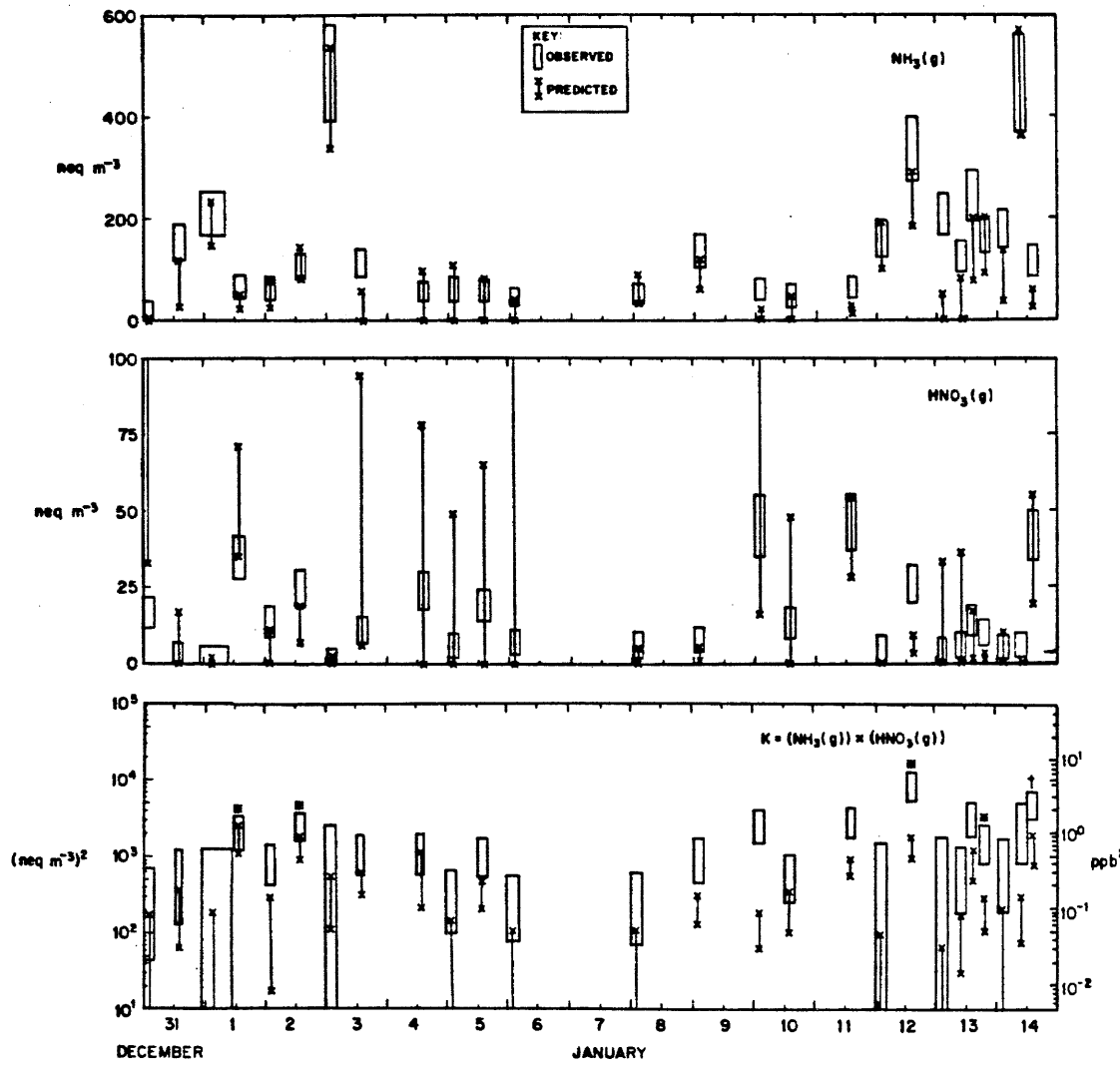
KEY:
OBSERVED
PREDICTED
$NH_3(g)$
neq m^{-3}
600
400
200
0
$HNO_3(g)$
neq m^{-3}
100
75
50
25
0
$K = (NH_3(g)) \times (HNO_3(g))$
$(neq\ m^{-3})^2$
10^5
10^4
10^3
10^2
10^1
ppb^2
10^1
10^0
10^{-1}
10^{-2}
31
1
2
3
4
5
6
7
8
9
10
11
12
13
14
DECEMBER
JANUARY

Figure 2a

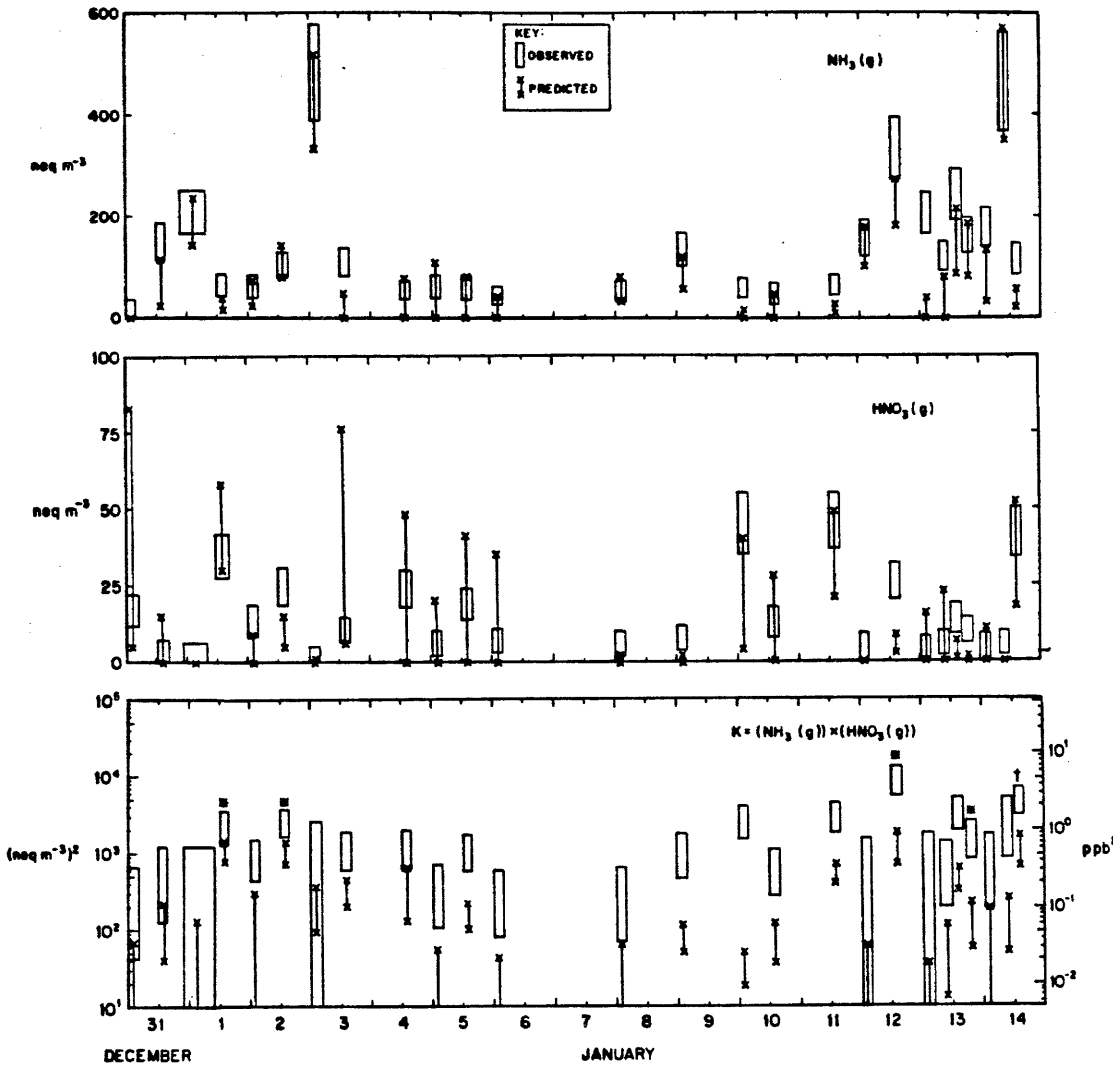
KEY:
OBSERVED
PREDICTED
NH3(g)
neq m-3
HNO3(g)
neq m-3
K = (NH3(g)) x (HNO3(g))
(neq m-3)2
ppb2
DECEMBER
JANUARY

Figure 2b

CHAPTER IX

FUTURE RESEARCH

The results of the research conducted so far have made the "acid fog" problem a serious environmental issue in California. Several studies on the environmental effects of acid fog have already been published, and more are under way. Eventually, regulatory action by air quality control agencies may be considered. Still, more research is needed to assess the extent of the "acid fog" problem, and to understand the means by which the acidity is produced. The following are a few questions which could be addressed in the next few years of research at Caltech.

1. Provide air quality control agencies with a fogwater collector suitable for routine monitoring. A screen collector has been developed for this purpose (Chapter 2) but has not yet been automated or experimentally calibrated. Another promising scheme for sampling fog droplets is by virtual impaction of fog droplets in a cavity. Such a method would have three major advantages over the screen collector:

1. Collection surfaces are easy to clean.
2. Droplets collect in a quiescent environment.
3. Fogs can be collected under freezing conditions.

On the other hand, two drawbacks of the jet impactor are:

1. Anisokinetic sampling biases.
2. Impaction on the inlet walls.

2. Fog and aerosol sampling in the Santa Barbara Channel. The Santa Barbara Channel has been found to contain considerable oil and gas

reserves, and the federal government is encouraging the development of these resources by proposing lease sales in the Outer Continental Shelf. This would considerably increase offshore SO_2 and NO_x emissions in an air basin where dense fogs are frequent and the acid-neutralizing capacity is low. Tracer studies have already been conducted, and have shown that offshore emissions affect the coastline. Further meteorological studies and tracer releases are planned by the California Air Resources Board. The fogwater acidity in the Santa Barbara Channel should be documented in detail, and predictions made of the increase in acidity to be expected from increased offshore activity.

3. Modeling of the smog-fog-smog cycle. One-dimensional models of fog microphysics have been proposed which predict droplet activation, growth, and evaporation over the course of a fog event. These models also predict the amount of liquid water deposited to the ground. It would be of great interest to interface such a model with chemistry packages for fogwater chemistry and the chemistry of non-activated aqueous aerosol. Considerable information would be gained regarding the effect of fog formation on the aerosol composition, and the importance of acid deposition during fogs.

4. Determine sulfate production rates in fogwater and aerosol. Such a project could be conducted in the southern San Joaquin Valley under stagnant conditions, with the help of tracer releases. Emissions of SO_2 in the Valley are concentrated in two small areas, and daily emission rates are available from the oil companies responsible for

these emissions. Tracer releases from both of these areas, followed by tracking of this tracer within the valley, would allow an estimate of sulfur transport. A the same time, a network of sites would be operated to monitor surface winds, mixing heights, SO_2 concentrations, aerosol and fogwater sulfate, and deposited sulfur. By a mass balance on sulfur it would be possible to determine SO_2 conversion rates.

5. Develop an engineering model for predicting fogwater mineral acidity in the San Joaquin Valley. At the present time, the San Joaquin Valley does not have a systematic "acid fog" problem. However, the decline of the cattle industry means that a decrease in NH_3 emissions is to be expected in the next few years. Since there is no foreseeable decrease of oil production activity, Kern county may soon be a "hot spot" for acid fog. The California Air Resources Board is currently working on a NO_x/O_3/hydrocarbons air quality model for the Valley. In parallel, a detailed inventory of ammonia emissions should be prepared. From this inventory, determinations of sulfate production rates, and results from Chapter 7, an "acid fog" simulation package can be written to interface with the Air Resources Board model. Chapter 7 shows that such a simple model can be expected to reliably predict inorganic acidities in fog.

APPENDIX A

INVENTORY OF AMMONIA EMISSIONS IN THE SOUTHERN SAN JOAQUIN VALLEY OF CALIFORNIA

The "southern San Joaquin Valley" is defined as that part of the valley south of the Kern county line (see Figure 1, Chapter VII). Area: 7930 km^2

Livestock

	number[1]	kg NH_3/day per head[2]	tons NH_3 day^{-1}
Cattle			
steers and cows	174,000	0.24[3]	41.2
calves	40,000	0.08[3]	3.2
Sheep	77,000	0.022	1.7
Hogs	6,000	0.036	0.2
Chickens and turkeys	<40,000	0.002	<0.1
		TOTAL	46.3

Soils

	area(km^2)[4]	kg NH_3/day per km^2[2]	tons NH_3 day^{-1}
built-up land	330 (4.2%)	0.45	0.1
cropland	3,470 (43.7%)	3.4	11.8
orchards	660 (8.3%)	3.6	2.4
rangeland	3,430 (43.3%)	1	3.4
forest land	40 (0.5%)	1	<0.1
		TOTAL	17.7

Fertilizer use

	tons fertilizer applied day^{-1}[5]	tons N applied day^{-1}[5]	% N loss[2]	tons NH_3 day^{-1}
dry	304	53.9	10	6.5
liquid	450	133.7	2	3.2
			TOTAL	9.7

Domestic

	number	H_3 emissions/head day^{-1} (2)	tons NH_3 day^{-1}
Humans (perspiration)	325,697 (6)	6.8×10^{4}	0.2
Dogs	283,000 (7)	6.9×10^{-3}	1.9
Cats	303,000 (7)	2.2×10^{-3}	0.6
		TOTAL	2.7

Fuel combustion - stationary sources

	barrels day^{-1}	BTU day^{-1} (8)	$kgNH_3/10^9$ BTU (2)	tons NH_3 day^{-1}
Steam generators				
oil	22,000	1.28×10^{11}	2.8	0.4
natural gas	57,300	3.44×10^{11}	1.4	0.5
Refineries				
oil	17,665	1.02×10^{11}	2.8	0.3
natural gas	39,900	2.39×10^{11}	1.4	0.3
			TOTAL	1.5

TOTAL NH3 EMISSIONS IN THE SOUTHERN SAN JOAQUIN VALLEY 77.9 tons NH_3 day-1

(1) county totals from McGregor et al.(1984). Fraction in SSJV obtained by personal communication from Evan Evans, Kern county Department of Agriculture. Number of calves estimated from personal communication by Neil Gum, California Crop and Livestock Reporting Service.
(2) from Cass et al.(1982).
(3) corrected by body weight from cow and steer emissions.
(4) measured from United States Geological Survey land use/land cover map (1980).
(5) California Department of Food and Agriculture (1984).
(6) U.S. population census (1980)
(7) county totals obtained by personal communication from the Kern county department of Animal Control. Numbers corrected by the fraction of the Kern county human population in the SSJV (81%, U.S. Census,1980).
(8) conversion factors from Cass(1978).

References.

California Department of Food and Agriculture, 1984. Fertilizing materials - tonnage report. January - February - March 1984. Feed, Fertilizer, and Livestock Drugs, Sacramento, CA 95814.

Cass, G.R. 1978. Methods for sulfate air quality managenement with examples to Los Angeles. Ph.D. thesis, California Institute of Technology, Pasadena, CA 91125.

Cass, G.R., Gharib, S., Peterson, M. and Tilden, J.W. 1982. The origin of ammonia emissions to the atmosphere in an urban area. Open file report 82-6, Environmental Quality Laboratory, California Institute of Technology, Pasadena, CA 91125.

McGregor, R.A., Tucker, G.N. Jr. and Gum, N. 1984. California Livestock: annual report 1983. California Crop and Livestock Reporting Service, California Department of Food and Agriculture, P.O. Box 1258, Sacramento, CA 95806.

APPENDIX B

CALCULATION OF SULFATE PRODUCTION IN FOGWATER FROM SUCCESSIVE SAMPLES COLLECTED AT ONE SITE

During the period 3 - 5 January 1984, a stratus cloud filled 1/4 to 1/2 of the boundary mixing layer in the southern San Joaquin Valley. Over that period, a sulfate production rate of the order of 2 % h^{-1} was observed in the overcast boundary layer (Chapter VII). This sulfate production could possibly have been due entirely to in-cloud S(IV) oxidation followed by downward transport of the produced sulfate. Alternatively, some of the sulfate could have been produced in the non-activated aerosol below the cloud. The enhanced SO_2 scavenging in fogs (Chapter VII)suggest that fog (or cloud) droplets could be a favorable environment for sulfate production. However, SO_2 scavenged in the fog may be stabilized as S(IV) by adduct formation (Chapter V) or removed from the atmosphere before undergoing oxidation.

Ideally, in-fog sulfate production rates should be determined by following the evolution of SO_2 and fogwater sulfate concentrations in a given air parcel. Dynamics of droplet growth and evaporation make this very difficult to achieve. The unknown errors in liquid water content measurement methods further complicate the estimate of in-fog sulfate production. In the San Joaquin Valley 1983-1984 study, we investigated sulfate production in fogwater by comparison of successive fog samples collected over the course of an event at a given site. The successive samples were identified by the subscripts 1 and 2, t_1 and t_2 being the corresponding midpoints of the sampling intervals. Samples were typically collected successively over intervals of 1 - 2 hours. The concentrations in samples 1 and 2 were assumed to be those of the fogwater at times t_1 and t_2, respectively.

Three processes could affect the sulfate concentration measured in fogwater: (i)change in the liquid water content, (ii) advection or deposition, and (iii) S(IV) oxidation reactions. We use the same notation as in Chapter 8 to describe concentrations in fogwater and concentrations in air. The time dependence of the sulfate fogwater loading $(S(VI))_f$ can be written:

$$\frac{d(S(VI))_f}{dt} = \left(\frac{d(S(VI))_f}{dt}\right)_{ox} + \left(\frac{d(S(VI))_f}{dt}\right)_{dep,adv} \quad . \tag{B1}$$

The deposition/advection term can be estimated by following the change in fogwater concentration for a component T assumed unreactive and with the same origin and behavior in the atmosphere as S(VI). Over a short time interval:

$$(d(S(VI))_f)_{dep,adv} = \frac{(S(VI))_f}{(T)_f}\, d(T)_f \quad . \tag{B2}$$

Assuming that $(T)_f$ varies linearly with time between t_1 and t_2, we obtain an expression for the oxidation term:

$$\int_{t_1}^{t_2} \left(\frac{d(S(VI))_f}{dt}\right)_{ox} = (S(VI))_{f,2} - (S(VI))_{f,1} - \frac{(T)_{f,2} - (T)_{f,1}}{(t_2 - t_1)} \int_{t_1}^{t_2} \frac{(S(VI))_f(t)}{(T)_f(t)}\, dt \quad . \tag{B3}$$

The integral on the right-hand side is estimated from an average of the $(S(VI))_f/(T)_f$ ratio at times t_1 and t_2:

$$\int_{t_1}^{t_2} \left(\frac{d(S(VI))_f}{dt}\right)_{ox} = \frac{(S(VI))_{f,2}-(S(VI))_{f,1}}{2} + \frac{(S(VI)_{f,2}(T)_{f,1}}{2(T)_{f,2}} - \frac{(S(VI))_{f,1}(T)_{f,2}}{2(T)_{f,1}} \quad . \tag{B4}$$

This oxidation rate was used to derive the pseudo first-order rate constant, k (% h^{-1}), for the conversion of $SO_2(g)$ to S(VI). By taking an average of P_{SO2} over the interval $[t_1, t_2]$:

$$k = \frac{100\ RT}{(t_2-t_1)\overline{P_{SO2}}} \int_{t_1}^{t_2} \left(\frac{d(S(VI))_f}{dt}\right)_{ox} dt \quad . \tag{B5}$$

We also obtained directly from the sulfate production rate a pseudo zero-order rate constant k' ($\underline{M}\ h^{-1}$) to describe an SO_2 conversion process limited by mass transfer of SO_2.

We calculated k and k' from our complete data set, using as tracers nickel and vanadium. Nickel and vanadium are almost exclusively contributed by fuel combustion, and therefore should trace sulfur concentrations. Results are shown in Table B1. No statistically significant conversion of $SO_2(g)$ to sulfate was observed from one sample to the next during fogs at any site. To test whether the lack of significance was due to short-term fluctuations, we examined separately a restricted data set with $(t_2-t_1) > 6$ hours. For these samples (all at McKittrick), the fluctuations for k were less, but the rates were still not significant.

It must be pointed out that the use of a pseudo first-order rate constant to calculate the in-fog sulfate production rate has the major fault that it ignores the dependence of the rate on the reactive species: oxidants, $SO_2.H_2O$, HSO_3^-, and SO_3^{2-}. The dependence of k on S(IV) speciation can be expressed by a function of the form:

$$k = a + \frac{b}{[H^+]} + \frac{c}{[H^+]^2} \quad . \tag{B6}$$

However, we were not able to find a significant fit of k to equation(B6).

In Chapter VI, we calculated sulfate production rates in winter 1982-1983 Bakersfield fogs by a method similar to the one used here (with nitrate as tracer, and approximating the right-hand side integral in (B3) using the $(S(VI))_f/(T)_f$ ratio at time t_2). We found rates of similar magnitude to those found here, and an average rate not significantly different from zero. It must be stressed that our failure to find significant sulfate production rates in fogwater does not constitute evidence that this production does not occur, but it does suggest that the production rate does not exceed a few percent per hour.

Table B1. Rates of sulfate production in fogwater.[a]

site	tracer	n	k (% h^{-1})	n	k[b]	n	$10^5 k'$ (nM m^{-3} h^{-1})
Bakersfield	nickel	3	2.3 ± 6.1			3	4 ± 20
	vanadium	3	1.1 ± 5.5			3	-1 ± 16
McKittrick	nickel	33	-0.1 ± 1.6	5	0.3 ± 0.6	33	0 ± 7
	vanadium	33	-0.4 ± 3.4	5	0.0 ± 0.7	33	0 ± 10
Buttonwillow	nickel					5	-4 ± 16
	vanadium					5	-4 ± 17
Visalia	nickel					2	3 ± 1
	vanadium					2	0 ± 1

(a) k is the pseudo first-order rate of SO_2 conversion. k' is the rate of sulfate production. k was not calculated for Buttonwillow (no SO_2 data) and for Visalia (SO_2 concentrations below detection limit of 10 ppb).
(b) calculated only from samples collected at 6-hour intervals.

APPENDIX C

FOGWATER CHEMICAL COMPOSITION: CALIFORNIA COAST, 1981 - 1983

TABLE 1. SAN DIEGO (DEL MAR) FOG - 08 JAN 83 $

#	TIME1	TIME2	DT(MIN)	MID T	PH	H	NA	K	NH4	CA	MG	F	CL	NO3	SO4	-/+
						MICRO EQ/LITER										
1	18.67	19.25	34.80	18.96	2.63	2340.0	1075.0	14.0	585.0	82.0	265.0	140.0	1300.0	2775.0	775.0	1.144
2	19.50	20.50	60.00	20.00	2.85	1410.0	590.0	14.0	815.0	61.0	155.0	50.0	565.0	1960.0	390.0	0.974
3	20.50	21.50	60.00	21.00	3.00	1000.0	355.0	5.9	1145.0	35.0	91.0	85.0	450.0	1695.0	445.0	1.016
4	21.75	22.50	45.00	22.13	2.98	1050.0	25.0	2.3	670.0	14.0	10.0	90.0	160.0	1140.0	310.0	0.960
5	22.50	23.00	30.00	22.75	3.72	191.0	16.0	3.9	890.0	20.0	9.1	47.0	65.0	765.0	200.0	0.953

TABLE 2. SAN DIEGO (DEL MAR) FOG - 08 JAN 83 $

#	TIME1	TIME2	DT(MIN)	-/+	CL/NA	MG/NA	CA/NA	SO4/NA	NO3/SO4	NH4/SO4	NH4/NO3	NH4/N+S	H/SO4	H/NO3	H/N+S	H+A/N+S
									EQUIVALENT RATIOS							
1	18.67	19.25	34.80	1.144	1.209	0.247	0.076	0.721	3.581	0.755	0.211	0.165	3.019	0.843	0.659	0.824
2	19.50	20.50	60.00	0.974	0.958	0.263	0.103	0.661	5.026	2.090	0.416	0.347	3.615	0.719	0.600	0.947
3	20.50	21.50	60.00	1.016	1.268	0.256	0.099	1.254	3.809	2.573	0.676	0.535	2.247	0.590	0.467	1.002
4	21.75	22.50	45.00	0.960	6.400	0.400	0.560	12.400	3.677	2.161	0.588	0.462	3.387	0.921	0.724	1.186
5	22.50	23.00	30.00	0.953	4.062	0.569	1.250	12.500	3.825	4.450	1.163	0.922	0.955	0.250	0.198	1.120
	SEASALT RATIOS				1.17	0.228	0.043	0.120								

REVISED 3/2/83

TABLE 3. SAN DIEGO (DEL MAR) FOG - 08 JAN 83 $

MASS SOLUTE PER M3 AIR IS BASED ON LIQUID WATER CONTENT EITHER MEASURED (IF AVAILABLE)
OR CALCULATED FROM THE VOLUME OF FOGWATER COLLECTED AND ASSUMING A SAMPLING RATE = 5 M3/MIN (AN UPPER BOUND)

#	TIME1	TIME2	DT (MIN)	VOL	LWC(G/M3) CALC.	LWC(G/M3) MEAS.	H	NA	K	NH4	CA	MG	F	CL	NO3	SO4	MASS
										MICROGRAM / CUBIC METER							
1	18.67	19.25	34.80	34.0	0.195	-1.0	0.457	4.831	0.107	2.058	0.320	0.629	0.520	9.005	33.619	7.269	58.816
2	19.50	20.50	60.00	56.0	0.187	-1.0	0.263	2.533	0.102	2.738	0.228	0.352	0.177	3.739	22.684	3.494	36.310
3	20.50	21.50	60.00	34.0	0.113	-1.0	0.113	0.925	0.026	2.336	0.079	0.125	0.183	1.808	11.910	2.421	19.927
4	21.75	22.50	45.00	34.0	0.151	-1.0	0.159	0.087	0.014	1.822	0.042	0.018	0.258	0.857	10.681	2.249	16.187
5	22.50	23.00	30.00	10.0	0.067	-1.0	0.013	0.025	0.010	1.068	0.027	0.007	0.060	0.154	3.162	0.640	5.165
	AVERAGE FOR 5. SAMPLES						0.201	1.680	0.052	2.004	0.139	0.226	0.240	3.113	16.411	3.215	27.281

TABLE 1. LONG BEACH (QUEEN MARY) FOG - 06 JAN 83

					MICRO EQ/LITER										
#	TIME1	TIME2	DT(MIN)	MID T	PH	H	NA	K	NH4	CA	MG	F	CL	NO3	SO4	-/+
1	3.50	4.00	30.00	3.75	4.78	16.6	43.5	12.4	710.0	46.0	16.0	66.0	375.0	621.0	362.0	1.686
2	4.00	4.50	30.00	4.25	4.82	15.1	28.0	4.1	608.0	19.0	10.0	30.0	170.0	195.0	321.0	1.046
3	4.50	5.00	30.00	4.75	5.32	4.8	180.0	42.1	1286.0	134.0	82.0	0.0	400.0	453.0	1070.0	1.112

REVISED 3/3/83

TABLE 2. LONG BEACH (QUEEN MARY) FOG - 06 JAN 83

					EQUIVALENT RATIOS										
#	TIME1	TIME2	DT(MIN)	-/+	CL/NA	MG/NA	CA/NA	SO4/NA	NO3/SO4	NH4/SO4	NH4/NO3	NH4/N+S	H/SO4	H/NO3	H/N+S	H+A/N+S
1	3.50	4.00	30.00	1.686	8.621	0.368	1.057	8.322	1.715	1.961	1.143	0.722	0.046	0.027	0.017	0.739
2	4.00	4.50	30.00	1.046	6.071	0.357	0.679	11.464	0.607	1.894	3.118	1.178	0.047	0.077	0.029	1.208
3	4.50	5.00	30.00	1.112	2.222	0.456	0.744	5.944	0.423	1.202	2.839	0.844	0.004	0.011	0.003	0.848
	SEASALT RATIOS				1.17	0.228	0.043	0.120								

REVISED 3/3/83

TABLE 3. LONG BEACH (QUEEN MARY) FOG - 06 JAN 83

MASS SOLUTE PER M3 AIR IS BASED ON LIQUID WATER CONTENT EITHER MEASURED (IF AVAILABLE)
OR CALCULATED FROM THE VOLUME OF FOGWATER COLLECTED AND ASSUMING A SAMPLING RATE = 5 M3/MIN (AN UPPER BOUND)

							MICROGRAM / CUBIC METER									
#	TIME1	TIME2	DT (MIN)	VOL	LWC(G/M3) CALC.	LWC(G/M3) MEAS.	H	NA	K	NH4	CA	MG	F	CL	NO3	SO4	MASS
1	3.50	4.00	30.00	50.0	0.333	-1.0	0.006	0.333	0.162	4.260	0.307	0.065	0.418	4.431	12.834	5.792	28.607
2	4.00	4.50	30.00	35.0	0.233	-1.0	0.004	0.150	0.037	2.554	0.089	0.028	0.133	1.406	2.821	3.595	10.817
3	4.50	5.00	30.00	10.0	0.067	-1.0	0.000	0.276	0.110	1.543	0.179	0.066	0.000	0.945	1.872	3.424	8.416
	AVERAGE FOR		3.	SAMPLES			0.016	0.314	0.105	2.899	0.188	0.054	0.197	2.376	6.578	4.371	17.099

REVISED 3/3/83

TABLE 1. LENNOX FOG - 06 JAN 83 $

#	TIME1	TIME2	DT(MIN)	MID T	PH	H	NA	K	NH4	CA	MG	F	CL	NO3	SO4	-/+
						MICRO EQ/LITER										
1	0.00	1.00	60.00	0.50	3.11	776.0	108.0	18.0	545.0	99.0	47.0	61.0	170.0	720.0	240.0	0.748
2	1.00	2.00	60.00	1.50	3.28	525.0	57.0	8.0	448.0	32.0	23.0	52.0	87.0	570.0	200.0	0.832
3	2.00	3.00	60.00	2.50	4.45	35.5	21.0	7.9	454.0	18.5	9.8	90.0	42.0	270.0	82.0	0.885
4	3.00	4.00	60.00	3.50	4.94	11.5	12.0	4.1	344.0	15.6	7.4	65.0	17.0	158.0	43.0	0.717
5	4.00	4.50	30.00	4.25	5.39	4.1	22.0	5.4	537.0	34.0	7.0	107.0	40.0	225.0	110.0	0.791
6	4.50	5.00	30.00	4.75	5.38	4.2	237.0	-0.1	1080.0	226.0	89.0	-0.1	-0.1	1738.0	1500.0	1.979
7	7.00	7.50	30.00	7.25	5.38	4.2	116.0	28.0	1990.0	200.0	275.0	150.0	150.0	1500.0	920.0	1.041
8	7.50	8.00	30.00	7.75	6.15	0.7	420.0	45.0	1330.0	330.0	170.0	420.0	580.0	1400.0	576.0	1.296

REVISED 3/3/83

TABLE 2. LENNOX FOG - 06 JAN 83 $

#	TIME1	TIME2	DT(MIN)	-/+	CL/NA	MG/NA	CA/NA	SO4/NA	NO3/SO4	NH4/SO4	NH4/NO3	NH4/N+S	H/SO4	H/NO3	H/N+S	H+A/N+S
									EQUIVALENT RATIOS							
1	0.00	1.00	60.00	0.748	1.574	0.435	0.917	2.222	3.000	2.271	0.757	0.568	3.233	1.078	0.808	1.376
2	1.00	2.00	60.00	0.832	1.526	0.404	0.561	3.509	2.850	2.240	0.786	0.582	2.625	0.921	0.682	1.264
3	2.00	3.00	60.00	0.885	2.000	0.467	0.881	3.905	3.293	5.537	1.681	1.290	0.433	0.131	0.101	1.391
4	3.00	4.00	60.00	0.717	1.417	0.617	1.300	3.583	3.674	8.000	2.177	1.711	0.267	0.073	0.057	1.769
5	4.00	4.50	30.00	0.791	1.818	0.318	1.545	5.000	2.045	4.882	2.387	1.603	0.037	0.018	0.012	1.615
6	4.50	5.00	30.00	1.979	-0.000	0.376	0.954	6.329	1.159	0.720	0.621	0.334	0.003	0.002	0.001	0.335
7	7.00	7.50	30.00	1.041	1.293	2.371	1.724	7.931	1.630	2.163	1.327	0.822	0.005	0.003	0.002	0.824
8	7.50	8.00	30.00	1.296	1.381	0.405	0.786	1.371	2.431	2.309	0.950	0.673	0.001	0.000	0.000	0.673
	SEASALT RATIOS				1.17	0.228	0.043	0.120								

REVISED 3/3/83

TABLE 3. LENNOX FOG - 06 JAN 83 $

MASS SOLUTE PER M3 AIR IS BASED ON LIQUID WATER CONTENT EITHER MEASURED (IF AVAILABLE)
OR CALCULATED FROM THE VOLUME OF FOGWATER COLLECTED AND ASSUMING A SAMPLING RATE = 5 M3/MIN (AN UPPER BOUND)

#	TIME1	TIME2	DT (MIN)	VOL	LWC(G/M3) CALC.	LWC(G/M3) MEAS.	H	NA	K	NH4	CA	MG	F	CL	NO3	SO4	MASS
							MICROGRAM / CUBIC METER										
1	0.00	1.00	60.00	30.0	0.100	-1.0	0.078	0.248	0.070	0.981	0.198	0.057	0.116	0.603	4.464	1.152	7.967
2	1.00	2.00	60.00	20.0	0.067	-1.0	0.035	0.087	0.021	0.538	0.043	0.019	0.066	0.206	2.356	0.640	4.010
3	2.00	3.00	60.00	34.0	0.113	-1.0	0.004	0.055	0.035	0.926	0.042	0.013	0.194	0.169	1.897	0.446	3.781
4	3.00	4.00	60.00	34.0	0.113	-1.0	0.001	0.031	0.018	0.702	0.035	0.010	0.140	0.068	1.110	0.234	2.350
5	4.00	4.50	30.00	16.0	0.107	-1.0	0.000	0.054	0.023	1.031	0.073	0.009	0.217	0.151	1.488	0.563	3.609
6	4.50	5.00	30.00	1.0	0.007	-1.0	0.000	0.036	-0.000	0.130	0.030	0.007	-0.000	-0.000	0.718	0.480	1.402
7	7.00	7.50	30.00	-9.0	-.060	-1.0	-0.000	-0.160	-0.066	-2.149	-0.240	-0.200	-0.171	-0.319	-5.580	-2.650	-11.53
8	7.50	8.00	30.00	-9.0	-.060	-1.0	-0.000	-0.580	-0.106	-1.436	-0.396	-0.124	-0.479	-1.234	-5.208	-1.659	-11.22
	AVERAGE FOR		8.	SAMPLES			0.040	0.182	0.006	0.341	-0.010	0.002	0.040	0.345	2.207	0.303	3.455

Site	Date	Time (local)	pH	Na^+	K^+	NH_4^+	Ca^{2+}	Mg^{2+}	Cl^-	NO_3^-	SO_4^{2-}	S(IV)	CH_2O	Fe	Mn	Pb	Cu	Ni	V	LWC
				$\mu eq\ \ell^{-1}$								μM		$\mu g\ \ell^{-1}$						$g\ m^{-3}$
Corona del Mar	12/7/82	2105-2150	2.16	725	71	2860	197	188	1050	7900	1290	-0.1	-0.1	-0.1	-0.1	-0.1	-0.1	-0.1	-0.1	0.11
San Nicholas Island	8/26/82	2115-2230	5.70	6975	170	444	485	1710	5900	328	1025	-0.1	198	244	132	73	59	325	41	0.062
		2235-0005	5.70	10200	240	507	705	2530	10400	1120	2960	18	-0.1	308	-0.1	-0.1	-0.1	-0.1	-0.1	0.044
		0007-0147	3.99	7270	175	455	565	1820	6700	1780	2390	-0.1	-0.1	331	87	26	57	15	12	0.040
		0150-0308	3.82	5610	130	328	400	1390	5800	1535	2080	19	447	-0.1	-0.1	-0.1	-0.1	-0.1	-0.1	0.051
		0310-0418	3.83	5940	140	523	430	1470	5300	2028	2320	-0.1	-0.1	342	77	30	45	46	8	0.049
		0420-0556	3.61	3435	95	463	270	825	2600	1940	1740	26	633	900	79	63	54	35	12	0.066
		0558-0755	3.53	4265	115	456	388	1090	3500	2520	2560	25	499	321	85	39	29	21	12	0.048
Morro Bay	7/14/82	0500-0600	6.09	441	17	100	91	113	597	144	188	13	204	192	21	11	57	21	-0.1	0.20
		0820-0900	6.53	1560	190	127	199	510	2814	34	285	-0.1	-0.1	-0.1	-0.1	-0.1	-0.1	-0.1	-0.1	0.075
Mt.Sutro	8/13/82	2125-2225	3.99	648	52	183	93	170	851	87	319	-0.1	-0.1	160	10	24	50	28	-0.1	0.056
Pt.Reyes	8/9/82	2202-0000	3.50	3520	91	327	242	890	3042	526	1281	19	538	484	67	67	87	209	-0.1	0.054
	8/10/82	0230-0328	4.49	2210	54	74	111	540	3230	23	363	8	29	148	8	7	20	63	-0.1	0.098
		0445-0621	4.28	2630	62	101	114	627	3549	32	389	9	98	540	7	16	44	44	-0.1	0.066
		1042-1115	4.72	4700	102	117	235	1200	7042	60	644	-0.1	-0.1	214	21	42	48	88	-0.1	0.081
	8/11/82	0200-0240	3.82	473	15	53	33	112	397	60	237	10	93	246	9	12	55	55	-0.1	0.15
		0241-0324	4.08	188	4	28	10	36	208	14	101	7	62	287	15	65	258	72	-0.1	0.30
		0536-0620	3.74	67	2	84	8	17	215	32	186	12	103	-0.1	-0.1	-0.1	-0.1	-0.1	-0.1	0.13
		0622-0707	3.88	54	2	47	0	12	112	32	101	-0.1	-0.1	80	2	20	70	53	-0.1	0.15
		0850-0958	3.69	993	31	119	55	290	1448	74	441	-0.1	-0.1	1072	4	12	47	21	-0.1	0.059
		1000-1101	3.83	1670	36	104	76	385	2301	69	413	16	268	-0.1	-0.1	-0.1	-0.1	-0.1	-0.1	0.077
		1103-1155	3.75	2440	56	101	124	580	3183	23	539	-0.1	-0.1	-0.1	-0.1	-0.1	-0.1	-0.1	-0.1	0.051
	8/12/82	0343-0427	4.75	97	4	30	8	26	91	12	74	11	142	-0.1	-0.1	-0.1	-0.1	-0.1	-0.1	0.18
		0429-0512	4.52	42	2	39	1	10	51	11	60	9	93	196	6	27	52	18	-0.1	0.19
		0513-0558	4.57	34	1	37	2	7	36	4	54	10	92	252	7	29	72	23	-0.1	0.19
		0559-0644	4.68	30	1	41	1	6	96	7	54	10	93	297	8	23	69	25	-0.1	0.19
		0645-0730	4.82	29	1	64	2	6	36	2	39	11	72	283	8	48	44	18	-0.1	0.19
		0731-0815	5.00	21	1	45	2	5	34	2	42	10	91	296	4	3	4	3	-0.1	0.19
San Marcos	8/20/83	2337-0000	4.41	15	2	128	7	6	42	104	49	-0.1	8	-0.1	-0.1	-0.1	-0.1	-0.1	-0.1	0.42
		0002-0058	4.22	8	2	93	3	3	40	126	52	-0.1	-0.1	-0.1	-0.1	-0.1	-0.1	-0.1	-0.1	0.42

Site	Date	Time (local)	pH	Na^+	K^+	NH_4^+	Ca^{2+}	Mg^{2+}	Cl^-	NO_3^-	SO_4^{2-}	S(IV)	CH_2O	Fe	Mn	Pb	Cu	Ni	V	LWC
				$\mu eq\ \ell^{-1}$								μM		$\mu g\ \ell^{-1}$						$g\ m^{-3}$
San Marcos Pass	8/20/83	2337–0000	4.41	15	2	128	7	6	42	104	49	-0.1	8	-0.1	-0.1	-0.1	-0.1	-0.1	-0.1	0.42
		0002–0058	4.22	8	2	93	3	3	40	126	52	-0.1	-0.1	-0.1	-0.1	-0.1	-0.1	-0.1	-0.1	0.42
		0100–0125	4.42	10	2	103	4	4	22	79	54	1	7	15	3	17	3	8	-0.1	0.51
		0125–0150	4.55	7	3	96	4	3	19	68	48	-0.1	-0.1	-0.1	-0.1	-0.1	-0.1	-0.1	-0.1	0.60
		0150–0203	4.66	9	3	109	2	4	13	68	54	-0.1	-0.1	-0.1	-0.1	-0.1	-0.1	-0.1	-0.1	0.59
		0300–0331	4.67	3	2	81	2	2	9	63	41	2	6	16	3	15	10	2	-0.1	0.54
		0400–0431	4.48	1	2	55	1	1	3	57	34	2	7	8	1	7	3	2	-0.1	0.51
		0600–0630	4.60	2	2	54	2	2	5	49	29	1	6	19	2	13	15	2	-0.1	0.59
		0632–0700	4.57	2	2	54	2	2	4	52	27	-0.1	-0.1	-0.1	-0.1	-0.1	-0.1	-0.1	-0.1	0.49
		0700–0800	4.53	7	9	94	3	3	11	69	49	2	7	22	3	37	5	1	-0.1	0.34
		0800–0900	4.41	10	2	107	2	4	17	65	72	1	10	35	3	38	22	10	-0.1	0.34
		0900–0958	4.68	28	3	198	4	9	43	96	126	4	12	76	3	39	14	10	-0.1	0.24
		1000–1058	4.52	39	4	154	8	12	42	87	118	4	-0.1	17	3	31	33	27	4	0.27
		1100–1200	4.27	41	4	161	10	13	45	121	153	3	14	30	5	43	17	9	-0.1	0.19

APPENDIX D

FOGWATER CHEMICAL COMPOSITION: BAKERSFIELD, CALIFORNIA, DECEMBER 1982 - JANUARY 1983

TABLE 1. BAKERSFIELD FOG - 29 DEC 82 $

#	TIME1	TIME2	PH	H	NA	K	NH4	CA	MG	F	CL	NO3	SO4	-/+	S(IV)	CH2O	TOC
				/ / / / / /				MICRO EQ/LITER				\ \ \ \ \ \			/ MICRO M/L \		/MM/L\
1	6.33	6.83	3.88	132.0	2160.0	700.0	30700.	2400.0	390.0	1430.0	1630.0	40800.	16720.	1.661	473.0	2866.	-1.0
2	6.83	7.83	6.00	1.0	2950.0	935.0	21100.	5180.0	655.0	1140.0	2800.0	11400.	15400.	0.997	-1.0	-1.0	-1.0

REVISED 2/25/83

TABLE 2. BAKERSFIELD FOG - 29 DEC 82 $

#	TIME1	TIME2	DT(MIN)	MIDT	-/+	CL/NA	NO3/NA	CA/NA	SO4/NA	NO3/SO4	NH4/N+S	H/N+S	H+A/N+S	S(IV)/SO4	S(IV)/CH2O
						EQUIVALENT RATIOS								MOLAR RATIOS	
1	6.33	6.83	30.00	6.58	1.661	0.755	0.181	1.111	7.741	2.440	0.534	0.002	0.536	0.057	0.165
2	6.83	7.83	60.00	7.33	0.997	0.949	0.222	1.736	5.220	0.740	0.787	0.000	0.787	-0.000	1.000
	SEA SALT RATIOS					1.17	0.228	0.043	0.120						

REVISED 2/25/83

TABLE 3. BAKERSFIELD FOG - 29 DEC 82 $

MASS SOLUTE PER M3 AIR IS BASED ON LIQUID WATER CONTENT EITHER MEASURED (IF AVAILABLE)
OR CALCULATED FROM THE VOLUME OF FOGWATER COLLECTED AND ASSUMING A SAMPLING RATE = 5 M3/MIN (A LOWER BOUND)

#	TIME1	TIME2	S(IV)	CH2O	TOC	LWC(G/M3) CALC.	LWC(G/M3) MEAS.	S(IV)	CH2O	TOC	-/+	'CORRECTED -/+'	PH	'PH-BY-DIFFERENCE'
			/ MICRO M/L \		/MM/L\			/ MICROGRAM / CUBIC METER \						
1	6.33	6.83	473.0	2866.	-1.0	0.007	-1.00	0.101	0.573	-1.000	1.661	1.619	3.88	1.64
2	6.83	7.83	-1.0	-1.0	-1.0	0.001	-1.00	-1.000	-1.000	-1.000	0.997	0.960	6.00	*****
TIME-WEIGHTED AVERAGE FOR 2. SAMPLES						0.003		0.101	0.573	0.000				

REVISED 2/25/83

TABLE 4. BAKERSFIELD FOG - 29 DEC 82 $

MASS SOLUTE PER M3 AIR IS BASED ON LIQUID WATER CONTENT EITHER MEASURED (IF AVAILABLE)
OR CALCULATED FROM THE VOLUME OF FOGWATER COLLECTED AND ASSUMING A SAMPLING RATE = 5 M3/MIN (AN LOWER BOUND)

#	TIME1	TIME2	DT (MIN)	VOL	LWC(G/M3) CALC.	LWC(G/M3) MEAS.	H	NA	K	NH4	CA	MG	F	CL	NO3	SO4	MASS
							MICROGRAM / CUBIC METER										
1	6.33	6.83	30.00	1.0	0.007	-1.00	0.001	0.331	0.182	3.684	0.320	0.032	0.181	0.385	16.864	5.350	27.331
2	6.83	7.83	60.00	0.7	0.001	-1.00	0.000	0.045	0.024	0.253	0.069	0.005	0.014	0.066	0.471	0.493	1.442
TIME-WEIGHTED AVERAGE FOR 2. SAMPLES					0.003		0.000	0.141	0.077	1.397	0.153	0.014	0.070	0.173	5.935	2.112	10.071

TABLE 5. BAKERSFIELD FOG - 29 DEC 82 $

#	TIME1	TIME2	PH	H	FE	MN	PB	CU	NI	V	FE	MN	PB	CU	NI	V
					MICROGRAM / LITER						MICROGRAM / CUBIC METER					
1	6.33	6.83	3.88	0.0	-0.1	13600.	11431.	-0.1	-0.1	-0.1	-0.000	0.091	0.076	-0.000	-0.000	-0.000
2	6.83	7.83	6.00	0.0	-0.1	1760.0	693.0	19000.	6370.0	-0.1	-0.000	0.001	0.000	0.013	0.004	-0.000

ENTERED 8/10/83

TABLE 1. BAKERSFIELD FOG - 31 DEC 82 $

				MICRO EQ/LITER										/ MICRO M/L \	/MM/L\
				/ / / / / /							\ \ \ \ \ \				
$	TIME1	TIME2	PH	H	NA	K	NH4	CA	NG	F	CL	NO3	SO4	-/+	S(IV)	CH2O	TOC
1	-2.83	-2.17	4.60	25.0	56.6	35.7	1840.0	66.2	7.8	170.0	117.0	970.0	680.0	0.954	395.0	245.0	6.3
2	-2.17	-1.58	4.25	56.0	29.4	14.2	1410.0	48.7	6.4	170.0	148.0	1025.0	730.0	1.325	256.0	218.0	6.3
3	-1.58	-1.00	4.09	81.0	28.1	12.1	1130.0	46.5	6.3	120.0	83.0	920.0	590.0	1.314	236.0	215.0	6.6
4	-0.42	0.08	4.08	83.0	24.1	11.3	1200.0	42.0	6.9	130.0	73.0	900.0	530.0	1.194	211.0	208.0	4.6
5	0.17	0.75	3.96	110.0	20.7	12.1	1400.0	44.3	7.9	140.0	99.0	940.0	530.0	1.071	232.0	237.0	4.7
6	1.50	2.58	4.16	69.0	8.9	7.4	1260.0	17.5	3.9	100.0	44.0	820.0	560.0	1.115	209.0	164.0	2.2
7	2.67	3.67	4.02	95.0	14.6	7.6	1600.0	52.4	9.0	89.0	47.0	1010.0	740.0	1.060	227.0	175.0	2.0
8	4.00	4.92	3.76	174.0	10.0	4.7	775.0	32.3	5.3	92.0	23.0	785.0	320.0	1.218	82.0	93.0	0.7
9	5.92	6.83	3.55	282.0	13.7	6.3	1000.0	23.4	4.8	80.0	65.0	815.0	640.0	1.203	100.0	140.0	1.5
10	7.00	7.92	3.45	358.0	12.7	6.3	1170.0	30.1	6.5	95.0	52.0	900.0	760.0	1.140	165.0	214.0	-1.0
11	8.00	9.00	3.94	115.0	12.5	6.7	1220.0	27.9	5.1	98.0	47.0	685.0	800.0	1.175	201.0	171.0	2.0
12	9.42	10.42	3.63	234.0	42.5	19.1	1465.0	218.0	29.3	-0.1	-0.1	891.0	1320.0	1.101	288.0	258.0	-1.0

REVISED 2/25/83

TABLE 2. BAKERSFIELD FOG - 31 DEC 82 $

						EQUIVALENT RATIOS							MOLAR RATIOS	
#	TIME1	TIME2	DT(MIN)	MIDT	-/+	CL/NA	NG/NA	CA/NA	SO4/NA	NO3/SO4	NH4/N+S	H/N+S	H+A/N+S	S(IV)/SO4	S(IV)/CH2O
1	-2.83	-2.17	39.60	-2.50	0.954	2.067	0.138	1.170	12.014	1.426	1.115	0.015	1.130	1.162	1.612
2	-2.17	-1.58	35.40	-1.88	1.325	5.034	0.218	1.656	24.830	1.404	0.803	0.032	0.835	0.701	1.174
3	-1.58	-1.00	34.80	-1.29	1.314	2.954	0.224	1.655	20.996	1.559	0.748	0.054	0.802	0.800	1.098
4	-0.42	0.08	30.00	-0.17	1.194	3.029	0.286	1.743	21.992	1.698	0.839	0.058	0.897	0.796	1.014
5	0.17	0.75	34.80	0.46	1.071	4.783	0.382	2.140	25.604	1.774	0.952	0.075	1.027	0.875	0.979
6	1.50	2.58	64.80	2.04	1.115	4.944	0.438	1.966	62.971	1.464	0.913	0.050	0.963	0.746	1.274
7	2.67	3.67	60.00	3.17	1.060	3.219	0.616	3.589	50.685	1.365	0.914	0.054	0.969	0.614	1.297
8	4.00	4.92	55.20	4.46	1.218	2.300	0.530	3.230	32.000	2.453	0.701	0.157	0.859	0.512	0.882
9	5.92	6.83	54.60	6.38	1.203	4.745	0.350	1.708	46.715	1.273	0.687	0.194	0.881	0.312	0.714
10	7.00	7.92	55.20	7.46	1.140	4.094	0.512	2.370	59.843	1.184	0.708	0.214	0.922	0.434	0.771
11	8.00	9.00	60.00	8.50	1.175	3.760	0.408	2.232	64.000	0.856	0.822	0.077	0.899	0.502	1.175
12	9.42	10.42	60.00	9.92	1.101	-0.002	0.689	5.129	31.059	0.675	0.663	0.106	0.768	0.436	1.116
	SEA SALT RATIOS					1.17	0.228	0.043	0.120						

REVISED 2/25/83

TABLE 3. BAKERSFIELD FOG - 31 DEC 82 $

MASS SOLUTE PER M3 AIR IS BASED ON LIQUID WATER CONTENT EITHER MEASURED (IF AVAILABLE)
OR CALCULATED FROM THE VOLUME OF FOGWATER COLLECTED AND ASSUMING A SAMPLING RATE = 5 M3/MIN (A LOWER BOUND)

			/ MICRO M/L \		/MM/L\	/ MICROGRAM / CUBIC METER \							
#	TIME1	TIME2	S(IV)	CH2O	TOC	LWC(G/M3) CALC.	LWC(G/M3) MEAS.	S(IV)	CH2O	TOC	-/+	'CORRECTED -/+'	PH	'PH-BY-DIFFERENCE'
1	-2.83	-2.17	395.0	245.0	6.3	0.323	-1.00	4.086	2.376	24.436	0.954	0.870	4.60	*****
2	-2.17	-1.58	256.0	218.0	6.3	0.294	-1.00	2.407	1.921	22.210	1.325	1.215	4.25	3.41
3	-1.58	-1.00	236.0	215.0	6.6	0.241	-1.00	1.823	1.557	19.117	1.314	1.220	4.09	3.43
4	-0.42	0.08	211.0	208.0	4.6	0.213	-1.00	1.440	1.331	11.776	1.194	1.098	4.08	3.66
5	0.17	0.75	232.0	237.0	4.7	0.161	-1.00	1.195	1.144	9.076	1.071	0.982	3.96	4.09
6	1.50	2.58	209.0	164.0	2.2	0.135	-1.00	1.239	0.911	4.889	1.115	1.041	4.16	3.90
7	2.67	3.67	227.0	175.0	2.0	0.080	-1.00	0.581	0.420	1.920	1.060	1.009	4.02	3.96
8	4.00	4.92	82.0	93.0	0.7	0.080	-1.00	0.209	0.222	0.679	1.218	1.124	3.76	3.53
9	5.92	6.83	100.0	140.0	1.5	0.103	-1.00	0.328	0.431	1.846	1.203	1.137	3.55	3.33
10	7.00	7.92	165.0	214.0	-1.0	0.072	-1.00	0.383	0.465	-1.000	1.140	1.073	3.45	3.33
11	8.00	9.00	201.0	171.0	2.0	0.093	-1.00	0.600	0.479	2.240	1.175	1.102	3.94	3.59
12	9.42	10.42	288.0	258.0	-1.0	0.033	-1.00	0.307	0.258	-1.000	1.101	1.095	3.63	3.37
TIME-WEIGHTED AVERAGE FOR 12. SAMPLES							0.140	1.053	0.832	6.084				

TABLE 4. BAKERSFIELD FOG - 31 DEC 82 $

MASS SOLUTE PER M3 AIR IS BASED ON LIQUID WATER CONTENT EITHER MEASURED (IF AVAILABLE)
OR CALCULATED FROM THE VOLUME OF FOGWATER COLLECTED AND ASSUMING A SAMPLING RATE = 5 M3/MIN (AN LOWER BOUND)

							MICROGRAM / CUBIC METER									
#	TIME1	TIME2	DT (MIN)	VOL	LWC(G/M3) CALC.	LWC(G/M3) MEAS.	H	NA	K	NH4	CA	MG	F	CL	NO3	SO4	MASS
1	-2.83	-2.17	39.60	64.0	0.323	-1.00	0.008	0.421	0.451	10.705	0.428	0.031	1.044	1.341	19.439	10.550	44.418
2	-2.17	-1.58	35.40	52.0	0.294	-1.00	0.016	0.199	0.163	7.456	0.286	0.023	0.949	1.541	18.670	10.294	39.598
3	-1.58	-1.00	34.80	42.0	0.241	-1.00	0.020	0.156	0.114	4.910	0.224	0.018	0.550	0.710	13.768	6.836	27.307
4	-0.42	0.08	30.00	32.0	0.213	-1.00	0.018	0.118	0.094	4.608	0.179	0.018	0.527	0.552	11.904	5.427	23.446
5	0.17	0.75	34.80	28.0	0.161	-1.00	0.018	0.077	0.076	4.055	0.143	0.015	0.428	0.565	9.378	4.094	18.849
6	1.50	2.58	64.80	60.0	0.185	-1.00	0.013	0.068	0.054	4.200	0.065	0.009	0.352	0.289	9.415	4.978	19.411
7	2.67	3.67	60.00	24.0	0.080	-1.00	0.008	0.027	0.024	2.304	0.064	0.009	0.135	0.133	5.010	2.842	10.575
8	4.00	4.92	55.20	22.0	0.080	-1.00	0.014	0.018	0.015	1.112	0.051	0.005	0.139	0.065	3.879	1.224	6.524
9	5.92	6.83	54.60	28.0	0.103	-1.00	0.029	0.032	0.025	1.846	0.048	0.006	0.156	0.236	5.183	3.151	10.712
10	7.00	7.92	55.20	20.0	0.072	-1.00	0.026	0.021	0.018	1.533	0.044	0.006	0.131	0.134	4.043	2.643	8.598
11	8.00	9.00	60.00	28.0	0.093	-1.00	0.011	0.027	0.024	2.050	0.052	0.006	0.174	0.156	3.964	3.584	10.047
12	9.42	10.42	60.00	10.0	0.033	-1.00	0.008	0.033	0.025	0.879	0.145	0.012	-0.100	-0.100	1.841	2.112	3.853
	TIME-WEIGHTED AVERAGE FOR 12. SAMPLES				0.140		0.015	0.080	0.076	3.373	0.127	0.012	0.361	0.436	7.824	4.356	16.660

TABLE 5. BAKERSFIELD FOG - 31 DEC 82 $

					MICROGRAM / LITER						MICROGRAM / CUBIC METER					
#	TIME1	TIME2	PH	H	FE	MN	PB	CU	NI	V	FE	MN	PB	CU	NI	V
1	-2.83	-2.17	4.60	0.0	419.0	14.0	166.0	70.0	61.0	32.0	0.135	0.005	0.054	0.023	0.020	0.010
2	-2.17	-1.58	4.25	0.0	280.0	11.0	268.0	70.0	48.4	35.0	0.082	0.003	0.078	0.021	0.014	0.010
3	-1.58	-1.00	4.09	0.0	117.0	6.0	228.0	18.0	34.6	31.0	0.028	0.001	0.055	0.004	0.008	0.007
4	-0.42	0.08	4.08	0.0	102.0	7.0	279.0	34.0	35.6	28.0	0.023	0.001	0.060	0.007	0.008	0.006
5	0.17	0.75	3.96	0.0	103.0	8.0	274.0	24.0	29.1	28.0	0.017	0.001	0.044	0.004	0.005	0.005
6	1.50	2.58	4.16	0.0	121.0	6.0	210.0	49.0	35.0	21.0	0.022	0.001	0.039	0.009	0.006	0.004
7	2.67	3.67	4.02	0.0	347.0	17.0	262.0	21.0	37.1	28.0	0.028	0.001	0.023	0.002	0.003	0.002
8	4.00	4.92	3.76	0.0	196.0	8.0	173.0	15.0	21.6	14.0	0.016	0.000	0.014	0.001	0.002	0.001
9	5.92	6.83	3.55	0.0	161.0	4.0	196.0	23.0	22.3	20.0	0.017	0.000	0.020	0.002	0.002	0.002
10	7.00	7.92	3.45	0.0	238.0	7.0	249.0	19.0	24.6	21.0	0.017	0.001	0.018	0.001	0.002	0.002
11	8.00	9.00	3.94	0.0	101.0	4.0	221.0	11.0	24.4	17.0	0.009	0.000	0.021	0.001	0.002	0.002
12	9.42	10.42	3.63	0.0	532.0	35.0	512.0	23.0	41.6	14.0	0.018	0.001	0.017	0.001	0.001	0.000

ENTERED 8/10/83

TABLE 1. BAKERSFIELD FOG - 01 JAN 83 $

				/ / / / / /	MICRO EQ/LITER					\ \ \ \ \ \				/ MICRO M/L \		/MM/L\
#	TIME1	TIME2	PH	H	NA	K	NH4	CA	MG	F	CL	NO3	SO4	-/+	S(IV)	CH2O	TOC
1	-4.25	-3.33	5.72	1.9	92.0	36.0	9110.0	355.0	56.0	630.0	405.0	1250.0	2200.0	0.467	45.0	105.0	-1.0
2	-3.17	-0.83	6.00	1.0	65.0	30.0	3980.0	423.0	70.0	190.0	88.0	1710.0	2080.0	0.890	309.0	132.0	8.0
3	-1.00	0.00	4.34	46.0	2.7	6.7	1950.0	54.0	5.5	150.0	198.0	540.0	1220.0	1.031	304.0	53.0	3.5
4	0.00	1.00	5.00	10.0	8.1	4.5	1970.0	16.5	4.0	150.0	34.0	520.0	1520.0	1.093	301.0	63.0	3.4
5	1.00	2.00	5.19	6.5	3.5	6.7	1800.0	20.0	4.4	150.0	150.0	540.0	800.0	0.891	-1.0	-1.0	-1.0
6	2.00	3.75	5.16	6.9	4.2	5.9	1620.0	23.0	5.0	160.0	34.0	590.0	820.0	0.963	295.0	75.0	2.8
7	3.75	5.15	4.85	14.0	28.0	12.2	1650.0	43.0	6.3	200.0	36.0	400.0	520.0	0.659	452.0	318.0	-1.0
8	5.50	6.58	4.89	13.0	47.0	27.0	2440.0	94.0	12.2	260.0	130.0	1040.0	1240.0	1.014	-1.0	-1.0	-1.0
9	6.58	8.50	5.96	1.1	121.0	59.0	2600.0	240.0	37.0	400.0	98.0	1080.0	1320.0	0.948	-1.0	-1.0	-1.0

REVISED 2/25/83

TABLE 2. BAKERSFIELD FOG - 01 JAN 83 $

						EQUIVALENT RATIOS							MOLAR RATIOS	
#	TIME1	TIME2	DT(MIN)	MIDT	-/+	CL/NA	MG/NA	CA/NA	SO4/NA	NO3/SO4	NH4/N+S	H/N+S	H+A/N+S	S(IV)/SO4	S(IV)/CH2O
1	-4.25	-3.33	55.20	-3.79	0.467	4.402	0.630	3.859	23.913	0.568	2.641	0.001	2.641	0.041	0.429
2	-3.17	-0.83	140.4	-2.00	0.890	1.354	1.077	6.538	32.000	0.822	1.050	0.000	1.050	0.297	2.341
3	-1.00	0.00	60.00	-0.50	1.031	73.333	2.037	12.593	451.85	0.443	1.108	0.026	1.134	0.498	5.736
4	0.00	1.00	60.00	0.50	1.093	4.198	0.494	2.284	187.65	0.342	0.975	0.005	0.980	0.396	4.778
5	1.00	2.00	60.00	1.50	0.891	42.857	1.257	5.714	228.57	0.675	1.343	0.005	1.348	-0.002	1.000
6	2.00	3.75	105.0	2.88	0.963	8.095	1.190	5.476	190.23	0.720	1.149	0.005	1.154	0.720	3.933
7	3.75	5.15	84.00	4.45	0.659	1.286	0.225	1.536	18.571	0.769	1.793	0.015	1.809	1.738	1.421
8	5.50	6.58	64.80	6.04	1.014	2.766	0.260	2.000	26.383	0.839	1.070	0.006	1.076	-0.002	1.000
9	6.58	8.50	115.2	7.54	0.948	0.810	0.306	1.983	10.909	0.818	1.083	0.000	1.084	-0.002	1.000
	SEA SALT RATIOS					1.17	0.228	0.043	0.120						

REVISED 2/25/83

TABLE 3. BAKERSFIELD FOG - 01 JAN 83 $

MASS SOLUTE PER M3 AIR IS BASED ON LIQUID WATER CONTENT EITHER MEASURED (IF AVAILABLE)
OR CALCULATED FROM THE VOLUME OF FOGWATER COLLECTED AND ASSUMING A SAMPLING RATE = 5 M3/MIN (A LOWER BOUND)

			/ MICRO M/L \		/MM/L\	/ MICROGRAM / CUBIC METER \							
#	TIME1	TIME2	S(IV)	CH2O	TOC	LWC(G/M3) CALC.	LWC(G/M3) MEAS.	S(IV)	CH2O	TOC	-/+	'CORRECTED -/+'	PH	'PH-BY-DIFFERENCE'
1	-4.25	-3.33	45.0	105.0	-1.0	0.043	-1.00	0.063	0.137	-1.000	0.467	0.399	5.72	*****
2	-3.17	-0.83	309.0	132.0	8.0	0.043	-1.00	0.423	0.169	4.103	0.890	0.848	6.00	*****
3	-1.00	0.00	304.0	53.0	3.5	0.113	-1.00	1.103	0.180	4.760	1.031	0.956	4.34	*****
4	0.00	1.00	301.0	63.0	3.4	0.100	-1.00	0.963	0.189	4.080	1.093	1.019	5.00	4.32
5	1.00	2.00	-1.0	-1.0	-1.0	0.087	-1.00	-1.000	-1.000	-1.000	0.891	0.809	5.19	*****
6	2.00	3.75	293.0	75.0	2.8	0.046	-1.00	0.432	0.103	1.536	0.963	0.867	5.16	*****
7	3.75	5.15	452.0	318.0	-1.0	0.019	-1.00	0.276	0.162	-1.000	0.659	0.545	4.85	*****
8	5.50	6.58	-1.0	-1.0	-1.0	0.012	-1.00	-1.000	-1.000	-1.000	1.014	0.915	4.89	*****
9	6.58	8.50	-1.0	-1.0	-1.0	0.003	-1.00	-1.000	-1.000	-1.000	0.948	0.817	5.96	*****
TIME-WEIGHTED AVERAGE FOR 9. SAMPLES							0.046	0.506	0.158	3.469				

REVISED 2/25/83

TABLE 4. BAKERSFIELD FOG - 01 JAN 83 $

MASS SOLUTE PER M3 AIR IS BASED ON LIQUID WATER CONTENT EITHER MEASURED (IF AVAILABLE)
OR CALCULATED FROM THE VOLUME OF FOGWATER COLLECTED AND ASSUMING A SAMPLING RATE = 5 M3/MIN (AN LOWER BOUND)

							MICROGRAM / CUBIC METER									
$	TIME1	TIME2	DT (MIN)	VOL	LWC(G/M3) CALC.	LWC(G/M3) MEAS.	H	NA	K	NH4	CA	MG	F	CL	NO3	SO4	MASS
1	-4.25	-3.33	55.20	12.0	0.043	-1.00	0.000	0.092	0.061	7.130	0.309	0.031	0.537	0.624	3.370	4.591	16.744
2	-3.17	-0.83	140.4	30.0	0.043	-1.00	0.000	0.064	0.050	3.062	0.363	0.036	0.154	0.133	4.531	4.267	12.660
3	-1.00	0.00	60.00	34.0	0.113	-1.00	0.005	0.007	0.030	3.978	0.077	0.008	0.323	0.795	3.794	6.637	15.654
4	0.00	1.00	60.00	30.0	0.100	-1.00	0.001	0.019	0.018	3.582	0.037	0.005	0.285	0.121	3.224	7.296	14.587
5	1.00	2.00	60.00	26.0	0.087	-1.00	0.001	0.007	0.023	2.808	0.035	0.005	0.247	0.461	2.902	3.328	9.815
6	2.00	3.75	105.0	24.0	0.046	-1.00	0.000	0.004	0.011	1.333	0.021	0.003	0.139	0.055	1.672	1.799	5.038
7	3.75	5.15	84.00	8.0	0.019	-1.00	0.000	0.012	0.009	0.566	0.016	0.001	0.072	0.024	0.472	0.475	1.650
8	5.50	6.58	64.80	4.0	0.012	-1.00	0.000	0.013	0.013	0.542	0.023	0.002	0.061	0.057	0.796	0.735	2.243
9	6.58	8.50	115.2	2.0	0.003	-1.00	0.000	0.010	0.008	0.162	0.017	0.002	0.026	0.012	0.233	0.220	0.689
TIME-WEIGHTED AVERAGE FOR 9. SAMPLES					0.046		0.001	0.026	0.025	2.265	0.113	0.011	0.175	0.200	2.298	2.941	8.055

TABLE 5. BAKERSFIELD FOG - 01 JAN 83 $

					MICROGRAM / LITER						MICROGRAM / CUBIC METER					
$	TIME1	TIME2	PH	H	FE	MN	PB	CU	NI	V	FE	MN	PB	CU	NI	V
1	-4.25	-3.33	5.72	0.0	1420.0	53.0	112.0	41.0	122.0	59.0	0.062	0.002	0.005	0.002	0.005	0.003
2	-3.17	-0.83	6.00	0.0	-0.1	123.0	303.0	46.0	257.0	175.0	-0.000	0.005	0.013	0.002	0.011	0.007
3	-1.00	0.00	4.34	0.0	1090.0	19.0	277.0	24.0	68.3	63.0	0.124	0.002	0.031	0.003	0.008	0.007
4	0.00	1.00	5.00	0.0	650.0	10.0	268.0	52.0	52.0	50.0	0.065	0.001	0.027	0.005	0.005	0.005
5	1.00	2.00	5.19	0.0	318.0	7.0	295.0	29.0	68.3	55.0	0.028	0.001	0.026	0.003	0.006	0.005
6	2.00	3.75	5.16	0.0	306.0	7.0	215.0	90.0	74.7	53.0	0.014	0.000	0.010	0.004	0.003	0.002
7	3.75	5.15	4.85	0.0	333.0	7.0	365.0	41.0	32.8	65.0	0.006	0.000	0.007	0.001	0.001	0.001
8	5.50	6.58	4.89	0.0	-0.1	-0.1	-0.1	-0.1	-0.1	-0.1	-0.000	-0.000	-0.000	-0.000	-0.000	-0.000
9	6.58	8.50	5.96	0.0	-0.1	-0.1	-0.1	-0.1	-0.1	-0.1	-0.000	-0.000	-0.000	-0.000	-0.000	-0.000

ENTERED 8/2/83

TABLE 1. BAKERSFIELD FOG - 02 JAN 83 $

#	TIME1	TIME2	PH	MICRO EQ/LITER H	NA	K	NH4	CA	MG	F	CL	NO3	SO4	-/+	MICRO M/L S(IV)	MM/L CH2O	MM/L TOC
1	7.67	8.67	5.07	8.5	210.0	79.0	5000.0	460.0	65.0	400.0	98.0	1080.0	1320.0	0.498	-1.0	-1.0	-1.0

REVISED 2/25/83

TABLE 2. BAKERSFIELD FOG - 02 JAN 83 $

#	TIME1	TIME2	DT(MIN)	NIDT	-/+	EQUIVALENT RATIOS CL/NA	MG/NA	CA/NA	SO4/NA	NO3/SO4	NH4/N+S	H/N+S	H+A/N+S	MOLAR RATIOS S(IV)/SO4	S(IV)/CH2O
1	7.67	8.67	60.00	8.17	0.498	0.467	0.310	2.190	6.286	0.818	2.083	0.004	2.087	-0.002	1.000
	SEA SALT RATIOS					1.17	0.228	0.043	0.120						

REVISED 2/25/83

TABLE 3. BAKERSFIELD FOG - 02 JAN 83 $

MASS SOLUTE PER M3 AIR IS BASED ON LIQUID WATER CONTENT EITHER MEASURED (IF AVAILABLE)
OR CALCULATED FROM THE VOLUME OF FOGWATER COLLECTED AND ASSUMING A SAMPLING RATE = 5 M3/MIN (A LOWER BOUND)

#	TIME1	TIME2	MICRO M/L S(IV)	MM/L CH2O	MM/L TOC	MICROGRAM / CUBIC METER LWC(G/M3) CALC.	LWC(G/M3) MEAS.	S(IV)	CH2O	TOC	-/+	*CORRECTED -/+*	PH	*PH-BY-DIFFERENCE*
1	7.67	8.67	-1.0	-1.0	-1.0	0.013	-1.00	-1.000	-1.000	-1.000	0.498	0.429	5.07	*****
TIME-WEIGHTED AVERAGE FOR 1. SAMPLES						0.013		0.000	0.000	0.000				

REVISED 2/25/83

TABLE 4. BAKERSFIELD FOG - 02 JAN 83 $

MASS SOLUTE PER M3 AIR IS BASED ON LIQUID WATER CONTENT EITHER MEASURED (IF AVAILABLE)
OR CALCULATED FROM THE VOLUME OF FOGWATER COLLECTED AND ASSUMING A SAMPLING RATE = 5 M3/MIN (AN LOWER BOUND)

#	TIME1	TIME2	DT (MIN)	VOL	LWC(G/M3) CALC.	LWC(G/M3) MEAS.	MICROGRAM / CUBIC METER H	NA	K	NH4	CA	MG	F	CL	NO3	SO4	MASS
1	7.67	8.67	60.00	4.0	0.013	-1.00	0.000	0.064	0.041	1.200	0.123	0.011	0.101	0.046	0.893	0.845	3.324
TIME-WEIGHTED AVERAGE FOR 1. SAMPLES					0.013		0.000	0.064	0.041	1.200	0.123	0.011	0.101	0.046	0.893	0.845	3.324

TABLE 5. BAKERSFIELD FOG - 02 JAN 83 $

#	TIME1	TIME2	PH	MICROGRAM / LITER H	FE	MN	PB	CU	NI	V	MICROGRAM / CUBIC METER FE	MN	PB	CU	NI	V
1	7.67	8.67	5.07	0.0	-0.1	-0.1	-0.1	-0.1	-0.1	-0.1	-0.000	-0.000	-0.000	-0.000	-0.000	-0.000

ENTERED 8/10/83

TABLE 1. BAKERSFIELD FOG - 03 JAN 83 $

#	TIME1	TIME2	PH	MICRO EQ/LITER H	NA	K	NH4	CA	MG	F	CL	NO3	SO4	-/+	MICRO M/L S(IV)	CH2O	/MM/L\ TOC
1	5.25	6.00	4.94	11.5	68.0	53.0	6710.0	54.0	11.0	450.0	123.0	2280.0	4760.0	1.102	596.0	118.0	7.0
2	6.00	6.83	5.47	3.4	48.0	-0.1	6590.0	-0.1	-0.1	550.0	143.0	3100.0	4600.0	1.264	-1.0	232.0	-1.0
3	6.92	7.92	4.98	10.5	197.0	-0.1	12260.	-0.1	-0.1	2100.0	4800.0	6800.0	9400.0	1.853	-1.0	-1.0	-1.0

REVISED 2/25/83

TABLE 2. BAKERSFIELD FOG - 03 JAN 83 $

#	TIME1	TIME2	DT(MIN)	MIDT	-/+	EQUIVALENT RATIOS CL/NA	MG/NA	CA/NA	SO4/NA	NO3/SO4	NH4/N+S	H/N+S	H+A/N+S	MOLAR RATIOS S(IV)/SO4	S(IV)/CH2O
1	5.25	6.00	45.00	5.62	1.102	1.809	0.162	0.794	70.000	0.479	0.953	0.002	0.955	0.250	5.051
2	6.00	6.83	49.80	6.41	1.264	2.979	-0.002	-0.002	95.833	0.674	0.856	0.000	0.856	-0.000	-0.004
3	6.92	7.92	60.00	7.42	1.853	24.365	-0.001	-0.001	47.716	0.723	0.757	0.001	0.757	-0.000	1.000
	SEA SALT RATIOS					1.17	0.228	0.043	0.120						

REVISED 2/25/83

TABLE 3. BAKERSFIELD FOG - 03 JAN 83 $

MASS SOLUTE PER M3 AIR IS BASED ON LIQUID WATER CONTENT EITHER MEASURED (IF AVAILABLE)
OR CALCULATED FROM THE VOLUME OF FOGWATER COLLECTED AND ASSUMING A SAMPLING RATE = 5 M3/MIN (A LOWER BOUND)

#	TIME1	TIME2	MICRO M/L S(IV)	CH2O	/MM/L\ TOC	LWC(G/M3) CALC.	MEAS.	MICROGRAM / CUBIC METER S(IV)	CH2O	TOC	-/+	'CORRECTED -/+'	PH	'PH-BY-DIFFERENCE'
1	5.25	6.00	596.0	118.0	7.0	0.044	-1.00	0.848	0.157	3.733	1.102	1.037	4.94	3.58
2	6.00	6.83	-1.0	232.0	-1.0	0.004	-1.00	-1.000	0.028	-1.000	1.264	1.181	5.47	2.92
3	6.92	7.92	-1.0	-1.0	-1.0	0.002	-1.00	-1.000	-1.000	-1.000	1.853	1.684	4.98	2.07
TIME-WEIGHTED AVERAGE FOR 3. SAMPLES						0.015		0.848	0.089	3.733				

REVISED 2/25/83

TABLE 4. BAKERSFIELD FOG - 03 JAN 83 $

MASS SOLUTE PER M3 AIR IS BASED ON LIQUID WATER CONTENT EITHER MEASURED (IF AVAILABLE)
OR CALCULATED FROM THE VOLUME OF FOGWATER COLLECTED AND ASSUMING A SAMPLING RATE = 5 M3/MIN (AN LOWER BOUND)

#	TIME1	TIME2	DT (MIN)	VOL	LWC(G/M3) CALC.	MEAS.	MICROGRAM / CUBIC METER H	NA	K	NH4	CA	MG	F	CL	NO3	SO4	MASS
1	5.25	6.00	45.00	10.0	0.044	-1.00	0.001	0.070	0.092	5.368	0.048	0.006	0.380	0.194	6.283	10.155	22.595
2	6.00	6.83	49.80	1.0	0.004	-1.00	0.000	0.004	-0.100	0.476	-0.100	-0.100	0.042	0.020	0.772	0.887	1.621
3	6.92	7.92	60.00	0.5	0.002	-1.00	0.000	0.008	-0.100	0.368	-0.100	-0.100	0.067	0.284	0.703	0.752	1.705
TIME-WEIGHTED AVERAGE FOR 3. SAMPLES					0.015		0.000	0.025	0.092	6.386	0.014	0.006	0.150	0.173	2.347	3.529	12.721

TABLE 5. BAKERSFIELD FOG - 03 JAN 83 *

*	TIME1	TIME2	PH	H	MICROGRAM / LITER FE	MN	PB	CU	NI	V	MICROGRAM / CUBIC METER FE	MN	PB	CU	NI	V
1	5.25	6.00	4.94	0.0	549.0	25.0	398.0	-0.1	-0.1	-0.1	0.024	0.001	0.018	-0.000	-0.000	-0.000
2	6.00	6.83	5.47	0.0	120.0	19.0	208.0	294.0	105.0	220.0	0.000	0.000	0.001	0.001	0.000	0.001
3	6.92	7.92	4.98	0.0	-0.1	-0.1	-0.1	-0.1	-0.1	-0.1	-0.000	-0.000	-0.000	-0.000	-0.000	-0.000

ENTERED 8/10/83

TABLE 1. BAKERSFIELD FOG - 04 JAN 83 *

#	TIME1	TIME2	PH	H	NA	K	NH4	CA	MG	F	CL	NO3	SO4	-/+	S(IV)	CH2O	TOC
				/ / / / / /				MICRO EQ/LITER				\ \ \ \ \ \			/ MICRO M/L \		/MM/L\
1	5.37	6.34	5.00	10.0	32.6	50.0	10000.	121.0	93.0	56.0	123.0	4400.0	4300.0	0.912	595.0	463.0	11.8
2	6.34	8.50	6.15	0.7	235.0	368.0	13280.	2270.0	295.0	880.0	973.0	5380.0	8600.0	0.953	-1.0	-1.0	-1.0

REVISED 2/25/83

TABLE 2. BAKERSFIELD FOG - 04 JAN 83 *

#	TIME1	TIME2	DT(MIN)	MIDT	-/+	CL/NA	NO3/NA	CA/NA	SO4/NA	NO3/SO4	NH4/N+S	H/N+S	H+A/N+S	S(IV)/SO4	S(IV)/CH2O
						EQUIVALENT RATIOS								MOLAR RATIOS	
1	5.37	6.34	58.20	5.86	0.912	3.844	2.906	3.781	134.37	1.023	1.149	0.001	1.151	0.277	1.285
2	6.34	8.50	129.6	7.42	0.953	4.149	1.085	9.660	36.596	0.626	0.950	0.000	0.950	-0.000	1.000
	SEA SALT RATIOS					1.17	0.228	0.043	0.120						

REVISED 2/25/83

TABLE 3. BAKERSFIELD FOG - 04 JAN 83 *

MASS SOLUTE PER M3 AIR IS BASED ON LIQUID WATER CONTENT EITHER MEASURED (IF AVAILABLE)
OR CALCULATED FROM THE VOLUME OF FOGWATER COLLECTED AND ASSUMING A SAMPLING RATE = 5 M3/MIN (A LOWER BOUND)

#	TIME1	TIME2	/ MICRO M/L \ S(IV)	CH2O	/MM/L\ TOC	LWC(G/M3) CALC.	MEAS.	/ MICROGRAM / CUBIC METER \ S(IV)	CH2O	TOC	-/+	*CORRECTED -/+*	PH	*PH-BY-DIFFERENCE*
1	5.37	6.34	595.0	463.0	11.8	0.021	-1.00	0.393	0.286	2.920	0.912	0.856	5.00	*****
2	6.34	8.50	-1.0	-1.0	-1.0	0.002	-1.00	-1.000	-1.000	-1.000	0.953	0.911	6.15	*****
TIME-WEIGHTED AVERAGE FOR 2. SAMPLES							0.007	0.393	0.286	2.920				

REVISED 2/25/83

TABLE 4. BAKERSFIELD FOG - 04 JAN 83 *

MASS SOLUTE PER M3 AIR IS BASED ON LIQUID WATER CONTENT EITHER MEASURED (IF AVAILABLE)
OR CALCULATED FROM THE VOLUME OF FOGWATER COLLECTED AND ASSUMING A SAMPLING RATE = 5 M3/MIN (AN LOWER BOUND)

#	TIME1	TIME2	DT (MIN)	VOL	LWC(G/M3) CALC.	MEAS.	H	NA	K	NH4	CA	MG	F	CL	NO3	SO4	MASS
											MICROGRAM / CUBIC METER						
1	5.37	6.34	58.20	6.0	0.021	-1.00	0.000	0.015	0.040	3.711	0.050	0.023	0.227	0.090	5.625	4.256	14.038
2	6.34	8.50	129.6	1.0	0.002	-1.00	0.000	0.008	0.022	0.369	0.070	0.005	0.020	0.053	0.515	0.637	1.699
TIME-WEIGHTED AVERAGE FOR 2. SAMPLES					0.007		0.000	0.010	0.028	1.405	0.064	0.011	0.084	0.065	2.098	1.758	5.523

TABLE 5. BAKERSFIELD FOG - 04 JAN 83 *

#	TIME1	TIME2	PH	H	FE	MN	PB	CU	NI	V	FE	MN	PB	CU	NI	V
					MICROGRAM / LITER						MICROGRAM / CUBIC METER					
1	5.37	6.34	5.00	0.0	296.0	19.0	379.0	82.0	235.0	200.0	0.006	0.000	0.008	0.002	0.005	0.004
2	6.34	8.50	6.15	0.0	-0.1	-0.1	-0.1	-0.1	-0.1	-0.1	-0.000	-0.000	-0.000	-0.000	-0.000	-0.000

ENTERED 8/10/83

TABLE 1. BAKERSFIELD FOG - 06 JAN 83 $

#	TIME1	TIME2	PH	MICRO EQ/LITER H	NA	K	NH4	CA	MG	F	CL	NO3	SO4	-/+	MICRO M/L S(IV)	MM/L CH2O	TOC
1	0.83	1.00	5.27	5.4	45.9	49.7	3980.0	181.0	28.8	168.0	960.0	1100.0	1920.0	0.967	1010.	377.0	-1.0
2	1.58	2.08	5.33	4.7	13.2	19.4	2050.0	52.0	5.4	212.0	260.0	440.0	880.0	0.836	505.0	174.0	4.3
3	2.33	3.00	5.30	5.0	40.7	35.3	2590.0	67.0	10.9	148.0	-0.1	840.0	1640.0	0.956	545.0	212.0	5.2
4	3.08	4.00	4.81	15.5	19.1	16.2	2400.0	38.0	6.4	87.0	24.0	850.0	1740.0	1.082	554.0	170.0	4.7
5	4.00	5.08	4.61	24.5	5.3	6.8	850.0	66.0	51.0	10.0	75.0	400.0	720.0	1.201	283.0	85.0	2.2
6	5.33	6.33	4.68	20.9	6.6	7.6	1330.0	48.0	4.4	87.0	3.4	380.0	940.0	0.995	481.0	95.0	1.5
7	6.42	7.17	5.08	8.3	7.0	9.0	1520.0	33.4	4.0	29.0	-0.1	330.0	880.0	0.783	482.0	103.0	2.1
8	7.17	8.17	4.84	14.5	8.3	11.9	1400.0	21.5	3.3	39.0	-0.1	430.0	1100.0	1.075	499.0	117.0	2.2
9	8.17	9.17	4.28	52.5	30.0	-0.1	1600.0	-0.1	-0.1	64.0	-0.1	540.0	1160.0	1.049	508.0	186.0	5.2
10	9.33	10.33	4.17	67.6	50.2	41.1	2330.0	545.0	64.0	142.0	48.0	1060.0	2040.0	1.062	838.0	350.0	12.5
11	10.33	11.08	4.84	14.5	65.3	55.8	3550.0	880.0	86.0	130.0	10.0	1400.0	2900.0	0.955	-1.0	-1.0	-1.0

REVISED 5/14/83

TABLE 2. BAKERSFIELD FOG - 06 JAN 83 $

#	TIME1	TIME2	DT(MIN)	MIDT	-/+	EQUIVALENT RATIOS CL/NA	NO3/NA	CA/NA	SO4/NA	NO3/SO4	NH4/N+S	H/N+S	H+A/N+S	MOLAR RATIOS S(IV)/SO4	S(IV)/CH2O
1	0.83	1.00	10.20	0.92	0.967	20.915	0.627	3.943	41.830	0.573	1.318	0.002	1.320	1.052	2.679
2	1.58	2.08	30.00	1.83	0.836	19.697	0.409	3.939	66.667	0.500	1.553	0.004	1.557	1.148	2.902
3	2.33	3.00	40.20	2.66	0.956	-0.002	0.268	1.646	40.295	0.512	1.044	0.002	1.046	0.665	2.571
4	3.08	4.00	55.20	3.54	1.082	1.257	0.335	1.990	91.099	0.489	0.927	0.006	0.933	0.637	3.259
5	4.00	5.08	64.80	4.54	1.201	14.151	9.623	12.453	135.84	0.596	0.759	0.022	0.781	0.786	3.329
6	5.33	6.33	60.00	5.83	0.995	0.515	0.667	7.273	142.42	0.404	1.008	0.016	1.023	1.023	5.063
7	6.42	7.17	45.00	6.80	0.783	-0.014	0.571	4.771	125.71	0.375	1.256	0.007	1.263	1.095	4.680
8	7.17	8.17	60.00	7.67	1.075	-0.012	0.398	2.590	132.53	0.391	0.915	0.009	0.925	0.907	4.265
9	8.17	9.17	60.00	8.67	1.049	-0.003	-0.003	-0.003	38.667	0.466	0.941	0.031	0.972	0.876	2.731
10	9.33	10.33	60.00	9.83	1.062	0.956	1.275	10.857	40.637	0.520	0.752	0.022	0.773	0.822	2.394
11	10.33	11.08	45.00	10.70	0.955	0.153	1.317	13.476	44.410	0.483	0.826	0.003	0.829	-0.001	1.000
	SEA SALT RATIOS					1.17	0.228	0.043	0.120						

REVISED 5/14/83

TABLE 3. BAKERSFIELD FOG - 06 JAN 83 $

MASS SOLUTE PER M3 AIR IS BASED ON LIQUID WATER CONTENT EITHER MEASURED (IF AVAILABLE)
OR CALCULATED FROM THE VOLUME OF FOGWATER COLLECTED AND ASSUMING A SAMPLING RATE = 5 M3/MIN (A LOWER BOUND)

#	TIME1	TIME2	MICRO M/L S(IV)	MM/L CH2O	TOC	MICROGRAM / CUBIC METER LWC(G/M3) CALC.	LWC(G/M3) MEAS.	S(IV)	CH2O	TOC	-/+	"CORRECTED -/+"	PH	"PH-BY-DIFFERENCE"
1	0.83	1.00	1010.	377.0	-1.0	0.157	0.140	4.525	1.583	-1.000	0.967	0.927	5.27	*****
2	1.58	2.08	505.0	174.0	4.3	0.133	0.140	2.262	0.731	7.224	0.836	0.737	5.33	*****
3	2.33	3.00	545.0	212.0	5.2	0.090	0.110	1.918	0.700	6.864	0.956	0.902	5.30	*****
4	3.08	4.00	554.0	170.0	4.7	0.087	0.140	2.482	0.714	7.856	1.082	1.047	4.81	3.08
5	4.00	5.08	283.0	85.0	2.2	0.111	0.165	1.494	0.421	4.356	1.201	1.190	4.61	3.67
6	5.33	6.33	481.0	95.0	1.5	0.067	0.150	2.309	0.438	2.700	0.995	0.933	4.68	*****
7	6.42	7.17	482.0	103.0	2.1	0.107	0.155	2.371	0.479	3.906	0.783	0.765	5.08	*****
8	7.17	8.17	499.0	117.0	2.2	0.073	0.150	2.393	0.527	3.960	1.075	1.048	4.84	4.07
9	8.17	9.17	508.0	186.0	5.2	0.053	0.036	0.585	0.201	2.246	1.049	1.009	4.28	4.17
10	9.33	10.33	838.0	350.0	12.5	0.033	0.010	0.764	0.165	1.500	1.062	1.014	4.17	3.95
11	10.33	11.08	-1.0	-1.0	-1.0	0.009	0.005	-1.000	-1.000	-1.000	0.955	0.926	4.84	*****
TIME-WEIGHTED AVERAGE FOR 11. SAMPLES							0.106	1.784	0.474	4.232				

REVISED 5/14/83

TABLE 4. BAKERSFIELD FOG - 06 JAN 83 $

MASS SOLUTE PER M3 AIR IS BASED ON LIQUID WATER CONTENT EITHER MEASURED (IF AVAILABLE)
OR CALCULATED FROM THE VOLUME OF FOGWATER COLLECTED AND ASSUMING A SAMPLING RATE = 5 M3/MIN (AN LOWER BOUND)

							MICROGRAM / CUBIC METER									
#	TIME1	TIME2	DT (MIN)	VOL	LWC(G/M3) CALC.	LWC(G/M3) MEAS.	H	NA	K	NH4	CA	MG	F	CL	NO3	SO4	MASS
1	0.83	1.00	10.20	8.0	0.157	0.140	0.001	0.146	0.272	10.030	0.507	0.049	0.447	4.764	9.548	12.902	38.668
2	1.58	2.08	30.00	20.0	0.133	0.140	0.001	0.043	0.106	5.166	0.146	0.009	0.564	1.290	3.819	5.914	17.057
3	2.33	3.00	40.20	18.0	0.090	0.110	0.001	0.103	0.152	5.128	0.147	0.015	0.309	-0.100	5.729	8.659	14.288
4	3.08	4.00	55.20	24.0	0.087	0.140	0.002	0.062	0.089	6.048	0.106	0.011	0.241	0.119	7.378	11.693	25.739
5	4.00	5.08	64.80	36.0	0.111	0.165	0.004	0.020	0.044	2.524	0.218	0.102	0.031	0.439	4.092	5.702	13.177
6	5.33	6.33	60.00	20.0	0.067	0.150	0.003	0.023	0.045	3.591	0.144	0.008	0.248	0.018	3.534	6.768	14.382
7	6.42	7.17	45.00	24.0	0.107	0.155	0.001	0.025	0.055	4.241	0.104	0.008	0.085	-0.100	3.171	6.547	9.618
8	7.17	8.17	60.00	22.0	0.073	0.150	0.002	0.029	0.070	3.780	0.065	0.006	0.111	-0.100	3.999	7.920	11.819
9	8.17	9.17	60.00	16.0	0.053	0.036	0.002	0.025	-0.100	1.037	-0.100	-0.100	0.044	-0.100	1.205	2.004	3.110
10	9.33	10.33	60.00	10.0	0.033	0.010	0.001	0.012	0.016	0.419	0.109	0.008	0.027	0.017	0.657	0.979	2.245
11	10.33	11.08	45.00	2.0	0.009	0.005	0.000	0.008	0.011	0.319	0.088	0.005	0.012	0.002	0.434	0.696	1.575
	TIME-WEIGHTED AVERAGE FOR 11. SAMPLES				0.106		0.002	0.035	0.065	3.605	0.119	0.022	0.149	0.483	3.470	5.766	13.615

TABLE 5. BAKERSFIELD FOG - 06 JAN 83 $

					MICROGRAM / LITER						MICROGRAM / CUBIC METER					
#	TIME1	TIME2	PH	H	FE	MN	PB	CU	NI	V	FE	MN	PB	CU	NI	V
1	0.83	1.00	5.27	0.0	670.0	144.0	1357.0	63.0	680.0	230.0	0.094	0.020	0.190	0.009	0.095	0.032
2	1.58	2.08	5.33	0.0	421.0	11.0	106.0	-0.1	71.5	70.0	0.059	0.002	0.015	-0.000	0.010	0.010
3	2.33	3.00	5.30	0.0	1010.0	23.0	222.0	-0.1	123.0	110.0	0.111	0.003	0.024	-0.000	0.014	0.012
4	3.08	4.00	4.81	0.0	1070.0	40.0	245.0	38.0	135.0	140.0	0.150	0.006	0.034	0.005	0.019	0.020
5	4.00	5.08	4.61	0.0	81.0	3.0	103.0	35.0	54.6	50.0	0.013	0.000	0.017	0.006	0.009	0.008
6	5.33	6.33	4.68	0.0	479.0	8.0	124.0	149.0	52.3	35.0	0.072	0.001	0.019	0.022	0.008	0.005
7	6.42	7.17	5.08	0.0	610.0	14.0	104.0	31.0	61.8	45.0	0.095	0.002	0.016	0.005	0.010	0.007
8	7.17	8.17	4.84	0.0	510.0	6.0	146.0	24.0	43.9	45.0	0.076	0.001	0.022	0.004	0.007	0.007
9	8.17	9.17	4.28	0.0	6300.0	30.0	450.0	46.0	58.2	50.0	0.227	0.001	0.016	0.002	0.002	0.002
10	9.33	10.33	4.17	0.0	-0.1	376.0	2580.0	404.0	-0.1	260.0	-0.000	0.004	0.024	0.004	-0.000	0.003
11	10.33	11.08	4.84	0.0	-0.1	-0.1	-0.1	-0.1	-0.1	-0.1	-0.000	-0.000	-0.000	-0.000	-0.000	-0.000

ENTERED 8/11/83

TABLE 1. BAKERSFIELD FOG - 07(A) JAN 83 $

#	TIME1	TIME2	PH	MICRO EQ/LITER / / / / / / H	NA	K	NH4	CA	MG	F	CL	\ \ \ \ \ \ NO3	SO4	-/+	/ MICRO M/L \ S(IV)	CH2O	/MM/L\ TOC
1	-5.17	-4.33	3.62	240.0	277.0	93.0	7510.0	1160.0	119.0	244.0	218.0	3760.0	8560.0	1.360	1180.	709.0	-1.0
2	-4.25	-2.83	3.65	224.0	233.0	247.0	5018.0	320.0	37.1	174.0	68.0	2540.0	4160.0	1.142	557.0	369.0	9.9
3	-2.83	-1.75	5.15	7.1	315.0	301.0	3490.0	193.0	20.9	136.0	86.0	1480.0	2640.0	1.002	-1.0	-1.0	9.6
4	-1.75	-0.50	4.34	45.7	64.0	64.0	4450.0	75.8	5.4	116.0	-0.1	1300.0	3560.0	1.058	580.0	253.0	5.3
5	0.25	1.75	4.28	52.5	10.5	17.0	2475.0	20.0	3.5	77.0	15.0	920.0	1480.0	0.966	575.0	191.0	-1.0
6	2.58	4.00	3.70	200.0	7.0	12.6	2050.0	14.0	1.6	390.0	340.0	840.0	1338.0	1.273	562.0	169.0	-1.0
7	4.67	6.00	3.62	240.0	24.2	16.2	2285.0	31.1	3.6	68.0	0.0	940.0	1320.0	0.884	489.0	163.0	-1.0
8	6.08	7.08	4.00	100.0	14.1	23.8	2560.0	37.1	4.9	96.0	0.0	900.0	1520.0	0.918	540.0	165.0	-1.0
9	7.08	9.08	3.63	234.0	57.1	26.6	3360.0	360.0	29.4	84.0	18.0	1440.0	2640.0	1.028	845.0	320.0	-1.0
10	9.08	11.25	3.23	590.0	50.0	37.8	3700.0	770.0	73.0	78.0	48.0	1840.0	3080.0	0.967	1046.	361.0	-1.0

REVISED 2/25/83

TABLE 2. BAKERSFIELD FOG - 07(A) JAN 83 $

#	TIME1	TIME2	DT(MIN)	NIDT	-/+	EQUIVALENT RATIOS CL/NA	MG/NA	CA/NA	SO4/NA	NO3/SO4	NH4/N+S	H/N+S	H+A/N+S	MOLAR RATIOS S(IV)/SO4	S(IV)/CH2O
1	-5.17	-4.33	50.40	-4.75	1.360	0.787	0.430	4.188	30.903	0.439	0.610	0.019	0.629	0.276	1.664
2	-4.25	-2.83	85.20	-3.54	1.142	0.292	0.159	1.373	17.854	0.611	0.749	0.033	0.782	0.268	1.509
3	-2.83	-1.75	64.80	-2.29	1.002	0.273	0.082	0.619	8.381	0.561	0.847	0.002	0.849	-0.001	1.000
4	-1.75	-0.50	75.00	-1.13	1.058	-0.002	0.084	1.184	55.625	0.365	0.916	0.009	0.925	0.326	2.292
5	0.25	1.75	90.00	1.00	0.966	1.429	0.333	1.905	140.95	0.622	1.031	0.022	1.053	0.777	3.010
6	2.58	4.00	85.20	3.29	1.273	48.571	0.229	2.000	191.14	0.628	0.941	0.092	1.033	0.840	3.325
7	4.67	6.00	79.80	5.34	0.884	0.000	0.149	1.285	54.545	0.712	1.011	0.106	1.117	0.741	3.000
8	6.08	7.08	60.00	6.58	0.918	0.000	0.348	2.631	107.80	0.592	1.058	0.041	1.099	0.711	3.273
9	7.08	9.08	120.0	8.08	1.028	0.315	0.515	6.305	46.235	0.545	0.824	0.057	0.881	0.640	2.641
10	9.08	11.25	130.2	10.16	0.967	0.960	1.460	15.400	61.600	0.597	0.752	0.120	0.872	0.679	2.898
	SEA SALT RATIOS					1.17	0.228	0.043	0.120						

REVISED 2/25/83

TABLE 3. BAKERSFIELD FOG - 07(A) JAN 83 $

MASS SOLUTE PER M3 AIR IS BASED ON LIQUID WATER CONTENT EITHER MEASURED (IF AVAILABLE) OR CALCULATED FROM THE VOLUME OF FOGWATER COLLECTED AND ASSUMING A SAMPLING RATE = 5 M3/MIN (A LOWER BOUND)

#	TIME1	TIME2	/ MICRO M/L \ S(IV)	CH2O	/MM/L\ TOC	LWC(G/M3) CALC.	MEAS.	/ MICROGRAM / CUBIC METER \ S(IV)	CH2O	TOC	-/+	'CORRECTED -/+'	PH	'PH-BY-DIFFERENCE'
1	-5.17	-4.33	1180.	709.0	-1.0	0.016	0.035	1.322	0.744	-1.000	1.360	1.325	3.62	2.48
2	-4.25	-2.83	557.0	369.0	9.9	0.047	0.055	0.990	0.609	6.534	1.142	1.107	3.65	3.06
3	-2.83	-1.75	-1.0	-1.0	9.6	0.049	0.070	-1.000	-1.000	8.064	1.002	0.970	5.15	*****
4	-1.75	-0.50	580.0	253.0	5.3	0.053	0.085	1.578	0.645	5.406	1.058	1.032	4.34	3.71
5	0.25	1.75	575.0	191.0	-1.0	0.067	0.095	1.748	0.544	-1.000	0.966	0.935	4.28	*****
6	2.58	4.00	562.0	169.0	-1.0	0.042	0.062	1.115	0.314	-1.000	1.273	1.097	3.70	3.37
7	4.67	6.00	489.0	163.0	-1.0	0.040	0.036	0.563	0.176	-1.000	0.884	0.864	3.62	*****
8	6.08	7.08	540.0	165.0	-1.0	0.033	0.023	0.397	0.114	-1.000	0.918	0.881	4.00	*****
9	7.08	9.08	845.0	320.0	-1.0	0.017	0.013	0.352	0.125	-1.000	1.028	1.001	3.63	3.62
10	9.08	11.25	1046.	361.0	-1.0	0.022	0.008	0.268	0.087	-1.000	0.967	0.938	3.23	3.58
TIME-WEIGHTED AVERAGE FOR 10. SAMPLES							0.045	0.859	0.336	6.599				

REVISED 2/25/83

TABLE 4. BAKERSFIELD FOG - 07(A) JAN 83 $

MASS SOLUTE PER M3 AIR IS BASED ON LIQUID WATER CONTENT EITHER MEASURED (IF AVAILABLE)
OR CALCULATED FROM THE VOLUME OF FOGWATER COLLECTED AND ASSUMING A SAMPLING RATE = 5 M3/MIN (AN LOWER BOUND)

							MICROGRAM / CUBIC METER									
#	TIME1	TIME2	DT (MIN)	VOL	LWC(G/M3) CALC.	LWC(G/M3) MEAS.	H	NA	K	NH4	CA	MG	F	CL	NO3	SO4	MASS
1	-5.17	-4.33	50.40	4.0	0.016	0.035	0.008	0.243	0.127	4.731	0.812	0.051	0.162	0.270	8.159	14.381	28.925
2	-4.25	-2.83	85.20	20.0	0.047	0.055	0.012	0.295	0.531	4.968	0.382	0.025	0.182	0.133	8.661	10.982	26.141
3	-2.83	-1.75	64.80	16.0	0.049	0.070	0.000	0.507	0.824	4.397	0.273	0.022	0.181	0.213	6.423	8.870	21.712
4	-1.75	-0.50	75.00	20.0	0.053	0.085	0.004	0.125	0.213	6.808	0.129	0.006	0.187	-0.100	6.851	14.525	21.276
5	0.25	1.75	90.00	30.0	0.067	0.095	0.005	0.023	0.063	4.232	0.038	0.004	0.139	0.051	5.419	6.749	16.722
6	2.58	4.00	85.20	18.0	0.042	0.062	0.012	0.010	0.031	2.288	0.017	0.001	0.459	0.747	3.229	3.982	10.777
7	4.67	6.00	79.80	16.0	0.040	0.036	0.009	0.020	0.023	1.481	0.022	0.002	0.026	0.000	2.098	2.281	5.961
8	6.08	7.08	60.00	10.0	0.033	0.023	0.002	0.007	0.021	1.060	0.017	0.001	0.042	0.000	1.283	1.678	4.113
9	7.08	9.08	120.0	10.0	0.017	0.013	0.003	0.017	0.014	0.786	0.094	0.005	0.021	0.008	1.161	1.647	3.755
10	9.08	11.25	130.2	14.0	0.022	0.008	0.005	0.009	0.012	0.533	0.123	0.007	0.012	0.014	0.913	1.183	2.810
	TIME-WEIGHTED AVERAGE FOR 10. SAMPLES				0.045		0.006	0.103	0.161	2.830	0.159	0.010	0.131	0.143	3.979	5.836	13.358

TABLE 5. BAKERSFIELD FOG - 07(A) JAN 83 $

					MICROGRAM / LITER						MICROGRAM / CUBIC METER					
#	TIME1	TIME2	PH	H	FE	MN	PB	CU	NI	V	FE	MN	PB	CU	NI	V
1	-5.17	-4.33	3.62	0.0	1900.0	525.0	628.0	48.0	1232.0	850.0	0.067	0.018	0.022	0.002	0.043	0.030
2	-4.25	-2.83	3.65	0.0	-0.1	100.0	796.0	202.0	367.0	375.0	-0.000	0.005	0.044	0.011	0.020	0.021
3	-2.83	-1.75	5.15	0.0	1900.0	46.0	372.0	24.0	286.0	370.0	0.133	0.003	0.027	0.002	0.019	0.026
4	-1.75	-0.50	4.34	0.0	1030.0	16.0	200.0	6.0	146.0	185.0	0.088	0.001	0.017	0.001	0.012	0.016
5	0.25	1.75	4.28	0.0	325.0	8.0	201.0	39.0	117.0	70.0	0.031	0.001	0.019	0.004	0.011	0.007
6	2.58	4.00	3.70	0.0	108.0	4.0	205.0	13.0	92.6	95.0	0.007	0.000	0.013	0.001	0.006	0.006
7	4.67	6.00	3.62	0.0	296.0	7.0	217.0	19.0	100.3	95.0	0.011	0.000	0.008	0.001	0.004	0.003
8	6.08	7.08	4.00	0.0	89.0	7.0	191.0	7.0	87.0	78.0	0.002	0.000	0.004	0.000	0.002	0.002
9	7.08	9.08	3.63	0.0	1248.0	49.0	711.0	59.0	137.0	175.0	0.016	0.001	0.009	0.001	0.002	0.002
10	9.08	11.25	3.23	0.0	2060.0	95.0	1233.0	83.0	150.0	150.0	0.016	0.001	0.010	0.001	0.001	0.001

ENTERED 8/11/83

TABLE 1. BAKERSFIELD FOG - 07(B) JAN 83 $

#	TIME1	TIME2	PH	H	NA	K	NH4	CA	MG	F	CL	NO3	SO4	-/+	S(IV)	CH2O	TOC
				/ / / / / /			MICRO EQ/LITER					\ \ \ \ \ \			/ MICRO M/L \		/MM/L\
1	18.92	19.92	2.93	1170.0	120.0	126.0	9700.0	1500.0	167.0	280.0	375.0	5100.0	6060.0	1.081	-1.0	-1.0	-1.0
2	19.92	22.00	2.99	1020.0	242.0	216.0	12000.	3500.0	427.0	430.0	575.0	8650.0	10000.	1.014	-1.0	-1.0	-1.0

REVISED 2/25/83

TABLE 2. BAKERSFIELD FOG - 07(B) JAN 83 $

#	TIME1	TIME2	DT(MIN)	MIDT	-/+	CL/NA	MG/NA	CA/NA	SO4/NA	NO3/SO4	NH4/N+S	H/N+S	H+A/N+S	S(IV)/SO4	S(IV)/CH2O
						EQUIVALENT RATIOS								MOLAR RATIOS	
1	18.92	19.92	60.00	19.42	1.081	3.125	1.408	12.500	67.167	0.633	0.737	0.087	0.826	-0.000	1.000
2	19.92	22.00	124.8	20.96	1.014	2.376	1.764	14.463	41.322	0.665	0.721	0.061	0.782	-0.000	1.000
	SEA SALT RATIOS					1.17	0.226	0.043	0.120						

REVISED 2/25/83

TABLE 3. BAKERSFIELD FOG - 07(B) JAN 83 $

MASS SOLUTE PER M3 AIR IS BASED ON LIQUID WATER CONTENT EITHER MEASURED (IF AVAILABLE)
OR CALCULATED FROM THE VOLUME OF FOGWATER COLLECTED AND ASSUMING A SAMPLING RATE = 5 M3/MIN (A LOWER BOUND)

#	TIME1	TIME2	S(IV)	CH2O	TOC	LWC(G/M3) CALC.	LWC(G/M3) MEAS.	S(IV)	CH2O	TOC	-/+	"CORRECTED -/+"	PH	"PH-BY-DIFFERENCE"
			/ MICRO M/L \		/MM/L\			/ MICROGRAM / CUBIC METER \						
1	18.92	19.92	-1.0	-1.0	-1.0	0.013	0.070	-1.000	-1.000	-1.000	1.081	1.031	2.93	2.81
2	19.92	22.00	-1.0	-1.0	-1.0	0.003	0.050	-1.000	-1.000	-1.000	1.014	0.967	2.99	3.35
TIME-WEIGHTED AVERAGE FOR 2. SAMPLES							0.056	0.000	0.000	0.000				

REVISED 2/25/83

TABLE 4. BAKERSFIELD FOG - 07(B) JAN 83 $

MASS SOLUTE PER M3 AIR IS BASED ON LIQUID WATER CONTENT EITHER MEASURED (IF AVAILABLE)
OR CALCULATED FROM THE VOLUME OF FOGWATER COLLECTED AND ASSUMING A SAMPLING RATE = 5 M3/MIN (AN LOWER BOUND)

#	TIME1	TIME2	DT (MIN)	VOL	LWC(G/M3) CALC.	LWC(G/M3) MEAS.	H	NA	K	NH4	CA	MG	F	CL	NO3	SO4	MASS
							MICROGRAM / CUBIC METER										
1	18.92	19.92	60.00	4.0	0.013	0.070	0.082	0.193	0.645	12.222	2.100	0.144	0.372	0.931	22.134	27.082	65.604
2	19.92	22.00	124.8	2.0	0.003	0.050	0.051	0.278	0.422	10.800	3.500	0.209	0.408	1.019	20.615	24.000	61.354
TIME-WEIGHTED AVERAGE FOR 2. SAMPLES					0.056		0.061	0.251	0.597	11.262	3.045	0.222	0.397	0.990	21.108	25.001	62.734

TABLE 5. BAKERSFIELD FOG - 07(B) JAN 83 $

#	TIME1	TIME2	PH	H	FE	MN	PB	CU	NI	V	FE	MN	PB	CU	NI	V
					MICROGRAM / LITER						MICROGRAM / CUBIC METER					
1	18.92	19.92	2.93	0.0	-0.1	-0.1	-0.1	-0.1	-0.1	-0.1	-0.000	-0.000	-0.000	-0.000	-0.000	-0.000
2	19.92	22.00	2.99	0.0	-0.1	-0.1	-0.1	-0.1	-0.1	-0.1	-0.000	-0.000	-0.000	-0.000	-0.000	-0.000

ENTERED 8/10/83

TABLE 1. BAKERSFIELD FOG - 08 JAN 83 *

#	TIME1	TIME2	PH	MICRO EQ/LITER / / / / / / H	NA	K	NH4	CA	MG	F	CL	\ \ \ \ \ NO3	SO4	-/+	/ MICRO M/L \ S(IV)	CH2O	/MM/L\ TOC
1	0.00	1.50	3.34	457.0	10.2	18.7	2780.0	132.0	29.3	140.0	10.0	1325.0	1500.0	0.868	258.0	170.0	13.0
2	1.50	3.75	3.44	363.0	13.6	24.3	2530.0	16.7	3.9	75.0	2.0	950.0	1300.0	0.788	217.0	195.0	5.7
3	3.75	5.50	4.54	29.0	3.9	5.6	1350.0	7.0	2.5	31.0	2.0	420.0	590.0	0.746	242.0	86.0	2.1
4	5.50	6.67	4.77	17.0	2.4	3.4	1440.0	27.5	3.5	34.0	2.0	385.0	1080.0	1.005	227.0	104.0	1.1
5	6.67	7.75	4.43	37.0	-0.1	-0.1	3390.0	304.0	28.0	39.0	2.0	680.0	1820.0	0.676	-1.0	-1.0	-1.0

REVISED 2/25/83

TABLE 2. BAKERSFIELD FOG - 08 JAN 83 *

#	TIME1	TIME2	DT(MIN)	NIDT	-/+	EQUIVALENT RATIOS CL/NA	MG/NA	CA/NA	SO4/NA	NO3/SO4	NH4/N+S	H/N+S	H+A/N+S	MOLAR RATIOS S(IV)/SO4	S(IV)/CH2O
1	0.00	1.50	90.00	0.75	0.868	0.980	2.873	12.941	147.05	0.883	0.984	0.162	1.146	0.344	1.518
2	1.50	3.75	135.0	2.63	0.788	0.147	0.267	1.228	95.588	0.731	1.124	0.161	1.286	0.334	1.113
3	3.75	5.50	105.0	4.63	0.746	0.513	0.641	1.795	151.28	0.712	1.337	0.029	1.365	0.820	2.814
4	5.50	6.67	70.20	6.09	1.005	0.833	1.458	11.458	450.00	0.356	0.983	0.012	0.995	0.420	2.183
5	6.67	7.75	64.80	7.21	0.676	-20.00	******	******	******	0.374	1.356	0.015	1.371	-0.001	1.000
	SEA SALT RATIOS					1.17	0.228	0.043	0.120						

REVISED 2/25/83

TABLE 3. BAKERSFIELD FOG - 08 JAN 83 *

MASS SOLUTE PER M3 AIR IS BASED ON LIQUID WATER CONTENT EITHER MEASURED (IF AVAILABLE)
OR CALCULATED FROM THE VOLUME OF FOGWATER COLLECTED AND ASSUMING A SAMPLING RATE = 5 M3/MIN (A LOWER BOUND)

#	TIME1	TIME2	/ MICRO M/L \ S(IV)	CH2O	/MM/L\ TOC	LWC(G/M3) CALC.	MEAS.	/ MICROGRAM / CUBIC METER \ S(IV)	CH2O	TOC	-/+	'CORRECTED -/+'	PH	'PH-BY-DIFFERENCE'
1	0.00	1.50	258.0	170.0	13.0	0.053	0.095	0.784	0.484	14.820	0.868	0.819	3.34	*****
2	1.50	3.75	217.0	195.0	5.7	0.053	0.100	0.694	0.583	6.840	0.788	0.757	3.44	*****
3	3.75	5.50	242.0	86.0	2.1	0.065	0.120	0.929	0.310	3.024	0.746	0.723	4.54	*****
4	5.50	6.67	227.0	104.0	1.1	0.051	0.032	0.232	0.100	0.422	1.005	0.982	4.77	*****
5	6.67	7.75	-1.0	-1.0	-1.0	0.003	0.005	-1.000	-1.000	-1.000	0.676	0.665	4.43	*****
TIME-WEIGHTED AVERAGE FOR 5. SAMPLES							0.080	0.693	0.405	6.508				

REVISED 2/25/83

TABLE 4. BAKERSFIELD FOG - 08 JAN 83 *

MASS SOLUTE PER M3 AIR IS BASED ON LIQUID WATER CONTENT EITHER MEASURED (IF AVAILABLE)
OR CALCULATED FROM THE VOLUME OF FOGWATER COLLECTED AND ASSUMING A SAMPLING RATE = 5 M3/MIN (AN LOWER BOUND)

#	TIME1	TIME2	DT (MIN)	VOL	LWC(G/M3) CALC.	MEAS.	MICROGRAM / CUBIC METER H	NA	K	NH4	CA	MG	F	CL	NO3	SO4	MASS
1	0.00	1.50	90.00	24.0	0.053	0.095	0.043	0.022	0.069	4.754	0.251	0.034	0.253	0.034	7.104	6.840	20.104
2	1.50	3.75	135.0	36.0	0.053	0.100	0.036	0.031	0.095	4.554	0.033	0.005	0.142	0.007	5.890	6.240	17.034
3	3.75	5.50	105.0	34.0	0.065	0.120	0.003	0.011	0.026	2.916	0.017	0.004	0.071	0.009	3.125	3.398	9.579
4	5.50	6.67	70.20	18.0	0.051	0.032	0.001	0.002	0.004	0.829	0.018	0.001	0.021	0.002	0.764	1.659	3.301
5	6.67	7.75	64.80	1.0	0.003	0.005	0.000	-0.100	-0.100	0.305	0.030	0.002	0.004	0.000	0.211	0.437	0.889
TIME-WEIGHTED AVERAGE FOR 5. SAMPLES					0.080		0.030	0.019	0.055	3.668	0.069	0.009	0.110	0.011	4.071	4.214	11.646

TABLE 5. BAKERSFIELD FOG - 04 JAN 83 $

#	TIME1	TIME2	PH	H	MICROGRAM / LITER FE	MN	PB	CU	NI	V	MICROGRAM / CUBIC METER FE	MN	PB	CU	NI	V
1	0.00	1.50	3.34	0.0	1860.0	41.0	903.0	243.0	180.0	126.0	0.177	0.004	0.086	0.023	0.017	0.012
2	1.50	3.75	3.44	0.0	647.0	7.0	612.0	51.0	140.0	80.0	0.065	0.001	0.061	0.005	0.014	0.008
3	3.75	5.50	4.54	0.0	158.0	5.0	61.0	23.0	36.2	27.0	0.019	0.001	0.007	0.003	0.004	0.003
4	5.50	6.67	4.77	0.0	262.0	30.0	90.0	11.0	33.0	24.0	0.008	0.001	0.003	0.000	0.001	0.001
5	6.67	7.75	4.43	0.0	-0.1	-0.1	-0.1	-0.1	-0.1	-0.1	-0.000	-0.000	-0.000	-0.000	-0.000	-0.000

ENTERED 8/11/83

TABLE 1. BAKERSFIELD FOG - 10 JAN 83 $

#	TIME1	TIME2	PH	MICRO EQ/LITER H	NA	K	NH4	CA	MG	F	CL	NO3	SO4	-/+	MICRO M/L S(IV)	CH2O	MM/L TOC
1	6.75	7.15	6.40	0.4	57.0	30.0	3070.0	335.0	44.0	320.0	225.0	780.0	1150.0	0.701	-1.0	-1.0	-1.0
2	7.15	7.75	6.70	0.2	34.0	21.0	3740.0	110.0	8.3	300.0	500.0	1120.0	1880.0	0.971	-1.0	-1.0	5.3
3	7.92	8.50	7.00	0.1	325.0	105.0	6260.0	3000.0	330.0	180.0	910.0	2800.0	4800.0	0.867	-1.0	-1.0	-1.0
4	9.42	10.42	6.00	1.0	250.0	50.0	4300.0	2135.0	224.0	400.0	600.0	2550.0	3580.0	1.024	-1.0	-1.0	-1.0

REVISED 5/14/83

TABLE 2. BAKERSFIELD FOG - 10 JAN 83 $

#	TIME1	TIME2	DT(MIN)	MIDT	-/+	EQUIVALENT RATIOS CL/NA	MG/NA	CA/NA	SO4/NA	NO3/SO4	NH4/N+S	H/N+S	H+A/N+S	MOLAR RATIOS S(IV)/SO4	S(IV)/CH2O
1	6.75	7.15	24.00	6.95	0.701	3.947	0.772	5.877	20.175	0.683	1.587	0.000	1.587	-0.002	1.000
2	7.15	7.75	36.00	7.45	0.971	14.706	0.144	3.235	55.294	0.596	1.247	0.000	1.247	-0.001	1.000
3	7.92	8.50	34.80	8.21	0.867	2.800	1.015	9.231	14.769	0.883	0.824	0.000	0.824	-0.000	1.000
4	9.42	10.42	60.00	9.92	1.024	2.400	0.896	8.540	14.320	0.712	0.701	0.000	0.702	-0.001	1.000
	SEA SALT RATIOS					1.17	0.228	0.043	0.120						

REVISED 5/14/83

TABLE 3. BAKERSFIELD FOG - 10 JAN 83 $

MASS SOLUTE PER M3 AIR IS BASED ON LIQUID WATER CONTENT EITHER MEASURED (IF AVAILABLE)
OR CALCULATED FROM THE VOLUME OF FOGWATER COLLECTED AND ASSUMING A SAMPLING RATE = 5 M3/MIN (A LOWER BOUND)

#	TIME1	TIME2	MICRO M/L S(IV)	MM/L CH2O	TOC	MICROGRAM / CUBIC METER LWC(G/M3) CALC.	LWC(G/M3) MEAS.	S(IV)	CH2O	TOC	-/+	"CORRECTED -/+"	PH	"PH-BY-DIFFERENCE"
1	6.75	7.15	-1.0	-1.0	-1.0	0.050	0.050	-1.000	-1.000	-1.000	0.701	0.611	6.40	*****
2	7.15	7.75	-1.0	-1.0	5.3	0.078	0.125	-1.000	-1.000	7.950	0.971	0.894	6.70	*****
3	7.92	8.50	-1.0	-1.0	-1.0	0.011	0.025	-1.000	-1.000	-1.000	0.867	0.849	7.00	*****
4	9.42	10.42	-1.0	-1.0	-1.0	0.007	0.010	-1.000	-1.000	-1.000	1.024	0.967	6.00	*****
TIME-WEIGHTED AVERAGE FOR 4. SAMPLES							0.046	0.000	0.000	7.950				

REVISED 5/14/83

TABLE 4. BAKERSFIELD FOG - 10 JAN 83 $

MASS SOLUTE PER M3 AIR IS BASED ON LIQUID WATER CONTENT EITHER MEASURED (IF AVAILABLE)
OR CALCULATED FROM THE VOLUME OF FOGWATER COLLECTED AND ASSUMING A SAMPLING RATE = 5 M3/MIN (AN LOWER BOUND)

#	TIME1	TIME2	DT (MIN)	VOL	MICROGRAM / CUBIC METER LWC(G/M3) CALC.	LWC(G/M3) MEAS.	H	NA	K	NH4	CA	MG	F	CL	NO3	SO4	MASS
1	6.75	7.15	24.00	6.0	0.050	0.050	0.000	0.066	0.059	2.763	0.335	0.027	0.304	0.399	2.434	2.760	9.145
2	7.15	7.75	36.00	14.0	0.078	0.125	0.000	0.098	0.103	8.415	0.275	0.013	0.712	2.216	8.680	11.280	31.791
3	7.92	8.50	34.80	2.0	0.011	0.025	0.000	0.187	0.103	2.817	1.500	0.100	0.085	0.806	4.340	5.760	15.699
4	9.42	10.42	60.00	2.0	0.007	0.010	0.000	0.058	0.020	0.774	0.427	0.027	0.076	0.213	1.581	1.718	4.893
TIME-WEIGHTED AVERAGE FOR 4. SAMPLES					0.046		0.000	0.097	0.064	3.319	0.619	0.040	0.262	0.841	3.984	5.012	14.237

TABLE 5. BAKERSFIELD FOG - 10 JAN 83 $

#	TIME1	TIME2	PH	H	MICROGRAM / LITER FE	MN	PB	CU	NI	V	MICROGRAM / CUBIC METER FE	MN	PB	CU	NI	V
1	6.75	7.15	6.40	0.0	1950.0	140.0	2280.0	456.0	392.0	187.0	0.097	0.007	0.114	0.023	0.020	0.009
2	7.15	7.75	6.70	0.0	4010.0	92.0	664.0	63.0	97.0	43.0	0.501	0.012	0.083	0.008	0.012	0.005
3	7.92	8.50	7.00	0.0	-0.1	-0.1	-0.1	-0.1	-0.1	-0.1	-0.000	-0.000	-0.000	-0.000	-0.000	-0.000
4	9.42	10.42	6.00	0.0	681.0	373.0	1012.0	175.0	-0.1	128.0	0.007	0.004	0.010	0.002	-0.000	0.001

ENTERED 8/11/83

TABLE 1. BAKERSFIELD FOG - 11 JAN 83 $

				/ / / / / /			MICRO EQ/LITER					\ \ \ \ \ \			/ MICRO M/L \	/MM/L\
$	TIME1	TIME2	PH	H	NA	K	NH4	CA	MG	F	CL	NO3	SO4	-/+	S(IV)	CH2O	TOC
1	1.33	2.00	5.05	9.0	19.8	4.4	762.0	30.9	3.1	66.0	22.0	405.0	194.0	0.829	400.0	105.0	2.2
2	2.00	3.00	5.30	5.0	9.3	4.1	777.0	16.0	1.8	58.0	42.0	405.0	210.0	0.876	573.0	114.0	1.8
3	3.00	4.00	5.15	7.0	9.5	4.8	885.0	12.3	1.4	65.0	21.0	470.0	290.0	0.920	692.0	117.0	1.7
4	4.00	5.00	4.64	23.0	11.2	-0.1	850.0	13.7	2.2	51.0	17.0	505.0	280.0	0.948	653.0	113.0	1.6
5	5.00	5.50	4.30	50.0	6.5	4.9	694.0	11.5	2.0	45.0	18.0	505.0	300.0	1.129	674.0	117.0	-1.0
6	5.50	6.00	3.93	117.0	10.6	10.3	930.0	22.2	4.5	0.0	0.0	723.0	430.0	1.053	389.0	108.0	1.9
7	6.00	6.50	3.80	158.0	7.6	4.9	762.0	16.0	2.4	36.0	54.0	625.0	330.0	1.099	332.0	106.0	-1.0
8	6.50	7.00	3.68	209.0	9.8	6.3	957.0	21.5	5.0	55.0	260.0	675.0	360.0	1.117	213.0	104.0	-1.0
9	7.00	7.50	3.66	219.0	7.6	5.6	892.0	18.2	3.8	40.0	30.0	740.0	354.0	1.016	152.0	66.0	-1.0
10	7.50	8.00	3.60	251.0	7.8	6.6	742.0	23.0	4.4	36.0	31.0	665.0	370.0	1.065	155.0	59.0	-1.0
11	8.00	8.50	3.48	331.0	12.3	5.6	864.0	25.6	4.7	36.0	190.0	710.0	470.0	1.131	157.0	99.0	-1.0
12	8.50	9.00	3.33	468.0	16.6	7.0	1085.0	37.1	8.3	10.0	40.0	935.0	858.0	1.136	-1.0	-1.0	-1.0
13	9.00	9.50	3.33	468.0	30.3	-0.1	1110.0	63.9	12.2	50.0	44.0	860.0	810.0	1.047	-1.0	233.0	-1.0
14	9.50	10.00	3.22	603.0	50.1	-0.1	1568.0	168.0	22.1	95.0	530.0	1190.0	1015.0	1.174	282.0	-1.0	-1.0
15	10.00	11.00	3.22	603.0	205.0	-0.1	2490.0	606.0	71.3	196.0	108.0	1790.0	1550.0	0.917	-1.0	-1.0	-1.0

REVISED 2/25/83

TABLE 2. BAKERSFIELD FOG - 11 JAN 83 $

						EQUIVALENT RATIOS								MOLAR RATIOS	
$	TIME1	TIME2	DT(MIN)	MIDT	-/+	CL/NA	MG/NA	CA/NA	SO4/NA	NO3/SO4	NH4/N+S	H/N+S	H+A/N+S	S(IV)/SO4	S(IV)/CH2O
1	1.33	2.00	40.20	1.67	0.829	1.111	0.157	1.561	9.798	2.088	1.272	0.015	1.287	4.124	3.810
2	2.00	3.00	60.00	2.50	0.876	4.516	0.194	1.720	22.581	1.929	1.263	0.008	1.272	5.457	5.026
3	3.00	4.00	60.00	3.50	0.920	2.211	0.147	1.295	30.526	1.621	1.164	0.009	1.174	4.772	5.915
4	4.00	5.00	60.00	4.50	0.948	1.518	0.196	1.223	25.000	1.804	1.083	0.029	1.112	4.664	5.779
5	5.00	5.50	30.00	5.25	1.129	2.769	0.308	1.769	46.154	1.683	0.862	0.062	0.924	4.493	5.761
6	5.50	6.00	30.00	5.75	1.053	0.000	0.425	2.094	40.566	1.681	0.807	0.101	0.908	1.809	3.602
7	6.00	6.50	30.00	6.25	1.099	7.105	0.316	2.105	43.421	1.894	0.798	0.165	0.963	2.012	3.132
8	6.50	7.00	30.00	6.75	1.117	26.531	0.510	2.194	36.735	1.675	0.925	0.202	1.127	1.183	2.048
9	7.00	7.50	30.00	7.25	1.016	3.947	0.500	2.395	46.579	2.090	0.815	0.200	1.016	0.859	2.303
10	7.50	8.00	30.00	7.75	1.065	3.974	0.564	2.949	47.436	1.797	0.717	0.243	0.959	0.838	2.627
11	8.00	8.50	30.00	8.25	1.131	15.447	0.382	2.081	38.211	1.511	0.732	0.281	1.013	0.668	1.586
12	8.50	9.00	30.00	8.75	1.136	2.410	0.500	2.235	51.687	1.090	0.605	0.261	0.866	-0.002	1.000
13	9.00	9.50	30.00	9.25	1.047	1.452	0.403	2.109	26.733	1.062	0.665	0.280	0.945	-0.002	-0.004
14	9.50	10.00	30.00	9.75	1.174	10.579	0.441	3.353	20.259	1.172	0.711	0.273	0.985	0.556	******
15	10.00	11.00	60.00	10.50	0.917	0.527	0.348	2.956	7.561	1.155	0.746	0.181	0.926	-0.001	1.000
		SEA SALT RATIOS				1.17	0.228	0.043	0.120						

REVISED 2/25/83

TABLE 3. BAKERSFIELD FOG - 11 JAN 83 $

MASS SOLUTE PER M3 AIR IS BASED ON LIQUID WATER CONTENT EITHER MEASURED (IF AVAILABLE)
OR CALCULATED FROM THE VOLUME OF FOGWATER COLLECTED AND ASSUMING A SAMPLING RATE = 5 M3/MIN (A LOWER BOUND)

			/ MICRO M/L \		/MM/L\	/ MICROGRAM / CUBIC METER \							
#	TIME1	TIME2	S(IV)	CH2O	TOC	LWC(G/M3) CALC.	LWC(G/M3) MEAS.	S(IV)	CH2O	TOC	-/+	*CORRECTED -/+*	PH	*PH-BY-DIFFERENCE*
1	1.33	2.00	400.0	105.0	2.2	0.159	0.310	3.968	0.976	8.184	0.829	0.749	5.05	*****
2	2.00	3.00	573.0	114.0	1.8	0.167	0.310	5.684	1.060	6.696	0.876	0.808	5.30	*****
3	3.00	4.00	692.0	117.0	1.7	0.147	0.300	6.643	1.053	6.120	0.920	0.849	5.15	*****
4	4.00	5.00	653.0	113.0	1.6	0.140	0.290	6.060	0.983	5.568	0.948	0.891	4.64	*****
5	5.00	5.50	674.0	117.0	-1.0	0.240	0.280	6.039	0.983	-1.000	1.129	1.070	4.30	3.99
6	5.50	6.00	389.0	108.0	1.9	0.160	0.270	3.361	0.875	6.156	1.053	1.051	3.93	3.76
7	6.00	6.50	332.0	106.0	-1.0	0.107	0.250	2.656	0.795	-1.000	1.099	1.059	3.80	3.67
8	6.50	7.00	213.0	104.0	-1.0	0.133	0.240	1.636	0.749	-1.000	1.117	1.069	3.68	3.53
9	7.00	7.50	152.0	66.0	-1.0	0.147	0.220	1.070	0.436	-1.000	1.016	0.978	3.66	3.71
10	7.50	8.00	155.0	59.0	-1.0	0.133	0.190	0.942	0.336	-1.000	1.065	1.026	3.60	*3.56
11	8.00	8.50	157.0	99.0	-1.0	0.093	0.160	0.804	0.475	-1.000	1.151	1.097	3.48	3.35
12	8.50	9.00	-1.0	-1.0	-1.0	0.067	0.080	-1.000	-1.000	-1.000	1.136	1.120	3.33	3.18
13	9.00	9.50	-1.0	233.0	-1.0	0.053	0.030	-1.000	0.210	-1.000	1.047	1.009	3.33	3.32
14	9.50	10.00	282.0	-1.0	-1.0	0.027	0.010	0.090	-1.000	-1.000	1.174	1.124	3.22	3.04
15	10.00	11.00	-1.0	-1.0	-1.0	0.020	-1.00	-1.000	-1.000	-1.000	0.917	0.858	3.22	4.41
TIME-WEIGHTED AVERAGE FOR 15. SAMPLES							0.206	3.826	0.806	6.462				

REVISED 2/25/83

TABLE 4. BAKERSFIELD FOG - 11 JAN 83 $

MASS SOLUTE PER M3 AIR IS BASED ON LIQUID WATER CONTENT EITHER MEASURED (IF AVAILABLE)
OR CALCULATED FROM THE VOLUME OF FOGWATER COLLECTED AND ASSUMING A SAMPLING RATE = 5 M3/MIN (AN LOWER BOUND)

							MICROGRAM / CUBIC METER								
#	TIME1	TIME2	DT (MIN)	VOL	LWC(G/M3) CALC.	LWC(G/M3) MEAS.	H	NA	K	NH4	CA	MG	F	CL	NO3	SO4	MASS
1	1.33	2.00	40.20	32.0	0.159	0.310	0.003	0.141	0.053	4.252	0.192	0.012	0.389	0.242	7.784	2.887	15.954
2	2.00	3.00	60.00	50.0	0.167	0.310	0.002	0.066	0.050	4.336	0.099	0.007	0.324	0.462	7.784	3.125	16.254
3	3.00	4.00	60.00	44.0	0.147	0.300	0.002	0.066	0.056	4.779	0.074	0.005	0.370	0.223	8.742	4.176	18.494
4	4.00	5.00	60.00	42.0	0.140	0.290	0.007	0.075	-0.100	4.437	0.079	0.008	0.281	0.175	9.080	3.898	17.857
5	5.00	5.50	30.00	36.0	0.240	0.280	0.014	0.042	0.054	3.498	0.064	0.007	0.239	0.179	8.767	4.032	16.895
6	5.50	6.00	30.00	24.0	0.160	0.270	0.032	0.066	0.109	4.526	0.120	0.015	0.000	0.000	12.103	5.573	22.536
7	6.00	6.50	30.00	16.0	0.107	0.250	0.040	0.044	0.048	3.429	0.080	0.007	0.171	0.479	9.687	3.960	17.944
8	6.50	7.00	30.00	20.0	0.133	0.240	0.050	0.054	0.059	4.134	0.103	0.015	0.251	2.212	10.044	4.147	21.069
9	7.00	7.50	30.00	22.0	0.147	0.220	0.048	0.038	0.048	3.532	0.080	0.010	0.167	0.234	10.094	3.738	17.990
10	7.50	8.00	30.00	20.0	0.133	0.190	0.048	0.034	0.049	2.536	0.087	0.010	0.150	0.209	7.834	3.374	14.313
11	8.00	8.50	30.00	14.0	0.093	0.160	0.053	0.045	0.035	2.488	0.082	0.009	0.109	1.078	7.043	3.610	14.553
12	8.50	9.00	30.00	10.0	0.067	0.080	0.037	0.031	0.022	1.562	0.059	0.008	0.015	0.113	4.638	3.295	9.781
13	9.00	9.50	30.00	8.0	0.053	0.030	0.014	0.021	-0.100	0.599	0.038	0.004	0.029	0.047	1.600	1.166	3.383
14	9.50	10.00	30.00	4.0	0.027	0.010	0.006	0.012	-0.100	0.282	0.034	0.003	0.018	0.186	0.738	0.467	1.649
15	10.00	11.00	60.00	6.0	0.020	-1.00	0.012	0.094	-0.100	0.896	0.242	0.017	0.074	0.077	2.220	1.468	4.915
TIME-WEIGHTED AVERAGE FOR 15. SAMPLES							0.206	0.020	0.061	0.053	3.163	0.103	0.009	0.194	0.359	7.168	3.258	14.368

TABLE 5. BAKERSFIELD FOG - 11 JAN 83 *

#	TIME1	TIME2	PH	H	MICROGRAM / LITER FE	MN	PB	CU	NI	V	MICROGRAM / CUBIC METER FE	MN	PB	CU	NI	V
1	1.33	2.00	5.05	0.0	296.0	9.0	77.0	18.0	10.0	7.0	0.092	0.003	0.024	0.006	0.003	0.002
2	2.00	3.00	5.30	0.0	100.0	3.0	47.9	7.0	6.6	7.0	0.031	0.001	0.015	0.002	0.002	0.002
3	3.00	4.00	5.15	0.0	255.0	3.0	78.0	15.0	7.7	12.0	0.076	0.001	0.024	0.004	0.002	0.004
4	4.00	5.00	4.64	0.0	313.0	5.0	113.0	7.0	11.0	12.0	0.091	0.001	0.034	0.003	0.003	0.003
5	5.00	5.50	4.30	0.0	-0.1	-0.1	-0.1	-0.1	-0.1	-0.1	-0.000	-0.000	-0.000	-0.000	-0.000	-0.000
6	5.50	6.00	3.93	0.0	151.0	3.0	197.0	85.0	21.0	19.0	0.041	0.001	0.053	0.024	0.006	0.005
7	6.00	6.50	3.80	0.0	-0.1	-0.1	-0.1	-0.1	-0.1	-0.1	-0.000	-0.000	-0.000	-0.000	-0.000	-0.000
8	6.50	7.00	3.68	0.0	216.0	5.0	891.0	6.0	16.0	17.0	0.052	0.001	0.214	0.001	0.004	0.004
9	7.00	7.50	3.66	0.0	-0.1	-0.1	-0.1	-0.1	-0.1	-0.1	-0.000	-0.000	-0.000	-0.000	-0.000	-0.000
10	7.50	8.00	3.60	0.0	-0.1	-0.1	-0.1	-0.1	-0.1	-0.1	-0.000	-0.000	-0.000	-0.000	-0.000	-0.000
11	8.00	8.50	3.48	0.0	-0.1	-0.1	-0.1	-0.1	-0.1	-0.1	-0.000	-0.000	-0.000	-0.000	-0.000	-0.000
12	8.50	9.00	3.33	0.0	487.0	11.0	263.0	17.0	16.0	16.0	0.039	0.001	0.021	0.001	0.001	0.001
13	9.00	9.50	3.33	0.0	-0.1	-0.1	-0.1	-0.1	-0.1	-0.1	-0.000	-0.000	-0.000	-0.000	-0.000	-0.000
14	9.50	10.00	3.22	0.0	-0.1	-0.1	-0.1	-0.1	-0.1	-0.1	-0.000	-0.000	-0.000	-0.000	-0.000	-0.000
15	10.00	11.00	3.22	0.0	-0.1	-0.1	-0.1	-0.1	-0.1	-0.1	-0.000	-0.000	-0.000	-0.000	-0.000	-0.000

ENTERED 8/11/83

TABLE 1. BAKERSFIELD FOG - 12 JAN 83 $

#	TIME1	TIME2	PH	/ / / / / / H	Na	K	NH4	Ca	Mg	F	Cl	\ \ \ \ \ \ NO3	SO4	-/+	/ MICRO M/L \ S(IV)	CH2O	/MM/L\ TOC
				MICRO EQ/LITER													
1	-4.92	-3.75	2.79	1620.0	293.0	-0.1	5645.0	2050.0	217.0	312.0	650.0	5250.0	7200.0	1.365	2980.	571.0	-1.0
2	-3.67	-2.00	3.09	813.0	83.1	-0.1	3890.0	180.0	20.0	172.0	210.0	3150.0	3370.0	1.390	1090.	-1.0	-1.0
3	-2.00	0.00	3.37	427.0	41.4	-0.1	4170.0	166.0	17.7	0.0	80.0	1940.0	2540.0	0.946	1140.	318.0	-1.0
4	0.00	2.00	3.53	295.0	16.8	22.4	2220.0	39.0	5.4	160.0	83.0	1000.0	1320.0	0.986	517.0	227.0	-1.0
5	2.00	4.83	3.53	295.0	13.1	12.4	1910.0	31.6	5.2	80.0	50.0	855.0	1570.0	1.039	711.0	-1.0	-1.0
6	4.83	7.00	3.66	219.0	15.5	12.1	1050.0	24.9	3.3	39.0	24.0	350.0	950.0	1.029	567.0	148.0	-1.0
7	7.00	9.50	3.58	263.0	24.8	-0.1	1100.0	102.0	13.9	0.0	0.0	395.0	1125.0	1.011	711.0	255.0	-1.0

REVISED 2/25/83

TABLE 2. BAKERSFIELD FOG - 12 JAN 83 $

#	TIME1	TIME2	DT(MIN)	MIDT	-/+	EQUIVALENT RATIOS CL/NA	NO3/NA	Ca/NA	SO4/NA	NO3/SO4	NH4/N+S	H/N+S	H+A/N+S	MOLAR RATIOS S(IV)/SO4	S(IV)/CH2O
1	-4.92	-3.75	70.20	-4.34	1.365	2.218	0.741	6.997	24.573	0.729	0.453	0.130	0.584	0.828	5.219
2	-3.67	-2.00	100.2	-2.84	1.390	2.527	0.241	1.925	40.554	0.935	0.597	0.125	0.721	0.647	******
3	-2.00	0.00	120.0	-1.00	0.946	1.932	0.428	4.010	61.353	0.764	0.931	0.095	1.026	0.898	3.585
4	0.00	2.00	120.0	1.00	0.986	4.940	0.321	2.321	78.571	0.758	0.957	0.127	1.084	0.783	2.278
5	2.00	4.83	169.8	3.41	1.039	3.817	0.397	2.412	119.84	0.417	0.858	0.133	0.991	0.906	******
6	4.83	7.00	130.2	5.91	1.029	1.548	0.213	1.606	61.290	0.368	0.808	0.168	0.976	1.194	3.831
7	7.00	9.50	150.0	8.25	1.011	0.000	0.560	4.113	45.363	0.351	0.724	0.173	0.897	1.264	2.788
	SEA SALT RATIOS					1.17	0.228	0.043	0.120						

REVISED 2/25/83

TABLE 3. BAKERSFIELD FOG - 12 JAN 83 $

MASS SOLUTE PER M3 AIR IS BASED ON LIQUID WATER CONTENT EITHER MEASURED (IF AVAILABLE)
OR CALCULATED FROM THE VOLUME OF FOGWATER COLLECTED AND ASSUMING A SAMPLING RATE = 5 M3/MIN (A LOWER BOUND)

#	TIME1	TIME2	/ MICRO M/L \ S(IV)	CH2O	/MM/L\ TOC	/ MICROGRAM / CUBIC METER \ LWC(G/M3) CALC.	MEAS.	S(IV)	CH2O	TOC	-/+	"CORRECTED -/+"	PH	"PH-BY-DIFFERENCE"
1	-4.92	-3.75	2980.	571.0	-1.0	0.017	-1.00	1.630	0.293	-1.000	1.365	1.290	2.79	2.35
2	-3.67	-2.00	1090.	-1.0	-1.0	0.020	0.009	0.314	-1.000	-1.000	1.390	1.334	3.09	2.61
3	-2.00	0.00	1140.	318.0	-1.0	0.040	0.058	2.116	0.553	-1.000	0.946	0.937	3.37	3.92
4	0.00	2.00	517.0	227.0	-1.0	0.060	0.110	1.820	0.749	-1.000	0.986	0.919	3.53	4.08
5	2.00	4.83	711.0	-1.0	-1.0	0.047	0.110	2.503	-1.000	-1.000	1.039	0.995	3.53	3.55
6	4.83	7.00	567.0	148.0	-1.0	0.061	0.085	1.542	0.377	-1.000	1.029	0.993	3.66	3.68
7	7.00	9.50	711.0	255.0	-1.0	0.027	0.055	1.251	0.421	-1.000	1.011	1.003	3.58	3.57
TIME-WEIGHTED AVERAGE FOR 7. SAMPLES							0.070	1.664	0.490	0.000				

REVISED 2/25/83

TABLE 4. BAKERSFIELD FOG - 12 JAN 83 $

MASS SOLUTE PER M3 AIR IS BASED ON LIQUID WATER CONTENT EITHER MEASURED (IF AVAILABLE)
OR CALCULATED FROM THE VOLUME OF FOGWATER COLLECTED AND ASSUMING A SAMPLING RATE = 5 M3/MIN (AN LOWER BOUND)

							MICROGRAM / CUBIC METER								
#	TIME1	TIME2	DT (MIN)	VOL	LWC(G/M3) CALC.	LWC(G/M3) MEAS.	H	NA	K	NH4	CA	MG	F	CL	NO3	SO4	MASS
1	-4.92	-3.75	70.20	6.0	0.017	-1.00	0.028	0.115	-0.100	1.737	0.701	0.045	0.101	0.394	5.564	5.908	14.750
2	-3.67	-2.00	100.2	10.0	0.020	0.009	0.007	0.017	-0.100	0.630	0.029	0.002	0.029	0.067	1.758	1.456	3.871
3	-2.00	0.00	120.0	24.0	0.040	0.058	0.025	0.055	-0.100	4.353	0.193	0.012	0.000	0.164	6.976	7.071	18.671
4	0.00	2.00	120.0	36.0	0.060	0.110	0.032	0.043	0.096	4.396	0.086	0.007	0.334	0.324	6.820	6.970	19.108
5	2.00	4.83	169.8	40.0	0.047	0.110	0.032	0.033	0.053	3.782	0.070	0.007	0.167	0.195	4.467	8.290	17.096
6	4.83	7.00	130.2	40.0	0.061	0.085	0.019	0.030	0.040	1.606	0.042	0.003	0.063	0.072	1.844	3.876	7.597
7	7.00	9.50	150.0	20.0	0.027	0.055	0.014	0.031	-0.100	1.089	0.112	0.009	0.000	0.000	1.347	2.970	5.427
TIME-WEIGHTED AVERAGE FOR 7. SAMPLES					0.070		0.023	0.042	0.062	2.615	0.139	0.010	0.101	0.157	3.978	5.350	12.477

TABLE 5. BAKERSFIELD FOG - 12 JAN 83 $

					MICROGRAM / LITER						MICROGRAM / CUBIC METER					
#	TIME1	TIME2	PH	H	FE	MN	PB	CU	NI	V	FE	MN	PB	CU	NI	V
1	-4.92	-3.75	2.79	0.0	6890.0	392.0	3340.0	717.0	214.0	85.0	0.118	0.007	0.057	0.012	0.004	0.001
2	-3.67	-2.00	3.09	0.0	3080.0	118.0	1754.0	173.0	95.0	61.0	0.028	0.001	0.016	0.002	0.001	0.001
3	-2.00	0.00	3.37	0.0	1420.0	49.0	1267.0	24.0	115.0	69.0	0.082	0.003	0.073	0.001	0.007	0.004
4	0.00	2.00	3.53	0.0	584.0	15.0	7815.0	12.0	76.0	48.0	0.064	0.002	0.860	0.001	0.008	0.005
5	2.00	4.83	3.53	0.0	302.0	9.0	393.0	9.0	77.7	61.0	0.033	0.001	0.043	0.001	0.009	0.007
6	4.83	7.00	3.66	0.0	670.0	12.0	214.0	26.0	169.0	106.0	0.057	0.001	0.018	0.002	0.014	0.009
7	7.00	9.50	3.58	0.0	636.0	19.0	543.0	15.0	106.0	88.0	0.035	0.001	0.030	0.001	0.006	0.005

ENTERED 8/11/83

TABLE 1. BAKERSFIELD FOG - 13 JAN 83 $

#	TIME1	TIME2	PH	MICRO EQ/LITER / / / / / / H	NA	K	NH4	CA	MG	F	CL	\ \ \ \ \ \ NO3	SO4	-/+	/ MICRO M/L \ S(IV)	CH2O	/MM/L\ TOC
1	-0.58	0.50	4.76	17.4	9.8	7.9	638.0	46.0	5.8	28.0	0.0	240.0	480.0	1.032	648.0	-1.0	1.8
2	0.83	2.08	4.62	24.0	5.5	9.3	488.0	25.2	3.2	20.0	19.0	200.0	400.0	1.151	547.0	-1.0	1.8
3	2.08	3.08	4.70	20.0	6.3	7.9	887.0	22.2	2.4	70.0	30.0	370.0	540.0	1.068	812.0	227.0	3.2
4	3.17	4.50	4.61	24.5	7.9	7.6	934.0	20.0	3.1	63.0	15.0	350.0	540.0	0.971	800.0	189.0	2.5
5	4.58	6.17	4.56	27.5	8.0	5.9	937.0	14.5	2.1	51.0	17.0	295.0	480.0	0.847	601.0	146.0	2.1
6	7.00	7.67	4.42	38.0	1.4	1.6	898.0	8.5	1.1	11.0	18.0	280.0	500.0	0.853	610.0	55.0	1.8
7	7.67	8.67	3.95	112.0	7.5	6.1	813.0	34.1	5.8	48.0	18.0	280.0	600.0	0.967	422.0	158.0	2.3
8	8.75	10.42	3.52	302.0	11.7	3.4	956.0	78.8	11.8	84.0	34.0	410.0	740.0	0.930	518.0	241.0	4.0
9	10.42	11.33	3.35	447.0	33.0	45.0	1708.0	1545.0	97.0	210.0	170.0	1280.0	2400.0	1.048	-1.0	-1.0	-1.0

REVISED 5/18/83

TABLE 2. BAKERSFIELD FOG - 13 JAN 83 $

#	TIME1	TIME2	DT(MIN)	MIDT	-/+	EQUIVALENT RATIOS CL/NA	MG/NA	CA/NA	SO4/NA	NO3/SO4	NH4/N+S	H/N+S	H+A/N+S	MOLAR RATIOS S(IV)/SO4	S(IV)/CH2O
1	-0.58	0.50	64.80	-0.04	1.032	0.000	0.592	4.694	48.980	0.500	0.886	0.024	0.910	2.700	******
2	0.83	2.08	75.00	1.45	1.151	3.455	0.582	4.582	72.727	0.500	0.813	0.040	0.853	2.735	******
3	2.08	3.08	60.00	2.58	1.068	4.762	0.381	3.524	85.714	0.685	0.975	0.022	0.997	3.007	3.577
4	3.17	4.50	79.80	3.84	0.971	1.899	0.392	2.532	68.354	0.648	1.049	0.028	1.077	2.963	4.233
5	4.58	6.17	95.40	5.38	0.847	2.125	0.262	1.813	60.000	0.615	1.209	0.035	1.245	2.504	4.116
6	7.00	7.67	40.20	7.34	0.853	12.857	0.786	6.071	357.14	0.560	1.151	0.049	1.200	2.440	11.091
7	7.67	8.67	60.00	8.17	0.967	2.400	0.773	4.547	80.000	0.467	0.924	0.127	1.051	1.407	2.671
8	8.75	10.42	100.2	9.59	0.930	2.906	1.009	6.735	63.248	0.554	0.831	0.263	1.094	1.400	2.149
9	10.42	11.33	54.60	10.88	1.048	5.152	2.939	46.818	72.727	0.543	0.464	0.121	0.586	-0.001	1.000
	SEA SALT RATIOS					1.17	0.228	0.043	0.120						

REVISED 5/18/83

TABLE 3. BAKERSFIELD FOG - 13 JAN 83 $

MASS SOLUTE PER M3 AIR IS BASED ON LIQUID WATER CONTENT EITHER MEASURED (IF AVAILABLE)
OR CALCULATED FROM THE VOLUME OF FOGWATER COLLECTED AND ASSUMING A SAMPLING RATE = 5 M3/MIN (A LOWER BOUND)

#	TIME1	TIME2	/ MICRO M/L \ S(IV)	CH2O	/MM/L\ TOC	LWC(G/M3) CALC.	MEAS.	/ MICROGRAM / CUBIC METER \ S(IV)	CH2O	TOC	-/+	"CORRECTED -/+"	PH	"PH-BY-DIFFERENCE"
1	-0.58	0.50	648.0	-1.0	1.8	0.049	0.110	2.281	-1.000	2.310	1.032	0.993	4.76	4.92
2	0.83	2.08	547.0	-1.0	1.8	0.080	0.175	3.063	-1.000	3.675	1.151	1.114	4.62	4.06
3	2.08	3.08	812.0	227.0	3.2	0.107	0.180	4.677	1.226	6.912	1.068	0.993	4.70	4.86
4	3.17	4.50	800.0	189.0	2.5	0.080	0.170	4.352	0.964	5.100	0.971	0.907	4.61	*****
5	4.58	6.17	601.0	146.0	2.1	0.113	0.155	2.981	0.679	3.906	0.847	0.795	4.56	*****
6	7.00	7.67	610.0	55.0	1.8	0.100	0.120	2.342	0.198	2.592	0.853	0.840	4.42	*****
7	7.67	8.67	422.0	158.0	2.3	0.067	0.100	1.350	0.474	2.760	0.967	0.915	3.95	4.54
8	8.75	10.42	518.0	241.0	4.0	0.048	0.040	0.663	0.289	1.920	0.930	0.862	3.52	3.95
9	10.42	11.33	-1.0	-1.0	-1.0	0.015	-1.00	-1.000	-1.000	-1.000	1.048	0.982	3.35	3.42
TIME-WEIGHTED AVERAGE FOR 9. SAMPLES							0.119	2.662	0.644	3.618				

REVISED 5/18/83

TABLE 4. BAKERSFIELD FOG - 13 JAN 83 $

MASS SOLUTE PER M3 AIR IS BASED ON LIQUID WATER CONTENT EITHER MEASURED (IF AVAILABLE)
OR CALCULATED FROM THE VOLUME OF FOGWATER COLLECTED AND ASSUMING A SAMPLING RATE = 5 M3/MIN (AN LOWER BOUND)

							MICROGRAM / CUBIC METER									
$	TIME1	TIME2	DT (MIN)	VOL	LWC(G/M3) CALC.	LWC(G/M3) MEAS.	H	NA	K	NH4	CA	MG	F	CL	NO3	SO4	MASS
1	-0.58	0.50	64.80	16.0	0.049	0.110	0.002	0.025	0.034	1.263	0.101	0.008	0.059	0.000	1.637	2.534	5.663
2	0.83	2.08	75.00	30.0	0.080	0.175	0.004	0.022	0.064	1.537	0.088	0.007	0.067	0.118	2.170	3.360	7.437
3	2.08	3.08	60.00	32.0	0.107	0.180	0.004	0.026	0.056	2.874	0.080	0.005	0.239	0.191	4.129	4.666	12.270
4	3.17	4.50	79.80	32.0	0.080	0.170	0.004	0.031	0.051	2.858	0.068	0.006	0.203	0.090	3.689	4.406	11.407
5	4.58	6.17	95.40	54.0	0.113	0.155	0.004	0.029	0.036	2.614	0.045	0.004	0.150	0.093	2.835	3.571	9.381
6	7.00	7.67	40.20	20.0	0.100	0.120	0.005	0.004	0.008	1.940	0.020	0.002	0.025	0.077	2.083	2.880	7.042
7	7.67	8.67	60.00	20.0	0.067	0.100	0.011	0.017	0.024	1.463	0.068	0.007	0.091	0.064	1.736	2.880	6.362
8	8.75	10.42	100.2	24.0	0.048	0.040	0.012	0.011	0.005	0.688	0.063	0.006	0.064	0.048	1.017	1.421	3.335
9	10.42	11.33	54.60	4.0	0.015	-1.00	0.007	0.011	0.026	0.450	0.453	0.017	0.058	0.088	1.163	1.688	3.961
	TIME-WEIGHTED AVERAGE FOR 9. SAMPLES				0.119		0.006	0.020	0.034	1.756	0.101	0.007	0.111	0.084	2.277	3.034	7.431

TABLE 5. BAKERSFIELD FOG - 13 JAN 83 $

					MICROGRAM / LITER						MICROGRAM / CUBIC METER					
$	TIME1	TIME2	PH	H	FE	MN	PB	CU	NI	V	FE	MN	PB	CU	NI	V
1	-0.58	0.50	4.76	0.0	216.0	3.0	114.0	15.0	64.3	51.0	0.024	0.000	0.013	0.002	0.007	0.006
2	0.83	2.08	4.62	0.0	96.0	1.0	53.0	23.0	23.6	25.0	0.017	0.000	0.009	0.004	0.004	0.004
3	2.08	3.08	4.70	0.0	375.0	7.0	41.8	31.0	32.1	27.0	0.068	0.001	0.008	0.006	0.006	0.005
4	3.17	4.50	4.61	0.0	420.0	9.0	141.0	21.0	48.0	54.0	0.071	0.002	0.024	0.004	0.008	0.009
5	4.58	6.17	4.56	0.0	241.0	5.0	99.4	56.0	38.1	40.0	0.037	0.001	0.015	0.009	0.006	0.006
6	7.00	7.67	4.42	0.0	307.0	75.0	249.0	13.0	49.5	42.0	0.037	0.009	0.029	0.002	0.006	0.005
7	7.67	8.67	3.95	0.0	350.0	8.0	322.0	25.0	43.4	48.0	0.035	0.001	0.032	0.002	0.004	0.005
8	8.75	10.42	3.52	0.0	507.0	16.0	511.0	27.0	50.4	52.0	0.020	0.001	0.020	0.001	0.002	0.002
9	10.42	11.33	3.35	0.0	-0.1	-0.1	-0.1	-0.1	-0.1	-0.1	-0.000	-0.000	-0.000	-0.000	-0.000	-0.000

ENTERED 8/11/83

TABLE 1. BAKERSFIELD FOG - 14 JAN 83 $

				MICRO EQ/LITER										MICRO M/L	MM/L
#	TIME1	TIME2	PH	H	NA	K	NH4	CA	MG	F	CL	NO3	SO4	-/+	S(IV)	CH2O	TOC
1	-5.50	-4.42	2.69	2040.0	62.7	45.9	4930.0	534.0	62.8	300.0	730.0	2500.0	4600.0	1.059	2100.	576.0	16.6
2	-4.42	-3.00	2.81	1550.0	55.2	38.7	3980.0	359.0	42.6	285.0	290.0	2400.0	3500.0	1.075	1240.	430.0	16.2
3	-2.92	-1.00	2.95	1120.0	28.3	22.5	3060.0	139.0	17.4	260.0	150.0	1550.0	2500.0	1.017	735.0	364.0	11.9
4	-0.17	2.00	3.22	603.0	13.5	16.2	2350.0	27.5	4.4	160.0	100.0	960.0	1760.0	0.989	573.0	293.0	7.8
5	2.08	5.08	3.41	389.0	9.6	14.0	1930.0	21.5	2.7	122.0	84.0	800.0	1360.0	1.000	535.0	179.0	22.8
6	5.08	7.33	3.50	316.0	14.9	18.0	2080.0	25.2	4.2	136.0	168.0	800.0	1280.0	0.970	540.0	283.0	4.6
7	7.33	9.42	3.33	468.0	16.7	23.8	1400.0	72.8	10.1	136.0	20.0	680.0	960.0	0.902	348.0	235.0	3.9
8	9.42	10.75	2.94	1150.0	40.3	32.3	1870.0	576.0	62.6	195.0	45.0	1350.0	2100.0	0.989	294.0	-1.0	-1.0

REVISED 2/25/83

TABLE 2. BAKERSFIELD FOG - 14 JAN 83 $

					EQUIVALENT RATIOS							MOLAR RATIOS	
#	TIME1	TIME2	DT(MIN)	MIDT	-/+	CL/NA	MG/NA	CA/NA	SO4/NA	NO3/SO4	NH4/N+S	H/N+S	H+A/N+S	S(IV)/SO4	S(IV)/CH2O
1	-5.50	-4.42	64.80	-4.96	1.059	11.643	1.002	8.517	73.365	0.543	0.694	0.287	0.982	0.913	3.646
2	-4.42	-3.00	85.20	-3.71	1.075	5.254	0.772	6.504	63.406	0.686	0.675	0.263	0.937	0.709	2.884
3	-2.92	-1.00	115.2	-1.96	1.017	5.300	0.615	4.912	88.339	0.620	0.756	0.277	1.032	0.588	2.019
4	-0.17	2.00	130.2	0.92	0.989	7.407	0.326	2.037	130.37	0.545	0.864	0.222	1.086	0.651	1.956
5	2.08	5.08	180.0	3.58	1.000	8.750	0.281	2.240	141.66	0.588	0.894	0.180	1.074	0.787	2.989
6	5.08	7.33	135.0	6.20	0.970	11.275	0.282	1.691	85.906	0.625	1.000	0.152	1.152	0.844	1.908
7	7.33	9.42	125.4	8.38	0.902	1.198	0.605	4.359	57.485	0.708	0.854	0.285	1.139	0.725	1.481
8	9.42	10.75	79.80	10.09	0.989	1.117	1.553	14.293	52.109	0.643	0.542	0.333	0.875	0.280	******
	SEA SALT RATIOS					1.17	0.228	0.043	0.120						

REVISED 2/25/83

TABLE 3. BAKERSFIELD FOG - 14 JAN 83 $

MASS SOLUTE PER M3 AIR IS BASED ON LIQUID WATER CONTENT EITHER MEASURED (IF AVAILABLE)
OR CALCULATED FROM THE VOLUME OF FOGWATER COLLECTED AND ASSUMING A SAMPLING RATE = 5 M3/MIN (A LOWER BOUND)

			MICRO M/L		MM/L	MICROGRAM / CUBIC METER							
#	TIME1	TIME2	S(IV)	CH2O	TOC	LWC(G/M3) CALC.	LWC(G/M3) MEAS.	S(IV)	CH2O	TOC	-/+	"CORRECTED -/+"	PH	"PH-BY-DIFFERENCE"
1	-5.50	-4.42	2100.	576.0	16.6	0.031	0.020	1.344	0.346	3.984	1.059	0.977	2.69	2.73
2	-4.42	-3.00	1240.	430.0	16.2	0.038	0.045	1.786	0.581	8.748	1.075	0.994	2.81	2.82
3	-2.92	-1.00	735.0	364.0	11.9	0.049	0.070	1.646	0.764	9.996	1.017	0.933	2.95	3.08
4	-0.17	2.00	573.0	293.0	7.8	0.058	0.090	1.650	0.791	8.424	0.989	0.921	3.22	3.44
5	2.08	5.08	535.0	179.0	22.8	0.040	0.095	1.626	0.510	25.992	1.000	0.939	3.41	3.61
6	5.08	7.33	540.0	283.0	4.6	0.033	0.090	1.555	0.764	4.968	0.970	0.908	3.50	4.05
7	7.33	9.42	348.0	235.0	3.9	0.045	0.055	0.612	0.388	2.574	0.902	0.825	3.33	3.93
8	9.42	10.75	294.0	-1.0	-1.0	0.005	0.001	0.009	-1.000	-1.000	0.989	0.912	2.94	3.09
TIME-WEIGHTED AVERAGE FOR 8. SAMPLES							0.067	1.337	0.606	10.677				

REVISED 2/25/83

TABLE 4. BAKERSFIELD FOG - 14 JAN 83 $

MASS SOLUTE PER M3 AIR IS BASED ON LIQUID WATER CONTENT EITHER MEASURED (IF AVAILABLE)
OR CALCULATED FROM THE VOLUME OF FOGWATER COLLECTED AND ASSUMING A SAMPLING RATE = 5 M3/MIN (AN LOWER BOUND)

							MICROGRAM / CUBIC METER									
$	TIME1	TIME2	DT (MIN)	VOL	LWC(G/M3) CALC.	LWC(G/M3) MEAS.	H	NA	K	NH4	CA	MG	F	CL	NO3	SO4	MASS
1	-5.50	-4.42	64.80	10.0	0.031	0.020	0.041	0.029	0.036	1.775	0.214	0.015	0.114	0.518	3.100	4.416	10.357
2	-4.42	-3.00	85.20	16.0	0.038	0.045	0.070	0.057	0.068	3.224	0.323	0.025	0.244	0.463	6.696	7.560	18.727
3	-2.92	-1.00	115.2	28.0	0.049	0.070	0.078	0.046	0.062	3.856	0.195	0.015	0.346	0.372	6.727	8.400	20.096
4	-0.17	2.00	130.2	36.0	0.058	0.090	0.054	0.028	0.057	3.807	0.050	0.005	0.274	0.319	5.357	7.603	17.353
5	2.08	5.08	180.0	36.0	0.040	0.095	0.037	0.021	0.052	3.300	0.041	0.003	0.220	0.283	4.712	6.202	14.871
6	5.08	7.33	135.0	22.0	0.033	0.090	0.028	0.031	0.063	3.370	0.045	0.005	0.233	0.536	4.464	5.530	14.304
7	7.33	9.42	125.4	28.0	0.045	0.055	0.026	0.021	0.051	1.386	0.080	0.007	0.142	0.039	2.319	2.534	6.605
8	9.42	10.75	79.80	2.0	0.005	0.001	0.001	0.001	0.001	0.034	0.012	0.001	0.004	0.002	0.084	0.101	0.239
	TIME-WEIGHTED AVERAGE FOR 8. SAMPLES				0.067		0.042	0.029	0.051	2.790	0.103	0.008	0.211	0.312	4.360	5.544	13.451

TABLE 5. BAKERSFIELD FOG - 14 JAN 83 $

					MICROGRAM / LITER						MICROGRAM / CUBIC METER					
$	TIME1	TIME2	PH	H	FE	MN	PB	CU	NI	V	FE	MN	PB	CU	NI	V
1	-5.50	-4.42	2.69	0.0	10700.	177.0	1704.0	103.0	386.0	324.0	0.214	0.004	0.034	0.002	0.008	0.006
2	-4.42	-3.00	2.81	0.0	2700.0	95.0	1582.0	70.0	582.0	246.0	0.122	0.004	0.071	0.003	0.026	0.011
3	-2.92	-1.00	2.95	0.0	1280.0	41.0	1075.0	50.0	273.0	205.0	0.090	0.003	0.075	0.004	0.019	0.014
4	-0.17	2.00	3.22	0.0	356.0	8.0	532.0	12.0	186.0	111.0	0.032	0.001	0.048	0.001	0.017	0.010
5	2.08	5.08	3.41	0.0	265.0	6.0	286.0	7.0	224.0	92.0	0.025	0.001	0.027	0.001	0.021	0.009
6	5.08	7.33	3.50	0.0	352.0	9.0	373.0	12.0	175.0	104.0	0.032	0.001	0.034	0.001	0.016	0.009
7	7.33	9.42	3.33	0.0	475.0	13.0	529.0	21.0	140.0	73.0	0.026	0.001	0.029	0.001	0.008	0.004
8	9.42	10.75	2.94	0.0	-0.1	-0.1	-0.1	-0.1	-0.1	-0.1	-0.000	-0.000	-0.000	-0.000	-0.000	-0.000

ENTERED 8/11/83

TABLE 1. BAKERSFIELD FOG - 15 JAN 83 *

				/ / / / / /			MICRO EQ/LITER				\ \ \ \ \ \			/ MICRO M/L \		/MM/L\
*	TIME1	TIME2	PH	H	NA	K	NH4	CA	MG	F	CL	NO3	SO4	-/+	S(IV)	CH2O	TOC
1	-1.25	-0.58	5.09	8.1	31.6	22.0	2415.0	358.0	41.5	190.0	140.0	920.0	1400.0	0.921	904.0	199.0	7.1
2	-0.58	1.25	4.42	38.0	8.9	7.4	1640.0	41.0	7.7	110.0	50.0	440.0	710.0	0.752	535.0	82.0	4.8
3	1.25	2.75	4.52	30.2	8.2	6.3	1070.0	26.0	4.5	105.0	42.0	380.0	490.0	0.888	585.0	93.0	4.7
4	2.75	4.25	4.41	38.9	5.7	5.9	780.0	18.6	2.2	100.0	42.0	415.0	445.0	1.177	631.0	153.0	3.8
5	4.25	6.00	4.65	22.4	5.0	7.0	1425.0	16.6	3.0	60.0	31.0	492.0	1180.0	1.190	802.0	170.0	3.2
6	6.00	7.25	4.60	25.1	2.2	4.5	1327.0	24.0	3.6	70.0	30.0	440.0	953.0	1.077	488.0	151.0	2.5
7	7.50	8.75	3.62	240.0	8.5	9.9	900.0	24.0	3.3	25.0	23.0	570.0	1050.0	1.407	428.0	114.0	4.8
8	8.75	9.75	3.06	871.0	22.8	5.9	1785.0	80.0	10.8	136.0	110.0	868.0	1550.0	0.960	750.0	279.0	6.0
9	9.75	10.50	2.80	1580.0	56.1	13.7	3310.0	470.0	32.0	178.0	108.0	1485.0	4200.0	1.093	1160.	304.0	-1.0
10	10.50	11.50	2.56	2750.0	202.0	53.4	5700.0	-0.1	-0.1	450.0	400.0	3140.0	9400.0	1.538	-1.0	-1.0	-1.0

REVISED 5/14/83

TABLE 2. BAKERSFIELD FOG - 15 JAN 83 *

					EQUIVALENT RATIOS								MOLAR RATIOS	
*	TIME1	TIME2	DT(MIN)	MIDT	-/+	CL/NA	MG/NA	CA/NA	SO4/NA	NO3/SO4	NH4/N+S	H/N+S	H+A/N+S	S(IV)/SO4	S(IV)/CH2O
1	-1.25	-0.58	40.20	-0.92	0.921	4.430	1.313	11.329	44.304	0.657	1.041	0.003	1.044	1.291	4.543
2	-0.58	1.25	109.8	0.34	0.752	5.618	0.865	4.607	79.775	0.620	1.426	0.033	1.459	1.507	6.524
3	1.25	2.75	90.00	2.00	0.888	5.122	0.549	3.171	59.756	0.776	1.230	0.035	1.265	2.388	6.290
4	2.75	4.25	90.00	3.50	1.177	7.368	0.386	3.263	78.070	0.933	0.907	0.045	0.952	2.836	4.124
5	4.25	6.00	105.0	5.13	1.190	6.200	0.600	3.720	236.00	0.417	0.852	0.013	0.866	1.359	4.718
6	6.00	7.25	75.00	6.63	1.077	13.636	1.636	10.909	433.18	0.462	0.953	0.018	0.971	1.024	3.232
7	7.50	8.75	75.00	8.12	1.407	2.706	0.388	2.824	123.52	0.843	0.556	0.148	0.704	0.815	3.754
8	8.75	9.75	60.00	9.25	0.960	4.825	0.474	3.509	67.982	0.560	0.738	0.360	1.098	0.968	2.688
9	9.75	10.50	45.00	10.13	1.093	1.925	0.570	8.378	74.866	0.354	0.582	0.278	0.860	0.552	3.816
10	10.50	11.50	60.00	11.00	1.538	1.980	-0.000	-0.000	46.535	0.354	0.455	0.219	0.674	-0.000	1.000
	SEA SALT RATIOS					1.17	0.228	0.043	0.120						

REVISED 5/14/83

TABLE 3. BAKERSFIELD FOG - 15 JAN 83 *

MASS SOLUTE PER M3 AIR IS BASED ON LIQUID WATER CONTENT EITHER MEASURED (IF AVAILABLE)
OR CALCULATED FROM THE VOLUME OF FOGWATER COLLECTED AND ASSUMING A SAMPLING RATE = 5 M3/MIN (A LOWER BOUND)

			/ MICRO M/L \		/MM/L\	/ MICROGRAM / CUBIC METER \							
*	TIME1	TIME2	S(IV)	CH2O	TOC	LWC(G/M3) CALC.	LWC(G/M3) MEAS.	S(IV)	CH2O	TOC	-/+	'CORRECTED -/+'	PH	'PH-BY-DIFFERENCE'
1	-1.25	-0.58	904.0	199.0	7.1	0.080	0.075	2.170	0.448	6.390	0.921	0.855	5.09	*****
2	-0.58	1.25	535.0	82.0	4.8	0.080	0.200	3.424	0.492	11.520	0.752	0.688	4.42	*****
3	1.25	2.75	585.0	93.0	4.7	0.111	0.200	3.744	0.558	11.280	0.888	0.796	4.52	*****
4	2.75	4.25	631.0	153.0	3.8	0.120	0.140	2.827	0.643	6.384	1.177	1.059	4.41	4.05
5	4.25	6.00	802.0	170.0	3.2	0.114	0.350	8.982	1.785	13.440	1.190	1.149	4.65	3.61
6	6.00	7.25	488.0	151.0	2.5	0.107	0.270	4.216	1.223	8.100	1.077	1.026	4.60	4.22
7	7.50	8.75	428.0	114.0	4.8	0.091	0.220	3.013	0.752	12.672	1.407	1.377	3.62	3.16
8	8.75	9.75	750.0	279.0	6.0	0.060	0.094	2.256	0.787	6.768	0.960	0.892	3.06	3.24
9	9.75	10.50	1160.	304.0	-1.0	0.044	0.023	0.854	0.210	-1.000	1.093	1.016	2.80	2.78
10	10.50	11.50	-1.0	-1.0	-1.0	0.007	0.005	-1.000	-1.000	-1.000	1.538	1.386	2.56	2.21
TIME-WEIGHTED AVERAGE FOR 10. SAMPLES							0.181	3.933	0.829	10.057				

TABLE 4. BAKERSFIELD FOG - 15 JAN 83 $

MASS SOLUTE PER M3 AIR IS BASED ON LIQUID WATER CONTENT EITHER MEASURED (IF AVAILABLE)
OR CALCULATED FROM THE VOLUME OF FOGWATER COLLECTED AND ASSUMING A SAMPLING RATE = 5 M3/MIN (AN LOWER BOUND)

							MICROGRAM / CUBIC METER									
#	TIME1	TIME2	DT (MIN)	VOL	LWC(G/M3) CALC.	LWC(G/M3) MEAS.	H	NA	K	NH4	CA	MG	F	CL	NO3	SO4	MASS
1	-1.25	-0.58	40.20	16.0	0.080	0.075	0.001	0.055	0.065	3.260	0.537	0.038	0.271	0.372	4.278	5.040	13.916
2	-0.58	1.25	109.8	44.0	0.080	0.200	0.008	0.041	0.058	5.904	0.164	0.019	0.418	0.354	5.456	6.816	19.238
3	1.25	2.75	90.00	50.0	0.111	0.200	0.006	0.038	0.049	3.852	0.104	0.011	0.399	0.298	4.712	4.704	14.173
4	2.75	4.25	90.00	54.0	0.120	0.140	0.005	0.018	0.032	1.966	0.052	0.004	0.266	0.208	3.602	2.990	9.145
5	4.25	6.00	105.0	60.0	0.114	0.350	0.008	0.040	0.096	8.977	0.130	0.013	0.399	0.385	10.676	19.824	40.548
6	6.00	7.25	75.00	40.0	0.107	0.270	0.007	0.014	0.048	6.449	0.130	0.012	0.359	0.287	7.366	12.351	27.021
7	7.50	8.75	75.00	34.0	0.091	0.220	0.053	0.043	0.085	3.564	0.106	0.009	0.104	0.179	7.775	11.088	23.006
8	8.75	9.75	60.00	18.0	0.060	0.094	0.082	0.049	0.022	3.020	0.150	0.012	0.243	0.367	5.059	6.994	15.998
9	9.75	10.50	45.00	10.0	0.044	0.023	0.036	0.030	0.012	1.370	0.216	0.009	0.078	0.088	2.118	4.637	8.594
10	10.50	11.50	60.00	2.0	0.007	0.005	0.014	0.023	0.010	0.513	-0.100	-0.100	0.043	0.071	0.973	2.256	3.243
	TIME-WEIGHTED AVERAGE FOR 10. SAMPLES				0.181		0.019	0.035	0.052	4.739	0.138	0.013	0.285	0.273	5.644	8.329	19.528

TABLE 5. BAKERSFIELD FOG - 15 JAN 83 $

					MICROGRAM / LITER						MICROGRAM / CUBIC METER					
#	TIME1	TIME2	PH	H	FE	MN	PB	CU	NI	V	FE	MN	PB	CU	NI	V
1	-1.25	-0.58	5.09	0.0	4320.0	216.0	552.0	410.0	704.0	55.6	0.324	0.016	0.041	0.031	0.053	0.004
2	-0.58	1.25	4.42	0.0	825.0	39.1	253.0	83.0	239.0	37.0	0.165	0.008	0.051	0.017	0.048	0.007
3	1.25	2.75	4.52	0.0	533.0	17.9	195.0	29.0	56.9	24.7	0.107	0.004	0.039	0.006	0.011	0.005
4	2.75	4.25	4.41	0.0	357.0	13.9	202.0	21.0	47.0	25.3	0.050	0.002	0.028	0.003	0.007	0.004
5	4.25	6.00	4.65	0.0	301.0	11.5	114.0	30.0	45.9	30.0	0.105	0.004	0.040	0.010	0.016	0.010
6	6.00	7.25	4.60	0.0	203.0	9.8	110.0	11.0	38.5	26.4	0.055	0.003	0.030	0.003	0.010	0.007
7	7.50	8.75	3.62	0.0	183.0	10.3	255.0	28.0	37.7	25.1	0.040	0.002	0.056	0.006	0.008	0.006
8	8.75	9.75	3.06	0.0	1023.0	36.9	665.0	32.0	67.0	41.5	0.096	0.003	0.063	0.003	0.006	0.004
9	9.75	10.50	2.80	0.0	-0.1	3480.0	-0.1	-0.1	1174.0	-0.1	-0.000	0.080	-0.000	-0.000	0.027	-0.000
10	10.50	11.50	2.56	0.0	-0.1	-0.1	-0.1	-0.1	-0.1	-0.1	-0.000	-0.000	-0.000	-0.000	-0.000	-0.000

ENTERED 8/11/83

APPENDIX E

FOGWATER AND AEROSOL CHEMICAL COMPOSITION, $HNO_3(g)$ AND $NH_3(g)$ CONCENTRATIONS: SAN JOAQUIN VALLEY, CALIFORNIA, DECEMBER 1983 - JANUARY 1984

** BAKERSFIELD **

DATE	T1	DT	NA+	K+	NH4+	CA++	MG++	CL-	NO3-	SO4--	S(IV)	HNO3G	NH3G	<H>	ERROR
12/15	0.000	3.970	-.001	-.001	-.001	-.001	-.001	0.034	0.126	0.134	0.054	-.001	-.001	0.299	0
12/15	12.67	3.850	-.001	-.001	0.043	-.001	-.001	0.000	0.022	0.013	0.026	-.001	-.001	-.004	0
12/16	0.000	4.040	-.001	-.001	-.001	-.001	-.001	-.001	-.001	-.001	0.053	-.001	-.001	0.002	0
12/16	12.00	3.980	-.001	-.001	0.486	-.001	-.001	0.017	0.293	0.293	0.305	-.001	-.001	0.121	0
12/17	2.500	3.900	0.015	0.007	0.256	0.025	0.006	0.013	0.201	0.107	0.060	-.001	-.001	0.012	0
12/17	19.00	3.840	0.119	0.000	0.217	0.021	0.005	0.026	0.104	0.091	0.026	-.001	-.001	-.141	0
12/18	14.42	3.900	0.012	0.000	0.419	0.036	0.007	0.000	0.308	0.154	0.065	-.001	-.001	-.012	0
12/19	14.00	4.030	0.008	0.000	0.149	0.050	0.007	0.000	0.083	0.033	-.001	-.001	-.001	-.098	0
12/20	12.00	4.050	0.012	0.006	0.148	0.032	0.006	0.000	0.148	0.058	0.043	-.001	-.001	0.002	0
12/27	8.500	9.310	0.009	0.004	0.023	0.090	0.007	0.011	0.013	0.014	-.001	0.035	0.124	-.095	0
12/31	0.000	3.750	0.008	0.016	0.573	0.028	0.006	0.067	0.351	0.351	0.046	0.017	0.019	0.138	0
12/31	12.00	4.210	0.007	0.006	0.669	0.029	0.005	0.004	0.467	0.297	0.032	0.004	0.158	0.052	1
1/ 1	-2.25	10.52	0.003	0.001	0.242	0.006	0.001	0.000	0.170	0.089	0.006	0.002	0.212	0.006	0
1/ 1	12.00	4.240	0.007	0.000	0.275	0.018	0.004	0.000	0.161	0.161	0.013	0.035	0.068	0.018	0
1/ 2	0.000	4.270	0.006	0.000	0.273	0.028	0.005	0.047	0.168	0.109	-.001	0.014	0.067	0.012	0
1/ 2	12.00	4.310	0.007	0.000	0.344	0.023	0.004	0.023	0.201	0.124	-.001	0.025	0.107	-.030	8
1/ 3	0.000	4.280	0.014	0.006	0.545	0.021	0.005	0.004	0.370	0.226	-.001	0.001	0.483	0.009	0
1/ 3	12.00	4.270	0.012	0.005	0.769	0.047	0.008	0.016	0.445	0.445	0.165	0.011	0.113	0.065	0
1/ 4	12.00	5.000	0.016	0.007	1.057	0.057	0.010	0.010	0.427	0.660	0.168	0.024	0.055	-.050	2
1/ 5	1.000	4.150	0.056	0.019	1.141	0.040	0.007	0.000	0.442	0.731	0.193	0.006	0.063	-.090	0
1/ 5	12.00	4.280	0.010	0.004	0.923	0.043	0.007	0.058	0.362	0.596	0.044	0.019	0.060	0.029	0
1/ 6	0.000	4.250	0.031	0.008	1.149	0.039	0.005	0.043	0.388	0.855	0.094	0.007	0.047	0.054	0
1/ 6	12.00	4.280	0.010	0.009	0.783	0.051	0.007	0.051	0.214	0.662	0.265	0.029	-.001	0.067	0
1/ 7	13.50	4.310	0.008	0.005	0.638	0.027	0.005	0.023	0.186	0.468	0.118	-.001	0.201	-.006	0
1/ 8	0.000	4.110	0.005	0.000	0.272	0.008	0.002	0.020	0.142	0.118	0.091	0.006	0.052	-.007	0
1/ 8	12.00	4.290	0.005	0.000	0.264	0.008	0.003	0.012	0.085	0.167	0.090	-.001	0.079	-.016	0
1/ 9	14.33	4.110	0.008	0.004	0.260	0.041	0.005	0.032	0.085	0.219	-.001	0.008	0.139	0.018	0
1/10	0.000	4.270	0.009	0.000	0.621	0.020	0.003	0.008	0.117	0.570	-.001	0.046	0.060	0.042	0
1/10	12.00	12.00	0.006	0.004	0.002	0.190	0.014	0.002	0.004	0.054	0.119	-.001	0.010	-.156	6
1/11	0.000	4.060	0.006	0.000	0.369	0.020	0.004	0.033	0.205	0.148	0.079	-.001	-.001	-.013	0
1/11	12.00	4.270	0.009	0.000	0.144	0.049	0.006	0.020	0.165	0.078	-.001	0.046	0.065	-.005	0
1/12	0.000	4.250	0.028	0.007	0.345	0.055	0.009	0.051	0.204	0.149	0.129	0.004	0.157	-.040	0
1/12	12.00	4.230	0.027	0.000	0.331	0.025	0.010	0.033	0.244	0.169	-.001	0.026	0.334	0.002	0
1/13	0.000	4.010	0.014	0.005	0.406	0.029	0.005	0.033	0.283	0.407	-.001	0.004	0.208	0.184	0
1/13	7.000	4.250	0.013	0.005	0.729	0.039	0.005	0.039	0.349	0.475	-.001	0.006	0.123	0.072	0
1/13	12.00	4.270	0.023	0.008	0.855	0.070	0.012	0.049	0.432	0.507	-.001	0.014	0.240	0.015	0
1/13	18.00	4.190	0.023	0.007	0.692	0.040	0.006	0.044	0.402	0.306	-.001	0.010	0.161	-.016	0
1/14	0.830	3.350	0.019	0.000	0.567	0.032	0.006	0.045	0.423	0.229	-.001	0.005	0.180	0.073	0
1/14	7.580	3.900	0.021	0.005	0.641	0.035	0.008	0.038	0.473	0.214	-.001	0.006	0.470	-.035	0
1/14	12.00	4.250	0.024	0.000	0.318	0.035	0.009	0.020	0.263	0.129	-.001	0.043	0.118	0.026	4

ALL CONCENTRATIONS ARE IN MICROEQ/M3 EXCEPT S(IV) WHICH IS IN MICROMOLES/M3. TIMES ARE GIVEN IN HOURS PST.
ERROR CODE: 1 = HANDLING, 2 = SAMPLING TIME, 4 = UNCERTAINTY T/AC/F, 8 = LOCAL SOURCE
WHEN -.001 IS DISPLAYED THE CONCENTRATION WAS NOT DETERMINED.
<H> IS CALCULATED BY IONIC BALANCE ON THE AEROSOL. PROOFED 6/18/84 - DJJ

** WASCO **

DATE	T1	DT	NA+	K+	NH4+	CA++	MG++	CL-	NO3-	SO4--	S(IV)	HNO3G	NH3G	(H)	ERROR
12/15	0.000	3.960	-.001	-.001	0.084	-.001	-.001	0.021	0.067	0.034	0.000	-.001	-.001	0.042	0
12/16	0.000	3.960	-.001	-.001	0.143	-.001	-.001	0.017	0.093	0.046	0.094	-.001	-.001	0.017	0
12/17	18.00	3.740	0.011	0.000	0.116	0.028	0.023	0.040	0.116	0.067	-.001	-.001	-.001	0.045	0
12/18	13.00	3.960	0.009	0.000	0.345	0.014	0.003	0.017	0.290	0.080	0.047	-.001	-.001	0.016	1
12/19	14.00	3.970	0.223	-.001	0.336	0.118	0.050	0.042	0.227	0.067	0.104	-.001	-.001	-.390	0
12/20	13.00	4.000	0.013	0.000	0.033	0.021	0.004	0.008	0.033	0.008	0.047	-.001	-.001	-.022	0
12/27	8.000	4.430	0.006	0.000	0.026	0.013	0.003	0.019	0.019	0.008	0.042	0.030	0.147	-.002	0
12/31	0.000	3.780	0.014	0.000	0.176	0.011	0.001	0.000	0.104	0.029	0.000	0.014	0.053	-.069	0
12/31	12.00	4.270	0.003	0.000	0.121	0.006	0.001	0.000	0.098	0.020	0.000	0.017	0.077	-.013	0
1/ 1	0.000	4.280	0.003	0.000	0.129	0.008	0.001	0.000	0.109	0.019	0.016	0.000	0.273	-.013	0
1/ 1	12.00	4.280	0.009	0.000	0.261	0.016	0.004	0.004	0.156	0.125	0.006	0.051	0.044	-.005	0
1/ 2	0.000	4.280	0.005	0.000	0.428	0.014	0.002	0.008	0.308	0.132	-.001	0.001	0.195	-.001	0
1/ 2	12.00	4.250	0.004	0.004	0.220	0.012	0.002	0.031	0.153	0.075	-.001	0.026	0.054	0.017	5
1/ 3	0.000	4.850	0.086	0.020	0.275	0.014	0.003	0.093	0.203	0.096	-.001	0.000	0.076	-.006	2
1/ 3	12.00	3.470	0.005	0.000	0.394	0.019	0.003	0.029	0.283	0.125	-.001	0.004	0.156	0.016	0
1/ 4	0.000	4.050	0.006	0.000	0.519	0.014	0.003	0.012	0.329	0.239	0.053	0.041	0.010	0.038	0
1/ 4	12.00	4.270	0.004	0.000	0.453	0.021	0.003	0.016	0.343	0.141	0.153	0.013	0.044	0.019	0
1/ 5	12.00	4.280	0.006	0.004	0.518	0.019	0.004	0.047	0.366	0.199	0.044	0.006	0.044	0.061	0
1/ 6	0.000	4.280	0.006	0.005	0.584	0.016	0.003	0.012	0.409	0.312	0.059	0.022	0.012	0.119	0
1/ 6	12.00	4.290	0.007	0.000	0.497	0.012	0.002	0.016	0.208	0.297	0.068	0.016	0.019	0.003	0
1/ 7	0.000	3.960	0.008	0.000	0.290	0.006	0.001	0.019	0.116	0.181	0.111	0.004	-.001	0.011	0
1/ 7	12.00	4.280	0.004	0.000	0.218	0.012	0.002	0.039	0.097	0.113	0.044	0.010	0.038	0.013	0
1/ 8	0.000	4.290	0.003	0.000	0.105	0.004	0.001	0.031	0.062	0.043	0.034	-.001	0.013	0.023	0
1/ 8	12.00	4.280	-.001	-.001	0.132	-.001	-.001	0.047	0.023	0.093	0.128	-.001	0.002	0.035	4
1/ 9	0.000	4.270	0.003	0.000	0.125	0.006	0.001	0.012	0.027	0.098	-.001	0.027	0.013	0.002	0
1/ 9	12.00	4.030	0.006	0.000	0.095	0.017	0.002	0.033	0.037	0.120	0.056	-.001	0.000	0.070	0
1/10	0.000	4.260	0.005	0.004	0.376	0.012	0.002	0.031	0.106	0.231	-.001	0.013	-.001	-.031	0
1/10	12.00	4.280	0.006	0.000	0.296	0.018	0.003	0.023	0.109	0.234	-.001	0.023	0.076	0.043	0
1/11	0.000	4.320	0.004	0.003	0.285	0.010	0.002	0.023	0.162	0.139	-.001	0.042	0.000	0.020	0
1/11	12.00	4.290	0.005	0.000	0.074	0.008	0.001	0.027	0.047	0.031	-.001	0.029	0.058	0.017	0
1/12	0.000	4.330	0.014	0.009	0.269	0.038	0.006	0.000	0.185	0.100	-.001	0.004	0.154	-.051	0
1/12	12.00	4.270	0.027	0.005	0.363	0.032	0.005	0.027	0.281	0.137	-.001	0.027	0.094	0.013	0
1/13	0.000	4.270	0.012	0.000	0.454	0.017	0.003	0.007	0.342	0.157	-.001	0.006	0.194	0.020	2
1/13	12.00	4.130	0.025	0.000	0.367	0.028	0.006	0.014	0.295	0.153	-.001	0.030	0.039	0.066	0
1/14	0.000	4.020	0.016	0.005	0.535	0.023	0.004	0.000	0.419	0.178	-.001	0.006	0.097	0.014	0
1/14	12.00	4.290	0.039	0.000	0.365	0.043	0.010	0.012	0.287	0.155	-.001	0.054	0.068	-.003	0

ALL CONCENTRATIONS ARE IN MICROEQ/M3 EXCEPT S(IV) WHICH IS IN MICROMOLES/M3. TIMES ARE GIVEN IN HOURS PST.
ERROR CODE: 1 = HANDLING, 2 = SAMPLING TIME, 4 = UNCERTAINTY T/AC/F, 8 = LOCAL SOURCE
WHERE -.001 IS DISPLAYED THE CONCENTRATION WAS NOT DETERMINED.
(H) IS CALCULATED BY IONIC BALANCE ON THE AEROSOL. PROOFED 6/18/84 - DJJ

AEROSOL, HNO3G, AND NH3G LOADINGS — SAN JOAQUIN VALLEY DEC.1983-JAN.1984 SAMPLING PROGRAM

** MC KITTRICK **

DATE	T1	DT	NA+	K+	NH4+	CA++	MG++	CL-	NO3-	SO4--	S(IV)	HNO3G	NH3G	<H>	ERROR
12/16	1.670	3.780	0.007	0.000	0.039	0.015	0.003	0.000	0.013	0.018	0.018	-.001	-.001	-.033	1
12/17	18.00	3.980	0.007	0.000	0.134	0.013	0.002	0.025	0.080	0.067	-.001	-.001	-.001	0.016	4
12/18	13.00	3.970	0.012	0.004	0.256	0.016	0.003	0.021	0.218	0.076	0.118	-.001	-.001	0.024	0
12/19	14.33	4.020	0.004	-.001	0.124	0.025	0.004	0.008	0.091	0.025	0.056	-.001	-.001	-.032	0
12/20	13.00	4.000	0.026	0.000	0.025	0.048	0.009	0.017	0.083	0.050	0.057	-.001	-.001	0.042	8
12/27	14.75	7.030	0.007	0.000	0.073	0.015	0.003	0.009	0.026	0.055	0.034	0.023	0.047	-.008	0
12/31	0.670	3.800	0.010	0.000	0.259	0.022	0.003	0.022	0.175	0.096	0.018	0.048	0.018	-.001	0
12/31	12.08	4.150	0.022	0.000	0.193	0.042	0.005	0.032	0.124	0.112	0.016	0.000	0.111	0.006	0
1/ 1	12.00	4.300	0.009	0.000	0.198	0.012	0.002	0.000	0.140	0.078	0.006	0.028	0.063	-.003	1
1/ 2	0.500	4.230	0.007	0.000	0.244	0.012	0.002	0.039	0.162	0.102	-.001	0.021	0.205	0.038	0
1/ 2	12.00	4.270	0.009	0.000	0.383	0.016	0.002	0.020	0.246	0.160	-.001	0.069	0.050	0.016	1
1/ 3	0.000	4.080	0.012	0.000	0.261	0.016	0.004	0.000	0.094	0.266	-.001	0.065	0.196	0.067	0
1/ 3	12.00	4.280	0.009	0.000	0.424	0.019	0.004	0.031	0.183	0.280	-.001	0.164	0.020	0.038	0
1/ 4	0.000	4.200	0.024	0.000	0.385	0.014	0.005	0.032	0.036	0.802	0.076	0.020	0.000	0.442	0
1/ 4	12.00	4.270	0.012	0.000	0.226	0.032	0.005	0.020	0.031	0.304	0.234	0.101	0.000	0.080	0
1/ 5	0.750	3.470	0.010	0.000	0.187	0.012	0.003	0.019	0.062	0.202	0.277	0.001	0.000	0.071	0
1/ 5	12.00	4.930	0.008	0.000	0.267	0.017	0.003	0.010	0.068	0.274	0.165	0.024	0.000	0.057	2
1/ 6	0.000	4.170	0.010	0.000	0.208	0.010	0.002	0.000	0.028	0.276	0.080	0.007	0.007	0.074	0
1/ 6	12.00	4.220	0.017	0.000	0.363	0.034	0.006	0.020	0.073	0.385	0.060	0.039	-.001	0.058	0
1/ 7	0.000	4.220	0.015	0.000	0.194	0.012	0.002	0.028	0.012	0.229	0.212	0.009	-.001	0.046	1
1/ 7	12.00	4.220	0.008	0.000	0.197	0.010	0.002	0.024	0.047	0.205	0.224	0.011	0.004	0.059	0
1/ 8	0.000	4.180	0.008	0.000	0.144	0.006	0.001	0.032	0.028	0.120	0.048	0.005	0.007	0.021	0
1/ 8	12.00	4.220	0.009	0.000	0.197	0.006	0.002	0.028	0.032	0.209	0.145	-.001	0.000	0.055	0
1/ 9	0.000	4.200	0.038	0.000	0.183	0.012	0.002	0.000	0.010	0.198	0.127	-.001	0.000	-.027	4
1/ 9	12.00	4.220	0.005	0.000	0.028	0.016	0.001	0.028	0.016	0.036	0.054	-.001	0.009	0.030	1
1/10	0.750	4.030	0.009	0.000	0.227	0.019	0.003	0.029	0.037	0.294	-.001	0.010	-.001	0.102	1
1/10	12.00	4.230	0.070	0.013	0.197	0.043	0.006	0.071	0.059	0.114	-.001	0.017	-.001	-.085	4
1/11	1.000	4.200	0.021	0.004	0.119	0.016	0.003	0.000	0.071	0.052	-.001	0.007	0.000	-.040	0
1/11	12.00	4.220	0.009	0.004	0.095	0.022	0.004	0.008	0.016	0.059	-.001	0.010	0.038	-.051	0
1/12	0.000	4.200	0.026	0.000	0.071	0.020	0.002	0.020	0.052	0.079	-.001	0.035	0.032	0.032	0
1/12	12.00	4.220	0.029	0.000	0.304	0.039	0.006	0.012	0.197	0.154	-.001	0.043	0.027	-.015	1
1/13	0.500	4.070	0.018	0.006	0.373	0.018	0.004	0.033	0.197	0.266	-.001	0.029	0.000	0.077	0
1/13	12.00	4.220	0.018	0.000	0.197	0.036	0.007	0.008	0.118	0.079	-.001	0.033	-.001	-.053	0
1/14	0.000	4.180	0.016	0.000	0.247	0.012	0.004	0.016	0.140	0.128	-.001	0.031	0.006	0.005	0
1/14	12.00	4.220	0.039	0.004	0.138	0.024	0.010	0.020	0.115	0.083	-.001	0.063	-.001	0.003	0

ALL CONCENTRATIONS ARE IN MICROEQ/M3 EXCEPT S(IV) WHICH IS IN MICROMOLES/M3. TIMES ARE GIVEN IN HOURS PST.
ERROR CODE: 1 = HANDLING, 2 = SAMPLING TIME, 4 = UNCERTAINTY T/AC/F, 8 = LOCAL SOURCE
WHEN -.001 IS DISPLAYED THE CONCENTRATION WAS NOT DETERMINED.
<H> IS CALCULATED BY IONIC BALANCE ON THE AEROSOL.

PROOFED 6/18/84 - DJJ

AEROSOL, HNO3G, AND NH3G LOADINGS — SAN JOAQUIN VALLEY DEC.1983-JAN.1984 SAMPLING PROGRAM

** LOST HILLS **

DATE	T1	DT	NA+	K+	NH4+	CA++	MG++	CL-	NO3-	SO4--	S(IV)	HNO3G	NH3G	(H)	ERROR
12/17	18.00	3.740	0.017	0.000	0.000	0.015	0.004	0.000	0.009	0.009	0.082	-.001	-.001	-.018	2
12/18	13.00	4.000	0.009	0.000	0.054	0.010	0.003	0.017	0.021	0.017	0.042	0.010	-.001	-.021	2
12/19	14.00	3.980	0.018	0.000	0.285	0.021	0.005	0.008	0.230	0.084	0.040	-.001	-.001	-.007	0
12/20	13.00	4.000	0.027	0.000	0.067	0.028	0.007	0.025	0.058	0.013	-.001	-.001	-.001	-.033	0
12/27	-3.83	5.670	0.012	0.000	0.018	0.007	0.003	0.021	0.029	0.026	0.031	0.033	0.061	0.036	0
12/31	0.000	3.830	0.006	0.000	0.218	0.009	0.002	0.017	0.170	0.061	0.000	0.017	0.052	0.013	2
12/31	12.00	4.270	0.010	0.000	0.156	0.008	0.002	0.000	0.109	0.035	0.006	0.035	0.034	-.032	0
1/ 1	0.000	4.300	0.009	0.000	0.066	0.012	0.002	0.000	0.054	0.016	0.006	0.005	0.078	-.019	0
1/ 2	0.000	4.280	0.004	0.000	0.202	0.008	0.001	0.004	0.152	0.055	-.001	0.002	0.000	-.004	0
1/ 2	12.00	4.250	0.003	0.000	0.294	0.014	0.002	0.008	0.188	0.102	-.001	0.065	0.043	-.015	0
1/ 3	0.000	4.300	0.008	0.000	0.422	0.014	0.002	0.019	0.310	0.128	-.001	0.001	0.041	0.011	0
1/ 3	12.00	4.030	0.020	0.000	0.397	0.029	0.005	0.000	0.240	0.182	-.001	0.174	0.024	-.029	4
1/ 4	12.00	4.250	0.006	0.000	0.404	0.025	0.004	0.024	0.184	0.235	0.056	0.075	0.009	0.004	0
1/ 5	12.00	4.250	0.007	0.004	0.553	0.014	0.003	0.024	0.267	0.314	0.176	0.034	0.064	0.024	0
1/ 6	12.00	4.270	0.005	0.000	0.383	0.032	0.002	0.016	0.152	0.250	0.044	0.033	0.016	-.004	0
1/ 7	0.000	4.620	0.006	0.000	0.299	0.005	0.001	0.025	0.083	0.227	0.052	0.005	-.001	0.024	2
1/ 7	12.33	4.220	0.007	0.000	0.071	0.016	0.002	0.000	0.024	0.021	0.101	-.001	-.001	-.051	0
1/ 8	0.000	4.000	0.003	0.000	0.075	0.008	0.001	0.017	0.050	0.033	0.070	-.001	0.006	0.013	0
1/ 8	12.23	4.170	0.002	0.000	0.080	0.004	0.000	0.024	0.048	0.032	0.035	-.001	0.000	0.018	0
1/ 9	0.000	4.170	0.003	0.000	0.148	0.012	0.001	0.000	0.048	0.112	-.001	0.047	0.000	-.004	0
1/ 9	12.00	4.230	0.006	0.000	0.055	0.016	0.002	0.008	0.004	0.032	0.142	0.049	0.000	-.035	0
1/10	0.000	4.020	0.008	0.000	0.133	0.021	0.003	0.000	0.028	0.066	-.001	0.012	-.001	-.071	0
1/10	12.00	4.270	0.004	0.000	0.215	0.014	0.001	0.016	0.070	0.168	-.001	0.038	0.044	0.020	0
1/11	0.000	4.230	0.004	0.000	0.154	0.006	0.001	0.000	0.099	0.055	-.001	0.010	0.002	-.011	0
1/11	12.00	4.270	0.012	0.000	0.094	0.012	0.001	0.016	0.059	0.039	-.001	0.015	0.087	-.005	0
1/12	0.000	4.030	0.023	0.007	0.132	0.021	0.003	0.017	0.103	0.054	-.001	0.005	0.088	-.012	0
1/12	12.00	4.250	0.040	0.000	0.192	0.057	0.007	0.020	0.188	0.133	-.001	0.095	0.047	0.045	0
1/13	12.00	4.250	0.022	0.000	0.176	0.024	0.004	0.012	0.173	0.114	-.001	0.063	0.000	0.073	4
1/14	0.000	4.020	0.013	0.004	0.398	0.015	0.004	0.021	0.286	0.108	-.001	0.022	0.026	-.019	0
1/14	12.00	4.270	0.048	0.000	0.269	0.025	0.011	0.043	0.215	0.121	-.001	0.078	0.020	0.026	0

ALL CONCENTRATIONS ARE IN MICROEQ/M3 EXCEPT S(IV) WHICH IS IN MICROMOLES/M3. TIMES ARE GIVEN IN HOURS PST.
ERROR CODE: 1 = HANDLING, 2 = SAMPLING TIME, 4 = UNCERTAINTY T/AC/F, 8 = LOCAL SOURCE
WHEN -.001 IS DISPLAYED THE CONCENTRATION WAS NOT DETERMINED.
(H) IS CALCULATED BY IONIC BALANCE ON THE AEROSOL.

PROOFED 6/18/84 - DJJ

** BUTTONWILLOW **

DATE	T1	DT	NA+	K+	NH4+	CA++	MG++	CL-	NO3-	SO4--	S(IV)	HNO3G	NH3G	(H)	ERROR
1/ 5	0.000	4.030	-.001	-.001	-.001	-.001	-.001	0.025	0.368	0.579	-.001	0.001	0.142	0.977	0
1/ 5	12.00	4.000	0.006	0.000	0.663	0.029	0.005	0.021	0.287	0.421	0.077	0.027	0.027	0.026	0
1/ 6	0.000	4.050	0.006	0.000	0.642	0.012	0.003	0.004	0.358	0.284	0.069	0.012	0.040	-.017	0
1/ 6	12.00	4.070	0.006	0.000	0.479	0.027	0.004	0.000	0.127	0.360	0.108	0.014	0.029	-.029	0
1/ 7	1.000	3.900	0.025	0.005	0.274	0.006	0.002	0.030	0.073	0.171	0.137	0.004	0.069	-.038	0
1/ 7	12.00	3.990	0.010	0.000	0.175	0.025	0.003	0.038	0.071	0.125	0.157	0.008	0.038	0.021	0
1/ 8	2.000	3.900	0.026	0.000	0.145	0.017	0.003	0.000	0.056	0.037	0.051	-.001	0.047	-.098	1
1/ 8	12.00	3.980	0.022	0.000	0.117	0.021	0.002	0.004	0.034	0.080	0.074	-.001	0.018	-.044	0
1/ 9	0.000	3.760	0.004	0.000	0.120	0.016	0.003	0.022	0.049	0.106	-.001	-.001	0.076	0.034	0
1/ 9	12.00	4.020	0.006	0.000	0.199	0.041	0.006	0.021	0.058	0.166	0.063	-.001	0.037	-.007	0
1/10	0.000	4.140	0.004	0.000	0.229	0.016	0.002	0.032	0.097	0.145	-.001	0.006	-.001	0.023	0
1/10	12.00	3.900	0.008	0.000	0.209	0.035	0.006	0.030	0.085	0.171	-.001	0.020	0.060	0.028	0
1/11	0.000	4.520	0.016	0.000	0.313	0.015	0.001	0.004	0.177	0.188	-.001	0.008	0.065	0.024	2
1/11	12.58	3.230	0.009	0.000	0.036	0.034	0.004	0.041	0.041	0.031	-.001	0.015	0.198	0.030	0
1/12	0.000	3.990	0.051	0.000	0.071	0.042	0.004	0.021	0.092	0.071	-.001	0.000	0.393	0.016	0
1/12	12.00	4.030	0.045	0.010	0.356	0.062	0.010	0.037	0.310	0.174	-.001	0.037	0.645	0.038	4
1/13	1.000	3.920	0.026	0.000	0.485	0.032	0.005	0.030	0.400	0.157	-.001	0.006	0.170	0.039	0
1/13	12.00	3.950	0.028	0.000	0.397	0.068	0.011	0.034	0.329	0.177	-.001	0.023	0.063	0.036	0
1/14	0.000	4.000	0.024	0.000	0.512	0.035	0.008	0.033	0.387	0.167	-.001	0.006	0.267	0.008	6
1/14	12.00	4.040	0.034	0.000	0.388	0.047	0.011	0.033	0.285	0.140	-.001	-.001	0.103	-.022	0

ALL CONCENTRATIONS ARE IN MICROEQ/M3 EXCEPT S(IV) WHICH IS IN MICROMOLES/M3. TIMES ARE GIVEN IN HOURS PST.
ERROR CODE: 1 = HANDLING, 2 = SAMPLING TIME, 4 = UNCERTAINTY T/AC/F, 8 = LOCAL SOURCE
WHEN -.001 IS DISPLAYED THE CONCENTRATION WAS NOT DETERMINED.
(H) IS CALCULATED BY IONIC BALANCE ON THE AEROSOL. PROOFED 6/18/84 - DJJ

AEROSOL, HNO3G, AND NH3G LOADINGS — SAN JOAQUIN VALLEY DEC.1983-JAN.1984 SAMPLING PROGRAM

** VISALIA **

DATE	T1	DT	NA+	K+	NH4+	CA++	MG++	CL-	NO3-	SO4--	S(IV)	HNO3G	NH3G	(H)	ERROR
12/17	14.50	4.200	0.000	0.000	0.317	0.000	0.000	0.020	0.230	0.071	0.000	-.001	-.001	0.004	0
12/18	3.000	4.200	0.006	0.004	0.472	0.015	0.003	0.008	0.345	0.115	0.040	-.001	-.001	-.032	0
12/18	12.00	4.200	0.004	0.004	0.365	0.019	0.004	0.000	0.254	0.071	0.000	-.001	-.001	-.071	0
12/19	11.67	6.980	0.031	0.012	0.308	0.031	0.007	0.021	0.213	0.096	-.001	-.001	-.001	-.059	0
1/ 1	-.250	7.070	0.004	0.004	0.108	0.006	0.003	0.033	0.078	0.035	0.000	0.010	0.599	0.021	0
1/ 1	11.75	6.670	0.003	0.002	0.267	0.015	0.003	0.022	0.192	0.092	0.030	0.012	0.280	0.016	0
1/ 2	0.500	3.900	0.007	0.006	0.252	0.013	0.002	0.017	0.184	0.073	0.000	0.015	0.316	-.006	0
1/ 2	12.00	3.970	0.005	0.000	0.281	0.021	0.003	0.017	0.202	0.097	0.000	0.008	0.588	0.006	0
1/ 3	0.000	3.970	0.006	0.007	0.218	0.010	0.002	0.025	0.168	0.059	0.000	0.002	0.395	0.009	0
1/ 3	12.00	4.020	0.016	0.006	0.249	0.034	0.005	0.041	0.191	0.079	0.007	0.007	0.235	0.001	0
1/ 4	0.000	3.980	0.009	0.000	0.348	0.026	0.005	0.008	0.318	0.096	0.000	0.004	0.184	0.034	0
1/ 4	12.00	3.950	0.005	0.000	0.359	0.037	0.004	0.000	0.283	0.101	0.007	0.005	0.405	-.021	0
1/ 5	0.000	4.000	0.003	0.000	0.354	0.010	0.002	0.021	0.275	0.112	0.040	0.003	0.467	0.039	0
1/ 5	12.00	3.980	0.009	0.000	0.180	0.034	0.005	0.025	0.121	0.080	0.047	0.011	0.662	-.002	0
1/ 6	0.000	5.230	0.004	0.000	0.166	0.016	0.002	0.013	0.108	0.076	0.028	0.003	0.535	0.009	0
1/ 7	1.750	1.830	0.008	0.000	0.128	0.018	0.005	0.018	0.073	0.046	0.066	0.000	0.592	-.022	0
1/ 7	12.00	4.020	0.007	0.000	0.203	0.015	0.003	0.004	0.083	0.129	0.113	0.005	0.589	-.012	0
1/14	1.500	3.750	-.001	-.001	-.001	-.001	-.001	-.001	-.001	-.001	0.039	0.007	0.427	0.002	0
1/14	12.00	4.020	0.012	0.000	0.435	0.037	0.005	0.012	0.369	0.133	0.050	0.018	0.522	0.025	0

ALL CONCENTRATIONS ARE IN MICROEQ/M3 EXCEPT S(IV) WHICH IS IN MICROMOLES/M3. TIMES ARE GIVEN IN HOURS PST.
ERROR CODE: 1 = HANDLING, 2 = SAMPLING TIME, 4 = UNCERTAINTY T/AC/F, 8 = LOCAL SOURCE
WHEN -.001 IS DISPLAYED THE CONCENTRATION WAS NOT DETERMINED.
(H) IS CALCULATED BY IONIC BALANCE ON THE AEROSOL.

PROOFED 6/18/84 - DJJ

AEROSOL, HNO3G, AND NH3G LOADINGS — SAN JOAQUIN VALLEY DEC.1983-JAN.1984 SAMPLING PROGRAM

** LAKE ISABELLA **

DATE	T1	DT	NA+	K+	NH4+	CA++	MG++	CL-	NO3-	SO4--	S(IV)	HNO3G	NH3G	(H)	ERROR
1/ 4	10.00	5.830	0.007	0.004	0.000	0.011	0.002	0.003	0.006	0.006	0.027	0.017	0.044	-.009	0
1/ 5	10.00	5.780	0.006	0.000	0.007	0.009	0.001	0.014	0.001	0.003	0.055	0.013	0.035	-.005	0
1/ 6	10.00	5.780	0.008	0.000	0.000	0.006	0.001	0.000	0.004	0.000	0.055	0.005	0.025	-.011	0
1/ 7	10.00	5.770	0.004	0.003	0.006	0.007	0.001	0.014	0.017	0.014	0.021	0.014	0.019	0.024	0
1/ 8	10.00	5.780	0.003	0.000	0.000	0.006	0.001	0.000	0.000	0.002	0.058	0.007	0.015	-.008	0
1/ 9	10.00	5.810	0.002	0.000	0.000	0.006	0.001	0.000	0.003	0.003	0.009	-.001	0.021	-.003	0
1/10	10.00	5.800	0.028	0.004	0.011	0.032	0.003	0.011	0.009	0.023	0.018	-.001	0.007	-.035	0
1/11	10.00	5.800	0.017	0.000	0.000	0.014	0.002	0.006	0.003	0.006	0.005	0.007	0.007	-.018	0
1/12	10.00	5.800	0.015	0.000	0.020	0.013	0.003	0.003	0.023	0.017	0.000	0.027	0.009	-.008	0
1/13	10.00	5.800	0.012	0.000	0.032	0.009	0.002	0.003	0.023	0.014	-.001	0.036	0.009	-.015	0

ALL CONCENTRATIONS ARE IN MICROEQ/M3 EXCEPT S(IV) WHICH IS IN MICROMOLES/M3. TIMES ARE GIVEN IN HOURS PST.
ERROR CODE: 1 = HANDLING, 2 = SAMPLING TIME, 4 = UNCERTAINTY T/AC/F, 8 = LOCAL SOURCE
WHEN -.001 IS DISPLAYED THE CONCENTRATION WAS NOT DETERMINED.
(H) IS CALCULATED BY IONIC BALANCE ON THE AEROSOL. PROOFED 6/18/84 - DJJ

AEROSOL, HNO3G, AND NH3G LOADINGS — SAN JOAQUIN VALLEY DEC.1983-JAN.1984 SAMPLING PROGRAM

** TEHACHAPI **

DATE	T1	DT	NA+	K+	NH4+	CA++	MG++	CL-	NO3-	SO4--	S(IV)	HNO3G	NH3G	<H>	ERROR
1/ 1	12.00	4.350	0.006	0.000	0.021	0.017	0.002	0.015	0.008	0.011	-.001	0.007	0.000	-.012	1
1/ 2	10.00	7.220	0.007	0.000	0.004	0.041	0.002	0.000	0.005	0.007	0.004	0.001	0.000	-.042	0
1/ 3	10.00	7.220	0.003	0.000	0.000	0.019	0.002	0.002	0.000	0.002	-.001	-.001	-.001	-.020	1
1/ 4	11.50	5.550	0.007	0.000	0.000	0.024	0.004	0.009	0.009	0.012	0.024	0.007	0.015	-.005	0
1/ 5	11.00	5.100	0.011	0.000	0.008	0.036	0.003	0.029	0.000	0.003	0.031	0.006	0.025	-.026	0
1/ 6	8.000	7.420	0.007	0.000	0.004	0.126	0.003	0.002	0.007	0.009	0.022	0.008	0.035	-.122	0
1/ 8	10.00	5.970	0.003	0.000	0.014	0.010	0.001	0.020	0.006	0.011	0.018	0.009	0.053	0.009	0
1/ 9	10.00	5.970	0.005	0.000	0.010	0.059	0.043	0.017	0.004	0.047	0.000	-.001	0.074	-.049	8
1/10	10.00	5.950	0.003	0.000	0.000	0.050	0.006	0.014	0.000	0.003	-.001	-.001	0.068	-.042	1
1/11	10.00	5.950	0.093	0.005	0.000	0.062	0.007	0.025	0.000	0.042	0.025	0.005	-.001	-.100	0
1/12	10.00	5.950	0.037	0.003	0.000	0.059	0.008	0.014	0.006	0.017	-.001	0.004	0.018	-.070	0
1/13	10.00	5.950	-.001	-.001	0.008	-.001	-.001	0.022	0.050	0.022	-.001	0.018	0.054	0.090	1
1/14	10.00	5.950	0.027	0.140	0.073	0.054	0.009	0.252	0.046	0.030	-.001	-.001	-.001	0.025	0

ALL CONCENTRATIONS ARE IN MICROEQ/M3 EXCEPT S(IV) WHICH IS IN MICROMOLES/M3. TIMES ARE GIVEN IN HOURS PST.
ERROR CODE: 1 = HANDLING, 2 = SAMPLING TIME, 4 = UNCERTAINTY T/AC/F, 8 = LOCAL SOURCE
WHEN -.001 IS DISPLAYED THE CONCENTRATION WAS NOT DETERMINED.
<H> IS CALCULATED BY IONIC BALANCE ON THE AEROSOL. PROOFED 6/18/84 - DJJ

TABLE 1. BAKERSFIELD FOG - 18 DEC 83 $

#	TIME1	TIME2	PH	MICRO EQ/LITER H	NA	NH4	CA	MG	CL	NO3	SO4	-/+	MICRO M/L S(IV)	CH2O	/MM/L\ TOC	/ML\ VOL
1	0.83	3.08	4.91	12.3	18.0	1640.0	70.0	15.0	27.0	427.0	983.0	0.753	115.0	43.0	5900.0	17.00
2	3.08	4.00	5.05	8.9	30.0	1030.0	50.0	3.0	10.0	192.0	896.0	0.865	128.0	74.0	-0.2	13.00
3	7.25	9.17	7.07	0.1	18.0	1970.0	50.0	8.0	-5.0	946.0	802.0	0.834	37.0	37.0	-0.2	14.00

REVISED 5/16/84

TABLE 2. BAKERSFIELD FOG - 18 DEC 83 $

#	TIME1	TIME2	MIDT	-/+	EQUIVALENT RATIOS CL/NA	MG/NA	CA/NA	SO4/NA	NO3/SO4	NH4/N+S	H/N+S	MOLAR RATIOS H+A/N+S	S(IV)/SO4	S(IV)/CH2O
1	0.83	3.08	1.95	0.753	1.500	0.833	3.889	54.611	0.434	1.163	0.009	1.172	0.234	2.674
2	3.08	4.00	3.54	0.865	0.333	0.100	1.667	29.867	0.214	0.947	0.008	0.955	0.286	1.730
3	7.25	9.17	8.21	0.834	-0.100	0.444	2.778	44.556	1.180	1.127	0.000	1.127	0.092	1.000
	SEA SALT RATIOS:				1.17	0.228	0.043	0.120						

REVISED 5/16/84

TABLE 3. BAKERSFIELD FOG - 18 DEC 83 $

MASS SOLUTE PER M3 OF AIR IS BASED ON LIQUID WATER CONTENT CALCULATED FROM THE VOLUME OF FOGWATER COLLECTED ASSUMING 50% EFFICIENCY AT A 5 M3/MIN SAMPLING RATE

#	TIME1	TIME2	MIDT	(MIN) DT	(ML) VOL	(G/M3) LWC	MICRO M/L S(IV)	CH2O	/MM/L\ TOC	MICROGRAM/CU. METER S(IV)	CH2O	TOC	-/+	"CORR" -/+	PH	"PH-BY-DIFFERENCE"
1	0.83	3.08	1.95	135.0	17.0	0.050	115.0	43.0	5900.0	0.186	0.065	3569.49	0.753	0.753	4.91	*****
2	3.08	4.00	3.54	55.2	13.0	0.094	128.0	74.0	-0.2	0.387	0.209	-0.100	0.865	0.864	5.05	*****
3	7.25	9.17	8.21	115.2	14.0	0.049	37.0	37.0	-0.2	0.058	0.054	-0.100	0.834	0.834	7.07	*****
	TIME-WEIGHTED AVERAGE FOR 3 SAMPLES					0.058				0.174	0.0873569.491					

REVISED 5/16/84

TABLE 4. BAKERSFIELD FOG - 18 DEC 83 $

MASS SOLUTE PER M3 OF AIR IS BASED ON LIQUID WATER CONTENT CALCULATED FROM THE VOLUME OF FOGWATER COLLECTED ASSUMING 50% EFFICIENCY AT A 5 M3/MIN SAMPLING RATE.

#	TIME1	TIME2	MIDT	(MIN) DT	(ML) VOL	(G/M3) LWC	/ / / / H	MICROGRAM / CUBIC METER NA	NH4	CA	MG	CL	NO3	SO4	\ \ \ \ SUM
1	0.83	3.08	1.95	135.0	17.0	0.050	0.001	0.021	1.490	0.071	0.009	0.048	1.334	2.378	5.351
2	3.08	4.00	3.54	55.2	13.0	0.094	0.001	0.065	1.750	0.094	0.003	0.043	1.121	4.054	7.123
3	7.25	9.17	8.21	115.2	14.0	0.049	0.000	0.020	1.728	0.049	0.005	-5.000	2.851	1.873	6.525
TIME-WEIGHTED AVERAGE FOR 3 SAMPLES						0.058	0.000	0.029	1.627	0.067	0.006	0.044	1.868	2.490	6.114

REVISED 5/16/84

TABLE 5. BAKERSFIELD FOG - 18 DEC 83 $

THE MASS LOADING OF TRACE METALS PER CU. METER OF AIR IS BASED ON LIQUID WATER CONTENT CALCULATED FROM THE VOLUME OF FOGWATER COLLECTED ASSUMING 50% EFFICIENCY AT A 5 M3/MIN SAMPLING RATE.

#	TIME1	TIME2	PH	/ / / / FE	MN	MICROGRAM / LITER PB	CU	NI	\ \ \ \ V	/ / / / FE	MN	MICROGRAM / CUBIC METER PB	CU	NI	\ \ \ \ V
1	0.83	3.08	4.91	605.0	57.0	48.0	111.0	91.9	23.0	0.030	0.003	0.002	0.006	0.005	0.001
2	3.08	4.00	5.05	159.0	10.0	86.0	10.4	33.5	19.0	0.015	0.001	0.008	0.001	0.003	0.002
3	7.25	9.17	7.07	118.0	-0.1	76.0	-0.1	-0.1	-0.1	0.006	-0.100	0.004	-0.100	-0.100	-0.100

REVISED 3/15/84

TABLE 1. BAKERSFIELD FOG - 19 DEC 83 $

#	TIME1	TIME2	PH	MICRO EQ/LITER H	NA	NH4	CA	MG	CL	NO3	SO4	-/+	MICRO M/L S(IV)	CH2O	/MM/L TOC	/ML VOL
1	0.67	1.67	7.10	0.1	7.0	970.0	16.0	3.0	33.0	280.0	426.0	0.727	15.0	27.0	5290.0	42.50
2	4.33	6.33	6.50	0.3	12.0	3130.0	64.0	8.0	10.0	391.0	2490.0	0.878	70.0	102.0	5400.0	11.50
3	8.25	9.50	6.69	0.2	104.0	8670.0	540.0	163.0	85.0	2470.0	7330.0	1.043	-0.1	-0.1	-0.2	2.70

REVISED 5/16/84

TABLE 2. BAKERSFIELD FOG - 19 DEC 83 $

#	TIME1	TIME2	MIDT	-/+	EQUIVALENT RATIOS CL/NA	MG/NA	CA/NA	SO4/NA	NO3/SO4	NH4/N+S	H/N+S	H+A/N+S	MOLAR RATIOS S(IV)/SO4	S(IV)/CH2O
1	0.67	1.67	1.17	0.727	4.714	0.429	2.286	60.857	0.657	1.374	0.000	1.374	0.070	0.556
2	4.33	6.33	5.33	0.878	0.833	0.667	5.333	207.500	0.157	1.086	0.000	1.087	0.056	0.686
3	8.25	9.50	8.88	1.043	0.817	1.567	5.192	70.481	0.337	0.885	0.000	0.885	-0.100	-0.100
	SEA SALT RATIOS:				1.17	0.228	0.043	0.120						

REVISED 5/16/84

ABLE 3. BAKERSFIELD FOG - 19 DEC 83 $

MASS SOLUTE PER M3 OF AIR IS BASED ON LIQUID WATER CONTENT CALCULATED FROM THE VOLUME OF FOGWATER COLLECTED ASSUMING 50% EFFICIENCY AT A 5 M3/MIN SAMPLING RATE

#	TIME1	TIME2	MIDT	(MIN) DT	(ML) VOL	(G/M3) LWC	MICRO M/L S(IV)	CH2O	/MM/L TOC	MICROGRAM/CU. METER S(IV)	CH2O	TOC	-/+	'CORR' -/+	PH	'PH-BY-DIFFERENCE'
1	0.67	1.67	1.17	60.0	42.5	0.283	15.0	27.0	5290.0	0.136	0.230	*******	0.727	0.727	7.10	*****
2	4.33	6.33	5.33	120.0	11.5	0.038	70.0	102.0	5400.0	0.086	0.117	2486.27	0.878	0.878	6.50	*****
3	8.25	9.50	8.88	75.0	2.7	0.014	-0.1	-0.1	-0.2	-0.100	-0.100	-0.100	1.043	1.043	6.69	3.39
	TIME-WEIGHTED AVERAGE FOR 3 SAMPLES					0.040				0.038	0.057	4376.198				

REVISED 5/16/84

TABLE 4. BAKERSFIELD FOG - 19 DEC 83 $

MASS SOLUTE PER M3 OF AIR IS BASED ON LIQUID WATER CONTENT CALCULATED FROM THE VOLUME OF FOGWATER COLLECTED ASSUMING 50% EFFICIENCY AT A 5 M3/MIN SAMPLING RATE.

#	TIME1	TIME2	MIDT	(MIN) DT	(ML) VOL	(G/M3) LWC	/ / / / H	NA	NH4	MICROGRAM / CUBIC METER CA	MG	CL	NO3	SO4	\ \ \ \ SUM
1	0.67	1.67	1.17	60.0	42.5	0.283	0.000	0.046	4.958	0.091	0.010	0.331	4.919	5.797	16.152
2	4.33	6.33	5.33	120.0	11.5	0.038	0.000	0.011	2.164	0.049	0.004	0.014	0.929	4.584	7.755
3	8.25	9.50	8.88	75.0	2.7	0.014	0.000	0.034	2.252	0.156	0.029	0.043	2.205	5.070	9.789
TIME-WEIGHTED AVERAGE FOR 3 SAMPLES						0.089	0.000	0.026	2.848	0.090	0.013	0.097	2.243	5.013	10.329

REVISED 5/16/84

TABLE 5. BAKERSFIELD FOG - 19 DEC 83 $

THE MASS LOADING OF TRACE METALS PER CU. METER OF AIR IS BASED ON LIQUID WATER CONTENT CALCULATED FROM THE VOLUME OF FOGWATER COLLECTED ASSUMING 50% EFFICIENCY AT A 5 M3/MIN SAMPLING RATE.

#	TIME1	TIME2	PH	/ / / / FE	MN	MICROGRAM / LITER PB	CU	NI	\ \ \ \ V	/ / / / FE	MN	MICROGRAM / CUBIC METER PB	CU	NI	\ \ \ \ V
1	0.67	1.67	7.10	369.0	7.0	29.0	15.0	6.6	5.4	0.105	0.002	0.008	0.004	0.002	0.002
2	4.33	6.33	6.50	-0.1	-0.1	-0.1	-0.1	-0.1	-0.1	-0.100	-0.100	-0.100	-0.100	-0.100	-0.100
3	8.25	9.50	6.69	281.0	14.0	70.0	30.0	18.2	17.0	0.004	0.000	0.001	0.000	0.000	0.000

REVISED 3/15/84

TABLE 1. BAKERSFIELD FOG - 31 DEC 83 $

#	TIME1	TIME2	PH	MICRO EQ/LITER H	NA	NH4	CA	MG	CL	NO3	SO4	-/+	MICRO M/L S(IV)	CH2O	/MM/L TOC	/ML VOL
1	1.25	2.50	5.99	1.0	40.0	1590.0	73.0	13.0	38.0	285.0	799.0	0.547	183.0	131.0	2800.0	28.50
2	3.08	4.25	5.63	2.3	27.0	2510.0	75.0	14.0	40.0	519.0	2360.0	0.889	583.0	498.0	5450.0	22.00
3	4.25	5.75	5.65	2.2	17.0	2320.0	-30.0	-10.0	42.0	613.0	1910.0	0.880	542.0	382.0	4400.0	17.00
4	5.75	7.75	6.49	0.3	38.0	3160.0	130.0	22.0	52.0	1370.0	1440.0	0.783	239.0	144.0	-0.2	13.50
5	7.75	9.25	6.79	0.2	-0.1	5010.0	196.0	-20.0	86.0	2260.0	2330.0	0.835	348.0	165.0	-0.2	4.00

REVISED 5/16/84

TABLE 2. BAKERSFIELD FOG - 31 DEC 83 $

#	TIME1	TIME2	MIDT	-/+	EQUIVALENT RATIOS CL/NA	MG/NA	CA/NA	SO4/NA	NO3/SO4	NH4/N+S	H/N+S	MOLAR RATIOS H+A/N+S	S(IV)/SO4	S(IV)/CH2O
1	1.25	2.50	1.87	0.547	0.950	0.325	1.825	19.975	0.357	1.467	0.001	1.468	0.458	1.397
2	3.08	4.25	3.66	0.889	1.481	0.519	2.778	87.407	0.220	0.872	0.001	0.873	0.494	1.171
3	4.25	5.75	5.00	0.880	2.471	-0.100	-0.100	112.353	0.321	0.920	0.001	0.920	0.568	1.419
4	5.75	7.75	6.75	0.783	1.368	0.579	3.421	37.895	0.951	1.125	0.000	1.125	0.332	1.660
5	7.75	9.25	8.50	0.835	-0.100	-0.100	-0.100	-0.100	0.970	1.092	0.000	1.092	0.299	2.109
	SEA SALT RATIOS:				1.17	0.228	0.043	0.120						

REVISED 5/16/84

TABLE 3. BAKERSFIELD FOG - 31 DEC 83 $

MASS SOLUTE PER M3 OF AIR IS BASED ON LIQUID WATER CONTENT CALCULATED FROM THE VOLUME OF FOGWATER COLLECTED ASSUMING 50% EFFICIENCY AT A 5 M3/MIN SAMPLING RATE

#	TIME1	TIME2	MIDT	(MIN) DT	(ML) VOL	(G/M3) LWC	MICRO M/L S(IV)	CH2O	/MM/L TOC	MICROGRAM/CU. METER S(IV)	CH2O	TOC	-/+	"CORR" -/+	PH	"PH-BY-DIFFERENCE"
1	1.25	2.50	1.87	75.0	28.5	0.152	183.0	131.0	2800.0	0.892	0.598	5111.88	0.547	0.547	5.99	*****
2	3.08	4.25	3.66	70.2	22.0	0.125	583.0	498.0	5450.0	2.343	1.875	8205.80	0.889	0.889	5.63	*****
3	4.25	5.75	5.00	90.0	17.0	0.076	542.0	382.0	4400.0	1.313	0.867	3992.99	0.880	0.880	5.65	*****
4	5.75	7.75	6.75	120.0	13.5	0.045	239.0	144.0	-0.2	0.345	0.195	-0.100	0.783	0.783	6.49	*****
5	7.75	9.25	8.50	90.0	4.0	0.018	348.0	165.0	-0.2	0.198	0.088	-0.100	0.835	0.835	6.79	*****
TIME-WEIGHTED AVERAGE FOR 5 SAMPLES						0.076				0.918	0.6425607.175					

REVISED 5/16/84

TABLE 4. BAKERSFIELD FOG - 31 DEC 83 $

MASS SOLUTE PER M3 OF AIR IS BASED ON LIQUID WATER CONTENT CALCULATED FROM THE VOLUME OF FOGWATER COLLECTED ASSUMING 50% EFFICIENCY AT A 5 M3/MIN SAMPLING RATE.

				(MIN)	(ML)	(G/M3)	/ / / /			MICROGRAM / CUBIC METER					\ \ \ \
#	TIME1	TIME2	MIDT	DT	VOL	LWC	H	NA	NH4	CA	MG	CL	NO3	SO4	SUM
1	1.25	2.50	1.87	75.0	28.5	0.152	0.000	0.140	4.360	0.222	0.024	0.205	2.686	5.833	13.470
2	3.08	4.25	3.66	70.2	22.0	0.125	0.000	0.078	5.676	0.188	0.021	0.178	4.034	14.209	24.385
3	4.25	5.75	5.00	90.0	17.0	0.076	0.000	0.030	3.162	-30.000	-10.000	0.112	2.872	6.931	13.107
4	5.75	7.75	6.75	120.0	13.5	0.045	0.000	0.039	2.565	0.117	0.012	0.083	3.822	3.112	9.751
5	7.75	9.25	8.50	90.0	4.0	0.018	0.000	-0.100	1.607	0.070	-20.000	0.054	2.491	1.990	6.211
TIME-WEIGHTED AVERAGE FOR 5 SAMPLES						0.076	0.000	0.066	3.285	0.141	0.018	0.119	3.203	5.866	12.648

REVISED 5/16/84

TABLE 5. BAKERSFIELD FOG - 31 DEC 83 $

THE MASS LOADING OF TRACE METALS PER CU. METER OF AIR IS BASED ON LIQUID WATER CONTENT CALCULATED FROM THE VOLUME OF FOGWATER COLLECTED ASSUMING 50% EFFICIENCY AT A 5 M3/MIN SAMPLING RATE.

				/ / / /		MICROGRAM / LITER			\ \ \ \	/ / / /	MICROGRAM / CUBIC METER				\ \ \ \
#	TIME1	TIME2	PH	FE	MN	PB	CU	NI	V	FE	MN	PB	CU	NI	V
1	1.25	2.50	5.99	283.0	26.0	132.0	13.0	25.5	19.0	0.043	0.004	0.020	0.002	0.004	0.003
2	3.08	4.25	5.63	284.0	24.0	100.0	16.0	30.2	34.0	0.036	0.003	0.013	0.002	0.004	0.004
3	4.25	5.75	5.65	260.0	15.0	110.0	15.0	39.3	45.0	0.020	0.001	0.008	0.001	0.003	0.003
4	5.75	7.75	6.49	190.0	33.0	75.0	20.0	24.3	30.0	0.009	0.001	0.003	0.001	0.001	0.001
5	7.75	9.25	6.79	-0.1	-0.1	-0.1	-0.1	-0.1	-0.1	-0.100	-0.100	-0.100	-0.100	-0.100	-0.100

REVISED 3/1/84

TABLE 1. BAKERSFIELD FOG - 7 JAN 84 $

#	TIME1	TIME2	PH	MICRO EQ/LITER H	NA	NH4	CA	MG	CL	NO3	SO4	-/+	MICRO M/L S(IV)	CH2O	MM/L TOC	ML VOL
1	-1.83	-0.83	5.11	7.8	47.0	5380.0	-0.1	92.0	191.0	1770.0	4680.0	1.102	549.0	354.0	-0.2	10.38
2	-0.80	0.17	5.15	7.1	29.0	5380.0	273.0	74.0	187.0	1700.0	4730.0	1.023	722.0	210.0	-0.2	6.76
3	0.18	1.17	5.10	7.9	-0.1	15600.0	-0.1	-0.1	704.0	4150.0	14670.0	1.251	-0.1	-0.1	-0.1	1.74
4	1.18	2.17	5.14	7.2	-0.1	7610.0	-0.1	-0.1	270.0	1980.0	7610.0	1.294	-0.1	-0.1	-0.1	3.12

REVISED 2/16/84

TABLE 2. BAKERSFIELD FOG - 7 JAN 84 $

#	TIME1	TIME2	MIDT	-/+	EQUIVALENT RATIOS CL/NA	MG/NA	CA/NA	SO4/NA	NO3/SO4	NH4/N+S	H/N+S	MOLAR RATIOS H+A/N+S	S(IV)/SO4	S(IV)/CH2O
1	-1.83	-0.83	-1.33	1.102	4.064	1.957	-0.100	99.574	0.378	0.834	0.001	0.835	0.235	1.551
2	-0.80	0.17	-0.31	1.023	6.448	2.552	9.414	163.103	0.359	0.837	0.001	0.838	0.305	3.438
3	0.18	1.17	0.68	1.251	-0.100	-0.100	-0.100	-0.100	0.283	0.829	0.000	0.829	-0.100	-0.100
4	1.18	2.17	1.68	1.294	-0.100	-0.100	-0.100	-0.100	0.260	0.794	0.001	0.794	-0.100	-0.100
	SEA SALT RATIOS:				1.17	0.228	0.043	0.120						

REVISED 2/16/84

ABLE 3. BAKERSFIELD FOG - 7 JAN 84 $

MASS SOLUTE PER M3 OF AIR IS BASED ON LIQUID WATER CONTENT CALCULATED FROM THE VOLUME OF FOGWATER COLLECTED ASSUMING 50% EFFICIENCY AT A 5 M3/MIN SAMPLING RATE

#	TIME1	TIME2	MIDT	(MIN) DT	(ML) VOL	(G/M3) LWC	MICRO M/L S(IV)	CH2O	MM/L TOC	MICROGRAM/CU. METER S(IV)	CH2O	TOC	-/+	"CORR" -/+	PH	"PH-BY-DIFFERENCE"
1	-1.83	-0.83	-1.33	60.0	10.4	0.069	549.0	354.0	-0.2	1.218	0.736	-0.100	1.102	1.102	5.11	3.24
2	-0.80	0.17	-0.31	58.2	6.8	0.046	722.0	210.0	-0.2	1.075	0.293	-0.100	1.023	1.023	5.15	3.86
3	0.18	1.17	0.68	59.4	1.7	0.012	-0.1	-0.1	-0.1	-0.100	-0.100	-0.100	1.251	1.251	5.10	2.41
4	1.18	2.17	1.68	59.4	3.1	0.021	-0.1	-0.1	-0.1	-0.100	-0.100	-0.100	1.294	1.294	5.14	2.65
	TIME-WEIGHTED AVERAGE FOR 4 SAMPLES					0.043				0.231	0.104	0.000				

REVISED 2/16/84

TABLE 4. BAKERSFIELD FOG - 7 JAN 84 $

MASS SOLUTE PER M3 OF AIR IS BASED ON LIQUID WATER CONTENT CALCULATED FROM THE VOLUME OF FOGWATER COLLECTED ASSUMING 50% EFFICIENCY AT A 5 M3/MIN SAMPLING RATE.

#	TIME1	TIME2	MIDT	(MIN) DT	(ML) VOL	(G/M3) LWC	MICROGRAM / CUBIC METER H	NA	NH4	CA	MG	CL	NO3	SO4	SUM
1	-1.83	-0.83	-1.33	60.0	10.4	0.069	0.001	0.075	6.716	-0.100	0.077	0.469	7.594	15.555	30.486
2	-0.80	0.17	-0.31	58.2	6.8	0.046	0.000	0.031	4.509	0.254	0.042	0.308	4.897	10.555	20.596
3	0.18	1.17	0.68	59.4	1.7	0.012	0.000	-0.100	3.297	-0.100	-0.100	0.292	3.015	8.256	14.861
4	1.18	2.17	1.68	59.4	3.1	0.021	0.000	-0.100	2.884	-0.100	-0.100	0.201	2.579	7.679	13.344
	TIME-WEIGHTED AVERAGE FOR 4 SAMPLES					0.037	0.000	0.053	4.357	0.254	0.060	0.318	4.527	10.524	19.845

REVISED 2/16/84

TABLE 5. BAKERSFIELD FOG - 7 JAN 84 $

THE MASS LOADING OF TRACE METALS PER CU. METER OF AIR IS BASED ON LIQUID WATER CONTENT
CALCULATED FROM THE VOLUME OF FOGWATER COLLECTED ASSUMING 50% EFFICIENCY AT A 5 M3/MIN SAMPLING RATE.

				/ / / / MICROGRAM / LITER \ \ \ \						/ / / / MICROGRAM / CUBIC METER \ \ \ \					
#	TIME1	TIME2	PH	FE	MN	PB	CU	NI	V	FE	MN	PB	CU	NI	V
1	-1.83	-0.83	5.11	1808.0	82.0	330.0	45.0	116.0	122.0	0.125	0.006	0.023	0.003	0.008	0.008
2	-0.80	0.17	5.15	-0.1	-0.1	-0.1	-0.1	-0.1	-0.1	-0.100	-0.100	-0.100	-0.100	-0.100	-0.100
3	0.18	1.17	5.10	-0.1	-0.1	-0.1	-0.1	-0.1	-0.1	-0.100	-0.100	-0.100	-0.100	-0.100	-0.100
4	1.18	2.17	5.14	-0.1	-0.1	-0.1	-0.1	-0.1	-0.1	-0.100	-0.100	-0.100	-0.100	-0.100	-0.100

REVISED 3/15/84

TABLE 1. BAKERSFIELD FOG - 13 JAN 84 $

#	TIME1	TIME2	PH	MICRO EQ/LITER H	NA	NH4	CA	MG	CL	NO3	SO4	-/+	MICRO M/L S(IV)	CH2O	MM/L TOC	ML VOL
1	1.50	2.00	6.38	0.4	59.0	3190.0	143.0	9.0	314.0	502.0	3250.0	1.094	344.0	122.0	3333.0	9.50
2	2.00	3.00	5.92	1.2	83.0	2800.0	175.0	16.0	180.0	425.0	2560.0	0.907	376.0	112.0	-0.2	19.80
3	3.00	3.50	6.72	0.2	-0.1	5920.0	492.0	52.0	211.0	1100.0	4920.0	0.964	-0.1	-0.1	-0.1	2.70
4	3.50	4.00	6.74	0.2	-0.1	3300.0	294.0	123.0	147.0	662.0	2940.0	0.927	302.0	149.0	-0.2	6.00
5	4.00	5.00	6.55	0.3	41.0	3100.0	117.0	9.0	149.0	475.0	3890.0	1.307	245.0	144.0	-0.2	15.60
6	5.00	6.00	6.92	0.1	-0.1	6230.0	587.0	55.0	206.0	1800.0	5460.0	1.086	-0.1	-0.1	-0.1	3.30

REVISED 5/16/84

TABLE 2. BAKERSFIELD FOG - 13 JAN 84 $

#	TIME1	TIME2	MIDT	-/+	EQUIVALENT RATIOS CL/NA	MG/NA	CA/NA	SO4/NA	NO3/SO4	NH4/N+S	H/N+S	MOLAR RATIOS H+A/N+S	S(IV)/SO4	S(IV)/CH2O
1	1.50	2.00	1.75	1.094	5.322	0.153	2.424	55.085	0.154	0.850	0.000	0.850	0.212	2.820
2	2.00	3.00	2.50	0.907	2.169	0.193	2.108	30.843	0.166	0.938	0.000	0.938	0.294	3.357
3	3.00	3.50	3.25	0.964	-0.100	-0.100	-0.100	-0.100	0.224	0.983	0.000	0.983	-0.100	-0.100
4	3.50	4.00	3.75	0.927	-0.100	-0.100	-0.100	-0.100	0.225	0.916	0.000	0.916	0.205	2.027
5	4.00	5.00	4.50	1.307	3.634	0.220	2.854	94.878	0.122	0.710	0.000	0.710	0.126	1.701
6	5.00	6.00	5.50	1.086	-0.100	-0.100	-0.100	-0.100	0.330	0.858	0.000	0.858	-0.100	-0.100
	SEA SALT RATIOS:				1.17	0.228	0.043	0.120						

REVISED 5/16/84

TABLE 3. BAKERSFIELD FOG - 13 JAN 84 $

MASS SOLUTE PER M3 OF AIR IS BASED ON LIQUID WATER CONTENT CALCULATED FROM THE VOLUME OF FOGWATER COLLECTED ASSUMING 50% EFFICIENCY AT A 5 M3/MIN SAMPLING RATE

#	TIME1	TIME2	MIDT	MIN DT	ML VOL	G/M3 LWC	MICRO M/L S(IV)	CH2O	MM/L TOC	MICROGRAM/CU. M S(IV)	CH2O	METER TOC	-/+	CORR -/+	PH	PH-BY-DIFFERENCE
1	1.50	2.00	1.75	30.0	9.5	0.127	344.0	122.0	3333.0	1.397	0.464	5070.80	1.094	1.094	6.38	3.49
2	2.00	3.00	2.50	60.0	19.8	0.132	376.0	112.0	-0.2	1.591	0.444	-0.100	0.907	0.907	5.92	*****
3	3.00	3.50	3.25	30.0	2.7	0.036	-0.1	-0.1	-0.1	-0.100	-0.100	-0.100	0.964	0.964	6.72	*****
4	3.50	4.00	3.75	30.0	6.0	0.080	302.0	149.0	-0.2	0.775	0.358	-0.100	0.927	0.927	6.74	*****
5	4.00	5.00	4.50	60.0	15.6	0.104	245.0	144.0	-0.2	0.817	0.450	-0.100	1.307	1.307	6.55	3.00
6	5.00	6.00	5.50	60.0	3.3	0.022	-0.1	-0.1	-0.1	-0.100	-0.100	-0.100	1.086	1.086	6.92	3.23
	TIME-WEIGHTED AVERAGE FOR 6 SAMPLES					0.084				1.165	0.435	5070.804				

REVISED 5/16/84

TABLE 4. BAKERSFIELD FOG - 13 JAN 84 $

MASS SOLUTE PER M3 OF AIR IS BASED ON LIQUID WATER CONTENT CALCULATED FROM THE VOLUME OF FOGWATER COLLECTED ASSUMING 50% EFFICIENCY AT A 5 M3/MIN SAMPLING RATE.

#	TIME1	TIME2	MIDT	(MIN) DT	(ML) VOL	(G/M3) LWC	/ / / / H	NA	NH4	MICROGRAM / CUBIC METER CA	MG	CL	NO3	SO4	\ \ \ \ SUM
1	1.50	2.00	1.75	30.0	9.5	0.127	0.000	0.172	7.289	0.363	0.014	1.410	3.942	19.772	32.963
2	2.00	3.00	2.50	60.0	19.8	0.132	0.000	0.252	6.668	0.463	0.026	0.842	3.478	16.230	27.959
3	3.00	3.50	3.25	30.0	2.7	0.036	0.000	-0.100	3.845	0.355	0.023	0.269	2.455	8.507	15.454
4	3.50	4.00	3.75	30.0	6.0	0.080	0.000	-0.100	4.763	0.471	0.120	0.417	3.284	11.297	20.351
5	4.00	5.00	4.50	60.0	15.6	0.104	0.000	0.098	5.816	0.244	0.011	0.549	3.063	19.431	29.213
6	5.00	6.00	5.50	60.0	3.3	0.022	0.000	-0.100	2.473	0.259	0.015	0.161	2.455	5.769	11.131
TIME-WEIGHTED AVERAGE FOR 6 SAMPLES						0.084	0.000	0.174	5.090	0.347	0.029	0.578	3.075	13.604	22.819

REVISED 5/16/84

TABLE 1. McKITTRICK FOG - 3 JAN 84 *

#	TIME1	TIME2	PH	MICRO EQ/LITER H	NA	NH4	CA	MG	CL	NO3	SO4	-/+	MICRO M/L S(IV)	CH2O	/MM/L\ TOC	/ML\ VOL
1	8.00	9.00	2.68	2089.3	-0.1	3560.0	580.0	83.0	110.0	4960.0	1960.0	1.101	80.0	51.0	-0.2	10.00
2	9.00	10.00	-0.10	-0.1	-0.1	4900.0	-0.1	94.0	351.0	6890.0	2910.0	2.014	95.0	36.0	-0.2	5.00

REVISED 5/16/84

TABLE 2. McKITTRICK FOG - 3 JAN 84 *

#	TIME1	TIME2	MIDT	EQUIVALENT RATIOS -/+	CL/NA	MG/NA	CA/NA	SO4/NA	NO3/SO4	NH4/N+S	H/N+S	MOLAR RATIOS H+A/N+S	S(IV)/SO4	S(IV)/CH2O
1	8.00	9.00	8.50	1.101	-0.100	-0.100	-0.100	-0.100	2.531	0.514	0.302	0.816	0.082	1.569
2	9.00	10.00	9.50	2.014	-0.100	-0.100	-0.100	-0.100	2.368	0.500	-0.100	0.500	0.065	2.639
	SEA SALT RATIOS:				1.17	0.228	0.043	0.120						

REVISED 5/16/84

TABLE 3. McKITTRICK FOG - 3 JAN 84 *

MASS SOLUTE PER M3 OF AIR IS BASED ON LIQUID WATER CONTENT CALCULATED FROM THE VOLUME OF FOGWATER COLLECTED ASSUMING 50% EFFICIENCY AT A 5 M3/MIN SAMPLING RATE

#	TIME1	TIME2	MIDT	(MIN) DT	(ML) VOL	(G/M3) LWC	MICRO M/L S(IV)	/MM/L\ CH2O	TOC	MICROGRAM/CU. METER S(IV)	CH2O	TOC	-/+	"CORR" -/+	PH	"PH-BY-DIFFERENCE"
1	8.00	9.00	8.50	60.0	10.0	0.067	80.0	51.0	-0.2	0.171	0.102	-0.100	1.101	1.078	2.68	2.59
2	9.00	10.00	9.50	60.0	5.0	0.033	95.0	36.0	-0.2	0.102	0.036	-0.100	2.014	2.014	-0.10	2.30
	TIME-WEIGHTED AVERAGE FOR 2 SAMPLES					0.050				0.136	0.069	0.000				

REVISED 5/16/84

TABLE 4. McKITTRICK FOG - 3 JAN 84 *

MASS SOLUTE PER M3 OF AIR IS BASED ON LIQUID WATER CONTENT CALCULATED FROM THE VOLUME OF FOGWATER COLLECTED ASSUMING 50% EFFICIENCY AT A 5 M3/MIN SAMPLING RATE.

#	TIME1	TIME2	MIDT	(MIN) DT	(ML) VOL	(G/M3) LWC	MICROGRAM / CUBIC METER H	NA	NH4	CA	MG	CL	NO3	SO4	SUM
1	8.00	9.00	8.50	60.0	10.0	0.067	0.141	-0.100	4.281	0.775	0.067	0.260	20.501	6.276	32.302
2	9.00	10.00	9.50	60.0	5.0	0.033	-0.100	-0.100	2.947	-0.100	0.038	0.415	14.239	4.659	22.298
	TIME-WEIGHTED AVERAGE FOR 2 SAMPLES					0.050	0.141	0.000	3.614	0.775	0.053	0.337	17.370	5.467	27.300

REVISED 5/16/84

TABLE 5. McKITTRICK FOG - 3 JAN 84 *

THE MASS LOADING OF TRACE METALS PER CU. METER OF AIR IS BASED ON LIQUID WATER CONTENT CALCULATED FROM THE VOLUME OF FOGWATER COLLECTED ASSUMING 50% EFFICIENCY AT A 5 M3/MIN SAMPLING RATE.

#	TIME1	TIME2	PH	MICROGRAM / LITER FE	MN	PB	CU	NI	V	MICROGRAM / CUBIC METER FE	MN	PB	CU	NI	V
1	8.00	9.00	2.68	1454.0	150.0	530.0	82.0	230.0	261.0	0.097	0.010	0.035	0.005	0.015	0.017
2	9.00	10.00	-0.10	-0.1	-0.1	-0.1	-0.1	-0.1	-0.1	-0.100	-0.100	-0.100	-0.100	-0.100	-0.100

TABLE 1. McKITTRICK FOG - 4 JAN 84 $

#	TIME1	TIME2	PH	H	NA	NH4	CA	MG	CL	NO3	SO4	-/+	S(IV)	CH2O	TOC	VOL
				/ / / / / /		MICRO EQ/LITER				\ \ \ \ \ \			/ MICRO M/L \		/MM/L\	/ML\
1	8.00	9.00	3.51	309.0	-0.1	882.0	55.0	10.0	60.0	654.0	670.0	1.077	31.0	18.0	3360.0	13.00
2	9.00	10.00	3.04	912.0	-0.1	2100.0	222.0	-20.0	42.0	1900.0	1680.0	1.127	-0.1	-0.1	-0.1	1.50

REVISED 5/16/84

TABLE 2. McKITTRICK FOG - 4 JAN 84 $

#	TIME1	TIME2	MIDT	-/+	CL/NA	MG/NA	CA/NA	SO4/NA	NO3/SO4	NH4/N+S	H/N+S	H+A/N+S	S(IV)/SO4	S(IV)/CH2O
				/ / / /			EQUIVALENT RATIOS					\ \ \ \ / / MOLAR RATIOS		\ \
1	8.00	9.00	8.50	1.077	-0.100	-0.100	-0.100	-0.100	0.976	0.666	0.233	0.900	0.093	1.722
2	9.00	10.00	9.50	1.127	-0.100	-0.100	-0.100	-0.100	1.131	0.587	0.255	0.841	-0.100	-0.100
	SEA SALT RATIOS:				1.17	0.228	0.043	0.120						

REVISED 5/16/84

ABLE 3. McKITTRICK FOG - 4 JAN 84 $

MASS SOLUTE PER M3 OF AIR IS BASED ON LIQUID WATER CONTENT CALCULATED FROM THE VOLUME OF FOGWATER COLLECTED ASSUMING 50% EFFICIENCY AT A 5 M3/MIN SAMPLING RATE

#	TIME1	TIME2	MIDT	(MIN) DT	(ML) VOL	(G/M3) LWC	/ MICRO M/L \ S(IV)	CH2O	/MM/L\ TOC	/ MICROGRAM/CU. METER \ S(IV)	CH2O	TOC	-/+	"CORR" -/+	PH	"PH-BY-DIFFERENCE"
1	8.00	9.00	8.50	60.0	13.0	0.087	31.0	18.0	3360.0	0.086	0.047	3497.60	1.077	1.071	3.51	3.40
2	9.00	10.00	9.50	60.0	1.5	0.010	-0.1	-0.1	-0.1	-0.100	-0.100	-0.100	1.127	1.109	3.04	2.90
	TIME-WEIGHTED AVERAGE FOR 2 SAMPLES					0.024				0.029	0.0163497.603					

REVISED 5/16/84

TABLE 4. McKITTRICK FOG - 4 JAN 84 $

MASS SOLUTE PER M3 OF AIR IS BASED ON LIQUID WATER CONTENT CALCULATED FROM THE VOLUME OF FOGWATER COLLECTED ASSUMING 50% EFFICIENCY AT A 5 M3/MIN SAMPLING RATE.

#	TIME1	TIME2	MIDT	(MIN) DT	(ML) VOL	(G/M3) LWC	/ / / / H	NA	NH4	MICROGRAM / CUBIC METER CA	MG	CL	NO3	SO4	\ \ \ \ SUM
1	8.00	9.00	8.50	60.0	13.0	0.087	0.027	-0.100	1.379	0.096	0.011	0.184	3.514	2.789	8.000
2	9.00	10.00	9.50	60.0	1.5	0.010	0.009	-0.100	0.379	0.044	-20.000	0.015	1.178	0.807	2.432
	TIME-WEIGHTED AVERAGE FOR 2 SAMPLES					0.048	0.018	0.000	0.879	0.070	0.011	0.100	2.346	1.798	5.216

REVISED 5/16/84

TABLE 5. McKITTRICK FOG - 4 JAN 84 $

THE MASS LOADING OF TRACE METALS PER CU. METER OF AIR IS BASED ON LIQUID WATER CONTENT CALCULATED FROM THE VOLUME OF FOGWATER COLLECTED ASSUMING 50% EFFICIENCY AT A 5 M3/MIN SAMPLING RATE.

#	TIME1	TIME2	PH	FE	MN	PB	CU	NI	V	FE	MN	PB	CU	NI	V
				/ / / /		MICROGRAM / LITER			\ \ \ \	/ / / /		MICROGRAM / CUBIC METER			\ \ \ \
1	8.00	9.00	3.51	204.0	17.0	96.0	24.0	95.1	150.0	0.018	0.001	0.008	0.002	0.008	0.013
2	9.00	10.00	3.04	-0.1	-0.1	-0.1	-0.1	-0.1	-0.1	-0.100	-0.100	-0.100	-0.100	-0.100	-0.100

TABLE 1. McKITTRICK FOG - 5 JAN 84 *

#	TIME1	TIME2	PH	MICRO EQ/LITER H	NA	NH4	CA	MG	CL	NO3	SO4	-/+	MICRO M/L S(IV)	CH2O	MM/L TOC	ML VOL
1	0.08	1.00	4.02	95.5	4.0	399.0	13.0	1.0	3.9	245.0	267.0	0.979	14.0	11.0	892.0	53.00
2	1.00	2.00	4.00	100.0	6.0	347.0	21.0	2.0	3.3	256.0	272.0	1.066	24.0	13.0	717.0	29.00
3	2.00	3.00	4.02	95.5	3.0	344.0	10.0	1.0	2.8	229.0	253.0	1.009	27.0	17.0	792.0	43.00
4	3.00	4.58	4.21	61.7	2.0	357.0	8.0	1.0	21.0	175.0	255.0	0.957	40.0	15.0	725.0	60.00
5	4.58	5.67	4.27	53.7	5.0	320.0	7.0	1.0	2.3	162.0	246.0	0.960	39.0	16.0	883.0	60.00
6	5.67	6.50	4.33	46.8	3.0	298.0	10.0	2.0	1.6	153.0	250.0	1.002	44.0	13.0	1070.0	19.00
7	6.50	7.00	5.23	5.9	-0.1	363.0	-0.1	-0.1	62.0	152.0	339.0	1.501	-0.1	-0.1	-0.1	1.50
8	7.80	8.83	4.47	33.9	10.0	399.0	25.0	3.0	7.6	140.0	392.0	1.025	57.0	14.0	-0.2	14.00
9	8.83	10.50	4.25	56.2	17.0	460.0	115.0	9.0	14.0	245.0	413.0	0.966	37.0	14.0	1480.0	30.00
10	10.92	12.70	3.94	114.8	15.0	725.0	213.0	16.0	33.0	414.0	684.0	1.010	36.0	17.0	1625.0	24.00

REVISED 5/16/84

TABLE 2. McKITTRICK FOG - 5 JAN 84 *

#	TIME1	TIME2	MIDT	EQUIVALENT RATIOS -/+	CL/NA	MG/NA	CA/NA	SO4/NA	NO3/SO4	NH4/N+S	H/N+S	MOLAR RATIOS H+A/N+S	S(IV)/SO4	S(IV)/CH2O
1	0.08	1.00	0.54	0.979	0.975	0.250	3.250	66.750	0.918	0.779	0.187	0.966	0.105	1.273
2	1.00	2.00	1.50	1.066	0.550	0.333	3.500	45.333	0.941	0.657	0.189	0.847	0.176	1.846
3	2.00	3.00	2.50	1.009	0.933	0.333	3.333	84.333	0.905	0.714	0.198	0.912	0.213	1.588
4	3.00	4.58	3.79	0.957	10.500	0.500	4.000	127.500	0.686	0.830	0.143	0.974	0.314	2.667
5	4.58	5.67	5.13	0.960	0.460	0.200	1.400	49.200	0.659	0.784	0.132	0.916	0.317	2.438
6	5.67	6.50	6.09	1.002	0.533	0.667	3.333	83.333	0.612	0.739	0.116	0.856	0.352	3.385
7	6.50	7.00	6.75	1.501	-0.100	-0.100	-0.100	-0.100	0.448	0.739	0.012	0.751	-0.100	-0.100
8	7.80	8.83	8.32	1.025	0.760	0.300	2.500	39.200	0.357	0.750	0.064	0.814	0.291	4.071
9	8.83	10.50	9.66	0.966	0.824	0.529	6.765	24.294	0.593	0.699	0.085	0.785	0.179	2.643
10	10.92	12.70	11.81	1.010	2.200	1.067	14.200	45.600	0.605	0.660	0.105	0.765	0.105	2.118
	SEA SALT RATIOS:				1.17	0.228	0.043	0.120						

REVISED 5/16/84

TABLE 3. McKITTRICK FOG - 5 JAN 84 *

MASS SOLUTE PER M3 OF AIR IS BASED ON LIQUID WATER CONTENT CALCULATED FROM THE VOLUME OF FOGWATER COLLECTED ASSUMING 50% EFFICIENCY AT A 5 M3/MIN SAMPLING RATE

#	TIME1	TIME2	MIDT	(MIN) DT	(ML) VOL	(G/M3) LWC	MICRO M/L S(IV)	CH2O	MM/L TOC	MICROGRAM/CU. METER S(IV)	CH2O	TOC	-/+	"CORR" -/+	PH	"PH-BY-DIFFERENCE"
1	0.08	1.00	0.54	55.2	53.0	0.384	14.0	11.0	892.0	0.172	0.127	4114.72	0.979	0.977	4.02	4.08
2	1.00	2.00	1.50	60.0	29.0	0.193	24.0	13.0	717.0	0.149	0.075	1664.96	1.066	1.063	4.00	3.89
3	2.00	3.00	2.50	60.0	43.0	0.287	27.0	17.0	792.0	0.248	0.146	2726.97	1.009	1.007	4.02	4.01
4	3.00	4.58	3.79	94.8	60.0	0.253	40.0	15.0	725.0	0.325	0.114	2204.55	0.957	0.955	4.21	4.37
5	4.58	5.67	5.13	65.4	60.0	0.367	39.0	16.0	883.0	0.459	0.176	3892.00	0.960	0.959	4.27	4.42
6	5.67	6.50	6.09	49.8	19.0	0.153	44.0	13.0	1070.0	0.215	0.060	1961.31	1.002	1.001	4.33	4.33
7	6.50	7.00	6.75	30.0	1.5	0.020	-0.1	-0.1	-0.1	-0.100	-0.100	-0.100	1.501	1.500	5.23	3.72
8	7.80	8.83	8.32	61.8	14.0	0.091	57.0	14.0	-0.2	0.166	0.038	-0.100	1.025	1.024	4.47	4.35
9	8.83	10.50	9.66	100.2	30.0	0.120	37.0	14.0	1480.0	0.142	0.050	2128.89	0.966	0.965	4.25	4.48
10	10.92	12.70	11.81	106.8	24.0	0.090	36.0	17.0	1625.0	0.104	0.046	1754.41	1.010	1.007	3.94	3.91
	TIME-WEIGHTED AVERAGE FOR 10 SAMPLES					0.195				0.215	0.089	2452.783				

REVISED 5/16/84

TABLE 4. McKITTRICK FOG - 5 JAN 84 $

MASS SOLUTE PER M3 OF AIR IS BASED ON LIQUID WATER CONTENT CALCULATED FROM THE VOLUME OF FOGWATER COLLECTED ASSUMING 50% EFFICIENCY AT A 5 M3/MIN SAMPLING RATE.

				(MIN)	(ML)	(G/M3)	/ / / /			MICROGRAM / CUBIC METER					\ \ \ \
#	TIME1	TIME2	MIDT	DT	VOL	LWC	H	NA	NH4	CA	MG	CL	NO3	SO4	SUM
1	0.08	1.00	0.54	55.2	53.0	0.384	0.037	0.035	2.764	0.100	0.005	0.053	5.834	4.925	13.754
2	1.00	2.00	1.50	60.0	29.0	0.193	0.020	0.027	1.210	0.081	0.005	0.023	3.069	2.526	6.959
3	2.00	3.00	2.50	60.0	43.0	0.287	0.028	0.020	1.779	0.057	0.003	0.028	4.070	3.483	9.469
4	3.00	4.58	3.79	94.8	60.0	0.253	0.016	0.012	1.630	0.041	0.003	0.188	2.747	3.101	7.737
5	4.58	5.67	5.13	65.4	60.0	0.367	0.020	0.042	2.118	0.051	0.004	0.030	3.686	4.336	10.288
6	5.67	6.50	6.09	49.8	19.0	0.153	0.007	0.011	0.820	0.031	0.004	0.009	1.448	1.832	4.161
7	6.50	7.00	6.75	30.0	1.5	0.020	0.000	-0.100	0.131	-0.100	-0.100	0.044	0.188	0.326	0.689
8	7.80	8.83	8.32	61.8	14.0	0.091	0.003	0.021	0.652	0.045	0.003	0.024	0.787	1.706	3.242
9	8.83	10.50	9.66	100.2	30.0	0.120	0.007	0.047	0.994	0.276	0.013	0.059	1.819	2.376	5.591
10	10.92	12.70	11.81	106.8	24.0	0.090	0.010	0.031	1.176	0.384	0.017	0.105	2.307	2.953	6.984
	TIME-WEIGHTED AVERAGE FOR 10 SAMPLES					0.195	0.015	0.028	1.367	0.144	0.007	0.068	2.642	2.880	7.143

REVISED 5/16/84

TABLE 5. McKITTRICK FOG - 5 JAN 84 $

THE MASS LOADING OF TRACE METALS PER CU. METER OF AIR IS BASED ON LIQUID WATER CONTENT CALCULATED FROM THE VOLUME OF FOGWATER COLLECTED ASSUMING 50% EFFICIENCY AT A 5 M3/MIN SAMPLING RATE.

				/ / / /	MICROGRAM / LITER				\ \ \ \	/ / / /	MICROGRAM / CUBIC METER				\ \ \ \
#	TIME1	TIME2	PH	FE	MN	PB	CU	NI	V	FE	MN	PB	CU	NI	V
1	0.08	1.00	4.02	39.0	3.0	34.0	16.0	31.0	38.0	0.015	0.001	0.013	0.006	0.012	0.015
2	1.00	2.00	4.00	60.0	3.0	40.0	3.0	30.0	50.0	0.012	0.001	0.008	0.001	0.006	0.010
3	2.00	3.00	4.02	12.0	2.0	30.0	4.0	24.0	43.0	0.003	0.001	0.009	0.001	0.007	0.012
4	3.00	4.58	4.21	8.0	2.0	23.0	4.0	23.0	28.0	0.002	0.001	0.006	0.001	0.006	0.007
5	4.58	5.67	4.27	14.0	2.0	26.0	10.0	29.0	51.0	0.005	0.001	0.010	0.004	0.011	0.019
6	5.67	6.50	4.33	56.0	2.0	31.0	7.0	35.0	51.0	0.009	0.000	0.005	0.001	0.005	0.008
7	6.50	7.00	5.23	-0.1	-0.1	-0.1	-0.1	-0.1	-0.1	-0.100	-0.100	-0.100	-0.100	-0.100	-0.100
8	7.80	8.83	4.47	28.0	3.0	16.0	8.0	39.0	65.0	0.003	0.000	0.001	0.001	0.004	0.006
9	8.83	10.50	4.25	94.0	11.0	37.0	8.0	50.0	100.0	0.011	0.001	0.004	0.001	0.006	0.012
10	10.92	12.70	3.94	261.0	25.0	51.0	20.0	62.0	119.0	0.023	0.002	0.005	0.002	0.006	0.011

REVISED 3/15/84

TABLE 1. McKITTRICK FOG - 6 JAN 84 *

#	TIME1	TIME2	PH	MICRO EQ/LITER H	NA	NH4	CA	MG	CL	NO3	SO4	-/+	MICRO M/L S(IV)	CH2O	/MM/L\ TOC	/ML\ VOL
1	0.55	1.00	4.23	58.9	8.0	241.0	10.0	1.0	8.0	59.0	250.0	0.862	42.0	11.0	-0.2	20.00
2	1.00	2.00	4.03	93.3	7.0	294.0	15.0	2.0	15.0	121.0	317.0	1.002	41.0	13.0	750.0	39.00
3	2.00	3.00	4.22	60.3	6.0	499.0	9.0	1.0	9.0	196.0	371.0	0.928	42.0	19.0	-0.2	30.00
4	3.00	4.00	4.20	63.1	11.0	333.0	10.0	1.0	8.0	158.0	310.0	1.050	37.0	11.0	1050.0	27.00
5	4.00	5.00	4.14	72.4	6.0	345.0	9.0	1.0	3.0	142.0	290.0	0.916	38.0	13.0	-0.2	21.00
6	5.00	6.00	4.31	49.0	4.0	301.0	6.0	0.9	15.0	128.0	247.0	0.981	37.0	15.0	-0.2	13.00
7	6.00	7.00	4.07	85.1	15.0	336.0	28.0	-0.1	15.0	108.0	390.0	0.994	52.0	10.0	-0.2	7.00
8	7.00	7.50	3.78	166.0	-0.1	490.0	-0.1	-0.1	19.0	80.0	633.0	1.117	-0.1	-0.1	-0.1	4.00

REVISED 3/21/84

TABLE 2. McKITTRICK FOG - 6 JAN 84 *

#	TIME1	TIME2	MIDT	EQUIVALENT RATIOS -/+	CL/NA	MG/NA	CA/NA	SO4/NA	NO3/SO4	NH4/N+S	H/N+S	MOLAR RATIOS H+A/N+S	S(IV)/SO4	S(IV)/CH2O
1	0.55	1.00	0.78	0.862	1.000	0.125	1.250	31.250	0.236	0.780	0.191	0.970	0.336	3.818
2	1.00	2.00	1.50	1.002	2.143	0.286	2.143	45.286	0.382	0.671	0.213	0.884	0.259	3.154
3	2.00	3.00	2.50	0.928	1.500	0.167	1.500	61.833	0.528	0.880	0.106	0.986	0.226	2.211
4	3.00	4.00	3.50	1.050	0.727	0.091	0.909	28.182	0.510	0.712	0.135	0.846	0.239	3.364
5	4.00	5.00	4.50	0.916	0.500	0.167	1.500	48.333	0.490	0.799	0.168	0.966	0.262	2.923
6	5.00	6.00	5.50	0.981	3.750	0.000	1.500	61.750	0.518	0.803	0.131	0.933	0.300	2.467
7	6.00	7.00	6.50	0.994	1.000	-0.100	1.867	26.000	0.277	0.675	0.171	0.846	0.267	5.200
8	7.00	7.50	7.25	1.117	-0.100	-0.100	-0.100	-0.100	0.126	0.687	0.233	0.920	-0.100	-0.100
	SEA SALT RATIOS:				1.17	0.228	0.043	0.120						

REVISED 3/21/84

TABLE 3. McKITTRICK FOG - 6 JAN 84 *

MASS SOLUTE PER M3 OF AIR IS BASED ON LIQUID WATER CONTENT CALCULATED FROM THE VOLUME OF FOGWATER COLLECTED ASSUMING 50% EFFICIENCY AT A 5 M3/MIN SAMPLING RATE

#	TIME1	TIME2	MIDT	(MIN) DT	(ML) VOL	(G/M3) LWC	MICRO M/L S(IV)	/MM/L\ CH2O	TOC	MICROGRAM/CU. METER S(IV)	CH2O	TOC	-/+	"CORR" -/+	PH	"PH-BY-DIFFERENCE"
1	0.55	1.00	0.78	27.0	20.0	0.296	42.0	11.0	-0.2	0.399	0.098	-0.100	0.862	0.860	4.23	4.84
2	1.00	2.00	1.50	60.0	39.0	0.260	41.0	13.0	750.0	0.342	0.102	2342.14	1.002	0.999	4.03	4.03
3	2.00	3.00	2.50	60.0	30.0	0.200	42.0	19.0	-0.2	0.269	0.114	-0.100	0.928	0.927	4.22	4.74
4	3.00	4.00	3.50	60.0	27.0	0.180	37.0	11.0	1050.0	0.214	0.059	2270.07	1.050	1.048	4.20	4.08
5	4.00	5.00	4.50	60.0	21.0	0.140	38.0	13.0	-0.2	0.171	0.055	-0.100	0.916	0.914	4.14	4.45
6	5.00	6.00	5.50	60.0	13.0	0.087	37.0	15.0	-0.2	0.103	0.039	-0.100	0.981	0.979	4.31	4.38
7	6.00	7.00	6.50	60.0	7.0	0.047	52.0	10.0	-0.2	0.078	0.014	-0.100	0.994	0.991	4.07	4.09
8	7.00	7.50	7.25	30.0	4.0	0.053	-0.1	-0.1	-0.1	-0.100	-0.100	-0.100	1.117	1.110	3.78	3.62
	TIME-WEIGHTED AVERAGE FOR 8 SAMPLES					0.154				0.210	0.0662306.112					

REVISED 3/21/84

TABLE 4. McKITTRICK FOG - 6 JAN 84 $

MASS SOLUTE PER M3 OF AIR IS BASED ON LIQUID WATER CONTENT CALCULATED FROM THE VOLUME OF FOGWATER COLLECTED ASSUMING 50% EFFICIENCY AT A 5 M3/MIN SAMPLING RATE.

#	TIME1	TIME2	MIDT	(MIN) DT	(ML) VOL	(G/M3) LWC	/ / / / H	MICROGRAM / CUBIC METER NA	NH4	CA	MG	CL	NO3	SO4	\ \ \ \ SUM
1	0.55	1.00	0.78	27.0	20.0	0.296	0.018	0.054	1.288	0.059	0.004	0.084	1.084	3.558	6.149
2	1.00	2.00	1.50	60.0	39.0	0.260	0.025	0.042	1.379	0.078	0.006	0.148	1.951	3.959	7.577
3	2.00	3.00	2.50	60.0	30.0	0.200	0.012	0.028	1.800	0.036	0.002	0.064	2.430	3.564	7.937
4	3.00	4.00	3.50	60.0	27.0	0.180	0.011	0.046	1.081	0.036	0.002	0.051	1.763	2.680	5.671
5	4.00	5.00	4.50	60.0	21.0	0.140	0.010	0.019	0.871	0.025	0.002	0.015	1.233	1.950	4.125
6	5.00	6.00	5.50	60.0	13.0	0.087	0.004	0.008	0.471	0.010	0.000	0.046	0.688	1.028	2.255
7	6.00	7.00	6.50	60.0	7.0	0.047	0.004	0.016	0.283	0.026	-0.100	0.025	0.312	0.874	1.541
8	7.00	7.50	7.25	30.0	4.0	0.053	0.009	-0.100	0.471	-0.100	-0.100	0.036	0.265	1.621	2.402
TIME-WEIGHTED AVERAGE FOR 8 SAMPLES						0.154	0.011	0.028	0.964	0.037	0.003	0.057	1.295	2.369	4.759

REVISED 3/21/84

TABLE 5. McKITTRICK FOG - 6 JAN 84 $

THE MASS LOADING OF TRACE METALS PER CU. METER OF AIR IS BASED ON LIQUID WATER CONTENT CALCULATED FROM THE VOLUME OF FOGWATER COLLECTED ASSUMING 50% EFFICIENCY AT A 5 M3/MIN SAMPLING RATE.

#	TIME1	TIME2	PH	/ / / / FE	MN	MICROGRAM / LITER PB	CU	NI	\ \ \ \ V	/ / / / FE	MN	MICROGRAM / CUBIC METER PB	CU	NI	\ \ \ \ V
1	0.55	1.00	4.23	29.0	2.0	6.0	8.0	38.0	69.0	0.009	0.001	0.002	0.002	0.011	0.020
2	1.00	2.00	4.03	35.0	4.0	19.0	13.0	65.0	124.0	0.009	0.001	0.005	0.003	0.022	0.032
3	2.00	3.00	4.22	33.0	3.0	21.0	11.0	69.0	89.0	0.007	0.001	0.004	0.002	0.014	0.018
4	3.00	4.00	4.20	36.0	1.0	24.0	11.0	62.0	88.0	0.006	0.000	0.004	0.002	0.011	0.016
5	4.00	5.00	4.14	38.0	2.0	19.0	5.0	62.0	93.0	0.005	0.000	0.003	0.001	0.009	0.013
6	5.00	6.00	4.31	19.0	1.0	11.0	3.0	48.0	78.0	0.002	0.000	0.001	0.000	0.004	0.007
7	6.00	7.00	4.07	-0.1	-0.1	-0.1	-0.1	-0.1	-0.1	-0.100	-0.100	-0.100	-0.100	-0.100	-0.100
8	7.00	7.50	3.78	-0.1	-0.1	-0.1	-0.1	-0.1	-0.1	-0.100	-0.100	-0.100	-0.100	-0.100	-0.100

REVISED 3/15/84

TABLE 1. MCKITTRICK FOG - 7 & 8 JAN 84 $

#	TIME1	TIME2	PH	MICRO EQ/LITER H	NA	NH4	CA	MG	CL	NO3	SO4	-/+	MICRO M/L S(IV)	CH2O	MM/L TOC	ML VOL
1	-3.08	-2.08	4.64	22.9	-0.1	278.0	13.0	2.0	3.3	44.0	267.0	0.824	54.0	28.0	1540.0	49.00
2	-1.50	-1.00	4.11	77.6	-0.1	146.0	14.0	1.0	5.0	41.0	225.0	0.968	40.0	29.0	-0.2	25.00
3	-1.00	0.00	4.21	61.7	-0.1	119.0	16.0	1.0	14.0	32.0	191.0	1.002	39.0	14.0	1150.0	40.00
4	0.00	1.00	3.96	109.6	-0.1	136.0	47.0	2.0	26.0	46.0	250.0	0.954	41.0	18.0	-0.2	35.00
5	1.25	1.87	4.41	38.9	-0.1	186.0	10.0	1.0	4.3	51.0	210.0	0.922	48.0	11.0	1720.0	33.00
6	2.00	3.00	4.26	55.0	-0.1	162.0	14.0	2.0	12.0	50.0	223.0	1.061	38.0	23.0	-0.2	38.00
7	3.00	4.00	4.40	39.8	-0.1	204.0	36.0	6.0	7.4	43.0	255.0	0.925	41.0	6.0	2300.0	12.00
8	4.00	5.00	4.44	36.3	-0.1	166.0	24.0	3.0	7.1	29.0	278.0	1.161	48.0	13.0	-0.2	36.00
9	5.00	5.50	4.41	38.9	-0.1	150.0	8.0	1.0	1.7	25.0	258.0	1.176	52.0	14.0	-0.2	16.00
10	6.00	7.00	4.71	19.5	-0.1	294.0	39.0	6.0	15.0	57.0	446.0	1.289	56.0	11.0	1500.0	12.00
11	7.00	9.00	4.47	33.9	-0.1	247.0	47.0	6.0	21.0	39.0	406.0	1.252	48.0	50.0	1920.0	25.00
12	9.50	10.50	4.44	36.3	-0.1	272.0	120.0	12.0	24.0	120.0	442.0	1.245	38.0	21.0	-0.2	12.00
13	10.50	12.50	4.23	58.9	-0.1	683.0	116.0	12.0	13.0	178.0	806.0	1.095	45.0	29.0	2250.0	35.00
14	12.50	14.67	4.24	57.5	-0.1	870.0	145.0	14.0	24.0	313.0	827.0	1.024	51.0	32.0	2810.0	28.00
15	14.67	15.67	4.28	52.5	-0.1	740.0	71.0	8.0	6.6	260.0	630.0	0.981	42.0	27.0	-0.2	30.00
16	15.67	16.92	4.12	75.9	-0.1	522.0	27.0	3.0	4.0	209.0	467.0	1.021	39.0	27.0	1870.0	50.00
17	16.92	18.50	3.93	117.5	-0.1	539.0	19.0	3.0	7.2	226.0	538.0	1.076	41.0	24.0	-0.2	42.00
18	18.50	19.58	3.80	158.5	-0.1	-0.1	-0.1	-0.1	-0.1	-0.1	-0.1	-0.001	-0.1	-0.1	-0.1	20.00
19	19.58	20.58	3.89	128.8	9.0	444.0	20.0	3.0	12.0	181.0	410.0	0.921	46.0	26.0	-0.2	18.00
20	20.58	24.58	4.18	66.1	12.0	599.0	12.0	2.0	9.0	222.0	546.0	1.029	66.0	30.0	2040.0	52.00
21	24.58	26.08	4.50	31.6	6.0	555.0	6.0	1.0	9.0	148.0	606.0	1.132	84.0	35.0	-0.2	18.00
22	26.08	28.08	5.01	9.8	16.0	658.0	15.0	10.0	10.0	152.0	600.0	1.075	-0.1	-0.1	-0.2	8.00

REVISED 5/16/84

TABLE 2. MCKITTRICK FOG - 7 & 8 JAN 84 $

#	TIME1	TIME2	MIDT	EQUIVALENT RATIOS -/+	CL/NA	MG/NA	CA/NA	SO4/NA	NO3/SO4	NH4/N+S	H/N+S	H+A/N+S	MOLAR RATIOS S(IV)/SO4	S(IV)/CH2O
1	-3.08	-2.08	-2.58	0.824	-0.100	-0.100	-0.100	-0.100	0.165	0.894	0.074	0.968	0.404	1.929
2	-1.50	-1.00	-1.25	0.968	-0.100	-0.100	-0.100	-0.100	0.182	0.549	0.292	0.841	0.356	1.379
3	-1.00	0.00	-0.50	1.002	-0.100	-0.100	-0.100	-0.100	0.168	0.534	0.276	0.810	0.408	2.786
4	0.00	1.00	0.50	0.954	-0.100	-0.100	-0.100	-0.100	0.184	0.459	0.370	0.830	0.328	2.278
5	1.25	1.87	1.56	0.922	-0.100	-0.100	-0.100	-0.100	0.243	0.713	0.149	0.862	0.457	4.364
6	2.00	3.00	2.50	1.061	-0.100	-0.100	-0.100	-0.100	0.224	0.593	0.201	0.795	0.341	1.652
7	3.00	4.00	3.50	0.925	-0.100	-0.100	-0.100	-0.100	0.169	0.685	0.134	0.818	0.322	6.833
8	4.00	5.00	4.50	1.161	-0.100	-0.100	-0.100	-0.100	0.104	0.541	0.118	0.659	0.345	3.692
9	5.00	5.50	5.25	1.176	-0.100	-0.100	-0.100	-0.100	0.097	0.530	0.137	0.668	0.403	3.714
10	6.00	7.00	6.50	1.289	-0.100	-0.100	-0.100	-0.100	0.128	0.584	0.039	0.623	0.251	5.091
11	7.00	9.00	8.00	1.252	-0.100	-0.100	-0.100	-0.100	0.096	0.555	0.076	0.631	0.236	0.960
12	9.50	10.50	10.00	1.245	-0.100	-0.100	-0.100	-0.100	0.271	0.484	0.065	0.549	0.172	1.810
13	10.50	12.50	11.50	1.095	-0.100	-0.100	-0.100	-0.100	0.221	0.694	0.060	0.754	0.112	1.552
14	12.50	14.67	13.59	1.024	-0.100	-0.100	-0.100	-0.100	0.378	0.763	0.050	0.814	0.123	1.594
15	14.67	15.67	15.17	0.981	-0.100	-0.100	-0.100	-0.100	0.413	0.831	0.059	0.890	0.133	1.556
16	15.67	16.92	16.30	1.021	-0.100	-0.100	-0.100	-0.100	0.448	0.772	0.112	0.884	0.167	1.444
17	16.92	18.50	17.71	1.076	-0.100	-0.100	-0.100	-0.100	0.420	0.705	0.154	0.859	0.152	1.708
18	18.50	19.58	19.04	-0.001	-0.100	-0.100	-0.100	-0.100	-0.100	-0.100	-0.100	-0.100	-0.100	-0.100
19	19.58	20.58	20.08	0.921	1.333	0.333	2.222	45.556	0.441	0.751	0.218	0.969	0.224	1.769
20	20.58	24.58	22.58	1.029	0.750	0.167	1.000	45.500	0.407	0.780	0.086	0.866	0.242	2.200
21	24.58	26.08	25.33	1.132	1.500	0.167	1.000	101.000	0.244	0.736	0.042	0.778	0.277	2.400
22	26.08	28.08	27.08	1.075	0.625	0.625	0.937	37.500	0.253	0.875	0.013	0.888	-0.100	-0.100
	SEA SALT RATIOS:				1.17	0.228	0.043	0.120						

REVISED 5/16/84

ABLE 3. MCKITTRICK FOG - 7 & 8 JAN 84 $

MASS SOLUTE PER M3 OF AIR IS BASED ON LIQUID WATER CONTENT CALCULATED FROM THE VOLUME OF FOGWATER COLLECTED ASSUMING 50% EFFICIENCY AT A 5 M3/MIN SAMPLING RATE

#	TIME1	TIME2	MIDT	(MIN) DT	(ML) VOL	(G/M3) LWC	/ MICRO M/L \ S(IV)	CH2O	/MM/L\ TOC	/ MICROGRAM/CU. METER \ S(IV)	CH2O	TOC	-/+	"CORR" -/+	PH	"PH-BY- DIFFERENCE"
1	-3.08	-2.08	-2.58	60.0	49.0	0.327	54.0	28.0	1540.0	0.566	0.275	6042.33	0.824	0.823	4.64	*****
2	-1.50	-1.00	-1.25	30.0	25.0	0.333	40.0	29.0	-0.2	0.427	0.290	-0.100	0.968	0.965	4.11	4.16
3	-1.00	0.00	-0.50	60.0	40.0	0.267	39.0	14.0	1150.0	0.333	0.112	3683.37	1.002	1.000	4.21	4.21
4	0.00	1.00	0.50	60.0	35.0	0.233	41.0	18.0	-0.2	0.307	0.126	-0.100	0.954	0.950	3.96	4.02
5	1.25	1.87	1.56	37.2	33.0	0.355	48.0	11.0	1720.0	0.546	0.117	7330.58	0.922	0.920	4.41	4.70
6	2.00	3.00	2.50	60.0	38.0	0.253	38.0	23.0	-0.2	0.309	0.175	-0.100	1.061	1.059	4.26	4.16
7	3.00	4.00	3.50	60.0	12.0	0.080	41.0	6.0	2300.0	0.105	0.014	2210.02	0.925	0.924	4.40	4.74
8	4.00	5.00	4.50	60.0	36.0	0.240	48.0	13.0	-0.2	0.369	0.094	-0.100	1.161	1.159	4.44	4.14
9	5.00	5.50	5.25	30.0	16.0	0.213	52.0	14.0	-0.2	0.356	0.090	-0.100	1.176	1.174	4.41	4.13
10	6.00	7.00	6.50	60.0	12.0	0.080	56.0	11.0	1500.0	0.144	0.026	1441.32	1.289	1.288	4.71	3.91
11	7.00	9.00	8.00	120.0	25.0	0.083	48.0	50.0	1920.0	0.128	0.125	1921.76	1.252	1.251	4.47	3.93
12	9.50	10.50	10.00	60.0	12.0	0.080	38.0	21.0	-0.2	0.097	0.050	-0.100	1.245	1.243	4.44	3.84
13	10.50	12.50	11.50	120.0	35.0	0.117	45.0	29.0	2250.0	0.168	0.102	3152.88	1.095	1.092	4.23	3.86
14	12.50	14.67	13.59	130.2	28.0	0.086	51.0	32.0	2810.0	0.141	0.083	2903.30	1.024	1.023	4.24	4.09
15	14.67	15.67	15.17	60.0	30.0	0.200	42.0	27.0	-0.2	0.269	0.162	-0.100	0.981	0.979	4.28	4.46
16	15.67	16.92	16.30	75.0	50.0	0.267	39.0	27.0	1870.0	0.333	0.216	5989.48	1.021	1.019	4.12	4.06
17	16.92	18.50	17.71	94.8	42.0	0.177	41.0	24.0	-0.2	0.233	0.128	-0.100	1.076	1.073	3.93	3.78
18	18.50	19.58	19.04	64.8	20.0	0.123	-0.1	-0.1	-0.1	-0.100	-0.100	-0.100	-0.001	-0.001	3.80	6.70
19	19.58	20.58	20.08	60.0	18.0	0.120	46.0	26.0	-0.2	0.177	0.094	-0.100	0.921	0.917	3.89	4.10
20	20.58	24.58	22.58	240.0	52.0	0.087	66.0	30.0	2040.0	0.183	0.078	2123.54	1.029	1.027	4.18	4.07
21	24.58	26.08	25.33	90.0	18.0	0.080	84.0	35.0	-0.2	0.215	0.084	-0.100	1.132	1.131	4.50	3.96
22	26.08	28.08	27.08	120.0	8.0	0.027	-0.1	-0.1	-0.2	-0.100	-0.100	-0.100	1.075	1.075	5.01	4.20
TIME-WEIGHTED AVERAGE FOR 22 SAMPLES						0.105				0.173	0.0832	644.565				

REVISED 5/16/84

TABLE 4. MCKITTRICK FOG - 7 & 8 JAN 84 $

MASS SOLUTE PER M3 OF AIR IS BASED ON LIQUID WATER CONTENT CALCULATED FROM THE VOLUME OF FOGWATER COLLECTED ASSUMING 50% EFFICIENCY AT A 5 M3/MIN SAMPLING RATE.

				(MIN)	(ML)	(G/M3)	/ / / /		MICROGRAM / CUBIC METER						\ \ \ \
#	TIME1	TIME2	MIDT	DT	VOL	LWC	H	NA	NH4	CA	MG	CL	NO3	SO4	SUM
1	-3.08	-2.08	-2.58	60.0	49.0	0.327	0.008	-0.100	1.638	0.085	0.008	0.038	0.891	4.189	6.857
2	-1.50	-1.00	-1.25	30.0	25.0	0.333	0.026	-0.100	0.878	0.094	0.004	0.059	0.847	3.602	5.510
3	-1.00	0.00	-0.50	60.0	40.0	0.267	0.017	-0.100	0.572	0.086	0.003	0.132	0.529	2.446	3.786
4	0.00	1.00	0.50	60.0	35.0	0.233	0.026	-0.100	0.572	0.220	0.006	0.215	0.665	2.802	4.506
5	1.25	1.87	1.56	37.2	33.0	0.355	0.014	-0.100	1.191	0.071	0.004	0.054	1.122	3.579	6.035
6	2.00	3.00	2.50	60.0	38.0	0.253	0.014	-0.100	0.740	0.071	0.006	0.108	0.785	2.713	4.438
7	3.00	4.00	3.50	60.0	12.0	0.080	0.003	-0.100	0.294	0.058	0.006	0.021	0.213	0.980	1.575
8	4.00	5.00	4.50	60.0	36.0	0.240	0.009	-0.100	0.719	0.115	0.009	0.060	0.432	3.205	4.548
9	5.00	5.50	5.25	30.0	16.0	0.213	0.008	-0.100	0.577	0.034	0.003	0.013	0.331	2.644	3.610
10	6.00	7.00	6.50	60.0	12.0	0.080	0.002	-0.100	0.424	0.063	0.006	0.043	0.283	1.714	2.533
11	7.00	9.00	8.00	120.0	25.0	0.083	0.003	-0.100	0.371	0.078	0.006	0.062	0.201	1.625	2.347
12	9.50	10.50	10.00	60.0	12.0	0.080	0.003	-0.100	0.393	0.192	0.012	0.068	0.595	1.698	2.961
13	10.50	12.50	11.50	120.0	35.0	0.117	0.007	-0.100	1.437	0.271	0.017	0.054	1.288	4.516	7.590
14	12.50	14.67	13.59	130.2	28.0	0.086	0.005	-0.100	1.350	0.250	0.015	0.073	1.669	3.417	6.779
15	14.67	15.67	15.17	60.0	30.0	0.200	0.011	-0.100	2.670	0.285	0.019	0.047	3.224	6.052	12.307
16	15.67	16.92	16.30	75.0	50.0	0.267	0.020	-0.100	2.511	0.144	0.010	0.038	3.455	5.981	12.160
17	16.92	18.50	17.71	94.8	42.0	0.177	0.021	-0.100	1.723	0.067	0.006	0.045	2.483	4.579	8.926
18	18.50	19.58	19.04	64.8	20.0	0.123	0.020	-0.100	-0.100	-0.100	-0.100	-0.100	-0.100	-0.100	0.020
19	19.58	20.58	20.08	60.0	18.0	0.120	0.016	0.025	0.961	0.048	0.004	0.051	1.347	2.363	4.815
20	20.58	24.58	22.58	240.0	52.0	0.087	0.006	0.024	0.937	0.021	0.002	0.028	1.193	2.273	4.482
21	24.58	26.08	25.33	90.0	18.0	0.080	0.003	0.011	0.801	0.010	0.001	0.026	0.734	2.328	3.913
22	26.08	28.08	27.08	120.0	8.0	0.027	0.000	0.010	0.317	0.008	0.003	0.009	0.251	0.768	1.367
TIME-WEIGHTED AVERAGE FOR 22 SAMPLES						0.145	0.009	0.018	1.011	0.106	0.007	0.054	1.119	2.917	5.037

REVISED 5/16/84

TABLE 5. McKITTRICK FOG - 7 & 8 JAN 84 $

THE MASS LOADING OF TRACE METALS PER CU. METER OF AIR IS BASED ON LIQUID WATER CONTENT
CALCULATED FROM THE VOLUME OF FOGWATER COLLECTED ASSUMING 50% EFFICIENCY AT A 5 M3/MIN SAMPLING RATE.

				MICROGRAM / LITER						MICROGRAM / CUBIC METER					
#	TIME1	TIME2	PH	FE	MN	PB	CU	NI	V	FE	MN	PB	CU	NI	V
1	-3.08	-2.08	4.64	52.0	4.0	10.0	7.0	30.0	53.0	0.017	0.001	0.003	0.002	0.010	0.017
2	-1.50	-1.00	4.11	63.0	2.0	16.0	7.0	40.0	111.0	0.021	0.001	0.005	0.002	0.013	0.037
3	-1.00	0.00	4.21	58.0	2.0	14.0	10.0	34.0	116.0	0.015	0.001	0.004	0.003	0.009	0.031
4	0.00	1.00	3.96	52.0	2.0	15.0	3.0	40.0	206.0	0.012	0.000	0.004	0.001	0.009	0.048
5	1.25	1.87	4.41	35.0	1.0	7.0	3.0	21.0	60.0	0.012	0.000	0.002	0.001	0.007	0.021
6	2.00	3.00	4.26	70.0	2.0	9.0	18.0	35.0	88.0	0.018	0.001	0.002	0.005	0.009	0.022
7	3.00	4.00	4.40	157.0	3.0	17.0	21.0	46.0	81.0	0.013	0.000	0.001	0.002	0.004	0.006
8	4.00	5.00	4.44	128.0	4.0	8.0	15.0	38.0	148.0	0.031	0.001	0.002	0.004	0.009	0.036
9	5.00	5.50	4.41	58.0	2.0	4.0	9.0	17.0	43.0	0.012	0.000	0.001	0.002	0.004	0.009
10	6.00	7.00	4.71	138.0	4.0	7.0	15.0	42.0	69.0	0.011	0.000	0.001	0.001	0.003	0.006
11	7.00	9.00	4.47	111.0	9.0	16.0	34.0	46.0	104.0	0.009	0.001	0.001	0.003	0.004	0.009
12	9.50	10.50	4.44	185.0	8.0	24.0	16.0	67.0	49.0	0.015	0.001	0.002	0.001	0.005	0.004
13	10.50	12.50	4.23	89.0	13.0	19.0	3.0	42.0	125.0	0.010	0.002	0.002	0.000	0.005	0.015
14	12.50	14.67	4.24	157.0	19.0	36.0	25.0	58.0	83.0	0.014	0.002	0.003	0.002	0.005	0.007
15	14.67	15.67	4.28	86.0	10.0	85.0	9.0	58.0	90.4	0.017	0.002	0.017	0.002	0.012	0.018
16	15.67	16.92	4.12	45.0	5.0	18.0	6.0	42.0	52.0	0.012	0.001	0.005	0.002	0.011	0.014
17	16.92	18.50	3.93	31.0	-0.1	25.0	4.0	54.0	102.0	0.005	-0.100	0.004	0.001	0.010	0.018
18	18.50	19.58	3.80	-0.1	-0.1	-0.1	-0.1	-0.1	-0.1	-0.100	-0.100	-0.100	-0.100	-0.100	-0.100
19	19.58	20.58	3.89	42.0	4.0	26.0	6.2	47.0	154.0	0.005	0.000	0.003	0.001	0.006	0.018
20	20.58	24.58	4.18	51.0	2.0	15.0	6.4	62.0	117.0	0.004	0.000	0.001	0.001	0.005	0.010
21	24.58	26.08	4.50	105.0	2.0	9.0	6.4	52.0	107.0	0.008	0.000	0.001	0.001	0.004	0.009
22	26.08	28.08	5.01	-0.1	-0.1	-0.1	-0.1	-0.1	-0.1	-0.100	-0.100	-0.100	-0.100	-0.100	-0.100

REVISED 3/15/84

TABLE 1. MCKITTRICK FOG - 8 JAN 84 $

#	TIME1	TIME2	PH	MICRO EQ/LITER H	NA	NH4	CA	MG	CL	NO3	SO4	-/+	MICRO M/L S(IV)	CH2O	MM/L TOC	ML VOL
1	8.25	9.58	4.44	36.3	62.0	1140.0	68.0	10.0	14.0	264.0	1170.0	1.100	-0.1	-0.1	-0.2	7.00
2	9.58	11.08	3.93	117.5	15.0	522.0	26.0	4.0	17.0	216.0	592.0	1.140	45.0	38.0	-0.2	8.00
3	11.25	12.33	3.80	158.5	17.0	636.0	-30.0	-0.1	16.0	240.0	684.0	1.203	-0.1	-0.1	-0.2	3.00

REVISED 5/16/84

TABLE 2. MCKITTRICK FOG - 8 JAN 84 $

#	TIME1	TIME2	MIDT	-/+	EQUIVALENT RATIOS CL/NA	MG/NA	CA/NA	SO4/NA	NO3/SO4	NH4/N+S	H/N+S	H+A/N+S	MOLAR RATIOS S(IV)/SO4	S(IV)/CH2O
1	8.25	9.58	8.91	1.100	0.226	0.161	1.097	18.871	0.226	0.795	0.025	0.820	-0.100	-0.100
2	9.58	11.08	10.33	1.140	1.133	0.267	1.733	39.467	0.365	0.646	0.145	0.791	0.152	1.184
3	11.25	12.33	11.79	1.203	0.941	-0.100	-0.100	40.235	0.351	0.688	0.172	0.860	-0.100	-0.100
	SEA SALT RATIOS:				1.17	0.228	0.043	0.120						

REVISED 5/16/84

ABLE 3. MCKITTRICK FOG - 8 JAN 84 $

MASS SOLUTE PER M3 OF AIR IS BASED ON LIQUID WATER CONTENT CALCULATED FROM THE VOLUME OF FOGWATER COLLECTED ASSUMING 50% EFFICIENCY AT A 5 M3/MIN SAMPLING RATE

#	TIME1	TIME2	MIDT	(MIN) DT	(ML) VOL	(G/M3) LWC	MICRO M/L S(IV)	CH2O	MM/L TOC	MICROGRAM/CU. METER S(IV)	CH2O	TOC	-/+	*CORR* -/+	PH	*PH-BY-DIFFERENCE*
1	8.25	9.58	8.91	79.8	7.0	0.035	-0.1	-0.1	-0.2	-0.100	-0.100	-0.100	1.100	1.099	4.44	3.78
2	9.58	11.08	10.33	90.0	8.0	0.036	45.0	38.0	-0.2	0.051	0.041	-0.100	1.140	1.135	3.93	3.68
3	11.25	12.33	11.79	64.8	3.0	0.019	-0.1	-0.1	-0.2	-0.100	-0.100	-0.100	1.203	1.197	3.80	3.50
	TIME-WEIGHTED AVERAGE FOR 3 SAMPLES					0.003				0.002	0.002	0.000				

REVISED 5/16/84

TABLE 4. MCKITTRICK FOG - 8 JAN 84 $

MASS SOLUTE PER M3 OF AIR IS BASED ON LIQUID WATER CONTENT CALCULATED FROM THE VOLUME OF FOGWATER COLLECTED ASSUMING 50% EFFICIENCY AT A 5 M3/MIN SAMPLING RATE.

#	TIME1	TIME2	MIDT	(MIN) DT	(ML) VOL	(G/M3) LWC	/ / / / H	NA	NH4	MICROGRAM / CUBIC METER CA	MG	CL	NO3	SO4	\ \ \ \ SUM
1	8.25	9.58	8.91	79.8	7.0	0.035	0.001	0.050	0.722	0.048	0.004	0.017	0.574	1.972	3.388
2	9.58	11.08	10.33	90.0	8.0	0.036	0.004	0.012	0.335	0.019	0.002	0.021	0.476	1.011	1.880
3	11.25	12.33	11.79	64.8	3.0	0.019	0.003	0.007	0.212	-30.000	-0.100	0.011	0.276	0.608	1.117
	TIME-WEIGHTED AVERAGE FOR 3 SAMPLES					0.031	0.003	0.024	0.433	0.032	0.003	0.017	0.454	1.227	2.182

REVISED 5/16/84

TABLE 5. McKITTRICK FOG - 8 JAN 84 $

THE MASS LOADING OF TRACE METALS PER CU. METER OF AIR IS BASED ON LIQUID WATER CONTENT CALCULATED FROM THE VOLUME OF FOGWATER COLLECTED ASSUMING 50% EFFICIENCY AT A 5 M3/MIN SAMPLING RATE.

#	TIME1	TIME2	PH	/ / / / FE	MN	MICROGRAM / LITER PB	CU	NI	\ \ \ \ V	/ / / / FE	MN	MICROGRAM / CUBIC METER PB	CU	NI	\ \ \ \ V
1	8.25	9.58	4.44	182.0	14.0	13.0	19.0	176.0	154.0	0.006	0.000	0.000	0.001	0.006	0.005
2	9.58	11.08	3.93	-0.1	-0.1	-0.1	-0.1	-0.1	-0.1	-0.100	-0.100	-0.100	-0.100	-0.100	-0.100
3	11.25	12.33	3.80	-0.1	-0.1	-0.1	-0.1	-0.1	-0.1	-0.100	-0.100	-0.100	-0.100	-0.100	-0.100

REVISED 3/15/84

TABLE 1. McKITTRICK FOG - 9 JAN 84 $

#	TIME1	TIME2	PH	MICRO EQ/LITER H	NA	NH4	CA	MG	CL	NO3	SO4	-/+	MICRO M/L S(IV)	CH2O	/MM/L TOC	/ML VOL
1	-5.75	-4.25	3.77	169.8	12.0	519.0	20.0	3.0	20.0	239.0	575.0	1.114	28.0	30.0	-0.2	8.00
2	9.00	11.00	3.55	281.8	34.0	686.0	73.0	14.0	32.0	379.0	767.0	1.082	-0.1	-0.1	-0.2	6.00
3	11.00	12.50	3.47	338.8	-0.1	912.0	-0.1	-0.1	-0.1	-0.1	-0.1	-0.000	-0.1	-0.1	-0.1	1.00

REVISED 2/17/84

TABLE 2. McKITTRICK FOG - 9 JAN 84 $

#	TIME1	TIME2	MIDT	-/+	EQUIVALENT RATIOS CL/NA	MG/NA	CA/NA	SO4/NA	NO3/SO4	NH4/N+S	H/N+S	MOLAR RATIOS H+A/N+S	S(IV)/SO4	S(IV)/CH2O
1	-5.75	-4.25	-5.00	1.114	1.667	0.250	1.667	47.917	0.416	0.638	0.209	0.846	0.097	0.933
2	9.00	11.00	10.00	1.082	0.941	0.412	2.147	22.559	0.494	0.599	0.246	0.845	-0.100	-0.100
3	11.00	12.50	11.75	-0.000	-0.100	-0.100	-0.100	-0.100	-0.100	-0.100	-0.100	-0.100	-0.100	-0.100
	SEA SALT RATIOS:				1.17	0.228	0.043	0.120						

REVISED 2/17/84

ABLE 3. McKITTRICK FOG - 9 JAN 84 $

MASS SOLUTE PER M3 OF AIR IS BASED ON LIQUID WATER CONTENT CALCULATED FROM THE VOLUME OF FOGWATER COLLECTED ASSUMING 50% EFFICIENCY AT A 5 M3/MIN SAMPLING RATE

#	TIME1	TIME2	MIDT	(MIN) DT	(ML) VOL	(G/M3) LWC	MICRO M/L S(IV)	/MM/L CH2O	TOC	MICROGRAM/CU. METER S(IV)	CH2O	TOC	-/+	"CORR" -/+	PH	"PH-BY-DIFFERENCE"
1	-5.75	-4.25	-5.00	90.0	8.0	0.036	28.0	30.0	-0.2	0.032	0.032	-0.100	1.114	1.108	3.77	3.61
2	9.00	11.00	10.00	120.0	6.0	0.020	-0.1	-0.1	-0.2	-0.100	-0.100	-0.100	1.082	1.074	3.55	3.44
3	11.00	12.50	11.75	90.0	1.0	0.004	-0.1	-0.1	-0.1	-0.100	-0.100	-0.100	-0.000	-0.000	3.47	*****
	TIME-WEIGHTED AVERAGE FOR 3 SAMPLES					0.011				0.011	0.011	0.000				

REVISED 2/17/84

TABLE 4. McKITTRICK FOG - 9 JAN 84 $

MASS SOLUTE PER M3 OF AIR IS BASED ON LIQUID WATER CONTENT CALCULATED FROM THE VOLUME OF FOGWATER COLLECTED ASSUMING 50% EFFICIENCY AT A 5 M3/MIN SAMPLING RATE.

#	TIME1	TIME2	MIDT	(MIN) DT	(ML) VOL	(G/M3) LWC	MICROGRAM / CUBIC METER H	NA	NH4	CA	MG	CL	NO3	SO4	SUM
1	-5.75	-4.25	-5.00	90.0	8.0	0.036	0.006	0.010	0.333	0.014	0.001	0.025	0.527	0.982	1.898
2	9.00	11.00	10.00	120.0	6.0	0.020	0.006	0.016	0.248	0.029	0.003	0.023	0.470	0.737	1.531
3	11.00	12.50	11.75	90.0	1.0	0.004	0.002	-0.100	0.073	-0.100	-0.100	-0.100	-0.100	-0.100	0.075
	TIME-WEIGHTED AVERAGE FOR 3 SAMPLES					0.020	0.005	0.013	0.221	0.023	0.003	0.024	0.494	0.842	1.204

REVISED 2/17/84

TABLE 1. McKITTRICK FOG - 10 JAN 84 *

#	TIME1	TIME2	PH	MICRO EQ/LITER H	NA	NH4	CA	MG	CL	NO3	SO4	-/+	MICRO M/L S(IV)	CH2O	MM/L TOC	ML VOL
1	0.17	1.33	3.71	195.0	28.0	845.0	78.0	8.0	30.0	270.0	842.0	0.939	58.0	77.0	2620.0	20.00
2	1.33	5.42	3.85	141.3	7.0	351.0	16.0	2.0	16.0	131.0	418.0	1.021	37.0	59.0	-0.2	55.00
3	5.42	6.83	3.96	109.6	10.0	610.0	16.0	3.0	16.0	212.0	538.0	0.952	53.0	63.0	-0.2	25.00
4	6.83	8.17	4.44	36.3	10.0	911.0	27.0	5.0	28.0	223.0	884.0	1.039	107.0	85.0	-0.2	20.00
5	8.17	9.50	4.09	81.3	10.0	840.0	29.0	4.0	9.0	238.0	778.0	0.981	79.0	93.0	-0.2	11.00

REVISED 3/21/84

TABLE 2. McKITTRICK FOG - 10 JAN 84 *

#	TIME1	TIME2	MIDT	-/+	EQUIVALENT RATIOS CL/NA	MG/NA	CA/NA	SO4/NA	NO3/SO4	NH4/N+S	H/N+S	MOLAR RATIOS H+A/N+S	S(IV)/SO4	S(IV)/CH2O
1	0.17	1.33	0.75	0.939	1.071	0.286	2.786	30.071	0.321	0.760	0.175	0.935	0.138	0.753
2	1.33	5.42	3.38	1.021	2.286	0.286	2.286	59.714	0.313	0.639	0.257	0.897	0.177	0.627
3	5.42	6.83	6.13	0.952	1.600	0.300	1.600	53.800	0.394	0.813	0.146	0.960	0.197	0.841
4	6.83	8.17	7.50	1.039	2.800	0.500	2.700	88.400	0.252	0.823	0.033	0.856	0.242	1.259
5	8.17	9.50	8.84	0.981	0.900	0.400	2.900	77.800	0.306	0.827	0.080	0.907	0.203	0.849
	SEA SALT RATIOS‡				1.17	0.228	0.043	0.120						

REVISED 3/21/84

ABLE 3. McKITTRICK FOG - 10 JAN 84 *

MASS SOLUTE PER M3 OF AIR IS BASED ON LIQUID WATER CONTENT CALCULATED FROM THE VOLUME OF FOGWATER COLLECTED ASSUMING 50% EFFICIENCY AT A 5 M3/MIN SAMPLING RATE

#	TIME1	TIME2	MIDT	(MIN) DT	(ML) VOL	(G/M3) LWC	MICRO M/L S(IV)	CH2O	MM/L TOC	MICROGRAM/CU. METER S(IV)	CH2O	TOC	-/+	"CORR" -/+	PH	"PH-BY-DIFFERENCE"
1	0.17	1.33	0.75	69.6	20.0	0.115	58.0	77.0	2620.0	0.214	0.266	3617.10	0.939	0.934	3.71	3.93
2	1.33	5.42	3.38	245.4	55.0	0.090	37.0	59.0	-0.2	0.106	0.159	-0.100	1.021	1.016	3.85	3.83
3	5.42	6.83	6.13	84.6	25.0	0.118	53.0	63.0	-0.2	0.201	0.224	-0.100	0.952	0.949	3.96	4.15
4	6.83	8.17	7.50	80.4	20.0	0.100	107.0	85.0	-0.2	0.341	0.254	-0.100	1.039	1.038	4.44	4.13
5	8.17	9.50	8.84	79.8	11.0	0.055	79.0	93.0	-0.2	0.140	0.154	-0.100	0.981	0.978	4.09	4.22
	TIME-WEIGHTED AVERAGE FOR 5 SAMPLES					0.025				0.065	0.069	375.972				

REVISED 3/21/84

TABLE 4. McKITTRICK FOG - 10 JAN 84 $

MASS SOLUTE PER M3 OF AIR IS BASED ON LIQUID WATER CONTENT CALCULATED FROM THE VOLUME OF FOGWATER COLLECTED ASSUMING 50% EFFICIENCY AT A 5 M3/MIN SAMPLING RATE.

#	TIME1	TIME2	MIDT	(MIN) DT	(ML) VOL	(G/M3) LWC	/ / / / H			MICROGRAM / CUBIC METER					\ \ \ \ SUM
								NA	NH4	CA	MG	CL	NO3	SO4	
1	0.17	1.33	0.75	69.6	20.0	0.115	0.023	0.074	1.752	0.180	0.011	0.122	1.924	4.648	8.734
2	1.33	5.42	3.38	245.4	55.0	0.090	0.013	0.014	0.568	0.029	0.002	0.051	0.728	1.800	3.205
3	5.42	6.83	6.13	84.6	25.0	0.118	0.013	0.027	1.301	0.038	0.004	0.067	1.554	3.054	6.058
4	6.83	8.17	7.50	80.4	20.0	0.100	0.004	0.023	1.635	0.054	0.006	0.099	1.376	4.225	7.421
5	8.17	9.50	8.84	79.8	11.0	0.055	0.005	0.013	0.836	0.032	0.003	0.018	0.814	2.060	3.779
TIME-WEIGHTED AVERAGE FOR 5 SAMPLES						0.094	0.012	0.025	1.017	0.053	0.004	0.064	1.107	2.729	5.011

REVISED 3/21/84

TABLE 5. McKITTRICK FOG - 10 JAN 84 $

THE MASS LOADING OF TRACE METALS PER CU. METER OF AIR IS BASED ON LIQUID WATER CONTENT CALCULATED FROM THE VOLUME OF FOGWATER COLLECTED ASSUMING 50% EFFICIENCY AT A 5 M3/MIN SAMPLING RATE.

#	TIME1	TIME2	PH	/ / / / FE	MN	MICROGRAM / LITER PB	CU	NI	\ \ \ \ V	/ / / / FE	MN	MICROGRAM / CUBIC METER PB	CU	NI	\ \ \ \ V
1	0.17	1.33	3.71	135.0	14.0	58.0	46.3	97.0	150.0	0.016	0.002	0.007	0.005	0.011	0.017
2	1.33	5.42	3.85	50.0	3.0	2.0	7.9	56.0	107.0	0.004	0.000	0.000	0.001	0.005	0.010
3	5.42	6.83	3.96	64.0	4.0	32.0	41.0	50.0	94.0	0.008	0.000	0.004	0.005	0.006	0.011
4	6.83	8.17	4.44	109.0	6.0	34.0	13.0	70.0	114.0	0.011	0.001	0.003	0.001	0.007	0.011
5	8.17	9.50	4.09	-0.1	-0.1	-0.1	-0.1	-0.1	-0.1	-0.100	-0.100	-0.100	-0.100	-0.100	-0.100

REVISED 3/15/84

TABLE 1. McKITTRICK FOG - 13 JAN 84 *

#	TIME1	TIME2	PH	MICRO EQ/LITER H	NA	NH4	CA	MG	CL	NO3	SO4	-/+	MICRO M/L S(IV)	CH2O	MM/L TOC	ML VOL
1	6.75	7.75	4.21	61.7	40.0	924.0	100.0	11.0	26.0	628.0	392.0	0.901	22.0	8.7	1250.0	28.00
2	7.75	8.75	4.23	58.9	27.0	598.0	72.0	13.0	17.0	431.0	379.0	1.031	34.0	14.9	3040.0	35.00
3	8.75	9.75	3.96	109.6	48.0	1070.0	59.0	8.0	24.0	828.0	540.0	1.053	29.0	18.7	2080.0	16.00

REVISED 3/21/84

TABLE 2. McKITTRICK FOG - 13 JAN 84 *

#	TIME1	TIME2	MIDT	-/+	EQUIVALENT RATIOS CL/NA	MG/NA	CA/NA	SO4/NA	NO3/SO4	NH4/N+S	H/N+S	MOLAR RATIOS H+A/N+S	S(IV)/SO4	S(IV)/CH2O
1	6.75	7.75	7.25	0.901	0.650	0.275	2.500	9.800	1.602	0.906	0.060	0.966	0.112	2.529
2	7.75	8.75	8.25	1.031	0.630	0.481	2.667	14.037	1.137	0.738	0.073	0.811	0.179	2.282
3	8.75	9.75	9.25	1.053	0.500	0.167	1.229	11.250	1.533	0.782	0.080	0.862	0.107	1.551
	SEA SALT RATIOS:				1.17	0.228	0.043	0.120						

REVISED 3/21/84

ABLE 3. McKITTRICK FOG - 13 JAN 84 *

MASS SOLUTE PER M3 OF AIR IS BASED ON LIQUID WATER CONTENT CALCULATED FROM THE VOLUME OF FOGWATER COLLECTED ASSUMING 50% EFFICIENCY AT A 5 M3/MIN SAMPLING RATE

#	TIME1	TIME2	MIDT	(MIN) DT	(ML) VOL	(G/M3) LWC	MICRO M/L S(IV)	CH2O	MM/L TOC	MICROGRAM/CU. METER S(IV)	CH2O	TOC	-/+	*CORR* -/+	PH	*PH-BY-DIFFERENCE*
1	6.75	7.75	7.25	60.0	28.0	0.187	22.0	8.7	1250.0	0.132	0.049	2802.56	0.901	0.900	4.21	*****
2	7.75	8.75	8.25	60.0	35.0	0.233	34.0	14.9	3040.0	0.254	0.104	8519.80	1.031	1.030	4.23	4.09
3	8.75	9.75	9.25	60.0	16.0	0.107	29.0	18.7	2080.0	0.099	0.060	2664.84	1.053	1.051	3.96	3.76
	TIME-WEIGHTED AVERAGE FOR 3 SAMPLES					0.042				0.065	0.028	3996.345				

REVISED 3/21/84

TABLE 4. McKITTRICK FOG - 13 JAN 84 *

MASS SOLUTE PER M3 OF AIR IS BASED ON LIQUID WATER CONTENT CALCULATED FROM THE VOLUME OF FOGWATER COLLECTED ASSUMING 50% EFFICIENCY AT A 5 M3/MIN SAMPLING RATE.

#	TIME1	TIME2	MIDT	(MIN) DT	(ML) VOL	(G/M3) LWC	MICROGRAM / CUBIC METER H	NA	NH4	CA	MG	CL	NO3	SO4	SUM
1	6.75	7.75	7.25	60.0	28.0	0.187	0.012	0.172	3.112	0.374	0.025	0.172	7.268	3.515	14.648
2	7.75	8.75	8.25	60.0	35.0	0.233	0.014	0.145	2.517	0.337	0.037	0.141	6.235	4.247	13.673
3	8.75	9.75	9.25	60.0	16.0	0.107	0.012	0.118	2.059	0.126	0.010	0.091	5.476	2.767	10.658
	TIME-WEIGHTED AVERAGE FOR 3 SAMPLES					0.176	0.012	0.145	2.563	0.279	0.024	0.134	6.326	3.509	12.993

REVISED 3/21/84

TABLE 1. BUTTONWILLOW FOG - 7 JAN 84 $

#	TIME1	TIME2	PH	H	NA	NH4	CA	MG	CL	NO3	SO4	-/+	S(IV)	CH2O	TOC	VOL
				/ / / / / /			MICRO EQ/LITER			\ \ \ \ \ \			/ MICRO M/L \		/MM/L\	/ML\
1	-0.50	0.67	5.01	9.8	15.0	1250.0	21.0	8.0	62.0	974.0	1099.0	1.578	78.0	115.0	3480.0	25.00
2	0.67	1.67	5.18	6.6	15.0	1270.0	18.0	4.0	56.0	1006.0	492.0	1.121	82.0	94.0	-0.2	15.00
3	1.67	4.17	5.40	4.0	8.0	969.0	29.0	5.0	18.0	331.0	916.0	1.175	72.0	72.0	2400.0	30.00
4	4.17	6.33	5.33	4.7	11.0	1070.0	27.0	5.0	27.0	318.0	900.0	1.045	77.0	83.0	-0.2	19.00
5	6.33	8.00	5.43	3.7	21.0	757.0	59.0	15.0	46.0	189.0	688.0	1.002	66.0	61.0	-0.2	15.00
6	8.00	11.00	5.34	4.6	15.0	1040.0	60.0	11.0	34.0	243.0	932.0	1.005	73.0	106.0	-0.2	14.00
7	11.00	13.00	6.79	0.2	-10.0	1170.0	2000.0	113.0	339.0	504.0	2281.0	0.954	-0.1	-0.1	-0.1	3.00

REVISED 5/16/84

TABLE 2. BUTTONWILLOW FOG - 7 JAN 84 $

#	TIME1	TIME2	MIDT	-/+	CL/NA	MG/NA	CA/NA	SO4/NA	NO3/SO4	NH4/N+S	H/N+S	H+A/N+S	S(IV)/SO4	S(IV)/CH2O
				/ / / /			EQUIVALENT RATIOS					\ \ \ \ / /	MOLAR RATIOS	\ \
1	-0.50	0.67	0.09	1.578	4.133	0.533	1.400	73.267	0.886	0.603	0.005	0.608	0.142	0.678
2	0.67	1.67	1.17	1.121	3.733	0.267	1.200	32.800	2.045	0.848	0.004	0.852	0.333	0.872
3	1.67	4.17	2.92	1.175	2.250	0.625	3.625	114.500	0.361	0.777	0.003	0.780	0.157	1.000
4	4.17	6.33	5.25	1.045	2.455	0.455	2.455	81.818	0.353	0.878	0.004	0.882	0.171	0.928
5	6.33	8.00	7.16	1.002	2.190	0.714	2.810	32.762	0.275	0.863	0.004	0.867	0.192	1.082
6	8.00	11.00	9.50	1.005	2.267	0.733	4.000	62.133	0.261	0.885	0.004	0.889	0.157	0.689
7	11.00	13.00	12.00	0.954	-0.100	-0.100	-0.100	-0.100	0.221	0.420	0.000	0.420	-0.100	-0.100
		SEA SALT RATIOS:			1.17	0.228	0.043	0.120						

REVISED 5/16/84

TABLE 3. BUTTONWILLOW FOG - 7 JAN 84 $

MASS SOLUTE PER M3 OF AIR IS BASED ON LIQUID WATER CONTENT CALCULATED FROM THE VOLUME OF FOGWATER COLLECTED ASSUMING 50% EFFICIENCY AT A 5 M3/MIN SAMPLING RATE

#	TIME1	TIME2	MIDT	(MIN) DT	(ML) VOL	(G/M3) LWC	/ MICRO M/L \ S(IV)	CH2O	/MM/L\ TOC	/ MICROGRAM/CU. METER \ S(IV)	CH2O	TOC	-/+	"CORR" -/+	PH	"PH-BY-DIFFERENCE"
1	-0.50	0.67	0.09	70.2	25.0	0.142	78.0	115.0	3480.0	0.356	0.492	5954.17	1.578	1.577	5.01	3.12
2	0.67	1.67	1.17	60.0	15.0	0.100	82.0	94.0	-0.2	0.263	0.282	-0.100	1.121	1.120	5.18	3.78
3	1.67	4.17	2.92	150.0	30.0	0.080	72.0	72.0	2400.0	0.185	0.173	2306.11	1.175	1.175	5.40	3.74
4	4.17	6.33	5.25	129.6	19.0	0.059	77.0	83.0	-0.2	0.145	0.146	-0.100	1.045	1.045	5.33	4.26
5	6.33	8.00	7.16	100.2	15.0	0.060	66.0	61.0	-0.2	0.127	0.110	-0.100	1.002	1.001	5.43	5.31
6	8.00	11.00	9.50	180.0	14.0	0.031	73.0	106.0	-0.2	0.073	0.099	-0.100	1.005	1.005	5.34	5.01
7	11.00	13.00	12.00	120.0	3.0	0.010	-0.1	-0.1	-0.1	-0.100	-0.100	-0.100	0.954	0.954	6.79	*****
	TIME-WEIGHTED AVERAGE FOR 7 SAMPLES					0.060				0.164	0.1813469.116					

REVISED 5/16/84

TABLE 4. BUTTONWILLOW FOG - 7 JAN 84 $

MASS SOLUTE PER M3 OF AIR IS BASED ON LIQUID WATER CONTENT CALCULATED FROM THE VOLUME OF FOGWATER COLLECTED ASSUMING 50% EFFICIENCY AT A 5 M3/MIN SAMPLING RATE.

#	TIME1	TIME2	MIDT	(MIN) DT	(ML) VOL	(G/M3) LWC	/ / / / H	NA	NH4	MICROGRAM / CUBIC METER CA	MG	CL	NO3	SO4	\ \ \ \ SUM
1	-0.50	0.67	0.09	70.2	25.0	0.142	0.001	0.049	3.212	0.060	0.014	0.313	8.602	7.519	19.771
2	0.67	1.67	1.17	60.0	15.0	0.100	0.001	0.034	2.291	0.036	0.005	0.199	6.237	2.363	11.166
3	1.67	4.17	2.92	150.0	30.0	0.080	0.000	0.015	1.398	0.046	0.005	0.051	1.642	3.520	6.677
4	4.17	6.33	5.25	129.6	19.0	0.059	0.000	0.015	1.132	0.032	0.004	0.056	1.156	2.535	4.930
5	6.33	8.00	7.16	100.2	15.0	0.060	0.000	0.029	0.818	0.071	0.011	0.098	0.702	1.979	3.707
6	8.00	11.00	9.50	180.0	14.0	0.031	0.000	0.011	0.584	0.037	0.004	0.037	0.469	1.393	2.535
7	11.00	13.00	12.00	120.0	3.0	0.010	0.000	-10.000	0.211	0.401	0.014	0.120	0.312	1.096	2.154
TIME-WEIGHTED AVERAGE FOR 7 SAMPLES						0.060	0.000	0.021	1.150	0.098	0.007	0.098	1.934	2.601	5.907

REVISED 5/16/84

TABLE 5. BUTTONWILLOW FOG - 7 JAN 84 $

THE MASS LOADING OF TRACE METALS PER CU. METER OF AIR IS BASED ON LIQUID WATER CONTENT CALCULATED FROM THE VOLUME OF FOGWATER COLLECTED ASSUMING 50% EFFICIENCY AT A 5 M3/MIN SAMPLING RATE.

#	TIME1	TIME2	PH	/ / / / FE	MN	MICROGRAM / LITER PB	CU	NI	\ \ \ \ V	/ / / / FE	MN	MICROGRAM / CUBIC METER PB	CU	NI	\ \ \ \ V
1	-0.50	0.67	5.01	142.0	48.0	39.0	36.0	48.0	34.0	0.020	0.007	0.006	0.005	0.007	0.005
2	0.67	1.67	5.18	115.0	8.0	42.0	29.0	48.0	35.0	0.012	0.001	0.004	0.003	0.005	0.004
3	1.67	4.17	5.40	44.0	6.0	34.0	270.0	40.7	34.0	0.004	0.000	0.003	0.022	0.003	0.003
4	4.17	6.33	5.33	93.0	7.0	37.0	6.0	42.5	38.0	0.005	0.000	0.002	0.000	0.002	0.002
5	6.33	8.00	5.43	444.0	15.0	70.0	4.0	38.2	30.0	0.027	0.001	0.004	0.000	0.002	0.002
6	8.00	11.00	5.34	123.0	12.0	54.0	4.0	47.3	16.0	0.004	0.000	0.002	0.000	0.001	0.000
7	11.00	13.00	6.79	-0.1	-0.1	-0.1	-0.1	-0.1	-0.1	-0.100	-0.100	-0.100	-0.100	-0.100	-0.100

REVISED 3/15/84

TABLE 1. VISALIA FOG - 18 DEC 83 *

#	TIME1	TIME2	PH	MICRO EQ/LITER H	NA	NH4	CA	MG	CL	NO3	SO4	-/+	MICRO M/L S(IV)	CH2O	/MM/L TOC	/ML VOL
1	2.33	2.75	-0.10	-0.1	560.0	2070.0	11800.0	230.0	496.0	6020.0	309.0	0.466	-0.1	-0.1	-0.1	1.00
2	6.67	7.58	5.81	1.5	45.0	2060.0	20.0	23.0	135.0	1300.0	447.0	0.871	10.0	30.0	3840.0	13.00
3	7.58	9.00	6.46	0.3	14.0	1100.0	33.0	5.0	112.0	483.0	186.0	0.676	2.0	22.0	2580.0	19.00
4	9.08	9.50	-0.10	-0.1	165.0	1500.0	0.0	46.0	229.0	464.0	390.0	0.633	-0.1	-0.1	-0.1	1.00

REVISED 5/16/84

TABLE 2. VISALIA FOG - 18 DEC 83 *

#	TIME1	TIME2	MIDT	EQUIVALENT RATIOS -/+	CL/NA	MG/NA	CA/NA	SO4/NA	NO3/SO4	NH4/N+S	H/N+S	MOLAR RATIOS H+A/N+S	S(IV)/SO4	S(IV)/CH2O
1	2.33	2.75	2.54	0.466	0.886	0.411	21.071	0.552	19.482	0.327	-0.100	0.327	-0.100	-0.100
2	6.67	7.58	7.13	0.871	3.000	0.511	0.444	9.933	2.908	1.179	0.001	1.180	0.045	0.333
3	7.58	9.00	8.29	0.676	8.000	0.357	2.357	13.286	2.597	1.644	0.001	1.645	0.022	0.091
4	9.08	9.50	9.29	0.633	1.308	0.279	0.000	2.364	1.190	1.756	-0.100	1.756	-0.100	-0.100
	SEA SALT RATIOS:				1.17	0.228	0.043	0.120						

REVISED 5/16/84

ABLE 3. VISALIA FOG - 18 DEC 83 *

MASS SOLUTE PER M3 OF AIR IS BASED ON LIQUID WATER CONTENT CALCULATED FROM THE VOLUME OF FOGWATER COLLECTED ASSUMING 50% EFFICIENCY AT A 5 M3/MIN SAMPLING RATE

#	TIME1	TIME2	MIDT	(MIN) DT	(ML) VOL	(G/M3) LWC	MICRO M/L S(IV)	/MM/L CH2O	TOC	MICROGRAM/CU. METER S(IV)	CH2O	TOC	-/+	*CORR* -/+	PH	*PH-BY-DIFFERENCE*
1	2.33	2.75	2.54	25.2	1.0	0.016	-0.1	-0.1	-0.1	-0.100	-0.100	-0.100	0.466	0.466	-0.10	*****
2	6.67	7.58	7.13	54.6	13.0	0.095	10.0	30.0	3840.0	0.031	0.086	4392.59	0.871	0.871	5.81	*****
3	7.58	9.00	8.29	85.2	19.0	0.089	2.0	22.0	2580.0	0.006	0.059	2764.22	0.676	0.676	6.46	*****
4	9.08	9.50	9.29	25.2	1.0	0.016	-0.1	-0.1	-0.1	-0.100	-0.100	-0.100	0.633	0.633	-0.10	*****
	TIME-WEIGHTED AVERAGE FOR 4 SAMPLES					0.006				0.001	0.006	587.284				

REVISED 5/16/84

TABLE 4. VISALIA FOG - 18 DEC 83 *

MASS SOLUTE PER M3 OF AIR IS BASED ON LIQUID WATER CONTENT CALCULATED FROM THE VOLUME OF FOGWATER COLLECTED ASSUMING 50% EFFICIENCY AT A 5 M3/MIN SAMPLING RATE.

#	TIME1	TIME2	MIDT	(MIN) DT	(ML) VOL	(G/M3) LWC	H	NA	NH4	MICROGRAM / CUBIC METER CA	MG	CL	NO3	SO4	SUM
1	2.33	2.75	2.54	25.2	1.0	0.016	-0.100	0.204	0.593	3.754	0.044	0.279	5.924	0.236	11.034
2	6.67	7.58	7.13	54.6	13.0	0.095	0.000	0.099	3.539	0.038	0.027	0.456	7.676	2.045	13.879
3	7.58	9.00	8.29	85.2	19.0	0.089	0.000	0.029	1.770	0.059	0.005	0.354	2.671	0.797	5.686
4	9.08	9.50	9.29	25.2	1.0	0.016	-0.100	0.060	0.430	0.000	0.009	0.129	0.457	0.297	1.381
	TIME-WEIGHTED AVERAGE FOR 4 SAMPLES					0.072	0.000	0.076	1.944	0.535	0.017	0.344	4.246	1.015	8.176

REVISED 5/14/84

TABLE 5. VISALIA FOG - 18 DEC 83 *

THE MASS LOADING OF TRACE METALS PER CU. METER OF AIR IS BASED ON LIQUID WATER CONTENT
CALCULATED FROM THE VOLUME OF FOGWATER COLLECTED ASSUMING 50% EFFICIENCY AT A 5 M3/MIN SAMPLING RATE.

				/ / / / MICROGRAM / LITER \ \ \ \						/ / / / MICROGRAM / CUBIC METER \ \ \ \					
*	TIME1	TIME2	PH	FE	MN	PB	CU	NI	V	FE	MN	PB	CU	NI	V
1	2.33	2.75	-0.10	-0.1	-0.1	-0.1	-0.1	-0.1	-0.1	-0.100	-0.100	-0.100	-0.100	-0.100	-0.100
2	6.67	7.58	5.81	846.0	88.0	184.0	69.0	192.0	10.0	0.081	0.008	0.018	0.007	0.018	0.001
3	7.58	9.00	6.46	153.0	22.0	47.0	28.0	43.6	11.0	0.014	0.002	0.004	0.002	0.004	0.001
4	9.08	9.50	-0.10	-0.1	-0.1	-0.1	-0.1	-0.1	-0.1	-0.100	-0.100	-0.100	-0.100	-0.100	-0.100

REVISED 3/15/84

TABLE 1. VISALIA FOG - 19 DEC 83 $

#	TIME1	TIME2	PH	MICRO EQ/LITER H	NA	NH4	CA	MG	CL	NO3	SO4	-/+	MICRO M/L S(IV)	CH2O	MM/L TOC	ML VOL
1	2.00	3.00	7.01	0.1	22.0	1170.0	20.0	2.0	39.0	296.0	115.0	0.371	0.0	26.0	-0.2	12.00
2	3.00	5.00	6.80	0.2	7.0	690.0	12.0	2.0	20.0	152.0	49.0	0.311	0.0	18.0	1830.0	20.00
3	5.00	7.00	6.74	0.2	3.0	750.0	12.0	2.0	26.0	220.0	295.0	0.701	3.0	24.0	1770.0	31.00
4	7.00	8.00	6.45	0.4	10.0	1120.0	55.0	4.0	58.0	412.0	566.0	0.837	40.0	33.0	3220.0	12.00
5	8.00	9.25	6.77	0.2	27.0	1800.0	60.0	18.0	116.0	868.0	638.0	0.842	17.0	55.0	-0.2	3.00

REVISED 3/21/84

TABLE 2. VISALIA FOG - 19 DEC 83 $

#	TIME1	TIME2	MIDT	-/+	EQUIVALENT RATIOS CL/NA	MG/NA	CA/NA	SO4/NA	NO3/SO4	NH4/N+S	H/N+S	H+A/N+S	MOLAR RATIOS S(IV)/SO4	S(IV)/CH2O
1	2.00	3.00	2.50	0.371	1.773	0.091	0.909	5.227	2.574	2.847	0.000	2.847	0.000	0.000
2	3.00	5.00	4.00	0.311	2.857	0.286	1.714	7.000	3.102	3.433	0.001	3.434	0.000	0.000
3	5.00	7.00	6.00	0.701	8.667	0.667	4.000	98.333	0.746	1.456	0.000	1.457	0.020	0.125
4	7.00	8.00	7.50	0.837	5.800	0.400	5.500	56.600	0.728	1.145	0.000	1.146	0.141	1.212
5	8.00	9.25	8.63	0.842	4.296	0.667	2.222	23.630	1.361	1.195	0.000	1.195	0.053	0.309
	SEA SALT RATIOS:				1.17	0.228	0.043	0.120						

REVISED 3/21/84

ABLE 3. VISALIA FOG - 19 DEC 83 $

MASS SOLUTE PER M3 OF AIR IS BASED ON LIQUID WATER CONTENT CALCULATED FROM THE VOLUME OF FOGWATER COLLECTED ASSUMING 50% EFFICIENCY AT A 5 M3/MIN SAMPLING RATE

#	TIME1	TIME2	MIDT	(MIN) DT	(ML) VOL	(G/M3) LWC	MICRO M/L S(IV)	CH2O	MM/L TOC	MICROGRAM/CU. METER S(IV)	CH2O	TOC	-/+	"CORR" -/+	PH	"PH-BY-DIFFERENCE"
1	2.00	3.00	2.50	60.0	12.0	0.080	0.0	26.0	-0.2	0.000	0.062	-0.100	0.371	0.371	7.01	*****
2	3.00	5.00	4.00	120.0	20.0	0.067	0.0	18.0	1830.0	0.000	0.036	1465.34	0.311	0.311	6.80	*****
3	5.00	7.00	6.00	120.0	31.0	0.103	3.0	24.0	1770.0	0.010	0.074	2196.81	0.701	0.701	6.74	*****
4	7.00	8.00	7.50	60.0	12.0	0.080	40.0	33.0	3220.0	0.103	0.079	3094.03	0.837	0.837	6.45	*****
5	8.00	9.25	8.63	75.0	3.0	0.016	17.0	55.0	-0.2	0.009	0.026	-0.100	0.842	0.842	6.77	*****
	TIME-WEIGHTED AVERAGE FOR 5 SAMPLES					0.011				0.004	0.011	563.458				

REVISED 3/21/84

TABLE 4. VISALIA FOG - 19 DEC 83 $

MASS SOLUTE PER M3 OF AIR IS BASED ON LIQUID WATER CONTENT CALCULATED FROM THE VOLUME OF FOGWATER COLLECTED ASSUMING 50% EFFICIENCY AT A 5 M3/MIN SAMPLING RATE.

#	TIME1	TIME2	MIDT	(MIN) DT	(ML) VOL	(G/M3) LWC	/ / / / H	NA	NH4	MICROGRAM / CUBIC METER CA	MG	CL	NO3	SO4	\ \ \ \ SUM
1	2.00	3.00	2.50	60.0	12.0	0.080	0.000	0.040	1.689	0.032	0.002	0.111	1.468	0.442	3.784
2	3.00	5.00	4.00	120.0	20.0	0.067	0.000	0.011	0.830	0.016	0.002	0.047	0.628	0.157	1.691
3	5.00	7.00	6.00	120.0	31.0	0.103	0.000	0.007	1.398	0.025	0.003	0.095	1.409	1.464	4.401
4	7.00	8.00	7.50	60.0	12.0	0.080	0.000	0.018	1.616	0.088	0.004	0.164	2.044	2.175	6.110
5	8.00	9.25	8.63	75.0	3.0	0.016	0.000	0.010	0.520	0.019	0.004	0.066	0.861	0.490	1.969
TIME-WEIGHTED AVERAGE FOR 5 SAMPLES						0.072	0.000	0.015	1.160	0.031	0.003	0.089	1.195	0.893	3.385

REVISED 3/21/84

TABLE 5. VISALIA FOG - 19 DEC 83 $

THE MASS LOADING OF TRACE METALS PER CU. METER OF AIR IS BASED ON LIQUID WATER CONTENT CALCULATED FROM THE VOLUME OF FOGWATER COLLECTED ASSUMING 50% EFFICIENCY AT A 5 M3/MIN SAMPLING RATE.

#	TIME1	TIME2	PH	/ / / / FE	MN	MICROGRAM / LITER PB	CU	NI	\ \ \ \ V	/ / / / FE	MN	MICROGRAM / CUBIC METER PB	CU	NI	\ \ \ \ V
1	2.00	3.00	7.01	228.0	38.0	29.0	17.0	73.0	7.0	0.018	0.003	0.002	0.001	0.006	0.001
2	3.00	5.00	6.80	18.0	7.0	10.0	4.0	13.5	7.0	0.001	0.000	0.001	0.000	0.001	0.000
3	5.00	7.00	6.74	107.0	6.0	44.0	632.0	639.0	9.0	0.011	0.001	0.005	0.065	0.066	0.001
4	7.00	8.00	6.45	153.0	9.0	75.0	14.3	9.9	9.0	0.012	0.001	0.006	0.001	0.001	0.001
5	8.00	9.25	6.77	-0.1	-0.1	-0.1	-0.1	-0.1	-0.1	-0.100	-0.100	-0.100	-0.100	-0.100	-0.100

REVISED 3/15/84

TABLE 1. VISALIA FOG - 3 JAN 84 $

#	TIME1	TIME2	PH	MICRO EQ/LITER H	NA	NH4	CA	MG	CL	NO3	SO4	-/+	MICRO M/L S(IV)	CH2O	/MM/L\ TOC	/ML\ VOL
1	-0.33	0.33	5.51	3.1	-0.1	3230.0	140.0	2.0	303.0	1000.0	410.0	0.508	-0.1	-0.1	-0.1	1.50

REVISED 5/17/84

TABLE 2. VISALIA FOG - 3 JAN 84 $

#	TIME1	TIME2	MIDT	-/+	EQUIVALENT RATIOS CL/NA	MG/NA	CA/NA	SO4/NA	NO3/SO4	NH4/N+S	H/N+S	MOLAR RATIOS H+A/N+S	S(IV)/SO4	S(IV)/CH2O
1	-0.33	0.33	0.00	0.508	-0.100	-0.100	-0.100	-0.100	2.439	2.291	0.002	2.293	-0.100	-0.100
	SEA SALT RATIOS:				1.17	0.228	0.043	0.120						

REVISED 5/17/84

ABLE 3. VISALIA FOG - 3 JAN 84 $

MASS SOLUTE PER M3 OF AIR IS BASED ON LIQUID WATER CONTENT CALCULATED FROM THE VOLUME OF FOGWATER COLLECTED ASSUMING 50% EFFICIENCY AT A 5 M3/MIN SAMPLING RATE

#	TIME1	TIME2	MIDT	(MIN) DT	(ML) VOL	(G/M3) LWC	MICRO M/L S(IV)	/MM/L\ CH2O	TOC	MICROGRAM/CU. METER S(IV)	CH2O	TOC	-/+	*CORR* -/+	PH	*PH-BY-DIFFERENCE*
1	-0.33	0.33	0.00	39.6	1.5	0.015	-0.1	-0.1	-0.1	-0.100	-0.100	-0.100	0.508	0.508	5.51	*****
	TIME-WEIGHTED AVERAGE FOR 1 SAMPLES					0.001				0.000	0.000	0.000				

REVISED 5/17/84

TABLE 4. VISALIA FOG - 3 JAN 84 $

MASS SOLUTE PER M3 OF AIR IS BASED ON LIQUID WATER CONTENT CALCULATED FROM THE VOLUME OF FOGWATER COLLECTED ASSUMING 50% EFFICIENCY AT A 5 M3/MIN SAMPLING RATE.

#	TIME1	TIME2	MIDT	(MIN) DT	(ML) VOL	(G/M3) LWC	MICROGRAM / CUBIC METER H	NA	NH4	CA	MG	CL	NO3	SO4	SUM
1	-0.33	0.33	0.00	39.6	1.5	0.015	0.000	-0.100	0.883	0.043	0.000	0.163	0.939	0.298	2.326
	TIME-WEIGHTED AVERAGE FOR 1 SAMPLES					0.015	0.000	0.000	0.883	0.043	0.000	0.163	0.939	0.298	2.326

REVISED 5/17/84

TABLE 1. VISALIA FOG - 5 JAN 84 $

#	TIME1	TIME2	PH	MICRO EQ/LITER H	NA	NH4	CA	MG	CL	NO3	SO4	-/+	MICRO M/L S(IV)	CH2O	/MM/L\ TOC	/ML\ VOL
1	3.63	4.00	6.90	0.1	2.0	2290.0	35.0	2.0	129.0	980.0	526.0	0.696	15.0	29.0	-0.2	5.00
2	4.00	4.50	6.89	0.1	2.0	1740.0	28.0	2.0	74.0	956.0	429.0	0.818	9.0	28.0	-0.2	4.00
3	4.55	5.52	-0.10	-0.1	23.0	2040.0	18.0	5.0	206.0	956.0	424.0	0.760	-0.1	-0.1	-0.2	4.00
4	5.53	6.50	7.13	0.1	12.0	1810.0	25.0	3.0	108.0	788.0	392.0	0.690	12.0	31.0	-0.2	5.00
5	6.50	7.00	7.13	0.1	10.0	1970.0	41.0	2.0	18.0	752.0	736.0	0.744	-0.1	-0.1	-0.2	4.00
6	7.00	8.00	7.06	0.1	8.0	1840.0	26.0	6.0	187.0	712.0	544.0	0.768	-0.1	-0.1	-0.2	9.00

REVISED 5/16/84

TABLE 2. VISALIA FOG - 5 JAN 84 $

#	TIME1	TIME2	MIDT	EQUIVALENT RATIOS -/+	CL/NA	MG/NA	CA/NA	SO4/NA	NO3/SO4	NH4/N+S	H/N+S	MOLAR RATIOS H+A/N+S	S(IV)/SO4	S(IV)/CH2O
1	3.63	4.00	3.82	0.696	64.500	1.000	17.500	263.000	1.863	1.521	0.000	1.521	0.057	0.517
2	4.00	4.50	4.25	0.818	37.000	1.000	14.000	214.500	2.228	1.256	0.000	1.256	0.042	0.321
3	4.55	5.52	5.04	0.760	8.957	0.217	0.783	18.435	2.255	1.478	-0.100	1.478	-0.100	-0.100
4	5.53	6.50	6.02	0.690	9.000	0.250	2.083	32.667	2.010	1.534	0.000	1.534	0.061	0.387
5	6.50	7.00	6.75	0.744	1.800	0.200	4.100	73.600	1.022	1.324	0.000	1.324	-0.100	-0.100
6	7.00	8.00	7.50	0.768	23.375	0.750	3.250	68.000	1.309	1.465	0.000	1.465	-0.100	-0.100
	SEA SALT RATIOS:				1.17	0.228	0.043	0.120						

REVISED 5/16/84

ABLE 3. VISALIA FOG - 5 JAN 84 $

MASS SOLUTE PER M3 OF AIR IS BASED ON LIQUID WATER CONTENT CALCULATED FROM THE VOLUME OF FOGWATER COLLECTED ASSUMING 50% EFFICIENCY AT A 5 M3/MIN SAMPLING RATE

#	TIME1	TIME2	MIDT	(MIN) DT	(ML) VOL	(G/M3) LWC	MICRO M/L S(IV)	/MM/L\ CH2O	TOC	MICROGRAM/CU. METER S(IV)	CH2O	TOC	-/+	"CORR" -/+	PH	"PH-BY-DIFFERENCE"
1	3.63	4.00	3.82	22.2	5.0	0.090	15.0	29.0	-0.2	0.043	0.078	-0.100	0.696	0.696	6.90	*****
2	4.00	4.50	4.25	30.0	4.0	0.053	9.0	28.0	-0.2	0.015	0.045	-0.100	0.818	0.818	6.89	*****
3	4.55	5.52	5.04	58.2	4.0	0.027	-0.1	-0.1	-0.2	-0.100	-0.100	-0.100	0.760	0.760	-0.10	*****
4	5.53	6.50	6.02	58.2	5.0	0.034	12.0	31.0	-0.2	0.013	0.032	-0.100	0.690	0.690	7.13	*****
5	6.50	7.00	6.75	30.0	4.0	0.053	-0.1	-0.1	-0.2	-0.100	-0.100	-0.100	0.744	0.744	7.13	*****
6	7.00	8.00	7.50	60.0	9.0	0.060	-0.1	-0.1	-0.2	-0.100	-0.100	-0.100	0.768	0.768	7.06	*****
TIME-WEIGHTED AVERAGE FOR 6 SAMPLES						0.012				0.004	0.009	0.000				

REVISED 5/16/84

TABLE 4. VISALIA FOG - 5 JAN 84 $

MASS SOLUTE PER M3 OF AIR IS BASED ON LIQUID WATER CONTENT CALCULATED FROM THE VOLUME OF FOGWATER COLLECTED ASSUMING 50% EFFICIENCY AT A 5 M3/MIN SAMPLING RATE.

#	TIME1	TIME2	MIDT	(MIN) DT	(ML) VOL	(G/M3) LWC	/ / / / H	MICROGRAM / CUBIC METER NA	NH4	CA	MG	CL	NO3	SO4	\ \ \ \ SUM
1	3.63	4.00	3.82	22.2	5.0	0.090	0.000	0.004	3.722	0.063	0.002	0.412	5.474	2.276	11.953
2	4.00	4.50	4.25	30.0	4.0	0.053	0.000	0.002	1.674	0.030	0.001	0.140	3.161	1.099	6.108
3	4.55	5.52	5.04	58.2	4.0	0.027	-0.100	0.015	1.012	0.010	0.002	0.201	1.629	0.560	3.428
4	5.53	6.50	6.02	58.2	5.0	0.034	0.000	0.009	1.122	0.017	0.001	0.132	1.679	0.647	3.607
5	6.50	7.00	6.75	30.0	4.0	0.053	0.000	0.012	1.895	0.044	0.001	0.034	2.487	1.885	6.359
6	7.00	8.00	7.50	60.0	9.0	0.060	0.000	0.011	1.992	0.031	0.004	0.398	2.649	1.568	6.652
TIME-WEIGHTED AVERAGE FOR 6 SAMPLES						0.048	0.000	0.010	1.676	0.027	0.002	0.223	2.484	1.177	5.599

REVISED 5/16/84

TABLE 5. VISALIA FOG - 5 JAN 84 $

THE MASS LOADING OF TRACE METALS PER CU. METER OF AIR IS BASED ON LIQUID WATER CONTENT CALCULATED FROM THE VOLUME OF FOGWATER COLLECTED ASSUMING 50% EFFICIENCY AT A 5 M3/MIN SAMPLING RATE.

#	TIME1	TIME2	PH	/ / / / FE	MN	MICROGRAM / LITER PB	CU	NI	\ \ \ \ V	/ / / / FE	MN	MICROGRAM / CUBIC METER PB	CU	NI	\ \ \ \ V
1	3.63	4.00	6.90	541.0	32.0	76.0	26.0	37.8	8.0	0.049	0.003	0.007	0.002	0.003	0.001
2	4.00	4.50	6.89	-0.1	-0.1	-0.1	-0.1	-0.1	-0.1	-0.100	-0.100	-0.100	-0.100	-0.100	-0.100
3	4.55	5.52	-0.10	-0.1	-0.1	-0.1	-0.1	-0.1	-0.1	-0.100	-0.100	-0.100	-0.100	-0.100	-0.100
4	5.53	6.50	7.13	441.0	13.0	350.0	32.0	16.4	6.0	0.015	0.000	0.012	0.001	0.001	0.000
5	6.50	7.00	7.13	-0.1	-0.1	-0.1	-0.1	-0.1	-0.1	-0.100	-0.100	-0.100	-0.100	-0.100	-0.100
6	7.00	8.00	7.06	-0.1	-0.1	-0.1	-0.1	-0.1	-0.1	-0.100	-0.100	-0.100	-0.100	-0.100	-0.100

REVISED 3/15/84

TABLE 1. VISALIA FOG - 7 JAN 84 $

#	TIME1	TIME2	PH	MICRO EQ/LITER / / / / / / H	NA	NH4	CA	MG	CL	NO3 \ \ \ \ \ \	SO4	-/+	MICRO M/L / S(IV)	CH2O \	/MM/L\ TOC	/ML\ VOL
1	1.33	2.83	6.97	0.1	9.0	860.0	11.0	2.0	25.0	198.0	176.0	0.452	-0.1	28.0	1720.0	16.00
2	2.83	4.50	7.23	0.1	4.0	678.0	6.0	1.0	2.0	162.0	122.0	0.409	4.0	22.0	1600.0	21.00
3	4.50	6.33	7.12	0.1	3.0	606.0	4.0	1.0	-0.1	117.0	150.0	0.418	10.0	22.0	1930.0	21.00
4	6.33	7.33	6.97	0.1	2.0	723.0	10.0	2.0	-0.1	99.0	179.0	0.351	19.0	31.0	-0.2	7.00
5	7.33	8.83	7.21	0.1	2.0	789.0	28.0	2.0	-0.1	98.0	390.0	0.565	24.0	65.0	2170.0	13.00
6	8.83	9.33	7.16	0.1	2.0	687.0	-10.0	2.0	1132.0	112.0	201.0	2.122	-0.1	-0.1	-0.2	3.00

REVISED 5/16/84

TABLE 2. VISALIA FOG - 7 JAN 84 $

#	TIME1	TIME2	MIDT	-/+	EQUIVALENT RATIOS / / / / CL/NA	MG/NA	CA/NA	SO4/NA	NO3/SO4	NH4/N+S	H/N+S	\ \ \ \ \ / / MOLAR RATIOS \ \ H+A/N+S	S(IV)/SO4	S(IV)/CH2O
1	1.33	2.83	2.08	0.452	2.778	0.222	1.222	19.556	1.125	2.299	0.000	2.300	-0.100	-0.100
2	2.83	4.50	3.66	0.409	0.500	0.250	1.500	30.500	1.328	2.387	0.000	2.388	0.066	0.182
3	4.50	6.33	5.41	0.418	-0.100	0.333	1.333	50.000	0.780	2.270	0.000	2.270	0.133	0.455
4	6.33	7.33	6.83	0.351	-0.100	1.000	5.000	89.500	0.553	2.601	0.000	2.601	0.212	0.613
5	7.33	8.83	8.08	0.565	-0.100	1.000	14.000	195.000	0.251	1.617	0.000	1.617	0.123	0.369
6	8.83	9.33	9.08	2.122	566.000	1.000	-0.100	100.500	0.557	2.195	0.000	2.195	-0.100	-0.100
	SEA SALT RATIOS:				1.17	0.228	0.043	0.120						

REVISED 5/16/84

ABLE 3. VISALIA FOG - 7 JAN 84 $

MASS SOLUTE PER M3 OF AIR IS BASED ON LIQUID WATER CONTENT CALCULATED FROM THE VOLUME OF FOGWATER COLLECTED ASSUMING 50% EFFICIENCY AT A 5 M3/MIN SAMPLING RATE

#	TIME1	TIME2	MIDT	(MIN) DT	(ML) VOL	(G/M3) LWC	/ MICRO M/L \ S(IV)	CH2O	/MM/L\ TOC	/ MICROGRAM/CU. METER \ S(IV)	CH2O	TOC	-/+	"CORR" -/+	PH	"PH-BY-DIFFERENCE"
1	1.33	2.83	2.08	90.0	16.0	0.071	-0.1	28.0	1720.0	-0.100	0.060	1469.07	0.452	0.452	6.97	*****
2	2.83	4.50	3.66	100.2	21.0	0.084	4.0	22.0	1600.0	0.011	0.055	1611.05	0.409	0.409	7.23	*****
3	4.50	6.33	5.41	109.8	21.0	0.077	10.0	22.0	1930.0	0.025	0.051	1773.42	0.418	0.418	7.12	*****
4	6.33	7.33	6.83	60.0	7.0	0.047	19.0	31.0	-0.2	0.028	0.043	-0.100	0.351	0.351	6.97	*****
5	7.33	8.83	8.08	90.0	13.0	0.058	24.0	65.0	2170.0	0.044	0.113	1505.91	0.565	0.565	7.21	*****
6	8.83	9.33	9.08	30.0	3.0	0.040	-0.1	-0.1	-0.2	-0.100	-0.100	-0.100	2.122	2.122	7.16	3.12
TIME-WEIGHTED AVERAGE FOR 6 SAMPLES						0.021				0.010	0.029	1039.832				

REVISED 5/16/84

TABLE 4. VISALIA FOG - 7 JAN 84 $

MASS SOLUTE PER M3 OF AIR IS BASED ON LIQUID WATER CONTENT CALCULATED FROM THE VOLUME OF FOGWATER COLLECTED ASSUMING 50% EFFICIENCY AT A 5 M3/MIN SAMPLING RATE.

				(MIN)	(ML)	(G/M3)	/ / / /	MICROGRAM / CUBIC METER						\ \ \ \
#	TIME1	TIME2	MIDT	DT	VOL	LWC	H	NA	NH4	CA	MG	CL	NO3	SO4	SUM
1	1.33	2.83	2.08	90.0	16.0	0.071	0.000	0.015	1.103	0.016	0.002	0.063	0.873	0.601	2.672
2	2.83	4.50	3.66	100.2	21.0	0.084	0.000	0.008	1.025	0.010	0.001	0.006	0.842	0.491	2.383
3	4.50	6.33	5.41	109.8	21.0	0.077	0.000	0.005	0.836	0.006	0.001	-0.100	0.555	0.551	1.955
4	6.33	7.33	6.83	60.0	7.0	0.047	0.000	0.002	0.609	0.009	0.001	-0.100	0.286	0.401	1.309
5	7.33	8.83	8.08	90.0	13.0	0.058	0.000	0.003	0.822	0.032	0.001	-0.100	0.351	1.082	2.292
6	8.83	9.33	9.08	30.0	3.0	0.040	0.000	0.002	0.496	-10.000	0.001	1.605	0.278	0.386	2.768
TIME-WEIGHTED AVERAGE FOR 6 SAMPLES						0.067	0.000	0.006	0.873	0.015	0.001	0.247	0.585	0.619	2.212

REVISED 5/16/84

TABLE 5. VISALIA FOG - 7 JAN 84 $

THE MASS LOADING OF TRACE METALS PER CU. METER OF AIR IS BASED ON LIQUID WATER CONTENT CALCULATED FROM THE VOLUME OF FOGWATER COLLECTED ASSUMING 50% EFFICIENCY AT A 5 M3/MIN SAMPLING RATE.

				/ / / /		MICROGRAM / LITER			\ \ \ \	/ / / /		MICROGRAM / CUBIC METER			\ \ \ \
#	TIME1	TIME2	PH	FE	MN	PB	CU	NI	V	FE	MN	PB	CU	NI	V
1	1.33	2.83	6.97	224.0	9.0	36.0	11.0	18.6	10.0	0.016	0.001	0.003	0.001	0.001	0.001
2	2.83	4.50	7.23	87.0	4.0	45.0	2.0	4.4	5.0	0.007	0.000	0.004	0.000	0.000	0.000
3	4.50	6.33	7.12	27.0	3.0	33.0	1.0	2.6	6.0	0.002	0.000	0.003	0.000	0.000	0.000
4	6.33	7.33	6.97	-0.1	-0.1	-0.1	-0.1	-0.1	-0.1	-0.100	-0.100	-0.100	-0.100	-0.100	-0.100
5	7.33	8.83	7.21	57.0	4.0	46.0	1.0	11.0	16.0	0.003	0.000	0.003	0.000	0.001	0.001
6	8.83	9.33	7.16	-0.1	-0.1	-0.1	-0.1	-0.1	-0.1	-0.100	-0.100	-0.100	-0.100	-0.100	-0.100

REVISED 3/15/84